



PATTERN RECOGNITION
AND MACHINE LEARNING

CHRISTOPHER M. BISHOP

Information Science and Statistics

Series Editors:

M. Jordan

J. Kleinberg

B. Schölkopf

Information Science and Statistics

Akaike and Kitagawa: The Practice of Time Series Analysis.

Bishop: Pattern Recognition and Machine Learning.

Cowell, Dawid, Lauritzen, and Spiegelhalter: Probabilistic Networks and Expert Systems.

Doucet, de Freitas, and Gordon: Sequential Monte Carlo Methods in Practice.

Fine: Feedforward Neural Network Methodology.

Hawkins and Olwell: Cumulative Sum Charts and Charting for Quality Improvement.

Jensen: Bayesian Networks and Decision Graphs.

Marchette: Computer Intrusion Detection and Network Monitoring:
A Statistical Viewpoint.

Rubinstein and Kroese: The Cross-Entropy Method: A Unified Approach to
Combinatorial Optimization, Monte Carlo Simulation, and Machine Learning.

Studený: Probabilistic Conditional Independence Structures.

Vapnik: The Nature of Statistical Learning Theory, Second Edition.

Wallace: Statistical and Inductive Inference by Minimum Message Length.

Christopher M. Bishop

Pattern Recognition and Machine Learning

Christopher M. Bishop F.R.Eng.
Assistant Director
Microsoft Research Ltd
Cambridge CB3 0FB, U.K.
cmbishop@microsoft.com
<http://research.microsoft.com/~cmbishop>

Series Editors

Michael Jordan
Department of Computer
Science and Department
of Statistics
University of California,
Berkeley
Berkeley, CA 94720
USA

Professor Jon Kleinberg
Department of Computer
Science
Cornell University
Ithaca, NY 14853
USA

Bernhard Schölkopf
Max Planck Institute for
Biological Cybernetics
Spemannstrasse 38
72076 Tübingen
Germany

Library of Congress Control Number: 2006922522

ISBN-10: 0-387-31073-8
ISBN-13: 978-0387-31073-2

Printed on acid-free paper.

© 2006 Springer Science+Business Media, LLC
All rights reserved. This work may not be translated or copied in whole or in part without the written permission of the publisher
(Springer Science+Business Media, LLC, 233 Spring Street, New York, NY 10013, USA), except for brief excerpts in connection
with reviews or scholarly analysis. Use in connection with any form of information storage and retrieval, electronic adaptation,
computer software, or by similar or dissimilar methodology now known or hereafter developed is forbidden.
The use in this publication of trade names, trademarks, service marks, and similar terms, even if they are not identified as such,
is not to be taken as an expression of opinion as to whether or not they are subject to proprietary rights.

Printed in Singapore. (KYO)

9 8 7 6 5 4 3 2 1

springer.com

This book is dedicated to my family:

Jenna, Mark, and Hugh



Total eclipse of the sun, Antalya, Turkey, 29 March 2006.

Preface

Pattern recognition has its origins in engineering, whereas machine learning grew out of computer science. However, these activities can be viewed as two facets of the same field, and together they have undergone substantial development over the past ten years. In particular, Bayesian methods have grown from a specialist niche to become mainstream, while graphical models have emerged as a general framework for describing and applying probabilistic models. Also, the practical applicability of Bayesian methods has been greatly enhanced through the development of a range of approximate inference algorithms such as variational Bayes and expectation propagation. Similarly, new models based on kernels have had significant impact on both algorithms and applications.

This new textbook reflects these recent developments while providing a comprehensive introduction to the fields of pattern recognition and machine learning. It is aimed at advanced undergraduates or first year PhD students, as well as researchers and practitioners, and assumes no previous knowledge of pattern recognition or machine learning concepts. Knowledge of multivariate calculus and basic linear algebra is required, and some familiarity with probabilities would be helpful though not essential as the book includes a self-contained introduction to basic probability theory.

Because this book has broad scope, it is impossible to provide a complete list of references, and in particular no attempt has been made to provide accurate historical attribution of ideas. Instead, the aim has been to give references that offer greater detail than is possible here and that hopefully provide entry points into what, in some cases, is a very extensive literature. For this reason, the references are often to more recent textbooks and review articles rather than to original sources.

The book is supported by a great deal of additional material, including lecture slides as well as the complete set of figures used in the book, and the reader is encouraged to visit the book web site for the latest information:

<http://research.microsoft.com/~cmbishop/PRML>

Exercises

The exercises that appear at the end of every chapter form an important component of the book. Each exercise has been carefully chosen to reinforce concepts explained in the text or to develop and generalize them in significant ways, and each is graded according to difficulty ranging from (\star), which denotes a simple exercise taking a few minutes to complete, through to ($\star\star\star$), which denotes a significantly more complex exercise.

It has been difficult to know to what extent these solutions should be made widely available. Those engaged in self study will find worked solutions very beneficial, whereas many course tutors request that solutions be available only via the publisher so that the exercises may be used in class. In order to try to meet these conflicting requirements, those exercises that help amplify key points in the text, or that fill in important details, have solutions that are available as a PDF file from the book web site. Such exercises are denoted by **www**. Solutions for the remaining exercises are available to course tutors by contacting the publisher (contact details are given on the book web site). Readers are strongly encouraged to work through the exercises unaided, and to turn to the solutions only as required.

Although this book focuses on concepts and principles, in a taught course the students should ideally have the opportunity to experiment with some of the key algorithms using appropriate data sets. A companion volume (Bishop and Nabney, 2008) will deal with practical aspects of pattern recognition and machine learning, and will be accompanied by Matlab software implementing most of the algorithms discussed in this book.

Acknowledgements

First of all I would like to express my sincere thanks to Markus Svensén who has provided immense help with preparation of figures and with the typesetting of the book in L^AT_EX. His assistance has been invaluable.

I am very grateful to Microsoft Research for providing a highly stimulating research environment and for giving me the freedom to write this book (the views and opinions expressed in this book, however, are my own and are therefore not necessarily the same as those of Microsoft or its affiliates).

Springer has provided excellent support throughout the final stages of preparation of this book, and I would like to thank my commissioning editor John Kimmel for his support and professionalism, as well as Joseph Piliero for his help in designing the cover and the text format and MaryAnn Brickner for her numerous contributions during the production phase. The inspiration for the cover design came from a discussion with Antonio Criminisi.

I also wish to thank Oxford University Press for permission to reproduce excerpts from an earlier textbook, *Neural Networks for Pattern Recognition* (Bishop, 1995a). The images of the Mark 1 perceptron and of Frank Rosenblatt are reproduced with the permission of Arvin Calspan Advanced Technology Center. I would also like to thank Asela Gunawardana for plotting the spectrogram in Figure 13.1, and Bernhard Schölkopf for permission to use his kernel PCA code to plot Figure 12.17.

Many people have helped by proofreading draft material and providing comments and suggestions, including Shivani Agarwal, Cédric Archambeau, Arik Azran, Andrew Blake, Hakan Cevikalp, Michael Fourman, Brendan Frey, Zoubin Ghahramani, Thore Graepel, Katherine Heller, Ralf Herbrich, Geoffrey Hinton, Adam Johansen, Matthew Johnson, Michael Jordan, Eva Kalyvianaki, Anitha Kannan, Julia Lasserre, David Liu, Tom Minka, Ian Nabney, Tonatiuh Pena, Yuan Qi, Sam Roweis, Balaji Sanjiya, Toby Sharp, Ana Costa e Silva, David Spiegelhalter, Jay Stokes, Tara Symeonides, Martin Szummer, Marshall Tappen, Ilkay Ulusoy, Chris Williams, John Winn, and Andrew Zisserman.

Finally, I would like to thank my wife Jenna who has been hugely supportive throughout the several years it has taken to write this book.

Chris Bishop
Cambridge
February 2006

Mathematical notation

I have tried to keep the mathematical content of the book to the minimum necessary to achieve a proper understanding of the field. However, this minimum level is nonzero, and it should be emphasized that a good grasp of calculus, linear algebra, and probability theory is essential for a clear understanding of modern pattern recognition and machine learning techniques. Nevertheless, the emphasis in this book is on conveying the underlying concepts rather than on mathematical rigour.

I have tried to use a consistent notation throughout the book, although at times this means departing from some of the conventions used in the corresponding research literature. Vectors are denoted by lower case bold Roman letters such as \mathbf{x} , and all vectors are assumed to be column vectors. A superscript T denotes the transpose of a matrix or vector, so that \mathbf{x}^T will be a row vector. Uppercase bold roman letters, such as \mathbf{M} , denote matrices. The notation (w_1, \dots, w_M) denotes a row vector with M elements, while the corresponding column vector is written as $\mathbf{w} = (w_1, \dots, w_M)^T$.

The notation $[a, b]$ is used to denote the *closed* interval from a to b , that is the interval including the values a and b themselves, while (a, b) denotes the corresponding *open* interval, that is the interval excluding a and b . Similarly, $[a, b)$ denotes an interval that includes a but excludes b . For the most part, however, there will be little need to dwell on such refinements as whether the end points of an interval are included or not.

The $M \times M$ identity matrix (also known as the unit matrix) is denoted \mathbf{I}_M , which will be abbreviated to \mathbf{I} where there is no ambiguity about its dimensionality. It has elements I_{ij} that equal 1 if $i = j$ and 0 if $i \neq j$.

A functional is denoted $f[y]$ where $y(x)$ is some function. The concept of a functional is discussed in Appendix D.

The notation $g(x) = O(f(x))$ denotes that $|f(x)/g(x)|$ is bounded as $x \rightarrow \infty$. For instance if $g(x) = 3x^2 + 2$, then $g(x) = O(x^2)$.

The expectation of a function $f(x, y)$ with respect to a random variable x is denoted by $\mathbb{E}_x[f(x, y)]$. In situations where there is no ambiguity as to which variable is being averaged over, this will be simplified by omitting the suffix, for instance

$\mathbb{E}[x]$. If the distribution of x is conditioned on another variable z , then the corresponding conditional expectation will be written $\mathbb{E}_x[f(x)|z]$. Similarly, the variance is denoted $\text{var}[f(x)]$, and for vector variables the covariance is written $\text{cov}[\mathbf{x}, \mathbf{y}]$. We shall also use $\text{cov}[\mathbf{x}]$ as a shorthand notation for $\text{cov}[\mathbf{x}, \mathbf{x}]$. The concepts of expectations and covariances are introduced in Section 1.2.2.

If we have N values $\mathbf{x}_1, \dots, \mathbf{x}_N$ of a D -dimensional vector $\mathbf{x} = (x_1, \dots, x_D)^T$, we can combine the observations into a data matrix \mathbf{X} in which the n^{th} row of \mathbf{X} corresponds to the row vector \mathbf{x}_n^T . Thus the n, i element of \mathbf{X} corresponds to the i^{th} element of the n^{th} observation \mathbf{x}_n . For the case of one-dimensional variables we shall denote such a matrix by \mathbf{x} , which is a column vector whose n^{th} element is x_n . Note that \mathbf{x} (which has dimensionality N) uses a different typeface to distinguish it from \mathbf{x} (which has dimensionality D).

Contents

| | |
|---|-------------|
| Preface | vii |
| Mathematical notation | xi |
| Contents | xiii |
| 1 Introduction | 1 |
| 1.1 Example: Polynomial Curve Fitting | 4 |
| 1.2 Probability Theory | 12 |
| 1.2.1 Probability densities | 17 |
| 1.2.2 Expectations and covariances | 19 |
| 1.2.3 Bayesian probabilities | 21 |
| 1.2.4 The Gaussian distribution | 24 |
| 1.2.5 Curve fitting re-visited | 28 |
| 1.2.6 Bayesian curve fitting | 30 |
| 1.3 Model Selection | 32 |
| 1.4 The Curse of Dimensionality | 33 |
| 1.5 Decision Theory | 38 |
| 1.5.1 Minimizing the misclassification rate | 39 |
| 1.5.2 Minimizing the expected loss | 41 |
| 1.5.3 The reject option | 42 |
| 1.5.4 Inference and decision | 42 |
| 1.5.5 Loss functions for regression | 46 |
| 1.6 Information Theory | 48 |
| 1.6.1 Relative entropy and mutual information | 55 |
| Exercises | 58 |

| | |
|--|------------|
| 2 Probability Distributions | 67 |
| 2.1 Binary Variables | 68 |
| 2.1.1 The beta distribution | 71 |
| 2.2 Multinomial Variables | 74 |
| 2.2.1 The Dirichlet distribution | 76 |
| 2.3 The Gaussian Distribution | 78 |
| 2.3.1 Conditional Gaussian distributions | 85 |
| 2.3.2 Marginal Gaussian distributions | 88 |
| 2.3.3 Bayes' theorem for Gaussian variables | 90 |
| 2.3.4 Maximum likelihood for the Gaussian | 93 |
| 2.3.5 Sequential estimation | 94 |
| 2.3.6 Bayesian inference for the Gaussian | 97 |
| 2.3.7 Student's t-distribution | 102 |
| 2.3.8 Periodic variables | 105 |
| 2.3.9 Mixtures of Gaussians | 110 |
| 2.4 The Exponential Family | 113 |
| 2.4.1 Maximum likelihood and sufficient statistics | 116 |
| 2.4.2 Conjugate priors | 117 |
| 2.4.3 Noninformative priors | 117 |
| 2.5 Nonparametric Methods | 120 |
| 2.5.1 Kernel density estimators | 122 |
| 2.5.2 Nearest-neighbour methods | 124 |
| Exercises | 127 |
| 3 Linear Models for Regression | 137 |
| 3.1 Linear Basis Function Models | 138 |
| 3.1.1 Maximum likelihood and least squares | 140 |
| 3.1.2 Geometry of least squares | 143 |
| 3.1.3 Sequential learning | 143 |
| 3.1.4 Regularized least squares | 144 |
| 3.1.5 Multiple outputs | 146 |
| 3.2 The Bias-Variance Decomposition | 147 |
| 3.3 Bayesian Linear Regression | 152 |
| 3.3.1 Parameter distribution | 152 |
| 3.3.2 Predictive distribution | 156 |
| 3.3.3 Equivalent kernel | 159 |
| 3.4 Bayesian Model Comparison | 161 |
| 3.5 The Evidence Approximation | 165 |
| 3.5.1 Evaluation of the evidence function | 166 |
| 3.5.2 Maximizing the evidence function | 168 |
| 3.5.3 Effective number of parameters | 170 |
| 3.6 Limitations of Fixed Basis Functions | 172 |
| Exercises | 173 |

| | |
|--|------------|
| 4 Linear Models for Classification | 179 |
| 4.1 Discriminant Functions | 181 |
| 4.1.1 Two classes | 181 |
| 4.1.2 Multiple classes | 182 |
| 4.1.3 Least squares for classification | 184 |
| 4.1.4 Fisher's linear discriminant | 186 |
| 4.1.5 Relation to least squares | 189 |
| 4.1.6 Fisher's discriminant for multiple classes | 191 |
| 4.1.7 The perceptron algorithm | 192 |
| 4.2 Probabilistic Generative Models | 196 |
| 4.2.1 Continuous inputs | 198 |
| 4.2.2 Maximum likelihood solution | 200 |
| 4.2.3 Discrete features | 202 |
| 4.2.4 Exponential family | 202 |
| 4.3 Probabilistic Discriminative Models | 203 |
| 4.3.1 Fixed basis functions | 204 |
| 4.3.2 Logistic regression | 205 |
| 4.3.3 Iterative reweighted least squares | 207 |
| 4.3.4 Multiclass logistic regression | 209 |
| 4.3.5 Probit regression | 210 |
| 4.3.6 Canonical link functions | 212 |
| 4.4 The Laplace Approximation | 213 |
| 4.4.1 Model comparison and BIC | 216 |
| 4.5 Bayesian Logistic Regression | 217 |
| 4.5.1 Laplace approximation | 217 |
| 4.5.2 Predictive distribution | 218 |
| Exercises | 220 |
| 5 Neural Networks | 225 |
| 5.1 Feed-forward Network Functions | 227 |
| 5.1.1 Weight-space symmetries | 231 |
| 5.2 Network Training | 232 |
| 5.2.1 Parameter optimization | 236 |
| 5.2.2 Local quadratic approximation | 237 |
| 5.2.3 Use of gradient information | 239 |
| 5.2.4 Gradient descent optimization | 240 |
| 5.3 Error Backpropagation | 241 |
| 5.3.1 Evaluation of error-function derivatives | 242 |
| 5.3.2 A simple example | 245 |
| 5.3.3 Efficiency of backpropagation | 246 |
| 5.3.4 The Jacobian matrix | 247 |
| 5.4 The Hessian Matrix | 249 |
| 5.4.1 Diagonal approximation | 250 |
| 5.4.2 Outer product approximation | 251 |
| 5.4.3 Inverse Hessian | 252 |

| | | |
|----------|---|------------|
| 5.4.4 | Finite differences | 252 |
| 5.4.5 | Exact evaluation of the Hessian | 253 |
| 5.4.6 | Fast multiplication by the Hessian | 254 |
| 5.5 | Regularization in Neural Networks | 256 |
| 5.5.1 | Consistent Gaussian priors | 257 |
| 5.5.2 | Early stopping | 259 |
| 5.5.3 | Invariances | 261 |
| 5.5.4 | Tangent propagation | 263 |
| 5.5.5 | Training with transformed data | 265 |
| 5.5.6 | Convolutional networks | 267 |
| 5.5.7 | Soft weight sharing | 269 |
| 5.6 | Mixture Density Networks | 272 |
| 5.7 | Bayesian Neural Networks | 277 |
| 5.7.1 | Posterior parameter distribution | 278 |
| 5.7.2 | Hyperparameter optimization | 280 |
| 5.7.3 | Bayesian neural networks for classification | 281 |
| | Exercises | 284 |
| 6 | Kernel Methods | 291 |
| 6.1 | Dual Representations | 293 |
| 6.2 | Constructing Kernels | 294 |
| 6.3 | Radial Basis Function Networks | 299 |
| 6.3.1 | Nadaraya-Watson model | 301 |
| 6.4 | Gaussian Processes | 303 |
| 6.4.1 | Linear regression revisited | 304 |
| 6.4.2 | Gaussian processes for regression | 306 |
| 6.4.3 | Learning the hyperparameters | 311 |
| 6.4.4 | Automatic relevance determination | 312 |
| 6.4.5 | Gaussian processes for classification | 313 |
| 6.4.6 | Laplace approximation | 315 |
| 6.4.7 | Connection to neural networks | 319 |
| | Exercises | 320 |
| 7 | Sparse Kernel Machines | 325 |
| 7.1 | Maximum Margin Classifiers | 326 |
| 7.1.1 | Overlapping class distributions | 331 |
| 7.1.2 | Relation to logistic regression | 336 |
| 7.1.3 | Multiclass SVMs | 338 |
| 7.1.4 | SVMs for regression | 339 |
| 7.1.5 | Computational learning theory | 344 |
| 7.2 | Relevance Vector Machines | 345 |
| 7.2.1 | RVM for regression | 345 |
| 7.2.2 | Analysis of sparsity | 349 |
| 7.2.3 | RVM for classification | 353 |
| | Exercises | 357 |

| | |
|---|------------|
| 8 Graphical Models | 359 |
| 8.1 Bayesian Networks | 360 |
| 8.1.1 Example: Polynomial regression | 362 |
| 8.1.2 Generative models | 365 |
| 8.1.3 Discrete variables | 366 |
| 8.1.4 Linear-Gaussian models | 370 |
| 8.2 Conditional Independence | 372 |
| 8.2.1 Three example graphs | 373 |
| 8.2.2 D-separation | 378 |
| 8.3 Markov Random Fields | 383 |
| 8.3.1 Conditional independence properties | 383 |
| 8.3.2 Factorization properties | 384 |
| 8.3.3 Illustration: Image de-noising | 387 |
| 8.3.4 Relation to directed graphs | 390 |
| 8.4 Inference in Graphical Models | 393 |
| 8.4.1 Inference on a chain | 394 |
| 8.4.2 Trees | 398 |
| 8.4.3 Factor graphs | 399 |
| 8.4.4 The sum-product algorithm | 402 |
| 8.4.5 The max-sum algorithm | 411 |
| 8.4.6 Exact inference in general graphs | 416 |
| 8.4.7 Loopy belief propagation | 417 |
| 8.4.8 Learning the graph structure | 418 |
| Exercises | 418 |
| 9 Mixture Models and EM | 423 |
| 9.1 K -means Clustering | 424 |
| 9.1.1 Image segmentation and compression | 428 |
| 9.2 Mixtures of Gaussians | 430 |
| 9.2.1 Maximum likelihood | 432 |
| 9.2.2 EM for Gaussian mixtures | 435 |
| 9.3 An Alternative View of EM | 439 |
| 9.3.1 Gaussian mixtures revisited | 441 |
| 9.3.2 Relation to K -means | 443 |
| 9.3.3 Mixtures of Bernoulli distributions | 444 |
| 9.3.4 EM for Bayesian linear regression | 448 |
| 9.4 The EM Algorithm in General | 450 |
| Exercises | 455 |
| 10 Approximate Inference | 461 |
| 10.1 Variational Inference | 462 |
| 10.1.1 Factorized distributions | 464 |
| 10.1.2 Properties of factorized approximations | 466 |
| 10.1.3 Example: The univariate Gaussian | 470 |
| 10.1.4 Model comparison | 473 |
| 10.2 Illustration: Variational Mixture of Gaussians | 474 |

| | | |
|-----------|---|------------|
| 10.2.1 | Variational distribution | 475 |
| 10.2.2 | Variational lower bound | 481 |
| 10.2.3 | Predictive density | 482 |
| 10.2.4 | Determining the number of components | 483 |
| 10.2.5 | Induced factorizations | 485 |
| 10.3 | Variational Linear Regression | 486 |
| 10.3.1 | Variational distribution | 486 |
| 10.3.2 | Predictive distribution | 488 |
| 10.3.3 | Lower bound | 489 |
| 10.4 | Exponential Family Distributions | 490 |
| 10.4.1 | Variational message passing | 491 |
| 10.5 | Local Variational Methods | 493 |
| 10.6 | Variational Logistic Regression | 498 |
| 10.6.1 | Variational posterior distribution | 498 |
| 10.6.2 | Optimizing the variational parameters | 500 |
| 10.6.3 | Inference of hyperparameters | 502 |
| 10.7 | Expectation Propagation | 505 |
| 10.7.1 | Example: The clutter problem | 511 |
| 10.7.2 | Expectation propagation on graphs | 513 |
| | Exercises | 517 |
| 11 | Sampling Methods | 523 |
| 11.1 | Basic Sampling Algorithms | 526 |
| 11.1.1 | Standard distributions | 526 |
| 11.1.2 | Rejection sampling | 528 |
| 11.1.3 | Adaptive rejection sampling | 530 |
| 11.1.4 | Importance sampling | 532 |
| 11.1.5 | Sampling-importance-resampling | 534 |
| 11.1.6 | Sampling and the EM algorithm | 536 |
| 11.2 | Markov Chain Monte Carlo | 537 |
| 11.2.1 | Markov chains | 539 |
| 11.2.2 | The Metropolis-Hastings algorithm | 541 |
| 11.3 | Gibbs Sampling | 542 |
| 11.4 | Slice Sampling | 546 |
| 11.5 | The Hybrid Monte Carlo Algorithm | 548 |
| 11.5.1 | Dynamical systems | 548 |
| 11.5.2 | Hybrid Monte Carlo | 552 |
| 11.6 | Estimating the Partition Function | 554 |
| | Exercises | 556 |
| 12 | Continuous Latent Variables | 559 |
| 12.1 | Principal Component Analysis | 561 |
| 12.1.1 | Maximum variance formulation | 561 |
| 12.1.2 | Minimum-error formulation | 563 |
| 12.1.3 | Applications of PCA | 565 |
| 12.1.4 | PCA for high-dimensional data | 569 |

| | |
|--|------------|
| 12.2 Probabilistic PCA | 570 |
| 12.2.1 Maximum likelihood PCA | 574 |
| 12.2.2 EM algorithm for PCA | 577 |
| 12.2.3 Bayesian PCA | 580 |
| 12.2.4 Factor analysis | 583 |
| 12.3 Kernel PCA | 586 |
| 12.4 Nonlinear Latent Variable Models | 591 |
| 12.4.1 Independent component analysis | 591 |
| 12.4.2 Autoassociative neural networks | 592 |
| 12.4.3 Modelling nonlinear manifolds | 595 |
| Exercises | 599 |
| 13 Sequential Data | 605 |
| 13.1 Markov Models | 607 |
| 13.2 Hidden Markov Models | 610 |
| 13.2.1 Maximum likelihood for the HMM | 615 |
| 13.2.2 The forward-backward algorithm | 618 |
| 13.2.3 The sum-product algorithm for the HMM | 625 |
| 13.2.4 Scaling factors | 627 |
| 13.2.5 The Viterbi algorithm | 629 |
| 13.2.6 Extensions of the hidden Markov model | 631 |
| 13.3 Linear Dynamical Systems | 635 |
| 13.3.1 Inference in LDS | 638 |
| 13.3.2 Learning in LDS | 642 |
| 13.3.3 Extensions of LDS | 644 |
| 13.3.4 Particle filters | 645 |
| Exercises | 646 |
| 14 Combining Models | 653 |
| 14.1 Bayesian Model Averaging | 654 |
| 14.2 Committees | 655 |
| 14.3 Boosting | 657 |
| 14.3.1 Minimizing exponential error | 659 |
| 14.3.2 Error functions for boosting | 661 |
| 14.4 Tree-based Models | 663 |
| 14.5 Conditional Mixture Models | 666 |
| 14.5.1 Mixtures of linear regression models | 667 |
| 14.5.2 Mixtures of logistic models | 670 |
| 14.5.3 Mixtures of experts | 672 |
| Exercises | 674 |
| Appendix A Data Sets | 677 |
| Appendix B Probability Distributions | 685 |
| Appendix C Properties of Matrices | 695 |

| | |
|--|------------|
| Appendix D Calculus of Variations | 703 |
| Appendix E Lagrange Multipliers | 707 |
| References | 711 |
| Index | 729 |



1

Introduction

The problem of searching for patterns in data is a fundamental one and has a long and successful history. For instance, the extensive astronomical observations of Tycho Brahe in the 16th century allowed Johannes Kepler to discover the empirical laws of planetary motion, which in turn provided a springboard for the development of classical mechanics. Similarly, the discovery of regularities in atomic spectra played a key role in the development and verification of quantum physics in the early twentieth century. The field of pattern recognition is concerned with the automatic discovery of regularities in data through the use of computer algorithms and with the use of these regularities to take actions such as classifying the data into different categories.

Consider the example of recognizing handwritten digits, illustrated in Figure 1.1. Each digit corresponds to a 28×28 pixel image and so can be represented by a vector \mathbf{x} comprising 784 real numbers. The goal is to build a machine that will take such a vector \mathbf{x} as input and that will produce the identity of the digit 0, ..., 9 as the output. This is a nontrivial problem due to the wide variability of handwriting. It could be

1. INTRODUCTION

Figure 1.1 Examples of hand-written digits taken from US zip codes.



tackled using handcrafted rules or heuristics for distinguishing the digits based on the shapes of the strokes, but in practice such an approach leads to a proliferation of rules and of exceptions to the rules and so on, and invariably gives poor results.

Far better results can be obtained by adopting a machine learning approach in which a large set of N digits $\{x_1, \dots, x_N\}$ called a *training set* is used to tune the parameters of an adaptive model. The categories of the digits in the training set are known in advance, typically by inspecting them individually and hand-labelling them. We can express the category of a digit using *target vector* t , which represents the identity of the corresponding digit. Suitable techniques for representing categories in terms of vectors will be discussed later. Note that there is one such target vector t for each digit image x .

The result of running the machine learning algorithm can be expressed as a function $y(x)$ which takes a new digit image x as input and that generates an output vector y , encoded in the same way as the target vectors. The precise form of the function $y(x)$ is determined during the *training* phase, also known as the *learning* phase, on the basis of the training data. Once the model is trained it can then determine the identity of new digit images, which are said to comprise a *test set*. The ability to categorize correctly new examples that differ from those used for training is known as *generalization*. In practical applications, the variability of the input vectors will be such that the training data can comprise only a tiny fraction of all possible input vectors, and so generalization is a central goal in pattern recognition.

For most practical applications, the original input variables are typically *preprocessed* to transform them into some new space of variables where, it is hoped, the pattern recognition problem will be easier to solve. For instance, in the digit recognition problem, the images of the digits are typically translated and scaled so that each digit is contained within a box of a fixed size. This greatly reduces the variability within each digit class, because the location and scale of all the digits are now the same, which makes it much easier for a subsequent pattern recognition algorithm to distinguish between the different classes. This pre-processing stage is sometimes also called *feature extraction*. Note that new test data must be pre-processed using the same steps as the training data.

Pre-processing might also be performed in order to speed up computation. For example, if the goal is real-time face detection in a high-resolution video stream, the computer must handle huge numbers of pixels per second, and presenting these directly to a complex pattern recognition algorithm may be computationally infeasible. Instead, the aim is to find useful features that are fast to compute, and yet that

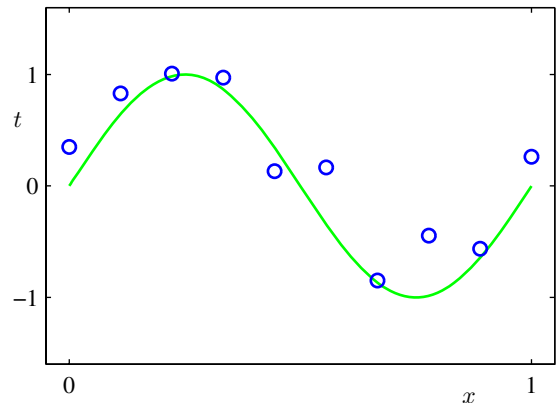
also preserve useful discriminatory information enabling faces to be distinguished from non-faces. These features are then used as the inputs to the pattern recognition algorithm. For instance, the average value of the image intensity over a rectangular subregion can be evaluated extremely efficiently (Viola and Jones, 2004), and a set of such features can prove very effective in fast face detection. Because the number of such features is smaller than the number of pixels, this kind of pre-processing represents a form of dimensionality reduction. Care must be taken during pre-processing because often information is discarded, and if this information is important to the solution of the problem then the overall accuracy of the system can suffer.

Applications in which the training data comprises examples of the input vectors along with their corresponding target vectors are known as *supervised learning* problems. Cases such as the digit recognition example, in which the aim is to assign each input vector to one of a finite number of discrete categories, are called *classification* problems. If the desired output consists of one or more continuous variables, then the task is called *regression*. An example of a regression problem would be the prediction of the yield in a chemical manufacturing process in which the inputs consist of the concentrations of reactants, the temperature, and the pressure.

In other pattern recognition problems, the training data consists of a set of input vectors \mathbf{x} without any corresponding target values. The goal in such *unsupervised learning* problems may be to discover groups of similar examples within the data, where it is called *clustering*, or to determine the distribution of data within the input space, known as *density estimation*, or to project the data from a high-dimensional space down to two or three dimensions for the purpose of *visualization*.

Finally, the technique of *reinforcement learning* (Sutton and Barto, 1998) is concerned with the problem of finding suitable actions to take in a given situation in order to maximize a reward. Here the learning algorithm is not given examples of optimal outputs, in contrast to supervised learning, but must instead discover them by a process of trial and error. Typically there is a sequence of states and actions in which the learning algorithm is interacting with its environment. In many cases, the current action not only affects the immediate reward but also has an impact on the reward at all subsequent time steps. For example, by using appropriate reinforcement learning techniques a neural network can learn to play the game of backgammon to a high standard (Tesauro, 1994). Here the network must learn to take a board position as input, along with the result of a dice throw, and produce a strong move as the output. This is done by having the network play against a copy of itself for perhaps a million games. A major challenge is that a game of backgammon can involve dozens of moves, and yet it is only at the end of the game that the reward, in the form of victory, is achieved. The reward must then be attributed appropriately to all of the moves that led to it, even though some moves will have been good ones and others less so. This is an example of a *credit assignment* problem. A general feature of reinforcement learning is the trade-off between *exploration*, in which the system tries out new kinds of actions to see how effective they are, and *exploitation*, in which the system makes use of actions that are known to yield a high reward. Too strong a focus on either exploration or exploitation will yield poor results. Reinforcement learning continues to be an active area of machine learning research. However, a

Figure 1.2 Plot of a training data set of $N = 10$ points, shown as blue circles, each comprising an observation of the input variable x along with the corresponding target variable t . The green curve shows the function $\sin(2\pi x)$ used to generate the data. Our goal is to predict the value of t for some new value of x , without knowledge of the green curve.



detailed treatment lies beyond the scope of this book.

Although each of these tasks needs its own tools and techniques, many of the key ideas that underpin them are common to all such problems. One of the main goals of this chapter is to introduce, in a relatively informal way, several of the most important of these concepts and to illustrate them using simple examples. Later in the book we shall see these same ideas re-emerge in the context of more sophisticated models that are applicable to real-world pattern recognition applications. This chapter also provides a self-contained introduction to three important tools that will be used throughout the book, namely probability theory, decision theory, and information theory. Although these might sound like daunting topics, they are in fact straightforward, and a clear understanding of them is essential if machine learning techniques are to be used to best effect in practical applications.

1.1. Example: Polynomial Curve Fitting

We begin by introducing a simple regression problem, which we shall use as a running example throughout this chapter to motivate a number of key concepts. Suppose we observe a real-valued input variable x and we wish to use this observation to predict the value of a real-valued target variable t . For the present purposes, it is instructive to consider an artificial example using **synthetically generated data** because we then know the precise process that generated the data for comparison against any learned model. The data for this example is generated from the function $\sin(2\pi x)$ with random noise included in the target values, as described in detail in Appendix A.

Now suppose that we are given a training set comprising N observations of x , written $\mathbf{x} \equiv (x_1, \dots, x_N)^T$, together with corresponding observations of the values of t , denoted $\mathbf{t} \equiv (t_1, \dots, t_N)^T$. Figure 1.2 shows a plot of a training set comprising $N = 10$ data points. The input data set \mathbf{x} in Figure 1.2 was generated by choosing values of x_n , for $n = 1, \dots, N$, spaced uniformly in range $[0, 1]$, and the target data set \mathbf{t} was obtained by first computing the corresponding values of the function

$\sin(2\pi x)$ and then adding a small level of random noise having a Gaussian distribution (the Gaussian distribution is discussed in Section 1.2.4) to each such point in order to obtain the corresponding value t_n . By generating data in this way, we are capturing a property of many real data sets, namely that they possess an underlying regularity, which we wish to learn, but that individual observations are corrupted by random noise. This noise might arise from intrinsically stochastic (i.e. random) processes such as radioactive decay but more typically is due to there being sources of variability that are themselves unobserved.

Our goal is to exploit this training set in order to make predictions of the value \hat{t} of the target variable for some new value \hat{x} of the input variable. As we shall see later, this involves implicitly trying to discover the underlying function $\sin(2\pi x)$. This is intrinsically a difficult problem as we have to generalize from a finite data set. Furthermore the observed data are corrupted with noise, and so for a given \hat{x} there is uncertainty as to the appropriate value for \hat{t} . Probability theory, discussed in Section 1.2, provides a framework for expressing such uncertainty in a precise and quantitative manner, and decision theory, discussed in Section 1.5, allows us to exploit this probabilistic representation in order to make predictions that are optimal according to appropriate criteria.

For the moment, however, we shall proceed rather informally and consider a simple approach based on curve fitting. In particular, we shall fit the data using a polynomial function of the form

$$y(x, \mathbf{w}) = w_0 + w_1x + w_2x^2 + \dots + w_Mx^M = \sum_{j=0}^M w_jx^j \quad (1.1)$$

where M is the *order* of the polynomial, and x^j denotes x raised to the power of j . The polynomial coefficients w_0, \dots, w_M are collectively denoted by the vector \mathbf{w} . Note that, although the polynomial function $y(x, \mathbf{w})$ is a nonlinear function of x , it is a linear function of the coefficients \mathbf{w} . Functions, such as the polynomial, which are linear in the unknown parameters have important properties and are called *linear models* and will be discussed extensively in Chapters 3 and 4.

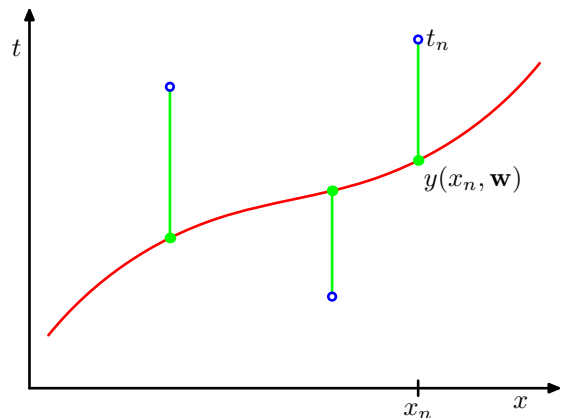
The values of the coefficients will be determined by fitting the polynomial to the training data. This can be done by minimizing an *error function* that measures the misfit between the function $y(x, \mathbf{w})$, for any given value of \mathbf{w} , and the training set data points. One simple choice of error function, which is widely used, is given by the sum of the squares of the errors between the predictions $y(x_n, \mathbf{w})$ for each data point x_n and the corresponding target values t_n , so that we minimize

$$E(\mathbf{w}) = \frac{1}{2} \sum_{n=1}^N \{y(x_n, \mathbf{w}) - t_n\}^2 \quad (1.2)$$

where the factor of $1/2$ is included for later convenience. We shall discuss the motivation for this choice of error function later in this chapter. For the moment we simply note that it is a nonnegative quantity that would be zero if, and only if, the

1. INTRODUCTION

Figure 1.3 The error function (1.2) corresponds to (one half of) the sum of the squares of the displacements (shown by the vertical green bars) of each data point from the function $y(x, \mathbf{w})$.



function $y(x, \mathbf{w})$ were to pass exactly through each training data point. The geometrical interpretation of the **sum-of-squares** error function is illustrated in Figure 1.3.

We can solve the curve fitting problem by choosing the value of \mathbf{w} for which $E(\mathbf{w})$ is as small as possible. Because the error function is a quadratic function of the coefficients \mathbf{w} , its derivatives with respect to the coefficients will be linear in the elements of \mathbf{w} , and so the minimization of the error function has a unique solution, denoted by \mathbf{w}^* , which can be found in closed form. The resulting polynomial is given by the function $y(x, \mathbf{w}^*)$.

Exercise 1.1

There remains the problem of choosing the order M of the polynomial, and as we shall see this will turn out to be an example of an important concept called **model comparison or model selection**. In Figure 1.4, we show four examples of the results of fitting polynomials having orders $M = 0, 1, 3$, and 9 to the data set shown in Figure 1.2.

We notice that the constant ($M = 0$) and first order ($M = 1$) polynomials give rather poor fits to the data and consequently rather poor representations of the function $\sin(2\pi x)$. The third order ($M = 3$) polynomial seems to give the best fit to the function $\sin(2\pi x)$ of the examples shown in Figure 1.4. When we go to a much higher order polynomial ($M = 9$), we obtain an excellent fit to the training data. In fact, the polynomial passes exactly through each data point and $E(\mathbf{w}^*) = 0$. However, the fitted curve oscillates wildly and gives a very poor representation of the function $\sin(2\pi x)$. This latter behaviour is known as **over-fitting**.

As we have noted earlier, the goal is to achieve good generalization by making accurate predictions for new data. We can obtain some quantitative insight into the dependence of the generalization performance on M by considering a separate test set comprising 100 data points generated using exactly the same procedure used to generate the training set points but with new choices for the random noise values included in the target values. For each choice of M , we can then evaluate the residual value of $E(\mathbf{w}^*)$ given by (1.2) for the training data, and we can also evaluate $E(\mathbf{w}^*)$ for the test data set. It is sometimes more convenient to use the **root-mean-square**



Figure 1.4 Plots of polynomials having various orders M , shown as red curves, fitted to the data set shown in Figure 1.2.

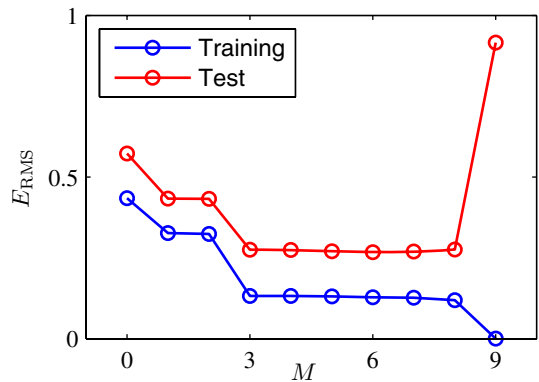
(RMS) error defined by

$$E_{\text{RMS}} = \sqrt{2E(\mathbf{w}^*)/N} \quad (1.3)$$

in which the division by N allows us to compare different sizes of data sets on an equal footing, and the square root ensures that E_{RMS} is measured on the same scale (and in the same units) as the target variable t . Graphs of the training and test set RMS errors are shown, for various values of M , in Figure 1.5. The test set error is a measure of how well we are doing in predicting the values of t for new data observations of x . We note from Figure 1.5 that small values of M give relatively large values of the test set error, and this can be attributed to the fact that the corresponding polynomials are rather inflexible and are incapable of capturing the oscillations in the function $\sin(2\pi x)$. Values of M in the range $3 \leq M \leq 8$ give small values for the test set error, and these also give reasonable representations of the generating function $\sin(2\pi x)$, as can be seen, for the case of $M = 3$, from Figure 1.4.

1. INTRODUCTION

Figure 1.5 Graphs of the root-mean-square error, defined by (1.3), evaluated on the training set and on an independent test set for various values of M .



For $M = 9$, the training set error goes to zero, as we might expect because this polynomial contains 10 degrees of freedom corresponding to the 10 coefficients w_0, \dots, w_9 , and so can be tuned exactly to the 10 data points in the training set. However, the test set error has become very large and, as we saw in Figure 1.4, the corresponding function $y(x, \mathbf{w}^*)$ exhibits wild oscillations.

This may seem paradoxical because a polynomial of given order contains all lower order polynomials as special cases. The $M = 9$ polynomial is therefore capable of generating results at least as good as the $M = 3$ polynomial. Furthermore, we might suppose that the best predictor of new data would be the function $\sin(2\pi x)$ from which the data was generated (and we shall see later that this is indeed the case). We know that a power series expansion of the function $\sin(2\pi x)$ contains terms of all orders, so we might expect that results should improve monotonically as we increase M .

We can gain some insight into the problem by examining the values of the coefficients \mathbf{w}^* obtained from polynomials of various order, as shown in Table 1.1. We see that, as M increases, the magnitude of the coefficients typically gets larger. In particular for the $M = 9$ polynomial, the coefficients have become finely tuned to the data by developing large positive and negative values so that the correspond-

Table 1.1

Table of the coefficients \mathbf{w}^* for polynomials of various order. Observe how the typical magnitude of the coefficients increases dramatically as the order of the polynomial increases.

| | $M = 0$ | $M = 1$ | $M = 6$ | $M = 9$ |
|---------|---------|---------|---------|-------------|
| w_0^* | 0.19 | 0.82 | 0.31 | 0.35 |
| w_1^* | | -1.27 | 7.99 | 232.37 |
| w_2^* | | | -25.43 | -5321.83 |
| w_3^* | | | 17.37 | 48568.31 |
| w_4^* | | | | -231639.30 |
| w_5^* | | | | 640042.26 |
| w_6^* | | | | -1061800.52 |
| w_7^* | | | | 1042400.18 |
| w_8^* | | | | -557682.99 |
| w_9^* | | | | 125201.43 |

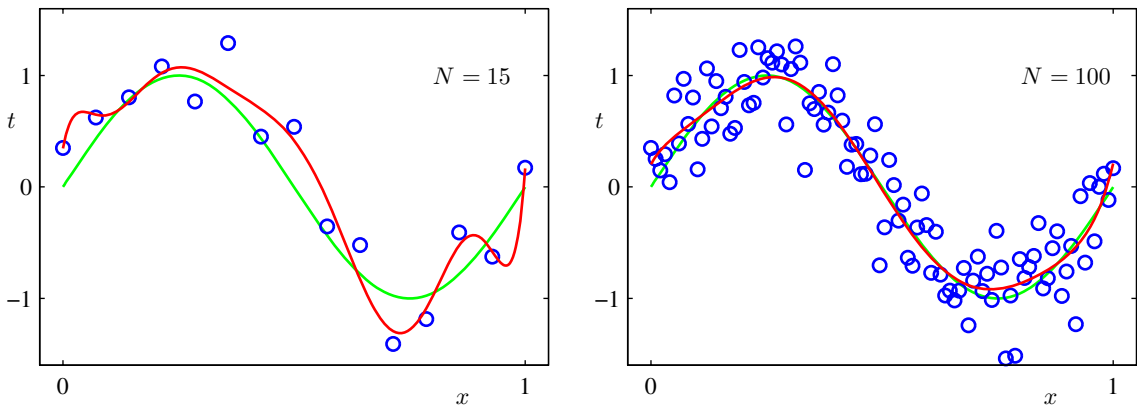


Figure 1.6 Plots of the solutions obtained by minimizing the sum-of-squares error function using the $M = 9$ polynomial for $N = 15$ data points (left plot) and $N = 100$ data points (right plot). We see that increasing the size of the data set reduces the over-fitting problem.

ing polynomial function matches each of the data points exactly, but between data points (particularly near the ends of the range) the function exhibits the large oscillations observed in Figure 1.4. Intuitively, what is happening is that the more flexible polynomials with larger values of M are becoming increasingly tuned to the random noise on the target values.

It is also interesting to examine the behaviour of a given model as the size of the data set is varied, as shown in Figure 1.6. We see that, for a given model complexity, the over-fitting problem become less severe as the size of the data set increases. Another way to say this is that the larger the data set, the more complex (in other words more flexible) the model that we can afford to fit to the data. One rough heuristic that is sometimes advocated is that the number of data points should be no less than some multiple (say 5 or 10) of the number of adaptive parameters in the model. However, as we shall see in Chapter 3, the number of parameters is not necessarily the most appropriate measure of model complexity.

Also, there is something rather unsatisfying about having to limit the number of parameters in a model according to the size of the available training set. It would seem more reasonable to choose the complexity of the model according to the complexity of the problem being solved. We shall see that the least squares approach to finding the model parameters represents a specific case of *maximum likelihood* (discussed in Section 1.2.5), and that the over-fitting problem can be understood as a general property of maximum likelihood. By adopting a *Bayesian* approach, the over-fitting problem can be avoided. We shall see that there is no difficulty from a Bayesian perspective in employing models for which the number of parameters greatly exceeds the number of data points. Indeed, in a Bayesian model the effective number of parameters adapts automatically to the size of the data set.

For the moment, however, it is instructive to continue with the current approach and to consider how in practice we can apply it to data sets of limited size where we

Section 3.4



Figure 1.7 Plots of $M = 9$ polynomials fitted to the data set shown in Figure 1.2 using the regularized error function (1.4) for two values of the regularization parameter λ corresponding to $\ln \lambda = -18$ and $\ln \lambda = 0$. The case of no regularizer, i.e., $\lambda = 0$, corresponding to $\ln \lambda = -\infty$, is shown at the bottom right of Figure 1.4.

may wish to use relatively complex and flexible models. One technique that is often used to control the over-fitting phenomenon in such cases is that of *regularization*, which involves adding a penalty term to the error function (1.2) in order to discourage the coefficients from reaching large values. The simplest such penalty term takes the form of a sum of squares of all of the coefficients, leading to a modified error function of the form

$$\tilde{E}(\mathbf{w}) = \frac{1}{2} \sum_{n=1}^N \{y(x_n, \mathbf{w}) - t_n\}^2 + \frac{\lambda}{2} \|\mathbf{w}\|^2 \quad (1.4)$$

where $\|\mathbf{w}\|^2 \equiv \mathbf{w}^T \mathbf{w} = w_0^2 + w_1^2 + \dots + w_M^2$, and the coefficient λ governs the relative importance of the regularization term compared with the sum-of-squares error term. Note that often the coefficient w_0 is omitted from the regularizer because its inclusion causes the results to depend on the choice of origin for the target variable (Hastie *et al.*, 2001), or it may be included but with its own regularization coefficient (we shall discuss this topic in more detail in Section 5.5.1). Again, the error function in (1.4) can be minimized exactly in closed form. Techniques such as this are known in the statistics literature as *shrinkage* methods because they reduce the value of the coefficients. The particular case of a quadratic regularizer is called *ridge regression* (Hoerl and Kennard, 1970). In the context of neural networks, this approach is known as *weight decay*.

Exercise 1.2

Figure 1.7 shows the results of fitting the polynomial of order $M = 9$ to the same data set as before but now using the regularized error function given by (1.4). We see that, for a value of $\ln \lambda = -18$, the over-fitting has been suppressed and we now obtain a much closer representation of the underlying function $\sin(2\pi x)$. If, however, we use too large a value for λ then we again obtain a poor fit, as shown in Figure 1.7 for $\ln \lambda = 0$. The corresponding coefficients from the fitted polynomials are given in Table 1.2, showing that regularization has the desired effect of reducing

Table 1.2 Table of the coefficients w^* for $M = 9$ polynomials with various values for the regularization parameter λ . Note that $\ln \lambda = -\infty$ corresponds to a model with no regularization, i.e., to the graph at the bottom right in Figure 1.4. We see that, as the value of λ increases, the typical magnitude of the coefficients gets smaller.

| | $\ln \lambda = -\infty$ | $\ln \lambda = -18$ | $\ln \lambda = 0$ |
|---------|-------------------------|---------------------|-------------------|
| w_0^* | 0.35 | 0.35 | 0.13 |
| w_1^* | 232.37 | 4.74 | -0.05 |
| w_2^* | -5321.83 | -0.77 | -0.06 |
| w_3^* | 48568.31 | -31.97 | -0.05 |
| w_4^* | -231639.30 | -3.89 | -0.03 |
| w_5^* | 640042.26 | 55.28 | -0.02 |
| w_6^* | -1061800.52 | 41.32 | -0.01 |
| w_7^* | 1042400.18 | -45.95 | -0.00 |
| w_8^* | -557682.99 | -91.53 | 0.00 |
| w_9^* | 125201.43 | 72.68 | 0.01 |

the magnitude of the coefficients.

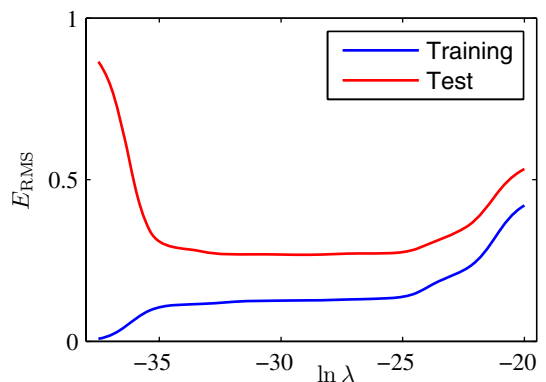
The impact of the regularization term on the generalization error can be seen by plotting the value of the RMS error (1.3) for both training and test sets against $\ln \lambda$, as shown in Figure 1.8. We see that in effect λ now controls the effective complexity of the model and hence determines the degree of over-fitting.

The issue of model complexity is an important one and will be discussed at length in Section 1.3. Here we simply note that, if we were trying to solve a practical application using this approach of minimizing an error function, we would have to find a way to determine a suitable value for the model complexity. The results above suggest a simple way of achieving this, namely by taking the available data and partitioning it into a training set, used to determine the coefficients w , and a separate validation set, also called a *hold-out* set, used to optimize the model complexity (either M or λ). In many cases, however, this will prove to be too wasteful of valuable training data, and we have to seek more sophisticated approaches.

Section 1.3

So far our discussion of polynomial curve fitting has appealed largely to intuition. We now seek a more principled approach to solving problems in pattern recognition by turning to a discussion of probability theory. As well as providing the foundation for nearly all of the subsequent developments in this book, it will also

Figure 1.8 Graph of the root-mean-square error (1.3) versus $\ln \lambda$ for the $M = 9$ polynomial.



give us some important insights into the concepts we have introduced in the context of polynomial curve fitting and will allow us to extend these to more complex situations.

1.2. Probability Theory

A key concept in the field of pattern recognition is that of uncertainty. It arises both through noise on measurements, as well as through the finite size of data sets. Probability theory provides a consistent framework for the quantification and manipulation of uncertainty and forms one of the central foundations for pattern recognition. When combined with decision theory, discussed in Section 1.5, it allows us to make optimal predictions given all the information available to us, even though that information may be incomplete or ambiguous.

We will introduce the basic concepts of probability theory by considering a simple example. Imagine we have two boxes, one red and one blue, and in the red box we have 2 apples and 6 oranges, and in the blue box we have 3 apples and 1 orange. This is illustrated in Figure 1.9. Now suppose we randomly pick one of the boxes and from that box we randomly select an item of fruit, and having observed which sort of fruit it is we replace it in the box from which it came. We could imagine repeating this process many times. Let us suppose that in so doing we pick the red box 40% of the time and we pick the blue box 60% of the time, and that when we remove an item of fruit from a box we are equally likely to select any of the pieces of fruit in the box.

In this example, the identity of the box that will be chosen is a random variable, which we shall denote by B . This random variable can take one of two possible values, namely r (corresponding to the red box) or b (corresponding to the blue box). Similarly, the identity of the fruit is also a random variable and will be denoted by F . It can take either of the values a (for apple) or o (for orange).

To begin with, we shall define the probability of an event to be the fraction of times that event occurs out of the total number of trials, in the limit that the total number of trials goes to infinity. Thus the probability of selecting the red box is 4/10

Figure 1.9 We use a simple example of two coloured boxes each containing fruit (apples shown in green and oranges shown in orange) to introduce the basic ideas of probability.



Figure 1.10 We can derive the sum and product rules of probability by considering two random variables, X , which takes the values $\{x_i\}$ where $i = 1, \dots, M$, and Y , which takes the values $\{y_j\}$ where $j = 1, \dots, L$. In this illustration we have $M = 5$ and $L = 3$. If we consider a total number N of instances of these variables, then we denote the number of instances where $X = x_i$ and $Y = y_j$ by n_{ij} , which is the number of points in the corresponding cell of the array. The number of points in column i , corresponding to $X = x_i$, is denoted by c_i , and the number of points in row j , corresponding to $Y = y_j$, is denoted by r_j .



and the probability of selecting the blue box is $6/10$. We write these probabilities as $p(B = r) = 4/10$ and $p(B = b) = 6/10$. Note that, by definition, probabilities must lie in the interval $[0, 1]$. Also, if the events are mutually exclusive and if they include all possible outcomes (for instance, in this example the box must be either red or blue), then we see that the probabilities for those events must sum to one.

We can now ask questions such as: “what is the overall probability that the selection procedure will pick an apple?”, or “given that we have chosen an orange, what is the probability that the box we chose was the blue one?”. We can answer questions such as these, and indeed much more complex questions associated with problems in pattern recognition, once we have equipped ourselves with the two elementary rules of probability, known as the *sum rule* and the *product rule*. Having obtained these rules, we shall then return to our boxes of fruit example.

In order to derive the rules of probability, consider the slightly more general example shown in Figure 1.10 involving two random variables X and Y (which could for instance be the Box and Fruit variables considered above). We shall suppose that X can take any of the values x_i where $i = 1, \dots, M$, and Y can take the values y_j where $j = 1, \dots, L$. Consider a total of N trials in which we sample both of the variables X and Y , and let the number of such trials in which $X = x_i$ and $Y = y_j$ be n_{ij} . Also, let the number of trials in which X takes the value x_i (irrespective of the value that Y takes) be denoted by c_i , and similarly let the number of trials in which Y takes the value y_j be denoted by r_j .

The probability that X will take the value x_i and Y will take the value y_j is written $p(X = x_i, Y = y_j)$ and is called the *joint* probability of $X = x_i$ and $Y = y_j$. It is given by the number of points falling in the cell i,j as a fraction of the total number of points, and hence

$$p(X = x_i, Y = y_j) = \frac{n_{ij}}{N}. \quad (1.5)$$

Here we are implicitly considering the limit $N \rightarrow \infty$. Similarly, the probability that X takes the value x_i irrespective of the value of Y is written as $p(X = x_i)$ and is given by the fraction of the total number of points that fall in column i , so that

$$p(X = x_i) = \frac{c_i}{N}. \quad (1.6)$$

Because the number of instances in column i in Figure 1.10 is just the sum of the number of instances in each cell of that column, we have $c_i = \sum_j n_{ij}$ and therefore,

from (1.5) and (1.6), we have

$$p(X = x_i) = \sum_{j=1}^L p(X = x_i, Y = y_j) \quad (1.7)$$

which is the **sum rule** of probability. Note that $p(X = x_i)$ is sometimes called the *marginal* probability, because it is obtained by marginalizing, or summing out, the other variables (in this case Y).

If we consider only those instances for which $X = x_i$, then the fraction of such instances for which $Y = y_j$ is written $p(Y = y_j | X = x_i)$ and is called the *conditional* probability of $Y = y_j$ given $X = x_i$. It is obtained by finding the fraction of those points in column i that fall in cell i,j and hence is given by

$$p(Y = y_j | X = x_i) = \frac{n_{ij}}{c_i}. \quad (1.8)$$

From (1.5), (1.6), and (1.8), we can then derive the following relationship

$$\begin{aligned} p(X = x_i, Y = y_j) &= \frac{n_{ij}}{N} = \frac{n_{ij}}{c_i} \cdot \frac{c_i}{N} \\ &= p(Y = y_j | X = x_i)p(X = x_i) \end{aligned} \quad (1.9)$$

which is the **product rule** of probability.

So far we have been quite careful to make a distinction between a random variable, such as the box B in the fruit example, and the values that the random variable can take, for example r if the box were the red one. Thus the probability that B takes the value r is denoted $p(B = r)$. Although this helps to avoid ambiguity, it leads to a rather cumbersome notation, and in many cases there will be no need for such pedantry. Instead, we may simply write $p(B)$ to denote a distribution over the random variable B , or $p(r)$ to denote the distribution evaluated for the particular value r , provided that the interpretation is clear from the context.

With this more compact notation, we can write the two fundamental rules of probability theory in the following form.

The Rules of Probability

| | | |
|-----------------|-------------------------|--------|
| sum rule | $p(X) = \sum_Y p(X, Y)$ | (1.10) |
|-----------------|-------------------------|--------|

| | | |
|---------------------|--------------------------|--------|
| product rule | $p(X, Y) = p(Y X)p(X)$. | (1.11) |
|---------------------|--------------------------|--------|

Here $p(X, Y)$ is a joint probability and is verbalized as “the probability of X and Y ”. Similarly, the quantity $p(Y|X)$ is a conditional probability and is verbalized as “the probability of Y given X ”, whereas the quantity $p(X)$ is a marginal probability

and is simply “the probability of X ”. These two simple rules form the basis for all of the probabilistic machinery that we use throughout this book.

From the product rule, together with the symmetry property $p(X, Y) = p(Y, X)$, we immediately obtain the following relationship between conditional probabilities

$$p(Y|X) = \frac{p(X|Y)p(Y)}{p(X)} \quad (1.12)$$

which is called *Bayes’ theorem* and which plays a central role in pattern recognition and machine learning. Using the sum rule, the denominator in Bayes’ theorem can be expressed in terms of the quantities appearing in the numerator

$$p(X) = \sum_Y p(X|Y)p(Y). \quad (1.13)$$

We can view the denominator in Bayes’ theorem as being the normalization constant required to ensure that the sum of the conditional probability on the left-hand side of (1.12) over all values of Y equals one.

In Figure 1.11, we show a simple example involving a joint distribution over two variables to illustrate the concept of marginal and conditional distributions. Here a finite sample of $N = 60$ data points has been drawn from the joint distribution and is shown in the top left. In the top right is a histogram of the fractions of data points having each of the two values of Y . From the definition of probability, these fractions would equal the corresponding probabilities $p(Y)$ in the limit $N \rightarrow \infty$. We can view the histogram as a simple way to model a probability distribution given only a finite number of points drawn from that distribution. Modelling distributions from data lies at the heart of statistical pattern recognition and will be explored in great detail in this book. The remaining two plots in Figure 1.11 show the corresponding histogram estimates of $p(X)$ and $p(X|Y = 1)$.

Let us now return to our example involving boxes of fruit. For the moment, we shall once again be explicit about distinguishing between the random variables and their instantiations. We have seen that the probabilities of selecting either the red or the blue boxes are given by

$$p(B = r) = 4/10 \quad (1.14)$$

$$p(B = b) = 6/10 \quad (1.15)$$

respectively. Note that these satisfy $p(B = r) + p(B = b) = 1$.

Now suppose that we pick a box at random, and it turns out to be the blue box. Then the probability of selecting an apple is just the fraction of apples in the blue box which is $3/4$, and so $p(F = a|B = b) = 3/4$. In fact, we can write out all four conditional probabilities for the type of fruit, given the selected box

$$p(F = a|B = r) = 1/4 \quad (1.16)$$

$$p(F = o|B = r) = 3/4 \quad (1.17)$$

$$p(F = a|B = b) = 3/4 \quad (1.18)$$

$$p(F = o|B = b) = 1/4. \quad (1.19)$$

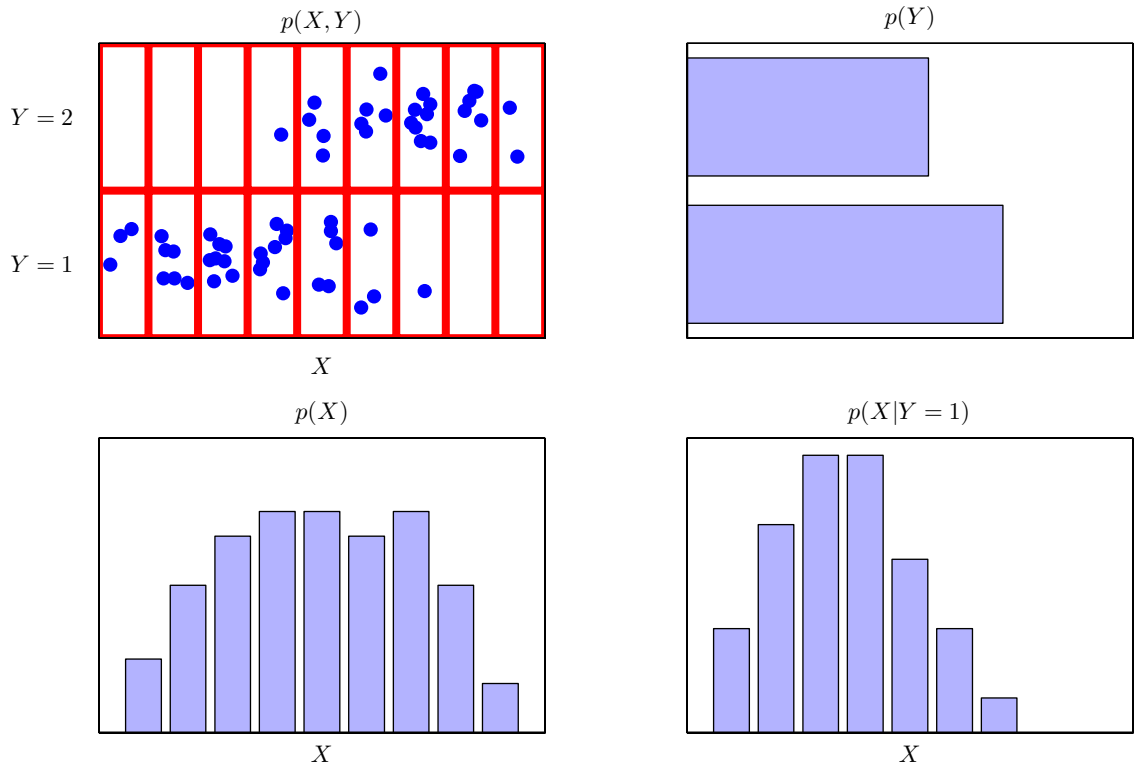


Figure 1.11 An illustration of a distribution over two variables, X , which takes 9 possible values, and Y , which takes two possible values. The top left figure shows a sample of 60 points drawn from a joint probability distribution over these variables. The remaining figures show histogram estimates of the marginal distributions $p(X)$ and $p(Y)$, as well as the conditional distribution $p(X|Y = 1)$ corresponding to the bottom row in the top left figure.

Again, note that these probabilities are normalized so that

$$p(F = a|B = r) + p(F = o|B = r) = 1 \quad (1.20)$$

and similarly

$$p(F = a|B = b) + p(F = o|B = b) = 1. \quad (1.21)$$

We can now use the sum and product rules of probability to evaluate the overall probability of choosing an apple

$$\begin{aligned} p(F = a) &= p(F = a|B = r)p(B = r) + p(F = a|B = b)p(B = b) \\ &= \frac{1}{4} \times \frac{4}{10} + \frac{3}{4} \times \frac{6}{10} = \frac{11}{20} \end{aligned} \quad (1.22)$$

from which it follows, using the sum rule, that $p(F = o) = 1 - 11/20 = 9/20$.

Suppose instead we are told that a piece of fruit has been selected and it is an orange, and we would like to know which box it came from. This requires that we evaluate the probability distribution over boxes conditioned on the identity of the fruit, whereas the probabilities in (1.16)–(1.19) give the probability distribution over the fruit conditioned on the identity of the box. We can solve the problem of reversing the conditional probability by using Bayes' theorem to give

$$p(B = r|F = o) = \frac{p(F = o|B = r)p(B = r)}{p(F = o)} = \frac{3}{4} \times \frac{4}{10} \times \frac{20}{9} = \frac{2}{3}. \quad (1.23)$$

From the sum rule, it then follows that $p(B = b|F = o) = 1 - 2/3 = 1/3$.

We can provide an important interpretation of Bayes' theorem as follows. If we had been asked which box had been chosen before being told the identity of the selected item of fruit, then the most complete information we have available is provided by the probability $p(B)$. We call this the *prior probability* because it is the probability available *before* we observe the identity of the fruit. Once we are told that the fruit is an orange, we can then use Bayes' theorem to compute the probability $p(B|F)$, which we shall call the *posterior probability* because it is the probability obtained *after* we have observed F . Note that in this example, the prior probability of selecting the red box was $4/10$, so that we were more likely to select the blue box than the red one. However, once we have observed that the piece of selected fruit is an orange, we find that the posterior probability of the red box is now $2/3$, so that it is now more likely that the box we selected was in fact the red one. This result accords with our intuition, as the proportion of oranges is much higher in the red box than it is in the blue box, and so the observation that the fruit was an orange provides significant evidence favouring the red box. In fact, the evidence is sufficiently strong that it outweighs the prior and makes it more likely that the red box was chosen rather than the blue one.

Finally, we note that if the joint distribution of two variables factorizes into the product of the marginals, so that $p(X, Y) = p(X)p(Y)$, then X and Y are said to be *independent*. From the product rule, we see that $p(Y|X) = p(Y)$, and so the conditional distribution of Y given X is indeed independent of the value of X . For instance, in our boxes of fruit example, if each box contained the same fraction of apples and oranges, then $p(F|B) = P(F)$, so that the probability of selecting, say, an apple is independent of which box is chosen.

1.2.1 Probability densities

As well as considering probabilities defined over discrete sets of events, we also wish to consider probabilities with respect to continuous variables. We shall limit ourselves to a relatively informal discussion. If the probability of a real-valued variable x falling in the interval $(x, x + \delta x)$ is given by $p(x)\delta x$ for $\delta x \rightarrow 0$, then $p(x)$ is called the *probability density* over x . This is illustrated in Figure 1.12. The probability that x will lie in an interval (a, b) is then given by

$$p(x \in (a, b)) = \int_a^b p(x) dx. \quad (1.24)$$

Figure 1.12 The concept of probability for discrete variables can be extended to that of a probability density $p(x)$ over a continuous variable x and is such that the probability of x lying in the interval $(x, x + \delta x)$ is given by $p(x)\delta x$ for $\delta x \rightarrow 0$. The probability density can be expressed as the derivative of a cumulative distribution function $P(x)$.



Because probabilities are nonnegative, and because the value of x must lie somewhere on the real axis, the probability density $p(x)$ must satisfy the two conditions

$$p(x) \geq 0 \quad (1.25)$$

$$\int_{-\infty}^{\infty} p(x) dx = 1. \quad (1.26)$$

Under a nonlinear change of variable, a probability density transforms differently from a simple function, due to the Jacobian factor. For instance, if we consider a change of variables $x = g(y)$, then a function $f(x)$ becomes $\tilde{f}(y) = f(g(y))$. Now consider a probability density $p_x(x)$ that corresponds to a density $p_y(y)$ with respect to the new variable y , where the suffices denote the fact that $p_x(x)$ and $p_y(y)$ are different densities. Observations falling in the range $(x, x + \delta x)$ will, for small values of δx , be transformed into the range $(y, y + \delta y)$ where $p_x(x)\delta x \simeq p_y(y)\delta y$, and hence

$$\begin{aligned} p_y(y) &= p_x(x) \left| \frac{dx}{dy} \right| \\ &= p_x(g(y)) |g'(y)|. \end{aligned} \quad (1.27)$$

One consequence of this property is that the concept of the maximum of a probability density is dependent on the choice of variable.

Exercise 1.4

The probability that x lies in the interval $(-\infty, z)$ is given by the *cumulative distribution function* defined by

$$P(z) = \int_{-\infty}^z p(x) dx \quad (1.28)$$

which satisfies $P'(x) = p(x)$, as shown in Figure 1.12.

If we have several continuous variables x_1, \dots, x_D , denoted collectively by the vector \mathbf{x} , then we can define a joint probability density $p(\mathbf{x}) = p(x_1, \dots, x_D)$ such

that the probability of \mathbf{x} falling in an infinitesimal volume $\delta\mathbf{x}$ containing the point \mathbf{x} is given by $p(\mathbf{x})\delta\mathbf{x}$. This multivariate probability density must satisfy

$$p(\mathbf{x}) \geq 0 \quad (1.29)$$

$$\int p(\mathbf{x}) d\mathbf{x} = 1 \quad (1.30)$$

in which the integral is taken over the whole of \mathbf{x} space. We can also consider joint probability distributions over a combination of discrete and continuous variables.

Note that if x is a discrete variable, then $p(x)$ is sometimes called a *probability mass function* because it can be regarded as a set of ‘probability masses’ concentrated at the allowed values of x .

The sum and product rules of probability, as well as Bayes’ theorem, apply equally to the case of probability densities, or to combinations of discrete and continuous variables. For instance, if x and y are two real variables, then the sum and product rules take the form

$$p(x) = \int p(x, y) dy \quad (1.31)$$

$$p(x, y) = p(y|x)p(x). \quad (1.32)$$

A formal justification of the sum and product rules for continuous variables (Feller, 1966) requires a branch of mathematics called *measure theory* and lies outside the scope of this book. Its validity can be seen informally, however, by dividing each real variable into intervals of width Δ and considering the discrete probability distribution over these intervals. Taking the limit $\Delta \rightarrow 0$ then turns sums into integrals and gives the desired result.

1.2.2 Expectations and covariances

One of the most important operations involving probabilities is that of finding weighted averages of functions. The average value of some function $f(x)$ under a probability distribution $p(x)$ is called the *expectation* of $f(x)$ and will be denoted by $\mathbb{E}[f]$. For a discrete distribution, it is given by

$$\mathbb{E}[f] = \sum_x p(x)f(x) \quad (1.33)$$

so that the average is weighted by the relative probabilities of the different values of x . In the case of continuous variables, expectations are expressed in terms of an integration with respect to the corresponding probability density

$$\mathbb{E}[f] = \int p(x)f(x) dx. \quad (1.34)$$

In either case, if we are given a finite number N of points drawn from the probability distribution or probability density, then the expectation can be approximated as a

finite sum over these points

$$\mathbb{E}[f] \simeq \frac{1}{N} \sum_{n=1}^N f(x_n). \quad (1.35)$$

We shall make extensive use of this result when we discuss sampling methods in Chapter 11. The approximation in (1.35) becomes exact in the limit $N \rightarrow \infty$.

Sometimes we will be considering expectations of functions of several variables, in which case we can use a subscript to indicate which variable is being averaged over, so that for instance

$$\mathbb{E}_x[f(x, y)] \quad (1.36)$$

denotes the average of the function $f(x, y)$ with respect to the distribution of x . Note that $\mathbb{E}_x[f(x, y)]$ will be a function of y .

We can also consider a *conditional expectation* with respect to a conditional distribution, so that

$$\mathbb{E}_x[f|y] = \sum_x p(x|y)f(x) \quad (1.37)$$

with an analogous definition for continuous variables.

The *variance* of $f(x)$ is defined by

$$\text{var}[f] = \mathbb{E}[(f(x) - \mathbb{E}[f(x)])^2] \quad (1.38)$$

and provides a measure of how much variability there is in $f(x)$ around its mean value $\mathbb{E}[f(x)]$. Expanding out the square, we see that the variance can also be written in terms of the expectations of $f(x)$ and $f(x)^2$

$$\text{var}[f] = \mathbb{E}[f(x)^2] - \mathbb{E}[f(x)]^2. \quad (1.39)$$

In particular, we can consider the variance of the variable x itself, which is given by

$$\text{var}[x] = \mathbb{E}[x^2] - \mathbb{E}[x]^2. \quad (1.40)$$

For two random variables x and y , the *covariance* is defined by

$$\begin{aligned} \text{cov}[x, y] &= \mathbb{E}_{x,y} [\{x - \mathbb{E}[x]\} \{y - \mathbb{E}[y]\}] \\ &= \mathbb{E}_{x,y}[xy] - \mathbb{E}[x]\mathbb{E}[y] \end{aligned} \quad (1.41)$$

which expresses the extent to which x and y vary together. If x and y are independent, then their covariance vanishes.

In the case of two vectors of random variables \mathbf{x} and \mathbf{y} , the covariance is a matrix

$$\begin{aligned} \text{cov}[\mathbf{x}, \mathbf{y}] &= \mathbb{E}_{\mathbf{x}, \mathbf{y}} [\{\mathbf{x} - \mathbb{E}[\mathbf{x}]\} \{\mathbf{y}^T - \mathbb{E}[\mathbf{y}^T]\}] \\ &= \mathbb{E}_{\mathbf{x}, \mathbf{y}}[\mathbf{x}\mathbf{y}^T] - \mathbb{E}[\mathbf{x}]\mathbb{E}[\mathbf{y}^T]. \end{aligned} \quad (1.42)$$

If we consider the covariance of the components of a vector \mathbf{x} with each other, then we use a slightly simpler notation $\text{cov}[\mathbf{x}] \equiv \text{cov}[\mathbf{x}, \mathbf{x}]$.

Exercise 1.5

Exercise 1.6

1.2.3 Bayesian probabilities

So far in this chapter, we have viewed probabilities in terms of the frequencies of random, repeatable events. We shall refer to this as the *classical* or *frequentist* interpretation of probability. Now we turn to the more general *Bayesian* view, in which probabilities provide a quantification of uncertainty.

Consider an uncertain event, for example whether the moon was once in its own orbit around the sun, or whether the Arctic ice cap will have disappeared by the end of the century. These are not events that can be repeated numerous times in order to define a notion of probability as we did earlier in the context of boxes of fruit. Nevertheless, we will generally have some idea, for example, of how quickly we think the polar ice is melting. If we now obtain fresh evidence, for instance from a new Earth observation satellite gathering novel forms of diagnostic information, we may revise our opinion on the rate of ice loss. Our assessment of such matters will affect the actions we take, for instance the extent to which we endeavour to reduce the emission of greenhouse gasses. In such circumstances, we would like to be able to quantify our expression of uncertainty and make precise revisions of uncertainty in the light of new evidence, as well as subsequently to be able to take optimal actions or decisions as a consequence. This can all be achieved through the elegant, and very general, Bayesian interpretation of probability.

The use of probability to represent uncertainty, however, is not an ad-hoc choice, but is inevitable if we are to respect common sense while making rational coherent inferences. For instance, Cox (1946) showed that if numerical values are used to represent degrees of belief, then a simple set of axioms encoding common sense properties of such beliefs leads uniquely to a set of rules for manipulating degrees of belief that are equivalent to the sum and product rules of probability. This provided the first rigorous proof that probability theory could be regarded as an extension of Boolean logic to situations involving uncertainty (Jaynes, 2003). Numerous other authors have proposed different sets of properties or axioms that such measures of uncertainty should satisfy (Ramsey, 1931; Good, 1950; Savage, 1961; deFinetti, 1970; Lindley, 1982). In each case, the resulting numerical quantities behave precisely according to the rules of probability. It is therefore natural to refer to these quantities as (Bayesian) probabilities.

In the field of pattern recognition, too, it is helpful to have a more general no-



Thomas Bayes
1701–1761

Thomas Bayes was born in Tunbridge Wells and was a clergyman as well as an amateur scientist and a mathematician. He studied logic and theology at Edinburgh University and was elected Fellow of the Royal Society in 1742. During the 18th century, issues regarding probability arose in connection with

gambling and with the new concept of insurance. One particularly important problem concerned so-called inverse probability. A solution was proposed by Thomas Bayes in his paper 'Essay towards solving a problem in the doctrine of chances', which was published in 1764, some three years after his death, in the *Philosophical Transactions of the Royal Society*. In fact, Bayes only formulated his theory for the case of a uniform prior, and it was Pierre-Simon Laplace who independently rediscovered the theory in general form and who demonstrated its broad applicability.

tion of probability. Consider the example of polynomial curve fitting discussed in Section 1.1. It seems reasonable to apply the frequentist notion of probability to the random values of the observed variables t_n . However, we would like to address and quantify the uncertainty that surrounds the appropriate choice for the model parameters \mathbf{w} . We shall see that, from a Bayesian perspective, we can use the machinery of probability theory to describe the uncertainty in model parameters such as \mathbf{w} , or indeed in the choice of model itself.

Bayes' theorem now acquires a new significance. Recall that in the boxes of fruit example, the observation of the identity of the fruit provided relevant information that altered the probability that the chosen box was the red one. In that example, Bayes' theorem was used to convert a prior probability into a posterior probability by incorporating the evidence provided by the observed data. As we shall see in detail later, we can adopt a similar approach when making inferences about quantities such as the parameters \mathbf{w} in the polynomial curve fitting example. We capture our assumptions about \mathbf{w} , before observing the data, in the form of a prior probability distribution $p(\mathbf{w})$. The effect of the observed data $\mathcal{D} = \{t_1, \dots, t_N\}$ is expressed through the conditional probability $p(\mathcal{D}|\mathbf{w})$, and we shall see later, in Section 1.2.5, how this can be represented explicitly. Bayes' theorem, which takes the form

$$p(\mathbf{w}|\mathcal{D}) = \frac{p(\mathcal{D}|\mathbf{w})p(\mathbf{w})}{p(\mathcal{D})} \quad (1.43)$$

then allows us to evaluate the uncertainty in \mathbf{w} *after* we have observed \mathcal{D} in the form of the posterior probability $p(\mathbf{w}|\mathcal{D})$.

The quantity $p(\mathcal{D}|\mathbf{w})$ on the right-hand side of Bayes' theorem is evaluated for the observed data set \mathcal{D} and can be viewed as a function of the parameter vector \mathbf{w} , in which case it is called the *likelihood function*. It expresses how probable the observed data set is for different settings of the parameter vector \mathbf{w} . Note that the likelihood is not a probability distribution over \mathbf{w} , and its integral with respect to \mathbf{w} does not (necessarily) equal one.

Given this definition of likelihood, we can state Bayes' theorem in words

$$\text{posterior} \propto \text{likelihood} \times \text{prior} \quad (1.44)$$

where all of these quantities are viewed as functions of \mathbf{w} . The denominator in (1.43) is the normalization constant, which ensures that the posterior distribution on the left-hand side is a valid probability density and integrates to one. Indeed, integrating both sides of (1.43) with respect to \mathbf{w} , we can express the denominator in Bayes' theorem in terms of the prior distribution and the likelihood function

$$p(\mathcal{D}) = \int p(\mathcal{D}|\mathbf{w})p(\mathbf{w}) d\mathbf{w}. \quad (1.45)$$

In both the Bayesian and frequentist paradigms, the likelihood function $p(\mathcal{D}|\mathbf{w})$ plays a central role. However, the manner in which it is used is fundamentally different in the two approaches. In a frequentist setting, \mathbf{w} is considered to be a fixed parameter, whose value is determined by some form of ‘estimator’, and error bars

on this estimate are obtained by considering the distribution of possible data sets \mathcal{D} . By contrast, from the Bayesian viewpoint there is only a single data set \mathcal{D} (namely the one that is actually observed), and the uncertainty in the parameters is expressed through a probability distribution over \mathbf{w} .

A widely used frequentist estimator is *maximum likelihood*, in which \mathbf{w} is set to the value that maximizes the likelihood function $p(\mathcal{D}|\mathbf{w})$. This corresponds to choosing the value of \mathbf{w} for which the probability of the observed data set is maximized. In the machine learning literature, the negative log of the likelihood function is called an *error function*. Because the negative logarithm is a monotonically decreasing function, maximizing the likelihood is equivalent to minimizing the error.

One approach to determining frequentist error bars is the *bootstrap* (Efron, 1979; Hastie *et al.*, 2001), in which multiple data sets are created as follows. Suppose our original data set consists of N data points $\mathbf{X} = \{\mathbf{x}_1, \dots, \mathbf{x}_N\}$. We can create a new data set \mathbf{X}_B by drawing N points at random from \mathbf{X} , with replacement, so that some points in \mathbf{X} may be replicated in \mathbf{X}_B , whereas other points in \mathbf{X} may be absent from \mathbf{X}_B . This process can be repeated L times to generate L data sets each of size N and each obtained by sampling from the original data set \mathbf{X} . The statistical accuracy of parameter estimates can then be evaluated by looking at the variability of predictions between the different bootstrap data sets.

One advantage of the Bayesian viewpoint is that the inclusion of prior knowledge arises naturally. Suppose, for instance, that a fair-looking coin is tossed three times and lands heads each time. A classical maximum likelihood estimate of the probability of landing heads would give 1, implying that all future tosses will land heads! By contrast, a Bayesian approach with any reasonable prior will lead to a much less extreme conclusion.

There has been much controversy and debate associated with the relative merits of the frequentist and Bayesian paradigms, which have not been helped by the fact that there is no unique frequentist, or even Bayesian, viewpoint. For instance, one common criticism of the Bayesian approach is that the prior distribution is often selected on the basis of mathematical convenience rather than as a reflection of any prior beliefs. Even the subjective nature of the conclusions through their dependence on the choice of prior is seen by some as a source of difficulty. Reducing the dependence on the prior is one motivation for so-called *noninformative* priors. However, these lead to difficulties when comparing different models, and indeed Bayesian methods based on poor choices of prior can give poor results with high confidence. Frequentist evaluation methods offer some protection from such problems, and techniques such as cross-validation remain useful in areas such as model comparison.

This book places a strong emphasis on the Bayesian viewpoint, reflecting the huge growth in the practical importance of Bayesian methods in the past few years, while also discussing useful frequentist concepts as required.

Although the Bayesian framework has its origins in the 18th century, the practical application of Bayesian methods was for a long time severely limited by the difficulties in carrying through the full Bayesian procedure, particularly the need to marginalize (sum or integrate) over the whole of parameter space, which, as we shall

Section 2.1

Section 2.4.3

Section 1.3

see, is required in order to make predictions or to compare different models. The development of sampling methods, such as Markov chain Monte Carlo (discussed in Chapter 11) along with dramatic improvements in the speed and memory capacity of computers, opened the door to the practical use of Bayesian techniques in an impressive range of problem domains. Monte Carlo methods are very flexible and can be applied to a wide range of models. However, they are computationally intensive and have mainly been used for small-scale problems.

More recently, highly efficient deterministic approximation schemes such as variational Bayes and expectation propagation (discussed in Chapter 10) have been developed. These offer a complementary alternative to sampling methods and have allowed Bayesian techniques to be used in large-scale applications (Blei *et al.*, 2003).

1.2.4 The Gaussian distribution

We shall devote the whole of Chapter 2 to a study of various probability distributions and their key properties. It is convenient, however, to introduce here one of the most important probability distributions for continuous variables, called the *normal* or *Gaussian* distribution. We shall make extensive use of this distribution in the remainder of this chapter and indeed throughout much of the book.

For the case of a single real-valued variable x , the Gaussian distribution is defined by

$$\mathcal{N}(x|\mu, \sigma^2) = \frac{1}{(2\pi\sigma^2)^{1/2}} \exp\left\{-\frac{1}{2\sigma^2}(x - \mu)^2\right\} \quad (1.46)$$

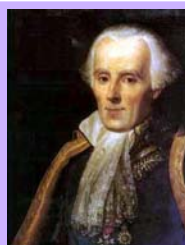
which is governed by two parameters: μ , called the *mean*, and σ^2 , called the *variance*. The square root of the variance, given by σ , is called the *standard deviation*, and the reciprocal of the variance, written as $\beta = 1/\sigma^2$, is called the *precision*. We shall see the motivation for these terms shortly. Figure 1.13 shows a plot of the Gaussian distribution.

From the form of (1.46) we see that the Gaussian distribution satisfies

$$\mathcal{N}(x|\mu, \sigma^2) > 0. \quad (1.47)$$

Exercise 1.7

Also it is straightforward to show that the Gaussian is normalized, so that

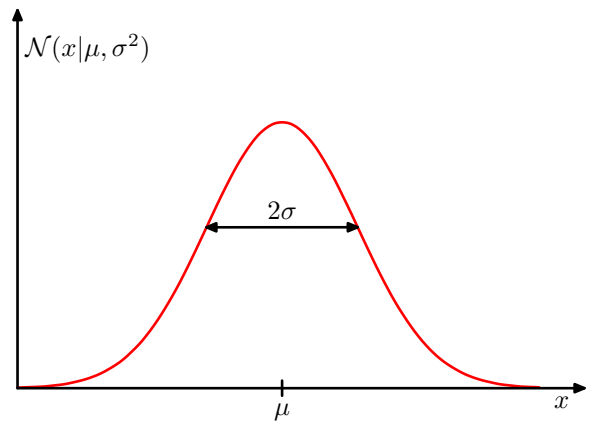


Pierre-Simon Laplace
1749–1827

It is said that Laplace was seriously lacking in modesty and at one point declared himself to be the best mathematician in France at the time, a claim that was arguably true. As well as being prolific in mathematics, he also made numerous contributions to astronomy, including the nebular hypothesis by which the

earth is thought to have formed from the condensation and cooling of a large rotating disk of gas and dust. In 1812 he published the first edition of *Théorie Analytique des Probabilités*, in which Laplace states that “probability theory is nothing but common sense reduced to calculation”. This work included a discussion of the inverse probability calculation (later termed Bayes’ theorem by Poincaré), which he used to solve problems in life expectancy, jurisprudence, planetary masses, triangulation, and error estimation.

Figure 1.13 Plot of the univariate Gaussian showing the mean μ and the standard deviation σ .



$$\int_{-\infty}^{\infty} \mathcal{N}(x|\mu, \sigma^2) dx = 1. \quad (1.48)$$

Thus (1.46) satisfies the two requirements for a valid probability density.

We can readily find expectations of functions of x under the Gaussian distribution. In particular, the average value of x is given by

$$\mathbb{E}[x] = \int_{-\infty}^{\infty} \mathcal{N}(x|\mu, \sigma^2) x dx = \mu. \quad (1.49)$$

Because the parameter μ represents the average value of x under the distribution, it is referred to as the mean. Similarly, for the second order moment

$$\mathbb{E}[x^2] = \int_{-\infty}^{\infty} \mathcal{N}(x|\mu, \sigma^2) x^2 dx = \mu^2 + \sigma^2. \quad (1.50)$$

From (1.49) and (1.50), it follows that the variance of x is given by

$$\text{var}[x] = \mathbb{E}[x^2] - \mathbb{E}[x]^2 = \sigma^2 \quad (1.51)$$

and hence σ^2 is referred to as the variance parameter. The maximum of a distribution is known as its mode. For a Gaussian, the mode coincides with the mean.

Exercise 1.9

We are also interested in the Gaussian distribution defined over a D -dimensional vector \mathbf{x} of continuous variables, which is given by

$$\mathcal{N}(\mathbf{x}|\boldsymbol{\mu}, \boldsymbol{\Sigma}) = \frac{1}{(2\pi)^{D/2}} \frac{1}{|\boldsymbol{\Sigma}|^{1/2}} \exp \left\{ -\frac{1}{2} (\mathbf{x} - \boldsymbol{\mu})^T \boldsymbol{\Sigma}^{-1} (\mathbf{x} - \boldsymbol{\mu}) \right\} \quad (1.52)$$

where the D -dimensional vector $\boldsymbol{\mu}$ is called the mean, the $D \times D$ matrix $\boldsymbol{\Sigma}$ is called the covariance, and $|\boldsymbol{\Sigma}|$ denotes the determinant of $\boldsymbol{\Sigma}$. We shall make use of the multivariate Gaussian distribution briefly in this chapter, although its properties will be studied in detail in Section 2.3.

Figure 1.14 Illustration of the likelihood function for a Gaussian distribution, shown by the red curve. Here the black points denote a data set of values $\{x_n\}$, and the likelihood function given by (1.53) corresponds to the product of the blue values. Maximizing the likelihood involves adjusting the mean and variance of the Gaussian so as to maximize this product.



Now suppose that we have a data set of observations $\mathbf{x} = (x_1, \dots, x_N)^T$, representing N observations of the scalar variable x . Note that we are using the typeface \mathbf{x} to distinguish this from a single observation of the vector-valued variable $(x_1, \dots, x_D)^T$, which we denote by \mathbf{x} . We shall suppose that the observations are drawn independently from a Gaussian distribution whose mean μ and variance σ^2 are unknown, and we would like to determine these parameters from the data set. Data points that are drawn independently from the same distribution are said to be **independent and identically distributed**, which is often abbreviated to i.i.d. We have seen that the joint probability of two independent events is given by the product of the marginal probabilities for each event separately. Because our data set \mathbf{x} is i.i.d., we can therefore write the probability of the data set, given μ and σ^2 , in the form

$$p(\mathbf{x}|\mu, \sigma^2) = \prod_{n=1}^N \mathcal{N}(x_n|\mu, \sigma^2). \quad (1.53)$$

When viewed as a function of μ and σ^2 , this is the likelihood function for the Gaussian and is interpreted diagrammatically in Figure 1.14.

One common criterion for determining the parameters in a probability distribution using an observed data set is to find the parameter values that maximize the likelihood function. This might seem like a strange criterion because, from our foregoing discussion of probability theory, it would seem more natural to maximize the probability of the parameters given the data, not the probability of the data given the parameters. In fact, these two criteria are related, as we shall discuss in the context of curve fitting.

For the moment, however, we shall determine values for the unknown parameters μ and σ^2 in the Gaussian by maximizing the likelihood function (1.53). In practice, it is more convenient to maximize the log of the likelihood function. Because the logarithm is a monotonically increasing function of its argument, maximization of the log of a function is equivalent to maximization of the function itself. Taking the log not only simplifies the subsequent mathematical analysis, but it also helps numerically because the product of a large number of small probabilities can easily underflow the numerical precision of the computer, and this is resolved by computing instead the sum of the log probabilities. From (1.46) and (1.53), the log likelihood

Section 1.2.5

function can be written in the form

$$\ln p(\mathbf{x}|\mu, \sigma^2) = -\frac{1}{2\sigma^2} \sum_{n=1}^N (x_n - \mu)^2 - \frac{N}{2} \ln \sigma^2 - \frac{N}{2} \ln(2\pi). \quad (1.54)$$

Maximizing (1.54) with respect to μ , we obtain the maximum likelihood solution given by

$$\mu_{\text{ML}} = \frac{1}{N} \sum_{n=1}^N x_n \quad (1.55)$$

which is the *sample mean*, i.e., the mean of the observed values $\{x_n\}$. Similarly, maximizing (1.54) with respect to σ^2 , we obtain the maximum likelihood solution for the variance in the form

$$\sigma_{\text{ML}}^2 = \frac{1}{N} \sum_{n=1}^N (x_n - \mu_{\text{ML}})^2 \quad (1.56)$$

which is the *sample variance* measured with respect to the sample mean μ_{ML} . Note that we are performing a joint maximization of (1.54) with respect to μ and σ^2 , but in the case of the Gaussian distribution the solution for μ decouples from that for σ^2 so that we can first evaluate (1.55) and then subsequently use this result to evaluate (1.56).

Later in this chapter, and also in subsequent chapters, we shall highlight the significant limitations of the maximum likelihood approach. Here we give an indication of the problem in the context of our solutions for the maximum likelihood parameter settings for the univariate Gaussian distribution. In particular, we shall show that the maximum likelihood approach systematically underestimates the variance of the distribution. This is an example of a phenomenon called *bias* and is related to the problem of over-fitting encountered in the context of polynomial curve fitting. We first note that the maximum likelihood solutions μ_{ML} and σ_{ML}^2 are functions of the data set values x_1, \dots, x_N . Consider the expectations of these quantities with respect to the data set values, which themselves come from a Gaussian distribution with parameters μ and σ^2 . It is straightforward to show that

$$\mathbb{E}[\mu_{\text{ML}}] = \mu \quad (1.57)$$

$$\mathbb{E}[\sigma_{\text{ML}}^2] = \left(\frac{N-1}{N}\right)\sigma^2 \quad (1.58)$$

so that on average the maximum likelihood estimate will obtain the correct mean but will underestimate the true variance by a factor $(N-1)/N$. The intuition behind this result is given by Figure 1.15.

From (1.58) it follows that the following estimate for the variance parameter is unbiased

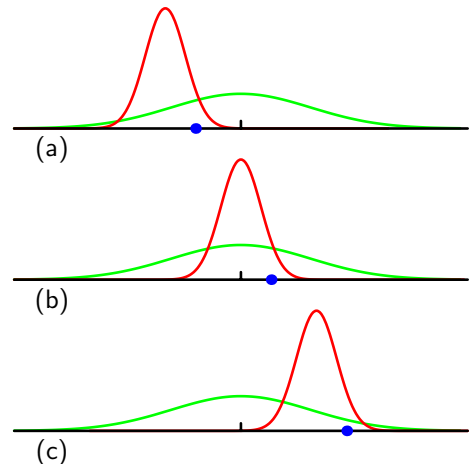
$$\tilde{\sigma}^2 = \frac{N}{N-1} \sigma_{\text{ML}}^2 = \frac{1}{N-1} \sum_{n=1}^N (x_n - \mu_{\text{ML}})^2. \quad (1.59)$$

Exercise 1.11

Section 1.1

Exercise 1.12

Figure 1.15 Illustration of how bias arises in using maximum likelihood to determine the variance of a Gaussian. The green curve shows the true Gaussian distribution from which data is generated, and the three red curves show the Gaussian distributions obtained by fitting to three data sets, each consisting of two data points shown in blue, using the maximum likelihood results (1.55) and (1.56). Averaged across the three data sets, the mean is correct, but the variance is systematically under-estimated because it is measured relative to the sample mean and not relative to the true mean.



In Section 10.1.3, we shall see how this result arises automatically when we adopt a Bayesian approach.

Note that the bias of the maximum likelihood solution becomes less significant as the number N of data points increases, and in the limit $N \rightarrow \infty$ the maximum likelihood solution for the variance equals the true variance of the distribution that generated the data. In practice, for anything other than small N , this bias will not prove to be a serious problem. However, throughout this book we shall be interested in more complex models with many parameters, for which the bias problems associated with maximum likelihood will be much more severe. In fact, as we shall see, the issue of bias in maximum likelihood lies at the root of the over-fitting problem that we encountered earlier in the context of polynomial curve fitting.

1.2.5 Curve fitting re-visited

Section 1.1

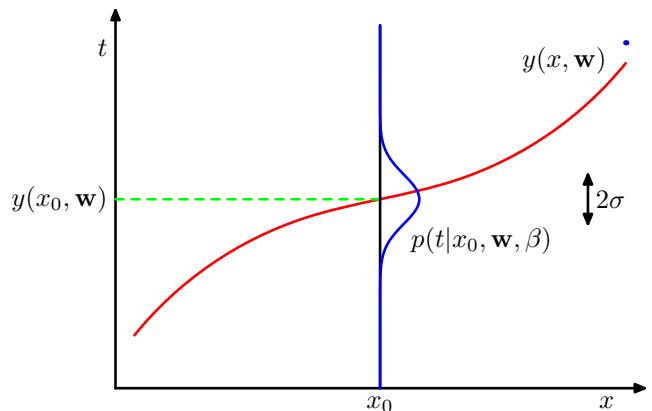
We have seen how the problem of polynomial curve fitting can be expressed in terms of error minimization. Here we return to the curve fitting example and view it from a probabilistic perspective, thereby gaining some insights into error functions and regularization, as well as taking us towards a full Bayesian treatment.

The goal in the curve fitting problem is to be able to make predictions for the target variable t given some new value of the input variable x on the basis of a set of training data comprising N input values $\mathbf{x} = (x_1, \dots, x_N)^T$ and their corresponding target values $\mathbf{t} = (t_1, \dots, t_N)^T$. We can express our uncertainty over the value of the target variable using a probability distribution. For this purpose, we shall assume that, given the value of x , the corresponding value of t has a Gaussian distribution with a mean equal to the value $y(x, \mathbf{w})$ of the polynomial curve given by (1.1). Thus we have

$$p(t|x, \mathbf{w}, \beta) = \mathcal{N}(t|y(x, \mathbf{w}), \beta^{-1}) \quad (1.60)$$

where, for consistency with the notation in later chapters, we have defined a precision parameter β corresponding to the inverse variance of the distribution. This is illustrated schematically in Figure 1.16.

Figure 1.16 Schematic illustration of a Gaussian conditional distribution for t given x given by (1.60), in which the mean is given by the polynomial function $y(x, \mathbf{w})$, and the precision is given by the parameter β , which is related to the variance by $\beta^{-1} = \sigma^2$.



We now use the training data $\{\mathbf{x}, \mathbf{t}\}$ to determine the values of the unknown parameters \mathbf{w} and β by maximum likelihood. If the data are assumed to be drawn independently from the distribution (1.60), then the likelihood function is given by

$$p(\mathbf{t}|\mathbf{x}, \mathbf{w}, \beta) = \prod_{n=1}^N \mathcal{N}(t_n | y(x_n, \mathbf{w}), \beta^{-1}). \quad (1.61)$$

As we did in the case of the simple Gaussian distribution earlier, it is convenient to maximize the logarithm of the likelihood function. Substituting for the form of the Gaussian distribution, given by (1.46), we obtain the log likelihood function in the form

$$\ln p(\mathbf{t}|\mathbf{x}, \mathbf{w}, \beta) = -\frac{\beta}{2} \sum_{n=1}^N \{y(x_n, \mathbf{w}) - t_n\}^2 + \frac{N}{2} \ln \beta - \frac{N}{2} \ln(2\pi). \quad (1.62)$$

Consider first the determination of the maximum likelihood solution for the polynomial coefficients, which will be denoted by \mathbf{w}_{ML} . These are determined by maximizing (1.62) with respect to \mathbf{w} . For this purpose, we can omit the last two terms on the right-hand side of (1.62) because they do not depend on \mathbf{w} . Also, we note that scaling the log likelihood by a positive constant coefficient does not alter the location of the maximum with respect to \mathbf{w} , and so we can replace the coefficient $\beta/2$ with $1/2$. Finally, instead of maximizing the log likelihood, we can equivalently minimize the negative log likelihood. We therefore see that maximizing likelihood is equivalent, so far as determining \mathbf{w} is concerned, to minimizing the *sum-of-squares error function* defined by (1.2). Thus the sum-of-squares error function has arisen as a consequence of maximizing likelihood under the assumption of a Gaussian noise distribution.

We can also use maximum likelihood to determine the precision parameter β of the Gaussian conditional distribution. Maximizing (1.62) with respect to β gives

$$\frac{1}{\beta_{\text{ML}}} = \frac{1}{N} \sum_{n=1}^N \{y(x_n, \mathbf{w}_{\text{ML}}) - t_n\}^2. \quad (1.63)$$

Section 1.2.4

Again we can first determine the parameter vector \mathbf{w}_{ML} governing the mean and subsequently use this to find the precision β_{ML} as was the case for the simple Gaussian distribution.

Having determined the parameters \mathbf{w} and β , we can now make predictions for new values of x . Because we now have a probabilistic model, these are expressed in terms of the *predictive distribution* that gives the probability distribution over t , rather than simply a point estimate, and is obtained by substituting the maximum likelihood parameters into (1.60) to give

$$p(t|x, \mathbf{w}_{\text{ML}}, \beta_{\text{ML}}) = \mathcal{N}(t|y(x, \mathbf{w}_{\text{ML}}), \beta_{\text{ML}}^{-1}). \quad (1.64)$$

Now let us take a step towards a more Bayesian approach and introduce a prior distribution over the polynomial coefficients \mathbf{w} . For simplicity, let us consider a Gaussian distribution of the form

$$p(\mathbf{w}|\alpha) = \mathcal{N}(\mathbf{w}|\mathbf{0}, \alpha^{-1}\mathbf{I}) = \left(\frac{\alpha}{2\pi}\right)^{(M+1)/2} \exp\left\{-\frac{\alpha}{2}\mathbf{w}^T\mathbf{w}\right\} \quad (1.65)$$

where α is the precision of the distribution, and $M+1$ is the total number of elements in the vector \mathbf{w} for an M^{th} order polynomial. Variables such as α , which control the distribution of model parameters, are called *hyperparameters*. Using Bayes' theorem, the posterior distribution for \mathbf{w} is proportional to the product of the prior distribution and the likelihood function

$$p(\mathbf{w}|\mathbf{x}, \mathbf{t}, \alpha, \beta) \propto p(\mathbf{t}|\mathbf{x}, \mathbf{w}, \beta)p(\mathbf{w}|\alpha). \quad (1.66)$$

We can now determine \mathbf{w} by finding the most probable value of \mathbf{w} given the data, in other words by maximizing the posterior distribution. This technique is called *maximum posterior*, or simply *MAP*. Taking the negative logarithm of (1.66) and combining with (1.62) and (1.65), we find that the maximum of the posterior is given by the minimum of

$$\frac{\beta}{2} \sum_{n=1}^N \{y(x_n, \mathbf{w}) - t_n\}^2 + \frac{\alpha}{2} \mathbf{w}^T \mathbf{w}. \quad (1.67)$$

Thus we see that maximizing the posterior distribution is equivalent to minimizing the regularized sum-of-squares error function encountered earlier in the form (1.4), with a regularization parameter given by $\lambda = \alpha/\beta$.

1.2.6 Bayesian curve fitting

Although we have included a prior distribution $p(\mathbf{w}|\alpha)$, we are so far still making a point estimate of \mathbf{w} and so this does not yet amount to a Bayesian treatment. In a fully Bayesian approach, we should consistently apply the sum and product rules of probability, which requires, as we shall see shortly, that we integrate over all values of \mathbf{w} . Such marginalizations lie at the heart of Bayesian methods for pattern recognition.

In the curve fitting problem, we are given the training data \mathbf{x} and \mathbf{t} , along with a new test point x , and our goal is to predict the value of t . We therefore wish to evaluate the predictive distribution $p(t|x, \mathbf{x}, \mathbf{t})$. Here we shall assume that the parameters α and β are fixed and known in advance (in later chapters we shall discuss how such parameters can be inferred from data in a Bayesian setting).

A Bayesian treatment simply corresponds to a consistent application of the sum and product rules of probability, which allow the predictive distribution to be written in the form

$$p(t|x, \mathbf{x}, \mathbf{t}) = \int p(t|x, \mathbf{w})p(\mathbf{w}|\mathbf{x}, \mathbf{t}) d\mathbf{w}. \quad (1.68)$$

Here $p(t|x, \mathbf{w})$ is given by (1.60), and we have omitted the dependence on α and β to simplify the notation. Here $p(\mathbf{w}|\mathbf{x}, \mathbf{t})$ is the posterior distribution over parameters, and can be found by normalizing the right-hand side of (1.66). We shall see in Section 3.3 that, for problems such as the curve-fitting example, this posterior distribution is a Gaussian and can be evaluated analytically. Similarly, the integration in (1.68) can also be performed analytically with the result that the predictive distribution is given by a Gaussian of the form

$$p(t|x, \mathbf{x}, \mathbf{t}) = \mathcal{N}(t|m(x), s^2(x)) \quad (1.69)$$

where the mean and variance are given by

$$m(x) = \beta \phi(x)^T \mathbf{S} \sum_{n=1}^N \phi(x_n) t_n \quad (1.70)$$

$$s^2(x) = \beta^{-1} + \phi(x)^T \mathbf{S} \phi(x). \quad (1.71)$$

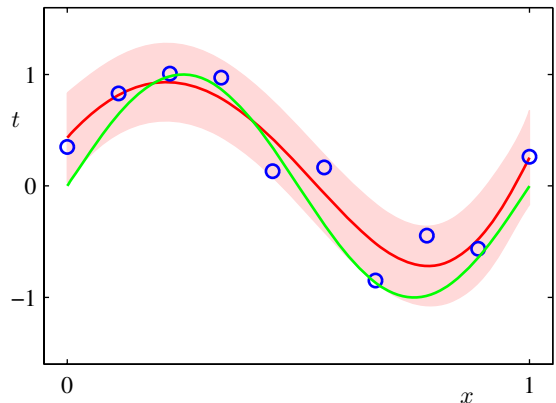
Here the matrix \mathbf{S} is given by

$$\mathbf{S}^{-1} = \alpha \mathbf{I} + \beta \sum_{n=1}^N \phi(x_n) \phi(x)^T \quad (1.72)$$

where \mathbf{I} is the unit matrix, and we have defined the vector $\phi(x)$ with elements $\phi_i(x) = x^i$ for $i = 0, \dots, M$.

We see that the variance, as well as the mean, of the predictive distribution in (1.69) is dependent on x . The first term in (1.71) represents the uncertainty in the predicted value of t due to the noise on the target variables and was expressed already in the maximum likelihood predictive distribution (1.64) through β_{ML}^{-1} . However, the second term arises from the uncertainty in the parameters \mathbf{w} and is a consequence of the Bayesian treatment. The predictive distribution for the synthetic sinusoidal regression problem is illustrated in Figure 1.17.

Figure 1.17 The predictive distribution resulting from a Bayesian treatment of polynomial curve fitting using an $M = 9$ polynomial, with the fixed parameters $\alpha = 5 \times 10^{-3}$ and $\beta = 11.1$ (corresponding to the known noise variance), in which the red curve denotes the mean of the predictive distribution and the red region corresponds to ± 1 standard deviation around the mean.



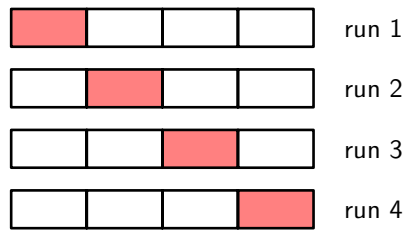
1.3. Model Selection

In our example of polynomial curve fitting using least squares, we saw that there was an optimal order of polynomial that gave the best generalization. The order of the polynomial controls the number of free parameters in the model and thereby governs the model complexity. With regularized least squares, the regularization coefficient λ also controls the effective complexity of the model, whereas for more complex models, such as mixture distributions or neural networks there may be multiple parameters governing complexity. In a practical application, we need to determine the values of such parameters, and the principal objective in doing so is usually to achieve the best predictive performance on new data. Furthermore, as well as finding the appropriate values for complexity parameters within a given model, we may wish to consider a range of different types of model in order to find the best one for our particular application.

We have already seen that, in the maximum likelihood approach, the performance on the training set is not a good indicator of predictive performance on unseen data due to the problem of over-fitting. If data is plentiful, then one approach is simply to use some of the available data to train a range of models, or a given model with a range of values for its complexity parameters, and then to compare them on independent data, sometimes called a *validation set*, and select the one having the best predictive performance. If the model design is iterated many times using a limited size data set, then some over-fitting to the validation data can occur and so it may be necessary to keep aside a third *test set* on which the performance of the selected model is finally evaluated.

In many applications, however, the supply of data for training and testing will be limited, and in order to build good models, we wish to use as much of the available data as possible for training. However, if the validation set is small, it will give a relatively noisy estimate of predictive performance. One solution to this dilemma is to use *cross-validation*, which is illustrated in Figure 1.18. This allows a proportion $(S - 1)/S$ of the available data to be used for training while making use of all of the

Figure 1.18 The technique of S -fold cross-validation, illustrated here for the case of $S = 4$, involves taking the available data and partitioning it into S groups (in the simplest case these are of equal size). Then $S - 1$ of the groups are used to train a set of models that are then evaluated on the remaining group. This procedure is then repeated for all S possible choices for the held-out group, indicated here by the red blocks, and the performance scores from the S runs are then averaged.



data to assess performance. When data is particularly scarce, it may be appropriate to consider the case $S = N$, where N is the total number of data points, which gives the *leave-one-out* technique.

One major drawback of cross-validation is that the number of training runs that must be performed is increased by a factor of S , and this can prove problematic for models in which the training is itself *computationally expensive*. A further problem with techniques such as cross-validation that use separate data to assess performance is that we might have multiple complexity parameters for a single model (for instance, there might be several regularization parameters). Exploring combinations of settings for such parameters could, in the worst case, require a number of training runs that is exponential in the number of parameters. Clearly, we need a better approach. Ideally, this should rely only on the training data and should allow multiple hyperparameters and model types to be compared in a single training run. We therefore need to find a measure of performance which depends only on the training data and which does not suffer from bias due to over-fitting.

Historically various ‘*information criteria*’ have been proposed that attempt to correct for the bias of maximum likelihood by the addition of a penalty term to compensate for the over-fitting of more complex models. For example, the *Akaike information criterion*, or AIC (Akaike, 1974), chooses the model for which the quantity

$$\ln p(\mathcal{D}|\mathbf{w}_{\text{ML}}) - M \quad (1.73)$$

is largest. Here $p(\mathcal{D}|\mathbf{w}_{\text{ML}})$ is the best-fit log likelihood, and M is the number of *adjustable parameters in the model*. A variant of this quantity, called the *Bayesian information criterion*, or *BIC*, will be discussed in Section 4.4.1. Such criteria do not take account of the uncertainty in the model parameters, however, and in practice they tend to favour overly simple models. We therefore turn in Section 3.4 to a fully Bayesian approach where we shall *see how complexity penalties arise in a natural and principled way*.

1.4. The Curse of Dimensionality

In the polynomial curve fitting example we had just one input variable x . For practical applications of pattern recognition, however, we will have to deal with spaces

Figure 1.19 Scatter plot of the oil flow data for input variables x_6 and x_7 , in which red denotes the ‘homogeneous’ class, green denotes the ‘annular’ class, and blue denotes the ‘laminar’ class. Our goal is to classify the new test point denoted by ‘ \times ’.

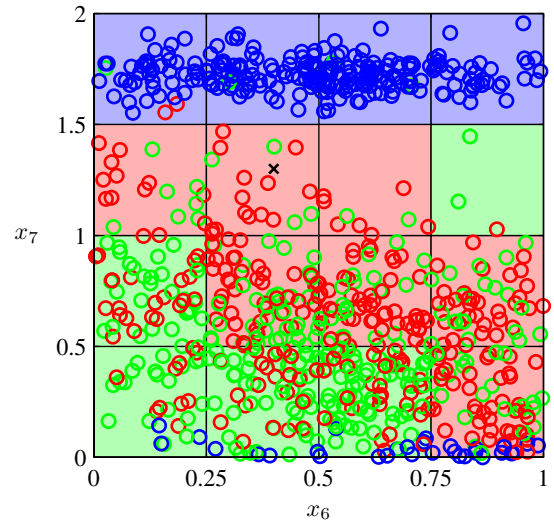


of high dimensionality comprising many input variables. As we now discuss, this poses some serious challenges and is an important factor influencing the design of pattern recognition techniques.

In order to illustrate the problem we consider a synthetically generated data set representing measurements taken from a pipeline containing a mixture of oil, water, and gas (Bishop and James, 1993). These three materials can be present in one of three different geometrical configurations known as ‘homogenous’, ‘annular’, and ‘laminar’, and the fractions of the three materials can also vary. Each data point comprises a 12-dimensional input vector consisting of measurements taken with gamma ray densitometers that measure the attenuation of gamma rays passing along narrow beams through the pipe. This data set is described in detail in Appendix A. Figure 1.19 shows 100 points from this data set on a plot showing two of the measurements x_6 and x_7 (the remaining ten input values are ignored for the purposes of this illustration). Each data point is labelled according to which of the three geometrical classes it belongs to, and our goal is to use this data as a training set in order to be able to classify a new observation (x_6, x_7) , such as the one denoted by the cross in Figure 1.19. We observe that the cross is surrounded by numerous red points, and so we might suppose that it belongs to the red class. However, there are also plenty of green points nearby, so we might think that it could instead belong to the green class. It seems unlikely that it belongs to the blue class. The intuition here is that the identity of the cross should be determined more strongly by nearby points from the training set and less strongly by more distant points. In fact, this intuition turns out to be reasonable and will be discussed more fully in later chapters.

How can we turn this intuition into a learning algorithm? One very simple approach would be to divide the input space into regular cells, as indicated in Figure 1.20. When we are given a test point and we wish to predict its class, we first decide which cell it belongs to, and we then find all of the training data points that

Figure 1.20 Illustration of a simple approach to the solution of a classification problem in which the input space is divided into cells and any new test point is assigned to the class that has a majority number of representatives in the same cell as the test point. As we shall see shortly, this simplistic approach has some severe shortcomings.



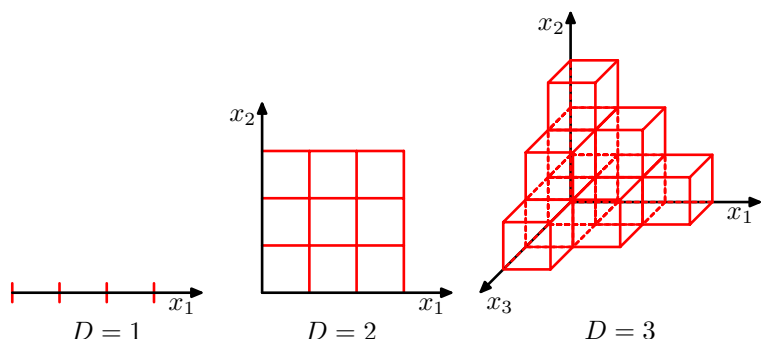
fall in the same cell. The identity of the test point is predicted as being the same as the class having the largest number of training points in the same cell as the test point (with ties being broken at random).

There are numerous problems with this naive approach, but one of the most severe becomes apparent when we consider its extension to problems having larger numbers of input variables, corresponding to input spaces of higher dimensionality. The origin of the problem is illustrated in Figure 1.21, which shows that, if we divide a region of a space into regular cells, then the number of such cells grows exponentially with the dimensionality of the space. The problem with an exponentially large number of cells is that we would need an exponentially large quantity of training data in order to ensure that the cells are not empty. Clearly, we have no hope of applying such a technique in a space of more than a few variables, and so we need to find a more sophisticated approach.

We can gain further insight into the problems of high-dimensional spaces by returning to the example of polynomial curve fitting and considering how we would

Section 1.1

Figure 1.21 Illustration of the curse of dimensionality, showing how the number of regions of a regular grid grows exponentially with the dimensionality D of the space. For clarity, only a subset of the cubical regions are shown for $D = 3$.



extend this approach to deal with input spaces having several variables. If we have D input variables, then a general polynomial with coefficients up to order 3 would take the form

$$y(\mathbf{x}, \mathbf{w}) = w_0 + \sum_{i=1}^D w_i x_i + \sum_{i=1}^D \sum_{j=1}^D w_{ij} x_i x_j + \sum_{i=1}^D \sum_{j=1}^D \sum_{k=1}^D w_{ijk} x_i x_j x_k. \quad (1.74)$$

As D increases, so the number of independent coefficients (not all of the coefficients are independent due to interchange symmetries amongst the x variables) grows proportionally to D^3 . In practice, to capture complex dependencies in the data, we may need to use a higher-order polynomial. For a polynomial of order M , the growth in the number of coefficients is like D^M . Although this is now a power law growth, rather than an exponential growth, it still points to the method becoming rapidly unwieldy and of limited practical utility.

Exercise 1.16

Our geometrical intuitions, formed through a life spent in a space of three dimensions, can fail badly when we consider spaces of higher dimensionality. As a simple example, consider a sphere of radius $r = 1$ in a space of D dimensions, and ask what is the fraction of the volume of the sphere that lies between radius $r = 1 - \epsilon$ and $r = 1$. We can evaluate this fraction by noting that the volume of a sphere of radius r in D dimensions must scale as r^D , and so we write

$$V_D(r) = K_D r^D \quad (1.75)$$

Exercise 1.18

where the constant K_D depends only on D . Thus the required fraction is given by

$$\frac{V_D(1) - V_D(1 - \epsilon)}{V_D(1)} = 1 - (1 - \epsilon)^D \quad (1.76)$$

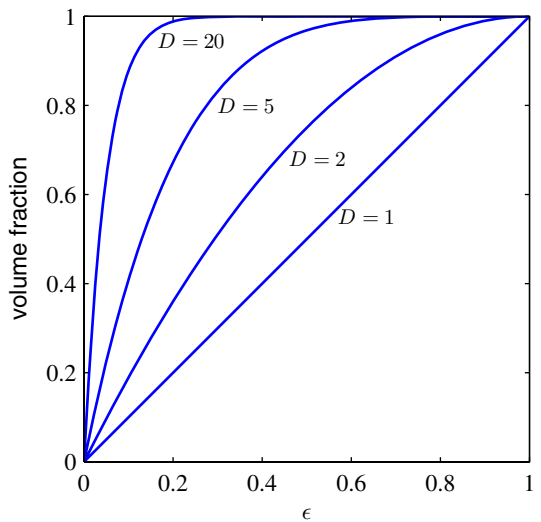
which is plotted as a function of ϵ for various values of D in Figure 1.22. We see that, for large D , this fraction tends to 1 even for small values of ϵ . **Thus, in spaces of high dimensionality, most of the volume of a sphere is concentrated in a thin shell near the surface!**

Exercise 1.20

As a further example, of direct relevance to pattern recognition, consider the behaviour of a Gaussian distribution in a high-dimensional space. If we transform from Cartesian to polar coordinates, and then integrate out the directional variables, we obtain an expression for the density $p(r)$ as a function of radius r from the origin. Thus $p(r)\delta r$ is the probability mass inside a thin shell of thickness δr located at radius r . This distribution is plotted, for various values of D , in Figure 1.23, and we see that for large D the probability mass of the Gaussian is concentrated in a thin shell.

The severe difficulty that can arise in spaces of many dimensions is sometimes called the **curse of dimensionality** (Bellman, 1961). In this book, we shall make extensive use of illustrative examples involving input spaces of one or two dimensions, because this makes it particularly easy to illustrate the techniques graphically. The reader should be warned, however, that not all intuitions developed in spaces of low dimensionality will generalize to spaces of many dimensions.

Figure 1.22 Plot of the fraction of the volume of a sphere lying in the range $r = 1 - \epsilon$ to $r = 1$ for various values of the dimensionality D .



Although the curse of dimensionality certainly raises important issues for pattern recognition applications, it does not prevent us from finding effective techniques applicable to high-dimensional spaces. The reasons for this are twofold. First, real data will often be confined to a region of the space having lower effective dimensionality, and in particular the directions over which important variations in the target variables occur may be so confined. Second, real data will typically exhibit some smoothness properties (at least locally) so that for the most part small changes in the input variables will produce small changes in the target variables, and so we can exploit local interpolation-like techniques to allow us to make predictions of the target variables for new values of the input variables. Successful pattern recognition techniques exploit one or both of these properties. Consider, for example, an application in manufacturing in which images are captured of identical planar objects on a conveyor belt, in which the goal is to determine their orientation. Each image is a point

Figure 1.23 Plot of the probability density with respect to radius r of a Gaussian distribution for various values of the dimensionality D . In a high-dimensional space, most of the probability mass of a Gaussian is located within a thin shell at a specific radius.



in a high-dimensional space whose dimensionality is determined by the number of pixels. Because the objects can occur at different positions within the image and in different orientations, there are three degrees of freedom of variability between images, and a set of images will live on a three dimensional *manifold* embedded within the high-dimensional space. Due to the complex relationships between the object position or orientation and the pixel intensities, this manifold will be highly nonlinear. If the goal is to learn a model that can take an input image and output the orientation of the object irrespective of its position, then there is only one degree of freedom of variability within the manifold that is significant.

1.5. Decision Theory

We have seen in Section 1.2 how probability theory provides us with a consistent mathematical framework for quantifying and manipulating uncertainty. Here we turn to a discussion of decision theory that, when combined with probability theory, allows us to make optimal decisions in situations involving uncertainty such as those encountered in pattern recognition.

Suppose we have an input vector \mathbf{x} together with a corresponding vector \mathbf{t} of target variables, and our goal is to predict \mathbf{t} given a new value for \mathbf{x} . For regression problems, \mathbf{t} will comprise continuous variables, whereas for classification problems \mathbf{t} will represent class labels. The joint probability distribution $p(\mathbf{x}, \mathbf{t})$ provides a complete summary of the uncertainty associated with these variables. Determination of $p(\mathbf{x}, \mathbf{t})$ from a set of training data is an example of *inference* and is typically a very difficult problem whose solution forms the subject of much of this book. In a practical application, however, we must often make a specific prediction for the value of \mathbf{t} , or more generally take a specific action based on our understanding of the values \mathbf{t} is likely to take, and this aspect is the subject of decision theory.

Consider, for example, a medical diagnosis problem in which we have taken an X-ray image of a patient, and we wish to determine whether the patient has cancer or not. In this case, the input vector \mathbf{x} is the set of pixel intensities in the image, and output variable t will represent the presence of cancer, which we denote by the class C_1 , or the absence of cancer, which we denote by the class C_2 . We might, for instance, choose t to be a binary variable such that $t = 0$ corresponds to class C_1 and $t = 1$ corresponds to class C_2 . We shall see later that this choice of label values is particularly convenient for probabilistic models. The general inference problem then involves determining the joint distribution $p(\mathbf{x}, C_k)$, or equivalently $p(\mathbf{x}, t)$, which gives us the most complete probabilistic description of the situation. Although this can be a very useful and informative quantity, in the end we must decide either to give treatment to the patient or not, and we would like this choice to be optimal in some appropriate sense (Duda and Hart, 1973). This is the *decision* step, and it is the subject of decision theory to tell us how to make optimal decisions given the appropriate probabilities. We shall see that the decision stage is generally very simple, even trivial, once we have solved the inference problem.

Here we give an introduction to the key ideas of decision theory as required for

the rest of the book. Further background, as well as more detailed accounts, can be found in Berger (1985) and Bather (2000).

Before giving a more detailed analysis, let us first consider informally how we might expect probabilities to play a role in making decisions. When we obtain the X-ray image \mathbf{x} for a new patient, our goal is to decide which of the two classes to assign to the image. We are interested in the probabilities of the two classes given the image, which are given by $p(\mathcal{C}_k|\mathbf{x})$. Using Bayes' theorem, these probabilities can be expressed in the form

$$p(\mathcal{C}_k|\mathbf{x}) = \frac{p(\mathbf{x}|\mathcal{C}_k)p(\mathcal{C}_k)}{p(\mathbf{x})}. \quad (1.77)$$

Note that any of the quantities appearing in Bayes' theorem can be obtained from the joint distribution $p(\mathbf{x}, \mathcal{C}_k)$ by either marginalizing or conditioning with respect to the appropriate variables. We can now interpret $p(\mathcal{C}_k)$ as the prior probability for the class \mathcal{C}_k , and $p(\mathcal{C}_k|\mathbf{x})$ as the corresponding posterior probability. Thus $p(\mathcal{C}_1)$ represents the probability that a person has cancer, before we take the X-ray measurement. Similarly, $p(\mathcal{C}_1|\mathbf{x})$ is the corresponding probability, revised using Bayes' theorem in light of the information contained in the X-ray. If our aim is to minimize the chance of assigning \mathbf{x} to the wrong class, then intuitively we would choose the class having the higher posterior probability. We now show that this intuition is correct, and we also discuss more general criteria for making decisions.

1.5.1 Minimizing the misclassification rate

Suppose that our goal is simply to make as few misclassifications as possible. We need a rule that assigns each value of \mathbf{x} to one of the available classes. Such a rule will divide the input space into regions \mathcal{R}_k called *decision regions*, one for each class, such that all points in \mathcal{R}_k are assigned to class \mathcal{C}_k . The boundaries between decision regions are called *decision boundaries* or *decision surfaces*. Note that each decision region need not be contiguous but could comprise some number of disjoint regions. We shall encounter examples of decision boundaries and decision regions in later chapters. In order to find the optimal decision rule, consider first of all the case of two classes, as in the cancer problem for instance. A mistake occurs when an input vector belonging to class \mathcal{C}_1 is assigned to class \mathcal{C}_2 or vice versa. The probability of this occurring is given by

$$\begin{aligned} p(\text{mistake}) &= p(\mathbf{x} \in \mathcal{R}_1, \mathcal{C}_2) + p(\mathbf{x} \in \mathcal{R}_2, \mathcal{C}_1) \\ &= \int_{\mathcal{R}_1} p(\mathbf{x}, \mathcal{C}_2) d\mathbf{x} + \int_{\mathcal{R}_2} p(\mathbf{x}, \mathcal{C}_1) d\mathbf{x}. \end{aligned} \quad (1.78)$$

We are free to choose the decision rule that assigns each point \mathbf{x} to one of the two classes. Clearly to minimize $p(\text{mistake})$ we should arrange that each \mathbf{x} is assigned to whichever class has the smaller value of the integrand in (1.78). Thus, if $p(\mathbf{x}, \mathcal{C}_1) > p(\mathbf{x}, \mathcal{C}_2)$ for a given value of \mathbf{x} , then we should assign that \mathbf{x} to class \mathcal{C}_1 . From the product rule of probability we have $p(\mathbf{x}, \mathcal{C}_k) = p(\mathcal{C}_k|\mathbf{x})p(\mathbf{x})$. Because the factor $p(\mathbf{x})$ is common to both terms, we can restate this result as saying that the minimum

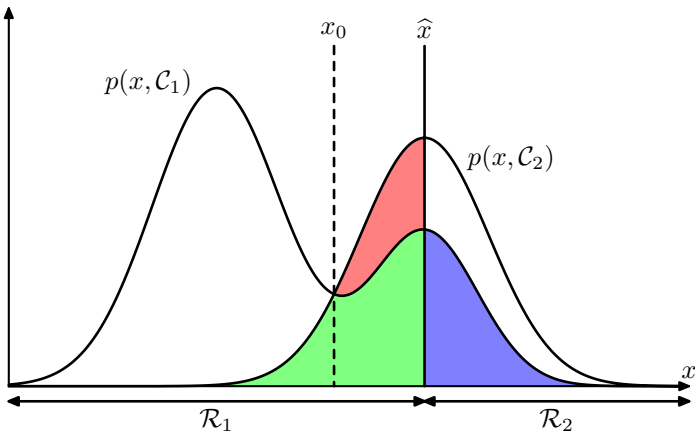


Figure 1.24 Schematic illustration of the joint probabilities $p(x, \mathcal{C}_k)$ for each of two classes plotted against x , together with the decision boundary $x = \hat{x}$. Values of $x \geq \hat{x}$ are classified as class \mathcal{C}_2 and hence belong to decision region \mathcal{R}_2 , whereas points $x < \hat{x}$ are classified as \mathcal{C}_1 and belong to \mathcal{R}_1 . Errors arise from the blue, green, and red regions, so that for $x < \hat{x}$ the errors are due to points from class \mathcal{C}_2 being misclassified as \mathcal{C}_1 (represented by the sum of the red and green regions), and conversely for points in the region $x \geq \hat{x}$ the errors are due to points from class \mathcal{C}_1 being misclassified as \mathcal{C}_2 (represented by the blue region). As we vary the location \hat{x} of the decision boundary, the combined areas of the blue and green regions remains constant, whereas the size of the red region varies. The optimal choice for \hat{x} is where the curves for $p(x, \mathcal{C}_1)$ and $p(x, \mathcal{C}_2)$ cross, corresponding to $\hat{x} = x_0$, because in this case the red region disappears. This is equivalent to the minimum misclassification rate decision rule, which assigns each value of x to the class having the higher posterior probability $p(\mathcal{C}_k|x)$.

probability of making a mistake is obtained if each value of x is assigned to the class for which the posterior probability $p(\mathcal{C}_k|x)$ is largest. This result is illustrated for two classes, and a single input variable x , in Figure 1.24.

For the more general case of K classes, it is slightly easier to maximize the probability of being correct, which is given by

$$\begin{aligned} p(\text{correct}) &= \sum_{k=1}^K p(\mathbf{x} \in \mathcal{R}_k, \mathcal{C}_k) \\ &= \sum_{k=1}^K \int_{\mathcal{R}_k} p(\mathbf{x}, \mathcal{C}_k) d\mathbf{x} \end{aligned} \quad (1.79)$$

which is maximized when the regions \mathcal{R}_k are chosen such that each \mathbf{x} is assigned to the class for which $p(\mathbf{x}, \mathcal{C}_k)$ is largest. Again, using the product rule $p(\mathbf{x}, \mathcal{C}_k) = p(\mathcal{C}_k|\mathbf{x})p(\mathbf{x})$, and noting that the factor of $p(\mathbf{x})$ is common to all terms, we see that each \mathbf{x} should be assigned to the class having the largest posterior probability $p(\mathcal{C}_k|\mathbf{x})$.

Figure 1.25 An example of a loss matrix with elements L_{kj} for the cancer treatment problem. The rows correspond to the true class, whereas the columns correspond to the assignment of class made by our decision criterion.

$$\begin{array}{cc} & \text{cancer} \quad \text{normal} \\ \text{cancer} & \left(\begin{array}{cc} 0 & 1000 \\ 1 & 0 \end{array} \right) \\ \text{normal} & \end{array}$$

1.5.2 Minimizing the expected loss

For many applications, our objective will be more complex than simply minimizing the number of misclassifications. Let us consider again the medical diagnosis problem. We note that, if a patient who does not have cancer is incorrectly diagnosed as having cancer, the consequences may be some patient distress plus the need for further investigations. Conversely, if a patient with cancer is diagnosed as healthy, the result may be premature death due to lack of treatment. Thus the consequences of these two types of mistake can be dramatically different. It would clearly be better to make fewer mistakes of the second kind, even if this was at the expense of making more mistakes of the first kind.

We can formalize such issues through the introduction of a *loss function*, also called a *cost function*, which is a single, overall measure of loss incurred in taking any of the available decisions or actions. Our goal is then to minimize the total loss incurred. Note that some authors consider instead a *utility function*, whose value they aim to maximize. These are equivalent concepts if we take the utility to be simply the negative of the loss, and throughout this text we shall use the loss function convention. Suppose that, for a new value of \mathbf{x} , the true class is \mathcal{C}_k and that we assign \mathbf{x} to class \mathcal{C}_j (where j may or may not be equal to k). In so doing, we incur some level of loss that we denote by L_{kj} , which we can view as the k, j element of a *loss matrix*. For instance, in our cancer example, we might have a loss matrix of the form shown in Figure 1.25. This particular loss matrix says that there is no loss incurred if the correct decision is made, there is a loss of 1 if a healthy patient is diagnosed as having cancer, whereas there is a loss of 1000 if a patient having cancer is diagnosed as healthy.

The optimal solution is the one which minimizes the loss function. However, the loss function depends on the true class, which is unknown. For a given input vector \mathbf{x} , our uncertainty in the true class is expressed through the joint probability distribution $p(\mathbf{x}, \mathcal{C}_k)$ and so we seek instead to minimize the average loss, where the average is computed with respect to this distribution, which is given by

$$\mathbb{E}[L] = \sum_k \sum_j \int_{\mathcal{R}_j} L_{kj} p(\mathbf{x}, \mathcal{C}_k) d\mathbf{x}. \quad (1.80)$$

Each \mathbf{x} can be assigned independently to one of the decision regions \mathcal{R}_j . Our goal is to choose the regions \mathcal{R}_j in order to minimize the expected loss (1.80), which implies that for each \mathbf{x} we should minimize $\sum_k L_{kj} p(\mathbf{x}, \mathcal{C}_k)$. As before, we can use the product rule $p(\mathbf{x}, \mathcal{C}_k) = p(\mathcal{C}_k | \mathbf{x}) p(\mathbf{x})$ to eliminate the common factor of $p(\mathbf{x})$. Thus the decision rule that minimizes the expected loss is the one that assigns each

Figure 1.26 Illustration of the reject option. Inputs x such that the larger of the two posterior probabilities is less than or equal to some threshold θ will be rejected.



new \mathbf{x} to the class j for which the quantity

$$\sum_k L_{kj} p(\mathcal{C}_k | \mathbf{x}) \quad (1.81)$$

is a minimum. This is clearly trivial to do, once we know the posterior class probabilities $p(\mathcal{C}_k | \mathbf{x})$.

1.5.3 The reject option

We have seen that classification errors arise from the regions of input space where the largest of the posterior probabilities $p(\mathcal{C}_k | \mathbf{x})$ is significantly less than unity, or equivalently where the joint distributions $p(\mathbf{x}, \mathcal{C}_k)$ have comparable values. These are the regions where we are relatively uncertain about class membership. In some applications, it will be appropriate to avoid making decisions on the difficult cases in anticipation of a lower error rate on those examples for which a classification decision is made. This is known as the *reject option*. For example, in our hypothetical medical illustration, it may be appropriate to use an automatic system to classify those X-ray images for which there is little doubt as to the correct class, while leaving a human expert to classify the more ambiguous cases. We can achieve this by introducing a threshold θ and rejecting those inputs \mathbf{x} for which the largest of the posterior probabilities $p(\mathcal{C}_k | \mathbf{x})$ is less than or equal to θ . This is illustrated for the case of two classes, and a single continuous input variable x , in Figure 1.26. Note that setting $\theta = 1$ will ensure that all examples are rejected, whereas if there are K classes then setting $\theta < 1/K$ will ensure that no examples are rejected. Thus the fraction of examples that get rejected is controlled by the value of θ .

We can easily extend the reject criterion to minimize the expected loss, when a loss matrix is given, taking account of the loss incurred when a reject decision is made.

Exercise 1.24

1.5.4 Inference and decision

We have broken the classification problem down into two separate stages, the *inference stage* in which we use training data to learn a model for $p(\mathcal{C}_k | \mathbf{x})$, and the

subsequent *decision stage* in which we use these posterior probabilities to make optimal class assignments. An alternative possibility would be to solve both problems together and simply learn a function that maps inputs \mathbf{x} directly into decisions. Such a function is called a *discriminant function*.

In fact, we can identify three distinct approaches to solving decision problems, all of which have been used in practical applications. These are given, in decreasing order of complexity, by:

- (a) First solve the inference problem of determining the class-conditional densities $p(\mathbf{x}|\mathcal{C}_k)$ for each class \mathcal{C}_k individually. Also separately infer the prior class probabilities $p(\mathcal{C}_k)$. Then use Bayes' theorem in the form

$$p(\mathcal{C}_k|\mathbf{x}) = \frac{p(\mathbf{x}|\mathcal{C}_k)p(\mathcal{C}_k)}{p(\mathbf{x})} \quad (1.82)$$

to find the posterior class probabilities $p(\mathcal{C}_k|\mathbf{x})$. As usual, the denominator in Bayes' theorem can be found in terms of the quantities appearing in the numerator, because

$$p(\mathbf{x}) = \sum_k p(\mathbf{x}|\mathcal{C}_k)p(\mathcal{C}_k). \quad (1.83)$$

Equivalently, we can model the joint distribution $p(\mathbf{x}, \mathcal{C}_k)$ directly and then normalize to obtain the posterior probabilities. Having found the posterior probabilities, we use decision theory to determine class membership for each new input \mathbf{x} . Approaches that explicitly or implicitly model the distribution of inputs as well as outputs are known as *generative models*, because by sampling from them it is possible to generate synthetic data points in the input space.

- (b) First solve the inference problem of determining the posterior class probabilities $p(\mathcal{C}_k|\mathbf{x})$, and then subsequently use decision theory to assign each new \mathbf{x} to one of the classes. Approaches that model the posterior probabilities directly are called *discriminative models*.
- (c) Find a function $f(\mathbf{x})$, called a discriminant function, which maps each input \mathbf{x} directly onto a class label. For instance, in the case of two-class problems, $f(\cdot)$ might be binary valued and such that $f = 0$ represents class \mathcal{C}_1 and $f = 1$ represents class \mathcal{C}_2 . In this case, probabilities play no role.

Let us consider the relative merits of these three alternatives. Approach (a) is the most demanding because it involves finding the joint distribution over both \mathbf{x} and \mathcal{C}_k . For many applications, \mathbf{x} will have high dimensionality, and consequently we may need a large training set in order to be able to determine the class-conditional densities to reasonable accuracy. Note that the class priors $p(\mathcal{C}_k)$ can often be estimated simply from the fractions of the training set data points in each of the classes. One advantage of approach (a), however, is that it also allows the marginal density of data $p(\mathbf{x})$ to be determined from (1.83). This can be useful for detecting new data points that have low probability under the model and for which the predictions may

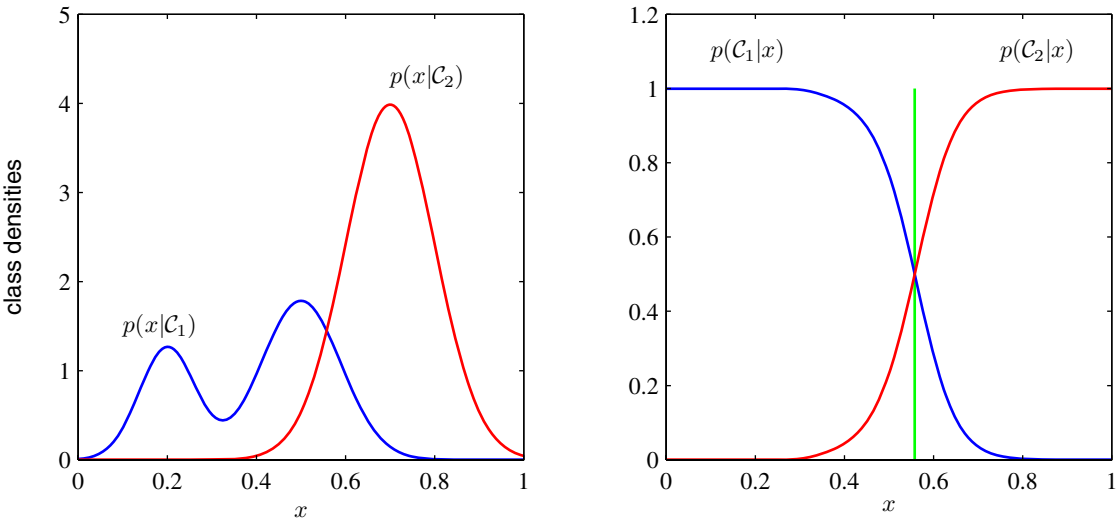


Figure 1.27 Example of the class-conditional densities for two classes having a single input variable x (left plot) together with the corresponding posterior probabilities (right plot). Note that the left-hand mode of the class-conditional density $p(x|\mathcal{C}_1)$, shown in blue on the left plot, has no effect on the posterior probabilities. The vertical green line in the right plot shows the decision boundary in x that gives the minimum misclassification rate.

be of low accuracy, which is known as *outlier detection* or *novelty detection* (Bishop, 1994; Tarassenko, 1995).

However, if we only wish to make classification decisions, then it can be wasteful of computational resources, and excessively demanding of data, to find the joint distribution $p(\mathbf{x}, \mathcal{C}_k)$ when in fact we only really need the posterior probabilities $p(\mathcal{C}_k|\mathbf{x})$, which can be obtained directly through approach (b). Indeed, the class-conditional densities may contain a lot of structure that has little effect on the posterior probabilities, as illustrated in Figure 1.27. There has been much interest in exploring the relative merits of generative and discriminative approaches to machine learning, and in finding ways to combine them (Jebara, 2004; Lasserre *et al.*, 2006).

An even simpler approach is (c) in which we use the training data to find a discriminant function $f(\mathbf{x})$ that maps each \mathbf{x} directly onto a class label, thereby combining the inference and decision stages into a single learning problem. In the example of Figure 1.27, this would correspond to finding the value of x shown by the vertical green line, because this is the decision boundary giving the minimum probability of misclassification.

With option (c), however, we no longer have access to the posterior probabilities $p(\mathcal{C}_k|\mathbf{x})$. There are many powerful reasons for wanting to compute the posterior probabilities, even if we subsequently use them to make decisions. These include:

Minimizing risk. Consider a problem in which the elements of the loss matrix are subjected to revision from time to time (such as might occur in a financial

application). If we know the posterior probabilities, we can trivially revise the minimum risk decision criterion by modifying (1.81) appropriately. If we have only a discriminant function, then any change to the loss matrix would require that we return to the training data and solve the classification problem afresh.

Reject option. Posterior probabilities allow us to determine a rejection criterion that will minimize the misclassification rate, or more generally the expected loss, for a given fraction of rejected data points.

Compensating for class priors. Consider our medical X-ray problem again, and suppose that we have collected a large number of X-ray images from the general population for use as training data in order to build an automated screening system. Because cancer is rare amongst the general population, we might find that, say, only 1 in every 1,000 examples corresponds to the presence of cancer. If we used such a data set to train an adaptive model, we could run into severe difficulties due to the small proportion of the cancer class. For instance, a classifier that assigned every point to the normal class would already achieve 99.9% accuracy and it would be difficult to avoid this trivial solution. Also, even a large data set will contain very few examples of X-ray images corresponding to cancer, and so the learning algorithm will not be exposed to a broad range of examples of such images and hence is not likely to generalize well. A balanced data set in which we have selected equal numbers of examples from each of the classes would allow us to find a more accurate model. However, we then have to compensate for the effects of our modifications to the training data. Suppose we have used such a modified data set and found models for the posterior probabilities. From Bayes' theorem (1.82), we see that the posterior probabilities are proportional to the prior probabilities, which we can interpret as the fractions of points in each class. We can therefore simply take the posterior probabilities obtained from our artificially balanced data set and first divide by the class fractions in that data set and then multiply by the class fractions in the population to which we wish to apply the model. Finally, we need to normalize to ensure that the new posterior probabilities sum to one. Note that this procedure cannot be applied if we have learned a discriminant function directly instead of determining posterior probabilities.

Combining models. For complex applications, we may wish to break the problem into a number of smaller subproblems each of which can be tackled by a separate module. For example, in our hypothetical medical diagnosis problem, we may have information available from, say, blood tests as well as X-ray images. Rather than combine all of this heterogeneous information into one huge input space, it may be more effective to build one system to interpret the X-ray images and a different one to interpret the blood data. As long as each of the two models gives posterior probabilities for the classes, we can combine the outputs systematically using the rules of probability. One simple way to do this is to assume that, for each class separately, the distributions of inputs for the X-ray images, denoted by \mathbf{x}_I , and the blood data, denoted by \mathbf{x}_B , are

independent, so that

$$p(\mathbf{x}_I, \mathbf{x}_B | \mathcal{C}_k) = p(\mathbf{x}_I | \mathcal{C}_k)p(\mathbf{x}_B | \mathcal{C}_k). \quad (1.84)$$

Section 8.2

This is an example of *conditional independence* property, because the independence holds when the distribution is conditioned on the class \mathcal{C}_k . The posterior probability, given both the X-ray and blood data, is then given by

$$\begin{aligned} p(\mathcal{C}_k | \mathbf{x}_I, \mathbf{x}_B) &\propto p(\mathbf{x}_I, \mathbf{x}_B | \mathcal{C}_k)p(\mathcal{C}_k) \\ &\propto p(\mathbf{x}_I | \mathcal{C}_k)p(\mathbf{x}_B | \mathcal{C}_k)p(\mathcal{C}_k) \\ &\propto \frac{p(\mathcal{C}_k | \mathbf{x}_I)p(\mathcal{C}_k | \mathbf{x}_B)}{p(\mathcal{C}_k)} \end{aligned} \quad (1.85)$$

Section 8.2.2

Thus we need the class prior probabilities $p(\mathcal{C}_k)$, which we can easily estimate from the fractions of data points in each class, and then we need to normalize the resulting posterior probabilities so they sum to one. The particular conditional independence assumption (1.84) is an example of the *naive Bayes model*. Note that the joint marginal distribution $p(\mathbf{x}_I, \mathbf{x}_B)$ will typically not factorize under this model. We shall see in later chapters how to construct models for combining data that do not require the conditional independence assumption (1.84).

1.5.5 Loss functions for regression

Section 1.1

So far, we have discussed decision theory in the context of classification problems. We now turn to the case of regression problems, such as the curve fitting example discussed earlier. The decision stage consists of choosing a specific estimate $y(\mathbf{x})$ of the value of t for each input \mathbf{x} . Suppose that in doing so, we incur a loss $L(t, y(\mathbf{x}))$. The average, or expected, loss is then given by

$$\mathbb{E}[L] = \iint L(t, y(\mathbf{x}))p(\mathbf{x}, t) d\mathbf{x} dt. \quad (1.86)$$

A common choice of loss function in regression problems is the squared loss given by $L(t, y(\mathbf{x})) = \{y(\mathbf{x}) - t\}^2$. In this case, the expected loss can be written

$$\mathbb{E}[L] = \iint \{y(\mathbf{x}) - t\}^2 p(\mathbf{x}, t) d\mathbf{x} dt. \quad (1.87)$$

Appendix D

Our goal is to choose $y(\mathbf{x})$ so as to minimize $\mathbb{E}[L]$. If we assume a completely flexible function $y(\mathbf{x})$, we can do this formally using the calculus of variations to give

$$\frac{\delta \mathbb{E}[L]}{\delta y(\mathbf{x})} = 2 \int \{y(\mathbf{x}) - t\} p(\mathbf{x}, t) dt = 0. \quad (1.88)$$

Solving for $y(\mathbf{x})$, and using the sum and product rules of probability, we obtain

$$y(\mathbf{x}) = \frac{\int tp(\mathbf{x}, t) dt}{p(\mathbf{x})} = \int tp(t|\mathbf{x}) dt = \mathbb{E}_t[t|\mathbf{x}] \quad (1.89)$$

Figure 1.28 The regression function $y(x)$, which minimizes the expected squared loss, is given by the mean of the conditional distribution $p(t|x)$.



which is the conditional average of t conditioned on \mathbf{x} and is known as the *regression function*. This result is illustrated in Figure 1.28. It can readily be extended to multiple target variables represented by the vector \mathbf{t} , in which case the optimal solution is the conditional average $\mathbf{y}(\mathbf{x}) = \mathbb{E}_t[\mathbf{t}|\mathbf{x}]$.

Exercise 1.25

We can also derive this result in a slightly different way, which will also shed light on the nature of the regression problem. Armed with the knowledge that the optimal solution is the conditional expectation, we can expand the square term as follows

$$\begin{aligned}\{y(\mathbf{x}) - t\}^2 &= \{y(\mathbf{x}) - \mathbb{E}[t|\mathbf{x}] + \mathbb{E}[t|\mathbf{x}] - t\}^2 \\ &= \{y(\mathbf{x}) - \mathbb{E}[t|\mathbf{x}]\}^2 + 2\{y(\mathbf{x}) - \mathbb{E}[t|\mathbf{x}]\}\{\mathbb{E}[t|\mathbf{x}] - t\} + \{\mathbb{E}[t|\mathbf{x}] - t\}^2\end{aligned}$$

where, to keep the notation uncluttered, we use $\mathbb{E}[t|\mathbf{x}]$ to denote $\mathbb{E}_t[t|\mathbf{x}]$. Substituting into the loss function and performing the integral over t , we see that the cross-term vanishes and we obtain an expression for the loss function in the form

$$\mathbb{E}[L] = \int \{y(\mathbf{x}) - \mathbb{E}[t|\mathbf{x}]\}^2 p(\mathbf{x}) d\mathbf{x} + \int \{\mathbb{E}[t|\mathbf{x}] - t\}^2 p(\mathbf{x}) d\mathbf{x}. \quad (1.90)$$

The function $y(\mathbf{x})$ we seek to determine enters only in the first term, which will be minimized when $y(\mathbf{x})$ is equal to $\mathbb{E}[t|\mathbf{x}]$, in which case this term will vanish. This is simply the result that we derived previously and that shows that the optimal least squares predictor is given by the conditional mean. The second term is the variance of the distribution of t , averaged over \mathbf{x} . It represents the intrinsic variability of the target data and can be regarded as noise. Because it is independent of $y(\mathbf{x})$, it represents the irreducible minimum value of the loss function.

As with the classification problem, we can either determine the appropriate probabilities and then use these to make optimal decisions, or we can build models that make decisions directly. Indeed, we can identify three distinct approaches to solving regression problems given, in order of decreasing complexity, by:

- (a) First solve the inference problem of determining the joint density $p(\mathbf{x}, t)$. Then normalize to find the conditional density $p(t|\mathbf{x})$, and finally marginalize to find the conditional mean given by (1.89).

(b) First solve the inference problem of determining the conditional density $p(t|\mathbf{x})$, and then subsequently marginalize to find the conditional mean given by (1.89).

(c) Find a regression function $y(\mathbf{x})$ directly from the training data.

The relative merits of these three approaches follow the same lines as for classification problems above.

The squared loss is not the only possible choice of loss function for regression. Indeed, there are situations in which squared loss can lead to very poor results and where we need to develop more sophisticated approaches. An important example concerns situations in which the conditional distribution $p(t|\mathbf{x})$ is multimodal, as often arises in the solution of inverse problems. Here we consider briefly one simple generalization of the squared loss, called the *Minkowski* loss, whose expectation is given by

$$\mathbb{E}[L_q] = \iint |y(\mathbf{x}) - t|^q p(\mathbf{x}, t) d\mathbf{x} dt \quad (1.91)$$

which reduces to the expected squared loss for $q = 2$. The function $|y - t|^q$ is plotted against $y - t$ for various values of q in Figure 1.29. The minimum of $\mathbb{E}[L_q]$ is given by the conditional mean for $q = 2$, the conditional median for $q = 1$, and the conditional mode for $q \rightarrow 0$.

Section 5.6

Exercise 1.27

1.6. Information Theory

In this chapter, we have discussed a variety of concepts from probability theory and decision theory that will form the foundations for much of the subsequent discussion in this book. We close this chapter by introducing some additional concepts from the field of information theory, which will also prove useful in our development of pattern recognition and machine learning techniques. Again, we shall focus only on the key concepts, and we refer the reader elsewhere for more detailed discussions (Viterbi and Omura, 1979; Cover and Thomas, 1991; MacKay, 2003).

We begin by considering a discrete random variable x and we ask how much information is received when we observe a specific value for this variable. The amount of information can be viewed as the ‘degree of surprise’ on learning the value of x . If we are told that a highly improbable event has just occurred, we will have received more information than if we were told that some very likely event has just occurred, and if we knew that the event was certain to happen we would receive no information. Our measure of information content will therefore depend on the probability distribution $p(x)$, and we therefore look for a quantity $h(x)$ that is a monotonic function of the probability $p(x)$ and that expresses the information content. The form of $h(\cdot)$ can be found by noting that if we have two events x and y that are unrelated, then the information gain from observing both of them should be the sum of the information gained from each of them separately, so that $h(x, y) = h(x) + h(y)$. Two unrelated events will be statistically independent and so $p(x, y) = p(x)p(y)$. From these two relationships, it is easily shown that $h(x)$ must be given by the logarithm of $p(x)$ and so we have

Exercise 1.28



Figure 1.29 Plots of the quantity $L_q = |y - t|^q$ for various values of q .

$$h(x) = -\log_2 p(x) \quad (1.92)$$

where the negative sign ensures that information is positive or zero. Note that low probability events x correspond to high information content. The choice of basis for the logarithm is arbitrary, and for the moment we shall adopt the convention prevalent in information theory of using logarithms to the base of 2. In this case, as we shall see shortly, the units of $h(x)$ are bits ('binary digits').

Now suppose that a sender wishes to transmit the value of a random variable to a receiver. The average amount of information that they transmit in the process is obtained by taking the expectation of (1.92) with respect to the distribution $p(x)$ and is given by

$$H[x] = - \sum_x p(x) \log_2 p(x). \quad (1.93)$$

This important quantity is called the *entropy* of the random variable x . Note that $\lim_{p \rightarrow 0} p \ln p = 0$ and so we shall take $p(x) \ln p(x) = 0$ whenever we encounter a value for x such that $p(x) = 0$.

So far we have given a rather heuristic motivation for the definition of informa-

tion (1.92) and the corresponding entropy (1.93). We now show that these definitions indeed possess useful properties. Consider a random variable x having 8 possible states, each of which is equally likely. In order to communicate the value of x to a receiver, we would need to transmit a message of length 3 bits. Notice that the entropy of this variable is given by

$$H[x] = -8 \times \frac{1}{8} \log_2 \frac{1}{8} = 3 \text{ bits.}$$

Now consider an example (Cover and Thomas, 1991) of a variable having 8 possible states $\{a, b, c, d, e, f, g, h\}$ for which the respective probabilities are given by $(\frac{1}{2}, \frac{1}{4}, \frac{1}{8}, \frac{1}{16}, \frac{1}{64}, \frac{1}{64}, \frac{1}{64}, \frac{1}{64})$. The entropy in this case is given by

$$H[x] = -\frac{1}{2} \log_2 \frac{1}{2} - \frac{1}{4} \log_2 \frac{1}{4} - \frac{1}{8} \log_2 \frac{1}{8} - \frac{1}{16} \log_2 \frac{1}{16} - \frac{4}{64} \log_2 \frac{1}{64} = 2 \text{ bits.}$$

We see that the nonuniform distribution has a smaller entropy than the uniform one, and we shall gain some insight into this shortly when we discuss the interpretation of entropy in terms of disorder. For the moment, let us consider how we would transmit the identity of the variable's state to a receiver. We could do this, as before, using a 3-bit number. However, we can take advantage of the nonuniform distribution by using shorter codes for the more probable events, at the expense of longer codes for the less probable events, in the hope of getting a shorter average code length. This can be done by representing the states $\{a, b, c, d, e, f, g, h\}$ using, for instance, the following set of code strings: 0, 10, 110, 1110, 111100, 111101, 111110, 111111. The average length of the code that has to be transmitted is then

$$\text{average code length} = \frac{1}{2} \times 1 + \frac{1}{4} \times 2 + \frac{1}{8} \times 3 + \frac{1}{16} \times 4 + 4 \times \frac{1}{64} \times 6 = 2 \text{ bits}$$

which again is the same as the entropy of the random variable. Note that shorter code strings cannot be used because it must be possible to disambiguate a concatenation of such strings into its component parts. For instance, 11001110 decodes uniquely into the state sequence c, a, d .

This relation between entropy and shortest coding length is a general one. The *noiseless coding theorem* (Shannon, 1948) states that the entropy is a lower bound on the number of bits needed to transmit the state of a random variable.

From now on, we shall switch to the use of natural logarithms in defining entropy, as this will provide a more convenient link with ideas elsewhere in this book. In this case, the entropy is measured in units of 'nats' instead of bits, which differ simply by a factor of $\ln 2$.

We have introduced the concept of entropy in terms of the average amount of information needed to specify the state of a random variable. In fact, the concept of entropy has much earlier origins in physics where it was introduced in the context of equilibrium thermodynamics and later given a deeper interpretation as a measure of disorder through developments in statistical mechanics. We can understand this alternative view of entropy by considering a set of N identical objects that are to be divided amongst a set of bins, such that there are n_i objects in the i^{th} bin. Consider

the number of different ways of allocating the objects to the bins. There are N ways to choose the first object, $(N - 1)$ ways to choose the second object, and so on, leading to a total of $N!$ ways to allocate all N objects to the bins, where $N!$ (pronounced ‘factorial N ’) denotes the product $N \times (N - 1) \times \dots \times 2 \times 1$. However, we don’t wish to distinguish between rearrangements of objects within each bin. In the i^{th} bin there are $n_i!$ ways of reordering the objects, and so the total number of ways of allocating the N objects to the bins is given by

$$W = \frac{N!}{\prod_i n_i!} \quad (1.94)$$

which is called the *multiplicity*. The entropy is then defined as the logarithm of the multiplicity scaled by an appropriate constant

$$H = \frac{1}{N} \ln W = \frac{1}{N} \ln N! - \frac{1}{N} \sum_i \ln n_i!. \quad (1.95)$$

We now consider the limit $N \rightarrow \infty$, in which the fractions n_i/N are held fixed, and apply Stirling’s approximation

$$\ln N! \simeq N \ln N - N \quad (1.96)$$

which gives

$$H = - \lim_{N \rightarrow \infty} \sum_i \left(\frac{n_i}{N} \right) \ln \left(\frac{n_i}{N} \right) = - \sum_i p_i \ln p_i \quad (1.97)$$

where we have used $\sum_i n_i = N$. Here $p_i = \lim_{N \rightarrow \infty} (n_i/N)$ is the probability of an object being assigned to the i^{th} bin. In physics terminology, the specific arrangements of objects in the bins is called a *microstate*, and the overall distribution of occupation numbers, expressed through the ratios n_i/N , is called a *macrostate*. The multiplicity W is also known as the *weight* of the macrostate.

We can interpret the bins as the states x_i of a discrete random variable X , where $p(X = x_i) = p_i$. The entropy of the random variable X is then

$$H[p] = - \sum_i p(x_i) \ln p(x_i). \quad (1.98)$$

Distributions $p(x_i)$ that are sharply peaked around a few values will have a relatively low entropy, whereas those that are spread more evenly across many values will have higher entropy, as illustrated in Figure 1.30. Because $0 \leq p_i \leq 1$, the entropy is nonnegative, and it will equal its minimum value of 0 when one of the $p_i = 1$ and all other $p_{j \neq i} = 0$. The maximum entropy configuration can be found by maximizing H using a Lagrange multiplier to enforce the normalization constraint on the probabilities. Thus we maximize

$$\tilde{H} = - \sum_i p(x_i) \ln p(x_i) + \lambda \left(\sum_i p(x_i) - 1 \right) \quad (1.99)$$



Figure 1.30 Histograms of two probability distributions over 30 bins illustrating the higher value of the entropy H for the broader distribution. The largest entropy would arise from a uniform distribution that would give $H = -\ln(1/30) = 3.40$.

from which we find that all of the $p(x_i)$ are equal and are given by $p(x_i) = 1/M$ where M is the total number of states x_i . The corresponding value of the entropy is then $H = \ln M$. This result can also be derived from Jensen's inequality (to be discussed shortly). To verify that the stationary point is indeed a maximum, we can evaluate the second derivative of the entropy, which gives

$$\frac{\partial \widetilde{H}}{\partial p(x_i) \partial p(x_j)} = -I_{ij} \frac{1}{p_i} \quad (1.100)$$

where I_{ij} are the elements of the identity matrix.

We can extend the definition of entropy to include distributions $p(x)$ over continuous variables x as follows. First divide x into bins of width Δ . Then, assuming $p(x)$ is continuous, the *mean value theorem* (Weisstein, 1999) tells us that, for each such bin, there must exist a value x_i such that

$$\int_{i\Delta}^{(i+1)\Delta} p(x) dx = p(x_i)\Delta. \quad (1.101)$$

We can now quantize the continuous variable x by assigning any value x to the value x_i whenever x falls in the i^{th} bin. The probability of observing the value x_i is then $p(x_i)\Delta$. This gives a discrete distribution for which the entropy takes the form

$$H_\Delta = - \sum_i p(x_i)\Delta \ln(p(x_i)\Delta) = - \sum_i p(x_i)\Delta \ln p(x_i) - \ln \Delta \quad (1.102)$$

where we have used $\sum_i p(x_i)\Delta = 1$, which follows from (1.101). We now omit the second term $-\ln \Delta$ on the right-hand side of (1.102) and then consider the limit

$\Delta \rightarrow 0$. The first term on the right-hand side of (1.102) will approach the integral of $p(x) \ln p(x)$ in this limit so that

$$\lim_{\Delta \rightarrow 0} \left\{ \sum_i p(x_i) \Delta \ln p(x_i) \right\} = - \int p(x) \ln p(x) dx \quad (1.103)$$

where the quantity on the right-hand side is called the *differential entropy*. We see that the discrete and continuous forms of the entropy differ by a quantity $\ln \Delta$, which diverges in the limit $\Delta \rightarrow 0$. This reflects the fact that to specify a continuous variable very precisely requires a large number of bits. For a density defined over multiple continuous variables, denoted collectively by the vector \mathbf{x} , the differential entropy is given by

$$H[\mathbf{x}] = - \int p(\mathbf{x}) \ln p(\mathbf{x}) d\mathbf{x}. \quad (1.104)$$

In the case of discrete distributions, we saw that the maximum entropy configuration corresponded to an equal distribution of probabilities across the possible states of the variable. Let us now consider the maximum entropy configuration for a continuous variable. In order for this maximum to be well defined, it will be necessary to constrain the first and second moments of $p(x)$ as well as preserving the normalization constraint. We therefore maximize the differential entropy with the



Ludwig Boltzmann
1844–1906

Ludwig Eduard Boltzmann was an Austrian physicist who created the field of statistical mechanics. Prior to Boltzmann, the concept of entropy was already known from classical thermodynamics where it quantifies the fact that when we take energy from a system, not all of that energy is typically available to do useful work. Boltzmann showed that the thermodynamic entropy S , a macroscopic quantity, could be related to the statistical properties at the microscopic level. This is expressed through the famous equation $S = k \ln W$ in which W represents the number of possible microstates in a macrostate, and $k \approx 1.38 \times 10^{-23}$ (in units of Joules per Kelvin) is known as Boltzmann's constant. Boltzmann's ideas were disputed by many scientists of the day. One difficulty they saw arose from the second law of thermo-

dynamics, which states that the entropy of a closed system tends to increase with time. By contrast, at the microscopic level the classical Newtonian equations of physics are reversible, and so they found it difficult to see how the latter could explain the former. They didn't fully appreciate Boltzmann's arguments, which were statistical in nature and which concluded not that entropy could never decrease over time but simply that with overwhelming probability it would generally increase. Boltzmann even had a long-running dispute with the editor of the leading German physics journal who refused to let him refer to atoms and molecules as anything other than convenient theoretical constructs. The continued attacks on his work lead to bouts of depression, and eventually he committed suicide. Shortly after Boltzmann's death, new experiments by Perrin on colloidal suspensions verified his theories and confirmed the value of the Boltzmann constant. The equation $S = k \ln W$ is carved on Boltzmann's tombstone.

three constraints

$$\int_{-\infty}^{\infty} p(x) dx = 1 \quad (1.105)$$

$$\int_{-\infty}^{\infty} xp(x) dx = \mu \quad (1.106)$$

$$\int_{-\infty}^{\infty} (x - \mu)^2 p(x) dx = \sigma^2. \quad (1.107)$$

Appendix E

The constrained maximization can be performed using Lagrange multipliers so that we maximize the following functional with respect to $p(x)$

$$\begin{aligned} & - \int_{-\infty}^{\infty} p(x) \ln p(x) dx + \lambda_1 \left(\int_{-\infty}^{\infty} p(x) dx - 1 \right) \\ & + \lambda_2 \left(\int_{-\infty}^{\infty} xp(x) dx - \mu \right) + \lambda_3 \left(\int_{-\infty}^{\infty} (x - \mu)^2 p(x) dx - \sigma^2 \right). \end{aligned}$$

Appendix D

Using the calculus of variations, we set the derivative of this functional to zero giving

$$p(x) = \exp \left\{ -1 + \lambda_1 + \lambda_2 x + \lambda_3 (x - \mu)^2 \right\}. \quad (1.108)$$

Exercise 1.34

The Lagrange multipliers can be found by back substitution of this result into the three constraint equations, leading finally to the result

$$p(x) = \frac{1}{(2\pi\sigma^2)^{1/2}} \exp \left\{ -\frac{(x - \mu)^2}{2\sigma^2} \right\} \quad (1.109)$$

and so the distribution that maximizes the differential entropy is the Gaussian. Note that we did not constrain the distribution to be nonnegative when we maximized the entropy. However, because the resulting distribution is indeed nonnegative, we see with hindsight that such a constraint is not necessary.

Exercise 1.35

If we evaluate the differential entropy of the Gaussian, we obtain

$$H[x] = \frac{1}{2} \left\{ 1 + \ln(2\pi\sigma^2) \right\}. \quad (1.110)$$

Thus we see again that the entropy increases as the distribution becomes broader, i.e., as σ^2 increases. This result also shows that the differential entropy, unlike the discrete entropy, can be negative, because $H(x) < 0$ in (1.110) for $\sigma^2 < 1/(2\pi e)$.

Suppose we have a joint distribution $p(\mathbf{x}, \mathbf{y})$ from which we draw pairs of values of \mathbf{x} and \mathbf{y} . If a value of \mathbf{x} is already known, then the additional information needed to specify the corresponding value of \mathbf{y} is given by $-\ln p(\mathbf{y}|\mathbf{x})$. Thus the average additional information needed to specify \mathbf{y} can be written as

$$H[\mathbf{y}|\mathbf{x}] = - \iint p(\mathbf{y}, \mathbf{x}) \ln p(\mathbf{y}|\mathbf{x}) d\mathbf{y} d\mathbf{x} \quad (1.111)$$

Exercise 1.37

which is called the *conditional entropy* of y given x . It is easily seen, using the product rule, that the conditional entropy satisfies the relation

$$H[x, y] = H[y|x] + H[x] \quad (1.112)$$

where $H[x, y]$ is the differential entropy of $p(x, y)$ and $H[x]$ is the differential entropy of the marginal distribution $p(x)$. Thus the information needed to describe x and y is given by the sum of the information needed to describe x alone plus the additional information required to specify y given x .

1.6.1 Relative entropy and mutual information

So far in this section, we have introduced a number of concepts from information theory, including the key notion of entropy. We now start to relate these ideas to pattern recognition. Consider some unknown distribution $p(x)$, and suppose that we have modelled this using an approximating distribution $q(x)$. If we use $q(x)$ to construct a coding scheme for the purpose of transmitting values of x to a receiver, then the average additional amount of information (in nats) required to specify the value of x (assuming we choose an efficient coding scheme) as a result of using $q(x)$ instead of the true distribution $p(x)$ is given by

$$\begin{aligned} KL(p\|q) &= - \int p(x) \ln q(x) dx - \left(- \int p(x) \ln p(x) dx \right) \\ &= - \int p(x) \ln \left\{ \frac{q(x)}{p(x)} \right\} dx. \end{aligned} \quad (1.113)$$

This is known as the *relative entropy* or *Kullback-Leibler divergence*, or *KL divergence* (Kullback and Leibler, 1951), between the distributions $p(x)$ and $q(x)$. Note that it is not a symmetrical quantity, that is to say $KL(p\|q) \neq KL(q\|p)$.

We now show that the Kullback-Leibler divergence satisfies $KL(p\|q) \geq 0$ with equality if, and only if, $p(x) = q(x)$. To do this we first introduce the concept of *convex functions*. A function $f(x)$ is said to be convex if it has the property that every chord lies on or above the function, as shown in Figure 1.31. Any value of x in the interval from $x = a$ to $x = b$ can be written in the form $\lambda a + (1 - \lambda)b$ where $0 \leq \lambda \leq 1$. The corresponding point on the chord is given by $\lambda f(a) + (1 - \lambda)f(b)$,



Claude Shannon
1916–2001

After graduating from Michigan and MIT, Shannon joined the AT&T Bell Telephone laboratories in 1941. His paper ‘A Mathematical Theory of Communication’ published in the *Bell System Technical Journal* in 1948 laid the foundations for modern information the-

ory. This paper introduced the word ‘bit’, and his concept that information could be sent as a stream of 1s and 0s paved the way for the communications revolution. It is said that von Neumann recommended to Shannon that he use the term entropy, not only because of its similarity to the quantity used in physics, but also because “nobody knows what entropy really is, so in any discussion you will always have an advantage”.

Figure 1.31 A convex function $f(x)$ is one for which every chord (shown in blue) lies on or above the function (shown in red).



and the corresponding value of the function is $f(\lambda a + (1 - \lambda)b)$. Convexity then implies

$$f(\lambda a + (1 - \lambda)b) \leq \lambda f(a) + (1 - \lambda)f(b). \quad (1.114)$$

Exercise 1.36

This is equivalent to the requirement that the second derivative of the function be everywhere positive. Examples of convex functions are $x \ln x$ (for $x > 0$) and x^2 . A function is called *strictly convex* if the equality is satisfied only for $\lambda = 0$ and $\lambda = 1$. If a function has the opposite property, namely that every chord lies on or below the function, it is called *concave*, with a corresponding definition for *strictly concave*. If a function $f(x)$ is convex, then $-f(x)$ will be concave.

Exercise 1.38

Using the technique of proof by induction, we can show from (1.114) that a convex function $f(x)$ satisfies

$$f\left(\sum_{i=1}^M \lambda_i x_i\right) \leq \sum_{i=1}^M \lambda_i f(x_i) \quad (1.115)$$

where $\lambda_i \geq 0$ and $\sum_i \lambda_i = 1$, for any set of points $\{x_i\}$. The result (1.115) is known as *Jensen's inequality*. If we interpret the λ_i as the probability distribution over a discrete variable x taking the values $\{x_i\}$, then (1.115) can be written

$$f(\mathbb{E}[x]) \leq \mathbb{E}[f(x)] \quad (1.116)$$

where $\mathbb{E}[\cdot]$ denotes the expectation. For continuous variables, Jensen's inequality takes the form

$$f\left(\int \mathbf{x} p(\mathbf{x}) d\mathbf{x}\right) \leq \int f(\mathbf{x}) p(\mathbf{x}) d\mathbf{x}. \quad (1.117)$$

We can apply Jensen's inequality in the form (1.117) to the Kullback-Leibler divergence (1.113) to give

$$\text{KL}(p\|q) = - \int p(\mathbf{x}) \ln \left\{ \frac{q(\mathbf{x})}{p(\mathbf{x})} \right\} d\mathbf{x} \geq - \ln \int q(\mathbf{x}) d\mathbf{x} = 0 \quad (1.118)$$

where we have used the fact that $-\ln x$ is a convex function, together with the normalization condition $\int q(\mathbf{x}) d\mathbf{x} = 1$. In fact, $-\ln x$ is a strictly convex function, so the equality will hold if, and only if, $q(\mathbf{x}) = p(\mathbf{x})$ for all \mathbf{x} . Thus we can interpret the Kullback-Leibler divergence as a measure of the dissimilarity of the two distributions $p(\mathbf{x})$ and $q(\mathbf{x})$.

We see that there is an intimate relationship between data compression and density estimation (i.e., the problem of modelling an unknown probability distribution) because the most efficient compression is achieved when we know the true distribution. If we use a distribution that is different from the true one, then we must necessarily have a less efficient coding, and on average the additional information that must be transmitted is (at least) equal to the Kullback-Leibler divergence between the two distributions.

Suppose that data is being generated from an unknown distribution $p(\mathbf{x})$ that we wish to model. We can try to approximate this distribution using some parametric distribution $q(\mathbf{x}|\boldsymbol{\theta})$, governed by a set of adjustable parameters $\boldsymbol{\theta}$, for example a multivariate Gaussian. One way to determine $\boldsymbol{\theta}$ is to minimize the Kullback-Leibler divergence between $p(\mathbf{x})$ and $q(\mathbf{x}|\boldsymbol{\theta})$ with respect to $\boldsymbol{\theta}$. We cannot do this directly because we don't know $p(\mathbf{x})$. Suppose, however, that we have observed a finite set of training points \mathbf{x}_n , for $n = 1, \dots, N$, drawn from $p(\mathbf{x})$. Then the expectation with respect to $p(\mathbf{x})$ can be approximated by a finite sum over these points, using (1.35), so that

$$\text{KL}(p\|q) \simeq \sum_{n=1}^N \{-\ln q(\mathbf{x}_n|\boldsymbol{\theta}) + \ln p(\mathbf{x}_n)\}. \quad (1.119)$$

The second term on the right-hand side of (1.119) is independent of $\boldsymbol{\theta}$, and the first term is the negative log likelihood function for $\boldsymbol{\theta}$ under the distribution $q(\mathbf{x}|\boldsymbol{\theta})$ evaluated using the training set. Thus we see that minimizing this Kullback-Leibler divergence is equivalent to maximizing the likelihood function.

Now consider the joint distribution between two sets of variables \mathbf{x} and \mathbf{y} given by $p(\mathbf{x}, \mathbf{y})$. If the sets of variables are independent, then their joint distribution will factorize into the product of their marginals $p(\mathbf{x}, \mathbf{y}) = p(\mathbf{x})p(\mathbf{y})$. If the variables are not independent, we can gain some idea of whether they are 'close' to being independent by considering the Kullback-Leibler divergence between the joint distribution and the product of the marginals, given by

$$\begin{aligned} I[\mathbf{x}, \mathbf{y}] &\equiv \text{KL}(p(\mathbf{x}, \mathbf{y})\|p(\mathbf{x})p(\mathbf{y})) \\ &= - \iint p(\mathbf{x}, \mathbf{y}) \ln \left(\frac{p(\mathbf{x})p(\mathbf{y})}{p(\mathbf{x}, \mathbf{y})} \right) d\mathbf{x} d\mathbf{y} \end{aligned} \quad (1.120)$$

which is called the *mutual information* between the variables \mathbf{x} and \mathbf{y} . From the properties of the Kullback-Leibler divergence, we see that $I(\mathbf{x}, \mathbf{y}) \geq 0$ with equality if, and only if, \mathbf{x} and \mathbf{y} are independent. Using the sum and product rules of probability, we see that the mutual information is related to the conditional entropy through

$$I[\mathbf{x}, \mathbf{y}] = H[\mathbf{x}] - H[\mathbf{x}|\mathbf{y}] = H[\mathbf{y}] - H[\mathbf{y}|\mathbf{x}]. \quad (1.121)$$

Thus we can view the mutual information as the reduction in the uncertainty about \mathbf{x} by virtue of being told the value of \mathbf{y} (or vice versa). From a Bayesian perspective, we can view $p(\mathbf{x})$ as the prior distribution for \mathbf{x} and $p(\mathbf{x}|\mathbf{y})$ as the posterior distribution after we have observed new data \mathbf{y} . The mutual information therefore represents the reduction in uncertainty about \mathbf{x} as a consequence of the new observation \mathbf{y} .

Exercises

- 1.1** (*) www Consider the sum-of-squares error function given by (1.2) in which the function $y(x, \mathbf{w})$ is given by the polynomial (1.1). Show that the coefficients $\mathbf{w} = \{w_i\}$ that minimize this error function are given by the solution to the following set of linear equations

$$\sum_{j=0}^M A_{ij} w_j = T_i \quad (1.122)$$

where

$$A_{ij} = \sum_{n=1}^N (x_n)^{i+j}, \quad T_i = \sum_{n=1}^N (x_n)^i t_n. \quad (1.123)$$

Here a suffix i or j denotes the index of a component, whereas $(x)^i$ denotes x raised to the power of i .

- 1.2** (*) Write down the set of coupled linear equations, analogous to (1.122), satisfied by the coefficients w_i which minimize the regularized sum-of-squares error function given by (1.4).
- 1.3** (**) Suppose that we have three coloured boxes r (red), b (blue), and g (green). Box r contains 3 apples, 4 oranges, and 3 limes, box b contains 1 apple, 1 orange, and 0 limes, and box g contains 3 apples, 3 oranges, and 4 limes. If a box is chosen at random with probabilities $p(r) = 0.2$, $p(b) = 0.2$, $p(g) = 0.6$, and a piece of fruit is removed from the box (with equal probability of selecting any of the items in the box), then what is the probability of selecting an apple? If we observe that the selected fruit is in fact an orange, what is the probability that it came from the green box?
- 1.4** (**) www Consider a probability density $p_x(x)$ defined over a continuous variable x , and suppose that we make a nonlinear change of variable using $x = g(y)$, so that the density transforms according to (1.27). By differentiating (1.27), show that the location \hat{y} of the maximum of the density in y is not in general related to the location \hat{x} of the maximum of the density over x by the simple functional relation $\hat{x} = g(\hat{y})$ as a consequence of the Jacobian factor. This shows that the maximum of a probability density (in contrast to a simple function) is dependent on the choice of variable. Verify that, in the case of a linear transformation, the location of the maximum transforms in the same way as the variable itself.
- 1.5** (*) Using the definition (1.38) show that $\text{var}[f(x)]$ satisfies (1.39).

1.6 (★) Show that if two variables x and y are independent, then their covariance is zero.

1.7 (★★) **www** In this exercise, we prove the normalization condition (1.48) for the univariate Gaussian. To do this consider, the integral

$$I = \int_{-\infty}^{\infty} \exp\left(-\frac{1}{2\sigma^2}x^2\right) dx \quad (1.124)$$

which we can evaluate by first writing its square in the form

$$I^2 = \int_{-\infty}^{\infty} \int_{-\infty}^{\infty} \exp\left(-\frac{1}{2\sigma^2}x^2 - \frac{1}{2\sigma^2}y^2\right) dx dy. \quad (1.125)$$

Now make the transformation from Cartesian coordinates (x, y) to polar coordinates (r, θ) and then substitute $u = r^2$. Show that, by performing the integrals over θ and u , and then taking the square root of both sides, we obtain

$$I = (2\pi\sigma^2)^{1/2}. \quad (1.126)$$

Finally, use this result to show that the Gaussian distribution $\mathcal{N}(x|\mu, \sigma^2)$ is normalized.

1.8 (★★) **www** By using a change of variables, verify that the univariate Gaussian distribution given by (1.46) satisfies (1.49). Next, by differentiating both sides of the normalization condition

$$\int_{-\infty}^{\infty} \mathcal{N}(x|\mu, \sigma^2) dx = 1 \quad (1.127)$$

with respect to σ^2 , verify that the Gaussian satisfies (1.50). Finally, show that (1.51) holds.

1.9 (★) **www** Show that the mode (i.e. the maximum) of the Gaussian distribution (1.46) is given by μ . Similarly, show that the mode of the multivariate Gaussian (1.52) is given by μ .

1.10 (★) **www** Suppose that the two variables x and z are statistically independent. Show that the mean and variance of their sum satisfies

$$\mathbb{E}[x + z] = \mathbb{E}[x] + \mathbb{E}[z] \quad (1.128)$$

$$\text{var}[x + z] = \text{var}[x] + \text{var}[z]. \quad (1.129)$$

1.11 (★) By setting the derivatives of the log likelihood function (1.54) with respect to μ and σ^2 equal to zero, verify the results (1.55) and (1.56).

- 1.12** (**) **www** Using the results (1.49) and (1.50), show that

$$\mathbb{E}[x_n x_m] = \mu^2 + I_{nm}\sigma^2 \quad (1.130)$$

where x_n and x_m denote data points sampled from a Gaussian distribution with mean μ and variance σ^2 , and I_{nm} satisfies $I_{nm} = 1$ if $n = m$ and $I_{nm} = 0$ otherwise. Hence prove the results (1.57) and (1.58).

- 1.13** (*) Suppose that the variance of a Gaussian is estimated using the result (1.56) but with the maximum likelihood estimate μ_{ML} replaced with the true value μ of the mean. Show that this estimator has the property that its expectation is given by the true variance σ^2 .

- 1.14** (**) Show that an arbitrary square matrix with elements w_{ij} can be written in the form $w_{ij} = w_{ij}^S + w_{ij}^A$ where w_{ij}^S and w_{ij}^A are symmetric and anti-symmetric matrices, respectively, satisfying $w_{ij}^S = w_{ji}^S$ and $w_{ij}^A = -w_{ji}^A$ for all i and j . Now consider the second order term in a higher order polynomial in D dimensions, given by

$$\sum_{i=1}^D \sum_{j=1}^D w_{ij} x_i x_j. \quad (1.131)$$

Show that

$$\sum_{i=1}^D \sum_{j=1}^D w_{ij} x_i x_j = \sum_{i=1}^D \sum_{j=1}^D w_{ij}^S x_i x_j \quad (1.132)$$

so that the contribution from the anti-symmetric matrix vanishes. We therefore see that, without loss of generality, the matrix of coefficients w_{ij} can be chosen to be symmetric, and so not all of the D^2 elements of this matrix can be chosen independently. Show that the number of independent parameters in the matrix w_{ij}^S is given by $D(D + 1)/2$.

- 1.15** (***) **www** In this exercise and the next, we explore how the number of independent parameters in a polynomial grows with the order M of the polynomial and with the dimensionality D of the input space. We start by writing down the M^{th} order term for a polynomial in D dimensions in the form

$$\sum_{i_1=1}^D \sum_{i_2=1}^D \cdots \sum_{i_M=1}^D w_{i_1 i_2 \cdots i_M} x_{i_1} x_{i_2} \cdots x_{i_M}. \quad (1.133)$$

The coefficients $w_{i_1 i_2 \cdots i_M}$ comprise D^M elements, but the number of independent parameters is significantly fewer due to the many interchange symmetries of the factor $x_{i_1} x_{i_2} \cdots x_{i_M}$. Begin by showing that the redundancy in the coefficients can be removed by rewriting this M^{th} order term in the form

$$\sum_{i_1=1}^D \sum_{i_2=1}^{i_1} \cdots \sum_{i_M=1}^{i_{M-1}} \tilde{w}_{i_1 i_2 \cdots i_M} x_{i_1} x_{i_2} \cdots x_{i_M}. \quad (1.134)$$

Note that the precise relationship between the \tilde{w} coefficients and w coefficients need not be made explicit. Use this result to show that the number of *independent* parameters $n(D, M)$, which appear at order M , satisfies the following recursion relation

$$n(D, M) = \sum_{i=1}^D n(i, M-1). \quad (1.135)$$

Next use proof by induction to show that the following result holds

$$\sum_{i=1}^D \frac{(i+M-2)!}{(i-1)! (M-1)!} = \frac{(D+M-1)!}{(D-1)! M!} \quad (1.136)$$

which can be done by first proving the result for $D = 1$ and arbitrary M by making use of the result $0! = 1$, then assuming it is correct for dimension D and verifying that it is correct for dimension $D + 1$. Finally, use the two previous results, together with proof by induction, to show

$$n(D, M) = \frac{(D+M-1)!}{(D-1)! M!}. \quad (1.137)$$

To do this, first show that the result is true for $M = 2$, and any value of $D \geq 1$, by comparison with the result of Exercise 1.14. Then make use of (1.135), together with (1.136), to show that, if the result holds at order $M - 1$, then it will also hold at order M .

- 1.16** (★★★) In Exercise 1.15, we proved the result (1.135) for the number of independent parameters in the M^{th} order term of a D -dimensional polynomial. We now find an expression for the total number $N(D, M)$ of independent parameters in all of the terms up to and including the M^{th} order. First show that $N(D, M)$ satisfies

$$N(D, M) = \sum_{m=0}^M n(D, m) \quad (1.138)$$

where $n(D, m)$ is the number of independent parameters in the term of order m . Now make use of the result (1.137), together with proof by induction, to show that

$$N(d, M) = \frac{(D+M)!}{D! M!}. \quad (1.139)$$

This can be done by first proving that the result holds for $M = 0$ and arbitrary $D \geq 1$, then assuming that it holds at order M , and hence showing that it holds at order $M + 1$. Finally, make use of Stirling's approximation in the form

$$n! \simeq n^n e^{-n} \quad (1.140)$$

for large n to show that, for $D \gg M$, the quantity $N(D, M)$ grows like D^M , and for $M \gg D$ it grows like M^D . Consider a cubic ($M = 3$) polynomial in D dimensions, and evaluate numerically the total number of independent parameters for (i) $D = 10$ and (ii) $D = 100$, which correspond to typical small-scale and medium-scale machine learning applications.

1.17 (**) **www** The gamma function is defined by

$$\Gamma(x) \equiv \int_0^\infty u^{x-1} e^{-u} du. \quad (1.141)$$

Using integration by parts, prove the relation $\Gamma(x+1) = x\Gamma(x)$. Show also that $\Gamma(1) = 1$ and hence that $\Gamma(x+1) = x!$ when x is an integer.

1.18 (**) **www** We can use the result (1.126) to derive an expression for the surface area S_D , and the volume V_D , of a sphere of unit radius in D dimensions. To do this, consider the following result, which is obtained by transforming from Cartesian to polar coordinates

$$\prod_{i=1}^D \int_{-\infty}^\infty e^{-x_i^2} dx_i = S_D \int_0^\infty e^{-r^2} r^{D-1} dr. \quad (1.142)$$

Using the definition (1.141) of the Gamma function, together with (1.126), evaluate both sides of this equation, and hence show that

$$S_D = \frac{2\pi^{D/2}}{\Gamma(D/2)}. \quad (1.143)$$

Next, by integrating with respect to radius from 0 to 1, show that the volume of the unit sphere in D dimensions is given by

$$V_D = \frac{S_D}{D}. \quad (1.144)$$

Finally, use the results $\Gamma(1) = 1$ and $\Gamma(3/2) = \sqrt{\pi}/2$ to show that (1.143) and (1.144) reduce to the usual expressions for $D = 2$ and $D = 3$.

1.19 (**) Consider a sphere of radius a in D -dimensions together with the concentric hypercube of side $2a$, so that the sphere touches the hypercube at the centres of each of its sides. By using the results of Exercise 1.18, show that the ratio of the volume of the sphere to the volume of the cube is given by

$$\frac{\text{volume of sphere}}{\text{volume of cube}} = \frac{\pi^{D/2}}{D2^{D-1}\Gamma(D/2)}. \quad (1.145)$$

Now make use of Stirling's formula in the form

$$\Gamma(x+1) \simeq (2\pi)^{1/2} e^{-x} x^{x+1/2} \quad (1.146)$$

which is valid for $x \gg 1$, to show that, as $D \rightarrow \infty$, the ratio (1.145) goes to zero. Show also that the ratio of the distance from the centre of the hypercube to one of the corners, divided by the perpendicular distance to one of the sides, is \sqrt{D} , which therefore goes to ∞ as $D \rightarrow \infty$. From these results we see that, in a space of high dimensionality, most of the volume of a cube is concentrated in the large number of corners, which themselves become very long 'spikes'!

- 1.20** (**) **www** In this exercise, we explore the behaviour of the Gaussian distribution in high-dimensional spaces. Consider a Gaussian distribution in D dimensions given by

$$p(\mathbf{x}) = \frac{1}{(2\pi\sigma^2)^{D/2}} \exp\left(-\frac{\|\mathbf{x}\|^2}{2\sigma^2}\right). \quad (1.147)$$

We wish to find the density with respect to radius in polar coordinates in which the direction variables have been integrated out. To do this, show that the integral of the probability density over a thin shell of radius r and thickness ϵ , where $\epsilon \ll 1$, is given by $p(r)\epsilon$ where

$$p(r) = \frac{S_D r^{D-1}}{(2\pi\sigma^2)^{D/2}} \exp\left(-\frac{r^2}{2\sigma^2}\right) \quad (1.148)$$

where S_D is the surface area of a unit sphere in D dimensions. Show that the function $p(r)$ has a single stationary point located, for large D , at $\hat{r} \simeq \sqrt{D}\sigma$. By considering $p(\hat{r} + \epsilon)$ where $\epsilon \ll \hat{r}$, show that for large D ,

$$p(\hat{r} + \epsilon) = p(\hat{r}) \exp\left(-\frac{3\epsilon^2}{2\sigma^2}\right) \quad (1.149)$$

which shows that \hat{r} is a maximum of the radial probability density and also that $p(r)$ decays exponentially away from its maximum at \hat{r} with length scale σ . We have already seen that $\sigma \ll \hat{r}$ for large D , and so we see that most of the probability mass is concentrated in a thin shell at large radius. Finally, show that the probability density $p(\mathbf{x})$ is larger at the origin than at the radius \hat{r} by a factor of $\exp(D/2)$. We therefore see that most of the probability mass in a high-dimensional Gaussian distribution is located at a different radius from the region of high probability density. This property of distributions in spaces of high dimensionality will have important consequences when we consider Bayesian inference of model parameters in later chapters.

- 1.21** (**) Consider two nonnegative numbers a and b , and show that, if $a \leq b$, then $a \leq (ab)^{1/2}$. Use this result to show that, if the decision regions of a two-class classification problem are chosen to minimize the probability of misclassification, this probability will satisfy

$$p(\text{mistake}) \leq \int \{p(\mathbf{x}, \mathcal{C}_1)p(\mathbf{x}, \mathcal{C}_2)\}^{1/2} d\mathbf{x}. \quad (1.150)$$

- 1.22** (*) **www** Given a loss matrix with elements L_{kj} , the expected risk is minimized if, for each \mathbf{x} , we choose the class that minimizes (1.81). Verify that, when the loss matrix is given by $L_{kj} = 1 - I_{kj}$, where I_{kj} are the elements of the identity matrix, this reduces to the criterion of choosing the class having the largest posterior probability. What is the interpretation of this form of loss matrix?

- 1.23** (*) Derive the criterion for minimizing the expected loss when there is a general loss matrix and general prior probabilities for the classes.

- 1.24** (**) **www** Consider a classification problem in which the loss incurred when an input vector from class \mathcal{C}_k is classified as belonging to class \mathcal{C}_j is given by the loss matrix L_{kj} , and for which the loss incurred in selecting the reject option is λ . Find the decision criterion that will give the minimum expected loss. Verify that this reduces to the reject criterion discussed in Section 1.5.3 when the loss matrix is given by $L_{kj} = 1 - I_{kj}$. What is the relationship between λ and the rejection threshold θ ?

- 1.25** (*) **www** Consider the generalization of the squared loss function (1.87) for a single target variable t to the case of multiple target variables described by the vector \mathbf{t} given by

$$\mathbb{E}[L(\mathbf{t}, \mathbf{y}(\mathbf{x}))] = \iint \|\mathbf{y}(\mathbf{x}) - \mathbf{t}\|^2 p(\mathbf{x}, \mathbf{t}) d\mathbf{x} d\mathbf{t}. \quad (1.151)$$

Using the calculus of variations, show that the function $\mathbf{y}(\mathbf{x})$ for which this expected loss is minimized is given by $\mathbf{y}(\mathbf{x}) = \mathbb{E}_{\mathbf{t}}[\mathbf{t}|\mathbf{x}]$. Show that this result reduces to (1.89) for the case of a single target variable t .

- 1.26** (*) By expansion of the square in (1.151), derive a result analogous to (1.90) and hence show that the function $\mathbf{y}(\mathbf{x})$ that minimizes the expected squared loss for the case of a vector \mathbf{t} of target variables is again given by the conditional expectation of \mathbf{t} .

- 1.27** (**) **www** Consider the expected loss for regression problems under the L_q loss function given by (1.91). Write down the condition that $y(\mathbf{x})$ must satisfy in order to minimize $\mathbb{E}[L_q]$. Show that, for $q = 1$, this solution represents the conditional median, i.e., the function $y(\mathbf{x})$ such that the probability mass for $t < y(\mathbf{x})$ is the same as for $t \geq y(\mathbf{x})$. Also show that the minimum expected L_q loss for $q \rightarrow 0$ is given by the conditional mode, i.e., by the function $y(\mathbf{x})$ equal to the value of t that maximizes $p(t|\mathbf{x})$ for each \mathbf{x} .

- 1.28** (*) In Section 1.6, we introduced the idea of entropy $h(x)$ as the information gained on observing the value of a random variable x having distribution $p(x)$. We saw that, for independent variables x and y for which $p(x, y) = p(x)p(y)$, the entropy functions are additive, so that $h(x, y) = h(x) + h(y)$. In this exercise, we derive the relation between h and p in the form of a function $h(p)$. First show that $h(p^2) = 2h(p)$, and hence by induction that $h(p^n) = nh(p)$ where n is a positive integer. Hence show that $h(p^{n/m}) = (n/m)h(p)$ where m is also a positive integer. This implies that $h(p^x) = xh(p)$ where x is a positive rational number, and hence by continuity when it is a positive real number. Finally, show that this implies $h(p)$ must take the form $h(p) \propto \ln p$.

- 1.29** (*) **www** Consider an M -state discrete random variable x , and use Jensen's inequality in the form (1.115) to show that the entropy of its distribution $p(x)$ satisfies $H[x] \leq \ln M$.

- 1.30** (**) Evaluate the Kullback-Leibler divergence (1.113) between two Gaussians $p(x) = \mathcal{N}(x|\mu, \sigma^2)$ and $q(x) = \mathcal{N}(x|m, s^2)$.

Table 1.3 The joint distribution $p(x, y)$ for two binary variables x and y used in Exercise 1.39.

| | | |
|-----|---|------------|
| | | y |
| | 0 | 0 1 |
| x | 0 | 1/3 1/3 |
| | 1 | 0 1/3 |

- 1.31** (**) **www** Consider two variables x and y having joint distribution $p(x, y)$. Show that the differential entropy of this pair of variables satisfies

$$H[x, y] \leq H[x] + H[y] \quad (1.152)$$

with equality if, and only if, x and y are statistically independent.

- 1.32** (*) Consider a vector \mathbf{x} of continuous variables with distribution $p(\mathbf{x})$ and corresponding entropy $H[\mathbf{x}]$. Suppose that we make a nonsingular linear transformation of \mathbf{x} to obtain a new variable $\mathbf{y} = \mathbf{Ax}$. Show that the corresponding entropy is given by $H[\mathbf{y}] = H[\mathbf{x}] + \ln |\mathbf{A}|$ where $|\mathbf{A}|$ denotes the determinant of \mathbf{A} .
- 1.33** (**) Suppose that the conditional entropy $H[y|x]$ between two discrete random variables x and y is zero. Show that, for all values of x such that $p(x) > 0$, the variable y must be a function of x , in other words for each x there is only one value of y such that $p(y|x) \neq 0$.
- 1.34** (**) **www** Use the calculus of variations to show that the stationary point of the functional (1.108) is given by (1.108). Then use the constraints (1.105), (1.106), and (1.107) to eliminate the Lagrange multipliers and hence show that the maximum entropy solution is given by the Gaussian (1.109).
- 1.35** (*) **www** Use the results (1.106) and (1.107) to show that the entropy of the univariate Gaussian (1.109) is given by (1.110).
- 1.36** (*) A strictly convex function is defined as one for which every chord lies above the function. Show that this is equivalent to the condition that the second derivative of the function be positive.
- 1.37** (*) Using the definition (1.111) together with the product rule of probability, prove the result (1.112).
- 1.38** (**) **www** Using proof by induction, show that the inequality (1.114) for convex functions implies the result (1.115).
- 1.39** (**) Consider two binary variables x and y having the joint distribution given in Table 1.3.

Evaluate the following quantities

(a) $H[x]$
(b) $H[y]$

(c) $H[y|x]$
(d) $H[x|y]$

(e) $H[x, y]$
(f) $I[x, y]$.

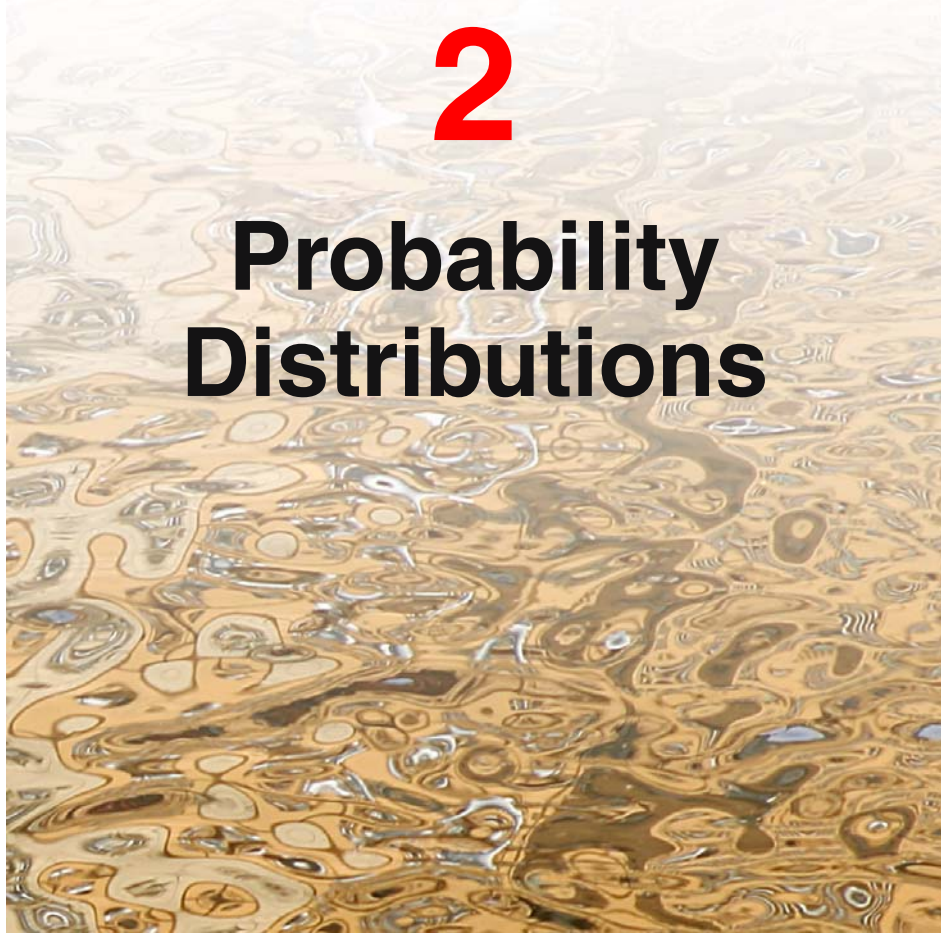
Draw a diagram to show the relationship between these various quantities.

1.40 (*) By applying Jensen's inequality (1.115) with $f(x) = \ln x$, show that the arithmetic mean of a set of real numbers is never less than their geometrical mean.

1.41 (*) **www** Using the sum and product rules of probability, show that the mutual information $I(\mathbf{x}, \mathbf{y})$ satisfies the relation (1.121).

2

Probability Distributions



In Chapter 1, we emphasized the central role played by probability theory in the solution of pattern recognition problems. We turn now to an exploration of some particular examples of probability distributions and their properties. As well as being of great interest in their own right, these distributions can form building blocks for more complex models and will be used extensively throughout the book. The distributions introduced in this chapter will also serve another important purpose, namely to provide us with the opportunity to discuss some key statistical concepts, such as Bayesian inference, in the context of simple models before we encounter them in more complex situations in later chapters.

One role for the distributions discussed in this chapter is to model the probability distribution $p(\mathbf{x})$ of a random variable \mathbf{x} , given a finite set $\mathbf{x}_1, \dots, \mathbf{x}_N$ of observations. This problem is known as *density estimation*. For the purposes of this chapter, we shall assume that the data points are independent and identically distributed. It should be emphasized that the problem of density estimation is fun-

damentally ill-posed, because there are infinitely many probability distributions that could have given rise to the observed finite data set. Indeed, any distribution $p(\mathbf{x})$ that is nonzero at each of the data points $\mathbf{x}_1, \dots, \mathbf{x}_N$ is a potential candidate. The issue of choosing an appropriate distribution relates to the problem of model selection that has already been encountered in the context of polynomial curve fitting in Chapter 1 and that is a central issue in pattern recognition.

We begin by considering the binomial and multinomial distributions for discrete random variables and the Gaussian distribution for continuous random variables. These are specific examples of *parametric* distributions, so-called because they are governed by a small number of adaptive parameters, such as the mean and variance in the case of a Gaussian for example. To apply such models to the problem of density estimation, we need a procedure for determining suitable values for the parameters, given an observed data set. In a frequentist treatment, we choose specific values for the parameters by optimizing some criterion, such as the likelihood function. By contrast, in a Bayesian treatment we introduce prior distributions over the parameters and then use Bayes' theorem to compute the corresponding posterior distribution given the observed data.

We shall see that an important role is played by *conjugate* priors, that lead to posterior distributions having the same functional form as the prior, and that therefore lead to a greatly simplified Bayesian analysis. For example, the conjugate prior for the parameters of the multinomial distribution is called the *Dirichlet* distribution, while the conjugate prior for the mean of a Gaussian is another Gaussian. All of these distributions are examples of the *exponential family* of distributions, which possess a number of important properties, and which will be discussed in some detail.

One limitation of the parametric approach is that it assumes a specific functional form for the distribution, which may turn out to be inappropriate for a particular application. An alternative approach is given by *nonparametric* density estimation methods in which the form of the distribution typically depends on the size of the data set. Such models still contain parameters, but these control the model complexity rather than the form of the distribution. We end this chapter by considering three nonparametric methods based respectively on histograms, nearest-neighbours, and kernels.

2.1. Binary Variables

We begin by considering a single binary random variable $x \in \{0, 1\}$. For example, x might describe the outcome of flipping a coin, with $x = 1$ representing ‘heads’, and $x = 0$ representing ‘tails’. We can imagine that this is a damaged coin so that the probability of landing heads is not necessarily the same as that of landing tails. The probability of $x = 1$ will be denoted by the parameter μ so that

$$p(x = 1|\mu) = \mu \tag{2.1}$$

where $0 \leq \mu \leq 1$, from which it follows that $p(x = 0|\mu) = 1 - \mu$. The probability distribution over x can therefore be written in the form

$$\text{Bern}(x|\mu) = \mu^x(1 - \mu)^{1-x} \quad (2.2)$$

Exercise 2.1

which is known as the *Bernoulli* distribution. It is easily verified that this distribution is normalized and that it has mean and variance given by

$$\mathbb{E}[x] = \mu \quad (2.3)$$

$$\text{var}[x] = \mu(1 - \mu). \quad (2.4)$$

Now suppose we have a data set $\mathcal{D} = \{x_1, \dots, x_N\}$ of observed values of x . We can construct the likelihood function, which is a function of μ , on the assumption that the observations are drawn independently from $p(x|\mu)$, so that

$$p(\mathcal{D}|\mu) = \prod_{n=1}^N p(x_n|\mu) = \prod_{n=1}^N \mu^{x_n}(1 - \mu)^{1-x_n}. \quad (2.5)$$

In a frequentist setting, we can estimate a value for μ by maximizing the likelihood function, or equivalently by maximizing the logarithm of the likelihood. In the case of the Bernoulli distribution, the log likelihood function is given by

$$\ln p(\mathcal{D}|\mu) = \sum_{n=1}^N \ln p(x_n|\mu) = \sum_{n=1}^N \{x_n \ln \mu + (1 - x_n) \ln(1 - \mu)\}. \quad (2.6)$$

At this point, it is worth noting that the log likelihood function depends on the N observations x_n only through their sum $\sum_n x_n$. This sum provides an example of a *sufficient statistic* for the data under this distribution, and we shall study the important role of sufficient statistics in some detail. If we set the derivative of $\ln p(\mathcal{D}|\mu)$ with respect to μ equal to zero, we obtain the maximum likelihood estimator

$$\mu_{\text{ML}} = \frac{1}{N} \sum_{n=1}^N x_n \quad (2.7)$$

Section 2.4



Jacob Bernoulli

1654–1705

Jacob Bernoulli, also known as Jacques or James Bernoulli, was a Swiss mathematician and was the first of many in the Bernoulli family to pursue a career in science and mathematics. Although compelled to study philosophy and theology against his will by his parents, he travelled extensively after graduating in order to meet with many of the leading scientists of

his time, including Boyle and Hooke in England. When he returned to Switzerland, he taught mechanics and became Professor of Mathematics at Basel in 1687. Unfortunately, rivalry between Jacob and his younger brother Johann turned an initially productive collaboration into a bitter and public dispute. Jacob's most significant contributions to mathematics appeared in *The Art of Conjecture* published in 1713, eight years after his death, which deals with topics in probability theory including what has become known as the Bernoulli distribution.

2. PROBABILITY DISTRIBUTIONS

Figure 2.1 Histogram plot of the binomial distribution (2.9) as a function of m for $N = 10$ and $\mu = 0.25$.



which is also known as the *sample mean*. If we denote the number of observations of $x = 1$ (heads) within this data set by m , then we can write (2.7) in the form

$$\mu_{\text{ML}} = \frac{m}{N} \quad (2.8)$$

so that the probability of landing heads is given, in this maximum likelihood framework, by the fraction of observations of heads in the data set.

Now suppose we flip a coin, say, 3 times and happen to observe 3 heads. Then $N = m = 3$ and $\mu_{\text{ML}} = 1$. In this case, the maximum likelihood result would predict that all future observations should give heads. Common sense tells us that this is unreasonable, and in fact this is an extreme example of the over-fitting associated with maximum likelihood. We shall see shortly how to arrive at more sensible conclusions through the introduction of a prior distribution over μ .

We can also work out the distribution of the number m of observations of $x = 1$, given that the data set has size N . This is called the *binomial* distribution, and from (2.5) we see that it is proportional to $\mu^m(1 - \mu)^{N-m}$. In order to obtain the normalization coefficient we note that out of N coin flips, we have to add up all of the possible ways of obtaining m heads, so that the binomial distribution can be written

$$\text{Bin}(m|N, \mu) = \binom{N}{m} \mu^m (1 - \mu)^{N-m} \quad (2.9)$$

where

$$\binom{N}{m} \equiv \frac{N!}{(N-m)!m!} \quad (2.10)$$

Exercise 2.3

is the number of ways of choosing m objects out of a total of N identical objects. Figure 2.1 shows a plot of the binomial distribution for $N = 10$ and $\mu = 0.25$.

The mean and variance of the binomial distribution can be found by using the result of Exercise 1.10, which shows that for independent events the mean of the sum is the sum of the means, and the variance of the sum is the sum of the variances. Because $m = x_1 + \dots + x_N$, and for each observation the mean and variance are

given by (2.3) and (2.4), respectively, we have

$$\mathbb{E}[m] \equiv \sum_{m=0}^N m \text{Bin}(m|N, \mu) = N\mu \quad (2.11)$$

$$\text{var}[m] \equiv \sum_{m=0}^N (m - \mathbb{E}[m])^2 \text{Bin}(m|N, \mu) = N\mu(1 - \mu). \quad (2.12)$$

Exercise 2.4

These results can also be proved directly using calculus.

2.1.1 The beta distribution

We have seen in (2.8) that the maximum likelihood setting for the parameter μ in the Bernoulli distribution, and hence in the binomial distribution, is given by the fraction of the observations in the data set having $x = 1$. As we have already noted, this can give severely over-fitted results for small data sets. In order to develop a Bayesian treatment for this problem, we need to introduce a prior distribution $p(\mu)$ over the parameter μ . Here we consider a form of prior distribution that has a simple interpretation as well as some useful analytical properties. To motivate this prior, we note that the likelihood function takes the form of the product of factors of the form $\mu^x(1 - \mu)^{1-x}$. If we choose a prior to be proportional to powers of μ and $(1 - \mu)$, then the posterior distribution, which is proportional to the product of the prior and the likelihood function, will have the same functional form as the prior. This property is called *conjugacy* and we will see several examples of it later in this chapter. We therefore choose a prior, called the *beta* distribution, given by

$$\text{Beta}(\mu|a, b) = \frac{\Gamma(a + b)}{\Gamma(a)\Gamma(b)} \mu^{a-1} (1 - \mu)^{b-1} \quad (2.13)$$

where $\Gamma(x)$ is the gamma function defined by (1.141), and the coefficient in (2.13) ensures that the beta distribution is normalized, so that

$$\int_0^1 \text{Beta}(\mu|a, b) d\mu = 1. \quad (2.14)$$

Exercise 2.5

The mean and variance of the beta distribution are given by

$$\mathbb{E}[\mu] = \frac{a}{a + b} \quad (2.15)$$

$$\text{var}[\mu] = \frac{ab}{(a + b)^2(a + b + 1)}. \quad (2.16)$$

The parameters a and b are often called *hyperparameters* because they control the distribution of the parameter μ . Figure 2.2 shows plots of the beta distribution for various values of the hyperparameters.

The posterior distribution of μ is now obtained by multiplying the beta prior (2.13) by the binomial likelihood function (2.9) and normalizing. Keeping only the factors that depend on μ , we see that this posterior distribution has the form

$$p(\mu|m, l, a, b) \propto \mu^{m+a-1} (1 - \mu)^{l+b-1} \quad (2.17)$$

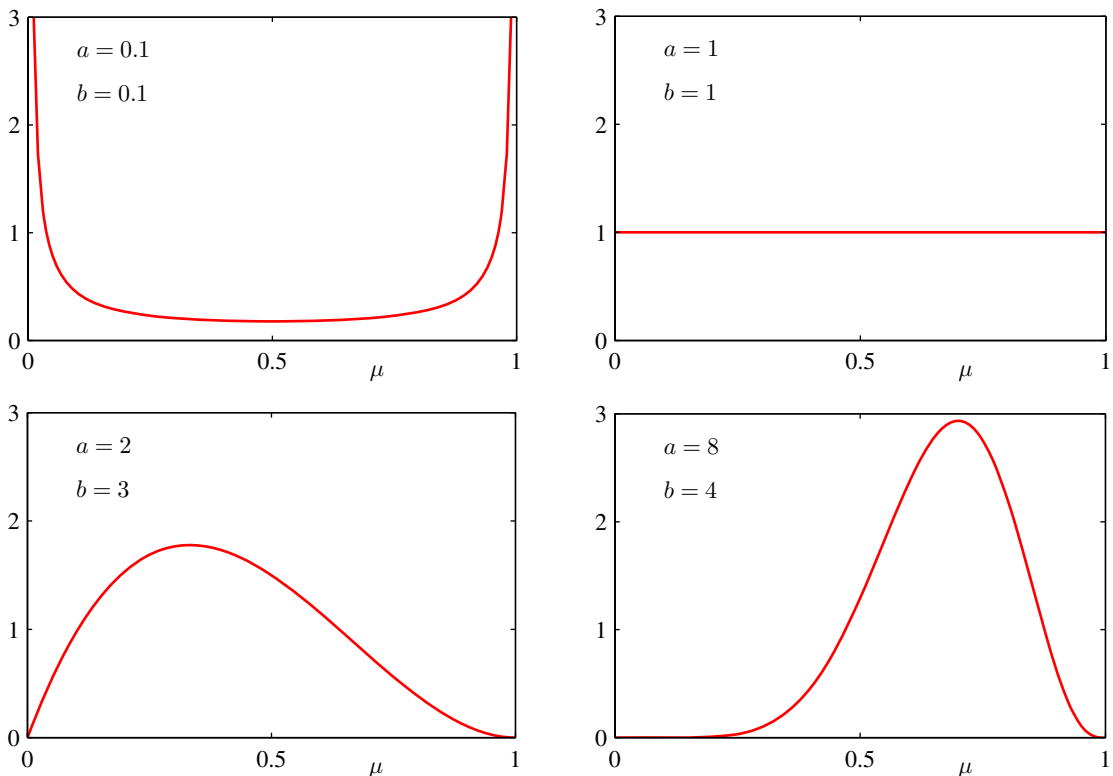


Figure 2.2 Plots of the beta distribution $\text{Beta}(\mu|a, b)$ given by (2.13) as a function of μ for various values of the hyperparameters a and b .

where $l = N - m$, and therefore corresponds to the number of ‘tails’ in the coin example. We see that (2.17) has the same functional dependence on μ as the prior distribution, reflecting the conjugacy properties of the prior with respect to the likelihood function. Indeed, it is simply another beta distribution, and its normalization coefficient can therefore be obtained by comparison with (2.13) to give

$$p(\mu|m, l, a, b) = \frac{\Gamma(m + a + l + b)}{\Gamma(m + a)\Gamma(l + b)} \mu^{m+a-1} (1 - \mu)^{l+b-1}. \quad (2.18)$$

We see that the effect of observing a data set of m observations of $x = 1$ and l observations of $x = 0$ has been to increase the value of a by m , and the value of b by l , in going from the prior distribution to the posterior distribution. This allows us to provide a simple interpretation of the hyperparameters a and b in the prior as an *effective number of observations* of $x = 1$ and $x = 0$, respectively. Note that a and b need not be integers. Furthermore, the posterior distribution can act as the prior if we subsequently observe additional data. To see this, we can imagine taking observations one at a time and after each observation updating the current posterior

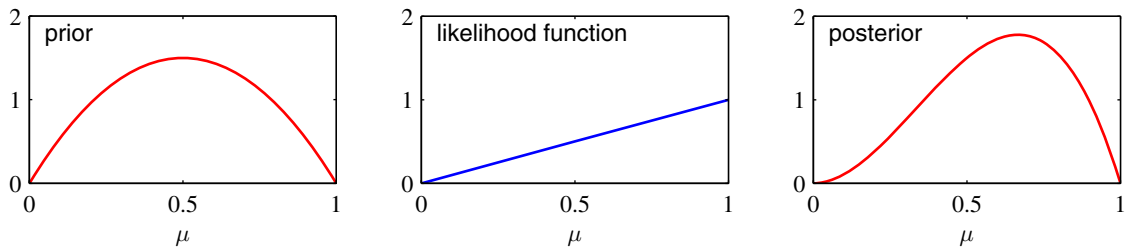


Figure 2.3 Illustration of one step of sequential Bayesian inference. The prior is given by a beta distribution with parameters $a = 2$, $b = 2$, and the likelihood function, given by (2.9) with $N = m = 1$, corresponds to a single observation of $x = 1$, so that the posterior is given by a beta distribution with parameters $a = 3$, $b = 2$.

distribution by multiplying by the likelihood function for the new observation and then normalizing to obtain the new, revised posterior distribution. At each stage, the posterior is a beta distribution with some total number of (prior and actual) observed values for $x = 1$ and $x = 0$ given by the parameters a and b . Incorporation of an additional observation of $x = 1$ simply corresponds to incrementing the value of a by 1, whereas for an observation of $x = 0$ we increment b by 1. Figure 2.3 illustrates one step in this process.

We see that this *sequential* approach to learning arises naturally when we adopt a Bayesian viewpoint. It is independent of the choice of prior and of the likelihood function and depends only on the assumption of i.i.d. data. Sequential methods make use of observations one at a time, or in small batches, and then discard them before the next observations are used. They can be used, for example, in real-time learning scenarios where a steady stream of data is arriving, and predictions must be made before all of the data is seen. Because they do not require the whole data set to be stored or loaded into memory, sequential methods are also useful for large data sets.

Maximum likelihood methods can also be cast into a sequential framework.

If our goal is to predict, as best we can, the outcome of the next trial, then we must evaluate the predictive distribution of x , given the observed data set \mathcal{D} . From the sum and product rules of probability, this takes the form

$$p(x = 1|\mathcal{D}) = \int_0^1 p(x = 1|\mu)p(\mu|\mathcal{D}) d\mu = \int_0^1 \mu p(\mu|\mathcal{D}) d\mu = \mathbb{E}[\mu|\mathcal{D}]. \quad (2.19)$$

Using the result (2.18) for the posterior distribution $p(\mu|\mathcal{D})$, together with the result (2.15) for the mean of the beta distribution, we obtain

$$p(x = 1|\mathcal{D}) = \frac{m + a}{m + a + l + b} \quad (2.20)$$

which has a simple interpretation as the total fraction of observations (both real observations and fictitious prior observations) that correspond to $x = 1$. Note that in the limit of an infinitely large data set $m, l \rightarrow \infty$ the result (2.20) reduces to the maximum likelihood result (2.8). As we shall see, it is a very general property that the Bayesian and maximum likelihood results will agree in the limit of an infinitely

Section 2.3.5

Exercise 2.7

large data set. For a finite data set, the posterior mean for μ always lies between the prior mean and the maximum likelihood estimate for μ corresponding to the relative frequencies of events given by (2.7).

From Figure 2.2, we see that as the number of observations increases, so the posterior distribution becomes more sharply peaked. This can also be seen from the result (2.16) for the variance of the beta distribution, in which we see that the variance goes to zero for $a \rightarrow \infty$ or $b \rightarrow \infty$. In fact, we might wonder whether it is a general property of Bayesian learning that, as we observe more and more data, the uncertainty represented by the posterior distribution will steadily decrease.

Exercise 2.8

To address this, we can take a frequentist view of Bayesian learning and show that, on average, such a property does indeed hold. Consider a general Bayesian inference problem for a parameter θ for which we have observed a data set \mathcal{D} , described by the joint distribution $p(\theta, \mathcal{D})$. The following result

$$\mathbb{E}_\theta[\theta] = \mathbb{E}_{\mathcal{D}} [\mathbb{E}_\theta[\theta | \mathcal{D}]] \quad (2.21)$$

where

$$\mathbb{E}_\theta[\theta] \equiv \int p(\theta) \theta d\theta \quad (2.22)$$

$$\mathbb{E}_{\mathcal{D}}[\mathbb{E}_\theta[\theta | \mathcal{D}]] \equiv \int \left\{ \int \theta p(\theta | \mathcal{D}) d\theta \right\} p(\mathcal{D}) d\mathcal{D} \quad (2.23)$$

says that the posterior mean of θ , averaged over the distribution generating the data, is equal to the prior mean of θ . Similarly, we can show that

$$\text{var}_\theta[\theta] = \mathbb{E}_{\mathcal{D}} [\text{var}_\theta[\theta | \mathcal{D}]] + \text{var}_{\mathcal{D}} [\mathbb{E}_\theta[\theta | \mathcal{D}]]. \quad (2.24)$$

The term on the left-hand side of (2.24) is the prior variance of θ . On the right-hand side, the first term is the average posterior variance of θ , and the second term measures the variance in the posterior mean of θ . Because this variance is a positive quantity, this result shows that, on average, the posterior variance of θ is smaller than the prior variance. The reduction in variance is greater if the variance in the posterior mean is greater. Note, however, that this result only holds on average, and that for a particular observed data set it is possible for the posterior variance to be larger than the prior variance.

2.2. Multinomial Variables

Binary variables can be used to describe quantities that can take one of two possible values. Often, however, we encounter discrete variables that can take on one of K possible mutually exclusive states. Although there are various alternative ways to express such variables, we shall see shortly that a particularly convenient representation is the 1-of- K scheme in which the variable is represented by a K -dimensional vector \mathbf{x} in which one of the elements x_k equals 1, and all remaining elements equal

0. So, for instance if we have a variable that can take $K = 6$ states and a particular observation of the variable happens to correspond to the state where $x_3 = 1$, then \mathbf{x} will be represented by

$$\mathbf{x} = (0, 0, 1, 0, 0, 0)^T. \quad (2.25)$$

Note that such vectors satisfy $\sum_{k=1}^K x_k = 1$. If we denote the probability of $x_k = 1$ by the parameter μ_k , then the distribution of \mathbf{x} is given

$$p(\mathbf{x}|\boldsymbol{\mu}) = \prod_{k=1}^K \mu_k^{x_k} \quad (2.26)$$

where $\boldsymbol{\mu} = (\mu_1, \dots, \mu_K)^T$, and the parameters μ_k are constrained to satisfy $\mu_k \geq 0$ and $\sum_k \mu_k = 1$, because they represent probabilities. The distribution (2.26) can be regarded as a generalization of the Bernoulli distribution to more than two outcomes. It is easily seen that the distribution is normalized

$$\sum_{\mathbf{x}} p(\mathbf{x}|\boldsymbol{\mu}) = \sum_{k=1}^K \mu_k = 1 \quad (2.27)$$

and that

$$\mathbb{E}[\mathbf{x}|\boldsymbol{\mu}] = \sum_{\mathbf{x}} p(\mathbf{x}|\boldsymbol{\mu}) \mathbf{x} = (\mu_1, \dots, \mu_M)^T = \boldsymbol{\mu}. \quad (2.28)$$

Now consider a data set \mathcal{D} of N independent observations $\mathbf{x}_1, \dots, \mathbf{x}_N$. The corresponding likelihood function takes the form

$$p(\mathcal{D}|\boldsymbol{\mu}) = \prod_{n=1}^N \prod_{k=1}^K \mu_k^{x_{nk}} = \prod_{k=1}^K \mu_k^{(\sum_n x_{nk})} = \prod_{k=1}^K \mu_k^{m_k}. \quad (2.29)$$

We see that the likelihood function depends on the N data points only through the K quantities

$$m_k = \sum_n x_{nk} \quad (2.30)$$

which represent the number of observations of $x_k = 1$. These are called the **sufficient statistics** for this distribution.

Section 2.4

Appendix E

In order to find the maximum likelihood solution for $\boldsymbol{\mu}$, we need to maximize $\ln p(\mathcal{D}|\boldsymbol{\mu})$ with respect to μ_k taking account of the constraint that the μ_k must sum to one. This can be achieved using a Lagrange multiplier λ and maximizing

$$\sum_{k=1}^K m_k \ln \mu_k + \lambda \left(\sum_{k=1}^K \mu_k - 1 \right). \quad (2.31)$$

Setting the derivative of (2.31) with respect to μ_k to zero, we obtain

$$\mu_k = -m_k/\lambda. \quad (2.32)$$

We can solve for the Lagrange multiplier λ by substituting (2.32) into the constraint $\sum_k \mu_k = 1$ to give $\lambda = -N$. Thus we obtain the maximum likelihood solution in the form

$$\mu_k^{\text{ML}} = \frac{m_k}{N} \quad (2.33)$$

which is the fraction of the N observations for which $x_k = 1$.

We can consider the joint distribution of the quantities m_1, \dots, m_K , conditioned on the parameters μ and on the total number N of observations. From (2.29) this takes the form

$$\text{Mult}(m_1, m_2, \dots, m_K | \boldsymbol{\mu}, N) = \binom{N}{m_1 m_2 \dots m_K} \prod_{k=1}^K \mu_k^{m_k} \quad (2.34)$$

which is known as the *multinomial* distribution. The normalization coefficient is the number of ways of partitioning N objects into K groups of size m_1, \dots, m_K and is given by

$$\binom{N}{m_1 m_2 \dots m_K} = \frac{N!}{m_1! m_2! \dots m_K!}. \quad (2.35)$$

Note that the variables m_k are subject to the constraint

$$\sum_{k=1}^K m_k = N. \quad (2.36)$$

2.2.1 The Dirichlet distribution

We now introduce a family of prior distributions for the parameters $\{\mu_k\}$ of the multinomial distribution (2.34). By inspection of the form of the multinomial distribution, we see that the conjugate prior is given by

$$p(\boldsymbol{\mu} | \boldsymbol{\alpha}) \propto \prod_{k=1}^K \mu_k^{\alpha_k - 1} \quad (2.37)$$

where $0 \leq \mu_k \leq 1$ and $\sum_k \mu_k = 1$. Here $\alpha_1, \dots, \alpha_K$ are the parameters of the distribution, and $\boldsymbol{\alpha}$ denotes $(\alpha_1, \dots, \alpha_K)^T$. Note that, because of the summation constraint, the distribution over the space of the $\{\mu_k\}$ is confined to a *simplex* of dimensionality $K - 1$, as illustrated for $K = 3$ in Figure 2.4.

Exercise 2.9

The normalized form for this distribution is by

$$\text{Dir}(\boldsymbol{\mu} | \boldsymbol{\alpha}) = \frac{\Gamma(\alpha_0)}{\Gamma(\alpha_1) \cdots \Gamma(\alpha_K)} \prod_{k=1}^K \mu_k^{\alpha_k - 1} \quad (2.38)$$

which is called the *Dirichlet* distribution. Here $\Gamma(x)$ is the gamma function defined by (1.141) while

$$\alpha_0 = \sum_{k=1}^K \alpha_k. \quad (2.39)$$

Figure 2.4 The Dirichlet distribution over three variables μ_1, μ_2, μ_3 is confined to a simplex (a bounded linear manifold) of the form shown, as a consequence of the constraints $0 \leq \mu_k \leq 1$ and $\sum_k \mu_k = 1$.



Plots of the Dirichlet distribution over the simplex, for various settings of the parameters α_k , are shown in Figure 2.5.

Multiplying the prior (2.38) by the likelihood function (2.34), we obtain the posterior distribution for the parameters $\{\mu_k\}$ in the form

$$p(\boldsymbol{\mu}|\mathcal{D}, \boldsymbol{\alpha}) \propto p(\mathcal{D}|\boldsymbol{\mu})p(\boldsymbol{\mu}|\boldsymbol{\alpha}) \propto \prod_{k=1}^K \mu_k^{\alpha_k + m_k - 1}. \quad (2.40)$$

We see that the posterior distribution again takes the form of a Dirichlet distribution, confirming that the Dirichlet is indeed a conjugate prior for the multinomial. This allows us to determine the normalization coefficient by comparison with (2.38) so that

$$\begin{aligned} p(\boldsymbol{\mu}|\mathcal{D}, \boldsymbol{\alpha}) &= \text{Dir}(\boldsymbol{\mu}|\boldsymbol{\alpha} + \mathbf{m}) \\ &= \frac{\Gamma(\alpha_0 + N)}{\Gamma(\alpha_1 + m_1) \cdots \Gamma(\alpha_K + m_K)} \prod_{k=1}^K \mu_k^{\alpha_k + m_k - 1} \end{aligned} \quad (2.41)$$

where we have denoted $\mathbf{m} = (m_1, \dots, m_K)^T$. As for the case of the binomial distribution with its beta prior, we can interpret the parameters α_k of the Dirichlet prior as an effective number of observations of $x_k = 1$.

Note that two-state quantities can either be represented as binary variables and



Lejeune Dirichlet
1805–1859

Johann Peter Gustav Lejeune Dirichlet was a modest and reserved mathematician who made contributions in number theory, mechanics, and astronomy, and who gave the first rigorous analysis of Fourier series. His family originated from Richelet in Belgium, and the name Lejeune Dirichlet comes

from ‘le jeune de Richelet’ (the young person from Richelet). Dirichlet’s first paper, which was published in 1825, brought him instant fame. It concerned Fermat’s last theorem, which claims that there are no positive integer solutions to $x^n + y^n = z^n$ for $n > 2$. Dirichlet gave a partial proof for the case $n = 5$, which was sent to Legendre for review and who in turn completed the proof. Later, Dirichlet gave a complete proof for $n = 14$, although a full proof of Fermat’s last theorem for arbitrary n had to wait until the work of Andrew Wiles in the closing years of the 20th century.



Figure 2.5 Plots of the Dirichlet distribution over three variables, where the two horizontal axes are coordinates in the plane of the simplex and the vertical axis corresponds to the value of the density. Here $\{\alpha_k\} = 0.1$ on the left plot, $\{\alpha_k\} = 1$ in the centre plot, and $\{\alpha_k\} = 10$ in the right plot.

modelled using the binomial distribution (2.9) or as 1-of-2 variables and modelled using the multinomial distribution (2.34) with $K = 2$.

2.3. The Gaussian Distribution

The Gaussian, also known as the normal distribution, is a widely used model for the distribution of continuous variables. In the case of a single variable x , the Gaussian distribution can be written in the form

$$\mathcal{N}(x|\mu, \sigma^2) = \frac{1}{(2\pi\sigma^2)^{1/2}} \exp\left\{-\frac{1}{2\sigma^2}(x - \mu)^2\right\} \quad (2.42)$$

where μ is the mean and σ^2 is the variance. For a D -dimensional vector \mathbf{x} , the multivariate Gaussian distribution takes the form

$$\mathcal{N}(\mathbf{x}|\boldsymbol{\mu}, \boldsymbol{\Sigma}) = \frac{1}{(2\pi)^{D/2}} \frac{1}{|\boldsymbol{\Sigma}|^{1/2}} \exp\left\{-\frac{1}{2}(\mathbf{x} - \boldsymbol{\mu})^T \boldsymbol{\Sigma}^{-1} (\mathbf{x} - \boldsymbol{\mu})\right\} \quad (2.43)$$

where $\boldsymbol{\mu}$ is a D -dimensional mean vector, $\boldsymbol{\Sigma}$ is a $D \times D$ covariance matrix, and $|\boldsymbol{\Sigma}|$ denotes the determinant of $\boldsymbol{\Sigma}$.

Section 1.6

The Gaussian distribution arises in many different contexts and can be motivated from a variety of different perspectives. For example, we have already seen that for a single real variable, the distribution that maximizes the entropy is the Gaussian. This property applies also to the multivariate Gaussian.

Exercise 2.14

Another situation in which the Gaussian distribution arises is when we consider the sum of multiple random variables. The *central limit theorem* (due to Laplace) tells us that, subject to certain mild conditions, the sum of a set of random variables, which is of course itself a random variable, has a distribution that becomes increasingly Gaussian as the number of terms in the sum increases (Walker, 1969). We can

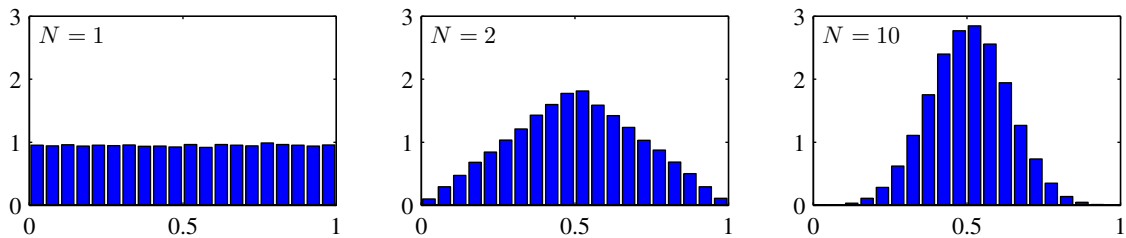


Figure 2.6 Histogram plots of the mean of N uniformly distributed numbers for various values of N . We observe that as N increases, the distribution tends towards a Gaussian.

illustrate this by considering N variables x_1, \dots, x_N each of which has a uniform distribution over the interval $[0, 1]$ and then considering the distribution of the mean $(x_1 + \dots + x_N)/N$. For large N , this distribution tends to a Gaussian, as illustrated in Figure 2.6. In practice, the convergence to a Gaussian as N increases can be very rapid. One consequence of this result is that the binomial distribution (2.9), which is a distribution over m defined by the sum of N observations of the random binary variable x , will tend to a Gaussian as $N \rightarrow \infty$ (see Figure 2.1 for the case of $N = 10$).

The Gaussian distribution has many important analytical properties, and we shall consider several of these in detail. As a result, this section will be rather more technically involved than some of the earlier sections, and will require familiarity with various matrix identities. However, we strongly encourage the reader to become proficient in manipulating Gaussian distributions using the techniques presented here as this will prove invaluable in understanding the more complex models presented in later chapters.

We begin by considering the geometrical form of the Gaussian distribution. The

Appendix C



Carl Friedrich Gauss
1777–1855

It is said that when Gauss went to elementary school at age 7, his teacher Büttner, trying to keep the class occupied, asked the pupils to sum the integers from 1 to 100. To the teacher's amazement, Gauss arrived at the answer in a matter of moments by noting that the sum can be represented as 50 pairs ($1 + 100$, $2 + 99$, etc.) each of which added to 101, giving the answer 5,050. It is now believed that the problem which was actually set was of the same form but somewhat harder in that the sequence had a larger starting value and a larger increment. Gauss was a German math-

ematician and scientist with a reputation for being a hard-working perfectionist. One of his many contributions was to show that least squares can be derived under the assumption of normally distributed errors. He also created an early formulation of non-Euclidean geometry (a self-consistent geometrical theory that violates the axioms of Euclid) but was reluctant to discuss it openly for fear that his reputation might suffer if it were seen that he believed in such a geometry. At one point, Gauss was asked to conduct a geodetic survey of the state of Hanover, which led to his formulation of the normal distribution, now also known as the Gaussian. After his death, a study of his diaries revealed that he had discovered several important mathematical results years or even decades before they were published by others.

functional dependence of the Gaussian on \mathbf{x} is through the quadratic form

$$\Delta^2 = (\mathbf{x} - \boldsymbol{\mu})^T \boldsymbol{\Sigma}^{-1} (\mathbf{x} - \boldsymbol{\mu}) \quad (2.44)$$

which appears in the exponent. The quantity Δ is called the *Mahalanobis distance* from $\boldsymbol{\mu}$ to \mathbf{x} and reduces to the Euclidean distance when $\boldsymbol{\Sigma}$ is the identity matrix. The Gaussian distribution will be constant on surfaces in \mathbf{x} -space for which this quadratic form is constant.

First of all, we note that the matrix $\boldsymbol{\Sigma}$ can be taken to be symmetric, without loss of generality, because any antisymmetric component would disappear from the exponent. Now consider the eigenvector equation for the covariance matrix

$$\boldsymbol{\Sigma} \mathbf{u}_i = \lambda_i \mathbf{u}_i \quad (2.45)$$

Exercise 2.17

Exercise 2.18

where $i = 1, \dots, D$. Because $\boldsymbol{\Sigma}$ is a real, symmetric matrix its eigenvalues will be real, and its eigenvectors can be chosen to form an orthonormal set, so that

$$\mathbf{u}_i^T \mathbf{u}_j = I_{ij} \quad (2.46)$$

where I_{ij} is the i, j element of the identity matrix and satisfies

$$I_{ij} = \begin{cases} 1, & \text{if } i = j \\ 0, & \text{otherwise.} \end{cases} \quad (2.47)$$

Exercise 2.19

The covariance matrix $\boldsymbol{\Sigma}$ can be expressed as an expansion in terms of its eigenvectors in the form

$$\boldsymbol{\Sigma} = \sum_{i=1}^D \lambda_i \mathbf{u}_i \mathbf{u}_i^T \quad (2.48)$$

and similarly the inverse covariance matrix $\boldsymbol{\Sigma}^{-1}$ can be expressed as

$$\boldsymbol{\Sigma}^{-1} = \sum_{i=1}^D \frac{1}{\lambda_i} \mathbf{u}_i \mathbf{u}_i^T. \quad (2.49)$$

Substituting (2.49) into (2.44), the quadratic form becomes

$$\Delta^2 = \sum_{i=1}^D \frac{y_i^2}{\lambda_i} \quad (2.50)$$

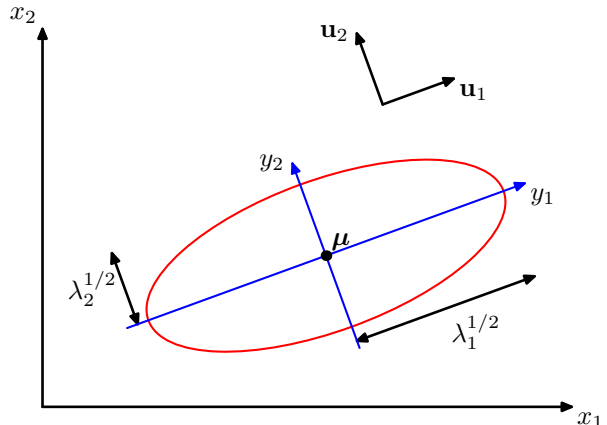
where we have defined

$$y_i = \mathbf{u}_i^T (\mathbf{x} - \boldsymbol{\mu}). \quad (2.51)$$

We can interpret $\{y_i\}$ as a new coordinate system defined by the orthonormal vectors \mathbf{u}_i that are shifted and rotated with respect to the original x_i coordinates. Forming the vector $\mathbf{y} = (y_1, \dots, y_D)^T$, we have

$$\mathbf{y} = \mathbf{U}(\mathbf{x} - \boldsymbol{\mu}) \quad (2.52)$$

Figure 2.7 The red curve shows the elliptical surface of constant probability density for a Gaussian in a two-dimensional space $\mathbf{x} = (x_1, x_2)$ on which the density is $\exp(-1/2)$ of its value at $\mathbf{x} = \mu$. The major axes of the ellipse are defined by the eigenvectors \mathbf{u}_i of the covariance matrix, with corresponding eigenvalues λ_i .



Appendix C

where \mathbf{U} is a matrix whose rows are given by \mathbf{u}_i^T . From (2.46) it follows that \mathbf{U} is an *orthogonal* matrix, i.e., it satisfies $\mathbf{U}\mathbf{U}^T = \mathbf{I}$, and hence also $\mathbf{U}^T\mathbf{U} = \mathbf{I}$, where \mathbf{I} is the identity matrix.

The quadratic form, and hence the Gaussian density, will be constant on surfaces for which (2.51) is constant. If all of the eigenvalues λ_i are positive, then these surfaces represent ellipsoids, with their centres at μ and their axes oriented along \mathbf{u}_i , and with scaling factors in the directions of the axes given by $\lambda_i^{1/2}$, as illustrated in Figure 2.7.

For the Gaussian distribution to be well defined, it is necessary for all of the eigenvalues λ_i of the covariance matrix to be strictly positive, otherwise the distribution cannot be properly normalized. A matrix whose eigenvalues are strictly positive is said to be *positive definite*. In Chapter 12, we will encounter Gaussian distributions for which one or more of the eigenvalues are zero, in which case the distribution is singular and is confined to a subspace of lower dimensionality. If all of the eigenvalues are nonnegative, then the covariance matrix is said to be *positive semidefinite*.

Now consider the form of the Gaussian distribution in the new coordinate system defined by the y_i . In going from the \mathbf{x} to the \mathbf{y} coordinate system, we have a Jacobian matrix \mathbf{J} with elements given by

$$J_{ij} = \frac{\partial x_i}{\partial y_j} = U_{ji} \quad (2.53)$$

where U_{ji} are the elements of the matrix \mathbf{U}^T . Using the orthonormality property of the matrix \mathbf{U} , we see that the square of the determinant of the Jacobian matrix is

$$|\mathbf{J}|^2 = |\mathbf{U}^T|^2 = |\mathbf{U}^T| |\mathbf{U}| = |\mathbf{U}^T \mathbf{U}| = |\mathbf{I}| = 1 \quad (2.54)$$

and hence $|\mathbf{J}| = 1$. Also, the determinant $|\Sigma|$ of the covariance matrix can be written

as the product of its eigenvalues, and hence

$$|\Sigma|^{1/2} = \prod_{j=1}^D \lambda_j^{1/2}. \quad (2.55)$$

Thus in the y_j coordinate system, the Gaussian distribution takes the form

$$p(\mathbf{y}) = p(\mathbf{x})|\mathbf{J}| = \prod_{j=1}^D \frac{1}{(2\pi\lambda_j)^{1/2}} \exp\left\{-\frac{y_j^2}{2\lambda_j}\right\} \quad (2.56)$$

which is the product of D independent univariate Gaussian distributions. The eigenvectors therefore define a new set of shifted and rotated coordinates with respect to which the joint probability distribution factorizes into a product of independent distributions. The integral of the distribution in the \mathbf{y} coordinate system is then

$$\int p(\mathbf{y}) d\mathbf{y} = \prod_{j=1}^D \int_{-\infty}^{\infty} \frac{1}{(2\pi\lambda_j)^{1/2}} \exp\left\{-\frac{y_j^2}{2\lambda_j}\right\} dy_j = 1 \quad (2.57)$$

where we have used the result (1.48) for the normalization of the univariate Gaussian. This confirms that the multivariate Gaussian (2.43) is indeed normalized.

We now look at the moments of the Gaussian distribution and thereby provide an interpretation of the parameters $\boldsymbol{\mu}$ and Σ . The expectation of \mathbf{x} under the Gaussian distribution is given by

$$\begin{aligned} \mathbb{E}[\mathbf{x}] &= \frac{1}{(2\pi)^{D/2}} \frac{1}{|\Sigma|^{1/2}} \int \exp\left\{-\frac{1}{2}(\mathbf{x} - \boldsymbol{\mu})^T \Sigma^{-1} (\mathbf{x} - \boldsymbol{\mu})\right\} \mathbf{x} d\mathbf{x} \\ &= \frac{1}{(2\pi)^{D/2}} \frac{1}{|\Sigma|^{1/2}} \int \exp\left\{-\frac{1}{2}\mathbf{z}^T \Sigma^{-1} \mathbf{z}\right\} (\mathbf{z} + \boldsymbol{\mu}) d\mathbf{z} \end{aligned} \quad (2.58)$$

where we have changed variables using $\mathbf{z} = \mathbf{x} - \boldsymbol{\mu}$. We now note that the exponent is an even function of the components of \mathbf{z} and, because the integrals over these are taken over the range $(-\infty, \infty)$, the term in \mathbf{z} in the factor $(\mathbf{z} + \boldsymbol{\mu})$ will vanish by symmetry. Thus

$$\mathbb{E}[\mathbf{x}] = \boldsymbol{\mu} \quad (2.59)$$

and so we refer to $\boldsymbol{\mu}$ as the mean of the Gaussian distribution.

We now consider second order moments of the Gaussian. In the univariate case, we considered the second order moment given by $\mathbb{E}[x^2]$. For the multivariate Gaussian, there are D^2 second order moments given by $\mathbb{E}[x_i x_j]$, which we can group together to form the matrix $\mathbb{E}[\mathbf{x}\mathbf{x}^T]$. This matrix can be written as

$$\begin{aligned} \mathbb{E}[\mathbf{x}\mathbf{x}^T] &= \frac{1}{(2\pi)^{D/2}} \frac{1}{|\Sigma|^{1/2}} \int \exp\left\{-\frac{1}{2}(\mathbf{x} - \boldsymbol{\mu})^T \Sigma^{-1} (\mathbf{x} - \boldsymbol{\mu})\right\} \mathbf{x}\mathbf{x}^T d\mathbf{x} \\ &= \frac{1}{(2\pi)^{D/2}} \frac{1}{|\Sigma|^{1/2}} \int \exp\left\{-\frac{1}{2}\mathbf{z}^T \Sigma^{-1} \mathbf{z}\right\} (\mathbf{z} + \boldsymbol{\mu})(\mathbf{z} + \boldsymbol{\mu})^T d\mathbf{z} \end{aligned}$$

where again we have changed variables using $\mathbf{z} = \mathbf{x} - \boldsymbol{\mu}$. Note that the cross-terms involving $\boldsymbol{\mu}\mathbf{z}^T$ and $\boldsymbol{\mu}^T\mathbf{z}$ will again vanish by symmetry. The term $\boldsymbol{\mu}\boldsymbol{\mu}^T$ is constant and can be taken outside the integral, which itself is unity because the Gaussian distribution is normalized. Consider the term involving $\mathbf{z}\mathbf{z}^T$. Again, we can make use of the eigenvector expansion of the covariance matrix given by (2.45), together with the completeness of the set of eigenvectors, to write

$$\mathbf{z} = \sum_{j=1}^D y_j \mathbf{u}_j \quad (2.60)$$

where $y_j = \mathbf{u}_j^T \mathbf{z}$, which gives

$$\begin{aligned} & \frac{1}{(2\pi)^{D/2}} \frac{1}{|\boldsymbol{\Sigma}|^{1/2}} \int \exp \left\{ -\frac{1}{2} \mathbf{z}^T \boldsymbol{\Sigma}^{-1} \mathbf{z} \right\} \mathbf{z} \mathbf{z}^T d\mathbf{z} \\ &= \frac{1}{(2\pi)^{D/2}} \frac{1}{|\boldsymbol{\Sigma}|^{1/2}} \sum_{i=1}^D \sum_{j=1}^D \mathbf{u}_i \mathbf{u}_j^T \int \exp \left\{ -\sum_{k=1}^D \frac{y_k^2}{2\lambda_k} \right\} y_i y_j dy \\ &= \sum_{i=1}^D \mathbf{u}_i \mathbf{u}_i^T \lambda_i = \boldsymbol{\Sigma} \end{aligned} \quad (2.61)$$

where we have made use of the eigenvector equation (2.45), together with the fact that the integral on the right-hand side of the middle line vanishes by symmetry unless $i = j$, and in the final line we have made use of the results (1.50) and (2.55), together with (2.48). Thus we have

$$\mathbb{E}[\mathbf{x}\mathbf{x}^T] = \boldsymbol{\mu}\boldsymbol{\mu}^T + \boldsymbol{\Sigma}. \quad (2.62)$$

For single random variables, we subtracted the mean before taking second moments in order to define a variance. Similarly, in the multivariate case it is again convenient to subtract off the mean, giving rise to the *covariance* of a random vector \mathbf{x} defined by

$$\text{cov}[\mathbf{x}] = \mathbb{E}[(\mathbf{x} - \mathbb{E}[\mathbf{x}])(\mathbf{x} - \mathbb{E}[\mathbf{x}])^T]. \quad (2.63)$$

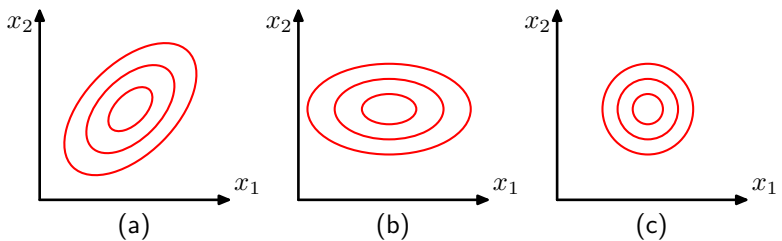
For the specific case of a Gaussian distribution, we can make use of $\mathbb{E}[\mathbf{x}] = \boldsymbol{\mu}$, together with the result (2.62), to give

$$\text{cov}[\mathbf{x}] = \boldsymbol{\Sigma}. \quad (2.64)$$

Because the parameter matrix $\boldsymbol{\Sigma}$ governs the covariance of \mathbf{x} under the Gaussian distribution, it is called **the covariance matrix**.

Although the Gaussian distribution (2.43) is widely used as a density model, it suffers from some significant limitations. Consider the number of free parameters in the distribution. A general symmetric covariance matrix $\boldsymbol{\Sigma}$ will have $D(D + 1)/2$ independent parameters, and there are another D independent parameters in $\boldsymbol{\mu}$, giving $D(D + 3)/2$ parameters in total. For large D , the total number of parameters

Figure 2.8 Contours of constant probability density for a Gaussian distribution in two dimensions in which the covariance matrix is (a) of general form, (b) diagonal, in which the elliptical contours are aligned with the coordinate axes, and (c) proportional to the identity matrix, in which the contours are concentric circles.



therefore grows quadratically with D , and the computational task of manipulating and inverting large matrices can become prohibitive. One way to address this problem is to use restricted forms of the covariance matrix. If we consider covariance matrices that are *diagonal*, so that $\Sigma = \text{diag}(\sigma_i^2)$, we then have a total of $2D$ independent parameters in the density model. The corresponding contours of constant density are given by axis-aligned ellipsoids. We could further restrict the covariance matrix to be proportional to the identity matrix, $\Sigma = \sigma^2 \mathbf{I}$, known as an *isotropic* covariance, giving $D + 1$ independent parameters in the model and spherical surfaces of constant density. The three possibilities of general, diagonal, and isotropic covariance matrices are illustrated in Figure 2.8. Unfortunately, whereas such approaches limit the number of degrees of freedom in the distribution and make inversion of the covariance matrix a much faster operation, they also greatly restrict the form of the probability density and limit its ability to capture interesting correlations in the data.

A further limitation of the Gaussian distribution is that it is intrinsically unimodal (i.e., has a single maximum) and so is unable to provide a good approximation to multimodal distributions. Thus the Gaussian distribution can be both too flexible, in the sense of having too many parameters, while also being too limited in the range of distributions that it can adequately represent. We will see later that the introduction of *latent variables*, also called *hidden* variables or *unobserved* variables, allows both of these problems to be addressed. In particular, a rich family of multimodal distributions is obtained by introducing discrete latent variables leading to mixtures of Gaussians, as discussed in Section 2.3.9. Similarly, the introduction of continuous latent variables, as described in Chapter 12, leads to models in which the number of free parameters can be controlled independently of the dimensionality D of the data space while still allowing the model to capture the dominant correlations in the data set. Indeed, these two approaches can be combined and further extended to derive a very rich set of hierarchical models that can be adapted to a broad range of practical applications.

Section 8.3

Section 13.3

For instance, the Gaussian version of the *Markov random field*, which is widely used as a probabilistic model of images, is a Gaussian distribution over the joint space of pixel intensities but rendered tractable through the imposition of considerable structure reflecting the spatial organization of the pixels. Similarly, the *linear dynamical system*, used to model time series data for applications such as tracking, is also a joint Gaussian distribution over a potentially large number of observed and latent variables and again is tractable due to the structure imposed on the distribution. A powerful framework for expressing the form and properties of

such complex distributions is that of probabilistic graphical models, which will form the subject of Chapter 8.

2.3.1 Conditional Gaussian distributions

An important property of the multivariate Gaussian distribution is that if two sets of variables are jointly Gaussian, then the conditional distribution of one set conditioned on the other is again Gaussian. Similarly, the marginal distribution of either set is also Gaussian.

Consider first the case of conditional distributions. Suppose \mathbf{x} is a D -dimensional vector with Gaussian distribution $\mathcal{N}(\mathbf{x}|\boldsymbol{\mu}, \boldsymbol{\Sigma})$ and that we partition \mathbf{x} into two disjoint subsets \mathbf{x}_a and \mathbf{x}_b . Without loss of generality, we can take \mathbf{x}_a to form the first M components of \mathbf{x} , with \mathbf{x}_b comprising the remaining $D - M$ components, so that

$$\mathbf{x} = \begin{pmatrix} \mathbf{x}_a \\ \mathbf{x}_b \end{pmatrix}. \quad (2.65)$$

We also define corresponding partitions of the mean vector $\boldsymbol{\mu}$ given by

$$\boldsymbol{\mu} = \begin{pmatrix} \boldsymbol{\mu}_a \\ \boldsymbol{\mu}_b \end{pmatrix} \quad (2.66)$$

and of the covariance matrix $\boldsymbol{\Sigma}$ given by

$$\boldsymbol{\Sigma} = \begin{pmatrix} \boldsymbol{\Sigma}_{aa} & \boldsymbol{\Sigma}_{ab} \\ \boldsymbol{\Sigma}_{ba} & \boldsymbol{\Sigma}_{bb} \end{pmatrix}. \quad (2.67)$$

Note that the symmetry $\boldsymbol{\Sigma}^T = \boldsymbol{\Sigma}$ of the covariance matrix implies that $\boldsymbol{\Sigma}_{aa}$ and $\boldsymbol{\Sigma}_{bb}$ are symmetric, while $\boldsymbol{\Sigma}_{ba} = \boldsymbol{\Sigma}_{ab}^T$.

In many situations, it will be convenient to work with the inverse of the covariance matrix

$$\boldsymbol{\Lambda} \equiv \boldsymbol{\Sigma}^{-1} \quad (2.68)$$

which is known as the *precision matrix*. In fact, we shall see that some properties of Gaussian distributions are most naturally expressed in terms of the covariance, whereas others take a simpler form when viewed in terms of the precision. We therefore also introduce the partitioned form of the precision matrix

$$\boldsymbol{\Lambda} = \begin{pmatrix} \boldsymbol{\Lambda}_{aa} & \boldsymbol{\Lambda}_{ab} \\ \boldsymbol{\Lambda}_{ba} & \boldsymbol{\Lambda}_{bb} \end{pmatrix} \quad (2.69)$$

Exercise 2.22 corresponding to the partitioning (2.65) of the vector \mathbf{x} . Because the inverse of a symmetric matrix is also symmetric, we see that $\boldsymbol{\Lambda}_{aa}$ and $\boldsymbol{\Lambda}_{bb}$ are symmetric, while $\boldsymbol{\Lambda}_{ab}^T = \boldsymbol{\Lambda}_{ba}$. It should be stressed at this point that, for instance, $\boldsymbol{\Lambda}_{aa}$ is not simply given by the inverse of $\boldsymbol{\Sigma}_{aa}$. In fact, we shall shortly examine the relation between the inverse of a partitioned matrix and the inverses of its partitions.

Let us begin by finding an expression for the conditional distribution $p(\mathbf{x}_a|\mathbf{x}_b)$. From the product rule of probability, we see that this conditional distribution can be

evaluated from the joint distribution $p(\mathbf{x}) = p(\mathbf{x}_a, \mathbf{x}_b)$ simply by fixing \mathbf{x}_b to the observed value and normalizing the resulting expression to obtain a valid probability distribution over \mathbf{x}_a . Instead of performing this normalization explicitly, we can obtain the solution more efficiently by considering the quadratic form in the exponent of the Gaussian distribution given by (2.44) and then reinstating the normalization coefficient at the end of the calculation. If we make use of the partitioning (2.65), (2.66), and (2.69), we obtain

$$\begin{aligned} -\frac{1}{2}(\mathbf{x} - \boldsymbol{\mu})^T \boldsymbol{\Sigma}^{-1} (\mathbf{x} - \boldsymbol{\mu}) &= \\ -\frac{1}{2}(\mathbf{x}_a - \boldsymbol{\mu}_a)^T \boldsymbol{\Lambda}_{aa} (\mathbf{x}_a - \boldsymbol{\mu}_a) - \frac{1}{2}(\mathbf{x}_a - \boldsymbol{\mu}_a)^T \boldsymbol{\Lambda}_{ab} (\mathbf{x}_b - \boldsymbol{\mu}_b) \\ -\frac{1}{2}(\mathbf{x}_b - \boldsymbol{\mu}_b)^T \boldsymbol{\Lambda}_{ba} (\mathbf{x}_a - \boldsymbol{\mu}_a) - \frac{1}{2}(\mathbf{x}_b - \boldsymbol{\mu}_b)^T \boldsymbol{\Lambda}_{bb} (\mathbf{x}_b - \boldsymbol{\mu}_b). \end{aligned} \quad (2.70)$$

We see that as a function of \mathbf{x}_a , this is again a quadratic form, and hence the corresponding conditional distribution $p(\mathbf{x}_a | \mathbf{x}_b)$ will be Gaussian. Because this distribution is completely characterized by its mean and its covariance, our goal will be to identify expressions for the mean and covariance of $p(\mathbf{x}_a | \mathbf{x}_b)$ by inspection of (2.70).

This is an example of a rather common operation associated with Gaussian distributions, sometimes called ‘completing the square’, in which we are given a quadratic form defining the exponent terms in a Gaussian distribution, and we need to determine the corresponding mean and covariance. Such problems can be solved straightforwardly by noting that the exponent in a general Gaussian distribution $\mathcal{N}(\mathbf{x} | \boldsymbol{\mu}, \boldsymbol{\Sigma})$ can be written

$$-\frac{1}{2}(\mathbf{x} - \boldsymbol{\mu})^T \boldsymbol{\Sigma}^{-1} (\mathbf{x} - \boldsymbol{\mu}) = -\frac{1}{2}\mathbf{x}^T \boldsymbol{\Sigma}^{-1} \mathbf{x} + \mathbf{x}^T \boldsymbol{\Sigma}^{-1} \boldsymbol{\mu} + \text{const} \quad (2.71)$$

where ‘const’ denotes terms which are independent of \mathbf{x} , and we have made use of the symmetry of $\boldsymbol{\Sigma}$. Thus if we take our general quadratic form and express it in the form given by the right-hand side of (2.71), then we can immediately equate the matrix of coefficients entering the second order term in \mathbf{x} to the inverse covariance matrix $\boldsymbol{\Sigma}^{-1}$ and the coefficient of the linear term in \mathbf{x} to $\boldsymbol{\Sigma}^{-1} \boldsymbol{\mu}$, from which we can obtain $\boldsymbol{\mu}$.

Now let us apply this procedure to the conditional Gaussian distribution $p(\mathbf{x}_a | \mathbf{x}_b)$ for which the quadratic form in the exponent is given by (2.70). We will denote the mean and covariance of this distribution by $\boldsymbol{\mu}_{a|b}$ and $\boldsymbol{\Sigma}_{a|b}$, respectively. Consider the functional dependence of (2.70) on \mathbf{x}_a in which \mathbf{x}_b is regarded as a constant. If we pick out all terms that are second order in \mathbf{x}_a , we have

$$-\frac{1}{2}\mathbf{x}_a^T \boldsymbol{\Lambda}_{aa} \mathbf{x}_a \quad (2.72)$$

from which we can immediately conclude that the covariance (inverse precision) of $p(\mathbf{x}_a | \mathbf{x}_b)$ is given by

$$\boldsymbol{\Sigma}_{a|b} = \boldsymbol{\Lambda}_{aa}^{-1}. \quad (2.73)$$

Now consider all of the terms in (2.70) that are linear in \mathbf{x}_a

$$\mathbf{x}_a^T \{ \boldsymbol{\Lambda}_{aa} \boldsymbol{\mu}_a - \boldsymbol{\Lambda}_{ab} (\mathbf{x}_b - \boldsymbol{\mu}_b) \} \quad (2.74)$$

where we have used $\boldsymbol{\Lambda}_{ba}^T = \boldsymbol{\Lambda}_{ab}$. From our discussion of the general form (2.71), the coefficient of \mathbf{x}_a in this expression must equal $\boldsymbol{\Sigma}_{a|b}^{-1} \boldsymbol{\mu}_{a|b}$ and hence

$$\begin{aligned} \boldsymbol{\mu}_{a|b} &= \boldsymbol{\Sigma}_{a|b} \{ \boldsymbol{\Lambda}_{aa} \boldsymbol{\mu}_a - \boldsymbol{\Lambda}_{ab} (\mathbf{x}_b - \boldsymbol{\mu}_b) \} \\ &= \boldsymbol{\mu}_a - \boldsymbol{\Lambda}_{aa}^{-1} \boldsymbol{\Lambda}_{ab} (\mathbf{x}_b - \boldsymbol{\mu}_b) \end{aligned} \quad (2.75)$$

where we have made use of (2.73).

The results (2.73) and (2.75) are expressed in terms of the partitioned precision matrix of the original joint distribution $p(\mathbf{x}_a, \mathbf{x}_b)$. We can also express these results in terms of the corresponding partitioned covariance matrix. To do this, we make use of the following identity for the inverse of a partitioned matrix

$$\begin{pmatrix} \mathbf{A} & \mathbf{B} \\ \mathbf{C} & \mathbf{D} \end{pmatrix}^{-1} = \begin{pmatrix} \mathbf{M} & -\mathbf{MBD}^{-1} \\ -\mathbf{D}^{-1}\mathbf{CM} & \mathbf{D}^{-1} + \mathbf{D}^{-1}\mathbf{CMBD}^{-1} \end{pmatrix} \quad (2.76)$$

where we have defined

$$\mathbf{M} = (\mathbf{A} - \mathbf{BD}^{-1}\mathbf{C})^{-1}. \quad (2.77)$$

The quantity \mathbf{M}^{-1} is known as the *Schur complement* of the matrix on the left-hand side of (2.76) with respect to the submatrix \mathbf{D} . Using the definition

$$\begin{pmatrix} \boldsymbol{\Sigma}_{aa} & \boldsymbol{\Sigma}_{ab} \\ \boldsymbol{\Sigma}_{ba} & \boldsymbol{\Sigma}_{bb} \end{pmatrix}^{-1} = \begin{pmatrix} \boldsymbol{\Lambda}_{aa} & \boldsymbol{\Lambda}_{ab} \\ \boldsymbol{\Lambda}_{ba} & \boldsymbol{\Lambda}_{bb} \end{pmatrix} \quad (2.78)$$

and making use of (2.76), we have

$$\boldsymbol{\Lambda}_{aa} = (\boldsymbol{\Sigma}_{aa} - \boldsymbol{\Sigma}_{ab} \boldsymbol{\Sigma}_{bb}^{-1} \boldsymbol{\Sigma}_{ba})^{-1} \quad (2.79)$$

$$\boldsymbol{\Lambda}_{ab} = -(\boldsymbol{\Sigma}_{aa} - \boldsymbol{\Sigma}_{ab} \boldsymbol{\Sigma}_{bb}^{-1} \boldsymbol{\Sigma}_{ba})^{-1} \boldsymbol{\Sigma}_{ab} \boldsymbol{\Sigma}_{bb}^{-1}. \quad (2.80)$$

From these we obtain the following expressions for the mean and covariance of the conditional distribution $p(\mathbf{x}_a | \mathbf{x}_b)$

$$\boldsymbol{\mu}_{a|b} = \boldsymbol{\mu}_a + \boldsymbol{\Sigma}_{ab} \boldsymbol{\Sigma}_{bb}^{-1} (\mathbf{x}_b - \boldsymbol{\mu}_b) \quad (2.81)$$

$$\boldsymbol{\Sigma}_{a|b} = \boldsymbol{\Sigma}_{aa} - \boldsymbol{\Sigma}_{ab} \boldsymbol{\Sigma}_{bb}^{-1} \boldsymbol{\Sigma}_{ba}. \quad (2.82)$$

Comparing (2.73) and (2.82), we see that the conditional distribution $p(\mathbf{x}_a | \mathbf{x}_b)$ takes a simpler form when expressed in terms of the partitioned precision matrix than when it is expressed in terms of the partitioned covariance matrix. Note that the mean of the conditional distribution $p(\mathbf{x}_a | \mathbf{x}_b)$, given by (2.81), is a linear function of \mathbf{x}_b and that the covariance, given by (2.82), is independent of \mathbf{x}_a . This represents an example of a *linear-Gaussian model*.

Section 8.1.4

2.3.2 Marginal Gaussian distributions

We have seen that if a joint distribution $p(\mathbf{x}_a, \mathbf{x}_b)$ is Gaussian, then the conditional distribution $p(\mathbf{x}_a | \mathbf{x}_b)$ will again be Gaussian. Now we turn to a discussion of the marginal distribution given by

$$p(\mathbf{x}_a) = \int p(\mathbf{x}_a, \mathbf{x}_b) d\mathbf{x}_b \quad (2.83)$$

which, as we shall see, is also Gaussian. Once again, our strategy for evaluating this distribution efficiently will be to focus on the quadratic form in the exponent of the joint distribution and thereby to identify the mean and covariance of the marginal distribution $p(\mathbf{x}_a)$.

The quadratic form for the joint distribution can be expressed, using the partitioned precision matrix, in the form (2.70). Because our goal is to integrate out \mathbf{x}_b , this is most easily achieved by first considering the terms involving \mathbf{x}_b and then completing the square in order to facilitate integration. Picking out just those terms that involve \mathbf{x}_b , we have

$$-\frac{1}{2} \mathbf{x}_b^T \boldsymbol{\Lambda}_{bb} \mathbf{x}_b + \mathbf{x}_b^T \mathbf{m} = -\frac{1}{2} (\mathbf{x}_b - \boldsymbol{\Lambda}_{bb}^{-1} \mathbf{m})^T \boldsymbol{\Lambda}_{bb} (\mathbf{x}_b - \boldsymbol{\Lambda}_{bb}^{-1} \mathbf{m}) + \frac{1}{2} \mathbf{m}^T \boldsymbol{\Lambda}_{bb}^{-1} \mathbf{m} \quad (2.84)$$

where we have defined

$$\mathbf{m} = \boldsymbol{\Lambda}_{bb} \boldsymbol{\mu}_b - \boldsymbol{\Lambda}_{ba} (\mathbf{x}_a - \boldsymbol{\mu}_a). \quad (2.85)$$

We see that the dependence on \mathbf{x}_b has been cast into the standard quadratic form of a Gaussian distribution corresponding to the first term on the right-hand side of (2.84), plus a term that does not depend on \mathbf{x}_b (but that does depend on \mathbf{x}_a). Thus, when we take the exponential of this quadratic form, we see that the integration over \mathbf{x}_b required by (2.83) will take the form

$$\int \exp \left\{ -\frac{1}{2} (\mathbf{x}_b - \boldsymbol{\Lambda}_{bb}^{-1} \mathbf{m})^T \boldsymbol{\Lambda}_{bb} (\mathbf{x}_b - \boldsymbol{\Lambda}_{bb}^{-1} \mathbf{m}) \right\} d\mathbf{x}_b. \quad (2.86)$$

This integration is easily performed by noting that it is the integral over an unnormalized Gaussian, and so the result will be the reciprocal of the normalization coefficient. We know from the form of the normalized Gaussian given by (2.43), that this coefficient is independent of the mean and depends only on the determinant of the covariance matrix. Thus, by completing the square with respect to \mathbf{x}_b , we can integrate out \mathbf{x}_b and the only term remaining from the contributions on the left-hand side of (2.84) that depends on \mathbf{x}_a is the last term on the right-hand side of (2.84) in which \mathbf{m} is given by (2.85). Combining this term with the remaining terms from

(2.70) that depend on \mathbf{x}_a , we obtain

$$\begin{aligned} & \frac{1}{2} [\Lambda_{bb}\boldsymbol{\mu}_b - \Lambda_{ba}(\mathbf{x}_a - \boldsymbol{\mu}_a)]^T \Lambda_{bb}^{-1} [\Lambda_{bb}\boldsymbol{\mu}_b - \Lambda_{ba}(\mathbf{x}_a - \boldsymbol{\mu}_a)] \\ & - \frac{1}{2} \mathbf{x}_a^T \Lambda_{aa} \mathbf{x}_a + \mathbf{x}_a^T (\Lambda_{aa}\boldsymbol{\mu}_a + \Lambda_{ab}\boldsymbol{\mu}_b) + \text{const} \\ = & -\frac{1}{2} \mathbf{x}_a^T (\Lambda_{aa} - \Lambda_{ab}\Lambda_{bb}^{-1}\Lambda_{ba}) \mathbf{x}_a \\ & + \mathbf{x}_a^T (\Lambda_{aa} - \Lambda_{ab}\Lambda_{bb}^{-1}\Lambda_{ba})^{-1} \boldsymbol{\mu}_a + \text{const} \end{aligned} \quad (2.87)$$

where ‘const’ denotes quantities independent of \mathbf{x}_a . Again, by comparison with (2.71), we see that the covariance of the marginal distribution of $p(\mathbf{x}_a)$ is given by

$$\Sigma_a = (\Lambda_{aa} - \Lambda_{ab}\Lambda_{bb}^{-1}\Lambda_{ba})^{-1}. \quad (2.88)$$

Similarly, the mean is given by

$$\Sigma_a (\Lambda_{aa} - \Lambda_{ab}\Lambda_{bb}^{-1}\Lambda_{ba}) \boldsymbol{\mu}_a = \boldsymbol{\mu}_a \quad (2.89)$$

where we have used (2.88). The covariance in (2.88) is expressed in terms of the partitioned precision matrix given by (2.69). We can rewrite this in terms of the corresponding partitioning of the covariance matrix given by (2.67), as we did for the conditional distribution. These partitioned matrices are related by

$$\begin{pmatrix} \Lambda_{aa} & \Lambda_{ab} \\ \Lambda_{ba} & \Lambda_{bb} \end{pmatrix}^{-1} = \begin{pmatrix} \Sigma_{aa} & \Sigma_{ab} \\ \Sigma_{ba} & \Sigma_{bb} \end{pmatrix} \quad (2.90)$$

Making use of (2.76), we then have

$$(\Lambda_{aa} - \Lambda_{ab}\Lambda_{bb}^{-1}\Lambda_{ba})^{-1} = \Sigma_{aa}. \quad (2.91)$$

Thus we obtain the intuitively satisfying result that the marginal distribution $p(\mathbf{x}_a)$ has mean and covariance given by

$$\mathbb{E}[\mathbf{x}_a] = \boldsymbol{\mu}_a \quad (2.92)$$

$$\text{cov}[\mathbf{x}_a] = \Sigma_{aa}. \quad (2.93)$$

We see that for a marginal distribution, the mean and covariance are most simply expressed in terms of the partitioned covariance matrix, in contrast to the conditional distribution for which the partitioned precision matrix gives rise to simpler expressions.

Our results for the marginal and conditional distributions of a partitioned Gaussian are summarized below.

Partitioned Gaussians

Given a joint Gaussian distribution $\mathcal{N}(\mathbf{x}|\boldsymbol{\mu}, \boldsymbol{\Sigma})$ with $\boldsymbol{\Lambda} \equiv \boldsymbol{\Sigma}^{-1}$ and

$$\mathbf{x} = \begin{pmatrix} \mathbf{x}_a \\ \mathbf{x}_b \end{pmatrix}, \quad \boldsymbol{\mu} = \begin{pmatrix} \boldsymbol{\mu}_a \\ \boldsymbol{\mu}_b \end{pmatrix} \quad (2.94)$$

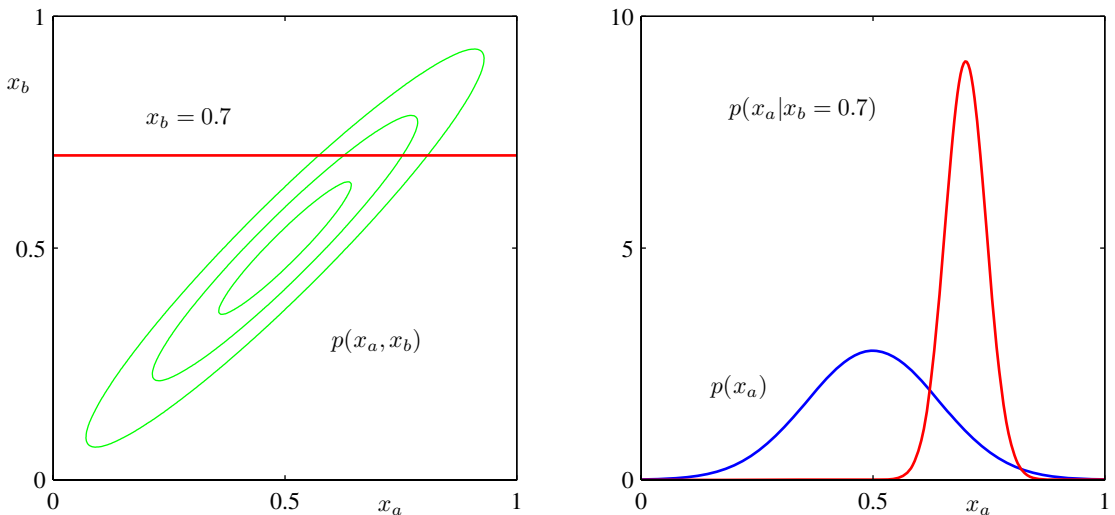


Figure 2.9 The plot on the left shows the contours of a Gaussian distribution $p(x_a, x_b)$ over two variables, and the plot on the right shows the marginal distribution $p(x_a)$ (blue curve) and the conditional distribution $p(x_a|x_b)$ for $x_b = 0.7$.

$$\Sigma = \begin{pmatrix} \Sigma_{aa} & \Sigma_{ab} \\ \Sigma_{ba} & \Sigma_{bb} \end{pmatrix}, \quad \Lambda = \begin{pmatrix} \Lambda_{aa} & \Lambda_{ab} \\ \Lambda_{ba} & \Lambda_{bb} \end{pmatrix}. \quad (2.95)$$

Conditional distribution:

$$p(\mathbf{x}_a|\mathbf{x}_b) = \mathcal{N}(\mathbf{x}_a|\boldsymbol{\mu}_{a|b}, \Lambda_{aa}^{-1}) \quad (2.96)$$

$$\boldsymbol{\mu}_{a|b} = \boldsymbol{\mu}_a - \Lambda_{aa}^{-1} \Lambda_{ab} (\mathbf{x}_b - \boldsymbol{\mu}_b). \quad (2.97)$$

Marginal distribution:

$$p(\mathbf{x}_a) = \mathcal{N}(\mathbf{x}_a|\boldsymbol{\mu}_a, \Sigma_{aa}). \quad (2.98)$$

We illustrate the idea of conditional and marginal distributions associated with a multivariate Gaussian using an example involving two variables in Figure 2.9.

2.3.3 Bayes' theorem for Gaussian variables

In Sections 2.3.1 and 2.3.2, we considered a Gaussian $p(\mathbf{x})$ in which we partitioned the vector \mathbf{x} into two subvectors $\mathbf{x} = (\mathbf{x}_a, \mathbf{x}_b)$ and then found expressions for the conditional distribution $p(\mathbf{x}_a|\mathbf{x}_b)$ and the marginal distribution $p(\mathbf{x}_a)$. We noted that the mean of the conditional distribution $p(\mathbf{x}_a|\mathbf{x}_b)$ was a linear function of \mathbf{x}_b . Here we shall suppose that we are given a Gaussian marginal distribution $p(\mathbf{x})$ and a Gaussian conditional distribution $p(\mathbf{y}|\mathbf{x})$ in which $p(\mathbf{y}|\mathbf{x})$ has a mean that is a linear function of \mathbf{x} , and a covariance which is independent of \mathbf{x} . This is an example of

a *linear Gaussian model* (Roweis and Ghahramani, 1999), which we shall study in greater generality in Section 8.1.4. We wish to find the marginal distribution $p(\mathbf{y})$ and the conditional distribution $p(\mathbf{x}|\mathbf{y})$. This is a problem that will arise frequently in subsequent chapters, and it will prove convenient to derive the general results here.

We shall take the marginal and conditional distributions to be

$$p(\mathbf{x}) = \mathcal{N}(\mathbf{x}|\boldsymbol{\mu}, \boldsymbol{\Lambda}^{-1}) \quad (2.99)$$

$$p(\mathbf{y}|\mathbf{x}) = \mathcal{N}(\mathbf{y}|\mathbf{Ax} + \mathbf{b}, \mathbf{L}^{-1}) \quad (2.100)$$

where $\boldsymbol{\mu}$, \mathbf{A} , and \mathbf{b} are parameters governing the means, and $\boldsymbol{\Lambda}$ and \mathbf{L} are precision matrices. If \mathbf{x} has dimensionality M and \mathbf{y} has dimensionality D , then the matrix \mathbf{A} has size $D \times M$.

First we find an expression for the joint distribution over \mathbf{x} and \mathbf{y} . To do this, we define

$$\mathbf{z} = \begin{pmatrix} \mathbf{x} \\ \mathbf{y} \end{pmatrix} \quad (2.101)$$

and then consider the log of the joint distribution

$$\begin{aligned} \ln p(\mathbf{z}) &= \ln p(\mathbf{x}) + \ln p(\mathbf{y}|\mathbf{x}) \\ &= -\frac{1}{2}(\mathbf{x} - \boldsymbol{\mu})^T \boldsymbol{\Lambda} (\mathbf{x} - \boldsymbol{\mu}) \\ &\quad -\frac{1}{2}(\mathbf{y} - \mathbf{Ax} - \mathbf{b})^T \mathbf{L} (\mathbf{y} - \mathbf{Ax} - \mathbf{b}) + \text{const} \end{aligned} \quad (2.102)$$

where ‘const’ denotes terms independent of \mathbf{x} and \mathbf{y} . As before, we see that this is a quadratic function of the components of \mathbf{z} , and hence $p(\mathbf{z})$ is Gaussian distribution. To find the precision of this Gaussian, we consider the second order terms in (2.102), which can be written as

$$\begin{aligned} &-\frac{1}{2}\mathbf{x}^T(\boldsymbol{\Lambda} + \mathbf{A}^T \mathbf{L} \mathbf{A})\mathbf{x} - \frac{1}{2}\mathbf{y}^T \mathbf{L} \mathbf{y} + \frac{1}{2}\mathbf{y}^T \mathbf{L} \mathbf{A} \mathbf{x} + \frac{1}{2}\mathbf{x}^T \mathbf{A}^T \mathbf{L} \mathbf{y} \\ &= -\frac{1}{2} \begin{pmatrix} \mathbf{x} \\ \mathbf{y} \end{pmatrix}^T \begin{pmatrix} \boldsymbol{\Lambda} + \mathbf{A}^T \mathbf{L} \mathbf{A} & -\mathbf{A}^T \mathbf{L} \\ -\mathbf{L} \mathbf{A} & \mathbf{L} \end{pmatrix} \begin{pmatrix} \mathbf{x} \\ \mathbf{y} \end{pmatrix} = -\frac{1}{2} \mathbf{z}^T \mathbf{R} \mathbf{z} \end{aligned} \quad (2.103)$$

and so the Gaussian distribution over \mathbf{z} has precision (inverse covariance) matrix given by

$$\mathbf{R} = \begin{pmatrix} \boldsymbol{\Lambda} + \mathbf{A}^T \mathbf{L} \mathbf{A} & -\mathbf{A}^T \mathbf{L} \\ -\mathbf{L} \mathbf{A} & \mathbf{L} \end{pmatrix}. \quad (2.104)$$

The covariance matrix is found by taking the inverse of the precision, which can be done using the matrix inversion formula (2.76) to give

$$\text{cov}[\mathbf{z}] = \mathbf{R}^{-1} = \begin{pmatrix} \boldsymbol{\Lambda}^{-1} & \boldsymbol{\Lambda}^{-1} \mathbf{A}^T \\ \mathbf{A} \boldsymbol{\Lambda}^{-1} & \mathbf{L}^{-1} + \mathbf{A} \boldsymbol{\Lambda}^{-1} \mathbf{A}^T \end{pmatrix}. \quad (2.105)$$

Exercise 2.29

Similarly, we can find the mean of the Gaussian distribution over \mathbf{z} by identifying the linear terms in (2.102), which are given by

$$\mathbf{x}^T \boldsymbol{\Lambda} \boldsymbol{\mu} - \mathbf{x}^T \mathbf{A}^T \mathbf{L} \mathbf{b} + \mathbf{y}^T \mathbf{L} \mathbf{b} = \begin{pmatrix} \mathbf{x} \\ \mathbf{y} \end{pmatrix}^T \begin{pmatrix} \boldsymbol{\Lambda} \boldsymbol{\mu} - \mathbf{A}^T \mathbf{L} \mathbf{b} \\ \mathbf{L} \mathbf{b} \end{pmatrix}. \quad (2.106)$$

Using our earlier result (2.71) obtained by completing the square over the quadratic form of a multivariate Gaussian, we find that the mean of \mathbf{z} is given by

$$\mathbb{E}[\mathbf{z}] = \mathbf{R}^{-1} \begin{pmatrix} \boldsymbol{\Lambda} \boldsymbol{\mu} - \mathbf{A}^T \mathbf{L} \mathbf{b} \\ \mathbf{L} \mathbf{b} \end{pmatrix}. \quad (2.107)$$

Exercise 2.30

Making use of (2.105), we then obtain

$$\mathbb{E}[\mathbf{z}] = \begin{pmatrix} \boldsymbol{\mu} \\ \mathbf{A} \boldsymbol{\mu} + \mathbf{b} \end{pmatrix}. \quad (2.108)$$

Section 2.3

Next we find an expression for the marginal distribution $p(\mathbf{y})$ in which we have marginalized over \mathbf{x} . Recall that the marginal distribution over a subset of the components of a Gaussian random vector takes a particularly simple form when expressed in terms of the partitioned covariance matrix. Specifically, its mean and covariance are given by (2.92) and (2.93), respectively. Making use of (2.105) and (2.108) we see that the mean and covariance of the marginal distribution $p(\mathbf{y})$ are given by

$$\mathbb{E}[\mathbf{y}] = \mathbf{A} \boldsymbol{\mu} + \mathbf{b} \quad (2.109)$$

$$\text{cov}[\mathbf{y}] = \mathbf{L}^{-1} + \mathbf{A} \boldsymbol{\Lambda}^{-1} \mathbf{A}^T. \quad (2.110)$$

Section 2.3

A special case of this result is when $\mathbf{A} = \mathbf{I}$, in which case it reduces to the convolution of two Gaussians, for which we see that the mean of the convolution is the sum of the mean of the two Gaussians, and the covariance of the convolution is the sum of their covariances.

Finally, we seek an expression for the conditional $p(\mathbf{x}|\mathbf{y})$. Recall that the results for the conditional distribution are most easily expressed in terms of the partitioned precision matrix, using (2.73) and (2.75). Applying these results to (2.105) and (2.108) we see that the conditional distribution $p(\mathbf{x}|\mathbf{y})$ has mean and covariance given by

$$\mathbb{E}[\mathbf{x}|\mathbf{y}] = (\boldsymbol{\Lambda} + \mathbf{A}^T \mathbf{L} \mathbf{A})^{-1} \{ \mathbf{A}^T \mathbf{L} (\mathbf{y} - \mathbf{b}) + \boldsymbol{\Lambda} \boldsymbol{\mu} \} \quad (2.111)$$

$$\text{cov}[\mathbf{x}|\mathbf{y}] = (\boldsymbol{\Lambda} + \mathbf{A}^T \mathbf{L} \mathbf{A})^{-1}. \quad (2.112)$$

The evaluation of this conditional can be seen as an example of Bayes' theorem. We can interpret the distribution $p(\mathbf{x})$ as a prior distribution over \mathbf{x} . If the variable \mathbf{y} is observed, then the conditional distribution $p(\mathbf{x}|\mathbf{y})$ represents the corresponding posterior distribution over \mathbf{x} . Having found the marginal and conditional distributions, we effectively expressed the joint distribution $p(\mathbf{z}) = p(\mathbf{x})p(\mathbf{y}|\mathbf{x})$ in the form $p(\mathbf{x}|\mathbf{y})p(\mathbf{y})$. These results are summarized below.

Marginal and Conditional Gaussians

Given a marginal Gaussian distribution for \mathbf{x} and a conditional Gaussian distribution for \mathbf{y} given \mathbf{x} in the form

$$p(\mathbf{x}) = \mathcal{N}(\mathbf{x}|\boldsymbol{\mu}, \boldsymbol{\Lambda}^{-1}) \quad (2.113)$$

$$p(\mathbf{y}|\mathbf{x}) = \mathcal{N}(\mathbf{y}|\mathbf{Ax} + \mathbf{b}, \mathbf{L}^{-1}) \quad (2.114)$$

the marginal distribution of \mathbf{y} and the conditional distribution of \mathbf{x} given \mathbf{y} are given by

$$p(\mathbf{y}) = \mathcal{N}(\mathbf{y}|\mathbf{A}\boldsymbol{\mu} + \mathbf{b}, \mathbf{L}^{-1} + \mathbf{A}\boldsymbol{\Lambda}^{-1}\mathbf{A}^T) \quad (2.115)$$

$$p(\mathbf{x}|\mathbf{y}) = \mathcal{N}(\mathbf{x}|\boldsymbol{\Sigma}\{\mathbf{A}^T\mathbf{L}(\mathbf{y} - \mathbf{b}) + \boldsymbol{\Lambda}\boldsymbol{\mu}\}, \boldsymbol{\Sigma}) \quad (2.116)$$

where

$$\boldsymbol{\Sigma} = (\boldsymbol{\Lambda} + \mathbf{A}^T\mathbf{L}\mathbf{A})^{-1}. \quad (2.117)$$

2.3.4 Maximum likelihood for the Gaussian

Given a data set $\mathbf{X} = (\mathbf{x}_1, \dots, \mathbf{x}_N)^T$ in which the observations $\{\mathbf{x}_n\}$ are assumed to be drawn independently from a multivariate Gaussian distribution, we can estimate the parameters of the distribution by maximum likelihood. The log likelihood function is given by

$$\ln p(\mathbf{X}|\boldsymbol{\mu}, \boldsymbol{\Sigma}) = -\frac{ND}{2} \ln(2\pi) - \frac{N}{2} \ln |\boldsymbol{\Sigma}| - \frac{1}{2} \sum_{n=1}^N (\mathbf{x}_n - \boldsymbol{\mu})^T \boldsymbol{\Sigma}^{-1} (\mathbf{x}_n - \boldsymbol{\mu}). \quad (2.118)$$

By simple rearrangement, we see that the likelihood function depends on the data set only through the two quantities

$$\sum_{n=1}^N \mathbf{x}_n, \quad \sum_{n=1}^N \mathbf{x}_n \mathbf{x}_n^T. \quad (2.119)$$

These are known as the *sufficient statistics* for the Gaussian distribution. Using Appendix C, the derivative of the log likelihood with respect to $\boldsymbol{\mu}$ is given by

$$\frac{\partial}{\partial \boldsymbol{\mu}} \ln p(\mathbf{X}|\boldsymbol{\mu}, \boldsymbol{\Sigma}) = \sum_{n=1}^N \boldsymbol{\Sigma}^{-1} (\mathbf{x}_n - \boldsymbol{\mu}) \quad (2.120)$$

and setting this derivative to zero, we obtain the solution for the maximum likelihood estimate of the mean given by

$$\boldsymbol{\mu}_{ML} = \frac{1}{N} \sum_{n=1}^N \mathbf{x}_n \quad (2.121)$$

Exercise 2.34

which is the mean of the observed set of data points. The maximization of (2.118) with respect to Σ is rather more involved. The simplest approach is to ignore the symmetry constraint and show that the resulting solution is symmetric as required. Alternative derivations of this result, which impose the symmetry and positive definiteness constraints explicitly, can be found in Magnus and Neudecker (1999). The result is as expected and takes the form

$$\boldsymbol{\Sigma}_{\text{ML}} = \frac{1}{N} \sum_{n=1}^N (\mathbf{x}_n - \boldsymbol{\mu}_{\text{ML}})(\mathbf{x}_n - \boldsymbol{\mu}_{\text{ML}})^T \quad (2.122)$$

which involves $\boldsymbol{\mu}_{\text{ML}}$ because this is the result of a joint maximization with respect to $\boldsymbol{\mu}$ and Σ . Note that the solution (2.121) for $\boldsymbol{\mu}_{\text{ML}}$ does not depend on $\boldsymbol{\Sigma}_{\text{ML}}$, and so we can first evaluate $\boldsymbol{\mu}_{\text{ML}}$ and then use this to evaluate $\boldsymbol{\Sigma}_{\text{ML}}$.

Exercise 2.35

If we evaluate the expectations of the maximum likelihood solutions under the true distribution, we obtain the following results

$$\mathbb{E}[\boldsymbol{\mu}_{\text{ML}}] = \boldsymbol{\mu} \quad (2.123)$$

$$\mathbb{E}[\boldsymbol{\Sigma}_{\text{ML}}] = \frac{N-1}{N} \boldsymbol{\Sigma}. \quad (2.124)$$

We see that the expectation of the maximum likelihood estimate for the mean is equal to the true mean. However, the maximum likelihood estimate for the covariance has an expectation that is less than the true value, and hence it is biased. We can correct this bias by defining a different estimator $\tilde{\boldsymbol{\Sigma}}$ given by

$$\tilde{\boldsymbol{\Sigma}} = \frac{1}{N-1} \sum_{n=1}^N (\mathbf{x}_n - \boldsymbol{\mu}_{\text{ML}})(\mathbf{x}_n - \boldsymbol{\mu}_{\text{ML}})^T. \quad (2.125)$$

Clearly from (2.122) and (2.124), the expectation of $\tilde{\boldsymbol{\Sigma}}$ is equal to $\boldsymbol{\Sigma}$.

2.3.5 Sequential estimation

Our discussion of the maximum likelihood solution for the parameters of a Gaussian distribution provides a convenient opportunity to give a more general discussion of the topic of sequential estimation for maximum likelihood. Sequential methods allow data points to be processed one at a time and then discarded and are important for on-line applications, and also where large data sets are involved so that batch processing of all data points at once is infeasible.

Consider the result (2.121) for the maximum likelihood estimator of the mean $\boldsymbol{\mu}_{\text{ML}}$, which we will denote by $\boldsymbol{\mu}_{\text{ML}}^{(N)}$ when it is based on N observations. If we

Figure 2.10 A schematic illustration of two correlated random variables z and θ , together with the regression function $f(\theta)$ given by the conditional expectation $\mathbb{E}[z|\theta]$. The Robbins-Monro algorithm provides a general sequential procedure for finding the root θ^* of such functions.



dissect out the contribution from the final data point \mathbf{x}_N , we obtain

$$\begin{aligned}
 \boldsymbol{\mu}_{\text{ML}}^{(N)} &= \frac{1}{N} \sum_{n=1}^N \mathbf{x}_n \\
 &= \frac{1}{N} \mathbf{x}_N + \frac{1}{N} \sum_{n=1}^{N-1} \mathbf{x}_n \\
 &= \frac{1}{N} \mathbf{x}_N + \frac{N-1}{N} \boldsymbol{\mu}_{\text{ML}}^{(N-1)} \\
 &= \boldsymbol{\mu}_{\text{ML}}^{(N-1)} + \frac{1}{N} (\mathbf{x}_N - \boldsymbol{\mu}_{\text{ML}}^{(N-1)}). \tag{2.126}
 \end{aligned}$$

This result has a nice interpretation, as follows. After observing $N-1$ data points we have estimated $\boldsymbol{\mu}$ by $\boldsymbol{\mu}_{\text{ML}}^{(N-1)}$. We now observe data point \mathbf{x}_N , and we obtain our revised estimate $\boldsymbol{\mu}_{\text{ML}}^{(N)}$ by moving the old estimate a small amount, proportional to $1/N$, in the direction of the ‘error signal’ $(\mathbf{x}_N - \boldsymbol{\mu}_{\text{ML}}^{(N-1)})$. Note that, as N increases, so the contribution from successive data points gets smaller.

The result (2.126) will clearly give the same answer as the batch result (2.121) because the two formulae are equivalent. However, we will not always be able to derive a sequential algorithm by this route, and so we seek a more general formulation of sequential learning, which leads us to the *Robbins-Monro* algorithm. Consider a pair of random variables θ and z governed by a joint distribution $p(z, \theta)$. The conditional expectation of z given θ defines a deterministic function $f(\theta)$ that is given by

$$f(\theta) \equiv \mathbb{E}[z|\theta] = \int z p(z|\theta) dz \tag{2.127}$$

and is illustrated schematically in Figure 2.10. Functions defined in this way are called *regression functions*.

Our goal is to find the root θ^* at which $f(\theta^*) = 0$. If we had a large data set of observations of z and θ , then we could model the regression function directly and then obtain an estimate of its root. Suppose, however, that we observe values of z one at a time and we wish to find a corresponding sequential estimation scheme for θ^* . The following general procedure for solving such problems was given by

Robbins and Monro (1951). We shall assume that the conditional variance of z is finite so that

$$\mathbb{E} [(z - f)^2 | \theta] < \infty \quad (2.128)$$

and we shall also, without loss of generality, consider the case where $f(\theta) > 0$ for $\theta > \theta^*$ and $f(\theta) < 0$ for $\theta < \theta^*$, as is the case in Figure 2.10. The Robbins-Monro procedure then defines a sequence of successive estimates of the root θ^* given by

$$\theta^{(N)} = \theta^{(N-1)} + a_{N-1} z(\theta^{(N-1)}) \quad (2.129)$$

where $z(\theta^{(N)})$ is an observed value of z when θ takes the value $\theta^{(N)}$. The coefficients $\{a_N\}$ represent a sequence of positive numbers that satisfy the conditions

$$\lim_{N \rightarrow \infty} a_N = 0 \quad (2.130)$$

$$\sum_{N=1}^{\infty} a_N = \infty \quad (2.131)$$

$$\sum_{N=1}^{\infty} a_N^2 < \infty. \quad (2.132)$$

It can then be shown (Robbins and Monro, 1951; Fukunaga, 1990) that the sequence of estimates given by (2.129) does indeed converge to the root with probability one. Note that the first condition (2.130) ensures that the successive corrections decrease in magnitude so that the process can converge to a limiting value. The second condition (2.131) is required to ensure that the algorithm does not converge short of the root, and the third condition (2.132) is needed to ensure that the accumulated noise has finite variance and hence does not spoil convergence.

Now let us consider how a general maximum likelihood problem can be solved sequentially using the Robbins-Monro algorithm. By definition, the maximum likelihood solution θ_{ML} is a stationary point of the log likelihood function and hence satisfies

$$\frac{\partial}{\partial \theta} \left\{ \frac{1}{N} \sum_{n=1}^N \ln p(\mathbf{x}_n | \theta) \right\} \Big|_{\theta_{ML}} = 0. \quad (2.133)$$

Exchanging the derivative and the summation, and taking the limit $N \rightarrow \infty$ we have

$$\lim_{N \rightarrow \infty} \frac{1}{N} \sum_{n=1}^N \frac{\partial}{\partial \theta} \ln p(x_n | \theta) = \mathbb{E}_x \left[\frac{\partial}{\partial \theta} \ln p(x | \theta) \right] \quad (2.134)$$

and so we see that finding the maximum likelihood solution corresponds to finding the root of a regression function. We can therefore apply the Robbins-Monro procedure, which now takes the form

$$\theta^{(N)} = \theta^{(N-1)} + a_{N-1} \frac{\partial}{\partial \theta^{(N-1)}} \ln p(x_N | \theta^{(N-1)}). \quad (2.135)$$

Figure 2.11 In the case of a Gaussian distribution, with θ corresponding to the mean μ , the regression function illustrated in Figure 2.10 takes the form of a straight line, as shown in red. In this case, the random variable z corresponds to the derivative of the log likelihood function and is given by $(x - \mu_{ML})/\sigma^2$, and its expectation that defines the regression function is a straight line given by $(\mu - \mu_{ML})/\sigma^2$. The root of the regression function corresponds to the maximum likelihood estimator μ_{ML} .



As a specific example, we consider once again the sequential estimation of the mean of a Gaussian distribution, in which case the parameter $\theta^{(N)}$ is the estimate $\mu_{ML}^{(N)}$ of the mean of the Gaussian, and the random variable z is given by

$$z = \frac{\partial}{\partial \mu_{ML}} \ln p(x|\mu_{ML}, \sigma^2) = \frac{1}{\sigma^2}(x - \mu_{ML}). \quad (2.136)$$

Thus the distribution of z is Gaussian with mean $\mu - \mu_{ML}$, as illustrated in Figure 2.11. Substituting (2.136) into (2.135), we obtain the univariate form of (2.126), provided we choose the coefficients a_N to have the form $a_N = \sigma^2/N$. Note that although we have focussed on the case of a single variable, the same technique, together with the same restrictions (2.130)–(2.132) on the coefficients a_N , apply equally to the multivariate case (Blum, 1965).

2.3.6 Bayesian inference for the Gaussian

The maximum likelihood framework gave point estimates for the parameters μ and Σ . Now we develop a Bayesian treatment by introducing prior distributions over these parameters. Let us begin with a simple example in which we consider a single Gaussian random variable x . We shall suppose that the variance σ^2 is known, and we consider the task of inferring the mean μ given a set of N observations $\mathbf{X} = \{x_1, \dots, x_N\}$. The likelihood function, that is the probability of the observed data given μ , viewed as a function of μ , is given by

$$p(\mathbf{X}|\mu) = \prod_{n=1}^N p(x_n|\mu) = \frac{1}{(2\pi\sigma^2)^{N/2}} \exp \left\{ -\frac{1}{2\sigma^2} \sum_{n=1}^N (x_n - \mu)^2 \right\}. \quad (2.137)$$

Again we emphasize that the likelihood function $p(\mathbf{X}|\mu)$ is not a probability distribution over μ and is not normalized.

We see that the likelihood function takes the form of the exponential of a quadratic form in μ . Thus if we choose a prior $p(\mu)$ given by a Gaussian, it will be a

conjugate distribution for this likelihood function because the corresponding posterior will be a product of two exponentials of quadratic functions of μ and hence will also be Gaussian. We therefore take our prior distribution to be

$$p(\mu) = \mathcal{N}(\mu|\mu_0, \sigma_0^2) \quad (2.138)$$

and the posterior distribution is given by

$$p(\mu|\mathbf{X}) \propto p(\mathbf{X}|\mu)p(\mu). \quad (2.139)$$

Exercise 2.38

Simple manipulation involving completing the square in the exponent shows that the posterior distribution is given by

$$p(\mu|\mathbf{X}) = \mathcal{N}(\mu|\mu_N, \sigma_N^2) \quad (2.140)$$

where

$$\mu_N = \frac{\sigma^2}{N\sigma_0^2 + \sigma^2}\mu_0 + \frac{N\sigma_0^2}{N\sigma_0^2 + \sigma^2}\mu_{ML} \quad (2.141)$$

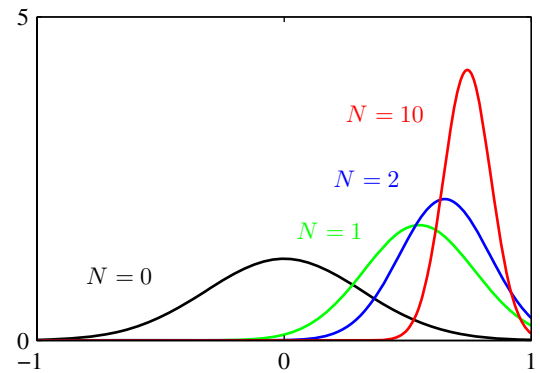
$$\frac{1}{\sigma_N^2} = \frac{1}{\sigma_0^2} + \frac{N}{\sigma^2} \quad (2.142)$$

in which μ_{ML} is the maximum likelihood solution for μ given by the sample mean

$$\mu_{ML} = \frac{1}{N} \sum_{n=1}^N x_n. \quad (2.143)$$

It is worth spending a moment studying the form of the posterior mean and variance. First of all, we note that the mean of the posterior distribution given by (2.141) is a compromise between the prior mean μ_0 and the maximum likelihood solution μ_{ML} . If the number of observed data points $N = 0$, then (2.141) reduces to the prior mean as expected. For $N \rightarrow \infty$, the posterior mean is given by the maximum likelihood solution. Similarly, consider the result (2.142) for the variance of the posterior distribution. **We see that this is most naturally expressed in terms of the inverse variance, which** is called the precision. Furthermore, the precisions are additive, so that the precision of the posterior is given by the precision of the prior plus one contribution of the data precision from each of the observed data points. As we increase the number of observed data points, the precision steadily increases, corresponding to a posterior distribution with steadily decreasing variance. With no observed data points, we have the prior variance, whereas if the number of data points $N \rightarrow \infty$, the variance σ_N^2 goes to zero and the posterior distribution becomes infinitely peaked around the maximum likelihood solution. We therefore see that the maximum likelihood result of a point estimate for μ given by (2.143) is recovered precisely from the Bayesian formalism in the limit of an infinite number of observations. Note also that for finite N , if we take the limit $\sigma_0^2 \rightarrow \infty$ in which the prior has infinite variance then the posterior mean (2.141) reduces to the maximum likelihood result, while from (2.142) the posterior variance is given by $\sigma_N^2 = \sigma^2/N$.

Figure 2.12 Illustration of Bayesian inference for the mean μ of a Gaussian distribution, in which the variance is assumed to be known. The curves show the prior distribution over μ (the curve labelled $N = 0$), which in this case is itself Gaussian, along with the posterior distribution given by (2.140) for increasing numbers N of data points. The data points are generated from a Gaussian of mean 0.8 and variance 0.1, and the prior is chosen to have mean 0. In both the prior and the likelihood function, the variance is set to the true value.



We illustrate our analysis of Bayesian inference for the mean of a Gaussian distribution in Figure 2.12. The generalization of this result to the case of a D -dimensional Gaussian random variable \mathbf{x} with known covariance and unknown mean is straightforward.

Exercise 2.40

Section 2.3.5

We have already seen how the maximum likelihood expression for the mean of a Gaussian can be re-cast as a sequential update formula in which the mean after observing N data points was expressed in terms of the mean after observing $N - 1$ data points together with the contribution from data point \mathbf{x}_N . In fact, the Bayesian paradigm leads very naturally to a sequential view of the inference problem. To see this in the context of the inference of the mean of a Gaussian, we write the posterior distribution with the contribution from the final data point \mathbf{x}_N separated out so that

$$p(\boldsymbol{\mu}|D) \propto \left[p(\boldsymbol{\mu}) \prod_{n=1}^{N-1} p(\mathbf{x}_n|\boldsymbol{\mu}) \right] p(\mathbf{x}_N|\boldsymbol{\mu}). \quad (2.144)$$

The term in square brackets is (up to a normalization coefficient) just the posterior distribution after observing $N - 1$ data points. We see that this can be viewed as a prior distribution, which is combined using Bayes' theorem with the likelihood function associated with data point \mathbf{x}_N to arrive at the posterior distribution after observing N data points. This sequential view of Bayesian inference is very general and applies to any problem in which the observed data are assumed to be independent and identically distributed.

So far, we have assumed that the variance of the Gaussian distribution over the data is known and our goal is to infer the mean. Now let us suppose that the mean is known and we wish to infer the variance. Again, our calculations will be greatly simplified if we choose a conjugate form for the prior distribution. It turns out to be most convenient to work with the precision $\lambda \equiv 1/\sigma^2$. The likelihood function for λ takes the form

$$p(\mathbf{X}|\lambda) = \prod_{n=1}^N \mathcal{N}(x_n|\mu, \lambda^{-1}) \propto \lambda^{N/2} \exp \left\{ -\frac{\lambda}{2} \sum_{n=1}^N (x_n - \mu)^2 \right\}. \quad (2.145)$$



Figure 2.13 Plot of the gamma distribution $\text{Gam}(\lambda|a, b)$ defined by (2.146) for various values of the parameters a and b .

The corresponding conjugate prior should therefore be proportional to the product of a power of λ and the exponential of a linear function of λ . This corresponds to the **gamma** distribution which is defined by

$$\text{Gam}(\lambda|a, b) = \frac{1}{\Gamma(a)} b^a \lambda^{a-1} \exp(-b\lambda). \quad (2.146)$$

Here $\Gamma(a)$ is the gamma function that is defined by (1.141) and that ensures that (2.146) is correctly normalized. The gamma distribution has a finite integral if $a > 0$, and the distribution itself is finite if $a \geq 1$. It is plotted, for various values of a and b , in Figure 2.13. The mean and variance of the gamma distribution are given by

$$\mathbb{E}[\lambda] = \frac{a}{b} \quad (2.147)$$

$$\text{var}[\lambda] = \frac{a}{b^2}. \quad (2.148)$$

Consider a prior distribution $\text{Gam}(\lambda|a_0, b_0)$. If we multiply by the likelihood function (2.145), then we obtain a posterior distribution

$$p(\lambda|\mathbf{X}) \propto \lambda^{a_0-1} \lambda^{N/2} \exp \left\{ -b_0 \lambda - \frac{\lambda}{2} \sum_{n=1}^N (x_n - \mu)^2 \right\} \quad (2.149)$$

which we recognize as a gamma distribution of the form $\text{Gam}(\lambda|a_N, b_N)$ where

$$a_N = a_0 + \frac{N}{2} \quad (2.150)$$

$$b_N = b_0 + \frac{1}{2} \sum_{n=1}^N (x_n - \mu)^2 = b_0 + \frac{N}{2} \sigma_{\text{ML}}^2 \quad (2.151)$$

where σ_{ML}^2 is the maximum likelihood estimator of the variance. Note that in (2.149) there is no need to keep track of the normalization constants in the prior and the likelihood function because, if required, the correct coefficient can be found at the end using the normalized form (2.146) for the gamma distribution.

Section 2.2

From (2.150), we see that the effect of observing N data points is to increase the value of the coefficient a by $N/2$. Thus we can interpret the parameter a_0 in the prior in terms of $2a_0$ ‘effective’ prior observations. Similarly, from (2.151) we see that the N data points contribute $N\sigma_{ML}^2/2$ to the parameter b , where σ_{ML}^2 is the variance, and so we can interpret the parameter b_0 in the prior as arising from the $2a_0$ ‘effective’ prior observations having variance $2b_0/(2a_0) = b_0/a_0$. Recall that we made an analogous interpretation for the Dirichlet prior. These distributions are examples of the exponential family, and we shall see that the interpretation of a conjugate prior in terms of effective fictitious data points is a general one for the exponential family of distributions.

Instead of working with the precision, we can consider the variance itself. The conjugate prior in this case is called the *inverse gamma* distribution, although we shall not discuss this further because we will find it more convenient to work with the precision.

Now suppose that both the mean and the precision are unknown. To find a conjugate prior, we consider the dependence of the likelihood function on μ and λ

$$\begin{aligned} p(\mathbf{X}|\mu, \lambda) &= \prod_{n=1}^N \left(\frac{\lambda}{2\pi} \right)^{1/2} \exp \left\{ -\frac{\lambda}{2}(x_n - \mu)^2 \right\} \\ &\propto \left[\lambda^{1/2} \exp \left(-\frac{\lambda\mu^2}{2} \right) \right]^N \exp \left\{ \lambda\mu \sum_{n=1}^N x_n - \frac{\lambda}{2} \sum_{n=1}^N x_n^2 \right\}. \end{aligned} \quad (2.152)$$

We now wish to identify a prior distribution $p(\mu, \lambda)$ that has the same functional dependence on μ and λ as the likelihood function and that should therefore take the form

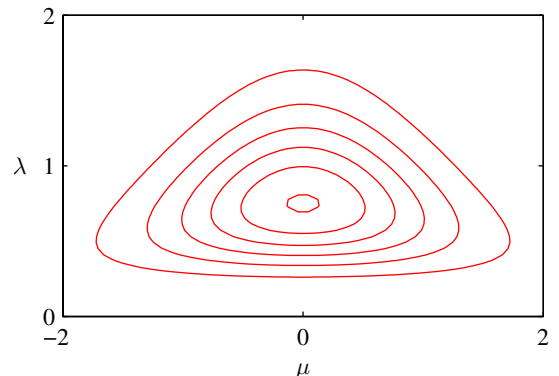
$$\begin{aligned} p(\mu, \lambda) &\propto \left[\lambda^{1/2} \exp \left(-\frac{\lambda\mu^2}{2} \right) \right]^\beta \exp \{c\lambda\mu - d\lambda\} \\ &= \exp \left\{ -\frac{\beta\lambda}{2}(\mu - c/\beta)^2 \right\} \lambda^{\beta/2} \exp \left\{ -\left(d - \frac{c^2}{2\beta} \right) \lambda \right\} \end{aligned} \quad (2.153)$$

where c , d , and β are constants. Since we can always write $p(\mu, \lambda) = p(\mu|\lambda)p(\lambda)$, we can find $p(\mu|\lambda)$ and $p(\lambda)$ by inspection. In particular, we see that $p(\mu|\lambda)$ is a Gaussian whose precision is a linear function of λ and that $p(\lambda)$ is a gamma distribution, so that the normalized prior takes the form

$$p(\mu, \lambda) = \mathcal{N}(\mu|\mu_0, (\beta\lambda)^{-1}) \text{Gam}(\lambda|a, b) \quad (2.154)$$

where we have defined new constants given by $\mu_0 = c/\beta$, $a = 1 + \beta/2$, $b = d - c^2/2\beta$. The distribution (2.154) is called the *normal-gamma* or *Gaussian-gamma* distribution and is plotted in Figure 2.14. Note that this is not simply the product of an independent Gaussian prior over μ and a gamma prior over λ , because the precision of μ is a linear function of λ . Even if we chose a prior in which μ and λ were independent, the posterior distribution would exhibit a coupling between the precision of μ and the value of λ .

Figure 2.14 Contour plot of the normal-gamma distribution (2.154) for parameter values $\mu_0 = 0$, $\beta = 2$, $a = 5$ and $b = 6$.



In the case of the multivariate Gaussian distribution $\mathcal{N}(\mathbf{x}|\boldsymbol{\mu}, \boldsymbol{\Lambda}^{-1})$ for a D -dimensional variable \mathbf{x} , the conjugate prior distribution for the mean $\boldsymbol{\mu}$, assuming the precision is known, is again a Gaussian. For known mean and unknown precision matrix $\boldsymbol{\Lambda}$, the conjugate prior is the *Wishart* distribution given by

$$\mathcal{W}(\boldsymbol{\Lambda}|\mathbf{W}, \nu) = B|\boldsymbol{\Lambda}|^{(\nu-D-1)/2} \exp\left(-\frac{1}{2}\text{Tr}(\mathbf{W}^{-1}\boldsymbol{\Lambda})\right) \quad (2.155)$$

where ν is called the number of *degrees of freedom* of the distribution, \mathbf{W} is a $D \times D$ scale matrix, and $\text{Tr}(\cdot)$ denotes the trace. The normalization constant B is given by

$$B(\mathbf{W}, \nu) = |\mathbf{W}|^{-\nu/2} \left(2^{\nu D/2} \pi^{D(D-1)/4} \prod_{i=1}^D \Gamma\left(\frac{\nu+1-i}{2}\right)\right)^{-1}. \quad (2.156)$$

Again, it is also possible to define a conjugate prior over the covariance matrix itself, rather than over the precision matrix, which leads to the *inverse Wishart* distribution, although we shall not discuss this further. If both the mean and the precision are unknown, then, following a similar line of reasoning to the univariate case, the conjugate prior is given by

$$p(\boldsymbol{\mu}, \boldsymbol{\Lambda}|\boldsymbol{\mu}_0, \beta, \mathbf{W}, \nu) = \mathcal{N}(\boldsymbol{\mu}|\boldsymbol{\mu}_0, (\beta\boldsymbol{\Lambda})^{-1}) \mathcal{W}(\boldsymbol{\Lambda}|\mathbf{W}, \nu) \quad (2.157)$$

which is known as the *normal-Wishart* or *Gaussian-Wishart* distribution.

2.3.7 Student's t-distribution

We have seen that the conjugate prior for the precision of a Gaussian is given by a gamma distribution. If we have a univariate Gaussian $\mathcal{N}(x|\mu, \tau^{-1})$ together with a Gamma prior $\text{Gam}(\tau|a, b)$ and we integrate out the precision, we obtain the marginal distribution of x in the form

Section 2.3.6

Exercise 2.46

Figure 2.15 Plot of Student's t-distribution (2.159) for $\mu = 0$ and $\lambda = 1$ for various values of ν . The limit $\nu \rightarrow \infty$ corresponds to a Gaussian distribution with mean μ and precision λ .



$$\begin{aligned}
 p(x|\mu, a, b) &= \int_0^\infty \mathcal{N}(x|\mu, \tau^{-1}) \text{Gam}(\tau|a, b) d\tau \quad (2.158) \\
 &= \int_0^\infty \frac{b^a e^{(-b\tau)} \tau^{a-1}}{\Gamma(a)} \left(\frac{\tau}{2\pi}\right)^{1/2} \exp\left\{-\frac{\tau}{2}(x-\mu)^2\right\} d\tau \\
 &= \frac{b^a}{\Gamma(a)} \left(\frac{1}{2\pi}\right)^{1/2} \left[b + \frac{(x-\mu)^2}{2}\right]^{-a-1/2} \Gamma(a+1/2)
 \end{aligned}$$

where we have made the change of variable $z = \tau[b + (x - \mu)^2/2]$. By convention we define new parameters given by $\nu = 2a$ and $\lambda = a/b$, in terms of which the distribution $p(x|\mu, a, b)$ takes the form

$$\text{St}(x|\mu, \lambda, \nu) = \frac{\Gamma(\nu/2 + 1/2)}{\Gamma(\nu/2)} \left(\frac{\lambda}{\pi\nu}\right)^{1/2} \left[1 + \frac{\lambda(x-\mu)^2}{\nu}\right]^{-\nu/2-1/2} \quad (2.159)$$

which is known as *Student's t-distribution*. The parameter λ is sometimes called the *precision* of the t-distribution, even though it is not in general equal to the inverse of the variance. The parameter ν is called the *degrees of freedom*, and its effect is illustrated in Figure 2.15. For the particular case of $\nu = 1$, the t-distribution reduces to the *Cauchy distribution*, while in the limit $\nu \rightarrow \infty$ the t-distribution $\text{St}(x|\mu, \lambda, \nu)$ becomes a Gaussian $\mathcal{N}(x|\mu, \lambda^{-1})$ with mean μ and precision λ .

Exercise 2.47

From (2.158), we see that Student's t-distribution is obtained by adding up an infinite number of Gaussian distributions having the same mean but different precisions. This can be interpreted as an infinite mixture of Gaussians (Gaussian mixtures will be discussed in detail in Section 2.3.9). The result is a distribution that in general has longer 'tails' than a Gaussian, as was seen in Figure 2.15. This gives the t-distribution an important property called *robustness*, which means that it is much less sensitive than the Gaussian to the presence of a few data points which are *outliers*. The robustness of the t-distribution is illustrated in Figure 2.16, which compares the maximum likelihood solutions for a Gaussian and a t-distribution. Note that the maximum likelihood solution for the t-distribution can be found using the expectation-maximization (EM) algorithm. Here we see that the effect of a small number of

Exercise 12.24

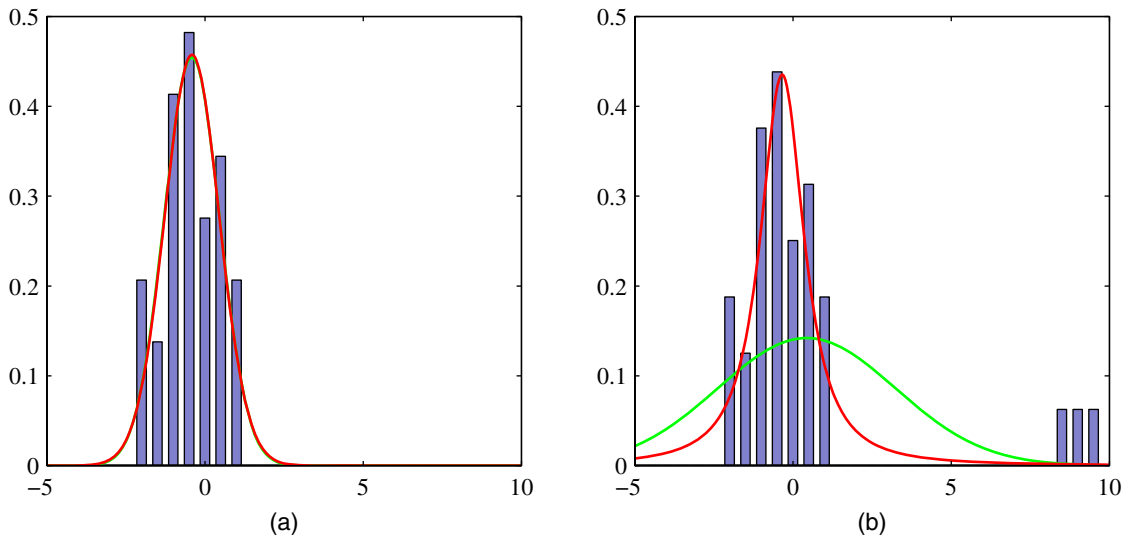


Figure 2.16 Illustration of the robustness of Student's t-distribution compared to a Gaussian. (a) Histogram distribution of 30 data points drawn from a Gaussian distribution, together with the maximum likelihood fit obtained from a t-distribution (red curve) and a Gaussian (green curve, largely hidden by the red curve). Because the t-distribution contains the Gaussian as a special case it gives almost the same solution as the Gaussian. (b) The same data set but with three additional outlying data points showing how the Gaussian (green curve) is strongly distorted by the outliers, whereas the t-distribution (red curve) is relatively unaffected.

outliers is much less significant for the t-distribution than for the Gaussian. Outliers can arise in practical applications either because the process that generates the data corresponds to a distribution having a heavy tail or simply through mislabelled data. Robustness is also an important property for regression problems. Unsurprisingly, the least squares approach to regression does not exhibit robustness, because it corresponds to maximum likelihood under a (conditional) Gaussian distribution. By basing a regression model on a heavy-tailed distribution such as a t-distribution, we obtain a more robust model.

If we go back to (2.158) and substitute the alternative parameters $\nu = 2a$, $\lambda = a/b$, and $\eta = \tau b/a$, we see that the t-distribution can be written in the form

$$\text{St}(x|\mu, \lambda, \nu) = \int_0^\infty \mathcal{N}(x|\mu, (\eta\lambda)^{-1}) \text{Gam}(\eta|\nu/2, \nu/2) d\eta. \quad (2.160)$$

We can then generalize this to a multivariate Gaussian $\mathcal{N}(\mathbf{x}|\boldsymbol{\mu}, \boldsymbol{\Lambda})$ to obtain the corresponding multivariate Student's t-distribution in the form

$$\text{St}(\mathbf{x}|\boldsymbol{\mu}, \boldsymbol{\Lambda}, \nu) = \int_0^\infty \mathcal{N}(\mathbf{x}|\boldsymbol{\mu}, (\eta\boldsymbol{\Lambda})^{-1}) \text{Gam}(\eta|\nu/2, \nu/2) d\eta. \quad (2.161)$$

Using the same technique as for the univariate case, we can evaluate this integral to give

$$\text{St}(\mathbf{x}|\boldsymbol{\mu}, \boldsymbol{\Lambda}, \nu) = \frac{\Gamma(D/2 + \nu/2)}{\Gamma(\nu/2)} \frac{|\boldsymbol{\Lambda}|^{1/2}}{(\pi\nu)^{D/2}} \left[1 + \frac{\Delta^2}{\nu} \right]^{-D/2 - \nu/2} \quad (2.162)$$

where D is the dimensionality of \mathbf{x} , and Δ^2 is the squared Mahalanobis distance defined by

$$\Delta^2 = (\mathbf{x} - \boldsymbol{\mu})^T \boldsymbol{\Lambda} (\mathbf{x} - \boldsymbol{\mu}). \quad (2.163)$$

This is the multivariate form of Student's t-distribution and satisfies the following properties

$$\mathbb{E}[\mathbf{x}] = \boldsymbol{\mu}, \quad \text{if } \nu > 1 \quad (2.164)$$

$$\text{cov}[\mathbf{x}] = \frac{\nu}{(\nu - 2)} \boldsymbol{\Lambda}^{-1}, \quad \text{if } \nu > 2 \quad (2.165)$$

$$\text{mode}[\mathbf{x}] = \boldsymbol{\mu} \quad (2.166)$$

with corresponding results for the univariate case.

2.3.8 Periodic variables

Although Gaussian distributions are of great practical significance, both in their own right and as building blocks for more complex probabilistic models, there are situations in which they are inappropriate as density models for continuous variables. One important case, which arises in practical applications, is that of periodic variables.

An example of a periodic variable would be the wind direction at a particular geographical location. We might, for instance, measure values of wind direction on a number of days and wish to summarize this using a parametric distribution. Another example is calendar time, where we may be interested in modelling quantities that are believed to be periodic over 24 hours or over an annual cycle. Such quantities can conveniently be represented using an angular (polar) coordinate $0 \leq \theta < 2\pi$.

We might be tempted to treat periodic variables by choosing some direction as the origin and then applying a conventional distribution such as the Gaussian. Such an approach, however, would give results that were strongly dependent on the arbitrary choice of origin. Suppose, for instance, that we have two observations at $\theta_1 = 1^\circ$ and $\theta_2 = 359^\circ$, and we model them using a standard univariate Gaussian distribution. If we choose the origin at 0° , then the sample mean of this data set will be 180° with standard deviation 179° , whereas if we choose the origin at 180° , then the mean will be 0° and the standard deviation will be 1° . We clearly need to develop a special approach for the treatment of periodic variables.

Let us consider the problem of evaluating the mean of a set of observations $\mathcal{D} = \{\theta_1, \dots, \theta_N\}$ of a periodic variable. From now on, we shall assume that θ is measured in radians. We have already seen that the simple average $(\theta_1 + \dots + \theta_N)/N$ will be strongly coordinate dependent. To find an invariant measure of the mean, we note that the observations can be viewed as points on the unit circle and can therefore be described instead by two-dimensional unit vectors $\mathbf{x}_1, \dots, \mathbf{x}_N$ where $\|\mathbf{x}_n\| = 1$ for $n = 1, \dots, N$, as illustrated in Figure 2.17. We can average the vectors $\{\mathbf{x}_n\}$

Exercise 2.49

Figure 2.17 Illustration of the representation of values θ_n of a periodic variable as two-dimensional vectors \mathbf{x}_n living on the unit circle. Also shown is the average $\bar{\mathbf{x}}$ of those vectors.



instead to give

$$\bar{\mathbf{x}} = \frac{1}{N} \sum_{n=1}^N \mathbf{x}_n \quad (2.167)$$

and then find the corresponding angle $\bar{\theta}$ of this average. Clearly, this definition will ensure that the location of the mean is independent of the origin of the angular coordinate. Note that $\bar{\mathbf{x}}$ will typically lie inside the unit circle. The Cartesian coordinates of the observations are given by $\mathbf{x}_n = (\cos \theta_n, \sin \theta_n)$, and we can write the Cartesian coordinates of the sample mean in the form $\bar{\mathbf{x}} = (\bar{r} \cos \bar{\theta}, \bar{r} \sin \bar{\theta})$. Substituting into (2.167) and equating the x_1 and x_2 components then gives

$$\bar{r} \cos \bar{\theta} = \frac{1}{N} \sum_{n=1}^N \cos \theta_n, \quad \bar{r} \sin \bar{\theta} = \frac{1}{N} \sum_{n=1}^N \sin \theta_n. \quad (2.168)$$

Taking the ratio, and using the identity $\tan \theta = \sin \theta / \cos \theta$, we can solve for $\bar{\theta}$ to give

$$\bar{\theta} = \tan^{-1} \left\{ \frac{\sum_n \sin \theta_n}{\sum_n \cos \theta_n} \right\}. \quad (2.169)$$

Shortly, we shall see how this result arises naturally as the maximum likelihood estimator for an appropriately defined distribution over a periodic variable.

We now consider a periodic generalization of the Gaussian called the *von Mises* distribution. Here we shall limit our attention to univariate distributions, although periodic distributions can also be found over hyperspheres of arbitrary dimension. For an extensive discussion of periodic distributions, see Mardia and Jupp (2000).

By convention, we will consider distributions $p(\theta)$ that have period 2π . Any probability density $p(\theta)$ defined over θ must not only be nonnegative and integrate

Figure 2.18 The von Mises distribution can be derived by considering a two-dimensional Gaussian of the form (2.173), whose density contours are shown in blue and conditioning on the unit circle shown in red.



to one, but it must also be periodic. Thus $p(\theta)$ must satisfy the three conditions

$$p(\theta) \geq 0 \quad (2.170)$$

$$\int_0^{2\pi} p(\theta) d\theta = 1 \quad (2.171)$$

$$p(\theta + 2\pi) = p(\theta). \quad (2.172)$$

From (2.172), it follows that $p(\theta + M2\pi) = p(\theta)$ for any integer M .

We can easily obtain a Gaussian-like distribution that satisfies these three properties as follows. Consider a Gaussian distribution over two variables $\mathbf{x} = (x_1, x_2)$ having mean $\mu = (\mu_1, \mu_2)$ and a covariance matrix $\Sigma = \sigma^2 \mathbf{I}$ where \mathbf{I} is the 2×2 identity matrix, so that

$$p(x_1, x_2) = \frac{1}{2\pi\sigma^2} \exp \left\{ -\frac{(x_1 - \mu_1)^2 + (x_2 - \mu_2)^2}{2\sigma^2} \right\}. \quad (2.173)$$

The contours of constant $p(\mathbf{x})$ are circles, as illustrated in Figure 2.18. Now suppose we consider the value of this distribution along a circle of fixed radius. Then by construction this distribution will be periodic, although it will not be normalized. We can determine the form of this distribution by transforming from Cartesian coordinates (x_1, x_2) to polar coordinates (r, θ) so that

$$x_1 = r \cos \theta, \quad x_2 = r \sin \theta. \quad (2.174)$$

We also map the mean μ into polar coordinates by writing

$$\mu_1 = r_0 \cos \theta_0, \quad \mu_2 = r_0 \sin \theta_0. \quad (2.175)$$

Next we substitute these transformations into the two-dimensional Gaussian distribution (2.173), and then condition on the unit circle $r = 1$, noting that we are interested only in the dependence on θ . Focussing on the exponent in the Gaussian distribution we have

$$\begin{aligned} & -\frac{1}{2\sigma^2} \{ (r \cos \theta - r_0 \cos \theta_0)^2 + (r \sin \theta - r_0 \sin \theta_0)^2 \} \\ &= -\frac{1}{2\sigma^2} \{ 1 + r_0^2 - 2r_0 \cos \theta \cos \theta_0 - 2r_0 \sin \theta \sin \theta_0 \} \\ &= \frac{r_0}{\sigma^2} \cos(\theta - \theta_0) + \text{const} \end{aligned} \quad (2.176)$$



Figure 2.19 The von Mises distribution plotted for two different parameter values, shown as a Cartesian plot on the left and as the corresponding polar plot on the right.

where ‘const’ denotes terms independent of θ , and we have made use of the following trigonometrical identities

$$\cos^2 A + \sin^2 A = 1 \quad (2.177)$$

$$\cos A \cos B + \sin A \sin B = \cos(A - B). \quad (2.178)$$

If we now define $m = r_0/\sigma^2$, we obtain our final expression for the distribution of $p(\theta)$ along the unit circle $r = 1$ in the form

$$p(\theta|\theta_0, m) = \frac{1}{2\pi I_0(m)} \exp \{m \cos(\theta - \theta_0)\} \quad (2.179)$$

which is called the *von Mises* distribution, or the *circular normal*. Here the parameter θ_0 corresponds to the mean of the distribution, while m , which is known as the *concentration* parameter, is analogous to the inverse variance (precision) for the Gaussian. The normalization coefficient in (2.179) is expressed in terms of $I_0(m)$, which is the zeroth-order Bessel function of the first kind (Abramowitz and Stegun, 1965) and is defined by

$$I_0(m) = \frac{1}{2\pi} \int_0^{2\pi} \exp \{m \cos \theta\} d\theta. \quad (2.180)$$

Exercise 2.52

For large m , the distribution becomes approximately Gaussian. The von Mises distribution is plotted in Figure 2.19, and the function $I_0(m)$ is plotted in Figure 2.20.

Now consider the maximum likelihood estimators for the parameters θ_0 and m for the von Mises distribution. The log likelihood function is given by

$$\ln p(\mathcal{D}|\theta_0, m) = -N \ln(2\pi) - N \ln I_0(m) + m \sum_{n=1}^N \cos(\theta_n - \theta_0). \quad (2.181)$$



Figure 2.20 Plot of the Bessel function $I_0(m)$ defined by (2.180), together with the function $A(m)$ defined by (2.186).

Setting the derivative with respect to θ_0 equal to zero gives

$$\sum_{n=1}^N \sin(\theta_n - \theta_0) = 0. \quad (2.182)$$

To solve for θ_0 , we make use of the trigonometric identity

$$\sin(A - B) = \cos B \sin A - \cos A \sin B \quad (2.183)$$

Exercise 2.53

from which we obtain

$$\theta_0^{\text{ML}} = \tan^{-1} \left\{ \frac{\sum_n \sin \theta_n}{\sum_n \cos \theta_n} \right\} \quad (2.184)$$

which we recognize as the result (2.169) obtained earlier for the mean of the observations viewed in a two-dimensional Cartesian space.

Similarly, maximizing (2.181) with respect to m , and making use of $I'_0(m) = I_1(m)$ (Abramowitz and Stegun, 1965), we have

$$A(m) = \frac{1}{N} \sum_{n=1}^N \cos(\theta_n - \theta_0^{\text{ML}}) \quad (2.185)$$

where we have substituted for the maximum likelihood solution for θ_0^{ML} (recalling that we are performing a joint optimization over θ and m), and we have defined

$$A(m) = \frac{I_1(m)}{I_0(m)}. \quad (2.186)$$

The function $A(m)$ is plotted in Figure 2.20. Making use of the trigonometric identity (2.178), we can write (2.185) in the form

$$A(m_{\text{ML}}) = \left(\frac{1}{N} \sum_{n=1}^N \cos \theta_n \right) \cos \theta_0^{\text{ML}} - \left(\frac{1}{N} \sum_{n=1}^N \sin \theta_n \right) \sin \theta_0^{\text{ML}}. \quad (2.187)$$

Figure 2.21 Plots of the ‘old faithful’ data in which the blue curves show contours of constant probability density. On the left is a single Gaussian distribution which has been fitted to the data using maximum likelihood. Note that this distribution fails to capture the two clumps in the data and indeed places much of its probability mass in the central region between the clumps where the data are relatively sparse. On the right the distribution is given by a linear combination of two Gaussians which has been fitted to the data by maximum likelihood using techniques discussed Chapter 9, and which gives a better representation of the data.



The right-hand side of (2.187) is easily evaluated, and the function $A(m)$ can be inverted numerically.

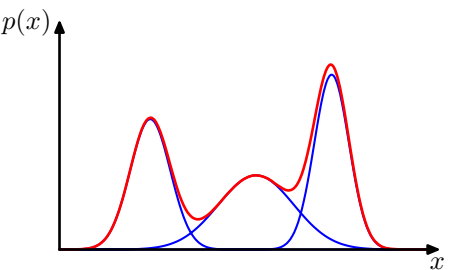
For completeness, we mention briefly some alternative techniques for the construction of periodic distributions. The simplest approach is to use a histogram of observations in which the angular coordinate is divided into fixed bins. This has the virtue of simplicity and flexibility but also suffers from significant limitations, as we shall see when we discuss histogram methods in more detail in Section 2.5. Another approach starts, like the von Mises distribution, from a Gaussian distribution over a Euclidean space but now marginalizes onto the unit circle rather than conditioning (Mardia and Jupp, 2000). However, this leads to more complex forms of distribution and will not be discussed further. Finally, any valid distribution over the real axis (such as a Gaussian) can be turned into a periodic distribution by mapping successive intervals of width 2π onto the periodic variable $(0, 2\pi)$, which corresponds to ‘wrapping’ the real axis around unit circle. Again, the resulting distribution is more complex to handle than the von Mises distribution.

One limitation of the von Mises distribution is that it is unimodal. By forming *mixtures* of von Mises distributions, we obtain a flexible framework for modelling periodic variables that can handle multimodality. For an example of a machine learning application that makes use of von Mises distributions, see Lawrence *et al.* (2002), and for extensions to modelling conditional densities for regression problems, see Bishop and Nabney (1996).

2.3.9 Mixtures of Gaussians

While the Gaussian distribution has some important analytical properties, it suffers from significant limitations when it comes to modelling real data sets. Consider the example shown in Figure 2.21. This is known as the ‘Old Faithful’ data set, and comprises 272 measurements of the eruption of the Old Faithful geyser at Yellowstone National Park in the USA. Each measurement comprises the duration of

Figure 2.22 Example of a Gaussian mixture distribution in one dimension showing three Gaussians (each scaled by a coefficient) in blue and their sum in red.



the eruption in minutes (horizontal axis) and the time in minutes to the next eruption (vertical axis). We see that the data set forms two dominant clumps, and that a simple Gaussian distribution is unable to capture this structure, whereas a linear superposition of two Gaussians gives a better characterization of the data set.

Such superpositions, formed by taking linear combinations of more basic distributions such as Gaussians, can be formulated as probabilistic models known as **mixture distributions** (McLachlan and Basford, 1988; McLachlan and Peel, 2000). In Figure 2.22 we see that a linear combination of Gaussians can give rise to very complex densities. By using a sufficient number of Gaussians, and by adjusting their means and covariances as well as the coefficients in the linear combination, almost any continuous density can be approximated to arbitrary accuracy.

We therefore consider a superposition of K Gaussian densities of the form

$$p(\mathbf{x}) = \sum_{k=1}^K \pi_k \mathcal{N}(\mathbf{x} | \boldsymbol{\mu}_k, \boldsymbol{\Sigma}_k) \quad (2.188)$$

which is called a *mixture of Gaussians*. Each Gaussian density $\mathcal{N}(\mathbf{x} | \boldsymbol{\mu}_k, \boldsymbol{\Sigma}_k)$ is called a *component* of the mixture and has its own mean $\boldsymbol{\mu}_k$ and covariance $\boldsymbol{\Sigma}_k$. Contour and surface plots for a Gaussian mixture having 3 components are shown in Figure 2.23.

In this section we shall consider Gaussian components to illustrate the framework of mixture models. More generally, mixture models can comprise linear combinations of other distributions. For instance, in Section 9.3.3 we shall consider mixtures of **Bernoulli distributions** as an example of a mixture model for discrete variables.

The parameters π_k in (2.188) are called *mixing coefficients*. If we integrate both sides of (2.188) with respect to \mathbf{x} , and note that both $p(\mathbf{x})$ and the individual Gaussian components are normalized, we obtain

$$\sum_{k=1}^K \pi_k = 1. \quad (2.189)$$

Also, the requirement that $p(\mathbf{x}) \geq 0$, together with $\mathcal{N}(\mathbf{x} | \boldsymbol{\mu}_k, \boldsymbol{\Sigma}_k) \geq 0$, implies $\pi_k \geq 0$ for all k . Combining this with the condition (2.189) we obtain

$$0 \leq \pi_k \leq 1. \quad (2.190)$$

Section 9.3.3



Figure 2.23 Illustration of a mixture of 3 Gaussians in a two-dimensional space. (a) Contours of constant density for each of the mixture components, in which the 3 components are denoted red, blue and green, and the values of the mixing coefficients are shown below each component. (b) Contours of the marginal probability density $p(\mathbf{x})$ of the mixture distribution. (c) A surface plot of the distribution $p(\mathbf{x})$.

We therefore see that the mixing coefficients satisfy the requirements to be probabilities.

From the sum and product rules, the marginal density is given by

$$p(\mathbf{x}) = \sum_{k=1}^K p(k)p(\mathbf{x}|k) \quad (2.191)$$

which is equivalent to (2.188) in which we can view $\pi_k = p(k)$ as the prior probability of picking the k^{th} component, and the density $\mathcal{N}(\mathbf{x}|\boldsymbol{\mu}_k, \boldsymbol{\Sigma}_k) = p(\mathbf{x}|k)$ as the probability of \mathbf{x} conditioned on k . As we shall see in later chapters, an important role is played by the posterior probabilities $p(k|\mathbf{x})$, which are also known as *responsibilities*. From Bayes' theorem these are given by

$$\begin{aligned} \gamma_k(\mathbf{x}) &\equiv p(k|\mathbf{x}) \\ &= \frac{p(k)p(\mathbf{x}|k)}{\sum_l p(l)p(\mathbf{x}|l)} \\ &= \frac{\pi_k \mathcal{N}(\mathbf{x}|\boldsymbol{\mu}_k, \boldsymbol{\Sigma}_k)}{\sum_l \pi_l \mathcal{N}(\mathbf{x}|\boldsymbol{\mu}_l, \boldsymbol{\Sigma}_l)}. \end{aligned} \quad (2.192)$$

We shall discuss the probabilistic interpretation of the mixture distribution in greater detail in Chapter 9.

The form of the Gaussian mixture distribution is governed by the parameters $\boldsymbol{\pi}$, $\boldsymbol{\mu}$ and $\boldsymbol{\Sigma}$, where we have used the notation $\boldsymbol{\pi} \equiv \{\pi_1, \dots, \pi_K\}$, $\boldsymbol{\mu} \equiv \{\boldsymbol{\mu}_1, \dots, \boldsymbol{\mu}_K\}$ and $\boldsymbol{\Sigma} \equiv \{\boldsymbol{\Sigma}_1, \dots, \boldsymbol{\Sigma}_K\}$. One way to set the values of these parameters is to use maximum likelihood. From (2.188) the log of the likelihood function is given by

$$\ln p(\mathbf{X}|\boldsymbol{\pi}, \boldsymbol{\mu}, \boldsymbol{\Sigma}) = \sum_{n=1}^N \ln \left\{ \sum_{k=1}^K \pi_k \mathcal{N}(\mathbf{x}_n|\boldsymbol{\mu}_k, \boldsymbol{\Sigma}_k) \right\} \quad (2.193)$$

where $\mathbf{X} = \{\mathbf{x}_1, \dots, \mathbf{x}_N\}$. We immediately see that the situation is now much more complex than with a single Gaussian, due to the presence of the summation over k inside the logarithm. As a result, the maximum likelihood solution for the parameters no longer has a closed-form analytical solution. One approach to maximizing the likelihood function is to use iterative numerical optimization techniques (Fletcher, 1987; Nocedal and Wright, 1999; Bishop and Nabney, 2008). Alternatively we can employ a powerful framework called *expectation maximization*, which will be discussed at length in Chapter 9.

2.4. The Exponential Family

The probability distributions that we have studied so far in this chapter (with the exception of the Gaussian mixture) are specific examples of a broad class of distributions called the *exponential family* (Duda and Hart, 1973; Bernardo and Smith, 1994). Members of the exponential family have many important properties in common, and it is illuminating to discuss these properties in some generality.

The exponential family of distributions over \mathbf{x} , given parameters $\boldsymbol{\eta}$, is defined to be the set of distributions of the form

$$p(\mathbf{x}|\boldsymbol{\eta}) = h(\mathbf{x})g(\boldsymbol{\eta}) \exp \left\{ \boldsymbol{\eta}^T \mathbf{u}(\mathbf{x}) \right\} \quad (2.194)$$

where \mathbf{x} may be scalar or vector, and may be discrete or continuous. Here $\boldsymbol{\eta}$ are called the *natural parameters* of the distribution, and $\mathbf{u}(\mathbf{x})$ is some function of \mathbf{x} . The function $g(\boldsymbol{\eta})$ can be interpreted as the coefficient that ensures that the distribution is normalized and therefore satisfies

$$g(\boldsymbol{\eta}) \int h(\mathbf{x}) \exp \left\{ \boldsymbol{\eta}^T \mathbf{u}(\mathbf{x}) \right\} d\mathbf{x} = 1 \quad (2.195)$$

where the integration is replaced by summation if \mathbf{x} is a discrete variable.

We begin by taking some examples of the distributions introduced earlier in the chapter and showing that they are indeed members of the exponential family. Consider first the Bernoulli distribution

$$p(x|\mu) = \text{Bern}(x|\mu) = \mu^x(1-\mu)^{1-x}. \quad (2.196)$$

Expressing the right-hand side as the exponential of the logarithm, we have

$$\begin{aligned} p(x|\mu) &= \exp \{x \ln \mu + (1-x) \ln(1-\mu)\} \\ &= (1-\mu) \exp \left\{ \ln \left(\frac{\mu}{1-\mu} \right) x \right\}. \end{aligned} \quad (2.197)$$

Comparison with (2.194) allows us to identify

$$\boldsymbol{\eta} = \ln \left(\frac{\mu}{1-\mu} \right) \quad (2.198)$$

which we can solve for μ to give $\mu = \sigma(\eta)$, where

$$\sigma(\eta) = \frac{1}{1 + \exp(-\eta)} \quad (2.199)$$

is called the *logistic sigmoid* function. Thus we can write the Bernoulli distribution using the standard representation (2.194) in the form

$$p(x|\eta) = \sigma(-\eta) \exp(\eta x) \quad (2.200)$$

where we have used $1 - \sigma(\eta) = \sigma(-\eta)$, which is easily proved from (2.199). Comparison with (2.194) shows that

$$u(x) = x \quad (2.201)$$

$$h(x) = 1 \quad (2.202)$$

$$g(\eta) = \sigma(-\eta). \quad (2.203)$$

Next consider the multinomial distribution that, for a single observation \mathbf{x} , takes the form

$$p(\mathbf{x}|\boldsymbol{\mu}) = \prod_{k=1}^M \mu_k^{x_k} = \exp \left\{ \sum_{k=1}^M x_k \ln \mu_k \right\} \quad (2.204)$$

where $\mathbf{x} = (x_1, \dots, x_N)^T$. Again, we can write this in the standard representation (2.194) so that

$$p(\mathbf{x}|\boldsymbol{\eta}) = \exp(\boldsymbol{\eta}^T \mathbf{x}) \quad (2.205)$$

where $\eta_k = \ln \mu_k$, and we have defined $\boldsymbol{\eta} = (\eta_1, \dots, \eta_M)^T$. Again, comparing with (2.194) we have

$$\mathbf{u}(\mathbf{x}) = \mathbf{x} \quad (2.206)$$

$$h(\mathbf{x}) = 1 \quad (2.207)$$

$$g(\boldsymbol{\eta}) = 1. \quad (2.208)$$

Note that the parameters η_k are not independent because the parameters μ_k are subject to the constraint

$$\sum_{k=1}^M \mu_k = 1 \quad (2.209)$$

so that, given any $M - 1$ of the parameters μ_k , the value of the remaining parameter is fixed. In some circumstances, it will be convenient to remove this constraint by expressing the distribution in terms of only $M - 1$ parameters. This can be achieved by using the relationship (2.209) to eliminate μ_M by expressing it in terms of the remaining $\{\mu_k\}$ where $k = 1, \dots, M - 1$, thereby leaving $M - 1$ parameters. Note that these remaining parameters are still subject to the constraints

$$0 \leq \mu_k \leq 1, \quad \sum_{k=1}^{M-1} \mu_k \leq 1. \quad (2.210)$$

Making use of the constraint (2.209), the multinomial distribution in this representation then becomes

$$\begin{aligned} & \exp \left\{ \sum_{k=1}^M x_k \ln \mu_k \right\} \\ = & \exp \left\{ \sum_{k=1}^{M-1} x_k \ln \mu_k + \left(1 - \sum_{k=1}^{M-1} x_k \right) \ln \left(1 - \sum_{k=1}^{M-1} \mu_k \right) \right\} \\ = & \exp \left\{ \sum_{k=1}^{M-1} x_k \ln \left(\frac{\mu_k}{1 - \sum_{j=1}^{M-1} \mu_j} \right) + \ln \left(1 - \sum_{k=1}^{M-1} \mu_k \right) \right\}. \quad (2.211) \end{aligned}$$

We now identify

$$\ln \left(\frac{\mu_k}{1 - \sum_j \mu_j} \right) = \eta_k \quad (2.212)$$

which we can solve for μ_k by first summing both sides over k and then rearranging and back-substituting to give

$$\mu_k = \frac{\exp(\eta_k)}{1 + \sum_j \exp(\eta_j)}. \quad (2.213)$$

This is called the *softmax* function, or the *normalized exponential*. In this representation, the multinomial distribution therefore takes the form

$$p(\mathbf{x}|\boldsymbol{\eta}) = \left(1 + \sum_{k=1}^{M-1} \exp(\eta_k) \right)^{-1} \exp(\boldsymbol{\eta}^T \mathbf{x}). \quad (2.214)$$

This is the standard form of the exponential family, with parameter vector $\boldsymbol{\eta} = (\eta_1, \dots, \eta_{M-1})^T$ in which

$$\mathbf{u}(\mathbf{x}) = \mathbf{x} \quad (2.215)$$

$$h(\mathbf{x}) = 1 \quad (2.216)$$

$$g(\boldsymbol{\eta}) = \left(1 + \sum_{k=1}^{M-1} \exp(\eta_k) \right)^{-1}. \quad (2.217)$$

Finally, let us consider the Gaussian distribution. For the univariate Gaussian, we have

$$p(x|\mu, \sigma^2) = \frac{1}{(2\pi\sigma^2)^{1/2}} \exp \left\{ -\frac{1}{2\sigma^2} (x - \mu)^2 \right\} \quad (2.218)$$

$$= \frac{1}{(2\pi\sigma^2)^{1/2}} \exp \left\{ -\frac{1}{2\sigma^2} x^2 + \frac{\mu}{\sigma^2} x - \frac{1}{2\sigma^2} \mu^2 \right\} \quad (2.219)$$

which, after some simple rearrangement, can be cast in the standard exponential family form (2.194) with

$$\boldsymbol{\eta} = \begin{pmatrix} \mu/\sigma^2 \\ -1/2\sigma^2 \end{pmatrix} \quad (2.220)$$

$$\mathbf{u}(x) = \begin{pmatrix} x \\ x^2 \end{pmatrix} \quad (2.221)$$

$$h(\mathbf{x}) = (2\pi)^{-1/2} \quad (2.222)$$

$$g(\boldsymbol{\eta}) = (-2\eta_2)^{1/2} \exp\left(\frac{\eta_1^2}{4\eta_2}\right). \quad (2.223)$$

2.4.1 Maximum likelihood and sufficient statistics

Let us now consider the problem of estimating the parameter vector $\boldsymbol{\eta}$ in the general exponential family distribution (2.194) using the technique of maximum likelihood. Taking the gradient of both sides of (2.195) with respect to $\boldsymbol{\eta}$, we have

$$\begin{aligned} & \nabla g(\boldsymbol{\eta}) \int h(\mathbf{x}) \exp\{\boldsymbol{\eta}^T \mathbf{u}(\mathbf{x})\} d\mathbf{x} \\ & + g(\boldsymbol{\eta}) \int h(\mathbf{x}) \exp\{\boldsymbol{\eta}^T \mathbf{u}(\mathbf{x})\} \mathbf{u}(\mathbf{x}) d\mathbf{x} = 0. \end{aligned} \quad (2.224)$$

Rearranging, and making use again of (2.195) then gives

$$-\frac{1}{g(\boldsymbol{\eta})} \nabla g(\boldsymbol{\eta}) = g(\boldsymbol{\eta}) \int h(\mathbf{x}) \exp\{\boldsymbol{\eta}^T \mathbf{u}(\mathbf{x})\} \mathbf{u}(\mathbf{x}) d\mathbf{x} = \mathbb{E}[\mathbf{u}(\mathbf{x})] \quad (2.225)$$

where we have used (2.194). We therefore obtain the result

$$-\nabla \ln g(\boldsymbol{\eta}) = \mathbb{E}[\mathbf{u}(\mathbf{x})]. \quad (2.226)$$

Exercise 2.58

Note that the covariance of $\mathbf{u}(\mathbf{x})$ can be expressed in terms of the second derivatives of $g(\boldsymbol{\eta})$, and similarly for higher order moments. Thus, provided we can normalize a distribution from the exponential family, we can always find its moments by simple differentiation.

Now consider a set of independent identically distributed data denoted by $\mathbf{X} = \{\mathbf{x}_1, \dots, \mathbf{x}_n\}$, for which the likelihood function is given by

$$p(\mathbf{X}|\boldsymbol{\eta}) = \left(\prod_{n=1}^N h(\mathbf{x}_n) \right) g(\boldsymbol{\eta})^N \exp\left\{ \boldsymbol{\eta}^T \sum_{n=1}^N \mathbf{u}(\mathbf{x}_n) \right\}. \quad (2.227)$$

Setting the gradient of $\ln p(\mathbf{X}|\boldsymbol{\eta})$ with respect to $\boldsymbol{\eta}$ to zero, we get the following condition to be satisfied by the maximum likelihood estimator $\boldsymbol{\eta}_{ML}$

$$-\nabla \ln g(\boldsymbol{\eta}_{ML}) = \frac{1}{N} \sum_{n=1}^N \mathbf{u}(\mathbf{x}_n) \quad (2.228)$$

which can in principle be solved to obtain $\boldsymbol{\eta}_{\text{ML}}$. We see that the solution for the maximum likelihood estimator depends on the data only through $\sum_n \mathbf{u}(\mathbf{x}_n)$, which is therefore called the *sufficient statistic* of the distribution (2.194). We do not need to store the entire data set itself but only the value of the sufficient statistic. For the Bernoulli distribution, for example, the function $\mathbf{u}(x)$ is given just by x and so we need only keep the sum of the data points $\{\mathbf{x}_n\}$, whereas for the Gaussian $\mathbf{u}(x) = (x, x^2)^T$, and so we should keep both the sum of $\{\mathbf{x}_n\}$ and the sum of $\{x_n^2\}$.

If we consider the limit $N \rightarrow \infty$, then the right-hand side of (2.228) becomes $\mathbb{E}[\mathbf{u}(\mathbf{x})]$, and so by comparing with (2.226) we see that in this limit $\boldsymbol{\eta}_{\text{ML}}$ will equal the true value $\boldsymbol{\eta}$.

In fact, this sufficiency property holds also for Bayesian inference, although we shall defer discussion of this until Chapter 8 when we have equipped ourselves with the tools of graphical models and can thereby gain a deeper insight into these important concepts.

2.4.2 Conjugate priors

We have already encountered the concept of a conjugate prior several times, for example in the context of the Bernoulli distribution (for which the conjugate prior is the beta distribution) or the Gaussian (where the conjugate prior for the mean is a Gaussian, and the conjugate prior for the precision is the Wishart distribution). In general, for a given probability distribution $p(\mathbf{x}|\boldsymbol{\eta})$, we can seek a prior $p(\boldsymbol{\eta})$ that is conjugate to the likelihood function, so that the posterior distribution has the same functional form as the prior. For any member of the exponential family (2.194), there exists a conjugate prior that can be written in the form

$$p(\boldsymbol{\eta}|\boldsymbol{\chi}, \nu) = f(\boldsymbol{\chi}, \nu)g(\boldsymbol{\eta})^\nu \exp \left\{ \nu \boldsymbol{\eta}^T \boldsymbol{\chi} \right\} \quad (2.229)$$

where $f(\boldsymbol{\chi}, \nu)$ is a normalization coefficient, and $g(\boldsymbol{\eta})$ is the same function as appears in (2.194). To see that this is indeed conjugate, let us multiply the prior (2.229) by the likelihood function (2.227) to obtain the posterior distribution, up to a normalization coefficient, in the form

$$p(\boldsymbol{\eta}|\mathbf{X}, \boldsymbol{\chi}, \nu) \propto g(\boldsymbol{\eta})^{\nu+N} \exp \left\{ \boldsymbol{\eta}^T \left(\sum_{n=1}^N \mathbf{u}(\mathbf{x}_n) + \nu \boldsymbol{\chi} \right) \right\}. \quad (2.230)$$

This again takes the same functional form as the prior (2.229), confirming conjugacy. Furthermore, we see that the parameter ν can be interpreted as a effective number of pseudo-observations in the prior, each of which has a value for the sufficient statistic $\mathbf{u}(\mathbf{x})$ given by $\boldsymbol{\chi}$.

2.4.3 Noninformative priors

In some applications of probabilistic inference, we may have prior knowledge that can be conveniently expressed through the prior distribution. For example, if the prior assigns zero probability to some value of variable, then the posterior distribution will necessarily also assign zero probability to that value, irrespective of

any subsequent observations of data. In many cases, however, we may have little idea of what form the distribution should take. We may then seek a form of prior distribution, called a *noninformative prior*, which is intended to have as little influence on the posterior distribution as possible (Jeffries, 1946; Box and Tao, 1973; Bernardo and Smith, 1994). This is sometimes referred to as ‘letting the data speak for themselves’.

If we have a distribution $p(x|\lambda)$ governed by a parameter λ , we might be tempted to propose a prior distribution $p(\lambda) = \text{const}$ as a suitable prior. If λ is a discrete variable with K states, this simply amounts to setting the prior probability of each state to $1/K$. In the case of continuous parameters, however, there are two potential difficulties with this approach. The first is that, if the domain of λ is unbounded, this prior distribution cannot be correctly normalized because the integral over λ diverges. Such priors are called *improper*. In practice, improper priors can often be used provided the corresponding posterior distribution is *proper*, i.e., that it can be correctly normalized. For instance, if we put a uniform prior distribution over the mean of a Gaussian, then the posterior distribution for the mean, once we have observed at least one data point, will be proper.

A second difficulty arises from the transformation behaviour of a probability density under a nonlinear change of variables, given by (1.27). If a function $h(\lambda)$ is constant, and we change variables to $\lambda = \eta^2$, then $\widehat{h}(\eta) = h(\eta^2)$ will also be constant. However, if we choose the density $p_\lambda(\lambda)$ to be constant, then the density of η will be given, from (1.27), by

$$p_\eta(\eta) = p_\lambda(\lambda) \left| \frac{d\lambda}{d\eta} \right| = p_\lambda(\eta^2) 2\eta \propto \eta \quad (2.231)$$

and so the density over η will not be constant. This issue does not arise when we use maximum likelihood, because the likelihood function $p(x|\lambda)$ is a simple function of λ and so we are free to use any convenient parameterization. If, however, we are to choose a prior distribution that is constant, we must take care to use an appropriate representation for the parameters.

Here we consider two simple examples of noninformative priors (Berger, 1985). First of all, if a density takes the form

$$p(x|\mu) = f(x - \mu) \quad (2.232)$$

then the parameter μ is known as a *location parameter*. This family of densities exhibits *translation invariance* because if we shift x by a constant to give $\widehat{x} = x + c$, then

$$p(\widehat{x}|\widehat{\mu}) = f(\widehat{x} - \widehat{\mu}) \quad (2.233)$$

where we have defined $\widehat{\mu} = \mu + c$. Thus the density takes the same form in the new variable as in the original one, and so the density is independent of the choice of origin. We would like to choose a prior distribution that reflects this translation invariance property, and so we choose a prior that assigns equal probability mass to

an interval $A \leq \mu \leq B$ as to the shifted interval $A - c \leq \mu \leq B - c$. This implies

$$\int_A^B p(\mu) d\mu = \int_{A-c}^{B-c} p(\mu) d\mu = \int_A^B p(\mu - c) d\mu \quad (2.234)$$

and because this must hold for all choices of A and B , we have

$$p(\mu - c) = p(\mu) \quad (2.235)$$

which implies that $p(\mu)$ is constant. An example of a location parameter would be the mean μ of a Gaussian distribution. As we have seen, the conjugate prior distribution for μ in this case is a Gaussian $p(\mu|\mu_0, \sigma_0^2) = \mathcal{N}(\mu|\mu_0, \sigma_0^2)$, and we obtain a noninformative prior by taking the limit $\sigma_0^2 \rightarrow \infty$. Indeed, from (2.141) and (2.142) we see that this gives a posterior distribution over μ in which the contributions from the prior vanish.

As a second example, consider a density of the form

$$p(x|\sigma) = \frac{1}{\sigma} f\left(\frac{x}{\sigma}\right) \quad (2.236)$$

Exercise 2.59

where $\sigma > 0$. Note that this will be a normalized density provided $f(x)$ is correctly normalized. The parameter σ is known as a *scale parameter*, and the density exhibits *scale invariance* because if we scale x by a constant to give $\hat{x} = cx$, then

$$p(\hat{x}|\hat{\sigma}) = \frac{1}{\hat{\sigma}} f\left(\frac{\hat{x}}{\hat{\sigma}}\right) \quad (2.237)$$

where we have defined $\hat{\sigma} = c\sigma$. This transformation corresponds to a change of scale, for example from meters to kilometers if x is a length, and we would like to choose a prior distribution that reflects this scale invariance. If we consider an interval $A \leq \sigma \leq B$, and a scaled interval $A/c \leq \sigma \leq B/c$, then the prior should assign equal probability mass to these two intervals. Thus we have

$$\int_A^B p(\sigma) d\sigma = \int_{A/c}^{B/c} p(\sigma) d\sigma = \int_A^B p\left(\frac{1}{c}\sigma\right) \frac{1}{c} d\sigma \quad (2.238)$$

and because this must hold for choices of A and B , we have

$$p(\sigma) = p\left(\frac{1}{c}\sigma\right) \frac{1}{c} \quad (2.239)$$

and hence $p(\sigma) \propto 1/\sigma$. Note that again this is an improper prior because the integral of the distribution over $0 \leq \sigma \leq \infty$ is divergent. It is sometimes also convenient to think of the prior distribution for a scale parameter in terms of the density of the log of the parameter. Using the transformation rule (1.27) for densities we see that $p(\ln \sigma) = \text{const}$. Thus, for this prior there is the same probability mass in the range $1 \leq \sigma \leq 10$ as in the range $10 \leq \sigma \leq 100$ and in $100 \leq \sigma \leq 1000$.

An example of a scale parameter would be the standard deviation σ of a Gaussian distribution, after we have taken account of the location parameter μ , because

$$\mathcal{N}(x|\mu, \sigma^2) \propto \sigma^{-1} \exp\left\{-\left(\tilde{x}/\sigma\right)^2\right\} \quad (2.240)$$

Section 2.3

where $\tilde{x} = x - \mu$. As discussed earlier, it is often more convenient to work in terms of the precision $\lambda = 1/\sigma^2$ rather than σ itself. Using the transformation rule for densities, we see that a distribution $p(\sigma) \propto 1/\sigma$ corresponds to a distribution over λ of the form $p(\lambda) \propto 1/\lambda$. We have seen that the conjugate prior for λ was the gamma distribution $\text{Gam}(\lambda|a_0, b_0)$ given by (2.146). The noninformative prior is obtained as the special case $a_0 = b_0 = 0$. Again, if we examine the results (2.150) and (2.151) for the posterior distribution of λ , we see that for $a_0 = b_0 = 0$, the posterior depends only on terms arising from the data and not from the prior.

2.5. Nonparametric Methods

Throughout this chapter, we have focussed on the use of probability distributions having specific functional forms governed by a small number of parameters whose values are to be determined from a data set. This is called the *parametric* approach to density modelling. An important limitation of this approach is that the chosen density might be a poor model of the distribution that generates the data, which can result in poor predictive performance. For instance, if the process that generates the data is multimodal, then this aspect of the distribution can never be captured by a Gaussian, which is necessarily unimodal.

In this final section, we consider some *nonparametric* approaches to density estimation that make few assumptions about the form of the distribution. Here we shall focus mainly on simple frequentist methods. The reader should be aware, however, that nonparametric Bayesian methods are attracting increasing interest (Walker *et al.*, 1999; Neal, 2000; Müller and Quintana, 2004; Teh *et al.*, 2006).

Let us start with a discussion of histogram methods for density estimation, which we have already encountered in the context of marginal and conditional distributions in Figure 1.11 and in the context of the central limit theorem in Figure 2.6. Here we explore the properties of histogram density models in more detail, focussing on the case of a single continuous variable x . Standard histograms simply partition x into distinct bins of width Δ_i and then count the number n_i of observations of x falling in bin i . In order to turn this count into a normalized probability density, we simply divide by the total number N of observations and by the width Δ_i of the bins to obtain probability values for each bin given by

$$p_i = \frac{n_i}{N\Delta_i} \quad (2.241)$$

for which it is easily seen that $\int p(x) dx = 1$. This gives a model for the density $p(x)$ that is constant over the width of each bin, and often the bins are chosen to have the same width $\Delta_i = \Delta$.

Figure 2.24 An illustration of the histogram approach to density estimation, in which a data set of 50 data points is generated from the distribution shown by the green curve. Histogram density estimates, based on (2.241), with a common bin width Δ are shown for various values of Δ .



In Figure 2.24, we show an example of histogram density estimation. Here the data is drawn from the distribution, corresponding to the green curve, which is formed from a mixture of two Gaussians. Also shown are three examples of histogram density estimates corresponding to three different choices for the bin width Δ . We see that when Δ is very small (top figure), the resulting density model is very spiky, with a lot of structure that is not present in the underlying distribution that generated the data set. Conversely, if Δ is too large (bottom figure) then the result is a model that is too smooth and that consequently fails to capture the bimodal property of the green curve. The best results are obtained for some intermediate value of Δ (middle figure). In principle, a histogram density model is also dependent on the choice of edge location for the bins, though this is typically much less significant than the value of Δ .

Note that the histogram method has the property (unlike the methods to be discussed shortly) that, once the histogram has been computed, the data set itself can be discarded, which can be advantageous if the data set is large. Also, the histogram approach is easily applied if the data points are arriving sequentially.

In practice, the histogram technique can be useful for obtaining a quick visualization of data in one or two dimensions but is unsuited to most density estimation applications. One obvious problem is that the estimated density has discontinuities that are due to the bin edges rather than any property of the underlying distribution that generated the data. Another major limitation of the histogram approach is its scaling with dimensionality. If we divide each variable in a D -dimensional space into M bins, then the total number of bins will be M^D . This exponential scaling with D is an example of the curse of dimensionality. In a space of high dimensionality, the quantity of data needed to provide meaningful estimates of local probability density would be prohibitive.

The histogram approach to density estimation does, however, teach us two important lessons. First, to estimate the probability density at a particular location, we should consider the data points that lie within some local neighbourhood of that point. Note that the concept of locality requires that we assume some form of distance measure, and here we have been assuming Euclidean distance. For histograms,

Section 1.4

this neighbourhood property was defined by the bins, and there is a natural ‘smoothing’ parameter describing the spatial extent of the local region, in this case the bin width. Second, the value of the smoothing parameter should be neither too large nor too small in order to obtain good results. This is reminiscent of the choice of model complexity in polynomial curve fitting discussed in Chapter 1 where the degree M of the polynomial, or alternatively the value α of the regularization parameter, was optimal for some intermediate value, neither too large nor too small. Armed with these insights, we turn now to a discussion of two widely used nonparametric techniques for density estimation, kernel estimators and nearest neighbours, which have better scaling with dimensionality than the simple histogram model.

2.5.1 Kernel density estimators

Let us suppose that observations are being drawn from some unknown probability density $p(\mathbf{x})$ in some D -dimensional space, which we shall take to be Euclidean, and we wish to estimate the value of $p(\mathbf{x})$. From our earlier discussion of locality, let us consider some small region \mathcal{R} containing \mathbf{x} . The probability mass associated with this region is given by

$$P = \int_{\mathcal{R}} p(\mathbf{x}) d\mathbf{x}. \quad (2.242)$$

Now suppose that we have collected a data set comprising N observations drawn from $p(\mathbf{x})$. Because each data point has a probability P of falling within \mathcal{R} , the total number K of points that lie inside \mathcal{R} will be distributed according to the binomial distribution

$$\text{Bin}(K|N, P) = \frac{N!}{K!(N-K)!} P^K (1-P)^{1-K}. \quad (2.243)$$

Using (2.11), we see that the mean fraction of points falling inside the region is $\mathbb{E}[K/N] = P$, and similarly using (2.12) we see that the variance around this mean is $\text{var}[K/N] = P(1-P)/N$. For large N , this distribution will be sharply peaked around the mean and so

$$K \simeq NP. \quad (2.244)$$

If, however, we also assume that the region \mathcal{R} is sufficiently small that the probability density $p(\mathbf{x})$ is roughly constant over the region, then we have

$$P \simeq p(\mathbf{x})V \quad (2.245)$$

where V is the volume of \mathcal{R} . Combining (2.244) and (2.245), we obtain our density estimate in the form

$$p(\mathbf{x}) = \frac{K}{NV}. \quad (2.246)$$

Note that the validity of (2.246) depends on two contradictory assumptions, namely that the region \mathcal{R} be sufficiently small that the density is approximately constant over the region and yet sufficiently large (in relation to the value of that density) that the number K of points falling inside the region is sufficient for the binomial distribution to be sharply peaked.

Section 2.1

We can exploit the result (2.246) in two different ways. Either we can fix K and determine the value of V from the data, which gives rise to the K -nearest-neighbour technique discussed shortly, or we can fix V and determine K from the data, giving rise to the kernel approach. It can be shown that both the K -nearest-neighbour density estimator and the kernel density estimator converge to the true probability density in the limit $N \rightarrow \infty$ provided V shrinks suitably with N , and K grows with N (Duda and Hart, 1973).

We begin by discussing the kernel method in detail, and to start with we take the region \mathcal{R} to be a small hypercube centred on the point \mathbf{x} at which we wish to determine the probability density. In order to count the number K of points falling within this region, it is convenient to define the following function

$$k(\mathbf{u}) = \begin{cases} 1, & |u_i| \leq 1/2, \\ 0, & \text{otherwise} \end{cases} \quad i = 1, \dots, D, \quad (2.247)$$

which represents a unit cube centred on the origin. The function $k(\mathbf{u})$ is an example of a *kernel function*, and in this context is also called a *Parzen window*. From (2.247), the quantity $k((\mathbf{x} - \mathbf{x}_n)/h)$ will be one if the data point \mathbf{x}_n lies inside a cube of side h centred on \mathbf{x} , and zero otherwise. The total number of data points lying inside this cube will therefore be

$$K = \sum_{n=1}^N k\left(\frac{\mathbf{x} - \mathbf{x}_n}{h}\right). \quad (2.248)$$

Substituting this expression into (2.246) then gives the following result for the estimated density at \mathbf{x}

$$p(\mathbf{x}) = \frac{1}{N} \sum_{n=1}^N \frac{1}{h^D} k\left(\frac{\mathbf{x} - \mathbf{x}_n}{h}\right) \quad (2.249)$$

where we have used $V = h^D$ for the volume of a hypercube of side h in D dimensions. Using the symmetry of the function $k(\mathbf{u})$, we can now re-interpret this equation, not as a single cube centred on \mathbf{x} but as the sum over N cubes centred on the N data points \mathbf{x}_n .

As it stands, the kernel density estimator (2.249) will suffer from one of the same problems that the histogram method suffered from, namely the presence of artificial discontinuities, in this case at the boundaries of the cubes. We can obtain a smoother density model if we choose a smoother kernel function, and a common choice is the Gaussian, which gives rise to the following kernel density model

$$p(\mathbf{x}) = \frac{1}{N} \sum_{n=1}^N \frac{1}{(2\pi h^2)^{1/2}} \exp\left\{-\frac{\|\mathbf{x} - \mathbf{x}_n\|^2}{2h^2}\right\} \quad (2.250)$$

where h represents the standard deviation of the Gaussian components. Thus our density model is obtained by placing a Gaussian over each data point and then adding up the contributions over the whole data set, and then dividing by N so that the density is correctly normalized. In Figure 2.25, we apply the model (2.250) to the data

Figure 2.25 Illustration of the kernel density model (2.250) applied to the same data set used to demonstrate the histogram approach in Figure 2.24. We see that h acts as a smoothing parameter and that if it is set too small (top panel), the result is a very noisy density model, whereas if it is set too large (bottom panel), then the bimodal nature of the underlying distribution from which the data is generated (shown by the green curve) is washed out. The best density model is obtained for some intermediate value of h (middle panel).



set used earlier to demonstrate the histogram technique. We see that, as expected, the parameter h plays the role of a smoothing parameter, and there is a trade-off between sensitivity to noise at small h and over-smoothing at large h . Again, the optimization of h is a problem in model complexity, analogous to the choice of bin width in histogram density estimation, or the degree of the polynomial used in curve fitting.

We can choose any other kernel function $k(\mathbf{u})$ in (2.249) subject to the conditions

$$k(\mathbf{u}) \geq 0, \quad (2.251)$$

$$\int k(\mathbf{u}) d\mathbf{u} = 1 \quad (2.252)$$

which ensure that the resulting probability distribution is nonnegative everywhere and integrates to one. The class of density model given by (2.249) is called a kernel density estimator, or *Parzen* estimator. It has a great merit that there is no computation involved in the ‘training’ phase because this simply requires storage of the training set. However, this is also one of its great weaknesses because the computational cost of evaluating the density grows linearly with the size of the data set.

2.5.2 Nearest-neighbour methods

One of the difficulties with the kernel approach to density estimation is that the parameter h governing the kernel width is fixed for all kernels. In regions of high data density, a large value of h may lead to over-smoothing and a washing out of structure that might otherwise be extracted from the data. However, reducing h may lead to noisy estimates elsewhere in data space where the density is smaller. Thus the optimal choice for h may be dependent on location within the data space. This issue is addressed by nearest-neighbour methods for density estimation.

We therefore return to our general result (2.246) for local density estimation, and instead of fixing V and determining the value of K from the data, we consider a fixed value of K and use the data to find an appropriate value for V . To do this, we consider a small sphere centred on the point \mathbf{x} at which we wish to estimate the

Figure 2.26 Illustration of K -nearest-neighbour density estimation using the same data set as in Figures 2.25 and 2.24. We see that the parameter K governs the degree of smoothing, so that a small value of K leads to a very noisy density model (top panel), whereas a large value (bottom panel) smoothes out the bimodal nature of the true distribution (shown by the green curve) from which the data set was generated.



density $p(\mathbf{x})$, and we allow the radius of the sphere to grow until it contains precisely K data points. The estimate of the density $p(\mathbf{x})$ is then given by (2.246) with V set to the volume of the resulting sphere. This technique is known as *K nearest neighbours* and is illustrated in Figure 2.26, for various choices of the parameter K , using the same data set as used in Figure 2.24 and Figure 2.25. We see that the value of K now governs the degree of smoothing and that again there is an optimum choice for K that is neither too large nor too small. Note that the model produced by K nearest neighbours is not a true density model because the integral over all space diverges.

Exercise 2.61

We close this chapter by showing how the K -nearest-neighbour technique for density estimation can be extended to the problem of classification. To do this, we apply the K -nearest-neighbour density estimation technique to each class separately and then make use of Bayes' theorem. Let us suppose that we have a data set comprising N_k points in class \mathcal{C}_k with N points in total, so that $\sum_k N_k = N$. If we wish to classify a new point \mathbf{x} , we draw a sphere centred on \mathbf{x} containing precisely K points irrespective of their class. Suppose this sphere has volume V and contains K_k points from class \mathcal{C}_k . Then (2.246) provides an estimate of the density associated with each class

$$p(\mathbf{x}|\mathcal{C}_k) = \frac{K_k}{N_k V}. \quad (2.253)$$

Similarly, the unconditional density is given by

$$p(\mathbf{x}) = \frac{K}{NV} \quad (2.254)$$

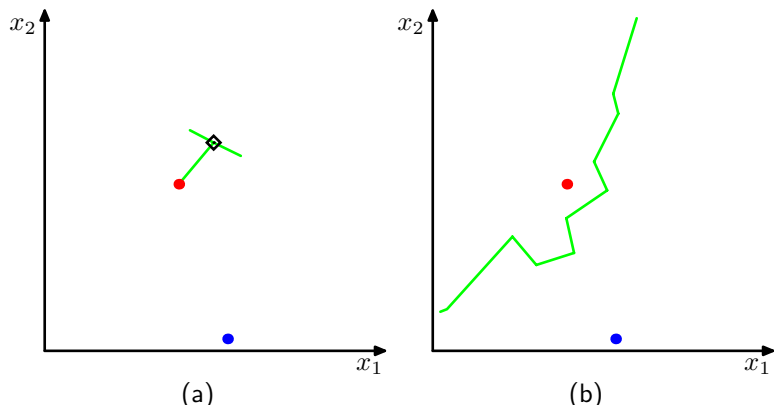
while the class priors are given by

$$p(\mathcal{C}_k) = \frac{N_k}{N}. \quad (2.255)$$

We can now combine (2.253), (2.254), and (2.255) using Bayes' theorem to obtain the posterior probability of class membership

$$p(\mathcal{C}_k|\mathbf{x}) = \frac{p(\mathbf{x}|\mathcal{C}_k)p(\mathcal{C}_k)}{p(\mathbf{x})} = \frac{K_k}{K}. \quad (2.256)$$

Figure 2.27 (a) In the K -nearest-neighbour classifier, a new point, shown by the black diamond, is classified according to the majority class membership of the K closest training data points, in this case $K = 3$. (b) In the nearest-neighbour ($K = 1$) approach to classification, the resulting decision boundary is composed of hyperplanes that form perpendicular bisectors of pairs of points from different classes.



If we wish to minimize the probability of misclassification, this is done by assigning the test point \mathbf{x} to the class having the largest posterior probability, corresponding to the largest value of K_k/K . Thus to classify a new point, we identify the K nearest points from the training data set and then assign the new point to the class having the largest number of representatives amongst this set. Ties can be broken at random. The particular case of $K = 1$ is called the *nearest-neighbour* rule, because a test point is simply assigned to the same class as the nearest point from the training set. These concepts are illustrated in Figure 2.27.

In Figure 2.28, we show the results of applying the K -nearest-neighbour algorithm to the oil flow data, introduced in Chapter 1, for various values of K . As expected, we see that K controls the degree of smoothing, so that small K produces many small regions of each class, whereas large K leads to fewer larger regions.



Figure 2.28 Plot of 200 data points from the oil data set showing values of x_6 plotted against x_7 , where the red, green, and blue points correspond to the ‘laminar’, ‘annular’, and ‘homogeneous’ classes, respectively. Also shown are the classifications of the input space given by the K -nearest-neighbour algorithm for various values of K .

An interesting property of the nearest-neighbour ($K = 1$) classifier is that, in the limit $N \rightarrow \infty$, the error rate is never more than twice the minimum achievable error rate of an optimal classifier, i.e., one that uses the true class distributions (Cover and Hart, 1967).

As discussed so far, both the K -nearest-neighbour method, and the kernel density estimator, require the entire training data set to be stored, leading to expensive computation if the data set is large. This effect can be offset, at the expense of some additional one-off computation, by constructing tree-based search structures to allow (approximate) near neighbours to be found efficiently without doing an exhaustive search of the data set. Nevertheless, these nonparametric methods are still severely limited. On the other hand, we have seen that simple parametric models are very restricted in terms of the forms of distribution that they can represent. We therefore need to find density models that are very flexible and yet for which the complexity of the models can be controlled independently of the size of the training set, and we shall see in subsequent chapters how to achieve this.

Exercises

- 2.1** (*) **www** Verify that the Bernoulli distribution (2.2) satisfies the following properties

$$\sum_{x=0}^1 p(x|\mu) = 1 \quad (2.257)$$

$$\mathbb{E}[x] = \mu \quad (2.258)$$

$$\text{var}[x] = \mu(1 - \mu). \quad (2.259)$$

Show that the entropy $H[x]$ of a Bernoulli distributed random binary variable x is given by

$$H[x] = -\mu \ln \mu - (1 - \mu) \ln(1 - \mu). \quad (2.260)$$

- 2.2** (**) The form of the Bernoulli distribution given by (2.2) is not symmetric between the two values of x . In some situations, it will be more convenient to use an equivalent formulation for which $x \in \{-1, 1\}$, in which case the distribution can be written

$$p(x|\mu) = \left(\frac{1-\mu}{2}\right)^{(1-x)/2} \left(\frac{1+\mu}{2}\right)^{(1+x)/2} \quad (2.261)$$

where $\mu \in [-1, 1]$. Show that the distribution (2.261) is normalized, and evaluate its mean, variance, and entropy.

- 2.3** (**) **www** In this exercise, we prove that the binomial distribution (2.9) is normalized. First use the definition (2.10) of the number of combinations of m identical objects chosen from a total of N to show that

$$\binom{N}{m} + \binom{N}{m-1} = \binom{N+1}{m}. \quad (2.262)$$

Use this result to prove by induction the following result

$$(1+x)^N = \sum_{m=0}^N \binom{N}{m} x^m \quad (2.263)$$

which is known as the *binomial theorem*, and which is valid for all real values of x . Finally, show that the binomial distribution is normalized, so that

$$\sum_{m=0}^N \binom{N}{m} \mu^m (1-\mu)^{N-m} = 1 \quad (2.264)$$

which can be done by first pulling out a factor $(1-\mu)^N$ out of the summation and then making use of the binomial theorem.

- 2.4** (**) Show that the mean of the binomial distribution is given by (2.11). To do this, differentiate both sides of the normalization condition (2.264) with respect to μ and then rearrange to obtain an expression for the mean of n . Similarly, by differentiating (2.264) twice with respect to μ and making use of the result (2.11) for the mean of the binomial distribution prove the result (2.12) for the variance of the binomial.
- 2.5** (**) **www** In this exercise, we prove that the beta distribution, given by (2.13), is correctly normalized, so that (2.14) holds. This is equivalent to showing that

$$\int_0^1 \mu^{a-1} (1-\mu)^{b-1} d\mu = \frac{\Gamma(a)\Gamma(b)}{\Gamma(a+b)}. \quad (2.265)$$

From the definition (1.141) of the gamma function, we have

$$\Gamma(a)\Gamma(b) = \int_0^\infty \exp(-x)x^{a-1} dx \int_0^\infty \exp(-y)y^{b-1} dy. \quad (2.266)$$

Use this expression to prove (2.265) as follows. First bring the integral over y inside the integrand of the integral over x , next make the change of variable $t = y + x$ where x is fixed, then interchange the order of the x and t integrations, and finally make the change of variable $x = t\mu$ where t is fixed.

- 2.6** (*) Make use of the result (2.265) to show that the mean, variance, and mode of the beta distribution (2.13) are given respectively by

$$\mathbb{E}[\mu] = \frac{a}{a+b} \quad (2.267)$$

$$\text{var}[\mu] = \frac{ab}{(a+b)^2(a+b+1)} \quad (2.268)$$

$$\text{mode}[\mu] = \frac{a-1}{a+b-2}. \quad (2.269)$$

- 2.7** (**) Consider a binomial random variable x given by (2.9), with prior distribution for μ given by the beta distribution (2.13), and suppose we have observed m occurrences of $x = 1$ and l occurrences of $x = 0$. Show that the posterior mean value of x lies between the prior mean and the maximum likelihood estimate for μ . To do this, show that the posterior mean can be written as λ times the prior mean plus $(1 - \lambda)$ times the maximum likelihood estimate, where $0 \leq \lambda \leq 1$. This illustrates the concept of the posterior distribution being a compromise between the prior distribution and the maximum likelihood solution.

- 2.8** (*) Consider two variables x and y with joint distribution $p(x, y)$. Prove the following two results

$$\mathbb{E}[x] = \mathbb{E}_y [\mathbb{E}_x[x|y]] \quad (2.270)$$

$$\text{var}[x] = \mathbb{E}_y [\text{var}_x[x|y]] + \text{var}_y [\mathbb{E}_x[x|y]]. \quad (2.271)$$

Here $\mathbb{E}_x[x|y]$ denotes the expectation of x under the conditional distribution $p(x|y)$, with a similar notation for the conditional variance.

- 2.9** (*** **www**) . In this exercise, we prove the normalization of the Dirichlet distribution (2.38) using induction. We have already shown in Exercise 2.5 that the beta distribution, which is a special case of the Dirichlet for $M = 2$, is normalized. We now assume that the Dirichlet distribution is normalized for $M - 1$ variables and prove that it is normalized for M variables. To do this, consider the Dirichlet distribution over M variables, and take account of the constraint $\sum_{k=1}^M \mu_k = 1$ by eliminating μ_M , so that the Dirichlet is written

$$p_M(\mu_1, \dots, \mu_{M-1}) = C_M \prod_{k=1}^{M-1} \mu_k^{\alpha_k-1} \left(1 - \sum_{j=1}^{M-1} \mu_j\right)^{\alpha_M-1} \quad (2.272)$$

and our goal is to find an expression for C_M . To do this, integrate over μ_{M-1} , taking care over the limits of integration, and then make a change of variable so that this integral has limits 0 and 1. By assuming the correct result for C_{M-1} and making use of (2.265), derive the expression for C_M .

- 2.10** (**) Using the property $\Gamma(x + 1) = x\Gamma(x)$ of the gamma function, derive the following results for the mean, variance, and covariance of the Dirichlet distribution given by (2.38)

$$\mathbb{E}[\mu_j] = \frac{\alpha_j}{\alpha_0} \quad (2.273)$$

$$\text{var}[\mu_j] = \frac{\alpha_j(\alpha_0 - \alpha_j)}{\alpha_0^2(\alpha_0 + 1)} \quad (2.274)$$

$$\text{cov}[\mu_j \mu_l] = -\frac{\alpha_j \alpha_l}{\alpha_0^2(\alpha_0 + 1)}, \quad j \neq l \quad (2.275)$$

where α_0 is defined by (2.39).

- 2.11** (*) **www** By expressing the expectation of $\ln \mu_j$ under the Dirichlet distribution (2.38) as a derivative with respect to α_j , show that

$$\mathbb{E}[\ln \mu_j] = \psi(\alpha_j) - \psi(\alpha_0) \quad (2.276)$$

where α_0 is given by (2.39) and

$$\psi(a) \equiv \frac{d}{da} \ln \Gamma(a) \quad (2.277)$$

is the *digamma* function.

- 2.12** (*) The uniform distribution for a continuous variable x is defined by

$$U(x|a, b) = \frac{1}{b - a}, \quad a \leq x \leq b. \quad (2.278)$$

Verify that this distribution is normalized, and find expressions for its mean and variance.

- 2.13** (**) Evaluate the Kullback-Leibler divergence (1.113) between two Gaussians $p(\mathbf{x}) = \mathcal{N}(\mathbf{x}|\boldsymbol{\mu}, \boldsymbol{\Sigma})$ and $q(\mathbf{x}) = \mathcal{N}(\mathbf{x}|\mathbf{m}, \mathbf{L})$.

- 2.14** (**) **www** This exercise demonstrates that the multivariate distribution with maximum entropy, for a given covariance, is a Gaussian. The entropy of a distribution $p(\mathbf{x})$ is given by

$$H[\mathbf{x}] = - \int p(\mathbf{x}) \ln p(\mathbf{x}) d\mathbf{x}. \quad (2.279)$$

We wish to maximize $H[\mathbf{x}]$ over all distributions $p(\mathbf{x})$ subject to the constraints that $p(\mathbf{x})$ be normalized and that it have a specific mean and covariance, so that

$$\int p(\mathbf{x}) d\mathbf{x} = 1 \quad (2.280)$$

$$\int p(\mathbf{x}) \mathbf{x} d\mathbf{x} = \boldsymbol{\mu} \quad (2.281)$$

$$\int p(\mathbf{x}) (\mathbf{x} - \boldsymbol{\mu})(\mathbf{x} - \boldsymbol{\mu})^T d\mathbf{x} = \boldsymbol{\Sigma}. \quad (2.282)$$

By performing a variational maximization of (2.279) and using Lagrange multipliers to enforce the constraints (2.280), (2.281), and (2.282), show that the maximum likelihood distribution is given by the Gaussian (2.43).

- 2.15** (**) Show that the entropy of the multivariate Gaussian $\mathcal{N}(\mathbf{x}|\boldsymbol{\mu}, \boldsymbol{\Sigma})$ is given by

$$H[\mathbf{x}] = \frac{1}{2} \ln |\boldsymbol{\Sigma}| + \frac{D}{2} (1 + \ln(2\pi)) \quad (2.283)$$

where D is the dimensionality of \mathbf{x} .

- 2.16** (★★★) **www** Consider two random variables x_1 and x_2 having Gaussian distributions with means μ_1, μ_2 and precisions τ_1, τ_2 respectively. Derive an expression for the differential entropy of the variable $x = x_1 + x_2$. To do this, first find the distribution of x by using the relation

$$p(x) = \int_{-\infty}^{\infty} p(x|x_2)p(x_2) dx_2 \quad (2.284)$$

and completing the square in the exponent. Then observe that this represents the convolution of two Gaussian distributions, which itself will be Gaussian, and finally make use of the result (1.110) for the entropy of the univariate Gaussian.

- 2.17** (*) **www** Consider the multivariate Gaussian distribution given by (2.43). By writing the precision matrix (inverse covariance matrix) Σ^{-1} as the sum of a symmetric and an anti-symmetric matrix, show that the anti-symmetric term does not appear in the exponent of the Gaussian, and hence that the precision matrix may be taken to be symmetric without loss of generality. Because the inverse of a symmetric matrix is also symmetric (see Exercise 2.22), it follows that the covariance matrix may also be chosen to be symmetric without loss of generality.
- 2.18** (★★★) Consider a real, symmetric matrix Σ whose eigenvalue equation is given by (2.45). By taking the complex conjugate of this equation and subtracting the original equation, and then forming the inner product with eigenvector \mathbf{u}_i , show that the eigenvalues λ_i are real. Similarly, use the symmetry property of Σ to show that two eigenvectors \mathbf{u}_i and \mathbf{u}_j will be orthogonal provided $\lambda_j \neq \lambda_i$. Finally, show that without loss of generality, the set of eigenvectors can be chosen to be orthonormal, so that they satisfy (2.46), even if some of the eigenvalues are zero.
- 2.19** (★★) Show that a real, symmetric matrix Σ having the eigenvector equation (2.45) can be expressed as an expansion in the eigenvectors, with coefficients given by the eigenvalues, of the form (2.48). Similarly, show that the inverse matrix Σ^{-1} has a representation of the form (2.49).
- 2.20** (★★) **www** A positive definite matrix Σ can be defined as one for which the quadratic form
- $$\mathbf{a}^T \Sigma \mathbf{a} \quad (2.285)$$
- is positive for any real value of the vector \mathbf{a} . Show that a necessary and sufficient condition for Σ to be positive definite is that all of the eigenvalues λ_i of Σ , defined by (2.45), are positive.
- 2.21** (*) Show that a real, symmetric matrix of size $D \times D$ has $D(D+1)/2$ independent parameters.
- 2.22** (*) **www** Show that the inverse of a symmetric matrix is itself symmetric.
- 2.23** (★★) By diagonalizing the coordinate system using the eigenvector expansion (2.45), show that the volume contained within the hyperellipsoid corresponding to a constant

Mahalanobis distance Δ is given by

$$V_D |\Sigma|^{1/2} \Delta^D \quad (2.286)$$

where V_D is the volume of the unit sphere in D dimensions, and the Mahalanobis distance is defined by (2.44).

- 2.24** (**) **www** Prove the identity (2.76) by multiplying both sides by the matrix

$$\begin{pmatrix} \mathbf{A} & \mathbf{B} \\ \mathbf{C} & \mathbf{D} \end{pmatrix} \quad (2.287)$$

and making use of the definition (2.77).

- 2.25** (**) In Sections 2.3.1 and 2.3.2, we considered the conditional and marginal distributions for a multivariate Gaussian. More generally, we can consider a partitioning of the components of \mathbf{x} into three groups \mathbf{x}_a , \mathbf{x}_b , and \mathbf{x}_c , with a corresponding partitioning of the mean vector μ and of the covariance matrix Σ in the form

$$\mu = \begin{pmatrix} \mu_a \\ \mu_b \\ \mu_c \end{pmatrix}, \quad \Sigma = \begin{pmatrix} \Sigma_{aa} & \Sigma_{ab} & \Sigma_{ac} \\ \Sigma_{ba} & \Sigma_{bb} & \Sigma_{bc} \\ \Sigma_{ca} & \Sigma_{cb} & \Sigma_{cc} \end{pmatrix}. \quad (2.288)$$

By making use of the results of Section 2.3, find an expression for the conditional distribution $p(\mathbf{x}_a | \mathbf{x}_b)$ in which \mathbf{x}_c has been marginalized out.

- 2.26** (**) A very useful result from linear algebra is the *Woodbury* matrix inversion formula given by

$$(\mathbf{A} + \mathbf{BCD})^{-1} = \mathbf{A}^{-1} - \mathbf{A}^{-1}\mathbf{B}(\mathbf{C}^{-1} + \mathbf{D}\mathbf{A}^{-1}\mathbf{B})^{-1}\mathbf{D}\mathbf{A}^{-1}. \quad (2.289)$$

By multiplying both sides by $(\mathbf{A} + \mathbf{BCD})$ prove the correctness of this result.

- 2.27** (*) Let \mathbf{x} and \mathbf{z} be two independent random vectors, so that $p(\mathbf{x}, \mathbf{z}) = p(\mathbf{x})p(\mathbf{z})$. Show that the mean of their sum $\mathbf{y} = \mathbf{x} + \mathbf{z}$ is given by the sum of the means of each of the variable separately. Similarly, show that the covariance matrix of \mathbf{y} is given by the sum of the covariance matrices of \mathbf{x} and \mathbf{z} . Confirm that this result agrees with that of Exercise 1.10.

- 2.28** (*** **www**) Consider a joint distribution over the variable

$$\mathbf{z} = \begin{pmatrix} \mathbf{x} \\ \mathbf{y} \end{pmatrix} \quad (2.290)$$

whose mean and covariance are given by (2.108) and (2.105) respectively. By making use of the results (2.92) and (2.93) show that the marginal distribution $p(\mathbf{x})$ is given (2.99). Similarly, by making use of the results (2.81) and (2.82) show that the conditional distribution $p(\mathbf{y}|\mathbf{x})$ is given by (2.100).

- 2.29** (**) Using the partitioned matrix inversion formula (2.76), show that the inverse of the precision matrix (2.104) is given by the covariance matrix (2.105).
- 2.30** (*) By starting from (2.107) and making use of the result (2.105), verify the result (2.108).
- 2.31** (**) Consider two multidimensional random vectors \mathbf{x} and \mathbf{z} having Gaussian distributions $p(\mathbf{x}) = \mathcal{N}(\mathbf{x}|\boldsymbol{\mu}_x, \boldsymbol{\Sigma}_x)$ and $p(\mathbf{z}) = \mathcal{N}(\mathbf{z}|\boldsymbol{\mu}_z, \boldsymbol{\Sigma}_z)$ respectively, together with their sum $\mathbf{y} = \mathbf{x} + \mathbf{z}$. Use the results (2.109) and (2.110) to find an expression for the marginal distribution $p(\mathbf{y})$ by considering the linear-Gaussian model comprising the product of the marginal distribution $p(\mathbf{x})$ and the conditional distribution $p(\mathbf{y}|\mathbf{x})$.
- 2.32** (***) **www** This exercise and the next provide practice at manipulating the quadratic forms that arise in linear-Gaussian models, as well as giving an independent check of results derived in the main text. Consider a joint distribution $p(\mathbf{x}, \mathbf{y})$ defined by the marginal and conditional distributions given by (2.99) and (2.100). By examining the quadratic form in the exponent of the joint distribution, and using the technique of ‘completing the square’ discussed in Section 2.3, find expressions for the mean and covariance of the marginal distribution $p(\mathbf{y})$ in which the variable \mathbf{x} has been integrated out. To do this, make use of the Woodbury matrix inversion formula (2.289). Verify that these results agree with (2.109) and (2.110) obtained using the results of Chapter 2.
- 2.33** (**) Consider the same joint distribution as in Exercise 2.32, but now use the technique of completing the square to find expressions for the mean and covariance of the conditional distribution $p(\mathbf{x}|\mathbf{y})$. Again, verify that these agree with the corresponding expressions (2.111) and (2.112).
- 2.34** (**) **www** To find the maximum likelihood solution for the covariance matrix of a multivariate Gaussian, we need to maximize the log likelihood function (2.118) with respect to $\boldsymbol{\Sigma}$, noting that the covariance matrix must be symmetric and positive definite. Here we proceed by ignoring these constraints and doing a straightforward maximization. Using the results (C.21), (C.26), and (C.28) from Appendix C, show that the covariance matrix $\boldsymbol{\Sigma}$ that maximizes the log likelihood function (2.118) is given by the sample covariance (2.122). We note that the final result is necessarily symmetric and positive definite (provided the sample covariance is nonsingular).
- 2.35** (**) Use the result (2.59) to prove (2.62). Now, using the results (2.59), and (2.62), show that
- $$\mathbb{E}[\mathbf{x}_n \mathbf{x}_m] = \boldsymbol{\mu} \boldsymbol{\mu}^T + I_{nm} \boldsymbol{\Sigma} \quad (2.291)$$
- where \mathbf{x}_n denotes a data point sampled from a Gaussian distribution with mean $\boldsymbol{\mu}$ and covariance $\boldsymbol{\Sigma}$, and I_{nm} denotes the (n, m) element of the identity matrix. Hence prove the result (2.124).
- 2.36** (**) **www** Using an analogous procedure to that used to obtain (2.126), derive an expression for the sequential estimation of the variance of a univariate Gaussian

distribution, by starting with the maximum likelihood expression

$$\sigma_{\text{ML}}^2 = \frac{1}{N} \sum_{n=1}^N (x_n - \mu)^2. \quad (2.292)$$

Verify that substituting the expression for a Gaussian distribution into the Robbins-Monro sequential estimation formula (2.135) gives a result of the same form, and hence obtain an expression for the corresponding coefficients a_N .

- 2.37** (**) Using an analogous procedure to that used to obtain (2.126), derive an expression for the sequential estimation of the covariance of a multivariate Gaussian distribution, by starting with the maximum likelihood expression (2.122). Verify that substituting the expression for a Gaussian distribution into the Robbins-Monro sequential estimation formula (2.135) gives a result of the same form, and hence obtain an expression for the corresponding coefficients a_N .
- 2.38** (*) Use the technique of completing the square for the quadratic form in the exponent to derive the results (2.141) and (2.142).
- 2.39** (**) Starting from the results (2.141) and (2.142) for the posterior distribution of the mean of a Gaussian random variable, dissect out the contributions from the first $N - 1$ data points and hence obtain expressions for the sequential update of μ_N and σ_N^2 . Now derive the same results starting from the posterior distribution $p(\mu|x_1, \dots, x_{N-1}) = \mathcal{N}(\mu|\mu_{N-1}, \sigma_{N-1}^2)$ and multiplying by the likelihood function $p(x_N|\mu) = \mathcal{N}(x_N|\mu, \sigma^2)$ and then completing the square and normalizing to obtain the posterior distribution after N observations.
- 2.40** (**) **www** Consider a D -dimensional Gaussian random variable \mathbf{x} with distribution $\mathcal{N}(\mathbf{x}|\boldsymbol{\mu}, \boldsymbol{\Sigma})$ in which the covariance $\boldsymbol{\Sigma}$ is known and for which we wish to infer the mean $\boldsymbol{\mu}$ from a set of observations $\mathbf{X} = \{\mathbf{x}_1, \dots, \mathbf{x}_N\}$. Given a prior distribution $p(\boldsymbol{\mu}) = \mathcal{N}(\boldsymbol{\mu}|\boldsymbol{\mu}_0, \boldsymbol{\Sigma}_0)$, find the corresponding posterior distribution $p(\boldsymbol{\mu}|\mathbf{X})$.
- 2.41** (*) Use the definition of the gamma function (1.141) to show that the gamma distribution (2.146) is normalized.
- 2.42** (**) Evaluate the mean, variance, and mode of the gamma distribution (2.146).
- 2.43** (*) The following distribution

$$p(x|\sigma^2, q) = \frac{q}{2(2\sigma^2)^{1/q}\Gamma(1/q)} \exp\left(-\frac{|x|^q}{2\sigma^2}\right) \quad (2.293)$$

is a generalization of the univariate Gaussian distribution. Show that this distribution is normalized so that

$$\int_{-\infty}^{\infty} p(x|\sigma^2, q) dx = 1 \quad (2.294)$$

and that it reduces to the Gaussian when $q = 2$. Consider a regression model in which the target variable is given by $t = y(\mathbf{x}, \mathbf{w}) + \epsilon$ and ϵ is a random noise

variable drawn from the distribution (2.293). Show that the log likelihood function over \mathbf{w} and σ^2 , for an observed data set of input vectors $\mathbf{X} = \{\mathbf{x}_1, \dots, \mathbf{x}_N\}$ and corresponding target variables $\mathbf{t} = (t_1, \dots, t_N)^T$, is given by

$$\ln p(\mathbf{t}|\mathbf{X}, \mathbf{w}, \sigma^2) = -\frac{1}{2\sigma^2} \sum_{n=1}^N |y(\mathbf{x}_n, \mathbf{w}) - t_n|^q - \frac{N}{q} \ln(2\sigma^2) + \text{const} \quad (2.295)$$

where ‘const’ denotes terms independent of both \mathbf{w} and σ^2 . Note that, as a function of \mathbf{w} , this is the L_q error function considered in Section 1.5.5.

- 2.44** (**) Consider a univariate Gaussian distribution $\mathcal{N}(x|\mu, \tau^{-1})$ having conjugate Gaussian-gamma prior given by (2.154), and a data set $\mathbf{x} = \{x_1, \dots, x_N\}$ of i.i.d. observations. Show that the posterior distribution is also a Gaussian-gamma distribution of the same functional form as the prior, and write down expressions for the parameters of this posterior distribution.
- 2.45** (*) Verify that the Wishart distribution defined by (2.155) is indeed a conjugate prior for the precision matrix of a multivariate Gaussian.
- 2.46** (*) **www** Verify that evaluating the integral in (2.158) leads to the result (2.159).
- 2.47** (*) **www** Show that in the limit $\nu \rightarrow \infty$, the t-distribution (2.159) becomes a Gaussian. Hint: ignore the normalization coefficient, and simply look at the dependence on x .
- 2.48** (*) By following analogous steps to those used to derive the univariate Student's t-distribution (2.159), verify the result (2.162) for the multivariate form of the Student's t-distribution, by marginalizing over the variable η in (2.161). Using the definition (2.161), show by exchanging integration variables that the multivariate t-distribution is correctly normalized.
- 2.49** (**) By using the definition (2.161) of the multivariate Student's t-distribution as a convolution of a Gaussian with a gamma distribution, verify the properties (2.164), (2.165), and (2.166) for the multivariate t-distribution defined by (2.162).
- 2.50** (*) Show that in the limit $\nu \rightarrow \infty$, the multivariate Student's t-distribution (2.162) reduces to a Gaussian with mean $\boldsymbol{\mu}$ and precision $\boldsymbol{\Lambda}$.
- 2.51** (*) **www** The various trigonometric identities used in the discussion of periodic variables in this chapter can be proven easily from the relation

$$\exp(iA) = \cos A + i \sin A \quad (2.296)$$

in which i is the square root of minus one. By considering the identity

$$\exp(iA) \exp(-iA) = 1 \quad (2.297)$$

prove the result (2.177). Similarly, using the identity

$$\cos(A - B) = \Re \exp\{i(A - B)\} \quad (2.298)$$

where \Re denotes the real part, prove (2.178). Finally, by using $\sin(A - B) = \Im \exp\{i(A - B)\}$, where \Im denotes the imaginary part, prove the result (2.183).

- 2.52** (**) For large m , the von Mises distribution (2.179) becomes sharply peaked around the mode θ_0 . By defining $\xi = m^{1/2}(\theta - \theta_0)$ and making the Taylor expansion of the cosine function given by

$$\cos \alpha = 1 - \frac{\alpha^2}{2} + O(\alpha^4) \quad (2.299)$$

show that as $m \rightarrow \infty$, the von Mises distribution tends to a Gaussian.

- 2.53** (*) Using the trigonometric identity (2.183), show that solution of (2.182) for θ_0 is given by (2.184).

- 2.54** (*) By computing first and second derivatives of the von Mises distribution (2.179), and using $I_0(m) > 0$ for $m > 0$, show that the maximum of the distribution occurs when $\theta = \theta_0$ and that the minimum occurs when $\theta = \theta_0 + \pi \pmod{2\pi}$.

- 2.55** (*) By making use of the result (2.168), together with (2.184) and the trigonometric identity (2.178), show that the maximum likelihood solution m_{ML} for the concentration of the von Mises distribution satisfies $A(m_{\text{ML}}) = \bar{r}$ where \bar{r} is the radius of the mean of the observations viewed as unit vectors in the two-dimensional Euclidean plane, as illustrated in Figure 2.17.

- 2.56** (**) **www** Express the beta distribution (2.13), the gamma distribution (2.146), and the von Mises distribution (2.179) as members of the exponential family (2.194) and thereby identify their natural parameters.

- 2.57** (*) Verify that the multivariate Gaussian distribution can be cast in exponential family form (2.194) and derive expressions for $\boldsymbol{\eta}$, $\mathbf{u}(\mathbf{x})$, $h(\mathbf{x})$ and $g(\boldsymbol{\eta})$ analogous to (2.220)–(2.223).

- 2.58** (*) The result (2.226) showed that the negative gradient of $\ln g(\boldsymbol{\eta})$ for the exponential family is given by the expectation of $\mathbf{u}(\mathbf{x})$. By taking the second derivatives of (2.195), show that

$$-\nabla \nabla \ln g(\boldsymbol{\eta}) = \mathbb{E}[\mathbf{u}(\mathbf{x})\mathbf{u}(\mathbf{x})^T] - \mathbb{E}[\mathbf{u}(\mathbf{x})]\mathbb{E}[\mathbf{u}(\mathbf{x})^T] = \text{cov}[\mathbf{u}(\mathbf{x})]. \quad (2.300)$$

- 2.59** (*) By changing variables using $y = x/\sigma$, show that the density (2.236) will be correctly normalized, provided $f(x)$ is correctly normalized.

- 2.60** (**) **www** Consider a histogram-like density model in which the space \mathbf{x} is divided into fixed regions for which the density $p(\mathbf{x})$ takes the constant value h_i over the i^{th} region, and that the volume of region i is denoted Δ_i . Suppose we have a set of N observations of \mathbf{x} such that n_i of these observations fall in region i . Using a Lagrange multiplier to enforce the normalization constraint on the density, derive an expression for the maximum likelihood estimator for the $\{h_i\}$.

- 2.61** (*) Show that the K -nearest-neighbour density model defines an improper distribution whose integral over all space is divergent.

3

Linear

Models for

Regression

The focus so far in this book has been on unsupervised learning, including topics such as density estimation and data clustering. We turn now to a discussion of supervised learning, starting with regression. The goal of regression is to predict the value of one or more continuous *target* variables t given the value of a D -dimensional vector \mathbf{x} of *input* variables. We have already encountered an example of a regression problem when we considered polynomial curve fitting in Chapter 1. The polynomial is a specific example of a broad class of functions called linear regression models, which share the property of being linear functions of the adjustable parameters, and which will form the focus of this chapter. The simplest form of linear regression models are also linear functions of the input variables. However, we can obtain a much more useful class of functions by taking linear combinations of a fixed set of nonlinear functions of the input variables, known as *basis functions*. Such models are linear functions of the parameters, which gives them simple analytical properties, and yet can be nonlinear with respect to the input variables.

Given a training data set comprising N observations $\{\mathbf{x}_n\}$, where $n = 1, \dots, N$, together with corresponding target values $\{t_n\}$, the goal is to predict the value of t for a new value of \mathbf{x} . In the simplest approach, this can be done by directly constructing an appropriate function $y(\mathbf{x})$ whose values for new inputs \mathbf{x} constitute the predictions for the corresponding values of t . More generally, from a probabilistic perspective, we aim to model the predictive distribution $p(t|\mathbf{x})$ because this expresses our uncertainty about the value of t for each value of \mathbf{x} . From this conditional distribution we can make predictions of t , for any new value of \mathbf{x} , in such a way as to minimize the expected value of a suitably chosen loss function. As discussed in Section 1.5.5, a common choice of loss function for real-valued variables is the squared loss, for which the optimal solution is given by the conditional expectation of t .

Although linear models have significant limitations as practical techniques for pattern recognition, particularly for problems involving input spaces of high dimensionality, they have nice analytical properties and form the foundation for more sophisticated models to be discussed in later chapters.

3.1. Linear Basis Function Models

The simplest linear model for regression is one that involves a linear combination of the input variables

$$y(\mathbf{x}, \mathbf{w}) = w_0 + w_1 x_1 + \dots + w_D x_D \quad (3.1)$$

where $\mathbf{x} = (x_1, \dots, x_D)^T$. This is often simply known as **linear regression**. The key property of this model is that it is a linear function of the parameters w_0, \dots, w_D . It is also, however, a linear function of the input variables x_i , and this imposes significant limitations on the model. We therefore extend the class of models by considering linear combinations of **fixed nonlinear functions of the input variables**, of the form

$$y(\mathbf{x}, \mathbf{w}) = w_0 + \sum_{j=1}^{M-1} w_j \phi_j(\mathbf{x}) \quad (3.2)$$

where $\phi_j(\mathbf{x})$ are known as **basis functions**. By denoting the maximum value of the index j by $M - 1$, the total number of parameters in this model will be M .

The parameter w_0 allows for any fixed offset in the data and is sometimes called a **bias** parameter (not to be confused with ‘bias’ in a statistical sense). It is often convenient to define an additional dummy ‘basis function’ $\phi_0(\mathbf{x}) = 1$ so that

$$y(\mathbf{x}, \mathbf{w}) = \sum_{j=0}^{M-1} w_j \phi_j(\mathbf{x}) = \mathbf{w}^T \boldsymbol{\phi}(\mathbf{x}) \quad (3.3)$$

where $\mathbf{w} = (w_0, \dots, w_{M-1})^T$ and $\boldsymbol{\phi} = (\phi_0, \dots, \phi_{M-1})^T$. In many practical applications of pattern recognition, we will apply some form of fixed pre-processing,

or feature extraction, to the original data variables. If the original variables comprise the vector \mathbf{x} , then the features can be expressed in terms of the basis functions $\{\phi_j(\mathbf{x})\}$.

By using nonlinear basis functions, we allow the function $y(\mathbf{x}, \mathbf{w})$ to be a nonlinear function of the input vector \mathbf{x} . Functions of the form (3.2) are called linear models, however, because this function is linear in \mathbf{w} . It is this linearity in the parameters that will greatly simplify the analysis of this class of models. However, it also leads to some significant limitations, as we discuss in Section 3.6.

The example of polynomial regression considered in Chapter 1 is a particular example of this model in which there is a single input variable x , and the basis functions take the form of powers of x so that $\phi_j(x) = x^j$. One limitation of polynomial basis functions is that they are global functions of the input variable, so that changes in one region of input space affect all other regions. This can be resolved by dividing the input space up into regions and fit a different polynomial in each region, leading to *spline functions* (Hastie *et al.*, 2001).

There are many other possible choices for the basis functions, for example

$$\phi_j(x) = \exp \left\{ -\frac{(x - \mu_j)^2}{2s^2} \right\} \quad (3.4)$$

where the μ_j govern the locations of the basis functions in input space, and the parameter s governs their spatial scale. These are usually referred to as ‘Gaussian’ basis functions, although it should be noted that they are not required to have a probabilistic interpretation, and in particular the normalization coefficient is unimportant because these basis functions will be multiplied by adaptive parameters w_j .

Another possibility is the sigmoidal basis function of the form

$$\phi_j(x) = \sigma \left(\frac{x - \mu_j}{s} \right) \quad (3.5)$$

where $\sigma(a)$ is the logistic sigmoid function defined by

$$\sigma(a) = \frac{1}{1 + \exp(-a)}. \quad (3.6)$$

Equivalently, we can use the ‘tanh’ function because this is related to the logistic sigmoid by $\tanh(a) = 2\sigma(a) - 1$, and so a general linear combination of logistic sigmoid functions is equivalent to a general linear combination of ‘tanh’ functions. These various choices of basis function are illustrated in Figure 3.1.

Yet another possible choice of basis function is the Fourier basis, which leads to an expansion in sinusoidal functions. Each basis function represents a specific frequency and has infinite spatial extent. By contrast, basis functions that are localized to finite regions of input space necessarily comprise a spectrum of different spatial frequencies. In many signal processing applications, it is of interest to consider basis functions that are localized in both space and frequency, leading to a class of functions known as *wavelets*. These are also defined to be mutually orthogonal, to simplify their application. Wavelets are most applicable when the input values live



Figure 3.1 Examples of basis functions, showing polynomials on the left, Gaussians of the form (3.4) in the centre, and sigmoidal of the form (3.5) on the right.

on a regular lattice, such as the successive time points in a temporal sequence, or the pixels in an image. Useful texts on wavelets include Ogden (1997), Mallat (1999), and Vidakovic (1999).

Most of the discussion in this chapter, however, is independent of the particular choice of basis function set, and so for most of our discussion we shall not specify the particular form of the basis functions, except for the purposes of numerical illustration. Indeed, much of our discussion will be equally applicable to the situation in which the vector $\phi(\mathbf{x})$ of basis functions is simply the identity $\phi(\mathbf{x}) = \mathbf{x}$. Furthermore, in order to keep the notation simple, we shall focus on the case of a single target variable t . However, in Section 3.1.5, we consider briefly the modifications needed to deal with multiple target variables.

3.1.1 Maximum likelihood and least squares

In Chapter 1, we fitted polynomial functions to data sets by minimizing a sum-of-squares error function. We also showed that this error function could be motivated as the maximum likelihood solution under an assumed Gaussian noise model. Let us return to this discussion and consider the least squares approach, and its relation to maximum likelihood, in more detail.

As before, we assume that the target variable t is given by a deterministic function $y(\mathbf{x}, \mathbf{w})$ with additive Gaussian noise so that

$$t = y(\mathbf{x}, \mathbf{w}) + \epsilon \quad (3.7)$$

where ϵ is a zero mean Gaussian random variable with precision (inverse variance) β . Thus we can write

$$p(t|\mathbf{x}, \mathbf{w}, \beta) = \mathcal{N}(t|y(\mathbf{x}, \mathbf{w}), \beta^{-1}). \quad (3.8)$$

Section 1.5.5

Recall that, if we assume a squared loss function, then the optimal prediction, for a new value of \mathbf{x} , will be given by the conditional mean of the target variable. In the case of a Gaussian conditional distribution of the form (3.8), the conditional mean

will be simply

$$\mathbb{E}[t|\mathbf{x}] = \int tp(t|\mathbf{x}) dt = y(\mathbf{x}, \mathbf{w}). \quad (3.9)$$

Note that the Gaussian noise assumption implies that the conditional distribution of t given \mathbf{x} is unimodal, which may be inappropriate for some applications. An extension to mixtures of conditional Gaussian distributions, which permit multimodal conditional distributions, will be discussed in Section 14.5.1.

Now consider a data set of inputs $\mathbf{X} = \{\mathbf{x}_1, \dots, \mathbf{x}_N\}$ with corresponding target values t_1, \dots, t_N . We group the target variables $\{t_n\}$ into a column vector that we denote by \mathbf{t} where the typeface is chosen to distinguish it from a single observation of a multivariate target, which would be denoted \mathbf{t} . Making the assumption that these data points are drawn independently from the distribution (3.8), we obtain the following expression for the likelihood function, which is a function of the adjustable parameters \mathbf{w} and β , in the form

$$p(\mathbf{t}|\mathbf{X}, \mathbf{w}, \beta) = \prod_{n=1}^N \mathcal{N}(t_n | \mathbf{w}^T \phi(\mathbf{x}_n), \beta^{-1}) \quad (3.10)$$

where we have used (3.3). Note that in supervised learning problems such as regression (and classification), we are not seeking to model the distribution of the input variables. Thus \mathbf{x} will always appear in the set of conditioning variables, and so from now on we will drop the explicit \mathbf{x} from expressions such as $p(\mathbf{t}|\mathbf{x}, \mathbf{w}, \beta)$ in order to keep the notation uncluttered. Taking the logarithm of the likelihood function, and making use of the standard form (1.46) for the univariate Gaussian, we have

$$\begin{aligned} \ln p(\mathbf{t}|\mathbf{w}, \beta) &= \sum_{n=1}^N \ln \mathcal{N}(t_n | \mathbf{w}^T \phi(\mathbf{x}_n), \beta^{-1}) \\ &= \frac{N}{2} \ln \beta - \frac{N}{2} \ln(2\pi) - \beta E_D(\mathbf{w}) \end{aligned} \quad (3.11)$$

where the sum-of-squares error function is defined by

$$E_D(\mathbf{w}) = \frac{1}{2} \sum_{n=1}^N \{t_n - \mathbf{w}^T \phi(\mathbf{x}_n)\}^2. \quad (3.12)$$

Having written down the likelihood function, we can use maximum likelihood to determine \mathbf{w} and β . Consider first the maximization with respect to \mathbf{w} . As observed already in Section 1.2.5, we see that maximization of the likelihood function under a conditional Gaussian noise distribution for a linear model is equivalent to minimizing a sum-of-squares error function given by $E_D(\mathbf{w})$. The gradient of the log likelihood function (3.11) takes the form

$$\nabla \ln p(\mathbf{t}|\mathbf{w}, \beta) = \sum_{n=1}^N \{t_n - \mathbf{w}^T \phi(\mathbf{x}_n)\} \phi(\mathbf{x}_n)^T. \quad (3.13)$$

Setting this gradient to zero gives

$$0 = \sum_{n=1}^N t_n \phi(\mathbf{x}_n)^T - \mathbf{w}^T \left(\sum_{n=1}^N \phi(\mathbf{x}_n) \phi(\mathbf{x}_n)^T \right). \quad (3.14)$$

Solving for \mathbf{w} we obtain

$$\mathbf{w}_{\text{ML}} = (\Phi^T \Phi)^{-1} \Phi^T \mathbf{t} \quad (3.15)$$

which are known as the *normal equations* for the least squares problem. Here Φ is an $N \times M$ matrix, called the *design matrix*, whose elements are given by $\Phi_{nj} = \phi_j(\mathbf{x}_n)$, so that

$$\Phi = \begin{pmatrix} \phi_0(\mathbf{x}_1) & \phi_1(\mathbf{x}_1) & \cdots & \phi_{M-1}(\mathbf{x}_1) \\ \phi_0(\mathbf{x}_2) & \phi_1(\mathbf{x}_2) & \cdots & \phi_{M-1}(\mathbf{x}_2) \\ \vdots & \vdots & \ddots & \vdots \\ \phi_0(\mathbf{x}_N) & \phi_1(\mathbf{x}_N) & \cdots & \phi_{M-1}(\mathbf{x}_N) \end{pmatrix}. \quad (3.16)$$

The quantity

$$\Phi^\dagger \equiv (\Phi^T \Phi)^{-1} \Phi^T \quad (3.17)$$

is known as the *Moore-Penrose pseudo-inverse* of the matrix Φ (Rao and Mitra, 1971; Golub and Van Loan, 1996). It can be regarded as a generalization of the notion of matrix inverse to nonsquare matrices. Indeed, if Φ is square and invertible, then using the property $(\mathbf{AB})^{-1} = \mathbf{B}^{-1} \mathbf{A}^{-1}$ we see that $\Phi^\dagger \equiv \Phi^{-1}$.

At this point, we can gain some insight into the role of the bias parameter w_0 . If we make the bias parameter explicit, then the error function (3.12) becomes

$$E_D(\mathbf{w}) = \frac{1}{2} \sum_{n=1}^N \{t_n - w_0 - \sum_{j=1}^{M-1} w_j \phi_j(\mathbf{x}_n)\}^2. \quad (3.18)$$

Setting the derivative with respect to w_0 equal to zero, and solving for w_0 , we obtain

$$w_0 = \bar{t} - \sum_{j=1}^{M-1} w_j \overline{\phi_j} \quad (3.19)$$

where we have defined

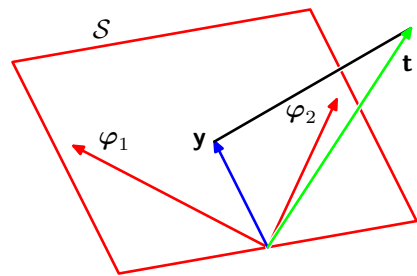
$$\bar{t} = \frac{1}{N} \sum_{n=1}^N t_n, \quad \overline{\phi_j} = \frac{1}{N} \sum_{n=1}^N \phi_j(\mathbf{x}_n). \quad (3.20)$$

Thus the bias w_0 compensates for the difference between the averages (over the training set) of the target values and the weighted sum of the averages of the basis function values.

We can also maximize the log likelihood function (3.11) with respect to the noise precision parameter β , giving

$$\frac{1}{\beta_{\text{ML}}} = \frac{1}{N} \sum_{n=1}^N \{t_n - \mathbf{w}_{\text{ML}}^T \phi(\mathbf{x}_n)\}^2 \quad (3.21)$$

Figure 3.2 Geometrical interpretation of the least-squares solution, in an N -dimensional space whose axes are the values of t_1, \dots, t_N . The least-squares regression function is obtained by finding the orthogonal projection of the data vector \mathbf{t} onto the subspace spanned by the basis functions $\phi_j(\mathbf{x})$ in which each basis function is viewed as a vector φ_j of length N with elements $\phi_j(\mathbf{x}_n)$.



and so we see that the inverse of the noise precision is given by the residual variance of the target values around the regression function.

3.1.2 Geometry of least squares

At this point, it is instructive to consider the geometrical interpretation of the least-squares solution. To do this we consider an N -dimensional space whose axes are given by the t_n , so that $\mathbf{t} = (t_1, \dots, t_N)^T$ is a vector in this space. Each basis function $\phi_j(\mathbf{x}_n)$, evaluated at the N data points, can also be represented as a vector in the same space, denoted by φ_j , as illustrated in Figure 3.2. Note that φ_j corresponds to the j^{th} column of Φ , whereas $\phi(\mathbf{x}_n)$ corresponds to the n^{th} row of Φ . If the number M of basis functions is smaller than the number N of data points, then the M vectors $\phi_j(\mathbf{x}_n)$ will span a linear subspace \mathcal{S} of dimensionality M . We define \mathbf{y} to be an N -dimensional vector whose n^{th} element is given by $y(\mathbf{x}_n, \mathbf{w})$, where $n = 1, \dots, N$. Because \mathbf{y} is an arbitrary linear combination of the vectors φ_j , it can live anywhere in the M -dimensional subspace. The sum-of-squares error (3.12) is then equal (up to a factor of $1/2$) to the squared Euclidean distance between \mathbf{y} and \mathbf{t} . Thus the least-squares solution for \mathbf{w} corresponds to that choice of \mathbf{y} that lies in subspace \mathcal{S} and that is closest to \mathbf{t} . Intuitively, from Figure 3.2, we anticipate that this solution corresponds to the orthogonal projection of \mathbf{t} onto the subspace \mathcal{S} . This is indeed the case, as can easily be verified by noting that the solution for \mathbf{y} is given by $\Phi \mathbf{w}_{\text{ML}}$, and then confirming that this takes the form of an orthogonal projection.

Exercise 3.2

In practice, a direct solution of the normal equations can lead to numerical difficulties when $\Phi^T \Phi$ is close to singular. In particular, when two or more of the basis vectors φ_j are co-linear, or nearly so, the resulting parameter values can have large magnitudes. Such near degeneracies will not be uncommon when dealing with real data sets. The resulting numerical difficulties can be addressed using the technique of *singular value decomposition*, or SVD (Press *et al.*, 1992; Bishop and Nabney, 2008). Note that the addition of a regularization term ensures that the matrix is non-singular, even in the presence of degeneracies.

3.1.3 Sequential learning

Batch techniques, such as the maximum likelihood solution (3.15), which involve processing the entire training set in one go, can be computationally costly for large data sets. As we have discussed in Chapter 1, if the data set is sufficiently large, it may be worthwhile to use *sequential* algorithms, also known as *on-line* algorithms,

in which the data points are considered one at a time, and the model parameters updated after each such presentation. Sequential learning is also appropriate for real-time applications in which the data observations are arriving in a continuous stream, and predictions must be made before all of the data points are seen.

We can obtain a sequential learning algorithm by applying the technique of *stochastic gradient descent*, also known as *sequential gradient descent*, as follows. If the error function comprises a sum over data points $E = \sum_n E_n$, then after presentation of pattern n , the stochastic gradient descent algorithm updates the parameter vector \mathbf{w} using

$$\mathbf{w}^{(\tau+1)} = \mathbf{w}^{(\tau)} - \eta \nabla E_n \quad (3.22)$$

where τ denotes the iteration number, and η is a learning rate parameter. We shall discuss the choice of value for η shortly. The value of \mathbf{w} is initialized to some starting vector $\mathbf{w}^{(0)}$. For the case of the sum-of-squares error function (3.12), this gives

$$\mathbf{w}^{(\tau+1)} = \mathbf{w}^{(\tau)} + \eta(t_n - \mathbf{w}^{(\tau)\text{T}} \phi_n) \phi_n \quad (3.23)$$

where $\phi_n = \phi(\mathbf{x}_n)$. This is known as *least-mean-squares* or the *LMS algorithm*. The value of η needs to be chosen with care to ensure that the algorithm converges (Bishop and Nabney, 2008).

3.1.4 Regularized least squares

In Section 1.1, we introduced the idea of adding a regularization term to an error function in order to control over-fitting, so that the total error function to be minimized takes the form

$$E_D(\mathbf{w}) + \lambda E_W(\mathbf{w}) \quad (3.24)$$

where λ is the regularization coefficient that controls the relative importance of the data-dependent error $E_D(\mathbf{w})$ and the regularization term $E_W(\mathbf{w})$. One of the simplest forms of regularizer is given by the sum-of-squares of the weight vector elements

$$E_W(\mathbf{w}) = \frac{1}{2} \mathbf{w}^{\text{T}} \mathbf{w}. \quad (3.25)$$

If we also consider the sum-of-squares error function given by

$$E(\mathbf{w}) = \frac{1}{2} \sum_{n=1}^N \{t_n - \mathbf{w}^{\text{T}} \phi(\mathbf{x}_n)\}^2 \quad (3.26)$$

then the total error function becomes

$$\frac{1}{2} \sum_{n=1}^N \{t_n - \mathbf{w}^{\text{T}} \phi(\mathbf{x}_n)\}^2 + \frac{\lambda}{2} \mathbf{w}^{\text{T}} \mathbf{w}. \quad (3.27)$$

This particular choice of regularizer is known in the machine learning literature as *weight decay* because in sequential learning algorithms, it encourages weight values to decay towards zero, unless supported by the data. In statistics, it provides an example of a *parameter shrinkage* method because it shrinks parameter values towards



Figure 3.3 Contours of the regularization term in (3.29) for various values of the parameter q .

zero. It has the advantage that the error function remains a quadratic function of \mathbf{w} , and so its exact minimizer can be found in closed form. Specifically, setting the gradient of (3.27) with respect to \mathbf{w} to zero, and solving for \mathbf{w} as before, we obtain

$$\mathbf{w} = (\lambda \mathbf{I} + \Phi^T \Phi)^{-1} \Phi^T \mathbf{t}. \quad (3.28)$$

This represents a simple extension of the least-squares solution (3.15).

A more general regularizer is sometimes used, for which the regularized error takes the form

$$\frac{1}{2} \sum_{n=1}^N \{t_n - \mathbf{w}^T \phi(\mathbf{x}_n)\}^2 + \frac{\lambda}{2} \sum_{j=1}^M |w_j|^q \quad (3.29)$$

where $q = 2$ corresponds to the quadratic regularizer (3.27). Figure 3.3 shows contours of the regularization function for different values of q .

The case of $q = 1$ is known as the *lasso* in the statistics literature (Tibshirani, 1996). It has the property that if λ is sufficiently large, some of the coefficients w_j are driven to zero, leading to a *sparse* model in which the corresponding basis functions play no role. To see this, we first note that minimizing (3.29) is equivalent to minimizing the unregularized sum-of-squares error (3.12) subject to the constraint

$$\sum_{j=1}^M |w_j|^q \leq \eta \quad (3.30)$$

Exercise 3.5

Appendix E

for an appropriate value of the parameter η , where the two approaches can be related using Lagrange multipliers. The origin of the sparsity can be seen from Figure 3.4, which shows that the minimum of the error function, subject to the constraint (3.30). As λ is increased, so an increasing number of parameters are driven to zero.

Regularization allows complex models to be trained on data sets of limited size without severe over-fitting, essentially by limiting the effective model complexity. However, the problem of determining the optimal model complexity is then shifted from one of finding the appropriate number of basis functions to one of determining a suitable value of the regularization coefficient λ . We shall return to the issue of model complexity later in this chapter.

Figure 3.4 Plot of the contours of the unregularized error function (blue) along with the constraint region (3.30) for the quadratic regularizer $q = 2$ on the left and the lasso regularizer $q = 1$ on the right, in which the optimum value for the parameter vector w is denoted by w^* . The lasso gives a sparse solution in which $w_1^* = 0$.



For the remainder of this chapter we shall focus on the quadratic regularizer (3.27) both for its practical importance and its analytical tractability.

3.1.5 Multiple outputs

So far, we have considered the case of a single target variable t . In some applications, we may wish to predict $K > 1$ target variables, which we denote collectively by the target vector \mathbf{t} . This could be done by introducing a different set of basis functions for each component of \mathbf{t} , leading to multiple, independent regression problems. However, a more interesting, and more common, approach is to use the same set of basis functions to model all of the components of the target vector so that

$$\mathbf{y}(\mathbf{x}, \mathbf{w}) = \mathbf{W}^T \phi(\mathbf{x}) \quad (3.31)$$

where \mathbf{y} is a K -dimensional column vector, \mathbf{W} is an $M \times K$ matrix of parameters, and $\phi(\mathbf{x})$ is an M -dimensional column vector with elements $\phi_j(\mathbf{x})$, with $\phi_0(\mathbf{x}) = 1$ as before. Suppose we take the conditional distribution of the target vector to be an isotropic Gaussian of the form

$$p(\mathbf{t}|\mathbf{x}, \mathbf{W}, \beta) = \mathcal{N}(\mathbf{t}|\mathbf{W}^T \phi(\mathbf{x}), \beta^{-1} \mathbf{I}). \quad (3.32)$$

If we have a set of observations $\mathbf{t}_1, \dots, \mathbf{t}_N$, we can combine these into a matrix \mathbf{T} of size $N \times K$ such that the n^{th} row is given by \mathbf{t}_n^T . Similarly, we can combine the input vectors $\mathbf{x}_1, \dots, \mathbf{x}_N$ into a matrix \mathbf{X} . The log likelihood function is then given by

$$\begin{aligned} \ln p(\mathbf{T}|\mathbf{X}, \mathbf{W}, \beta) &= \sum_{n=1}^N \ln \mathcal{N}(\mathbf{t}_n|\mathbf{W}^T \phi(\mathbf{x}_n), \beta^{-1} \mathbf{I}) \\ &= \frac{NK}{2} \ln \left(\frac{\beta}{2\pi} \right) - \frac{\beta}{2} \sum_{n=1}^N \|\mathbf{t}_n - \mathbf{W}^T \phi(\mathbf{x}_n)\|^2. \end{aligned} \quad (3.33)$$

As before, we can maximize this function with respect to \mathbf{W} , giving

$$\mathbf{W}_{\text{ML}} = (\Phi^T \Phi)^{-1} \Phi^T \mathbf{T}. \quad (3.34)$$

If we examine this result for each target variable t_k , we have

$$\mathbf{w}_k = (\Phi^T \Phi)^{-1} \Phi^T \mathbf{t}_k = \Phi^\dagger \mathbf{t}_k \quad (3.35)$$

where \mathbf{t}_k is an N -dimensional column vector with components t_{nk} for $n = 1, \dots, N$. Thus the solution to the regression problem decouples between the different target variables, and we need only compute a single pseudo-inverse matrix Φ^\dagger , which is shared by all of the vectors \mathbf{w}_k .

Exercise 3.6

The extension to general Gaussian noise distributions having arbitrary covariance matrices is straightforward. Again, this leads to a decoupling into K independent regression problems. This result is unsurprising because the parameters \mathbf{W} define only the mean of the Gaussian noise distribution, and we know from Section 2.3.4 that the maximum likelihood solution for the mean of a multivariate Gaussian is independent of the covariance. From now on, we shall therefore consider a single target variable t for simplicity.

3.2. The Bias-Variance Decomposition

So far in our discussion of linear models for regression, we have assumed that the form and number of basis functions are both fixed. As we have seen in Chapter 1, the use of maximum likelihood, or equivalently least squares, can lead to severe over-fitting if complex models are trained using data sets of limited size. However, limiting the number of basis functions in order to avoid over-fitting has the side effect of limiting the flexibility of the model to capture interesting and important trends in the data. Although the introduction of regularization terms can control over-fitting for models with many parameters, this raises the question of how to determine a suitable value for the regularization coefficient λ . Seeking the solution that minimizes the regularized error function with respect to both the weight vector \mathbf{w} and the regularization coefficient λ is clearly not the right approach since this leads to the unregularized solution with $\lambda = 0$.

As we have seen in earlier chapters, the phenomenon of over-fitting is really an unfortunate property of maximum likelihood and does not arise when we marginalize over parameters in a Bayesian setting. In this chapter, we shall consider the Bayesian view of model complexity in some depth. Before doing so, however, it is instructive to consider a frequentist viewpoint of the model complexity issue, known as the bias-variance trade-off. Although we shall introduce this concept in the context of linear basis function models, where it is easy to illustrate the ideas using simple examples, the discussion has more general applicability.

In Section 1.5.5, when we discussed decision theory for regression problems, we considered various loss functions each of which leads to a corresponding optimal prediction once we are given the conditional distribution $p(t|\mathbf{x})$. A popular choice is

the squared loss function, for which the optimal prediction is given by the conditional expectation, which we denote by $h(\mathbf{x})$ and which is given by

$$h(\mathbf{x}) = \mathbb{E}[t|\mathbf{x}] = \int tp(t|\mathbf{x}) dt. \quad (3.36)$$

At this point, it is worth distinguishing between the squared loss function arising from decision theory and the sum-of-squares error function that arose in the maximum likelihood estimation of model parameters. We might use more sophisticated techniques than least squares, for example regularization or a fully Bayesian approach, to determine the conditional distribution $p(t|\mathbf{x})$. These can all be combined with the squared loss function for the purpose of making predictions.

We showed in Section 1.5.5 that the expected squared loss can be written in the form

$$\mathbb{E}[L] = \int \{y(\mathbf{x}) - h(\mathbf{x})\}^2 p(\mathbf{x}) d\mathbf{x} + \int \{h(\mathbf{x}) - t\}^2 p(\mathbf{x}, t) d\mathbf{x} dt. \quad (3.37)$$

Recall that the second term, which is independent of $y(\mathbf{x})$, arises from the intrinsic noise on the data and represents the minimum achievable value of the expected loss. The first term depends on our choice for the function $y(\mathbf{x})$, and we will seek a solution for $y(\mathbf{x})$ which makes this term a minimum. Because it is nonnegative, the smallest that we can hope to make this term is zero. If we had an unlimited supply of data (and unlimited computational resources), we could in principle find the regression function $h(\mathbf{x})$ to any desired degree of accuracy, and this would represent the optimal choice for $y(\mathbf{x})$. However, in practice we have a data set \mathcal{D} containing only a finite number N of data points, and consequently we do not know the regression function $h(\mathbf{x})$ exactly.

If we model the $h(\mathbf{x})$ using a parametric function $y(\mathbf{x}; \mathbf{w})$ governed by a parameter vector \mathbf{w} , then from a Bayesian perspective the uncertainty in our model is expressed through a posterior distribution over \mathbf{w} . A frequentist treatment, however, involves making a point estimate of \mathbf{w} based on the data set \mathcal{D} , and tries instead to interpret the uncertainty of this estimate through the following thought experiment. Suppose we had a large number of data sets each of size N and each drawn independently from the distribution $p(t, \mathbf{x})$. For any given data set \mathcal{D} , we can run our learning algorithm and obtain a prediction function $y(\mathbf{x}; \mathcal{D})$. Different data sets from the ensemble will give different functions and consequently different values of the squared loss. The performance of a particular learning algorithm is then assessed by taking the average over this ensemble of data sets.

Consider the integrand of the first term in (3.37), which for a particular data set \mathcal{D} takes the form

$$\{y(\mathbf{x}; \mathcal{D}) - h(\mathbf{x})\}^2. \quad (3.38)$$

Because this quantity will be dependent on the particular data set \mathcal{D} , we take its average over the ensemble of data sets. If we add and subtract the quantity $\mathbb{E}_{\mathcal{D}}[y(\mathbf{x}; \mathcal{D})]$

inside the braces, and then expand, we obtain

$$\begin{aligned} & \{y(\mathbf{x}; \mathcal{D}) - \mathbb{E}_{\mathcal{D}}[y(\mathbf{x}; \mathcal{D})] + \mathbb{E}_{\mathcal{D}}[y(\mathbf{x}; \mathcal{D})] - h(\mathbf{x})\}^2 \\ &= \{y(\mathbf{x}; \mathcal{D}) - \mathbb{E}_{\mathcal{D}}[y(\mathbf{x}; \mathcal{D})]\}^2 + \{\mathbb{E}_{\mathcal{D}}[y(\mathbf{x}; \mathcal{D})] - h(\mathbf{x})\}^2 \\ &\quad + 2\{y(\mathbf{x}; \mathcal{D}) - \mathbb{E}_{\mathcal{D}}[y(\mathbf{x}; \mathcal{D})]\}\{\mathbb{E}_{\mathcal{D}}[y(\mathbf{x}; \mathcal{D})] - h(\mathbf{x})\}. \end{aligned} \quad (3.39)$$

We now take the expectation of this expression with respect to \mathcal{D} and note that the final term will vanish, giving

$$\begin{aligned} & \mathbb{E}_{\mathcal{D}} [\{y(\mathbf{x}; \mathcal{D}) - h(\mathbf{x})\}^2] \\ &= \underbrace{\{\mathbb{E}_{\mathcal{D}}[y(\mathbf{x}; \mathcal{D})] - h(\mathbf{x})\}^2}_{\text{(bias)}^2} + \underbrace{\mathbb{E}_{\mathcal{D}} [\{y(\mathbf{x}; \mathcal{D}) - \mathbb{E}_{\mathcal{D}}[y(\mathbf{x}; \mathcal{D})]\}^2]}_{\text{variance}}. \end{aligned} \quad (3.40)$$

We see that the expected squared difference between $y(\mathbf{x}; \mathcal{D})$ and the regression function $h(\mathbf{x})$ can be expressed as the sum of two terms. The first term, called the squared **bias**, represents the extent to which the average prediction over all data sets differs from the desired regression function. The second term, called the **variance**, measures the extent to which the solutions for individual data sets vary around their average, and hence this measures the extent to which the function $y(\mathbf{x}; \mathcal{D})$ is sensitive to the particular choice of data set. We shall provide some intuition to support these definitions shortly when we consider a simple example.

So far, we have considered a single input value \mathbf{x} . If we substitute this expansion back into (3.37), we obtain the following decomposition of the expected squared loss

$$\text{expected loss} = (\text{bias})^2 + \text{variance} + \text{noise} \quad (3.41)$$

where

$$(\text{bias})^2 = \int \{\mathbb{E}_{\mathcal{D}}[y(\mathbf{x}; \mathcal{D})] - h(\mathbf{x})\}^2 p(\mathbf{x}) d\mathbf{x} \quad (3.42)$$

$$\text{variance} = \int \mathbb{E}_{\mathcal{D}} [\{y(\mathbf{x}; \mathcal{D}) - \mathbb{E}_{\mathcal{D}}[y(\mathbf{x}; \mathcal{D})]\}^2] p(\mathbf{x}) d\mathbf{x} \quad (3.43)$$

$$\text{noise} = \int \{h(\mathbf{x}) - t\}^2 p(\mathbf{x}, t) d\mathbf{x} dt \quad (3.44)$$

and the bias and variance terms now refer to integrated quantities.

Our goal is to minimize the expected loss, which we have decomposed into the sum of a (squared) bias, a variance, and a constant noise term. As we shall see, there is a trade-off between bias and variance, with very flexible models having low bias and high variance, and relatively rigid models having high bias and low variance. The model with the optimal predictive capability is the one that leads to the best balance between bias and variance. This is illustrated by considering the sinusoidal data set from Chapter 1. Here we generate 100 data sets, each containing $N = 25$ data points, independently from the sinusoidal curve $h(x) = \sin(2\pi x)$. The data sets are indexed by $l = 1, \dots, L$, where $L = 100$, and for each data set $\mathcal{D}^{(l)}$ we



Figure 3.5 Illustration of the dependence of bias and variance on model complexity, governed by a regularization parameter λ , using the sinusoidal data set from Chapter 1. There are $L = 100$ data sets, each having $N = 25$ data points, and there are 24 Gaussian basis functions in the model so that the total number of parameters is $M = 25$ including the bias parameter. The left column shows the result of fitting the model to the data sets for various values of $\ln \lambda$ (for clarity, only 20 of the 100 fits are shown). The right column shows the corresponding average of the 100 fits (red) along with the sinusoidal function from which the data sets were generated (green).

Figure 3.6 Plot of squared bias and variance, together with their sum, corresponding to the results shown in Figure 3.5. Also shown is the average test set error for a test data set size of 1000 points. The minimum value of $(\text{bias})^2 + \text{variance}$ occurs around $\ln \lambda = -0.31$, which is close to the value that gives the minimum error on the test data.



fit a model with 24 Gaussian basis functions by minimizing the regularized error function (3.27) to give a prediction function $y^{(l)}(x)$ as shown in Figure 3.5. The top row corresponds to a large value of the regularization coefficient λ that gives low variance (because the red curves in the left plot look similar) but high bias (because the two curves in the right plot are very different). Conversely on the bottom row, for which λ is small, there is large variance (shown by the high variability between the red curves in the left plot) but low bias (shown by the good fit between the average model fit and the original sinusoidal function). Note that the result of averaging many solutions for the complex model with $M = 25$ is a very good fit to the regression function, which suggests that averaging may be a beneficial procedure. Indeed, a weighted averaging of multiple solutions lies at the heart of a Bayesian approach, although the averaging is with respect to the posterior distribution of parameters, not with respect to multiple data sets.

We can also examine the bias-variance trade-off quantitatively for this example. The average prediction is estimated from

$$\bar{y}(x) = \frac{1}{L} \sum_{l=1}^L y^{(l)}(x) \quad (3.45)$$

and the integrated squared bias and integrated variance are then given by

$$(\text{bias})^2 = \frac{1}{N} \sum_{n=1}^N \{\bar{y}(x_n) - h(x_n)\}^2 \quad (3.46)$$

$$\text{variance} = \frac{1}{N} \sum_{n=1}^N \frac{1}{L} \sum_{l=1}^L \{y^{(l)}(x_n) - \bar{y}(x_n)\}^2 \quad (3.47)$$

where the integral over x weighted by the distribution $p(x)$ is approximated by a finite sum over data points drawn from that distribution. These quantities, along with their sum, are plotted as a function of $\ln \lambda$ in Figure 3.6. We see that small values of λ allow the model to become finely tuned to the noise on each individual

data set leading to large variance. Conversely, a large value of λ pulls the weight parameters towards zero leading to large bias.

Although the bias-variance decomposition may provide some interesting insights into the model complexity issue from a frequentist perspective, it is of limited practical value, because the bias-variance decomposition is based on averages with respect to ensembles of data sets, whereas in practice we have only the single observed data set. If we had a large number of independent training sets of a given size, we would be better off combining them into a single large training set, which of course would reduce the level of over-fitting for a given model complexity.

Given these limitations, we turn in the next section to a Bayesian treatment of linear basis function models, which not only provides powerful insights into the issues of over-fitting but which also leads to practical techniques for addressing the question model complexity.

3.3. Bayesian Linear Regression

In our discussion of maximum likelihood for setting the parameters of a linear regression model, we have seen that the effective model complexity, governed by the number of basis functions, needs to be controlled according to the size of the data set. Adding a regularization term to the log likelihood function means the effective model complexity can then be controlled by the value of the regularization coefficient, although the choice of the number and form of the basis functions is of course still important in determining the overall behaviour of the model.

This leaves the issue of deciding the appropriate model complexity for the particular problem, which cannot be decided simply by maximizing the likelihood function, because this always leads to excessively complex models and over-fitting. Independent hold-out data can be used to determine model complexity, as discussed in Section 1.3, but this can be both computationally expensive and wasteful of valuable data. We therefore turn to a Bayesian treatment of linear regression, which will avoid the over-fitting problem of maximum likelihood, and which will also lead to automatic methods of determining model complexity using the training data alone. Again, for simplicity we will focus on the case of a single target variable t . Extension to multiple target variables is straightforward and follows the discussion of Section 3.1.5.

3.3.1 Parameter distribution

We begin our discussion of the Bayesian treatment of linear regression by introducing a prior probability distribution over the model parameters w . For the moment, we shall treat the noise precision parameter β as a known constant. First note that the likelihood function $p(t|w)$ defined by (3.10) is the exponential of a quadratic function of w . The corresponding conjugate prior is therefore given by a Gaussian distribution of the form

$$p(w) = \mathcal{N}(w|m_0, S_0) \quad (3.48)$$

having mean m_0 and covariance S_0 .

Next we compute the posterior distribution, which is proportional to the product of the likelihood function and the prior. Due to the choice of a conjugate Gaussian prior distribution, the posterior will also be Gaussian. We can evaluate this distribution by the usual procedure of completing the square in the exponential, and then finding the normalization coefficient using the standard result for a normalized Gaussian. However, we have already done the necessary work in deriving the general result (2.116), which allows us to write down the posterior distribution directly in the form

$$p(\mathbf{w}|\mathbf{t}) = \mathcal{N}(\mathbf{w}|\mathbf{m}_N, \mathbf{S}_N) \quad (3.49)$$

where

$$\mathbf{m}_N = \mathbf{S}_N (\mathbf{S}_0^{-1} \mathbf{m}_0 + \beta \Phi^T \mathbf{t}) \quad (3.50)$$

$$\mathbf{S}_N^{-1} = \mathbf{S}_0^{-1} + \beta \Phi^T \Phi. \quad (3.51)$$

Note that because the posterior distribution is Gaussian, its mode coincides with its mean. Thus the maximum posterior weight vector is simply given by $\mathbf{w}_{\text{MAP}} = \mathbf{m}_N$. If we consider an infinitely broad prior $\mathbf{S}_0 = \alpha^{-1} \mathbf{I}$ with $\alpha \rightarrow 0$, the mean \mathbf{m}_N of the posterior distribution reduces to the maximum likelihood value \mathbf{w}_{ML} given by (3.15). Similarly, if $N = 0$, then the posterior distribution reverts to the prior. Furthermore, if data points arrive sequentially, then the posterior distribution at any stage acts as the prior distribution for the subsequent data point, such that the new posterior distribution is again given by (3.49).

Exercise 3.8

For the remainder of this chapter, we shall consider a particular form of Gaussian prior in order to simplify the treatment. Specifically, we consider a zero-mean isotropic Gaussian governed by a single precision parameter α so that

$$p(\mathbf{w}|\alpha) = \mathcal{N}(\mathbf{w}|\mathbf{0}, \alpha^{-1} \mathbf{I}) \quad (3.52)$$

and the corresponding posterior distribution over \mathbf{w} is then given by (3.49) with

$$\mathbf{m}_N = \beta \mathbf{S}_N \Phi^T \mathbf{t} \quad (3.53)$$

$$\mathbf{S}_N^{-1} = \alpha \mathbf{I} + \beta \Phi^T \Phi. \quad (3.54)$$

The log of the posterior distribution is given by the sum of the log likelihood and the log of the prior and, as a function of \mathbf{w} , takes the form

$$\ln p(\mathbf{w}|\mathbf{t}) = -\frac{\beta}{2} \sum_{n=1}^N \{t_n - \mathbf{w}^T \phi(\mathbf{x}_n)\}^2 - \frac{\alpha}{2} \mathbf{w}^T \mathbf{w} + \text{const.} \quad (3.55)$$

Maximization of this posterior distribution with respect to \mathbf{w} is therefore equivalent to the minimization of the sum-of-squares error function with the addition of a quadratic regularization term, corresponding to (3.27) with $\lambda = \alpha/\beta$.

We can illustrate Bayesian learning in a linear basis function model, as well as the sequential update of a posterior distribution, using a simple example involving straight-line fitting. Consider a single input variable x , a single target variable t and

a linear model of the form $y(x, \mathbf{w}) = w_0 + w_1x$. Because this has just two adaptive parameters, we can plot the prior and posterior distributions directly in parameter space. We generate synthetic data from the function $f(x, \mathbf{a}) = a_0 + a_1x$ with parameter values $a_0 = -0.3$ and $a_1 = 0.5$ by first choosing values of x_n from the uniform distribution $U(x| -1, 1)$, then evaluating $f(x_n, \mathbf{a})$, and finally adding Gaussian noise with standard deviation of 0.2 to obtain the target values t_n . Our goal is to recover the values of a_0 and a_1 from such data, and we will explore the dependence on the size of the data set. We assume here that the noise variance is known and hence we set the precision parameter to its true value $\beta = (1/0.2)^2 = 25$. Similarly, we fix the parameter α to 2.0. We shall shortly discuss strategies for determining α and β from the training data. Figure 3.7 shows the results of Bayesian learning in this model as the size of the data set is increased and demonstrates the sequential nature of Bayesian learning in which the current posterior distribution forms the prior when a new data point is observed. It is worth taking time to study this figure in detail as it illustrates several important aspects of Bayesian inference. The first row of this figure corresponds to the situation before any data points are observed and shows a plot of the prior distribution in \mathbf{w} space together with six samples of the function $y(x, \mathbf{w})$ in which the values of \mathbf{w} are drawn from the prior. In the second row, we see the situation after observing a single data point. The location (x, t) of the data point is shown by a blue circle in the right-hand column. In the left-hand column is a plot of the likelihood function $p(t|x, \mathbf{w})$ for this data point as a function of \mathbf{w} . Note that the likelihood function provides a soft constraint that the line must pass close to the data point, where close is determined by the noise precision β . For comparison, the true parameter values $a_0 = -0.3$ and $a_1 = 0.5$ used to generate the data set are shown by a white cross in the plots in the left column of Figure 3.7. When we multiply this likelihood function by the prior from the top row, and normalize, we obtain the posterior distribution shown in the middle plot on the second row. Samples of the regression function $y(x, \mathbf{w})$ obtained by drawing samples of \mathbf{w} from this posterior distribution are shown in the right-hand plot. Note that these sample lines all pass close to the data point. The third row of this figure shows the effect of observing a second data point, again shown by a blue circle in the plot in the right-hand column. The corresponding likelihood function for this second data point alone is shown in the left plot. When we multiply this likelihood function by the posterior distribution from the second row, we obtain the posterior distribution shown in the middle plot of the third row. Note that this is exactly the same posterior distribution as would be obtained by combining the original prior with the likelihood function for the two data points. This posterior has now been influenced by two data points, and because two points are sufficient to define a line this already gives a relatively compact posterior distribution. Samples from this posterior distribution give rise to the functions shown in red in the third column, and we see that these functions pass close to both of the data points. The fourth row shows the effect of observing a total of 20 data points. The left-hand plot shows the likelihood function for the 20th data point alone, and the middle plot shows the resulting posterior distribution that has now absorbed information from all 20 observations. Note how the posterior is much sharper than in the third row. In the limit of an infinite number of data points, the



Figure 3.7 Illustration of sequential Bayesian learning for a simple linear model of the form $y(x, \mathbf{w}) = w_0 + w_1 x$. A detailed description of this figure is given in the text.

posterior distribution would become a delta function centred on the true parameter values, shown by the white cross.

Other forms of prior over the parameters can be considered. For instance, we can generalize the Gaussian prior to give

$$p(\mathbf{w}|\alpha) = \left[\frac{q}{2} \left(\frac{\alpha}{2} \right)^{1/q} \frac{1}{\Gamma(1/q)} \right]^M \exp \left(-\frac{\alpha}{2} \sum_{j=1}^M |w_j|^q \right) \quad (3.56)$$

in which $q = 2$ corresponds to the Gaussian distribution, and only in this case is the prior conjugate to the likelihood function (3.10). Finding the maximum of the posterior distribution over \mathbf{w} corresponds to minimization of the regularized error function (3.29). In the case of the Gaussian prior, the mode of the posterior distribution was equal to the mean, although this will no longer hold if $q \neq 2$.

3.3.2 Predictive distribution

In practice, we are not usually interested in the value of \mathbf{w} itself but rather in making predictions of t for new values of \mathbf{x} . This requires that we evaluate the *predictive distribution* defined by

$$p(t|\mathbf{t}, \alpha, \beta) = \int p(t|\mathbf{w}, \beta)p(\mathbf{w}|\mathbf{t}, \alpha, \beta) d\mathbf{w} \quad (3.57)$$

in which \mathbf{t} is the vector of target values from the training set, and we have omitted the corresponding input vectors from the right-hand side of the conditioning statements to simplify the notation. The conditional distribution $p(t|\mathbf{x}, \mathbf{w}, \beta)$ of the target variable is given by (3.8), and the posterior weight distribution is given by (3.49). We see that (3.57) involves the convolution of two Gaussian distributions, and so making use of the result (2.115) from Section 8.1.4, we see that the predictive distribution takes the form

$$p(t|\mathbf{x}, \mathbf{t}, \alpha, \beta) = \mathcal{N}(t|\mathbf{m}_N^T \boldsymbol{\phi}(\mathbf{x}), \sigma_N^2(\mathbf{x})) \quad (3.58)$$

where the variance $\sigma_N^2(\mathbf{x})$ of the predictive distribution is given by

$$\sigma_N^2(\mathbf{x}) = \frac{1}{\beta} + \boldsymbol{\phi}(\mathbf{x})^T \mathbf{S}_N \boldsymbol{\phi}(\mathbf{x}). \quad (3.59)$$

The first term in (3.59) represents the noise on the data whereas the second term reflects the uncertainty associated with the parameters \mathbf{w} . Because the noise process and the distribution of \mathbf{w} are independent Gaussians, their variances are additive. Note that, as additional data points are observed, the posterior distribution becomes narrower. As a consequence it can be shown (Qazaz *et al.*, 1997) that $\sigma_{N+1}^2(\mathbf{x}) \leq \sigma_N^2(\mathbf{x})$. In the limit $N \rightarrow \infty$, the second term in (3.59) goes to zero, and the variance of the predictive distribution arises solely from the additive noise governed by the parameter β .

Exercise 3.10

Exercise 3.11

As an illustration of the predictive distribution for Bayesian linear regression models, let us return to the synthetic sinusoidal data set of Section 1.1. In Figure 3.8,



Figure 3.8 Examples of the predictive distribution (3.58) for a model consisting of 9 Gaussian basis functions of the form (3.4) using the synthetic sinusoidal data set of Section 1.1. See the text for a detailed discussion.

we fit a model comprising a linear combination of Gaussian basis functions to data sets of various sizes and then look at the corresponding posterior distributions. Here the green curves correspond to the function $\sin(2\pi x)$ from which the data points were generated (with the addition of Gaussian noise). Data sets of size $N = 1$, $N = 2$, $N = 4$, and $N = 25$ are shown in the four plots by the blue circles. For each plot, the red curve shows the mean of the corresponding Gaussian predictive distribution, and the red shaded region spans one standard deviation either side of the mean. Note that the predictive uncertainty depends on x and is smallest in the neighbourhood of the data points. Also note that the level of uncertainty decreases as more data points are observed.

The plots in Figure 3.8 only show the point-wise predictive variance as a function of x . In order to gain insight into the covariance between the predictions at different values of x , we can draw samples from the posterior distribution over \mathbf{w} , and then plot the corresponding functions $y(x, \mathbf{w})$, as shown in Figure 3.9.



Figure 3.9 Plots of the function $y(x, \mathbf{w})$ using samples from the posterior distributions over \mathbf{w} corresponding to the plots in Figure 3.8.

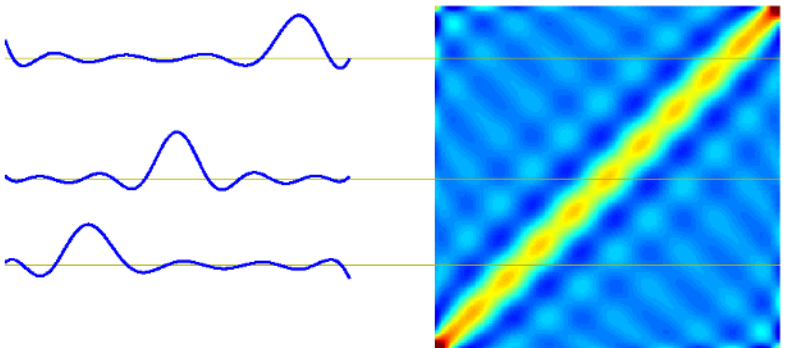
If we used localized basis functions such as Gaussians, then in regions away from the basis function centres, the contribution from the second term in the predictive variance (3.59) will go to zero, leaving only the noise contribution β^{-1} . Thus, the model becomes very confident in its predictions when extrapolating outside the region occupied by the basis functions, which is generally an undesirable behaviour. This problem can be avoided by adopting an alternative Bayesian approach to regression known as a Gaussian process.

Section 6.4

Exercise 3.12
Exercise 3.13

Note that, if both \mathbf{w} and β are treated as unknown, then we can introduce a conjugate prior distribution $p(\mathbf{w}, \beta)$ that, from the discussion in Section 2.3.6, will be given by a Gaussian-gamma distribution (Denison *et al.*, 2002). In this case, the predictive distribution is a Student's t-distribution.

Figure 3.10 The equivalent kernel $k(x, x')$ for the Gaussian basis functions in Figure 3.1, shown as a plot of x versus x' , together with three slices through this matrix corresponding to three different values of x . The data set used to generate this kernel comprised 200 values of x equally spaced over the interval $(-1, 1)$.



3.3.3 Equivalent kernel

Chapter 6

The posterior mean solution (3.53) for the linear basis function model has an interesting interpretation that will set the stage for kernel methods, including Gaussian processes. If we substitute (3.53) into the expression (3.3), we see that the predictive mean can be written in the form

$$y(\mathbf{x}, \mathbf{m}_N) = \mathbf{m}_N^T \phi(\mathbf{x}) = \beta \phi(\mathbf{x})^T \mathbf{S}_N \Phi^T \mathbf{t} = \sum_{n=1}^N \beta \phi(\mathbf{x})^T \mathbf{S}_N \phi(\mathbf{x}_n) t_n \quad (3.60)$$

where \mathbf{S}_N is defined by (3.51). Thus the mean of the predictive distribution at a point \mathbf{x} is given by a linear combination of the training set target variables t_n , so that we can write

$$y(\mathbf{x}, \mathbf{m}_N) = \sum_{n=1}^N k(\mathbf{x}, \mathbf{x}_n) t_n \quad (3.61)$$

where the function

$$k(\mathbf{x}, \mathbf{x}') = \beta \phi(\mathbf{x})^T \mathbf{S}_N \phi(\mathbf{x}') \quad (3.62)$$

is known as the *smoother matrix* or the *equivalent kernel*. Regression functions, such as this, which make predictions by taking linear combinations of the training set target values are known as *linear smoothers*. Note that the equivalent kernel depends on the input values \mathbf{x}_n from the data set because these appear in the definition of \mathbf{S}_N . The equivalent kernel is illustrated for the case of Gaussian basis functions in Figure 3.10 in which the kernel functions $k(x, x')$ have been plotted as a function of x' for three different values of x . We see that they are localized around x , and so the mean of the predictive distribution at x , given by $y(\mathbf{x}, \mathbf{m}_N)$, is obtained by forming a weighted combination of the target values in which data points close to x are given higher weight than points further removed from x . Intuitively, it seems reasonable that we should weight local evidence more strongly than distant evidence. Note that this localization property holds not only for the localized Gaussian basis functions but also for the nonlocal polynomial and sigmoidal basis functions, as illustrated in Figure 3.11.

Figure 3.11 Examples of equivalent kernels $k(x, x')$ for $x = 0$ plotted as a function of x' , corresponding (left) to the polynomial basis functions and (right) to the sigmoidal basis functions shown in Figure 3.1. Note that these are localized functions of x' even though the corresponding basis functions are nonlocal.



Further insight into the role of the equivalent kernel can be obtained by considering the covariance between $y(\mathbf{x})$ and $y(\mathbf{x}')$, which is given by

$$\begin{aligned}\text{cov}[y(\mathbf{x}), y(\mathbf{x}')] &= \text{cov}[\phi(\mathbf{x})^T \mathbf{w}, \mathbf{w}^T \phi(\mathbf{x}')] \\ &= \phi(\mathbf{x})^T \mathbf{S}_N \phi(\mathbf{x}') = \beta^{-1} k(\mathbf{x}, \mathbf{x}')\end{aligned}\quad (3.63)$$

where we have made use of (3.49) and (3.62). From the form of the equivalent kernel, we see that the predictive mean at nearby points will be highly correlated, whereas for more distant pairs of points the correlation will be smaller.

The predictive distribution shown in Figure 3.8 allows us to visualize the pointwise uncertainty in the predictions, governed by (3.59). However, by drawing samples from the posterior distribution over \mathbf{w} , and plotting the corresponding model functions $y(\mathbf{x}, \mathbf{w})$ as in Figure 3.9, we are visualizing the joint uncertainty in the posterior distribution between the y values at two (or more) x values, as governed by the equivalent kernel.

The formulation of linear regression in terms of a kernel function suggests an alternative approach to regression as follows. Instead of introducing a set of basis functions, which implicitly determines an equivalent kernel, we can instead define a localized kernel directly and use this to make predictions for new input vectors \mathbf{x} , given the observed training set. This leads to a practical framework for regression (and classification) called *Gaussian processes*, which will be discussed in detail in Section 6.4.

We have seen that the effective kernel defines the weights by which the training set target values are combined in order to make a prediction at a new value of \mathbf{x} , and it can be shown that these weights sum to one, in other words

$$\sum_{n=1}^N k(\mathbf{x}, \mathbf{x}_n) = 1 \quad (3.64)$$

Exercise 3.14

for all values of \mathbf{x} . This intuitively pleasing result can easily be proven informally by noting that the summation is equivalent to considering the predictive mean $\hat{y}(\mathbf{x})$ for a set of target data in which $t_n = 1$ for all n . Provided the basis functions are linearly independent, that there are more data points than basis functions, and that one of the basis functions is constant (corresponding to the bias parameter), then it is clear that we can fit the training data exactly and hence that the predictive mean will

be simply $\hat{y}(\mathbf{x}) = 1$, from which we obtain (3.64). Note that the kernel function can be negative as well as positive, so although it satisfies a summation constraint, the corresponding predictions are not necessarily convex combinations of the training set target variables.

Chapter 6

Finally, we note that the equivalent kernel (3.62) satisfies an important property shared by kernel functions in general, namely that it can be expressed in the form an inner product with respect to a vector $\psi(\mathbf{x})$ of nonlinear functions, so that

$$k(\mathbf{x}, \mathbf{z}) = \psi(\mathbf{x})^T \psi(\mathbf{z}) \quad (3.65)$$

where $\psi(\mathbf{x}) = \beta^{1/2} \mathbf{S}_N^{1/2} \phi(\mathbf{x})$.

3.4. Bayesian Model Comparison

In Chapter 1, we highlighted the problem of over-fitting as well as the use of cross-validation as a technique for setting the values of regularization parameters or for choosing between alternative models. Here we consider the problem of model selection from a Bayesian perspective. In this section, our discussion will be very general, and then in Section 3.5 we shall see how these ideas can be applied to the determination of regularization parameters in linear regression.

As we shall see, the over-fitting associated with maximum likelihood can be avoided by marginalizing (summing or integrating) over the model parameters instead of making point estimates of their values. Models can then be compared directly on the training data, without the need for a validation set. This allows all available data to be used for training and avoids the multiple training runs for each model associated with cross-validation. It also allows multiple complexity parameters to be determined simultaneously as part of the training process. For example, in Chapter 7 we shall introduce the *relevance vector machine*, which is a Bayesian model having one complexity parameter for every training data point.

Section 1.5.4

The Bayesian view of model comparison simply involves the use of probabilities to represent uncertainty in the choice of model, along with a consistent application of the sum and product rules of probability. Suppose we wish to compare a set of L models $\{\mathcal{M}_i\}$ where $i = 1, \dots, L$. Here a model refers to a probability distribution over the observed data \mathcal{D} . In the case of the polynomial curve-fitting problem, the distribution is defined over the set of target values \mathbf{t} , while the set of input values \mathbf{X} is assumed to be known. Other types of model define a joint distributions over \mathbf{X} and \mathbf{t} . We shall suppose that the data is generated from one of these models but we are uncertain which one. Our uncertainty is expressed through a prior probability distribution $p(\mathcal{M}_i)$. Given a training set \mathcal{D} , we then wish to evaluate the posterior distribution

$$p(\mathcal{M}_i | \mathcal{D}) \propto p(\mathcal{M}_i) p(\mathcal{D} | \mathcal{M}_i). \quad (3.66)$$

The prior allows us to express a preference for different models. Let us simply assume that all models are given equal prior probability. The interesting term is the *model evidence* $p(\mathcal{D} | \mathcal{M}_i)$ which expresses the preference shown by the data for

different models, and we shall examine this term in more detail shortly. The model evidence is sometimes also called the *marginal likelihood* because it can be viewed as a likelihood function over the space of models, in which the parameters have been marginalized out. The ratio of model evidences $p(\mathcal{D}|\mathcal{M}_i)/p(\mathcal{D}|\mathcal{M}_j)$ for two models is known as a *Bayes factor* (Kass and Raftery, 1995).

Once we know the posterior distribution over models, the predictive distribution is given, from the sum and product rules, by

$$p(t|\mathbf{x}, \mathcal{D}) = \sum_{i=1}^L p(t|\mathbf{x}, \mathcal{M}_i, \mathcal{D})p(\mathcal{M}_i|\mathcal{D}). \quad (3.67)$$

This is an example of a *mixture distribution* in which the overall predictive distribution is obtained by averaging the predictive distributions $p(t|\mathbf{x}, \mathcal{M}_i, \mathcal{D})$ of individual models, weighted by the posterior probabilities $p(\mathcal{M}_i|\mathcal{D})$ of those models. For instance, if we have two models that are a-posteriori equally likely and one predicts a narrow distribution around $t = a$ while the other predicts a narrow distribution around $t = b$, the overall predictive distribution will be a bimodal distribution with modes at $t = a$ and $t = b$, not a single model at $t = (a + b)/2$.

A simple approximation to model averaging is to use the single most probable model alone to make predictions. This is known as *model selection*.

For a model governed by a set of parameters \mathbf{w} , the model evidence is given, from the sum and product rules of probability, by

$$p(\mathcal{D}|\mathcal{M}_i) = \int p(\mathcal{D}|\mathbf{w}, \mathcal{M}_i)p(\mathbf{w}|\mathcal{M}_i) d\mathbf{w}. \quad (3.68)$$

Chapter 11

From a sampling perspective, the marginal likelihood can be viewed as the probability of generating the data set \mathcal{D} from a model whose parameters are sampled at random from the prior. It is also interesting to note that the evidence is precisely the normalizing term that appears in the denominator in Bayes' theorem when evaluating the posterior distribution over parameters because

$$p(\mathbf{w}|\mathcal{D}, \mathcal{M}_i) = \frac{p(\mathcal{D}|\mathbf{w}, \mathcal{M}_i)p(\mathbf{w}|\mathcal{M}_i)}{p(\mathcal{D}|\mathcal{M}_i)}. \quad (3.69)$$

We can obtain some insight into the model evidence by making a simple approximation to the integral over parameters. Consider first the case of a model having a single parameter w . The posterior distribution over parameters is proportional to $p(\mathcal{D}|w)p(w)$, where we omit the dependence on the model \mathcal{M}_i to keep the notation uncluttered. If we assume that the posterior distribution is sharply peaked around the most probable value w_{MAP} , with width $\Delta w_{\text{posterior}}$, then we can approximate the integral by the value of the integrand at its maximum times the width of the peak. If we further assume that the prior is flat with width Δw_{prior} so that $p(w) = 1/\Delta w_{\text{prior}}$, then we have

$$p(\mathcal{D}) = \int p(\mathcal{D}|w)p(w) dw \simeq p(\mathcal{D}|w_{\text{MAP}}) \frac{\Delta w_{\text{posterior}}}{\Delta w_{\text{prior}}} \quad (3.70)$$

Figure 3.12 We can obtain a rough approximation to the model evidence if we assume that the posterior distribution over parameters is sharply peaked around its mode w_{MAP} .



and so taking logs we obtain

$$\ln p(\mathcal{D}) \simeq \ln p(\mathcal{D}|w_{\text{MAP}}) + \ln \left(\frac{\Delta w_{\text{posterior}}}{\Delta w_{\text{prior}}} \right). \quad (3.71)$$

This approximation is illustrated in Figure 3.12. The first term represents the fit to the data given by the most probable parameter values, and for a flat prior this would correspond to the log likelihood. The second term penalizes the model according to its complexity. Because $\Delta w_{\text{posterior}} < \Delta w_{\text{prior}}$ this term is negative, and it increases in magnitude as the ratio $\Delta w_{\text{posterior}}/\Delta w_{\text{prior}}$ gets smaller. Thus, if parameters are finely tuned to the data in the posterior distribution, then the penalty term is large.

For a model having a set of M parameters, we can make a similar approximation for each parameter in turn. Assuming that all parameters have the same ratio of $\Delta w_{\text{posterior}}/\Delta w_{\text{prior}}$, we obtain

$$\ln p(\mathcal{D}) \simeq \ln p(\mathcal{D}|w_{\text{MAP}}) + M \ln \left(\frac{\Delta w_{\text{posterior}}}{\Delta w_{\text{prior}}} \right). \quad (3.72)$$

Thus, in this very simple approximation, the size of the complexity penalty increases linearly with the number M of adaptive parameters in the model. As we increase the complexity of the model, the first term will typically decrease, because a more complex model is better able to fit the data, whereas the second term will increase due to the dependence on M . The optimal model complexity, as determined by the maximum evidence, will be given by a trade-off between these two competing terms. We shall later develop a more refined version of this approximation, based on a Gaussian approximation to the posterior distribution.

Section 4.4.1

We can gain further insight into Bayesian model comparison and understand how the marginal likelihood can favour models of intermediate complexity by considering Figure 3.13. Here the horizontal axis is a one-dimensional representation of the space of possible data sets, so that each point on this axis corresponds to a specific data set. We now consider three models \mathcal{M}_1 , \mathcal{M}_2 and \mathcal{M}_3 of successively increasing complexity. Imagine running these models generatively to produce example data sets, and then looking at the distribution of data sets that result. Any given

Figure 3.13 Schematic illustration of the distribution of data sets for three models of different complexity, in which \mathcal{M}_1 is the simplest and \mathcal{M}_3 is the most complex. Note that the distributions are normalized. In this example, for the particular observed data set \mathcal{D}_0 , the model \mathcal{M}_2 with intermediate complexity has the largest evidence.



model can generate a variety of different data sets since the parameters are governed by a prior probability distribution, and for any choice of the parameters there may be random noise on the target variables. To generate a particular data set from a specific model, we first choose the values of the parameters from their prior distribution $p(\mathbf{w})$, and then for these parameter values we sample the data from $p(\mathcal{D}|\mathbf{w})$. A simple model (for example, based on a first order polynomial) has little variability and so will generate data sets that are fairly similar to each other. Its distribution $p(\mathcal{D})$ is therefore confined to a relatively small region of the horizontal axis. By contrast, a complex model (such as a ninth order polynomial) can generate a great variety of different data sets, and so its distribution $p(\mathcal{D})$ is spread over a large region of the space of data sets. Because the distributions $p(\mathcal{D}|\mathcal{M}_i)$ are normalized, we see that the particular data set \mathcal{D}_0 can have the highest value of the evidence for the model of intermediate complexity. Essentially, the simpler model cannot fit the data well, whereas the more complex model spreads its predictive probability over too broad a range of data sets and so assigns relatively small probability to any one of them.

Implicit in the Bayesian model comparison framework is the assumption that the true distribution from which the data are generated is contained within the set of models under consideration. Provided this is so, we can show that Bayesian model comparison will on average favour the correct model. To see this, consider two models \mathcal{M}_1 and \mathcal{M}_2 in which the truth corresponds to \mathcal{M}_1 . For a given finite data set, it is possible for the Bayes factor to be larger for the incorrect model. However, if we average the Bayes factor over the distribution of data sets, we obtain the expected Bayes factor in the form

$$\int p(\mathcal{D}|\mathcal{M}_1) \ln \frac{p(\mathcal{D}|\mathcal{M}_1)}{p(\mathcal{D}|\mathcal{M}_2)} d\mathcal{D} \quad (3.73)$$

where the average has been taken with respect to the true distribution of the data. This quantity is an example of the *Kullback-Leibler* divergence and satisfies the property of always being positive unless the two distributions are equal in which case it is zero. Thus on average the Bayes factor will always favour the correct model.

We have seen that the Bayesian framework avoids the problem of over-fitting and allows models to be compared on the basis of the training data alone. However,

a Bayesian approach, like any approach to pattern recognition, needs to make assumptions about the form of the model, and if these are invalid then the results can be misleading. In particular, we see from Figure 3.12 that the model evidence can be sensitive to many aspects of the prior, such as the behaviour in the tails. Indeed, the evidence is not defined if the prior is improper, as can be seen by noting that an improper prior has an arbitrary scaling factor (in other words, the normalization coefficient is not defined because the distribution cannot be normalized). If we consider a proper prior and then take a suitable limit in order to obtain an improper prior (for example, a Gaussian prior in which we take the limit of infinite variance) then the evidence will go to zero, as can be seen from (3.70) and Figure 3.12. It may, however, be possible to consider the evidence ratio between two models first and then take a limit to obtain a meaningful answer.

In a practical application, therefore, it will be wise to keep aside an independent test set of data on which to evaluate the overall performance of the final system.

3.5. The Evidence Approximation

In a fully Bayesian treatment of the linear basis function model, we would introduce prior distributions over the hyperparameters α and β and make predictions by marginalizing with respect to these hyperparameters as well as with respect to the parameters \mathbf{w} . However, although we can integrate analytically over either \mathbf{w} or over the hyperparameters, the complete marginalization over all of these variables is analytically intractable. Here we discuss an approximation in which we set the hyperparameters to specific values determined by maximizing the *marginal likelihood function* obtained by first integrating over the parameters \mathbf{w} . This framework is known in the statistics literature as *empirical Bayes* (Bernardo and Smith, 1994; Gelman *et al.*, 2004), or *type 2 maximum likelihood* (Berger, 1985), or *generalized maximum likelihood* (Wahba, 1975), and in the machine learning literature is also called the *evidence approximation* (Gull, 1989; MacKay, 1992a).

If we introduce hyperpriors over α and β , the predictive distribution is obtained by marginalizing over \mathbf{w} , α and β so that

$$p(t|\mathbf{t}) = \iiint p(t|\mathbf{w}, \beta) p(\mathbf{w}|\mathbf{t}, \alpha, \beta) p(\alpha, \beta|\mathbf{t}) d\mathbf{w} d\alpha d\beta \quad (3.74)$$

where $p(t|\mathbf{w}, \beta)$ is given by (3.8) and $p(\mathbf{w}|\mathbf{t}, \alpha, \beta)$ is given by (3.49) with \mathbf{m}_N and \mathbf{S}_N defined by (3.53) and (3.54) respectively. Here we have omitted the dependence on the input variable \mathbf{x} to keep the notation uncluttered. If the posterior distribution $p(\alpha, \beta|\mathbf{t})$ is sharply peaked around values $\hat{\alpha}$ and $\hat{\beta}$, then the predictive distribution is obtained simply by marginalizing over \mathbf{w} in which α and β are fixed to the values $\hat{\alpha}$ and $\hat{\beta}$, so that

$$p(t|\mathbf{t}) \simeq p(t|\mathbf{t}, \hat{\alpha}, \hat{\beta}) = \int p(t|\mathbf{w}, \hat{\beta}) p(\mathbf{w}|\mathbf{t}, \hat{\alpha}, \hat{\beta}) d\mathbf{w}. \quad (3.75)$$

From Bayes' theorem, the posterior distribution for α and β is given by

$$p(\alpha, \beta | \mathbf{t}) \propto p(\mathbf{t} | \alpha, \beta) p(\alpha, \beta). \quad (3.76)$$

If the prior is relatively flat, then in the evidence framework the values of $\hat{\alpha}$ and $\hat{\beta}$ are obtained by maximizing the marginal likelihood function $p(\mathbf{t} | \alpha, \beta)$. We shall proceed by evaluating the marginal likelihood for the linear basis function model and then finding its maxima. This will allow us to determine values for these hyperparameters from the training data alone, without recourse to cross-validation. Recall that the ratio α/β is analogous to a regularization parameter.

As an aside it is worth noting that, if we define conjugate (Gamma) prior distributions over α and β , then the marginalization over these hyperparameters in (3.74) can be performed analytically to give a Student's t-distribution over \mathbf{w} (see Section 2.3.7). Although the resulting integral over \mathbf{w} is no longer analytically tractable, it might be thought that approximating this integral, for example using the Laplace approximation discussed (Section 4.4) which is based on a local Gaussian approximation centred on the mode of the posterior distribution, might provide a practical alternative to the evidence framework (Buntine and Weigend, 1991). However, the integrand as a function of \mathbf{w} typically has a strongly skewed mode so that the Laplace approximation fails to capture the bulk of the probability mass, leading to poorer results than those obtained by maximizing the evidence (MacKay, 1999).

Returning to the evidence framework, we note that there are two approaches that we can take to the maximization of the log evidence. We can evaluate the evidence function analytically and then set its derivative equal to zero to obtain re-estimation equations for α and β , which we shall do in Section 3.5.2. Alternatively we use a technique called the expectation maximization (EM) algorithm, which will be discussed in Section 9.3.4 where we shall also show that these two approaches converge to the same solution.

3.5.1 Evaluation of the evidence function

The marginal likelihood function $p(\mathbf{t} | \alpha, \beta)$ is obtained by integrating over the weight parameters \mathbf{w} , so that

$$p(\mathbf{t} | \alpha, \beta) = \int p(\mathbf{t} | \mathbf{w}, \beta) p(\mathbf{w} | \alpha) d\mathbf{w}. \quad (3.77)$$

One way to evaluate this integral is to make use once again of the result (2.115) for the conditional distribution in a linear-Gaussian model. Here we shall evaluate the integral instead by completing the square in the exponent and making use of the standard form for the normalization coefficient of a Gaussian.

Exercise 3.16

Exercise 3.17

From (3.11), (3.12), and (3.52), we can write the evidence function in the form

$$p(\mathbf{t} | \alpha, \beta) = \left(\frac{\beta}{2\pi} \right)^{N/2} \left(\frac{\alpha}{2\pi} \right)^{M/2} \int \exp \{-E(\mathbf{w})\} d\mathbf{w} \quad (3.78)$$

where M is the dimensionality of \mathbf{w} , and we have defined

$$\begin{aligned} E(\mathbf{w}) &= \beta E_D(\mathbf{w}) + \alpha E_W(\mathbf{w}) \\ &= \frac{\beta}{2} \|\mathbf{t} - \Phi\mathbf{w}\|^2 + \frac{\alpha}{2} \mathbf{w}^T \mathbf{w}. \end{aligned} \quad (3.79)$$

We recognize (3.79) as being equal, up to a constant of proportionality, to the regularized sum-of-squares error function (3.27). We now complete the square over \mathbf{w} giving

$$E(\mathbf{w}) = E(\mathbf{m}_N) + \frac{1}{2}(\mathbf{w} - \mathbf{m}_N)^T \mathbf{A}(\mathbf{w} - \mathbf{m}_N) \quad (3.80)$$

where we have introduced

$$\mathbf{A} = \alpha \mathbf{I} + \beta \Phi^T \Phi \quad (3.81)$$

together with

$$E(\mathbf{m}_N) = \frac{\beta}{2} \|\mathbf{t} - \Phi \mathbf{m}_N\|^2 + \frac{\alpha}{2} \mathbf{m}_N^T \mathbf{m}_N. \quad (3.82)$$

Note that \mathbf{A} corresponds to the matrix of second derivatives of the error function

$$\mathbf{A} = \nabla \nabla E(\mathbf{w}) \quad (3.83)$$

and is known as the *Hessian matrix*. Here we have also defined \mathbf{m}_N given by

$$\mathbf{m}_N = \beta \mathbf{A}^{-1} \Phi^T \mathbf{t}. \quad (3.84)$$

Using (3.54), we see that $\mathbf{A} = \mathbf{S}_N^{-1}$, and hence (3.84) is equivalent to the previous definition (3.53), and therefore represents the mean of the posterior distribution.

The integral over \mathbf{w} can now be evaluated simply by appealing to the standard result for the normalization coefficient of a multivariate Gaussian, giving

$$\begin{aligned} &\int \exp \{-E(\mathbf{w})\} d\mathbf{w} \\ &= \exp \{-E(\mathbf{m}_N)\} \int \exp \left\{ -\frac{1}{2}(\mathbf{w} - \mathbf{m}_N)^T \mathbf{A}(\mathbf{w} - \mathbf{m}_N) \right\} d\mathbf{w} \\ &= \exp \{-E(\mathbf{m}_N)\} (2\pi)^{M/2} |\mathbf{A}|^{-1/2}. \end{aligned} \quad (3.85)$$

Using (3.78) we can then write the log of the marginal likelihood in the form

$$\ln p(\mathbf{t} | \alpha, \beta) = \frac{M}{2} \ln \alpha + \frac{N}{2} \ln \beta - E(\mathbf{m}_N) - \frac{1}{2} \ln |\mathbf{A}| - \frac{N}{2} \ln(2\pi) \quad (3.86)$$

which is the required expression for the evidence function.

Returning to the polynomial regression problem, we can plot the model evidence against the order of the polynomial, as shown in Figure 3.14. Here we have assumed a prior of the form (1.65) with the parameter α fixed at $\alpha = 5 \times 10^{-3}$. The form of this plot is very instructive. Referring back to Figure 1.4, we see that the $M = 0$ polynomial has very poor fit to the data and consequently gives a relatively low value

Exercise 3.18

Exercise 3.19

Figure 3.14 Plot of the model evidence versus the order M , for the polynomial regression model, showing that the evidence favours the model with $M = 3$.



for the evidence. Going to the $M = 1$ polynomial greatly improves the data fit, and hence the evidence is significantly higher. However, in going to $M = 2$, the data fit is improved only very marginally, due to the fact that the underlying sinusoidal function from which the data is generated is an odd function and so has no even terms in a polynomial expansion. Indeed, Figure 1.5 shows that the residual data error is reduced only slightly in going from $M = 1$ to $M = 2$. Because this richer model suffers a greater complexity penalty, the evidence actually falls in going from $M = 1$ to $M = 2$. When we go to $M = 3$ we obtain a significant further improvement in data fit, as seen in Figure 1.4, and so the evidence is increased again, giving the highest overall evidence for any of the polynomials. Further increases in the value of M produce only small improvements in the fit to the data but suffer increasing complexity penalty, leading overall to a decrease in the evidence values. Looking again at Figure 1.5, we see that the generalization error is roughly constant between $M = 3$ and $M = 8$, and it would be difficult to choose between these models on the basis of this plot alone. The evidence values, however, show a clear preference for $M = 3$, since this is the simplest model which gives a good explanation for the observed data.

3.5.2 Maximizing the evidence function

Let us first consider the maximization of $p(\mathbf{t}|\alpha, \beta)$ with respect to α . This can be done by first defining the following eigenvector equation

$$(\beta \Phi^T \Phi) \mathbf{u}_i = \lambda_i \mathbf{u}_i. \quad (3.87)$$

From (3.81), it then follows that \mathbf{A} has eigenvalues $\alpha + \lambda_i$. Now consider the derivative of the term involving $\ln |\mathbf{A}|$ in (3.86) with respect to α . We have

$$\frac{d}{d\alpha} \ln |\mathbf{A}| = \frac{d}{d\alpha} \ln \prod_i (\lambda_i + \alpha) = \frac{d}{d\alpha} \sum_i \ln(\lambda_i + \alpha) = \sum_i \frac{1}{\lambda_i + \alpha}. \quad (3.88)$$

Thus the stationary points of (3.86) with respect to α satisfy

$$0 = \frac{M}{2\alpha} - \frac{1}{2} \mathbf{m}_N^T \mathbf{m}_N - \frac{1}{2} \sum_i \frac{1}{\lambda_i + \alpha}. \quad (3.89)$$

Multiplying through by 2α and rearranging, we obtain

$$\alpha \mathbf{m}_N^T \mathbf{m}_N = M - \alpha \sum_i \frac{1}{\lambda_i + \alpha} = \gamma. \quad (3.90)$$

Since there are M terms in the sum over i , the quantity γ can be written

$$\gamma = \sum_i \frac{\lambda_i}{\alpha + \lambda_i}. \quad (3.91)$$

The interpretation of the quantity γ will be discussed shortly. From (3.90) we see that the value of α that maximizes the marginal likelihood satisfies

$$\alpha = \frac{\gamma}{\mathbf{m}_N^T \mathbf{m}_N}. \quad (3.92)$$

Note that this is an implicit solution for α not only because γ depends on α , but also because the mode \mathbf{m}_N of the posterior distribution itself depends on the choice of α . We therefore adopt an iterative procedure in which we make an initial choice for α and use this to find \mathbf{m}_N , which is given by (3.53), and also to evaluate γ , which is given by (3.91). These values are then used to re-estimate α using (3.92), and the process repeated until convergence. Note that because the matrix $\Phi^T \Phi$ is fixed, we can compute its eigenvalues once at the start and then simply multiply these by β to obtain the λ_i .

It should be emphasized that the value of α has been determined purely by looking at the training data. In contrast to maximum likelihood methods, no independent data set is required in order to optimize the model complexity.

We can similarly maximize the log marginal likelihood (3.86) with respect to β . To do this, we note that the eigenvalues λ_i defined by (3.87) are proportional to β , and hence $d\lambda_i/d\beta = \lambda_i/\beta$ giving

$$\frac{d}{d\beta} \ln |\mathbf{A}| = \frac{d}{d\beta} \sum_i \ln(\lambda_i + \alpha) = \frac{1}{\beta} \sum_i \frac{\lambda_i}{\lambda_i + \alpha} = \frac{\gamma}{\beta}. \quad (3.93)$$

The stationary point of the marginal likelihood therefore satisfies

$$0 = \frac{N}{2\beta} - \frac{1}{2} \sum_{n=1}^N \{t_n - \mathbf{m}_N^T \phi(\mathbf{x}_n)\}^2 - \frac{\gamma}{2\beta} \quad (3.94)$$

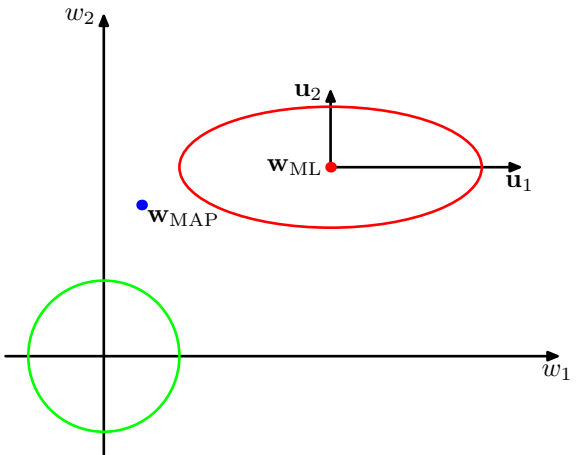
Exercise 3.22

and rearranging we obtain

$$\frac{1}{\beta} = \frac{1}{N - \gamma} \sum_{n=1}^N \{t_n - \mathbf{m}_N^T \phi(\mathbf{x}_n)\}^2. \quad (3.95)$$

Again, this is an implicit solution for β and can be solved by choosing an initial value for β and then using this to calculate \mathbf{m}_N and γ and then re-estimate β using (3.95), repeating until convergence. If both α and β are to be determined from the data, then their values can be re-estimated together after each update of γ .

Figure 3.15 Contours of the likelihood function (red) and the prior (green) in which the axes in parameter space have been rotated to align with the eigenvectors \mathbf{u}_i of the Hessian. For $\alpha = 0$, the mode of the posterior is given by the maximum likelihood solution \mathbf{w}_{ML} , whereas for nonzero α the mode is at $\mathbf{w}_{\text{MAP}} = \mathbf{m}_N$. In the direction w_1 the eigenvalue λ_1 , defined by (3.87), is small compared with α and so the quantity $\lambda_1/(\lambda_1 + \alpha)$ is close to zero, and the corresponding MAP value of w_1 is also close to zero. By contrast, in the direction w_2 the eigenvalue λ_2 is large compared with α and so the quantity $\lambda_2/(\lambda_2 + \alpha)$ is close to unity, and the MAP value of w_2 is close to its maximum likelihood value.



3.5.3 Effective number of parameters

The result (3.92) has an elegant interpretation (MacKay, 1992a), which provides insight into the Bayesian solution for α . To see this, consider the contours of the likelihood function and the prior as illustrated in Figure 3.15. Here we have implicitly transformed to a rotated set of axes in parameter space aligned with the eigenvectors \mathbf{u}_i defined in (3.87). Contours of the likelihood function are then axis-aligned ellipses. The eigenvalues λ_i measure the curvature of the likelihood function, and so in Figure 3.15 the eigenvalue λ_1 is small compared with λ_2 (because a smaller curvature corresponds to a greater elongation of the contours of the likelihood function). Because $\beta\Phi^T\Phi$ is a positive definite matrix, it will have positive eigenvalues, and so the ratio $\lambda_i/(\lambda_i + \alpha)$ will lie between 0 and 1. Consequently, the quantity γ defined by (3.91) will lie in the range $0 \leq \gamma \leq M$. For directions in which $\lambda_i \gg \alpha$, the corresponding parameter w_i will be close to its maximum likelihood value, and the ratio $\lambda_i/(\lambda_i + \alpha)$ will be close to 1. Such parameters are called *well determined* because their values are tightly constrained by the data. Conversely, for directions in which $\lambda_i \ll \alpha$, the corresponding parameters w_i will be close to zero, as will the ratios $\lambda_i/(\lambda_i + \alpha)$. These are directions in which the likelihood function is relatively insensitive to the parameter value and so the parameter has been set to a small value by the prior. The quantity γ defined by (3.91) therefore measures the effective total number of well determined parameters.

We can obtain some insight into the result (3.95) for re-estimating β by comparing it with the corresponding maximum likelihood result given by (3.21). Both of these formulae express the variance (the inverse precision) as an average of the squared differences between the targets and the model predictions. However, they differ in that the number of data points N in the denominator of the maximum likelihood result is replaced by $N - \gamma$ in the Bayesian result. We recall from (1.56) that the maximum likelihood estimate of the variance for a Gaussian distribution over a

single variable x is given by

$$\sigma_{\text{ML}}^2 = \frac{1}{N} \sum_{n=1}^N (x_n - \mu_{\text{ML}})^2 \quad (3.96)$$

and that this estimate is biased because the maximum likelihood solution μ_{ML} for the mean has fitted some of the noise on the data. In effect, this has used up one degree of freedom in the model. The corresponding unbiased estimate is given by (1.59) and takes the form

$$\sigma_{\text{MAP}}^2 = \frac{1}{N-1} \sum_{n=1}^N (x_n - \mu_{\text{ML}})^2. \quad (3.97)$$

We shall see in Section 10.1.3 that this result can be obtained from a Bayesian treatment in which we marginalize over the unknown mean. The factor of $N-1$ in the denominator of the Bayesian result takes account of the fact that one degree of freedom has been used in fitting the mean and removes the bias of maximum likelihood. Now consider the corresponding results for the linear regression model. The mean of the target distribution is now given by the function $\mathbf{w}^T \phi(\mathbf{x})$, which contains M parameters. However, not all of these parameters are tuned to the data. The effective number of parameters that are determined by the data is γ , with the remaining $M-\gamma$ parameters set to small values by the prior. This is reflected in the Bayesian result for the variance that has a factor $N-\gamma$ in the denominator, thereby correcting for the bias of the maximum likelihood result.

We can illustrate the evidence framework for setting hyperparameters using the sinusoidal synthetic data set from Section 1.1, together with the Gaussian basis function model comprising 9 basis functions, so that the total number of parameters in the model is given by $M = 10$ including the bias. Here, for simplicity of illustration, we have set β to its true value of 11.1 and then used the evidence framework to determine α , as shown in Figure 3.16.

We can also see how the parameter α controls the magnitude of the parameters $\{w_i\}$, by plotting the individual parameters versus the effective number γ of parameters, as shown in Figure 3.17.

If we consider the limit $N \gg M$ in which the number of data points is large in relation to the number of parameters, then from (3.87) all of the parameters will be well determined by the data because $\Phi^T \Phi$ involves an implicit sum over data points, and so the eigenvalues λ_i increase with the size of the data set. In this case, $\gamma = M$, and the re-estimation equations for α and β become

$$\alpha = \frac{M}{2E_W(\mathbf{m}_N)} \quad (3.98)$$

$$\beta = \frac{N}{2E_D(\mathbf{m}_N)} \quad (3.99)$$

where E_W and E_D are defined by (3.25) and (3.26), respectively. These results can be used as an easy-to-compute approximation to the full evidence re-estimation



Figure 3.16 The left plot shows γ (red curve) and $2\alpha E_W(m_N)$ (blue curve) versus $\ln \alpha$ for the sinusoidal synthetic data set. It is the intersection of these two curves that defines the optimum value for α given by the evidence procedure. The right plot shows the corresponding graph of log evidence $\ln p(t|\alpha, \beta)$ versus $\ln \alpha$ (red curve) showing that the peak coincides with the crossing point of the curves in the left plot. Also shown is the test set error (blue curve) showing that the evidence maximum occurs close to the point of best generalization.

formulae, because they do not require evaluation of the eigenvalue spectrum of the Hessian.

Figure 3.17 Plot of the 10 parameters w_i from the Gaussian basis function model versus the effective number of parameters γ , in which the hyperparameter α is varied in the range $0 \leq \alpha \leq \infty$ causing γ to vary in the range $0 \leq \gamma \leq M$.



3.6. Limitations of Fixed Basis Functions

Throughout this chapter, we have focussed on models comprising a linear combination of fixed, nonlinear basis functions. We have seen that the assumption of linearity in the parameters led to a range of useful properties including closed-form solutions to the least-squares problem, as well as a tractable Bayesian treatment. Furthermore, for a suitable choice of basis functions, we can model arbitrary nonlinearities in the

mapping from input variables to targets. In the next chapter, we shall study an analogous class of models for classification.

It might appear, therefore, that such linear models constitute a general purpose framework for solving problems in pattern recognition. Unfortunately, there are some significant shortcomings with linear models, which will cause us to turn in later chapters to more complex models such as support vector machines and neural networks.

The difficulty stems from the assumption that the basis functions $\phi_j(\mathbf{x})$ are fixed before the training data set is observed and is a manifestation of the curse of dimensionality discussed in Section 1.4. As a consequence, the number of basis functions needs to grow rapidly, often exponentially, with the dimensionality D of the input space.

Fortunately, there are two properties of real data sets that we can exploit to help alleviate this problem. First of all, the data vectors $\{\mathbf{x}_n\}$ typically lie close to a non-linear manifold whose intrinsic dimensionality is smaller than that of the input space as a result of strong correlations between the input variables. We will see an example of this when we consider images of handwritten digits in Chapter 12. If we are using localized basis functions, we can arrange that they are scattered in input space only in regions containing data. This approach is used in radial basis function networks and also in support vector and relevance vector machines. Neural network models, which use adaptive basis functions having sigmoidal nonlinearities, can adapt the parameters so that the regions of input space over which the basis functions vary corresponds to the data manifold. The second property is that target variables may have significant dependence on only a small number of possible directions within the data manifold. Neural networks can exploit this property by choosing the directions in input space to which the basis functions respond.

Exercises

- 3.1** (*) **www** Show that the ‘tanh’ function and the logistic sigmoid function (3.6) are related by

$$\tanh(a) = 2\sigma(2a) - 1. \quad (3.100)$$

Hence show that a general linear combination of logistic sigmoid functions of the form

$$y(x, \mathbf{w}) = w_0 + \sum_{j=1}^M w_j \sigma\left(\frac{x - \mu_j}{s}\right) \quad (3.101)$$

is equivalent to a linear combination of ‘tanh’ functions of the form

$$y(x, \mathbf{u}) = u_0 + \sum_{j=1}^M u_j \tanh\left(\frac{x - \mu_j}{s}\right) \quad (3.102)$$

and find expressions to relate the new parameters $\{u_1, \dots, u_M\}$ to the original parameters $\{w_1, \dots, w_M\}$.

- 3.2** (**) Show that the matrix

$$\Phi(\Phi^T \Phi)^{-1} \Phi^T \quad (3.103)$$

takes any vector \mathbf{v} and projects it onto the space spanned by the columns of Φ . Use this result to show that the least-squares solution (3.15) corresponds to an orthogonal projection of the vector \mathbf{t} onto the manifold \mathcal{S} as shown in Figure 3.2.

- 3.3** (*) Consider a data set in which each data point t_n is associated with a weighting factor $r_n > 0$, so that the sum-of-squares error function becomes

$$E_D(\mathbf{w}) = \frac{1}{2} \sum_{n=1}^N r_n \{t_n - \mathbf{w}^T \phi(\mathbf{x}_n)\}^2. \quad (3.104)$$

Find an expression for the solution \mathbf{w}^* that minimizes this error function. Give two alternative interpretations of the weighted sum-of-squares error function in terms of (i) data dependent noise variance and (ii) replicated data points.

- 3.4** (*) **www** Consider a linear model of the form

$$y(x, \mathbf{w}) = w_0 + \sum_{i=1}^D w_i x_i \quad (3.105)$$

together with a sum-of-squares error function of the form

$$E_D(\mathbf{w}) = \frac{1}{2} \sum_{n=1}^N \{y(x_n, \mathbf{w}) - t_n\}^2. \quad (3.106)$$

Now suppose that Gaussian noise ϵ_i with zero mean and variance σ^2 is added independently to each of the input variables x_i . By making use of $\mathbb{E}[\epsilon_i] = 0$ and $\mathbb{E}[\epsilon_i \epsilon_j] = \delta_{ij} \sigma^2$, show that minimizing E_D averaged over the noise distribution is equivalent to minimizing the sum-of-squares error for noise-free input variables with the addition of a weight-decay regularization term, in which the bias parameter w_0 is omitted from the regularizer.

- 3.5** (*) **www** Using the technique of Lagrange multipliers, discussed in Appendix E, show that minimization of the regularized error function (3.29) is equivalent to minimizing the unregularized sum-of-squares error (3.12) subject to the constraint (3.30). Discuss the relationship between the parameters η and λ .

- 3.6** (*) **www** Consider a linear basis function regression model for a multivariate target variable \mathbf{t} having a Gaussian distribution of the form

$$p(\mathbf{t}|\mathbf{W}, \Sigma) = \mathcal{N}(\mathbf{t}|\mathbf{y}(\mathbf{x}, \mathbf{W}), \Sigma) \quad (3.107)$$

where

$$\mathbf{y}(\mathbf{x}, \mathbf{W}) = \mathbf{W}^T \phi(\mathbf{x}) \quad (3.108)$$

together with a training data set comprising input basis vectors $\phi(\mathbf{x}_n)$ and corresponding target vectors \mathbf{t}_n , with $n = 1, \dots, N$. Show that the maximum likelihood solution \mathbf{W}_{ML} for the parameter matrix \mathbf{W} has the property that each column is given by an expression of the form (3.15), which was the solution for an isotropic noise distribution. Note that this is independent of the covariance matrix Σ . Show that the maximum likelihood solution for Σ is given by

$$\Sigma = \frac{1}{N} \sum_{n=1}^N (\mathbf{t}_n - \mathbf{W}_{\text{ML}}^T \phi(\mathbf{x}_n)) (\mathbf{t}_n - \mathbf{W}_{\text{ML}}^T \phi(\mathbf{x}_n))^T. \quad (3.109)$$

- 3.7** (*) By using the technique of completing the square, verify the result (3.49) for the posterior distribution of the parameters \mathbf{w} in the linear basis function model in which \mathbf{m}_N and \mathbf{S}_N are defined by (3.50) and (3.51) respectively.
- 3.8** (**) **www** Consider the linear basis function model in Section 3.1, and suppose that we have already observed N data points, so that the posterior distribution over \mathbf{w} is given by (3.49). This posterior can be regarded as the prior for the next observation. By considering an additional data point $(\mathbf{x}_{N+1}, t_{N+1})$, and by completing the square in the exponential, show that the resulting posterior distribution is again given by (3.49) but with \mathbf{S}_N replaced by \mathbf{S}_{N+1} and \mathbf{m}_N replaced by \mathbf{m}_{N+1} .
- 3.9** (**) Repeat the previous exercise but instead of completing the square by hand, make use of the general result for linear-Gaussian models given by (2.116).
- 3.10** (**) **www** By making use of the result (2.115) to evaluate the integral in (3.57), verify that the predictive distribution for the Bayesian linear regression model is given by (3.58) in which the input-dependent variance is given by (3.59).
- 3.11** (**) We have seen that, as the size of a data set increases, the uncertainty associated with the posterior distribution over model parameters decreases. Make use of the matrix identity (Appendix C)

$$(\mathbf{M} + \mathbf{v}\mathbf{v}^T)^{-1} = \mathbf{M}^{-1} - \frac{(\mathbf{M}^{-1}\mathbf{v})(\mathbf{v}^T\mathbf{M}^{-1})}{1 + \mathbf{v}^T\mathbf{M}^{-1}\mathbf{v}} \quad (3.110)$$

to show that the uncertainty $\sigma_N^2(\mathbf{x})$ associated with the linear regression function given by (3.59) satisfies

$$\sigma_{N+1}^2(\mathbf{x}) \leq \sigma_N^2(\mathbf{x}). \quad (3.111)$$

- 3.12** (**) We saw in Section 2.3.6 that the conjugate prior for a Gaussian distribution with unknown mean and unknown precision (inverse variance) is a normal-gamma distribution. This property also holds for the case of the conditional Gaussian distribution $p(t|\mathbf{x}, \mathbf{w}, \beta)$ of the linear regression model. If we consider the likelihood function (3.10), then the conjugate prior for \mathbf{w} and β is given by

$$p(\mathbf{w}, \beta) = \mathcal{N}(\mathbf{w}|\mathbf{m}_0, \beta^{-1}\mathbf{S}_0)\text{Gam}(\beta|a_0, b_0). \quad (3.112)$$

Show that the corresponding posterior distribution takes the same functional form, so that

$$p(\mathbf{w}, \beta | \mathbf{t}) = \mathcal{N}(\mathbf{w} | \mathbf{m}_N, \beta^{-1} \mathbf{S}_N) \text{Gam}(\beta | a_N, b_N) \quad (3.113)$$

and find expressions for the posterior parameters \mathbf{m}_N , \mathbf{S}_N , a_N , and b_N .

- 3.13** (**) Show that the predictive distribution $p(t|\mathbf{x}, \mathbf{t})$ for the model discussed in Exercise 3.12 is given by a Student's t-distribution of the form

$$p(t|\mathbf{x}, \mathbf{t}) = \text{St}(t|\mu, \lambda, \nu) \quad (3.114)$$

and obtain expressions for μ , λ and ν .

- 3.14** (**) In this exercise, we explore in more detail the properties of the equivalent kernel defined by (3.62), where \mathbf{S}_N is defined by (3.54). Suppose that the basis functions $\phi_j(\mathbf{x})$ are linearly independent and that the number N of data points is greater than the number M of basis functions. Furthermore, let one of the basis functions be constant, say $\phi_0(\mathbf{x}) = 1$. By taking suitable linear combinations of these basis functions, we can construct a new basis set $\psi_j(\mathbf{x})$ spanning the same space but that are orthonormal, so that

$$\sum_{n=1}^N \psi_j(\mathbf{x}_n) \psi_k(\mathbf{x}_n) = I_{jk} \quad (3.115)$$

where I_{jk} is defined to be 1 if $j = k$ and 0 otherwise, and we take $\psi_0(\mathbf{x}) = 1$. Show that for $\alpha = 0$, the equivalent kernel can be written as $k(\mathbf{x}, \mathbf{x}') = \boldsymbol{\psi}(\mathbf{x})^T \boldsymbol{\psi}(\mathbf{x}')$ where $\boldsymbol{\psi} = (\psi_1, \dots, \psi_M)^T$. Use this result to show that the kernel satisfies the summation constraint

$$\sum_{n=1}^N k(\mathbf{x}, \mathbf{x}_n) = 1. \quad (3.116)$$

- 3.15** (*) **www** Consider a linear basis function model for regression in which the parameters α and β are set using the evidence framework. Show that the function $E(\mathbf{m}_N)$ defined by (3.82) satisfies the relation $2E(\mathbf{m}_N) = N$.

- 3.16** (**) Derive the result (3.86) for the log evidence function $p(\mathbf{t}|\alpha, \beta)$ of the linear regression model by making use of (2.115) to evaluate the integral (3.77) directly.

- 3.17** (*) Show that the evidence function for the Bayesian linear regression model can be written in the form (3.78) in which $E(\mathbf{w})$ is defined by (3.79).

- 3.18** (**) **www** By completing the square over \mathbf{w} , show that the error function (3.79) in Bayesian linear regression can be written in the form (3.80).

- 3.19** (**) Show that the integration over \mathbf{w} in the Bayesian linear regression model gives the result (3.85). Hence show that the log marginal likelihood is given by (3.86).

- 3.20** (**) **www** Starting from (3.86) verify all of the steps needed to show that maximization of the log marginal likelihood function (3.86) with respect to α leads to the re-estimation equation (3.92).
- 3.21** (**) An alternative way to derive the result (3.92) for the optimal value of α in the evidence framework is to make use of the identity

$$\frac{d}{d\alpha} \ln |\mathbf{A}| = \text{Tr} \left(\mathbf{A}^{-1} \frac{d}{d\alpha} \mathbf{A} \right). \quad (3.117)$$

Prove this identity by considering the eigenvalue expansion of a real, symmetric matrix \mathbf{A} , and making use of the standard results for the determinant and trace of \mathbf{A} expressed in terms of its eigenvalues (Appendix C). Then make use of (3.117) to derive (3.92) starting from (3.86).

- 3.22** (**) Starting from (3.86) verify all of the steps needed to show that maximization of the log marginal likelihood function (3.86) with respect to β leads to the re-estimation equation (3.95).
- 3.23** (**) **www** Show that the marginal probability of the data, in other words the model evidence, for the model described in Exercise 3.12 is given by

$$p(\mathbf{t}) = \frac{1}{(2\pi)^{N/2}} \frac{b_0^{a_0}}{b_N^{a_N}} \frac{\Gamma(a_N)}{\Gamma(a_0)} \frac{|\mathbf{S}_N|^{1/2}}{|\mathbf{S}_0|^{1/2}} \quad (3.118)$$

by first marginalizing with respect to \mathbf{w} and then with respect to β .

- 3.24** (**) Repeat the previous exercise but now use Bayes' theorem in the form

$$p(\mathbf{t}) = \frac{p(\mathbf{t}|\mathbf{w}, \beta)p(\mathbf{w}, \beta)}{p(\mathbf{w}, \beta|\mathbf{t})} \quad (3.119)$$

and then substitute for the prior and posterior distributions and the likelihood function in order to derive the result (3.118).



4

Linear

Models for

Classification

In the previous chapter, we explored a class of regression models having particularly simple analytical and computational properties. We now discuss an analogous class of models for solving classification problems. The goal in classification is to take an input vector \mathbf{x} and to assign it to one of K discrete classes \mathcal{C}_k where $k = 1, \dots, K$. In the most common scenario, the classes are taken to be disjoint, so that each input is assigned to one and only one class. The input space is thereby divided into *decision regions* whose boundaries are called *decision boundaries* or *decision surfaces*. In this chapter, we consider linear models for classification, by which we mean that the decision surfaces are linear functions of the input vector \mathbf{x} and hence are defined by $(D - 1)$ -dimensional hyperplanes within the D -dimensional input space. Data sets whose classes can be separated exactly by linear decision surfaces are said to be *linearly separable*.

For regression problems, the target variable t was simply the vector of real numbers whose values we wish to predict. In the case of classification, there are various

ways of using target values to represent class labels. For probabilistic models, the most convenient, in the case of two-class problems, is the binary representation in which there is a single target variable $t \in \{0, 1\}$ such that $t = 1$ represents class \mathcal{C}_1 and $t = 0$ represents class \mathcal{C}_2 . We can interpret the value of t as the probability that the class is \mathcal{C}_1 , with the values of probability taking only the extreme values of 0 and 1. For $K > 2$ classes, it is convenient to use a 1-of- K coding scheme in which \mathbf{t} is a vector of length K such that if the class is \mathcal{C}_j , then all elements t_k of \mathbf{t} are zero except element t_j , which takes the value 1. For instance, if we have $K = 5$ classes, then a pattern from class 2 would be given the target vector

$$\mathbf{t} = (0, 1, 0, 0, 0)^T. \quad (4.1)$$

Again, we can interpret the value of t_k as the probability that the class is \mathcal{C}_k . For nonprobabilistic models, alternative choices of target variable representation will sometimes prove convenient.

In Chapter 1, we identified three distinct approaches to the classification problem. The simplest involves constructing a *discriminant function* that directly assigns each vector \mathbf{x} to a specific class. A more powerful approach, however, models the conditional probability distribution $p(\mathcal{C}_k|\mathbf{x})$ in an inference stage, and then subsequently uses this distribution to make optimal decisions. By separating inference and decision, we gain numerous benefits, as discussed in Section 1.5.4. There are two different approaches to determining the conditional probabilities $p(\mathcal{C}_k|\mathbf{x})$. One technique is to model them directly, for example by representing them as parametric models and then optimizing the parameters using a training set. Alternatively, we can adopt a generative approach in which we model the class-conditional densities given by $p(\mathbf{x}|\mathcal{C}_k)$, together with the prior probabilities $p(\mathcal{C}_k)$ for the classes, and then we compute the required posterior probabilities using Bayes' theorem

$$p(\mathcal{C}_k|\mathbf{x}) = \frac{p(\mathbf{x}|\mathcal{C}_k)p(\mathcal{C}_k)}{p(\mathbf{x})}. \quad (4.2)$$

We shall discuss examples of all three approaches in this chapter.

In the linear regression models considered in Chapter 3, the model prediction $y(\mathbf{x}, \mathbf{w})$ was given by a linear function of the parameters \mathbf{w} . In the simplest case, the model is also linear in the input variables and therefore takes the form $y(\mathbf{x}) = \mathbf{w}^T \mathbf{x} + w_0$, so that y is a real number. For classification problems, however, we wish to predict discrete class labels, or more generally posterior probabilities that lie in the range $(0, 1)$. To achieve this, we consider a generalization of this model in which we transform the linear function of \mathbf{w} using a nonlinear function $f(\cdot)$ so that

$$y(\mathbf{x}) = f(\mathbf{w}^T \mathbf{x} + w_0). \quad (4.3)$$

In the machine learning literature $f(\cdot)$ is known as an *activation function*, whereas its inverse is called a *link function* in the statistics literature. The decision surfaces correspond to $y(\mathbf{x}) = \text{constant}$, so that $\mathbf{w}^T \mathbf{x} + w_0 = \text{constant}$ and hence the decision surfaces are linear functions of \mathbf{x} , even if the function $f(\cdot)$ is nonlinear. For this reason, the class of models described by (4.3) are called *generalized linear models*

(McCullagh and Nelder, 1989). Note, however, that in contrast to the models used for regression, they are no longer linear in the parameters due to the presence of the nonlinear function $f(\cdot)$. This will lead to more complex analytical and computational properties than for linear regression models. Nevertheless, these models are still relatively simple compared to the more general nonlinear models that will be studied in subsequent chapters.

The algorithms discussed in this chapter will be equally applicable if we first make a fixed nonlinear transformation of the input variables using a vector of basis functions $\phi(\mathbf{x})$ as we did for regression models in Chapter 3. We begin by considering classification directly in the original input space \mathbf{x} , while in Section 4.3 we shall find it convenient to switch to a notation involving basis functions for consistency with later chapters.

4.1. Discriminant Functions

A discriminant is a function that takes an input vector \mathbf{x} and assigns it to one of K classes, denoted \mathcal{C}_k . In this chapter, we shall restrict attention to *linear discriminants*, namely those for which the decision surfaces are hyperplanes. To simplify the discussion, we consider first the case of two classes and then investigate the extension to $K > 2$ classes.

4.1.1 Two classes

The simplest representation of a linear discriminant function is obtained by taking a linear function of the input vector so that

$$y(\mathbf{x}) = \mathbf{w}^T \mathbf{x} + w_0 \quad (4.4)$$

where \mathbf{w} is called a *weight vector*, and w_0 is a *bias* (not to be confused with bias in the statistical sense). The negative of the bias is sometimes called a *threshold*. An input vector \mathbf{x} is assigned to class \mathcal{C}_1 if $y(\mathbf{x}) \geq 0$ and to class \mathcal{C}_2 otherwise. The corresponding decision boundary is therefore defined by the relation $y(\mathbf{x}) = 0$, which corresponds to a $(D - 1)$ -dimensional hyperplane within the D -dimensional input space. Consider two points \mathbf{x}_A and \mathbf{x}_B both of which lie on the decision surface. Because $y(\mathbf{x}_A) = y(\mathbf{x}_B) = 0$, we have $\mathbf{w}^T(\mathbf{x}_A - \mathbf{x}_B) = 0$ and hence the vector \mathbf{w} is orthogonal to every vector lying within the decision surface, and so \mathbf{w} determines the orientation of the decision surface. Similarly, if \mathbf{x} is a point on the decision surface, then $y(\mathbf{x}) = 0$, and so the normal distance from the origin to the decision surface is given by

$$\frac{\mathbf{w}^T \mathbf{x}}{\|\mathbf{w}\|} = -\frac{w_0}{\|\mathbf{w}\|}. \quad (4.5)$$

We therefore see that the bias parameter w_0 determines the location of the decision surface. These properties are illustrated for the case of $D = 2$ in Figure 4.1.

Furthermore, we note that the value of $y(\mathbf{x})$ gives a signed measure of the perpendicular distance r of the point \mathbf{x} from the decision surface. To see this, consider

Figure 4.1 Illustration of the geometry of a linear discriminant function in two dimensions. The decision surface, shown in red, is perpendicular to \mathbf{w} , and its displacement from the origin is controlled by the bias parameter w_0 . Also, the signed orthogonal distance of a general point \mathbf{x} from the decision surface is given by $y(\mathbf{x})/\|\mathbf{w}\|$.



an arbitrary point \mathbf{x} and let \mathbf{x}_\perp be its orthogonal projection onto the decision surface, so that

$$\mathbf{x} = \mathbf{x}_\perp + r \frac{\mathbf{w}}{\|\mathbf{w}\|}. \quad (4.6)$$

Multiplying both sides of this result by \mathbf{w}^T and adding w_0 , and making use of $y(\mathbf{x}) = \mathbf{w}^T \mathbf{x} + w_0$ and $y(\mathbf{x}_\perp) = \mathbf{w}^T \mathbf{x}_\perp + w_0 = 0$, we have

$$r = \frac{y(\mathbf{x})}{\|\mathbf{w}\|}. \quad (4.7)$$

This result is illustrated in Figure 4.1.

As with the linear regression models in Chapter 3, it is sometimes convenient to use a more compact notation in which we introduce an additional dummy ‘input’ value $x_0 = 1$ and then define $\tilde{\mathbf{w}} = (w_0, \mathbf{w})$ and $\tilde{\mathbf{x}} = (x_0, \mathbf{x})$ so that

$$y(\mathbf{x}) = \tilde{\mathbf{w}}^T \tilde{\mathbf{x}}. \quad (4.8)$$

In this case, the decision surfaces are D -dimensional hyperplanes passing through the origin of the $D + 1$ -dimensional expanded input space.

4.1.2 Multiple classes

Now consider the extension of linear discriminants to $K > 2$ classes. We might be tempted to build a K -class discriminant by combining a number of two-class discriminant functions. However, this leads to some serious difficulties (Duda and Hart, 1973) as we now show.

Consider the use of $K - 1$ classifiers each of which solves a two-class problem of separating points in a particular class \mathcal{C}_k from points not in that class. This is known as a *one-versus-the-rest* classifier. The left-hand example in Figure 4.2 shows an



Figure 4.2 Attempting to construct a K class discriminant from a set of two class discriminants leads to ambiguous regions, shown in green. On the left is an example involving the use of two discriminants designed to distinguish points in class C_k from points not in class C_k . On the right is an example involving three discriminant functions each of which is used to separate a pair of classes C_k and C_j .

example involving three classes where this approach leads to regions of input space that are ambiguously classified.

An alternative is to introduce $K(K - 1)/2$ binary discriminant functions, one for every possible pair of classes. This is known as a *one-versus-one* classifier. Each point is then classified according to a majority vote amongst the discriminant functions. However, this too runs into the problem of ambiguous regions, as illustrated in the right-hand diagram of Figure 4.2.

We can avoid these difficulties by considering a single K -class discriminant comprising K linear functions of the form

$$y_k(\mathbf{x}) = \mathbf{w}_k^T \mathbf{x} + w_{k0} \quad (4.9)$$

and then assigning a point \mathbf{x} to class C_k if $y_k(\mathbf{x}) > y_j(\mathbf{x})$ for all $j \neq k$. The decision boundary between class C_k and class C_j is therefore given by $y_k(\mathbf{x}) = y_j(\mathbf{x})$ and hence corresponds to a $(D - 1)$ -dimensional hyperplane defined by

$$(\mathbf{w}_k - \mathbf{w}_j)^T \mathbf{x} + (w_{k0} - w_{j0}) = 0. \quad (4.10)$$

This has the same form as the decision boundary for the two-class case discussed in Section 4.1.1, and so analogous geometrical properties apply.

The decision regions of such a discriminant are always singly connected and convex. To see this, consider two points \mathbf{x}_A and \mathbf{x}_B both of which lie inside decision region \mathcal{R}_k , as illustrated in Figure 4.3. Any point $\hat{\mathbf{x}}$ that lies on the line connecting \mathbf{x}_A and \mathbf{x}_B can be expressed in the form

$$\hat{\mathbf{x}} = \lambda \mathbf{x}_A + (1 - \lambda) \mathbf{x}_B \quad (4.11)$$

Figure 4.3 Illustration of the decision regions for a multiclass linear discriminant, with the decision boundaries shown in red. If two points \mathbf{x}_A and \mathbf{x}_B both lie inside the same decision region \mathcal{R}_k , then any point $\hat{\mathbf{x}}$ that lies on the line connecting these two points must also lie in \mathcal{R}_k , and hence the decision region must be singly connected and convex.



where $0 \leq \lambda \leq 1$. From the linearity of the discriminant functions, it follows that

$$y_k(\hat{\mathbf{x}}) = \lambda y_k(\mathbf{x}_A) + (1 - \lambda)y_k(\mathbf{x}_B). \quad (4.12)$$

Because both \mathbf{x}_A and \mathbf{x}_B lie inside \mathcal{R}_k , it follows that $y_k(\mathbf{x}_A) > y_j(\mathbf{x}_A)$, and $y_k(\mathbf{x}_B) > y_j(\mathbf{x}_B)$, for all $j \neq k$, and hence $y_k(\hat{\mathbf{x}}) > y_j(\hat{\mathbf{x}})$, and so $\hat{\mathbf{x}}$ also lies inside \mathcal{R}_k . Thus \mathcal{R}_k is singly connected and convex.

Note that for two classes, we can either employ the formalism discussed here, based on two discriminant functions $y_1(\mathbf{x})$ and $y_2(\mathbf{x})$, or else use the simpler but equivalent formulation described in Section 4.1.1 based on a single discriminant function $y(\mathbf{x})$.

We now explore three approaches to learning the parameters of linear discriminant functions, based on least squares, Fisher's linear discriminant, and the perceptron algorithm.

4.1.3 Least squares for classification

In Chapter 3, we considered models that were linear functions of the parameters, and we saw that the minimization of a sum-of-squares error function led to a simple closed-form solution for the parameter values. It is therefore tempting to see if we can apply the same formalism to classification problems. Consider a general classification problem with K classes, with a 1-of- K binary coding scheme for the target vector \mathbf{t} . One justification for using least squares in such a context is that it approximates the conditional expectation $\mathbb{E}[\mathbf{t}|\mathbf{x}]$ of the target values given the input vector. For the binary coding scheme, this conditional expectation is given by the vector of posterior class probabilities. Unfortunately, however, these probabilities are typically approximated rather poorly, indeed the approximations can have values outside the range $(0, 1)$, due to the limited flexibility of a linear model as we shall see shortly.

Each class \mathcal{C}_k is described by its own linear model so that

$$y_k(\mathbf{x}) = \mathbf{w}_k^T \mathbf{x} + w_{k0} \quad (4.13)$$

where $k = 1, \dots, K$. We can conveniently group these together using vector notation so that

$$\mathbf{y}(\mathbf{x}) = \widetilde{\mathbf{W}}^T \widetilde{\mathbf{x}} \quad (4.14)$$

where $\tilde{\mathbf{W}}$ is a matrix whose k^{th} column comprises the $D + 1$ -dimensional vector $\tilde{\mathbf{w}}_k = (w_{k0}, \mathbf{w}_k^T)^T$ and $\tilde{\mathbf{x}}$ is the corresponding augmented input vector $(1, \mathbf{x}^T)^T$ with a dummy input $x_0 = 1$. This representation was discussed in detail in Section 3.1. A new input \mathbf{x} is then assigned to the class for which the output $y_k = \tilde{\mathbf{w}}_k^T \tilde{\mathbf{x}}$ is largest.

We now determine the parameter matrix $\tilde{\mathbf{W}}$ by minimizing a sum-of-squares error function, as we did for regression in Chapter 3. Consider a training data set $\{\mathbf{x}_n, \mathbf{t}_n\}$ where $n = 1, \dots, N$, and define a matrix \mathbf{T} whose n^{th} row is the vector \mathbf{t}_n^T , together with a matrix $\tilde{\mathbf{X}}$ whose n^{th} row is $\tilde{\mathbf{x}}_n^T$. The sum-of-squares error function can then be written as

$$E_D(\tilde{\mathbf{W}}) = \frac{1}{2} \text{Tr} \left\{ (\tilde{\mathbf{X}} \tilde{\mathbf{W}} - \mathbf{T})^T (\tilde{\mathbf{X}} \tilde{\mathbf{W}} - \mathbf{T}) \right\}. \quad (4.15)$$

Setting the derivative with respect to $\tilde{\mathbf{W}}$ to zero, and rearranging, we then obtain the solution for $\tilde{\mathbf{W}}$ in the form

$$\tilde{\mathbf{W}} = (\tilde{\mathbf{X}}^T \tilde{\mathbf{X}})^{-1} \tilde{\mathbf{X}}^T \mathbf{T} = \tilde{\mathbf{X}}^\dagger \mathbf{T} \quad (4.16)$$

where $\tilde{\mathbf{X}}^\dagger$ is the pseudo-inverse of the matrix $\tilde{\mathbf{X}}$, as discussed in Section 3.1.1. We then obtain the discriminant function in the form

$$\mathbf{y}(\mathbf{x}) = \tilde{\mathbf{W}}^T \tilde{\mathbf{x}} = \mathbf{T}^T \left(\tilde{\mathbf{X}}^\dagger \right)^T \tilde{\mathbf{x}}. \quad (4.17)$$

An interesting property of least-squares solutions with multiple target variables is that if every target vector in the training set satisfies some linear constraint

$$\mathbf{a}^T \mathbf{t}_n + b = 0 \quad (4.18)$$

for some constants \mathbf{a} and b , then the model prediction for any value of \mathbf{x} will satisfy the same constraint so that

$$\mathbf{a}^T \mathbf{y}(\mathbf{x}) + b = 0. \quad (4.19)$$

Thus if we use a 1-of- K coding scheme for K classes, then the predictions made by the model will have the property that the elements of $\mathbf{y}(\mathbf{x})$ will sum to 1 for any value of \mathbf{x} . However, this summation constraint alone is not sufficient to allow the model outputs to be interpreted as probabilities because they are not constrained to lie within the interval $(0, 1)$.

The least-squares approach gives an exact closed-form solution for the discriminant function parameters. However, even as a discriminant function (where we use it to make decisions directly and dispense with any probabilistic interpretation) it suffers from some severe problems. We have already seen that least-squares solutions lack robustness to outliers, and this applies equally to the classification application, as illustrated in Figure 4.4. Here we see that the additional data points in the right-hand figure produce a significant change in the location of the decision boundary, even though these point would be correctly classified by the original decision boundary in the left-hand figure. The sum-of-squares error function penalizes predictions that are ‘too correct’ in that they lie a long way on the correct side of the decision

Exercise 4.2

Section 2.3.7



Figure 4.4 The left plot shows data from two classes, denoted by red crosses and blue circles, together with the decision boundary found by least squares (magenta curve) and also by the logistic regression model (green curve), which is discussed later in Section 4.3.2. The right-hand plot shows the corresponding results obtained when extra data points are added at the bottom left of the diagram, showing that least squares is highly sensitive to outliers, unlike logistic regression.

boundary. In Section 7.1.2, we shall consider several alternative error functions for classification and we shall see that they do not suffer from this difficulty.

However, problems with least squares can be more severe than simply lack of robustness, as illustrated in Figure 4.5. This shows a synthetic data set drawn from three classes in a two-dimensional input space (x_1, x_2), having the property that linear decision boundaries can give excellent separation between the classes. Indeed, the technique of logistic regression, described later in this chapter, gives a satisfactory solution as seen in the right-hand plot. However, the least-squares solution gives poor results, with only a small region of the input space assigned to the green class.

The failure of least squares should not surprise us when we recall that it corresponds to maximum likelihood under the assumption of a Gaussian conditional distribution, whereas binary target vectors clearly have a distribution that is far from Gaussian. By adopting more appropriate probabilistic models, we shall obtain classification techniques with much better properties than least squares. For the moment, however, we continue to explore alternative nonprobabilistic methods for setting the parameters in the linear classification models.

4.1.4 Fisher's linear discriminant

One way to view a linear classification model is in terms of dimensionality reduction. Consider first the case of two classes, and suppose we take the D -



Figure 4.5 Example of a synthetic data set comprising three classes, with training data points denoted in red (\times), green (+), and blue (\circ). Lines denote the decision boundaries, and the background colours denote the respective classes of the decision regions. On the left is the result of using a least-squares discriminant. We see that the region of input space assigned to the green class is too small and so most of the points from this class are misclassified. On the right is the result of using logistic regressions as described in Section 4.3.2 showing correct classification of the training data.

dimensional input vector \mathbf{x} and project it down to one dimension using

$$y = \mathbf{w}^T \mathbf{x}. \quad (4.20)$$

If we place a threshold on y and classify $y \geq -w_0$ as class \mathcal{C}_1 , and otherwise class \mathcal{C}_2 , then we obtain our standard linear classifier discussed in the previous section. In general, the projection onto one dimension leads to a considerable loss of information, and classes that are well separated in the original D -dimensional space may become strongly overlapping in one dimension. However, by adjusting the components of the weight vector \mathbf{w} , we can select a projection that maximizes the class separation. To begin with, consider a two-class problem in which there are N_1 points of class \mathcal{C}_1 and N_2 points of class \mathcal{C}_2 , so that the mean vectors of the two classes are given by

$$\mathbf{m}_1 = \frac{1}{N_1} \sum_{n \in \mathcal{C}_1} \mathbf{x}_n, \quad \mathbf{m}_2 = \frac{1}{N_2} \sum_{n \in \mathcal{C}_2} \mathbf{x}_n. \quad (4.21)$$

The simplest measure of the separation of the classes, when projected onto \mathbf{w} , is the separation of the projected class means. This suggests that we might choose \mathbf{w} so as to maximize

$$m_2 - m_1 = \mathbf{w}^T (\mathbf{m}_2 - \mathbf{m}_1) \quad (4.22)$$

where

$$m_k = \mathbf{w}^T \mathbf{m}_k \quad (4.23)$$



Figure 4.6 The left plot shows samples from two classes (depicted in red and blue) along with the histograms resulting from projection onto the line joining the class means. Note that there is considerable class overlap in the projected space. The right plot shows the corresponding projection based on the Fisher linear discriminant, showing the greatly improved class separation.

Appendix E
Exercise 4.4

is the mean of the projected data from class \mathcal{C}_k . However, this expression can be made arbitrarily large simply by increasing the magnitude of \mathbf{w} . To solve this problem, we could constrain \mathbf{w} to have unit length, so that $\sum_i w_i^2 = 1$. Using a Lagrange multiplier to perform the constrained maximization, we then find that $\mathbf{w} \propto (\mathbf{m}_2 - \mathbf{m}_1)$. There is still a problem with this approach, however, as illustrated in Figure 4.6. This shows two classes that are well separated in the original two-dimensional space (x_1, x_2) but that have considerable overlap when projected onto the line joining their means. This difficulty arises from the strongly nondiagonal covariances of the class distributions. The idea proposed by Fisher is to maximize a function that will give a large separation between the projected class means while also giving a small variance within each class, thereby minimizing the class overlap.

The projection formula (4.20) transforms the set of labelled data points in \mathbf{x} into a labelled set in the one-dimensional space y . The within-class variance of the transformed data from class \mathcal{C}_k is therefore given by

$$s_k^2 = \sum_{n \in \mathcal{C}_k} (y_n - m_k)^2 \quad (4.24)$$

where $y_n = \mathbf{w}^T \mathbf{x}_n$. We can define the total within-class variance for the whole data set to be simply $s_1^2 + s_2^2$. The Fisher criterion is defined to be the ratio of the between-class variance to the within-class variance and is given by

$$J(\mathbf{w}) = \frac{(m_2 - m_1)^2}{s_1^2 + s_2^2}. \quad (4.25)$$

We can make the dependence on \mathbf{w} explicit by using (4.20), (4.23), and (4.24) to rewrite the Fisher criterion in the form

$$J(\mathbf{w}) = \frac{\mathbf{w}^T \mathbf{S}_B \mathbf{w}}{\mathbf{w}^T \mathbf{S}_W \mathbf{w}} \quad (4.26)$$

where \mathbf{S}_B is the *between-class* covariance matrix and is given by

$$\mathbf{S}_B = (\mathbf{m}_2 - \mathbf{m}_1)(\mathbf{m}_2 - \mathbf{m}_1)^T \quad (4.27)$$

and \mathbf{S}_W is the total *within-class* covariance matrix, given by

$$\mathbf{S}_W = \sum_{n \in \mathcal{C}_1} (\mathbf{x}_n - \mathbf{m}_1)(\mathbf{x}_n - \mathbf{m}_1)^T + \sum_{n \in \mathcal{C}_2} (\mathbf{x}_n - \mathbf{m}_2)(\mathbf{x}_n - \mathbf{m}_2)^T. \quad (4.28)$$

Differentiating (4.26) with respect to \mathbf{w} , we find that $J(\mathbf{w})$ is maximized when

$$(\mathbf{w}^T \mathbf{S}_B \mathbf{w}) \mathbf{S}_W \mathbf{w} = (\mathbf{w}^T \mathbf{S}_W \mathbf{w}) \mathbf{S}_B \mathbf{w}. \quad (4.29)$$

From (4.27), we see that $\mathbf{S}_B \mathbf{w}$ is always in the direction of $(\mathbf{m}_2 - \mathbf{m}_1)$. Furthermore, we do not care about the magnitude of \mathbf{w} , only its direction, and so we can drop the scalar factors $(\mathbf{w}^T \mathbf{S}_B \mathbf{w})$ and $(\mathbf{w}^T \mathbf{S}_W \mathbf{w})$. Multiplying both sides of (4.29) by \mathbf{S}_W^{-1} we then obtain

$$\mathbf{w} \propto \mathbf{S}_W^{-1}(\mathbf{m}_2 - \mathbf{m}_1). \quad (4.30)$$

Note that if the within-class covariance is isotropic, so that \mathbf{S}_W is proportional to the unit matrix, we find that \mathbf{w} is proportional to the difference of the class means, as discussed above.

The result (4.30) is known as *Fisher's linear discriminant*, although strictly it is not a discriminant but rather a specific choice of direction for projection of the data down to one dimension. However, the projected data can subsequently be used to construct a discriminant, by choosing a threshold y_0 so that we classify a new point as belonging to \mathcal{C}_1 if $y(\mathbf{x}) \geq y_0$ and classify it as belonging to \mathcal{C}_2 otherwise. For example, we can model the class-conditional densities $p(y|\mathcal{C}_k)$ using Gaussian distributions and then use the techniques of Section 1.2.4 to find the parameters of the Gaussian distributions by maximum likelihood. Having found Gaussian approximations to the projected classes, the formalism of Section 1.5.1 then gives an expression for the optimal threshold. Some justification for the Gaussian assumption comes from the central limit theorem by noting that $y = \mathbf{w}^T \mathbf{x}$ is the sum of a set of random variables.

4.1.5 Relation to least squares

The least-squares approach to the determination of a linear discriminant was based on the goal of making the model predictions as close as possible to a set of target values. By contrast, the Fisher criterion was derived by requiring maximum class separation in the output space. It is interesting to see the relationship between these two approaches. In particular, we shall show that, for the two-class problem, the Fisher criterion can be obtained as a special case of least squares.

So far we have considered 1-of- K coding for the target values. If, however, we adopt a slightly different target coding scheme, then the least-squares solution for

the weights becomes equivalent to the Fisher solution (Duda and Hart, 1973). In particular, we shall take the targets for class \mathcal{C}_1 to be N/N_1 , where N_1 is the number of patterns in class \mathcal{C}_1 , and N is the total number of patterns. This target value approximates the reciprocal of the prior probability for class \mathcal{C}_1 . For class \mathcal{C}_2 , we shall take the targets to be $-N/N_2$, where N_2 is the number of patterns in class \mathcal{C}_2 .

The sum-of-squares error function can be written

$$E = \frac{1}{2} \sum_{n=1}^N (\mathbf{w}^T \mathbf{x}_n + w_0 - t_n)^2. \quad (4.31)$$

Setting the derivatives of E with respect to w_0 and \mathbf{w} to zero, we obtain respectively

$$\sum_{n=1}^N (\mathbf{w}^T \mathbf{x}_n + w_0 - t_n) = 0 \quad (4.32)$$

$$\sum_{n=1}^N (\mathbf{w}^T \mathbf{x}_n + w_0 - t_n) \mathbf{x}_n = 0. \quad (4.33)$$

From (4.32), and making use of our choice of target coding scheme for the t_n , we obtain an expression for the bias in the form

$$w_0 = -\mathbf{w}^T \mathbf{m} \quad (4.34)$$

where we have used

$$\sum_{n=1}^N t_n = N_1 \frac{N}{N_1} - N_2 \frac{N}{N_2} = 0 \quad (4.35)$$

and where \mathbf{m} is the mean of the total data set and is given by

$$\mathbf{m} = \frac{1}{N} \sum_{n=1}^N \mathbf{x}_n = \frac{1}{N} (N_1 \mathbf{m}_1 + N_2 \mathbf{m}_2). \quad (4.36)$$

After some straightforward algebra, and again making use of the choice of t_n , the second equation (4.33) becomes

$$\left(\mathbf{S}_W + \frac{N_1 N_2}{N} \mathbf{S}_B \right) \mathbf{w} = N(\mathbf{m}_1 - \mathbf{m}_2) \quad (4.37)$$

where \mathbf{S}_W is defined by (4.28), \mathbf{S}_B is defined by (4.27), and we have substituted for the bias using (4.34). Using (4.27), we note that $\mathbf{S}_B \mathbf{w}$ is always in the direction of $(\mathbf{m}_2 - \mathbf{m}_1)$. Thus we can write

$$\mathbf{w} \propto \mathbf{S}_W^{-1} (\mathbf{m}_2 - \mathbf{m}_1) \quad (4.38)$$

where we have ignored irrelevant scale factors. Thus the weight vector coincides with that found from the Fisher criterion. In addition, we have also found an expression for the bias value w_0 given by (4.34). This tells us that a new vector \mathbf{x} should be classified as belonging to class \mathcal{C}_1 if $y(\mathbf{x}) = \mathbf{w}^T (\mathbf{x} - \mathbf{m}) > 0$ and class \mathcal{C}_2 otherwise.

Exercise 4.6

4.1.6 Fisher's discriminant for multiple classes

We now consider the generalization of the Fisher discriminant to $K > 2$ classes, and we shall assume that the dimensionality D of the input space is greater than the number K of classes. Next, we introduce $D' > 1$ linear ‘features’ $y_k = \mathbf{w}_k^T \mathbf{x}$, where $k = 1, \dots, D'$. These feature values can conveniently be grouped together to form a vector \mathbf{y} . Similarly, the weight vectors $\{\mathbf{w}_k\}$ can be considered to be the columns of a matrix \mathbf{W} , so that

$$\mathbf{y} = \mathbf{W}^T \mathbf{x}. \quad (4.39)$$

Note that again we are not including any bias parameters in the definition of \mathbf{y} . The generalization of the within-class covariance matrix to the case of K classes follows from (4.28) to give

$$\mathbf{S}_W = \sum_{k=1}^K \mathbf{S}_k \quad (4.40)$$

where

$$\mathbf{S}_k = \sum_{n \in \mathcal{C}_k} (\mathbf{x}_n - \mathbf{m}_k)(\mathbf{x}_n - \mathbf{m}_k)^T \quad (4.41)$$

$$\mathbf{m}_k = \frac{1}{N_k} \sum_{n \in \mathcal{C}_k} \mathbf{x}_n \quad (4.42)$$

and N_k is the number of patterns in class \mathcal{C}_k . In order to find a generalization of the between-class covariance matrix, we follow Duda and Hart (1973) and consider first the total covariance matrix

$$\mathbf{S}_T = \sum_{n=1}^N (\mathbf{x}_n - \mathbf{m})(\mathbf{x}_n - \mathbf{m})^T \quad (4.43)$$

where \mathbf{m} is the mean of the total data set

$$\mathbf{m} = \frac{1}{N} \sum_{n=1}^N \mathbf{x}_n = \frac{1}{N} \sum_{k=1}^K N_k \mathbf{m}_k \quad (4.44)$$

and $N = \sum_k N_k$ is the total number of data points. The total covariance matrix can be decomposed into the sum of the within-class covariance matrix, given by (4.40) and (4.41), plus an additional matrix \mathbf{S}_B , which we identify as a measure of the between-class covariance

$$\mathbf{S}_T = \mathbf{S}_W + \mathbf{S}_B \quad (4.45)$$

where

$$\mathbf{S}_B = \sum_{k=1}^K N_k (\mathbf{m}_k - \mathbf{m})(\mathbf{m}_k - \mathbf{m})^T. \quad (4.46)$$

These covariance matrices have been defined in the original \mathbf{x} -space. We can now define similar matrices in the projected D' -dimensional \mathbf{y} -space

$$\mathbf{s}_W = \sum_{k=1}^K \sum_{n \in C_k} (\mathbf{y}_n - \boldsymbol{\mu}_k)(\mathbf{y}_n - \boldsymbol{\mu}_k)^T \quad (4.47)$$

and

$$\mathbf{s}_B = \sum_{k=1}^K N_k (\boldsymbol{\mu}_k - \boldsymbol{\mu})(\boldsymbol{\mu}_k - \boldsymbol{\mu})^T \quad (4.48)$$

where

$$\boldsymbol{\mu}_k = \frac{1}{N_k} \sum_{n \in C_k} \mathbf{y}_n, \quad \boldsymbol{\mu} = \frac{1}{N} \sum_{k=1}^K N_k \boldsymbol{\mu}_k. \quad (4.49)$$

Again we wish to construct a scalar that is large when the between-class covariance is large and when the within-class covariance is small. There are now many possible choices of criterion (Fukunaga, 1990). One example is given by

$$J(\mathbf{W}) = \text{Tr} \{ \mathbf{s}_W^{-1} \mathbf{s}_B \}. \quad (4.50)$$

This criterion can then be rewritten as an explicit function of the projection matrix \mathbf{W} in the form

$$J(\mathbf{w}) = \text{Tr} \{ (\mathbf{W} \mathbf{S}_W \mathbf{W}^T)^{-1} (\mathbf{W} \mathbf{S}_B \mathbf{W}^T) \}. \quad (4.51)$$

Maximization of such criteria is straightforward, though somewhat involved, and is discussed at length in Fukunaga (1990). The weight values are determined by those eigenvectors of $\mathbf{S}_W^{-1} \mathbf{S}_B$ that correspond to the D' largest eigenvalues.

There is one important result that is common to all such criteria, which is worth emphasizing. We first note from (4.46) that \mathbf{S}_B is composed of the sum of K matrices, each of which is an outer product of two vectors and therefore of rank 1. In addition, only $(K - 1)$ of these matrices are independent as a result of the constraint (4.44). Thus, \mathbf{S}_B has rank at most equal to $(K - 1)$ and so there are at most $(K - 1)$ nonzero eigenvalues. This shows that the projection onto the $(K - 1)$ -dimensional subspace spanned by the eigenvectors of \mathbf{S}_B does not alter the value of $J(\mathbf{w})$, and so we are therefore unable to find more than $(K - 1)$ linear ‘features’ by this means (Fukunaga, 1990).

4.1.7 The perceptron algorithm

Another example of a linear discriminant model is the perceptron of Rosenblatt (1962), which occupies an important place in the history of pattern recognition algorithms. It corresponds to a two-class model in which the input vector \mathbf{x} is first transformed using a fixed nonlinear transformation to give a feature vector $\phi(\mathbf{x})$, and this is then used to construct a generalized linear model of the form

$$y(\mathbf{x}) = f(\mathbf{w}^T \phi(\mathbf{x})) \quad (4.52)$$

where the nonlinear activation function $f(\cdot)$ is given by a step function of the form

$$f(a) = \begin{cases} +1, & a \geq 0 \\ -1, & a < 0. \end{cases} \quad (4.53)$$

The vector $\phi(\mathbf{x})$ will typically include a bias component $\phi_0(\mathbf{x}) = 1$. In earlier discussions of two-class classification problems, we have focussed on a target coding scheme in which $t \in \{0, 1\}$, which is appropriate in the context of probabilistic models. For the perceptron, however, it is more convenient to use target values $t = +1$ for class C_1 and $t = -1$ for class C_2 , which matches the choice of activation function.

The algorithm used to determine the parameters \mathbf{w} of the perceptron can most easily be motivated by error function minimization. A natural choice of error function would be the total number of misclassified patterns. However, this does not lead to a simple learning algorithm because the error is a piecewise constant function of \mathbf{w} , with discontinuities wherever a change in \mathbf{w} causes the decision boundary to move across one of the data points. Methods based on changing \mathbf{w} using the gradient of the error function cannot then be applied, because the gradient is zero almost everywhere.

We therefore consider an alternative error function known as the *perceptron criterion*. To derive this, we note that we are seeking a weight vector \mathbf{w} such that patterns \mathbf{x}_n in class C_1 will have $\mathbf{w}^T \phi(\mathbf{x}_n) > 0$, whereas patterns \mathbf{x}_n in class C_2 have $\mathbf{w}^T \phi(\mathbf{x}_n) < 0$. Using the $t \in \{-1, +1\}$ target coding scheme it follows that we would like all patterns to satisfy $\mathbf{w}^T \phi(\mathbf{x}_n) t_n > 0$. The perceptron criterion associates zero error with any pattern that is correctly classified, whereas for a misclassified pattern \mathbf{x}_n it tries to minimize the quantity $-\mathbf{w}^T \phi(\mathbf{x}_n) t_n$. The perceptron criterion is therefore given by

$$E_P(\mathbf{w}) = - \sum_{n \in \mathcal{M}} \mathbf{w}^T \phi_n t_n \quad (4.54)$$



Frank Rosenblatt
1928–1969

Rosenblatt's perceptron played an important role in the history of machine learning. Initially, Rosenblatt simulated the perceptron on an IBM 704 computer at Cornell in 1957, but by the early 1960s he had built special-purpose hardware that provided a direct, parallel implementation of perceptron learning. Many of his ideas were encapsulated in "Principles of Neurodynamics: Perceptrons and the Theory of Brain Mechanisms" published in 1962. Rosenblatt's work was criticized by Marvin Minsky, whose objections were published in the book "Perceptrons", co-authored with

Seymour Papert. This book was widely misinterpreted at the time as showing that neural networks were fatally flawed and could only learn solutions for linearly separable problems. In fact, it only proved such limitations in the case of single-layer networks such as the perceptron and merely conjectured (incorrectly) that they applied to more general network models. Unfortunately, however, this book contributed to the substantial decline in research funding for neural computing, a situation that was not reversed until the mid-1980s. Today, there are many hundreds, if not thousands, of applications of neural networks in widespread use, with examples in areas such as handwriting recognition and information retrieval being used routinely by millions of people.

where \mathcal{M} denotes the set of all misclassified patterns. The contribution to the error associated with a particular misclassified pattern is a linear function of \mathbf{w} in regions of \mathbf{w} space where the pattern is misclassified and zero in regions where it is correctly classified. The total error function is therefore piecewise linear.

Section 3.1.3

We now apply the stochastic gradient descent algorithm to this error function. The change in the weight vector \mathbf{w} is then given by

$$\mathbf{w}^{(\tau+1)} = \mathbf{w}^{(\tau)} - \eta \nabla E_P(\mathbf{w}) = \mathbf{w}^{(\tau)} + \eta \phi_n t_n \quad (4.55)$$

where η is the learning rate parameter and τ is an integer that indexes the steps of the algorithm. Because the perceptron function $y(\mathbf{x}, \mathbf{w})$ is unchanged if we multiply \mathbf{w} by a constant, we can set the learning rate parameter η equal to 1 without loss of generality. Note that, as the weight vector evolves during training, the set of patterns that are misclassified will change.

The perceptron learning algorithm has a simple interpretation, as follows. We cycle through the training patterns in turn, and for each pattern \mathbf{x}_n we evaluate the perceptron function (4.52). If the pattern is correctly classified, then the weight vector remains unchanged, whereas if it is incorrectly classified, then for class C_1 we add the vector $\phi(\mathbf{x}_n)$ onto the current estimate of weight vector \mathbf{w} while for class C_2 we subtract the vector $\phi(\mathbf{x}_n)$ from \mathbf{w} . The perceptron learning algorithm is illustrated in Figure 4.7.

If we consider the effect of a single update in the perceptron learning algorithm, we see that the contribution to the error from a misclassified pattern will be reduced because from (4.55) we have

$$-\mathbf{w}^{(\tau+1)\top} \phi_n t_n = -\mathbf{w}^{(\tau)\top} \phi_n t_n - (\phi_n t_n)^\top \phi_n t_n < -\mathbf{w}^{(\tau)\top} \phi_n t_n \quad (4.56)$$

where we have set $\eta = 1$, and made use of $\|\phi_n t_n\|^2 > 0$. Of course, this does not imply that the contribution to the error function from the other misclassified patterns will have been reduced. Furthermore, the change in weight vector may have caused some previously correctly classified patterns to become misclassified. Thus the perceptron learning rule is not guaranteed to reduce the total error function at each stage.

However, the *perceptron convergence theorem* states that if there exists an exact solution (in other words, if the training data set is linearly separable), then the perceptron learning algorithm is guaranteed to find an exact solution in a finite number of steps. Proofs of this theorem can be found for example in Rosenblatt (1962), Block (1962), Nilsson (1965), Minsky and Papert (1969), Hertz *et al.* (1991), and Bishop (1995a). Note, however, that the number of steps required to achieve convergence could still be substantial, and in practice, until convergence is achieved, we will not be able to distinguish between a nonseparable problem and one that is simply slow to converge.

Even when the data set is linearly separable, there may be many solutions, and which one is found will depend on the initialization of the parameters and on the order of presentation of the data points. Furthermore, for data sets that are not linearly separable, the perceptron learning algorithm will never converge.



Figure 4.7 Illustration of the convergence of the perceptron learning algorithm, showing data points from two classes (red and blue) in a two-dimensional feature space (ϕ_1, ϕ_2). The top left plot shows the initial parameter vector w shown as a black arrow together with the corresponding decision boundary (black line), in which the arrow points towards the decision region which classified as belonging to the red class. The data point circled in green is misclassified and so its feature vector is added to the current weight vector, giving the new decision boundary shown in the top right plot. The bottom left plot shows the next misclassified point to be considered, indicated by the green circle, and its feature vector is again added to the weight vector giving the decision boundary shown in the bottom right plot for which all data points are correctly classified.



Figure 4.8 Illustration of the Mark 1 perceptron hardware. The photograph on the left shows how the inputs were obtained using a simple camera system in which an input scene, in this case a printed character, was illuminated by powerful lights, and an image focussed onto a 20×20 array of cadmium sulphide photocells, giving a primitive 400 pixel image. The perceptron also had a patch board, shown in the middle photograph, which allowed different configurations of input features to be tried. Often these were wired up at random to demonstrate the ability of the perceptron to learn without the need for precise wiring, in contrast to a modern digital computer. The photograph on the right shows one of the racks of adaptive weights. Each weight was implemented using a rotary variable resistor, also called a potentiometer, driven by an electric motor thereby allowing the value of the weight to be adjusted automatically by the learning algorithm.

Aside from difficulties with the learning algorithm, the perceptron does not provide probabilistic outputs, nor does it generalize readily to $K > 2$ classes. The most important limitation, however, arises from the fact that (in common with all of the models discussed in this chapter and the previous one) it is based on linear combinations of fixed basis functions. More detailed discussions of the limitations of perceptrons can be found in Minsky and Papert (1969) and Bishop (1995a).

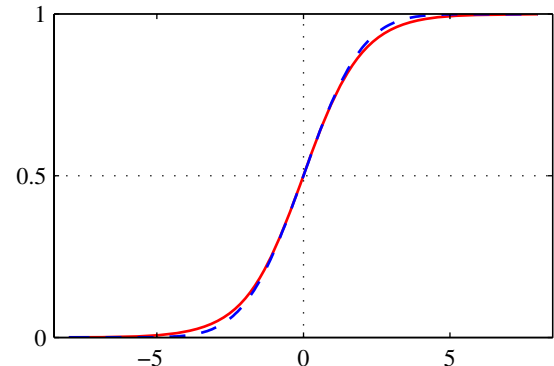
Analogue hardware implementations of the perceptron were built by Rosenblatt, based on motor-driven variable resistors to implement the adaptive parameters w_j . These are illustrated in Figure 4.8. The inputs were obtained from a simple camera system based on an array of photo-sensors, while the basis functions ϕ could be chosen in a variety of ways, for example based on simple fixed functions of randomly chosen subsets of pixels from the input image. Typical applications involved learning to discriminate simple shapes or characters.

At the same time that the perceptron was being developed, a closely related system called the *adaline*, which is short for ‘adaptive linear element’, was being explored by Widrow and co-workers. The functional form of the model was the same as for the perceptron, but a different approach to training was adopted (Widrow and Hoff, 1960; Widrow and Lehr, 1990).

4.2. Probabilistic Generative Models

We turn next to a probabilistic view of classification and show how models with linear decision boundaries arise from simple assumptions about the distribution of the data. In Section 1.5.4, we discussed the distinction between the discriminative and the generative approaches to classification. Here we shall adopt a generative

Figure 4.9 Plot of the logistic sigmoid function $\sigma(a)$ defined by (4.59), shown in red, together with the scaled probit function $\Phi(\lambda a)$, for $\lambda^2 = \pi/8$, shown in dashed blue, where $\Phi(a)$ is defined by (4.114). The scaling factor $\pi/8$ is chosen so that the derivatives of the two curves are equal for $a = 0$.



approach in which we model the class-conditional densities $p(\mathbf{x}|\mathcal{C}_k)$, as well as the class priors $p(\mathcal{C}_k)$, and then use these to compute posterior probabilities $p(\mathcal{C}_k|\mathbf{x})$ through Bayes' theorem.

Consider first of all the case of two classes. The posterior probability for class \mathcal{C}_1 can be written as

$$\begin{aligned} p(\mathcal{C}_1|\mathbf{x}) &= \frac{p(\mathbf{x}|\mathcal{C}_1)p(\mathcal{C}_1)}{p(\mathbf{x}|\mathcal{C}_1)p(\mathcal{C}_1) + p(\mathbf{x}|\mathcal{C}_2)p(\mathcal{C}_2)} \\ &= \frac{1}{1 + \exp(-a)} = \sigma(a) \end{aligned} \quad (4.57)$$

where we have defined

$$a = \ln \frac{p(\mathbf{x}|\mathcal{C}_1)p(\mathcal{C}_1)}{p(\mathbf{x}|\mathcal{C}_2)p(\mathcal{C}_2)} \quad (4.58)$$

and $\sigma(a)$ is the *logistic sigmoid* function defined by

$$\sigma(a) = \frac{1}{1 + \exp(-a)} \quad (4.59)$$

which is plotted in Figure 4.9. The term ‘sigmoid’ means S-shaped. This type of function is sometimes also called a ‘squashing function’ because it maps the whole real axis into a finite interval. The logistic sigmoid has been encountered already in earlier chapters and plays an important role in many classification algorithms. It satisfies the following symmetry property

$$\sigma(-a) = 1 - \sigma(a) \quad (4.60)$$

as is easily verified. The inverse of the logistic sigmoid is given by

$$a = \ln \left(\frac{\sigma}{1 - \sigma} \right) \quad (4.61)$$

and is known as the *logit* function. It represents the log of the ratio of probabilities $\ln [p(\mathcal{C}_1|\mathbf{x})/p(\mathcal{C}_2|\mathbf{x})]$ for the two classes, also known as the *log odds*.

Note that in (4.57) we have simply rewritten the posterior probabilities in an equivalent form, and so the appearance of the logistic sigmoid may seem rather vacuous. However, it will have significance provided $a(\mathbf{x})$ takes a simple functional form. We shall shortly consider situations in which $a(\mathbf{x})$ is a linear function of \mathbf{x} , in which case the posterior probability is governed by a generalized linear model.

For the case of $K > 2$ classes, we have

$$\begin{aligned} p(\mathcal{C}_k|\mathbf{x}) &= \frac{p(\mathbf{x}|\mathcal{C}_k)p(\mathcal{C}_k)}{\sum_j p(\mathbf{x}|\mathcal{C}_j)p(\mathcal{C}_j)} \\ &= \frac{\exp(a_k)}{\sum_j \exp(a_j)} \end{aligned} \quad (4.62)$$

which is known as the *normalized exponential* and can be regarded as a multiclass generalization of the logistic sigmoid. Here the quantities a_k are defined by

$$a_k = \ln p(\mathbf{x}|\mathcal{C}_k)p(\mathcal{C}_k). \quad (4.63)$$

The normalized exponential is also known as the *softmax function*, as it represents a smoothed version of the ‘max’ function because, if $a_k \gg a_j$ for all $j \neq k$, then $p(\mathcal{C}_k|\mathbf{x}) \simeq 1$, and $p(\mathcal{C}_j|\mathbf{x}) \simeq 0$.

We now investigate the consequences of choosing specific forms for the class-conditional densities, looking first at continuous input variables \mathbf{x} and then discussing briefly the case of discrete inputs.

4.2.1 Continuous inputs

Let us assume that the class-conditional densities are Gaussian and then explore the resulting form for the posterior probabilities. To start with, we shall assume that all classes share the same covariance matrix. Thus the density for class \mathcal{C}_k is given by

$$p(\mathbf{x}|\mathcal{C}_k) = \frac{1}{(2\pi)^{D/2}} \frac{1}{|\boldsymbol{\Sigma}|^{1/2}} \exp \left\{ -\frac{1}{2} (\mathbf{x} - \boldsymbol{\mu}_k)^T \boldsymbol{\Sigma}^{-1} (\mathbf{x} - \boldsymbol{\mu}_k) \right\}. \quad (4.64)$$

Consider first the case of two classes. From (4.57) and (4.58), we have

$$p(\mathcal{C}_1|\mathbf{x}) = \sigma(\mathbf{w}^T \mathbf{x} + w_0) \quad (4.65)$$

where we have defined

$$\mathbf{w} = \boldsymbol{\Sigma}^{-1}(\boldsymbol{\mu}_1 - \boldsymbol{\mu}_2) \quad (4.66)$$

$$w_0 = -\frac{1}{2} \boldsymbol{\mu}_1^T \boldsymbol{\Sigma}^{-1} \boldsymbol{\mu}_1 + \frac{1}{2} \boldsymbol{\mu}_2^T \boldsymbol{\Sigma}^{-1} \boldsymbol{\mu}_2 + \ln \frac{p(\mathcal{C}_1)}{p(\mathcal{C}_2)}. \quad (4.67)$$

We see that the quadratic terms in \mathbf{x} from the exponents of the Gaussian densities have cancelled (due to the assumption of common covariance matrices) leading to a linear function of \mathbf{x} in the argument of the logistic sigmoid. This result is illustrated for the case of a two-dimensional input space \mathbf{x} in Figure 4.10. The resulting



Figure 4.10 The left-hand plot shows the class-conditional densities for two classes, denoted red and blue. On the right is the corresponding posterior probability $p(C_1|x)$, which is given by a logistic sigmoid of a linear function of x . The surface in the right-hand plot is coloured using a proportion of red ink given by $p(C_1|x)$ and a proportion of blue ink given by $p(C_2|x) = 1 - p(C_1|x)$.

decision boundaries correspond to surfaces along which the posterior probabilities $p(C_k|x)$ are constant and so will be given by linear functions of x , and therefore the decision boundaries are linear in input space. The prior probabilities $p(C_k)$ enter only through the bias parameter w_0 so that changes in the priors have the effect of making parallel shifts of the decision boundary and more generally of the parallel contours of constant posterior probability.

For the general case of K classes we have, from (4.62) and (4.63),

$$a_k(\mathbf{x}) = \mathbf{w}_k^T \mathbf{x} + w_{k0} \quad (4.68)$$

where we have defined

$$\mathbf{w}_k = \Sigma^{-1} \boldsymbol{\mu}_k \quad (4.69)$$

$$w_{k0} = -\frac{1}{2} \boldsymbol{\mu}_k^T \Sigma^{-1} \boldsymbol{\mu}_k + \ln p(C_k). \quad (4.70)$$

We see that the $a_k(\mathbf{x})$ are again linear functions of \mathbf{x} as a consequence of the cancellation of the quadratic terms due to the shared covariances. The resulting decision boundaries, corresponding to the minimum misclassification rate, will occur when two of the posterior probabilities (the two largest) are equal, and so will be defined by linear functions of \mathbf{x} , and so again we have a generalized linear model.

If we relax the assumption of a shared covariance matrix and allow each class-conditional density $p(\mathbf{x}|C_k)$ to have its own covariance matrix Σ_k , then the earlier cancellations will no longer occur, and we will obtain quadratic functions of \mathbf{x} , giving rise to a *quadratic discriminant*. The linear and quadratic decision boundaries are illustrated in Figure 4.11.



Figure 4.11 The left-hand plot shows the class-conditional densities for three classes each having a Gaussian distribution, coloured red, green, and blue, in which the red and green classes have the same covariance matrix. The right-hand plot shows the corresponding posterior probabilities, in which the RGB colour vector represents the posterior probabilities for the respective three classes. The decision boundaries are also shown. Notice that the boundary between the red and green classes, which have the same covariance matrix, is linear, whereas those between the other pairs of classes are quadratic.

4.2.2 Maximum likelihood solution

Once we have specified a parametric functional form for the class-conditional densities $p(\mathbf{x}|\mathcal{C}_k)$, we can then determine the values of the parameters, together with the prior class probabilities $p(\mathcal{C}_k)$, using maximum likelihood. This requires a data set comprising observations of \mathbf{x} along with their corresponding class labels.

Consider first the case of two classes, each having a Gaussian class-conditional density with a shared covariance matrix, and suppose we have a data set $\{\mathbf{x}_n, t_n\}$ where $n = 1, \dots, N$. Here $t_n = 1$ denotes class \mathcal{C}_1 and $t_n = 0$ denotes class \mathcal{C}_2 . We denote the prior class probability $p(\mathcal{C}_1) = \pi$, so that $p(\mathcal{C}_2) = 1 - \pi$. For a data point \mathbf{x}_n from class \mathcal{C}_1 , we have $t_n = 1$ and hence

$$p(\mathbf{x}_n, \mathcal{C}_1) = p(\mathcal{C}_1)p(\mathbf{x}_n|\mathcal{C}_1) = \pi \mathcal{N}(\mathbf{x}_n|\boldsymbol{\mu}_1, \boldsymbol{\Sigma}).$$

Similarly for class \mathcal{C}_2 , we have $t_n = 0$ and hence

$$p(\mathbf{x}_n, \mathcal{C}_2) = p(\mathcal{C}_2)p(\mathbf{x}_n|\mathcal{C}_2) = (1 - \pi) \mathcal{N}(\mathbf{x}_n|\boldsymbol{\mu}_2, \boldsymbol{\Sigma}).$$

Thus the likelihood function is given by

$$p(\mathbf{t}|\pi, \boldsymbol{\mu}_1, \boldsymbol{\mu}_2, \boldsymbol{\Sigma}) = \prod_{n=1}^N [\pi \mathcal{N}(\mathbf{x}_n|\boldsymbol{\mu}_1, \boldsymbol{\Sigma})]^{t_n} [(1 - \pi) \mathcal{N}(\mathbf{x}_n|\boldsymbol{\mu}_2, \boldsymbol{\Sigma})]^{1-t_n} \quad (4.71)$$

where $\mathbf{t} = (t_1, \dots, t_N)^T$. As usual, it is convenient to maximize the log of the likelihood function. Consider first the maximization with respect to π . The terms in

the log likelihood function that depend on π are

$$\sum_{n=1}^N \{t_n \ln \pi + (1 - t_n) \ln(1 - \pi)\}. \quad (4.72)$$

Setting the derivative with respect to π equal to zero and rearranging, we obtain

$$\pi = \frac{1}{N} \sum_{n=1}^N t_n = \frac{N_1}{N} = \frac{N_1}{N_1 + N_2} \quad (4.73)$$

where N_1 denotes the total number of data points in class \mathcal{C}_1 , and N_2 denotes the total number of data points in class \mathcal{C}_2 . Thus the maximum likelihood estimate for π is simply the fraction of points in class \mathcal{C}_1 as expected. This result is easily generalized to the multiclass case where again the maximum likelihood estimate of the prior probability associated with class \mathcal{C}_k is given by the fraction of the training set points assigned to that class.

Exercise 4.9

Now consider the maximization with respect to $\boldsymbol{\mu}_1$. Again we can pick out of the log likelihood function those terms that depend on $\boldsymbol{\mu}_1$ giving

$$\sum_{n=1}^N t_n \ln \mathcal{N}(\mathbf{x}_n | \boldsymbol{\mu}_1, \boldsymbol{\Sigma}) = -\frac{1}{2} \sum_{n=1}^N t_n (\mathbf{x}_n - \boldsymbol{\mu}_1)^T \boldsymbol{\Sigma}^{-1} (\mathbf{x}_n - \boldsymbol{\mu}_1) + \text{const.} \quad (4.74)$$

Setting the derivative with respect to $\boldsymbol{\mu}_1$ to zero and rearranging, we obtain

$$\boldsymbol{\mu}_1 = \frac{1}{N_1} \sum_{n=1}^N t_n \mathbf{x}_n \quad (4.75)$$

which is simply the mean of all the input vectors \mathbf{x}_n assigned to class \mathcal{C}_1 . By a similar argument, the corresponding result for $\boldsymbol{\mu}_2$ is given by

$$\boldsymbol{\mu}_2 = \frac{1}{N_2} \sum_{n=1}^N (1 - t_n) \mathbf{x}_n \quad (4.76)$$

which again is the mean of all the input vectors \mathbf{x}_n assigned to class \mathcal{C}_2 .

Finally, consider the maximum likelihood solution for the shared covariance matrix $\boldsymbol{\Sigma}$. Picking out the terms in the log likelihood function that depend on $\boldsymbol{\Sigma}$, we have

$$\begin{aligned} & -\frac{1}{2} \sum_{n=1}^N t_n \ln |\boldsymbol{\Sigma}| - \frac{1}{2} \sum_{n=1}^N t_n (\mathbf{x}_n - \boldsymbol{\mu}_1)^T \boldsymbol{\Sigma}^{-1} (\mathbf{x}_n - \boldsymbol{\mu}_1) \\ & - \frac{1}{2} \sum_{n=1}^N (1 - t_n) \ln |\boldsymbol{\Sigma}| - \frac{1}{2} \sum_{n=1}^N (1 - t_n) (\mathbf{x}_n - \boldsymbol{\mu}_2)^T \boldsymbol{\Sigma}^{-1} (\mathbf{x}_n - \boldsymbol{\mu}_2) \\ & = -\frac{N}{2} \ln |\boldsymbol{\Sigma}| - \frac{N}{2} \text{Tr} \{ \boldsymbol{\Sigma}^{-1} \mathbf{S} \} \end{aligned} \quad (4.77)$$

where we have defined

$$\mathbf{S} = \frac{N_1}{N} \mathbf{S}_1 + \frac{N_2}{N} \mathbf{S}_2 \quad (4.78)$$

$$\mathbf{S}_1 = \frac{1}{N_1} \sum_{n \in \mathcal{C}_1} (\mathbf{x}_n - \boldsymbol{\mu}_1)(\mathbf{x}_n - \boldsymbol{\mu}_1)^T \quad (4.79)$$

$$\mathbf{S}_2 = \frac{1}{N_2} \sum_{n \in \mathcal{C}_2} (\mathbf{x}_n - \boldsymbol{\mu}_2)(\mathbf{x}_n - \boldsymbol{\mu}_2)^T. \quad (4.80)$$

Using the standard result for the maximum likelihood solution for a Gaussian distribution, we see that $\Sigma = \mathbf{S}$, which represents a weighted average of the covariance matrices associated with each of the two classes separately.

This result is easily extended to the K class problem to obtain the corresponding maximum likelihood solutions for the parameters in which each class-conditional density is Gaussian with a shared covariance matrix. Note that the approach of fitting Gaussian distributions to the classes is not robust to outliers, because the maximum likelihood estimation of a Gaussian is not robust.

Exercise 4.10

Section 2.3.7

Section 8.2.2

Exercise 4.11

4.2.3 Discrete features

Let us now consider the case of discrete feature values x_i . For simplicity, we begin by looking at binary feature values $x_i \in \{0, 1\}$ and discuss the extension to more general discrete features shortly. If there are D inputs, then a general distribution would correspond to a table of 2^D numbers for each class, containing $2^D - 1$ independent variables (due to the summation constraint). Because this grows exponentially with the number of features, we might seek a more restricted representation. Here we will make the *naive Bayes* assumption in which the feature values are treated as independent, conditioned on the class \mathcal{C}_k . Thus we have class-conditional distributions of the form

$$p(\mathbf{x}|\mathcal{C}_k) = \prod_{i=1}^D \mu_{ki}^{x_i} (1 - \mu_{ki})^{1-x_i} \quad (4.81)$$

which contain D independent parameters for each class. Substituting into (4.63) then gives

$$a_k(\mathbf{x}) = \sum_{i=1}^D \{x_i \ln \mu_{ki} + (1 - x_i) \ln(1 - \mu_{ki})\} + \ln p(\mathcal{C}_k) \quad (4.82)$$

which again are linear functions of the input values x_i . For the case of $K = 2$ classes, we can alternatively consider the logistic sigmoid formulation given by (4.57). Analogous results are obtained for discrete variables each of which can take $M > 2$ states.

4.2.4 Exponential family

As we have seen, for both Gaussian distributed and discrete inputs, the posterior class probabilities are given by generalized linear models with logistic sigmoid ($K =$

2 classes) or softmax ($K \geq 2$ classes) activation functions. These are particular cases of a more general result obtained by assuming that the class-conditional densities $p(\mathbf{x}|\mathcal{C}_k)$ are members of the exponential family of distributions.

Using the form (2.194) for members of the exponential family, we see that the distribution of \mathbf{x} can be written in the form

$$p(\mathbf{x}|\boldsymbol{\lambda}_k) = h(\mathbf{x})g(\boldsymbol{\lambda}_k) \exp \left\{ \boldsymbol{\lambda}_k^T \mathbf{u}(\mathbf{x}) \right\}. \quad (4.83)$$

We now restrict attention to the subclass of such distributions for which $\mathbf{u}(\mathbf{x}) = \mathbf{x}$. Then we make use of (2.236) to introduce a scaling parameter s , so that we obtain the restricted set of exponential family class-conditional densities of the form

$$p(\mathbf{x}|\boldsymbol{\lambda}_k, s) = \frac{1}{s} h\left(\frac{1}{s}\mathbf{x}\right) g(\boldsymbol{\lambda}_k) \exp \left\{ \frac{1}{s} \boldsymbol{\lambda}_k^T \mathbf{x} \right\}. \quad (4.84)$$

Note that we are allowing each class to have its own parameter vector $\boldsymbol{\lambda}_k$ but we are assuming that the classes share the same scale parameter s .

For the two-class problem, we substitute this expression for the class-conditional densities into (4.58) and we see that the posterior class probability is again given by a logistic sigmoid acting on a linear function $a(\mathbf{x})$ which is given by

$$a(\mathbf{x}) = (\boldsymbol{\lambda}_1 - \boldsymbol{\lambda}_2)^T \mathbf{x} + \ln g(\boldsymbol{\lambda}_1) - \ln g(\boldsymbol{\lambda}_2) + \ln p(\mathcal{C}_1) - \ln p(\mathcal{C}_2). \quad (4.85)$$

Similarly, for the K -class problem, we substitute the class-conditional density expression into (4.63) to give

$$a_k(\mathbf{x}) = \boldsymbol{\lambda}_k^T \mathbf{x} + \ln g(\boldsymbol{\lambda}_k) + \ln p(\mathcal{C}_k) \quad (4.86)$$

and so again is a linear function of \mathbf{x} .

4.3. Probabilistic Discriminative Models

For the two-class classification problem, we have seen that the posterior probability of class \mathcal{C}_1 can be written as a logistic sigmoid acting on a linear function of \mathbf{x} , for a wide choice of class-conditional distributions $p(\mathbf{x}|\mathcal{C}_k)$. Similarly, for the multiclass case, the posterior probability of class \mathcal{C}_k is given by a softmax transformation of a linear function of \mathbf{x} . For specific choices of the class-conditional densities $p(\mathbf{x}|\mathcal{C}_k)$, we have used maximum likelihood to determine the parameters of the densities as well as the class priors $p(\mathcal{C}_k)$ and then used Bayes' theorem to find the posterior class probabilities.

However, an alternative approach is to use the functional form of the generalized linear model explicitly and to determine its parameters directly by using maximum likelihood. We shall see that there is an efficient algorithm finding such solutions known as *iterative reweighted least squares*, or *IRLS*.

The indirect approach to finding the parameters of a generalized linear model, by fitting class-conditional densities and class priors separately and then applying

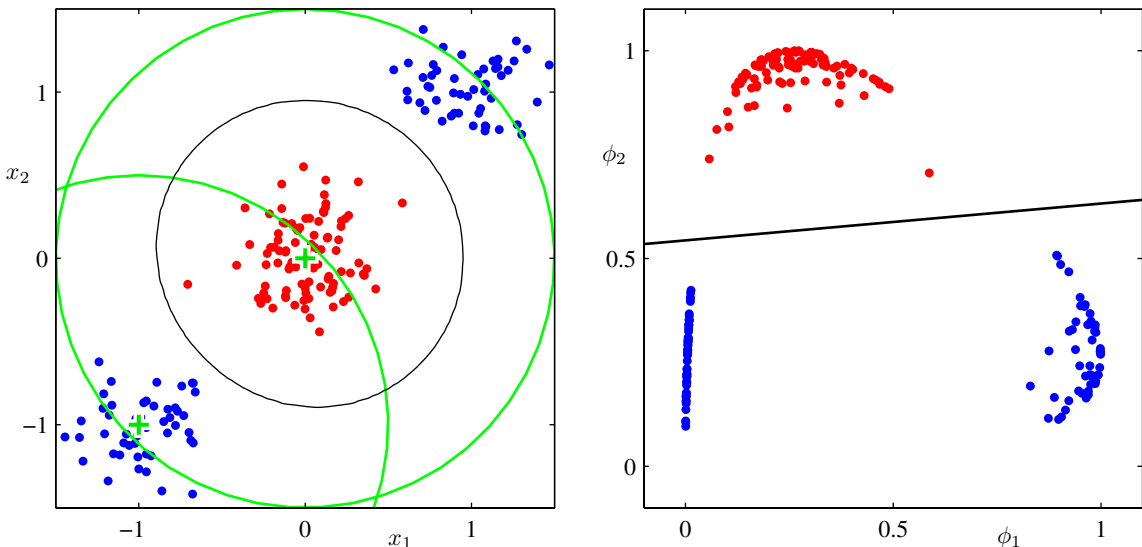


Figure 4.12 Illustration of the role of nonlinear basis functions in linear classification models. The left plot shows the original input space (x_1, x_2) together with data points from two classes labelled red and blue. Two ‘Gaussian’ basis functions $\phi_1(\mathbf{x})$ and $\phi_2(\mathbf{x})$ are defined in this space with centres shown by the green crosses and with contours shown by the green circles. The right-hand plot shows the corresponding feature space (ϕ_1, ϕ_2) together with the linear decision boundary obtained given by a logistic regression model of the form discussed in Section 4.3.2. This corresponds to a nonlinear decision boundary in the original input space, shown by the black curve in the left-hand plot.

Bayes’ theorem, represents an example of *generative* modelling, because we could take such a model and generate synthetic data by drawing values of \mathbf{x} from the marginal distribution $p(\mathbf{x})$. In the direct approach, we are maximizing a likelihood function defined through the conditional distribution $p(C_k|\mathbf{x})$, which represents a form of *discriminative* training. One advantage of the discriminative approach is that there will typically be fewer adaptive parameters to be determined, as we shall see shortly. It may also lead to improved predictive performance, particularly when the class-conditional density assumptions give a poor approximation to the true distributions.

4.3.1 Fixed basis functions

So far in this chapter, we have considered classification models that work directly with the original input vector \mathbf{x} . However, all of the algorithms are equally applicable if we first make a fixed nonlinear transformation of the inputs using a vector of basis functions $\phi(\mathbf{x})$. The resulting decision boundaries will be linear in the feature space ϕ , and these correspond to nonlinear decision boundaries in the original \mathbf{x} space, as illustrated in Figure 4.12. Classes that are linearly separable in the feature space $\phi(\mathbf{x})$ need not be linearly separable in the original observation space \mathbf{x} . Note that as in our discussion of linear models for regression, one of the

basis functions is typically set to a constant, say $\phi_0(\mathbf{x}) = 1$, so that the corresponding parameter w_0 plays the role of a bias. For the remainder of this chapter, we shall include a fixed basis function transformation $\phi(\mathbf{x})$, as this will highlight some useful similarities to the regression models discussed in Chapter 3.

For many problems of practical interest, there is significant overlap between the class-conditional densities $p(\mathbf{x}|\mathcal{C}_k)$. This corresponds to posterior probabilities $p(\mathcal{C}_k|\mathbf{x})$, which, for at least some values of \mathbf{x} , are not 0 or 1. In such cases, the optimal solution is obtained by modelling the posterior probabilities accurately and then applying standard decision theory, as discussed in Chapter 1. Note that nonlinear transformations $\phi(\mathbf{x})$ cannot remove such class overlap. Indeed, they can increase the level of overlap, or create overlap where none existed in the original observation space. However, suitable choices of nonlinearity can make the process of modelling the posterior probabilities easier.

Section 3.6

Such fixed basis function models have important limitations, and these will be resolved in later chapters by allowing the basis functions themselves to adapt to the data. Notwithstanding these limitations, models with fixed nonlinear basis functions play an important role in applications, and a discussion of such models will introduce many of the key concepts needed for an understanding of their more complex counterparts.

4.3.2 Logistic regression

We begin our treatment of generalized linear models by considering the problem of two-class classification. In our discussion of generative approaches in Section 4.2, we saw that under rather general assumptions, the posterior probability of class \mathcal{C}_1 can be written as a logistic sigmoid acting on a linear function of the feature vector ϕ so that

$$p(\mathcal{C}_1|\phi) = y(\phi) = \sigma(\mathbf{w}^T \phi) \quad (4.87)$$

with $p(\mathcal{C}_2|\phi) = 1 - p(\mathcal{C}_1|\phi)$. Here $\sigma(\cdot)$ is the *logistic sigmoid* function defined by (4.59). In the terminology of statistics, this model is known as *logistic regression*, although it should be emphasized that this is a model for classification rather than regression.

For an M -dimensional feature space ϕ , this model has M adjustable parameters. By contrast, if we had fitted Gaussian class conditional densities using maximum likelihood, we would have used $2M$ parameters for the means and $M(M+1)/2$ parameters for the (shared) covariance matrix. Together with the class prior $p(\mathcal{C}_1)$, this gives a total of $M(M+5)/2 + 1$ parameters, which grows quadratically with M , in contrast to the linear dependence on M of the number of parameters in logistic regression. For large values of M , there is a clear advantage in working with the logistic regression model directly.

We now use maximum likelihood to determine the parameters of the logistic regression model. To do this, we shall make use of the derivative of the logistic sigmoid function, which can conveniently be expressed in terms of the sigmoid function itself

$$\frac{d\sigma}{da} = \sigma(1 - \sigma). \quad (4.88)$$

Exercise 4.12

For a data set $\{\phi_n, t_n\}$, where $t_n \in \{0, 1\}$ and $\phi_n = \phi(\mathbf{x}_n)$, with $n = 1, \dots, N$, the likelihood function can be written

$$p(\mathbf{t}|\mathbf{w}) = \prod_{n=1}^N y_n^{t_n} \{1 - y_n\}^{1-t_n} \quad (4.89)$$

where $\mathbf{t} = (t_1, \dots, t_N)^T$ and $y_n = p(\mathcal{C}_1|\phi_n)$. As usual, we can define an error function by taking the negative logarithm of the likelihood, which gives the *cross-entropy* error function in the form

$$E(\mathbf{w}) = -\ln p(\mathbf{t}|\mathbf{w}) = -\sum_{n=1}^N \{t_n \ln y_n + (1 - t_n) \ln(1 - y_n)\} \quad (4.90)$$

where $y_n = \sigma(a_n)$ and $a_n = \mathbf{w}^T \phi_n$. Taking the gradient of the error function with respect to \mathbf{w} , we obtain

$$\nabla E(\mathbf{w}) = \sum_{n=1}^N (y_n - t_n) \phi_n \quad (4.91)$$

where we have made use of (4.88). We see that the factor involving the derivative of the logistic sigmoid has cancelled, leading to a simplified form for the gradient of the log likelihood. In particular, the contribution to the gradient from data point n is given by the ‘error’ $y_n - t_n$ between the target value and the prediction of the model, times the basis function vector ϕ_n . Furthermore, comparison with (3.13) shows that this takes precisely the same form as the gradient of the sum-of-squares error function for the linear regression model.

Section 3.1.1

If desired, we could make use of the result (4.91) to give a sequential algorithm in which patterns are presented one at a time, in which each of the weight vectors is updated using (3.22) in which ∇E_n is the n^{th} term in (4.91).

Exercise 4.14

It is worth noting that maximum likelihood can exhibit severe over-fitting for data sets that are linearly separable. This arises because the maximum likelihood solution occurs when the hyperplane corresponding to $\sigma = 0.5$, equivalent to $\mathbf{w}^T \phi = 0$, separates the two classes and the magnitude of \mathbf{w} goes to infinity. In this case, the logistic sigmoid function becomes infinitely steep in feature space, corresponding to a Heaviside step function, so that every training point from each class k is assigned a posterior probability $p(\mathcal{C}_k|\mathbf{x}) = 1$. Furthermore, there is typically a continuum of such solutions because any separating hyperplane will give rise to the same posterior probabilities at the training data points, as will be seen later in Figure 10.13. Maximum likelihood provides no way to favour one such solution over another, and which solution is found in practice will depend on the choice of optimization algorithm and on the parameter initialization. Note that the problem will arise even if the number of data points is large compared with the number of parameters in the model, so long as the training data set is linearly separable. The singularity can be avoided by inclusion of a prior and finding a MAP solution for \mathbf{w} , or equivalently by adding a regularization term to the error function.

4.3.3 Iterative reweighted least squares

In the case of the linear regression models discussed in Chapter 3, the maximum likelihood solution, on the assumption of a Gaussian noise model, leads to a closed-form solution. This was a consequence of the quadratic dependence of the log likelihood function on the parameter vector \mathbf{w} . For logistic regression, there is no longer a closed-form solution, due to the nonlinearity of the logistic sigmoid function. However, the departure from a quadratic form is not substantial. To be precise, the error function is concave, as we shall see shortly, and hence has a unique minimum. Furthermore, the error function can be minimized by an efficient iterative technique based on the *Newton-Raphson* iterative optimization scheme, which uses a local quadratic approximation to the log likelihood function. The Newton-Raphson update, for minimizing a function $E(\mathbf{w})$, takes the form (Fletcher, 1987; Bishop and Nabney, 2008)

$$\mathbf{w}^{(\text{new})} = \mathbf{w}^{(\text{old})} - \mathbf{H}^{-1} \nabla E(\mathbf{w}). \quad (4.92)$$

where \mathbf{H} is the Hessian matrix whose elements comprise the second derivatives of $E(\mathbf{w})$ with respect to the components of \mathbf{w} .

Let us first of all apply the Newton-Raphson method to the linear regression model (3.3) with the sum-of-squares error function (3.12). The gradient and Hessian of this error function are given by

$$\nabla E(\mathbf{w}) = \sum_{n=1}^N (\mathbf{w}^T \phi_n - t_n) \phi_n = \Phi^T \Phi \mathbf{w} - \Phi^T \mathbf{t} \quad (4.93)$$

$$\mathbf{H} = \nabla \nabla E(\mathbf{w}) = \sum_{n=1}^N \phi_n \phi_n^T = \Phi^T \Phi \quad (4.94)$$

Section 3.1.1

where Φ is the $N \times M$ design matrix, whose n^{th} row is given by ϕ_n^T . The Newton-Raphson update then takes the form

$$\begin{aligned} \mathbf{w}^{(\text{new})} &= \mathbf{w}^{(\text{old})} - (\Phi^T \Phi)^{-1} \{ \Phi^T \Phi \mathbf{w}^{(\text{old})} - \Phi^T \mathbf{t} \} \\ &= (\Phi^T \Phi)^{-1} \Phi^T \mathbf{t} \end{aligned} \quad (4.95)$$

which we recognize as the standard least-squares solution. Note that the error function in this case is quadratic and hence the Newton-Raphson formula gives the exact solution in one step.

Now let us apply the Newton-Raphson update to the cross-entropy error function (4.90) for the logistic regression model. From (4.91) we see that the gradient and Hessian of this error function are given by

$$\nabla E(\mathbf{w}) = \sum_{n=1}^N (y_n - t_n) \phi_n = \Phi^T (\mathbf{y} - \mathbf{t}) \quad (4.96)$$

$$\mathbf{H} = \nabla \nabla E(\mathbf{w}) = \sum_{n=1}^N y_n (1 - y_n) \phi_n \phi_n^T = \Phi^T \mathbf{R} \Phi \quad (4.97)$$

where we have made use of (4.88). Also, we have introduced the $N \times N$ diagonal matrix \mathbf{R} with elements

$$R_{nn} = y_n(1 - y_n). \quad (4.98)$$

We see that the Hessian is no longer constant but depends on \mathbf{w} through the weighting matrix \mathbf{R} , corresponding to the fact that the error function is no longer quadratic. Using the property $0 < y_n < 1$, which follows from the form of the logistic sigmoid function, we see that $\mathbf{u}^T \mathbf{H} \mathbf{u} > 0$ for an arbitrary vector \mathbf{u} , and so the Hessian matrix \mathbf{H} is positive definite. It follows that the error function is a concave function of \mathbf{w} and hence has a unique minimum.

Exercise 4.15

The Newton-Raphson update formula for the logistic regression model then becomes

$$\begin{aligned} \mathbf{w}^{(\text{new})} &= \mathbf{w}^{(\text{old})} - (\Phi^T \mathbf{R} \Phi)^{-1} \Phi^T (\mathbf{y} - \mathbf{t}) \\ &= (\Phi^T \mathbf{R} \Phi)^{-1} \{ \Phi^T \mathbf{R} \Phi \mathbf{w}^{(\text{old})} - \Phi^T (\mathbf{y} - \mathbf{t}) \} \\ &= (\Phi^T \mathbf{R} \Phi)^{-1} \Phi^T \mathbf{R} \mathbf{z} \end{aligned} \quad (4.99)$$

where \mathbf{z} is an N -dimensional vector with elements

$$\mathbf{z} = \Phi \mathbf{w}^{(\text{old})} - \mathbf{R}^{-1} (\mathbf{y} - \mathbf{t}). \quad (4.100)$$

We see that the update formula (4.99) takes the form of a set of normal equations for a weighted least-squares problem. Because the weighing matrix \mathbf{R} is not constant but depends on the parameter vector \mathbf{w} , we must apply the normal equations iteratively, each time using the new weight vector \mathbf{w} to compute a revised weighing matrix \mathbf{R} . For this reason, the algorithm is known as *iterative reweighted least squares*, or *IRLS* (Rubin, 1983). As in the weighted least-squares problem, the elements of the diagonal weighting matrix \mathbf{R} can be interpreted as variances because the mean and variance of t in the logistic regression model are given by

$$\mathbb{E}[t] = \sigma(\mathbf{x}) = y \quad (4.101)$$

$$\text{var}[t] = \mathbb{E}[t^2] - \mathbb{E}[t]^2 = \sigma(\mathbf{x}) - \sigma(\mathbf{x})^2 = y(1 - y) \quad (4.102)$$

where we have used the property $t^2 = t$ for $t \in \{0, 1\}$. In fact, we can interpret IRLS as the solution to a linearized problem in the space of the variable $a = \mathbf{w}^T \phi$. The quantity z_n , which corresponds to the n^{th} element of \mathbf{z} , can then be given a simple interpretation as an effective target value in this space obtained by making a local linear approximation to the logistic sigmoid function around the current operating point $\mathbf{w}^{(\text{old})}$

$$\begin{aligned} a_n(\mathbf{w}) &\simeq a_n(\mathbf{w}^{(\text{old})}) + \frac{da_n}{dy_n} \Big|_{\mathbf{w}^{(\text{old})}} (t_n - y_n) \\ &= \phi_n^T \mathbf{w}^{(\text{old})} - \frac{(y_n - t_n)}{y_n(1 - y_n)} = z_n. \end{aligned} \quad (4.103)$$

4.3.4 Multiclass logistic regression

Section 4.2

In our discussion of generative models for multiclass classification, we have seen that for a large class of distributions, the posterior probabilities are given by a softmax transformation of linear functions of the feature variables, so that

$$p(\mathcal{C}_k|\phi) = y_k(\phi) = \frac{\exp(a_k)}{\sum_j \exp(a_j)} \quad (4.104)$$

where the ‘activations’ a_k are given by

$$a_k = \mathbf{w}_k^T \phi. \quad (4.105)$$

There we used maximum likelihood to determine separately the class-conditional densities and the class priors and then found the corresponding posterior probabilities using Bayes’ theorem, thereby implicitly determining the parameters $\{\mathbf{w}_k\}$. Here we consider the use of maximum likelihood to determine the parameters $\{\mathbf{w}_k\}$ of this model directly. To do this, we will require the derivatives of y_k with respect to all of the activations a_j . These are given by

$$\frac{\partial y_k}{\partial a_j} = y_k(I_{kj} - y_j) \quad (4.106)$$

where I_{kj} are the elements of the identity matrix.

Next we write down the likelihood function. This is most easily done using the 1-of- K coding scheme in which the target vector \mathbf{t}_n for a feature vector ϕ_n belonging to class \mathcal{C}_k is a binary vector with all elements zero except for element k , which equals one. The likelihood function is then given by

$$p(\mathbf{T}|\mathbf{w}_1, \dots, \mathbf{w}_K) = \prod_{n=1}^N \prod_{k=1}^K p(\mathcal{C}_k|\phi_n)^{t_{nk}} = \prod_{n=1}^N \prod_{k=1}^K y_{nk}^{t_{nk}} \quad (4.107)$$

where $y_{nk} = y_k(\phi_n)$, and \mathbf{T} is an $N \times K$ matrix of target variables with elements t_{nk} . Taking the negative logarithm then gives

$$E(\mathbf{w}_1, \dots, \mathbf{w}_K) = -\ln p(\mathbf{T}|\mathbf{w}_1, \dots, \mathbf{w}_K) = -\sum_{n=1}^N \sum_{k=1}^K t_{nk} \ln y_{nk} \quad (4.108)$$

which is known as the *cross-entropy* error function for the multiclass classification problem.

We now take the gradient of the error function with respect to one of the parameter vectors \mathbf{w}_j . Making use of the result (4.106) for the derivatives of the softmax function, we obtain

$$\nabla_{\mathbf{w}_j} E(\mathbf{w}_1, \dots, \mathbf{w}_K) = \sum_{n=1}^N (y_{nj} - t_{nj}) \phi_n \quad (4.109)$$

Exercise 4.17

where we have made use of $\sum_k t_{nk} = 1$. Once again, we see the same form arising for the gradient as was found for the sum-of-squares error function with the linear model and the cross-entropy error for the logistic regression model, namely the product of the error $(y_{nj} - t_{nj})$ times the basis function ϕ_n . Again, we could use this to formulate a sequential algorithm in which patterns are presented one at a time, in which each of the weight vectors is updated using (3.22).

We have seen that the derivative of the log likelihood function for a linear regression model with respect to the parameter vector w for a data point n took the form of the ‘error’ $y_n - t_n$ times the feature vector ϕ_n . Similarly, for the combination of logistic sigmoid activation function and cross-entropy error function (4.90), and for the softmax activation function with the multiclass cross-entropy error function (4.108), we again obtain this same simple form. This is an example of a more general result, as we shall see in Section 4.3.6.

To find a batch algorithm, we again appeal to the Newton-Raphson update to obtain the corresponding IRLS algorithm for the multiclass problem. This requires evaluation of the Hessian matrix that comprises blocks of size $M \times M$ in which block j, k is given by

$$\nabla_{w_k} \nabla_{w_j} E(w_1, \dots, w_K) = - \sum_{n=1}^N y_{nk} (I_{kj} - y_{nj}) \phi_n \phi_n^T. \quad (4.110)$$

As with the two-class problem, the Hessian matrix for the multiclass logistic regression model is positive definite and so the error function again has a unique minimum. Practical details of IRLS for the multiclass case can be found in Bishop and Nabney (2008).

Exercise 4.20

4.3.5 Probit regression

We have seen that, for a broad range of class-conditional distributions, described by the exponential family, the resulting posterior class probabilities are given by a logistic (or softmax) transformation acting on a linear function of the feature variables. However, not all choices of class-conditional density give rise to such a simple form for the posterior probabilities (for instance, if the class-conditional densities are modelled using Gaussian mixtures). This suggests that it might be worth exploring other types of discriminative probabilistic model. For the purposes of this chapter, however, we shall return to the two-class case, and again remain within the framework of generalized linear models so that

$$p(t = 1 | a) = f(a) \quad (4.111)$$

where $a = w^T \phi$, and $f(\cdot)$ is the activation function.

One way to motivate an alternative choice for the link function is to consider a noisy threshold model, as follows. For each input ϕ_n , we evaluate $a_n = w^T \phi_n$ and then we set the target value according to

$$\begin{cases} t_n = 1 & \text{if } a_n \geq \theta \\ t_n = 0 & \text{otherwise.} \end{cases} \quad (4.112)$$

Figure 4.13 Schematic example of a probability density $p(\theta)$ shown by the blue curve, given in this example by a mixture of two Gaussians, along with its cumulative distribution function $f(a)$, shown by the red curve. Note that the value of the blue curve at any point, such as that indicated by the vertical green line, corresponds to the slope of the red curve at the same point. Conversely, the value of the red curve at this point corresponds to the area under the blue curve indicated by the shaded green region. In the stochastic threshold model, the class label takes the value $t = 1$ if the value of $a = \mathbf{w}^T \phi$ exceeds a threshold, otherwise it takes the value $t = 0$. This is equivalent to an activation function given by the cumulative distribution function $f(a)$.



If the value of θ is drawn from a probability density $p(\theta)$, then the corresponding activation function will be given by the cumulative distribution function

$$f(a) = \int_{-\infty}^a p(\theta) d\theta \quad (4.113)$$

as illustrated in Figure 4.13.

As a specific example, suppose that the density $p(\theta)$ is given by a zero mean, unit variance Gaussian. The corresponding cumulative distribution function is given by

$$\Phi(a) = \int_{-\infty}^a \mathcal{N}(\theta|0, 1) d\theta \quad (4.114)$$

which is known as the *probit* function. It has a sigmoidal shape and is compared with the logistic sigmoid function in Figure 4.9. Note that the use of a more general Gaussian distribution does not change the model because this is equivalent to a re-scaling of the linear coefficients w . Many numerical packages provide for the evaluation of a closely related function defined by

$$\text{erf}(a) = \frac{2}{\sqrt{\pi}} \int_0^a \exp(-\theta^2/2) d\theta \quad (4.115)$$

and known as the *erf function* or *error function* (not to be confused with the error function of a machine learning model). It is related to the probit function by

$$\Phi(a) = \frac{1}{2} \left\{ 1 + \frac{1}{\sqrt{2}} \text{erf}(a) \right\}. \quad (4.116)$$

The generalized linear model based on a probit activation function is known as *probit regression*.

We can determine the parameters of this model using maximum likelihood, by a straightforward extension of the ideas discussed earlier. In practice, the results found using probit regression tend to be similar to those of logistic regression. We shall,

Exercise 4.21

however, find another use for the probit model when we discuss Bayesian treatments of logistic regression in Section 4.5.

One issue that can occur in practical applications is that of *outliers*, which can arise for instance through errors in measuring the input vector \mathbf{x} or through mislabelling of the target value t . Because such points can lie a long way to the wrong side of the ideal decision boundary, they can seriously distort the classifier. Note that the logistic and probit regression models behave differently in this respect because the tails of the logistic sigmoid decay asymptotically like $\exp(-x)$ for $x \rightarrow \infty$, whereas for the probit activation function they decay like $\exp(-x^2)$, and so the probit model can be significantly more sensitive to outliers.

However, both the logistic and the probit models assume the data is correctly labelled. The effect of mislabelling is easily incorporated into a probabilistic model by introducing a probability ϵ that the target value t has been flipped to the wrong value (Opper and Winther, 2000a), leading to a target value distribution for data point \mathbf{x} of the form

$$\begin{aligned} p(t|\mathbf{x}) &= (1 - \epsilon)\sigma(\mathbf{x}) + \epsilon(1 - \sigma(\mathbf{x})) \\ &= \epsilon + (1 - 2\epsilon)\sigma(\mathbf{x}) \end{aligned} \quad (4.117)$$

where $\sigma(\mathbf{x})$ is the activation function with input vector \mathbf{x} . Here ϵ may be set in advance, or it may be treated as a hyperparameter whose value is inferred from the data.

4.3.6 Canonical link functions

For the linear regression model with a Gaussian noise distribution, the error function, corresponding to the negative log likelihood, is given by (3.12). If we take the derivative with respect to the parameter vector \mathbf{w} of the contribution to the error function from a data point n , this takes the form of the ‘error’ $y_n - t_n$ times the feature vector ϕ_n , where $y_n = \mathbf{w}^T \phi_n$. Similarly, for the combination of the logistic sigmoid activation function and the cross-entropy error function (4.90), and for the softmax activation function with the multiclass cross-entropy error function (4.108), we again obtain this same simple form. We now show that this is a general result of assuming a conditional distribution for the target variable from the exponential family, along with a corresponding choice for the activation function known as the *canonical link function*.

We again make use of the restricted form (4.84) of exponential family distributions. Note that here we are applying the assumption of exponential family distribution to the target variable t , in contrast to Section 4.2.4 where we applied it to the input vector \mathbf{x} . We therefore consider conditional distributions of the target variable of the form

$$p(t|\eta, s) = \frac{1}{s} h\left(\frac{t}{s}\right) g(\eta) \exp\left\{\frac{\eta t}{s}\right\}. \quad (4.118)$$

Using the same line of argument as led to the derivation of the result (2.226), we see that the conditional mean of t , which we denote by y , is given by

$$y \equiv \mathbb{E}[t|\eta] = -s \frac{d}{d\eta} \ln g(\eta). \quad (4.119)$$

Thus y and η must be related, and we denote this relation through $\eta = \psi(y)$.

Following Nelder and Wedderburn (1972), we define a *generalized linear model* to be one for which y is a nonlinear function of a linear combination of the input (or feature) variables so that

$$y = f(\mathbf{w}^T \boldsymbol{\phi}) \quad (4.120)$$

where $f(\cdot)$ is known as the *activation function* in the machine learning literature, and $f^{-1}(\cdot)$ is known as the *link function* in statistics.

Now consider the log likelihood function for this model, which, as a function of η , is given by

$$\ln p(\mathbf{t}|\eta, s) = \sum_{n=1}^N \ln p(t_n|\eta, s) = \sum_{n=1}^N \left\{ \ln g(\eta_n) + \frac{\eta_n t_n}{s} \right\} + \text{const} \quad (4.121)$$

where we are assuming that all observations share a common scale parameter (which corresponds to the noise variance for a Gaussian distribution for instance) and so s is independent of n . The derivative of the log likelihood with respect to the model parameters \mathbf{w} is then given by

$$\begin{aligned} \nabla_{\mathbf{w}} \ln p(\mathbf{t}|\eta, s) &= \sum_{n=1}^N \left\{ \frac{d}{d\eta_n} \ln g(\eta_n) + \frac{t_n}{s} \right\} \frac{d\eta_n}{dy_n} \frac{dy_n}{da_n} \nabla a_n \\ &= \sum_{n=1}^N \frac{1}{s} \{t_n - y_n\} \psi'(y_n) f'(a_n) \boldsymbol{\phi}_n \end{aligned} \quad (4.122)$$

where $a_n = \mathbf{w}^T \boldsymbol{\phi}_n$, and we have used $y_n = f(a_n)$ together with the result (4.119) for $\mathbb{E}[t|\eta]$. We now see that there is a considerable simplification if we choose a particular form for the link function $f^{-1}(y)$ given by

$$f^{-1}(y) = \psi(y) \quad (4.123)$$

which gives $f(\psi(y)) = y$ and hence $f'(\psi)\psi'(y) = 1$. Also, because $a = f^{-1}(y)$, we have $a = \psi$ and hence $f'(a)\psi'(y) = 1$. In this case, the gradient of the error function reduces to

$$\nabla \ln E(\mathbf{w}) = \frac{1}{s} \sum_{n=1}^N \{y_n - t_n\} \boldsymbol{\phi}_n. \quad (4.124)$$

For the Gaussian $s = \beta^{-1}$, whereas for the logistic model $s = 1$.

4.4. The Laplace Approximation

In Section 4.5 we shall discuss the Bayesian treatment of logistic regression. As we shall see, this is more complex than the Bayesian treatment of linear regression models, discussed in Sections 3.3 and 3.5. In particular, we cannot integrate exactly

over the parameter vector \mathbf{w} since the posterior distribution is no longer Gaussian. It is therefore necessary to introduce some form of approximation. Later in the book we shall consider a range of techniques based on analytical approximations and numerical sampling.

Here we introduce a simple, but widely used, framework called the Laplace approximation, that aims to find a Gaussian approximation to a probability density defined over a set of continuous variables. Consider first the case of a single continuous variable z , and suppose the distribution $p(z)$ is defined by

$$p(z) = \frac{1}{Z} f(z) \quad (4.125)$$

where $Z = \int f(z) dz$ is the normalization coefficient. We shall suppose that the value of Z is unknown. In the Laplace method the goal is to find a Gaussian approximation $q(z)$ which is centred on a mode of the distribution $p(z)$. The first step is to find a mode of $p(z)$, in other words a point z_0 such that $p'(z_0) = 0$, or equivalently

$$\left. \frac{df(z)}{dz} \right|_{z=z_0} = 0. \quad (4.126)$$

A Gaussian distribution has the property that its logarithm is a quadratic function of the variables. We therefore consider a Taylor expansion of $\ln f(z)$ centred on the mode z_0 so that

$$\ln f(z) \simeq \ln f(z_0) - \frac{1}{2} A(z - z_0)^2 \quad (4.127)$$

where

$$A = -\left. \frac{d^2}{dz^2} \ln f(z) \right|_{z=z_0}. \quad (4.128)$$

Note that the first-order term in the Taylor expansion does not appear since z_0 is a local maximum of the distribution. Taking the exponential we obtain

$$f(z) \simeq f(z_0) \exp \left\{ -\frac{A}{2}(z - z_0)^2 \right\}. \quad (4.129)$$

We can then obtain a normalized distribution $q(z)$ by making use of the standard result for the normalization of a Gaussian, so that

$$q(z) = \left(\frac{A}{2\pi} \right)^{1/2} \exp \left\{ -\frac{A}{2}(z - z_0)^2 \right\}. \quad (4.130)$$

The Laplace approximation is illustrated in Figure 4.14. Note that the Gaussian approximation will only be well defined if its precision $A > 0$, in other words the stationary point z_0 must be a local maximum, so that the second derivative of $f(z)$ at the point z_0 is negative.



Figure 4.14 Illustration of the Laplace approximation applied to the distribution $p(z) \propto \exp(-z^2/2)\sigma(20z + 4)$ where $\sigma(z)$ is the logistic sigmoid function defined by $\sigma(z) = (1 + e^{-z})^{-1}$. The left plot shows the normalized distribution $p(z)$ in yellow, together with the Laplace approximation centred on the mode z_0 of $p(z)$ in red. The right plot shows the negative logarithms of the corresponding curves.

We can extend the Laplace method to approximate a distribution $p(\mathbf{z}) = f(\mathbf{z})/Z$ defined over an M -dimensional space \mathbf{z} . At a stationary point \mathbf{z}_0 the gradient $\nabla f(\mathbf{z})$ will vanish. Expanding around this stationary point we have

$$\ln f(\mathbf{z}) \simeq \ln f(\mathbf{z}_0) - \frac{1}{2}(\mathbf{z} - \mathbf{z}_0)^T \mathbf{A}(\mathbf{z} - \mathbf{z}_0) \quad (4.131)$$

where the $M \times M$ Hessian matrix \mathbf{A} is defined by

$$\mathbf{A} = -\nabla\nabla \ln f(\mathbf{z})|_{\mathbf{z}=\mathbf{z}_0} \quad (4.132)$$

and ∇ is the gradient operator. Taking the exponential of both sides we obtain

$$f(\mathbf{z}) \simeq f(\mathbf{z}_0) \exp \left\{ -\frac{1}{2}(\mathbf{z} - \mathbf{z}_0)^T \mathbf{A}(\mathbf{z} - \mathbf{z}_0) \right\}. \quad (4.133)$$

The distribution $q(\mathbf{z})$ is proportional to $f(\mathbf{z})$ and the appropriate normalization coefficient can be found by inspection, using the standard result (2.43) for a normalized multivariate Gaussian, giving

$$q(\mathbf{z}) = \frac{|\mathbf{A}|^{1/2}}{(2\pi)^{M/2}} \exp \left\{ -\frac{1}{2}(\mathbf{z} - \mathbf{z}_0)^T \mathbf{A}(\mathbf{z} - \mathbf{z}_0) \right\} = \mathcal{N}(\mathbf{z} | \mathbf{z}_0, \mathbf{A}^{-1}) \quad (4.134)$$

where $|\mathbf{A}|$ denotes the determinant of \mathbf{A} . This Gaussian distribution will be well defined provided its precision matrix, given by \mathbf{A} , is positive definite, which implies that the stationary point \mathbf{z}_0 must be a local maximum, not a minimum or a saddle point.

In order to apply the Laplace approximation we first need to find the mode \mathbf{z}_0 , and then evaluate the Hessian matrix at that mode. In practice a mode will typically be found by running some form of numerical optimization algorithm (Bishop

and Nabney, 2008). Many of the distributions encountered in practice will be multimodal and so there will be different Laplace approximations according to which mode is being considered. Note that the normalization constant Z of the true distribution does not need to be known in order to apply the Laplace method. As a result of the central limit theorem, the posterior distribution for a model is expected to become increasingly better approximated by a Gaussian as the number of observed data points is increased, and so we would expect the Laplace approximation to be most useful in situations where the number of data points is relatively large.

One major weakness of the Laplace approximation is that, since it is based on a Gaussian distribution, it is only directly applicable to real variables. In other cases it may be possible to apply the Laplace approximation to a transformation of the variable. For instance if $0 \leq \tau < \infty$ then we can consider a Laplace approximation of $\ln \tau$. The most serious limitation of the Laplace framework, however, is that it is based purely on the aspects of the true distribution at a specific value of the variable, and so can fail to capture important global properties. In Chapter 10 we shall consider alternative approaches which adopt a more global perspective.

4.4.1 Model comparison and BIC

As well as approximating the distribution $p(\mathbf{z})$ we can also obtain an approximation to the normalization constant Z . Using the approximation (4.133) we have

$$\begin{aligned} Z &= \int f(\mathbf{z}) d\mathbf{z} \\ &\simeq f(\mathbf{z}_0) \int \exp \left\{ -\frac{1}{2} (\mathbf{z} - \mathbf{z}_0)^T \mathbf{A} (\mathbf{z} - \mathbf{z}_0) \right\} d\mathbf{z} \\ &= f(\mathbf{z}_0) \frac{(2\pi)^{M/2}}{|\mathbf{A}|^{1/2}} \end{aligned} \quad (4.135)$$

where we have noted that the integrand is Gaussian and made use of the standard result (2.43) for a normalized Gaussian distribution. We can use the result (4.135) to obtain an approximation to the model evidence which, as discussed in Section 3.4, plays a central role in Bayesian model comparison.

Consider a data set \mathcal{D} and a set of models $\{\mathcal{M}_i\}$ having parameters $\{\boldsymbol{\theta}_i\}$. For each model we define a likelihood function $p(\mathcal{D}|\boldsymbol{\theta}_i, \mathcal{M}_i)$. If we introduce a prior $p(\boldsymbol{\theta}_i|\mathcal{M}_i)$ over the parameters, then we are interested in computing the model evidence $p(\mathcal{D}|\mathcal{M}_i)$ for the various models. From now on we omit the conditioning on \mathcal{M}_i to keep the notation uncluttered. From Bayes' theorem the model evidence is given by

$$p(\mathcal{D}) = \int p(\mathcal{D}|\boldsymbol{\theta}) p(\boldsymbol{\theta}) d\boldsymbol{\theta}. \quad (4.136)$$

Identifying $f(\boldsymbol{\theta}) = p(\mathcal{D}|\boldsymbol{\theta})p(\boldsymbol{\theta})$ and $Z = p(\mathcal{D})$, and applying the result (4.135), we obtain

$$\ln p(\mathcal{D}) \simeq \ln p(\mathcal{D}|\boldsymbol{\theta}_{\text{MAP}}) + \underbrace{\ln p(\boldsymbol{\theta}_{\text{MAP}}) + \frac{M}{2} \ln(2\pi) - \frac{1}{2} \ln |\mathbf{A}|}_{\text{Occam factor}} \quad (4.137)$$

Exercise 4.22

where $\boldsymbol{\theta}_{\text{MAP}}$ is the value of $\boldsymbol{\theta}$ at the mode of the posterior distribution, and \mathbf{A} is the *Hessian* matrix of second derivatives of the negative log posterior

$$\mathbf{A} = -\nabla\nabla \ln p(\mathcal{D}|\boldsymbol{\theta}_{\text{MAP}})p(\boldsymbol{\theta}_{\text{MAP}}) = -\nabla\nabla \ln p(\boldsymbol{\theta}_{\text{MAP}}|\mathcal{D}). \quad (4.138)$$

The first term on the right hand side of (4.137) represents the log likelihood evaluated using the optimized parameters, while the remaining three terms comprise the ‘Occam factor’ which penalizes model complexity.

If we assume that the Gaussian prior distribution over parameters is broad, and that the Hessian has full rank, then we can approximate (4.137) very roughly using

$$\ln p(\mathcal{D}) \simeq \ln p(\mathcal{D}|\boldsymbol{\theta}_{\text{MAP}}) - \frac{1}{2}M \ln N \quad (4.139)$$

where N is the number of data points, M is the number of parameters in $\boldsymbol{\theta}$ and we have omitted additive constants. This is known as the *Bayesian Information Criterion* (BIC) or the *Schwarz criterion* (Schwarz, 1978). Note that, compared to AIC given by (1.73), this penalizes model complexity more heavily.

Complexity measures such as AIC and BIC have the virtue of being easy to evaluate, but can also give misleading results. In particular, the assumption that the Hessian matrix has full rank is often not valid since many of the parameters are not ‘well-determined’. We can use the result (4.137) to obtain a more accurate estimate of the model evidence starting from the Laplace approximation, as we illustrate in the context of neural networks in Section 5.7.

Section 3.5.3

4.5. Bayesian Logistic Regression

We now turn to a Bayesian treatment of logistic regression. Exact Bayesian inference for logistic regression is intractable. In particular, evaluation of the posterior distribution would require normalization of the product of a prior distribution and a likelihood function that itself comprises a product of logistic sigmoid functions, one for every data point. Evaluation of the predictive distribution is similarly intractable. Here we consider the application of the Laplace approximation to the problem of Bayesian logistic regression (Spiegelhalter and Lauritzen, 1990; MacKay, 1992b).

4.5.1 Laplace approximation

Recall from Section 4.4 that the Laplace approximation is obtained by finding the mode of the posterior distribution and then fitting a Gaussian centred at that mode. This requires evaluation of the second derivatives of the log posterior, which is equivalent to finding the Hessian matrix.

Because we seek a Gaussian representation for the posterior distribution, it is natural to begin with a Gaussian prior, which we write in the general form

$$p(\mathbf{w}) = \mathcal{N}(\mathbf{w}|\mathbf{m}_0, \mathbf{S}_0) \quad (4.140)$$

where \mathbf{m}_0 and \mathbf{S}_0 are fixed hyperparameters. The posterior distribution over \mathbf{w} is given by

$$p(\mathbf{w}|\mathbf{t}) \propto p(\mathbf{w})p(\mathbf{t}|\mathbf{w}) \quad (4.141)$$

where $\mathbf{t} = (t_1, \dots, t_N)^T$. Taking the log of both sides, and substituting for the prior distribution using (4.140), and for the likelihood function using (4.89), we obtain

$$\begin{aligned} \ln p(\mathbf{w}|\mathbf{t}) &= -\frac{1}{2}(\mathbf{w} - \mathbf{m}_0)^T \mathbf{S}_0^{-1} (\mathbf{w} - \mathbf{m}_0) \\ &\quad + \sum_{n=1}^N \{t_n \ln y_n + (1 - t_n) \ln(1 - y_n)\} + \text{const} \end{aligned} \quad (4.142)$$

where $y_n = \sigma(\mathbf{w}^T \phi_n)$. To obtain a Gaussian approximation to the posterior distribution, we first maximize the posterior distribution to give the MAP (maximum posterior) solution \mathbf{w}_{MAP} , which defines the mean of the Gaussian. The covariance is then given by the inverse of the matrix of second derivatives of the negative log likelihood, which takes the form

$$\mathbf{S}_N = -\nabla \nabla \ln p(\mathbf{w}|\mathbf{t}) = \mathbf{S}_0^{-1} + \sum_{n=1}^N y_n(1 - y_n) \phi_n \phi_n^T. \quad (4.143)$$

The Gaussian approximation to the posterior distribution therefore takes the form

$$q(\mathbf{w}) = \mathcal{N}(\mathbf{w}|\mathbf{w}_{\text{MAP}}, \mathbf{S}_N). \quad (4.144)$$

Having obtained a Gaussian approximation to the posterior distribution, there remains the task of marginalizing with respect to this distribution in order to make predictions.

4.5.2 Predictive distribution

The predictive distribution for class \mathcal{C}_1 , given a new feature vector $\phi(\mathbf{x})$, is obtained by marginalizing with respect to the posterior distribution $p(\mathbf{w}|\mathbf{t})$, which is itself approximated by a Gaussian distribution $q(\mathbf{w})$ so that

$$p(\mathcal{C}_1|\phi, \mathbf{t}) = \int p(\mathcal{C}_1|\phi, \mathbf{w}) p(\mathbf{w}|\mathbf{t}) d\mathbf{w} \simeq \int \sigma(\mathbf{w}^T \phi) q(\mathbf{w}) d\mathbf{w} \quad (4.145)$$

with the corresponding probability for class \mathcal{C}_2 given by $p(\mathcal{C}_2|\phi, \mathbf{t}) = 1 - p(\mathcal{C}_1|\phi, \mathbf{t})$. To evaluate the predictive distribution, we first note that the function $\sigma(\mathbf{w}^T \phi)$ depends on \mathbf{w} only through its projection onto ϕ . Denoting $a = \mathbf{w}^T \phi$, we have

$$\sigma(\mathbf{w}^T \phi) = \int \delta(a - \mathbf{w}^T \phi) \sigma(a) da \quad (4.146)$$

where $\delta(\cdot)$ is the Dirac delta function. From this we obtain

$$\int \sigma(\mathbf{w}^T \phi) q(\mathbf{w}) d\mathbf{w} = \int \sigma(a) p(a) da \quad (4.147)$$

where

$$p(a) = \int \delta(a - \mathbf{w}^T \boldsymbol{\phi}) q(\mathbf{w}) d\mathbf{w}. \quad (4.148)$$

We can evaluate $p(a)$ by noting that the delta function imposes a linear constraint on \mathbf{w} and so forms a marginal distribution from the joint distribution $q(\mathbf{w})$ by integrating out all directions orthogonal to $\boldsymbol{\phi}$. Because $q(\mathbf{w})$ is Gaussian, we know from Section 2.3.2 that the marginal distribution will also be Gaussian. We can evaluate the mean and covariance of this distribution by taking moments, and interchanging the order of integration over a and \mathbf{w} , so that

$$\mu_a = \mathbb{E}[a] = \int p(a) a da = \int q(\mathbf{w}) \mathbf{w}^T \boldsymbol{\phi} d\mathbf{w} = \mathbf{w}_{\text{MAP}}^T \boldsymbol{\phi} \quad (4.149)$$

where we have used the result (4.144) for the variational posterior distribution $q(\mathbf{w})$. Similarly

$$\begin{aligned} \sigma_a^2 &= \text{var}[a] = \int p(a) \{a^2 - \mathbb{E}[a]^2\} da \\ &= \int q(\mathbf{w}) \{(\mathbf{w}^T \boldsymbol{\phi})^2 - (\mathbf{m}_N^T \boldsymbol{\phi})^2\} d\mathbf{w} = \boldsymbol{\phi}^T \mathbf{S}_N \boldsymbol{\phi}. \end{aligned} \quad (4.150)$$

Note that the distribution of a takes the same form as the predictive distribution (3.58) for the linear regression model, with the noise variance set to zero. Thus our variational approximation to the predictive distribution becomes

$$p(\mathcal{C}_1 | \mathbf{t}) = \int \sigma(a) p(a) da = \int \sigma(a) \mathcal{N}(a | \mu_a, \sigma_a^2) da. \quad (4.151)$$

This result can also be derived directly by making use of the results for the marginal of a Gaussian distribution given in Section 2.3.2.

Exercise 4.24

The integral over a represents the convolution of a Gaussian with a logistic sigmoid, and cannot be evaluated analytically. We can, however, obtain a good approximation (Spiegelhalter and Lauritzen, 1990; MacKay, 1992b; Barber and Bishop, 1998a) by making use of the close similarity between the logistic sigmoid function $\sigma(a)$ defined by (4.59) and the probit function $\Phi(a)$ defined by (4.114). In order to obtain the best approximation to the logistic function we need to re-scale the horizontal axis, so that we approximate $\sigma(a)$ by $\Phi(\lambda a)$. We can find a suitable value of λ by requiring that the two functions have the same slope at the origin, which gives $\lambda^2 = \pi/8$. The similarity of the logistic sigmoid and the probit function, for this choice of λ , is illustrated in Figure 4.9.

Exercise 4.25

The advantage of using a probit function is that its convolution with a Gaussian can be expressed analytically in terms of another probit function. Specifically we can show that

$$\int \Phi(\lambda a) \mathcal{N}(a | \mu, \sigma^2) da = \Phi\left(\frac{\mu}{(\lambda^{-2} + \sigma^2)^{1/2}}\right). \quad (4.152)$$

Exercise 4.26

We now apply the approximation $\sigma(a) \simeq \Phi(\lambda a)$ to the probit functions appearing on both sides of this equation, leading to the following approximation for the convolution of a logistic sigmoid with a Gaussian

$$\int \sigma(a)\mathcal{N}(a|\mu, \sigma^2) da \simeq \sigma(\kappa(\sigma^2)\mu) \quad (4.153)$$

where we have defined

$$\kappa(\sigma^2) = (1 + \pi\sigma^2/8)^{-1/2}. \quad (4.154)$$

Applying this result to (4.151) we obtain the approximate predictive distribution in the form

$$p(C_1|\phi, \mathbf{t}) = \sigma(\kappa(\sigma_a^2)\mu_a) \quad (4.155)$$

where μ_a and σ_a^2 are defined by (4.149) and (4.150), respectively, and $\kappa(\sigma_a^2)$ is defined by (4.154).

Note that the decision boundary corresponding to $p(C_1|\phi, \mathbf{t}) = 0.5$ is given by $\mu_a = 0$, which is the same as the decision boundary obtained by using the MAP value for \mathbf{w} . Thus if the decision criterion is based on minimizing misclassification rate, with equal prior probabilities, then the marginalization over \mathbf{w} has no effect. However, for more complex decision criteria it will play an important role. Marginalization of the logistic sigmoid model under a Gaussian approximation to the posterior distribution will be illustrated in the context of variational inference in Figure 10.13.

Exercises

- 4.1** (**) Given a set of data points $\{\mathbf{x}_n\}$, we can define the *convex hull* to be the set of all points \mathbf{x} given by

$$\mathbf{x} = \sum_n \alpha_n \mathbf{x}_n \quad (4.156)$$

where $\alpha_n \geq 0$ and $\sum_n \alpha_n = 1$. Consider a second set of points $\{\mathbf{y}_n\}$ together with their corresponding convex hull. By definition, the two sets of points will be linearly separable if there exists a vector $\hat{\mathbf{w}}$ and a scalar w_0 such that $\hat{\mathbf{w}}^T \mathbf{x}_n + w_0 > 0$ for all \mathbf{x}_n , and $\hat{\mathbf{w}}^T \mathbf{y}_n + w_0 < 0$ for all \mathbf{y}_n . Show that if their convex hulls intersect, the two sets of points cannot be linearly separable, and conversely that if they are linearly separable, their convex hulls do not intersect.

- 4.2** (**) **www** Consider the minimization of a sum-of-squares error function (4.15), and suppose that all of the target vectors in the training set satisfy a linear constraint

$$\mathbf{a}^T \mathbf{t}_n + b = 0 \quad (4.157)$$

where \mathbf{t}_n corresponds to the n^{th} row of the matrix \mathbf{T} in (4.15). Show that as a consequence of this constraint, the elements of the model prediction $\mathbf{y}(\mathbf{x})$ given by the least-squares solution (4.17) also satisfy this constraint, so that

$$\mathbf{a}^T \mathbf{y}(\mathbf{x}) + b = 0. \quad (4.158)$$

To do so, assume that one of the basis functions $\phi_0(\mathbf{x}) = 1$ so that the corresponding parameter w_0 plays the role of a bias.

- 4.3** (**) Extend the result of Exercise 4.2 to show that if multiple linear constraints are satisfied simultaneously by the target vectors, then the same constraints will also be satisfied by the least-squares prediction of a linear model.
- 4.4** (*) **www** Show that maximization of the class separation criterion given by (4.23) with respect to \mathbf{w} , using a Lagrange multiplier to enforce the constraint $\mathbf{w}^T \mathbf{w} = 1$, leads to the result that $\mathbf{w} \propto (\mathbf{m}_2 - \mathbf{m}_1)$.
- 4.5** (*) By making use of (4.20), (4.23), and (4.24), show that the Fisher criterion (4.25) can be written in the form (4.26).
- 4.6** (*) Using the definitions of the between-class and within-class covariance matrices given by (4.27) and (4.28), respectively, together with (4.34) and (4.36) and the choice of target values described in Section 4.1.5, show that the expression (4.33) that minimizes the sum-of-squares error function can be written in the form (4.37).
- 4.7** (*) **www** Show that the logistic sigmoid function (4.59) satisfies the property $\sigma(-a) = 1 - \sigma(a)$ and that its inverse is given by $\sigma^{-1}(y) = \ln\{y/(1-y)\}$.
- 4.8** (*) Using (4.57) and (4.58), derive the result (4.65) for the posterior class probability in the two-class generative model with Gaussian densities, and verify the results (4.66) and (4.67) for the parameters \mathbf{w} and w_0 .
- 4.9** (*) **www** Consider a generative classification model for K classes defined by prior class probabilities $p(\mathcal{C}_k) = \pi_k$ and general class-conditional densities $p(\phi|\mathcal{C}_k)$ where ϕ is the input feature vector. Suppose we are given a training data set $\{\phi_n, \mathbf{t}_n\}$ where $n = 1, \dots, N$, and \mathbf{t}_n is a binary target vector of length K that uses the 1-of- K coding scheme, so that it has components $t_{nj} = I_{jk}$ if pattern n is from class \mathcal{C}_k . Assuming that the data points are drawn independently from this model, show that the maximum-likelihood solution for the prior probabilities is given by

$$\pi_k = \frac{N_k}{N} \quad (4.159)$$

where N_k is the number of data points assigned to class \mathcal{C}_k .

- 4.10** (**) Consider the classification model of Exercise 4.9 and now suppose that the class-conditional densities are given by Gaussian distributions with a shared covariance matrix, so that

$$p(\phi|\mathcal{C}_k) = \mathcal{N}(\phi|\boldsymbol{\mu}_k, \boldsymbol{\Sigma}). \quad (4.160)$$

Show that the maximum likelihood solution for the mean of the Gaussian distribution for class \mathcal{C}_k is given by

$$\boldsymbol{\mu}_k = \frac{1}{N_k} \sum_{n=1}^{N_k} t_{nk} \phi_n \quad (4.161)$$

which represents the mean of those feature vectors assigned to class \mathcal{C}_k . Similarly, show that the maximum likelihood solution for the shared covariance matrix is given by

$$\Sigma = \sum_{k=1}^K \frac{N_k}{N} \mathbf{S}_k \quad (4.162)$$

where

$$\mathbf{S}_k = \frac{1}{N_k} \sum_{n=1}^N t_{nk} (\phi_n - \mu_k)(\phi_n - \mu_k)^T. \quad (4.163)$$

Thus Σ is given by a weighted average of the covariances of the data associated with each class, in which the weighting coefficients are given by the prior probabilities of the classes.

- 4.11** (★) Consider a classification problem with K classes for which the feature vector ϕ has M components each of which can take L discrete states. Let the values of the components be represented by a 1-of- L binary coding scheme. Further suppose that, conditioned on the class \mathcal{C}_k , the M components of ϕ are independent, so that the class-conditional density factorizes with respect to the feature vector components. Show that the quantities a_k given by (4.63), which appear in the argument to the softmax function describing the posterior class probabilities, are linear functions of the components of ϕ . Note that this represents an example of the naive Bayes model which is discussed in Section 8.2.2.
- 4.12** (★) **www** Verify the relation (4.88) for the derivative of the logistic sigmoid function defined by (4.59).
- 4.13** (★) **www** By making use of the result (4.88) for the derivative of the logistic sigmoid, show that the derivative of the error function (4.90) for the logistic regression model is given by (4.91).
- 4.14** (★) Show that for a linearly separable data set, the maximum likelihood solution for the logistic regression model is obtained by finding a vector w whose decision boundary $w^T \phi(x) = 0$ separates the classes and then taking the magnitude of w to infinity.
- 4.15** (★) Show that the Hessian matrix H for the logistic regression model, given by (4.97), is positive definite. Here R is a diagonal matrix with elements $y_n(1 - y_n)$, and y_n is the output of the logistic regression model for input vector x_n . Hence show that the error function is a concave function of w and that it has a unique minimum.
- 4.16** (★) Consider a binary classification problem in which each observation x_n is known to belong to one of two classes, corresponding to $t = 0$ and $t = 1$, and suppose that the procedure for collecting training data is imperfect, so that training points are sometimes mislabelled. For every data point x_n , instead of having a value t for the class label, we have instead a value π_n representing the probability that $t_n = 1$. Given a probabilistic model $p(t = 1|\phi)$, write down the log likelihood function appropriate to such a data set.

- 4.17** (★) **www** Show that the derivatives of the softmax activation function (4.104), where the a_k are defined by (4.105), are given by (4.106).
- 4.18** (★) Using the result (4.91) for the derivatives of the softmax activation function, show that the gradients of the cross-entropy error (4.108) are given by (4.109).
- 4.19** (★) **www** Write down expressions for the gradient of the log likelihood, as well as the corresponding Hessian matrix, for the probit regression model defined in Section 4.3.5. These are the quantities that would be required to train such a model using IRLS.
- 4.20** (★★) Show that the Hessian matrix for the multiclass logistic regression problem, defined by (4.110), is positive semidefinite. Note that the full Hessian matrix for this problem is of size $MK \times MK$, where M is the number of parameters and K is the number of classes. To prove the positive semidefinite property, consider the product $\mathbf{u}^T \mathbf{H} \mathbf{u}$ where \mathbf{u} is an arbitrary vector of length MK , and then apply Jensen's inequality.
- 4.21** (★) Show that the probit function (4.114) and the erf function (4.115) are related by (4.116).
- 4.22** (★) Using the result (4.135), derive the expression (4.137) for the log model evidence under the Laplace approximation.
- 4.23** (★★) **www** In this exercise, we derive the BIC result (4.139) starting from the Laplace approximation to the model evidence given by (4.137). Show that if the prior over parameters is Gaussian of the form $p(\boldsymbol{\theta}) = \mathcal{N}(\boldsymbol{\theta} | \mathbf{m}, \mathbf{V}_0)$, the log model evidence under the Laplace approximation takes the form

$$\ln p(\mathcal{D}) \simeq \ln p(\mathcal{D} | \boldsymbol{\theta}_{\text{MAP}}) - \frac{1}{2} (\boldsymbol{\theta}_{\text{MAP}} - \mathbf{m})^T \mathbf{V}_0^{-1} (\boldsymbol{\theta}_{\text{MAP}} - \mathbf{m}) - \frac{1}{2} \ln |\mathbf{H}| + \text{const}$$

where \mathbf{H} is the matrix of second derivatives of the log likelihood $\ln p(\mathcal{D} | \boldsymbol{\theta})$ evaluated at $\boldsymbol{\theta}_{\text{MAP}}$. Now assume that the prior is broad so that \mathbf{V}_0^{-1} is small and the second term on the right-hand side above can be neglected. Furthermore, consider the case of independent, identically distributed data so that \mathbf{H} is the sum of terms one for each data point. Show that the log model evidence can then be written approximately in the form of the BIC expression (4.139).

- 4.24** (★★) Use the results from Section 2.3.2 to derive the result (4.151) for the marginalization of the logistic regression model with respect to a Gaussian posterior distribution over the parameters \mathbf{w} .
- 4.25** (★★) Suppose we wish to approximate the logistic sigmoid $\sigma(a)$ defined by (4.59) by a scaled probit function $\Phi(\lambda a)$, where $\Phi(a)$ is defined by (4.114). Show that if λ is chosen so that the derivatives of the two functions are equal at $a = 0$, then $\lambda^2 = \pi/8$.

4.26 (**) In this exercise, we prove the relation (4.152) for the convolution of a probit function with a Gaussian distribution. To do this, show that the derivative of the left-hand side with respect to μ is equal to the derivative of the right-hand side, and then integrate both sides with respect to μ and then show that the constant of integration vanishes. Note that before differentiating the left-hand side, it is convenient first to introduce a change of variable given by $a = \mu + \sigma z$ so that the integral over a is replaced by an integral over z . When we differentiate the left-hand side of the relation (4.152), we will then obtain a Gaussian integral over z that can be evaluated analytically.

5

Neural Networks



In Chapters 3 and 4 we considered models for regression and classification that comprised linear combinations of fixed basis functions. We saw that such models have useful analytical and computational properties but that their practical applicability was limited by the curse of dimensionality. In order to apply such models to large-scale problems, it is necessary to adapt the basis functions to the data.

Support vector machines (SVMs), discussed in Chapter 7, address this by first defining basis functions that are centred on the training data points and then selecting a subset of these during training. One advantage of SVMs is that, although the training involves nonlinear optimization, the objective function is convex, and so the solution of the optimization problem is relatively straightforward. The number of basis functions in the resulting models is generally much smaller than the number of training points, although it is often still relatively large and typically increases with the size of the training set. The relevance vector machine, discussed in Section 7.2, also chooses a subset from a fixed set of basis functions and typically results in much

sparser models. Unlike the SVM it also produces probabilistic outputs, although this is at the expense of a nonconvex optimization during training.

An alternative approach is to fix the number of basis functions in advance but allow them to be adaptive, in other words to use parametric forms for the basis functions in which the parameter values are adapted during training. The most successful model of this type in the context of pattern recognition is the feed-forward neural network, also known as the *multilayer perceptron*, discussed in this chapter. In fact, ‘multilayer perceptron’ is really a misnomer, because the model comprises multiple layers of logistic regression models (with continuous nonlinearities) rather than multiple perceptrons (with discontinuous nonlinearities). For many applications, the resulting model can be significantly more compact, and hence faster to evaluate, than a support vector machine having the same generalization performance. The price to be paid for this compactness, as with the relevance vector machine, is that the likelihood function, which forms the basis for network training, is no longer a convex function of the model parameters. In practice, however, it is often worth investing substantial computational resources during the training phase in order to obtain a compact model that is fast at processing new data.

The term ‘neural network’ has its origins in attempts to find mathematical representations of information processing in biological systems (McCulloch and Pitts, 1943; Widrow and Hoff, 1960; Rosenblatt, 1962; Rumelhart *et al.*, 1986). Indeed, it has been used very broadly to cover a wide range of different models, many of which have been the subject of exaggerated claims regarding their biological plausibility. From the perspective of practical applications of pattern recognition, however, biological realism would impose entirely unnecessary constraints. Our focus in this chapter is therefore on neural networks as efficient models for statistical pattern recognition. In particular, we shall restrict our attention to the specific class of neural networks that have proven to be of greatest practical value, namely the multilayer perceptron.

We begin by considering the functional form of the network model, including the specific parameterization of the basis functions, and we then discuss the problem of determining the network parameters within a maximum likelihood framework, which involves the solution of a nonlinear optimization problem. This requires the evaluation of derivatives of the log likelihood function with respect to the network parameters, and we shall see how these can be obtained efficiently using the technique of *error backpropagation*. We shall also show how the backpropagation framework can be extended to allow other derivatives to be evaluated, such as the Jacobian and Hessian matrices. Next we discuss various approaches to regularization of neural network training and the relationships between them. We also consider some extensions to the neural network model, and in particular we describe a general framework for modelling conditional probability distributions known as *mixture density networks*. Finally, we discuss the use of Bayesian treatments of neural networks. Additional background on neural network models can be found in Bishop (1995a).

5.1. Feed-forward Network Functions

The linear models for regression and classification discussed in Chapters 3 and 4, respectively, are based on linear combinations of fixed nonlinear basis functions $\phi_j(\mathbf{x})$ and take the form

$$y(\mathbf{x}, \mathbf{w}) = f \left(\sum_{j=1}^M w_j \phi_j(\mathbf{x}) \right) \quad (5.1)$$

where $f(\cdot)$ is a nonlinear activation function in the case of classification and is the identity in the case of regression. Our goal is to extend this model by making the basis functions $\phi_j(\mathbf{x})$ depend on parameters and then to allow these parameters to be adjusted, along with the coefficients $\{w_j\}$, during training. There are, of course, many ways to construct parametric nonlinear basis functions. Neural networks use basis functions that follow the same form as (5.1), so that each basis function is itself a nonlinear function of a linear combination of the inputs, where the coefficients in the linear combination are adaptive parameters.

This leads to the basic neural network model, which can be described a series of functional transformations. First we construct M linear combinations of the input variables x_1, \dots, x_D in the form

$$a_j = \sum_{i=1}^D w_{ji}^{(1)} x_i + w_{j0}^{(1)} \quad (5.2)$$

where $j = 1, \dots, M$, and the superscript (1) indicates that the corresponding parameters are in the first ‘layer’ of the network. We shall refer to the parameters $w_{ji}^{(1)}$ as *weights* and the parameters $w_{j0}^{(1)}$ as *biases*, following the nomenclature of Chapter 3. The quantities a_j are known as *activations*. Each of them is then transformed using a differentiable, nonlinear *activation function* $h(\cdot)$ to give

$$z_j = h(a_j). \quad (5.3)$$

These quantities correspond to the outputs of the basis functions in (5.1) that, in the context of neural networks, are called *hidden units*. The nonlinear functions $h(\cdot)$ are generally chosen to be sigmoidal functions such as the logistic sigmoid or the ‘tanh’ function. Following (5.1), these values are again linearly combined to give *output unit activations*

$$a_k = \sum_{j=1}^M w_{kj}^{(2)} z_j + w_{k0}^{(2)} \quad (5.4)$$

where $k = 1, \dots, K$, and K is the total number of outputs. This transformation corresponds to the second layer of the network, and again the $w_{k0}^{(2)}$ are bias parameters. Finally, the output unit activations are transformed using an appropriate activation function to give a set of network outputs y_k . The choice of activation function is determined by the nature of the data and the assumed distribution of target variables

Exercise 5.1

Figure 5.1 Network diagram for the two-layer neural network corresponding to (5.7). The input, hidden, and output variables are represented by nodes, and the weight parameters are represented by links between the nodes, in which the bias parameters are denoted by links coming from additional input and hidden variables x_0 and z_0 . Arrows denote the direction of information flow through the network during forward propagation.



and follows the same considerations as for linear models discussed in Chapters 3 and 4. Thus for standard regression problems, the activation function is the identity so that $y_k = a_k$. Similarly, for multiple binary classification problems, each output unit activation is transformed using a logistic sigmoid function so that

$$y_k = \sigma(a_k) \quad (5.5)$$

where

$$\sigma(a) = \frac{1}{1 + \exp(-a)}. \quad (5.6)$$

Finally, for multiclass problems, a softmax activation function of the form (4.62) is used. The choice of output unit activation function is discussed in detail in Section 5.2.

We can combine these various stages to give the overall network function that, for sigmoidal output unit activation functions, takes the form

$$y_k(\mathbf{x}, \mathbf{w}) = \sigma \left(\sum_{j=1}^M w_{kj}^{(2)} h \left(\sum_{i=1}^D w_{ji}^{(1)} x_i + w_{j0}^{(1)} \right) + w_{k0}^{(2)} \right) \quad (5.7)$$

where the set of all weight and bias parameters have been grouped together into a vector \mathbf{w} . Thus the neural network model is simply a nonlinear function from a set of input variables $\{x_i\}$ to a set of output variables $\{y_k\}$ controlled by a vector \mathbf{w} of adjustable parameters.

This function can be represented in the form of a network diagram as shown in Figure 5.1. The process of evaluating (5.7) can then be interpreted as a *forward propagation* of information through the network. It should be emphasized that these diagrams do not represent probabilistic graphical models of the kind to be considered in Chapter 8 because the internal nodes represent deterministic variables rather than stochastic ones. For this reason, we have adopted a slightly different graphical

notation for the two kinds of model. We shall see later how to give a probabilistic interpretation to a neural network.

As discussed in Section 3.1, the bias parameters in (5.2) can be absorbed into the set of weight parameters by defining an additional input variable x_0 whose value is clamped at $x_0 = 1$, so that (5.2) takes the form

$$a_j = \sum_{i=0}^D w_{ji}^{(1)} x_i. \quad (5.8)$$

We can similarly absorb the second-layer biases into the second-layer weights, so that the overall network function becomes

$$y_k(\mathbf{x}, \mathbf{w}) = \sigma \left(\sum_{j=0}^M w_{kj}^{(2)} h \left(\sum_{i=0}^D w_{ji}^{(1)} x_i \right) \right). \quad (5.9)$$

As can be seen from Figure 5.1, the neural network model comprises two stages of processing, each of which resembles the perceptron model of Section 4.1.7, and for this reason the neural network is also known as the *multilayer perceptron*, or MLP. A key difference compared to the perceptron, however, is that the neural network uses continuous sigmoidal nonlinearities in the hidden units, whereas the perceptron uses step-function nonlinearities. This means that the neural network function is differentiable with respect to the network parameters, and this property will play a central role in network training.

If the activation functions of all the hidden units in a network are taken to be linear, then for any such network we can always find an equivalent network without hidden units. This follows from the fact that the composition of successive linear transformations is itself a linear transformation. However, if the number of hidden units is smaller than either the number of input or output units, then the transformations that the network can generate are not the most general possible linear transformations from inputs to outputs because information is lost in the dimensionality reduction at the hidden units. In Section 12.4.2, we show that networks of linear units give rise to principal component analysis. In general, however, there is little interest in multilayer networks of linear units.

The network architecture shown in Figure 5.1 is the most commonly used one in practice. However, it is easily generalized, for instance by considering additional layers of processing each consisting of a weighted linear combination of the form (5.4) followed by an element-wise transformation using a nonlinear activation function. Note that there is some confusion in the literature regarding the terminology for counting the number of layers in such networks. Thus the network in Figure 5.1 may be described as a 3-layer network (which counts the number of layers of units, and treats the inputs as units) or sometimes as a single-hidden-layer network (which counts the number of layers of hidden units). We recommend a terminology in which Figure 5.1 is called a two-layer network, because it is the number of layers of adaptive weights that is important for determining the network properties.

Another generalization of the network architecture is to include *skip-layer* connections, each of which is associated with a corresponding adaptive parameter. For

Figure 5.2 Example of a neural network having a general feed-forward topology. Note that each hidden and output unit has an associated bias parameter (omitted for clarity).



instance, in a two-layer network these would go directly from inputs to outputs. In principle, a network with sigmoidal hidden units can always mimic skip layer connections (for bounded input values) by using a sufficiently small first-layer weight that, over its operating range, the hidden unit is effectively linear, and then compensating with a large weight value from the hidden unit to the output. In practice, however, it may be advantageous to include skip-layer connections explicitly.

Furthermore, the network can be sparse, with not all possible connections within a layer being present. We shall see an example of a sparse network architecture when we consider convolutional neural networks in Section 5.5.6.

Because there is a direct correspondence between a network diagram and its mathematical function, we can develop more general network mappings by considering more complex network diagrams. However, these must be restricted to a *feed-forward* architecture, in other words to one having no closed directed cycles, to ensure that the outputs are deterministic functions of the inputs. This is illustrated with a simple example in Figure 5.2. Each (hidden or output) unit in such a network computes a function given by

$$z_k = h \left(\sum_i w_{kj} z_j \right) \quad (5.10)$$

where the sum runs over all units that send connections to unit k (and a bias parameter is included in the summation). For a given set of values applied to the inputs of the network, successive application of (5.10) allows the activations of all units in the network to be evaluated including those of the output units.

The approximation properties of feed-forward networks have been widely studied (Funahashi, 1989; Cybenko, 1989; Hornik *et al.*, 1989; Stinchcombe and White, 1989; Cotter, 1990; Ito, 1991; Hornik, 1991; Kreinovich, 1991; Ripley, 1996) and found to be very general. Neural networks are therefore said to be *universal approximators*. For example, a two-layer network with linear outputs can uniformly approximate any continuous function on a compact input domain to arbitrary accuracy provided the network has a sufficiently large number of hidden units. This result holds for a wide range of hidden unit activation functions, but excluding polynomials. Although such theorems are reassuring, the key problem is how to find suitable parameter values given a set of training data, and in later sections of this chapter we

Figure 5.3 Illustration of the capability of a multilayer perceptron to approximate four different functions comprising (a) $f(x) = x^2$, (b) $f(x) = \sin(x)$, (c), $f(x) = |x|$, and (d) $f(x) = H(x)$ where $H(x)$ is the Heaviside step function. In each case, $N = 50$ data points, shown as blue dots, have been sampled uniformly in x over the interval $(-1, 1)$ and the corresponding values of $f(x)$ evaluated. These data points are then used to train a two-layer network having 3 hidden units with ‘tanh’ activation functions and linear output units. The resulting network functions are shown by the red curves, and the outputs of the three hidden units are shown by the three dashed curves.



will show that there exist effective solutions to this problem based on both maximum likelihood and Bayesian approaches.

The capability of a two-layer network to model a broad range of functions is illustrated in Figure 5.3. This figure also shows how individual hidden units work collaboratively to approximate the final function. The role of hidden units in a simple classification problem is illustrated in Figure 5.4 using the synthetic classification data set described in Appendix A.

5.1.1 Weight-space symmetries

One property of feed-forward networks, which will play a role when we consider Bayesian model comparison, is that multiple distinct choices for the weight vector w can all give rise to the same mapping function from inputs to outputs (Chen *et al.*, 1993). Consider a two-layer network of the form shown in Figure 5.1 with M hidden units having ‘tanh’ activation functions and full connectivity in both layers. If we change the sign of all of the weights and the bias feeding into a particular hidden unit, then, for a given input pattern, the sign of the activation of the hidden unit will be reversed, because ‘tanh’ is an odd function, so that $\tanh(-a) = -\tanh(a)$. This transformation can be exactly compensated by changing the sign of all of the weights leading out of that hidden unit. Thus, by changing the signs of a particular group of weights (and a bias), the input–output mapping function represented by the network is unchanged, and so we have found two different weight vectors that give rise to the same mapping function. For M hidden units, there will be M such ‘sign-flip’

Figure 5.4 Example of the solution of a simple two-class classification problem involving synthetic data using a neural network having two inputs, two hidden units with ‘tanh’ activation functions, and a single output having a logistic sigmoid activation function. The dashed blue lines show the $z = 0.5$ contours for each of the hidden units, and the red line shows the $y = 0.5$ decision surface for the network. For comparison, the green line denotes the optimal decision boundary computed from the distributions used to generate the data.



symmetries, and thus any given weight vector will be one of a set 2^M equivalent weight vectors .

Similarly, imagine that we interchange the values of all of the weights (and the bias) leading both into and out of a particular hidden unit with the corresponding values of the weights (and bias) associated with a different hidden unit. Again, this clearly leaves the network input–output mapping function unchanged, but it corresponds to a different choice of weight vector. For M hidden units, any given weight vector will belong to a set of $M!$ equivalent weight vectors associated with this interchange symmetry, corresponding to the $M!$ different orderings of the hidden units. The network will therefore have an overall weight-space symmetry factor of $M!2^M$. For networks with more than two layers of weights, the total level of symmetry will be given by the product of such factors, one for each layer of hidden units.

It turns out that these factors account for all of the symmetries in weight space (except for possible accidental symmetries due to specific choices for the weight values). Furthermore, the existence of these symmetries is not a particular property of the ‘tanh’ function but applies to a wide range of activation functions (Kúrková and Kainen, 1994). In many cases, these symmetries in weight space are of little practical consequence, although in Section 5.7 we shall encounter a situation in which we need to take them into account.

5.2. Network Training

So far, we have viewed neural networks as a general class of parametric nonlinear functions from a vector \mathbf{x} of input variables to a vector \mathbf{y} of output variables. A simple approach to the problem of determining the network parameters is to make an analogy with the discussion of polynomial curve fitting in Section 1.1, and therefore to minimize a sum-of-squares error function. Given a training set comprising a set of input vectors $\{\mathbf{x}_n\}$, where $n = 1, \dots, N$, together with a corresponding set of

target vectors $\{\mathbf{t}_n\}$, we minimize the error function

$$E(\mathbf{w}) = \frac{1}{2} \sum_{n=1}^N \|y(\mathbf{x}_n, \mathbf{w}) - t_n\|^2. \quad (5.11)$$

However, we can provide a much more general view of network training by first giving a probabilistic interpretation to the network outputs. We have already seen many advantages of using probabilistic predictions in Section 1.5.4. Here it will also provide us with a clearer motivation both for the choice of output unit nonlinearity and the choice of error function.

We start by discussing regression problems, and for the moment we consider a single target variable t that can take any real value. Following the discussions in Section 1.2.5 and 3.1, we assume that t has a Gaussian distribution with an \mathbf{x} -dependent mean, which is given by the output of the neural network, so that

$$p(t|\mathbf{x}, \mathbf{w}) = \mathcal{N}(t|y(\mathbf{x}, \mathbf{w}), \beta^{-1}) \quad (5.12)$$

where β is the precision (inverse variance) of the Gaussian noise. Of course this is a somewhat restrictive assumption, and in Section 5.6 we shall see how to extend this approach to allow for more general conditional distributions. For the conditional distribution given by (5.12), it is sufficient to take the output unit activation function to be the identity, because such a network can approximate any continuous function from \mathbf{x} to y . Given a data set of N independent, identically distributed observations $\mathbf{X} = \{\mathbf{x}_1, \dots, \mathbf{x}_N\}$, along with corresponding target values $\mathbf{t} = \{t_1, \dots, t_N\}$, we can construct the corresponding likelihood function

$$p(\mathbf{t}|\mathbf{X}, \mathbf{w}, \beta) = \prod_{n=1}^N p(t_n|\mathbf{x}_n, \mathbf{w}, \beta).$$

Taking the negative logarithm, we obtain the error function

$$\frac{\beta}{2} \sum_{n=1}^N \{y(\mathbf{x}_n, \mathbf{w}) - t_n\}^2 - \frac{N}{2} \ln \beta + \frac{N}{2} \ln(2\pi) \quad (5.13)$$

which can be used to learn the parameters \mathbf{w} and β . In Section 5.7, we shall discuss the Bayesian treatment of neural networks, while here we consider a maximum likelihood approach. Note that in the neural networks literature, it is usual to consider the minimization of an error function rather than the maximization of the (log) likelihood, and so here we shall follow this convention. Consider first the determination of \mathbf{w} . Maximizing the likelihood function is equivalent to minimizing the sum-of-squares error function given by

$$E(\mathbf{w}) = \frac{1}{2} \sum_{n=1}^N \{y(\mathbf{x}_n, \mathbf{w}) - t_n\}^2 \quad (5.14)$$

where we have discarded additive and multiplicative constants. The value of \mathbf{w} found by minimizing $E(\mathbf{w})$ will be denoted \mathbf{w}_{ML} because it corresponds to the maximum likelihood solution. In practice, the nonlinearity of the network function $y(\mathbf{x}_n, \mathbf{w})$ causes the error $E(\mathbf{w})$ to be nonconvex, and so in practice local maxima of the likelihood may be found, corresponding to local minima of the error function, as discussed in Section 5.2.1.

Having found \mathbf{w}_{ML} , the value of β can be found by minimizing the negative log likelihood to give

$$\frac{1}{\beta_{\text{ML}}} = \frac{1}{N} \sum_{n=1}^N \{y(\mathbf{x}_n, \mathbf{w}_{\text{ML}}) - t_n\}^2. \quad (5.15)$$

Note that this can be evaluated once the iterative optimization required to find \mathbf{w}_{ML} is completed. If we have multiple target variables, and we assume that they are independent conditional on \mathbf{x} and \mathbf{w} with shared noise precision β , then the conditional distribution of the target values is given by

$$p(\mathbf{t}|\mathbf{x}, \mathbf{w}) = \mathcal{N}(\mathbf{t}|y(\mathbf{x}, \mathbf{w}), \beta^{-1}\mathbf{I}). \quad (5.16)$$

Following the same argument as for a single target variable, we see that the maximum likelihood weights are determined by minimizing the sum-of-squares error function (5.11). The noise precision is then given by

$$\frac{1}{\beta_{\text{ML}}} = \frac{1}{NK} \sum_{n=1}^N \|y(\mathbf{x}_n, \mathbf{w}_{\text{ML}}) - \mathbf{t}_n\|^2 \quad (5.17)$$

where K is the number of target variables. The assumption of independence can be dropped at the expense of a slightly more complex optimization problem.

Exercise 5.2

Recall from Section 4.3.6 that there is a natural pairing of the error function (given by the negative log likelihood) and the output unit activation function. In the regression case, we can view the network as having an output activation function that is the identity, so that $y_k = a_k$. The corresponding sum-of-squares error function has the property

$$\frac{\partial E}{\partial a_k} = y_k - t_k \quad (5.18)$$

which we shall make use of when discussing error backpropagation in Section 5.3.

Now consider the case of binary classification in which we have a single target variable t such that $t = 1$ denotes class C_1 and $t = 0$ denotes class C_2 . Following the discussion of canonical link functions in Section 4.3.6, we consider a network having a single output whose activation function is a logistic sigmoid

$$y = \sigma(a) \equiv \frac{1}{1 + \exp(-a)} \quad (5.19)$$

so that $0 \leq y(\mathbf{x}, \mathbf{w}) \leq 1$. We can interpret $y(\mathbf{x}, \mathbf{w})$ as the conditional probability $p(C_1|\mathbf{x})$, with $p(C_2|\mathbf{x})$ given by $1 - y(\mathbf{x}, \mathbf{w})$. The conditional distribution of targets given inputs is then a Bernoulli distribution of the form

$$p(t|\mathbf{x}, \mathbf{w}) = y(\mathbf{x}, \mathbf{w})^t \{1 - y(\mathbf{x}, \mathbf{w})\}^{1-t}. \quad (5.20)$$

If we consider a training set of independent observations, then the error function, which is given by the negative log likelihood, is then a *cross-entropy* error function of the form

$$E(\mathbf{w}) = - \sum_{n=1}^N \{t_n \ln y_n + (1 - t_n) \ln(1 - y_n)\} \quad (5.21)$$

where y_n denotes $y(\mathbf{x}_n, \mathbf{w})$. Note that there is no analogue of the noise precision β because the target values are assumed to be correctly labelled. However, the model is easily extended to allow for labelling errors. Simard *et al.* (2003) found that using the *cross-entropy error* function instead of the sum-of-squares for a classification problem leads to faster training as well as improved generalization.

If we have K separate binary classifications to perform, then we can use a network having K outputs each of which has a logistic sigmoid activation function. Associated with each output is a binary class label $t_k \in \{0, 1\}$, where $k = 1, \dots, K$. If we assume that the class labels are independent, given the input vector, then the conditional distribution of the targets is

$$p(\mathbf{t}|\mathbf{x}, \mathbf{w}) = \prod_{k=1}^K y_k(\mathbf{x}, \mathbf{w})^{t_k} [1 - y_k(\mathbf{x}, \mathbf{w})]^{1-t_k}. \quad (5.22)$$

Taking the negative logarithm of the corresponding likelihood function then gives the following error function

$$E(\mathbf{w}) = - \sum_{n=1}^N \sum_{k=1}^K \{t_{nk} \ln y_{nk} + (1 - t_{nk}) \ln(1 - y_{nk})\} \quad (5.23)$$

where y_{nk} denotes $y_k(\mathbf{x}_n, \mathbf{w})$. Again, the derivative of the error function with respect to the activation for a particular output unit takes the form (5.18) just as in the regression case.

It is interesting to contrast the neural network solution to this problem with the corresponding approach based on a linear classification model of the kind discussed in Chapter 4. Suppose that we are using a standard two-layer network of the kind shown in Figure 5.1. We see that the weight parameters in the first layer of the network are shared between the various outputs, whereas in the linear model each classification problem is solved independently. The first layer of the network can be viewed as performing a nonlinear feature extraction, and the sharing of features between the different outputs can save on computation and can also lead to improved generalization.

Finally, we consider the standard multiclass classification problem in which each input is assigned to one of K mutually exclusive classes. The binary target variables $t_k \in \{0, 1\}$ have a 1-of- K coding scheme indicating the class, and the network outputs are interpreted as $y_k(\mathbf{x}, \mathbf{w}) = p(t_k = 1|\mathbf{x})$, leading to the following error function

$$E(\mathbf{w}) = - \sum_{n=1}^N \sum_{k=1}^K t_{kn} \ln y_k(\mathbf{x}_n, \mathbf{w}). \quad (5.24)$$

Exercise 5.4

Exercise 5.5

Exercise 5.6

Figure 5.5 Geometrical view of the error function $E(\mathbf{w})$ as a surface sitting over weight space. Point \mathbf{w}_A is a local minimum and \mathbf{w}_B is the global minimum. At any point \mathbf{w}_C , the local gradient of the error surface is given by the vector ∇E .



Following the discussion of Section 4.3.4, we see that the output unit activation function, which corresponds to the canonical link, is given by the softmax function

$$y_k(\mathbf{x}, \mathbf{w}) = \frac{\exp(a_k(\mathbf{x}, \mathbf{w}))}{\sum_j \exp(a_j(\mathbf{x}, \mathbf{w}))} \quad (5.25)$$

which satisfies $0 \leq y_k \leq 1$ and $\sum_k y_k = 1$. Note that the $y_k(\mathbf{x}, \mathbf{w})$ are unchanged if a constant is added to all of the $a_k(\mathbf{x}, \mathbf{w})$, causing the error function to be constant for some directions in weight space. This degeneracy is removed if an appropriate regularization term (Section 5.5) is added to the error function.

Once again, the derivative of the error function with respect to the activation for a particular output unit takes the familiar form (5.18).

In summary, there is a natural choice of both output unit activation function and matching error function, according to the type of problem being solved. For regression we use linear outputs and a sum-of-squares error, for (multiple independent) binary classifications we use logistic sigmoid outputs and a cross-entropy error function, and for multiclass classification we use softmax outputs with the corresponding multiclass cross-entropy error function. For classification problems involving two classes, we can use a single logistic sigmoid output, or alternatively we can use a network with two outputs having a softmax output activation function.

5.2.1 Parameter optimization

We turn next to the task of finding a weight vector \mathbf{w} which minimizes the chosen function $E(\mathbf{w})$. At this point, it is useful to have a geometrical picture of the error function, which we can view as a surface sitting over weight space as shown in Figure 5.5. First note that if we make a small step in weight space from \mathbf{w} to $\mathbf{w} + \delta\mathbf{w}$ then the change in the error function is $\delta E \simeq \delta\mathbf{w}^T \nabla E(\mathbf{w})$, where the vector $\nabla E(\mathbf{w})$ points in the direction of greatest rate of increase of the error function. Because the error $E(\mathbf{w})$ is a smooth continuous function of \mathbf{w} , its smallest value will occur at a

Exercise 5.7

point in weight space such that the gradient of the error function vanishes, so that

$$\nabla E(\mathbf{w}) = 0 \quad (5.26)$$

as otherwise we could make a small step in the direction of $-\nabla E(\mathbf{w})$ and thereby further reduce the error. Points at which the gradient vanishes are called stationary points, and may be further classified into minima, maxima, and saddle points.

Our goal is to find a vector \mathbf{w} such that $E(\mathbf{w})$ takes its smallest value. However, the error function typically has a highly nonlinear dependence on the weights and bias parameters, and so there will be many points in weight space at which the gradient vanishes (or is numerically very small). Indeed, from the discussion in Section 5.1.1 we see that for any point \mathbf{w} that is a local minimum, there will be other points in weight space that are equivalent minima. For instance, in a two-layer network of the kind shown in Figure 5.1, with M hidden units, each point in weight space is a member of a family of $M!2^M$ equivalent points.

Section 5.1.1

Furthermore, there will typically be multiple inequivalent stationary points and in particular multiple inequivalent minima. A minimum that corresponds to the smallest value of the error function for any weight vector is said to be a **global minimum**. Any other minima corresponding to higher values of the error function are said to be *local minima*. For a successful application of neural networks, it may not be necessary to find the global minimum (and in general it will not be known whether the global minimum has been found) but it may be necessary to compare several local minima in order to find a sufficiently good solution.

Because there is clearly no hope of finding an analytical solution to the equation $\nabla E(\mathbf{w}) = 0$ we resort to iterative numerical procedures. The optimization of continuous nonlinear functions is a widely studied problem and there exists an extensive literature on how to solve it efficiently. Most techniques involve choosing some initial value $\mathbf{w}^{(0)}$ for the weight vector and then moving through weight space in a succession of steps of the form

$$\mathbf{w}^{(\tau+1)} = \mathbf{w}^{(\tau)} + \Delta\mathbf{w}^{(\tau)} \quad (5.27)$$

where τ labels the iteration step. Different algorithms involve different choices for the weight vector update $\Delta\mathbf{w}^{(\tau)}$. Many algorithms make use of gradient information and therefore require that, after each update, the value of $\nabla E(\mathbf{w})$ is evaluated at the new weight vector $\mathbf{w}^{(\tau+1)}$. In order to understand the importance of gradient information, it is useful to consider a local approximation to the error function based on a Taylor expansion.

5.2.2 Local quadratic approximation

Insight into the optimization problem, and into the various techniques for solving it, can be obtained by considering a local quadratic approximation to the error function.

Consider the Taylor expansion of $E(\mathbf{w})$ around some point $\hat{\mathbf{w}}$ in weight space

$$E(\mathbf{w}) \simeq E(\hat{\mathbf{w}}) + (\mathbf{w} - \hat{\mathbf{w}})^T \mathbf{b} + \frac{1}{2} (\mathbf{w} - \hat{\mathbf{w}})^T \mathbf{H} (\mathbf{w} - \hat{\mathbf{w}}) \quad (5.28)$$

where cubic and higher terms have been omitted. Here \mathbf{b} is defined to be the gradient of E evaluated at $\hat{\mathbf{w}}$

$$\mathbf{b} \equiv \nabla E|_{\mathbf{w}=\hat{\mathbf{w}}} \quad (5.29)$$

and the Hessian matrix $\mathbf{H} = \nabla \nabla E$ has elements

$$(\mathbf{H})_{ij} \equiv \left. \frac{\partial E}{\partial w_i \partial w_j} \right|_{\mathbf{w}=\hat{\mathbf{w}}}. \quad (5.30)$$

From (5.28), the corresponding local approximation to the gradient is given by

$$\nabla E \simeq \mathbf{b} + \mathbf{H}(\mathbf{w} - \hat{\mathbf{w}}). \quad (5.31)$$

For points \mathbf{w} that are sufficiently close to $\hat{\mathbf{w}}$, these expressions will give reasonable approximations for the error and its gradient.

Consider the particular case of a local quadratic approximation around a point \mathbf{w}^* that is a minimum of the error function. In this case there is no linear term, because $\nabla E = 0$ at \mathbf{w}^* , and (5.28) becomes

$$E(\mathbf{w}) = E(\mathbf{w}^*) + \frac{1}{2}(\mathbf{w} - \mathbf{w}^*)^T \mathbf{H}(\mathbf{w} - \mathbf{w}^*) \quad (5.32)$$

where the Hessian \mathbf{H} is evaluated at \mathbf{w}^* . In order to interpret this geometrically, consider the eigenvalue equation for the Hessian matrix

$$\mathbf{H}\mathbf{u}_i = \lambda_i \mathbf{u}_i \quad (5.33)$$

where the eigenvectors \mathbf{u}_i form a complete orthonormal set (Appendix C) so that

$$\mathbf{u}_i^T \mathbf{u}_j = \delta_{ij}. \quad (5.34)$$

We now expand $(\mathbf{w} - \mathbf{w}^*)$ as a linear combination of the eigenvectors in the form

$$\mathbf{w} - \mathbf{w}^* = \sum_i \alpha_i \mathbf{u}_i. \quad (5.35)$$

This can be regarded as a transformation of the coordinate system in which the origin is translated to the point \mathbf{w}^* , and the axes are rotated to align with the eigenvectors (through the orthogonal matrix whose columns are the \mathbf{u}_i), and is discussed in more detail in Appendix C. Substituting (5.35) into (5.32), and using (5.33) and (5.34), allows the error function to be written in the form

$$E(\mathbf{w}) = E(\mathbf{w}^*) + \frac{1}{2} \sum_i \lambda_i \alpha_i^2. \quad (5.36)$$

A matrix \mathbf{H} is said to be *positive definite* if, and only if,

$$\mathbf{v}^T \mathbf{H} \mathbf{v} > 0 \quad \text{for all } \mathbf{v}. \quad (5.37)$$

Figure 5.6 In the neighbourhood of a minimum \mathbf{w}^* , the error function can be approximated by a quadratic. Contours of constant error are then ellipses whose axes are aligned with the eigenvectors \mathbf{u}_i of the Hessian matrix, with lengths that are inversely proportional to the square roots of the corresponding eigenvectors λ_i .



Because the eigenvectors $\{\mathbf{u}_i\}$ form a complete set, an arbitrary vector \mathbf{v} can be written in the form

$$\mathbf{v} = \sum_i c_i \mathbf{u}_i. \quad (5.38)$$

From (5.33) and (5.34), we then have

$$\mathbf{v}^T \mathbf{H} \mathbf{v} = \sum_i c_i^2 \lambda_i \quad (5.39)$$

Exercise 5.10

Exercise 5.11

Exercise 5.12

and so \mathbf{H} will be positive definite if, and only if, all of its eigenvalues are positive. In the new coordinate system, whose basis vectors are given by the eigenvectors $\{\mathbf{u}_i\}$, the contours of constant E are ellipses centred on the origin, as illustrated in Figure 5.6. For a one-dimensional weight space, a stationary point w^* will be a minimum if

$$\left. \frac{\partial^2 E}{\partial w^2} \right|_{w^*} > 0. \quad (5.40)$$

The corresponding result in D -dimensions is that the Hessian matrix, evaluated at \mathbf{w}^* , should be positive definite.

5.2.3 Use of gradient information

As we shall see in Section 5.3, it is possible to evaluate the gradient of an error function efficiently by means of the backpropagation procedure. The use of this gradient information can lead to significant improvements in the speed with which the minima of the error function can be located. We can see why this is so, as follows.

In the quadratic approximation to the error function, given in (5.28), the error surface is specified by the quantities \mathbf{b} and \mathbf{H} , which contain a total of $W(W + 3)/2$ independent elements (because the matrix \mathbf{H} is symmetric), where W is the dimensionality of \mathbf{w} (i.e., the total number of adaptive parameters in the network). The location of the minimum of this quadratic approximation therefore depends on $O(W^2)$ parameters, and we should not expect to be able to locate the minimum until we have gathered $O(W^2)$ independent pieces of information. If we do not make use of gradient information, we would expect to have to perform $O(W^2)$ function

Exercise 5.13

evaluations, each of which would require $O(W)$ steps. Thus, the computational effort needed to find the minimum using such an approach would be $O(W^3)$.

Now compare this with an algorithm that makes use of the gradient information. Because each evaluation of ∇E brings W items of information, we might hope to find the minimum of the function in $O(W)$ gradient evaluations. As we shall see, by using error backpropagation, each such evaluation takes only $O(W)$ steps and so the minimum can now be found in $O(W^2)$ steps. For this reason, the use of gradient information forms the basis of practical algorithms for training neural networks.

5.2.4 Gradient descent optimization

The simplest approach to using gradient information is to choose the weight update in (5.27) to comprise a small step in the direction of the negative gradient, so that

$$\mathbf{w}^{(\tau+1)} = \mathbf{w}^{(\tau)} - \eta \nabla E(\mathbf{w}^{(\tau)}) \quad (5.41)$$

where the parameter $\eta > 0$ is known as the *learning rate*. After each such update, the gradient is re-evaluated for the new weight vector and the process repeated. Note that the error function is defined with respect to a training set, and so each step requires that the entire training set be processed in order to evaluate ∇E . Techniques that use the whole data set at once are called *batch* methods. At each step the weight vector is moved in the direction of the greatest rate of decrease of the error function, and so this approach is known as *gradient descent* or *steepest descent*. Although such an approach might intuitively seem reasonable, in fact it turns out to be a poor algorithm, for reasons discussed in Bishop and Nabney (2008).

For batch optimization, there are more efficient methods, such as *conjugate gradients* and *quasi-Newton* methods, which are much more robust and much faster than simple gradient descent (Gill *et al.*, 1981; Fletcher, 1987; Nocedal and Wright, 1999). Unlike gradient descent, these algorithms have the property that the error function always decreases at each iteration unless the weight vector has arrived at a local or global minimum.

In order to find a sufficiently good minimum, it may be necessary to run a gradient-based algorithm multiple times, each time using a different randomly chosen starting point, and comparing the resulting performance on an independent validation set.

There is, however, an on-line version of gradient descent that has proved useful in practice for training neural networks on large data sets (Le Cun *et al.*, 1989). Error functions based on maximum likelihood for a set of independent observations comprise a sum of terms, one for each data point

$$E(\mathbf{w}) = \sum_{n=1}^N E_n(\mathbf{w}). \quad (5.42)$$

On-line gradient descent, also known as *sequential gradient descent* or *stochastic gradient descent*, makes an update to the weight vector based on one data point at a time, so that

$$\mathbf{w}^{(\tau+1)} = \mathbf{w}^{(\tau)} - \eta \nabla E_n(\mathbf{w}^{(\tau)}). \quad (5.43)$$

This update is repeated by cycling through the data either in sequence or by selecting points at random with replacement. There are of course intermediate scenarios in which the updates are based on batches of data points.

One advantage of on-line methods compared to batch methods is that the former handle redundancy in the data much more efficiently. To see, this consider an extreme example in which we take a data set and double its size by duplicating every data point. Note that this simply multiplies the error function by a factor of 2 and so is equivalent to using the original error function. Batch methods will require double the computational effort to evaluate the batch error function gradient, whereas on-line methods will be unaffected. Another property of on-line gradient descent is the possibility of escaping from local minima, since a stationary point with respect to the error function for the whole data set will generally not be a stationary point for each data point individually.

Nonlinear optimization algorithms, and their practical application to neural network training, are discussed in detail in Bishop and Nabney (2008).

5.3. Error Backpropagation

Our goal in this section is to find an efficient technique for evaluating the gradient of an error function $E(\mathbf{w})$ for a feed-forward neural network. We shall see that this can be achieved using a local message passing scheme in which information is sent alternately forwards and backwards through the network and is known as *error backpropagation*, or sometimes simply as *backprop*.

It should be noted that the term backpropagation is used in the neural computing literature to mean a variety of different things. For instance, the multilayer perceptron architecture is sometimes called a backpropagation network. The term backpropagation is also used to describe the training of a multilayer perceptron using gradient descent applied to a sum-of-squares error function. In order to clarify the terminology, it is useful to consider the nature of the training process more carefully. Most training algorithms involve an iterative procedure for minimization of an error function, with adjustments to the weights being made in a sequence of steps. At each such step, we can distinguish between two distinct stages. In the first stage, the derivatives of the error function with respect to the weights must be evaluated. As we shall see, the important contribution of the backpropagation technique is in providing a computationally efficient method for evaluating such derivatives. Because it is at this stage that errors are propagated backwards through the network, we shall use the term backpropagation specifically to describe the evaluation of derivatives. In the second stage, the derivatives are then used to compute the adjustments to be made to the weights. The simplest such technique, and the one originally considered by Rumelhart *et al.* (1986), involves gradient descent. It is important to recognize that the two stages are distinct. Thus, the first stage, namely the propagation of errors backwards through the network in order to evaluate derivatives, can be applied to many other kinds of network and not just the multilayer perceptron. It can also be applied to error functions other than just the simple sum-of-squares, and to the eval-

uation of other derivatives such as the Jacobian and Hessian matrices, as we shall see later in this chapter. Similarly, the second stage of weight adjustment using the calculated derivatives can be tackled using a variety of optimization schemes, many of which are substantially more powerful than simple gradient descent.

5.3.1 Evaluation of error-function derivatives

We now derive the backpropagation algorithm for a general network having arbitrary feed-forward topology, arbitrary differentiable nonlinear activation functions, and a broad class of error function. The resulting formulae will then be illustrated using a simple layered network structure having a single layer of sigmoidal hidden units together with a sum-of-squares error.

Many error functions of practical interest, for instance those defined by maximum likelihood for a set of i.i.d. data, comprise a sum of terms, one for each data point in the training set, so that

$$E(\mathbf{w}) = \sum_{n=1}^N E_n(\mathbf{w}). \quad (5.44)$$

Here we shall consider the problem of evaluating $\nabla E_n(\mathbf{w})$ for one such term in the error function. This may be used directly for sequential optimization, or the results can be accumulated over the training set in the case of batch methods.

Consider first a simple linear model in which the outputs y_k are linear combinations of the input variables x_i so that

$$y_k = \sum_i w_{ki} x_i \quad (5.45)$$

together with an error function that, for a particular input pattern n , takes the form

$$E_n = \frac{1}{2} \sum_k (y_{nk} - t_{nk})^2 \quad (5.46)$$

where $y_{nk} = y_k(\mathbf{x}_n, \mathbf{w})$. The gradient of this error function with respect to a weight w_{ji} is given by

$$\frac{\partial E_n}{\partial w_{ji}} = (y_{nj} - t_{nj}) x_{ni} \quad (5.47)$$

which can be interpreted as a ‘local’ computation involving the product of an ‘error signal’ $y_{nj} - t_{nj}$ associated with the output end of the link w_{ji} and the variable x_{ni} associated with the input end of the link. In Section 4.3.2, we saw how a similar formula arises with the logistic sigmoid activation function together with the cross entropy error function, and similarly for the softmax activation function together with its matching cross-entropy error function. We shall now see how this simple result extends to the more complex setting of multilayer feed-forward networks.

In a general feed-forward network, each unit computes a weighted sum of its inputs of the form

$$a_j = \sum_i w_{ji} z_i \quad (5.48)$$

where z_i is the activation of a unit, or input, that sends a connection to unit j , and w_{ji} is the weight associated with that connection. In Section 5.1, we saw that biases can be included in this sum by introducing an extra unit, or input, with activation fixed at +1. We therefore do not need to deal with biases explicitly. The sum in (5.48) is transformed by a nonlinear activation function $h(\cdot)$ to give the activation z_j of unit j in the form

$$z_j = h(a_j). \quad (5.49)$$

Note that one or more of the variables z_i in the sum in (5.48) could be an input, and similarly, the unit j in (5.49) could be an output.

For each pattern in the training set, we shall suppose that we have supplied the corresponding input vector to the network and calculated the activations of all of the hidden and output units in the network by successive application of (5.48) and (5.49). This process is often called *forward propagation* because it can be regarded as a forward flow of information through the network.

Now consider the evaluation of the derivative of E_n with respect to a weight w_{ji} . The outputs of the various units will depend on the particular input pattern n . However, in order to keep the notation uncluttered, we shall omit the subscript n from the network variables. First we note that E_n depends on the weight w_{ji} only via the summed input a_j to unit j . We can therefore apply the chain rule for partial derivatives to give

$$\frac{\partial E_n}{\partial w_{ji}} = \frac{\partial E_n}{\partial a_j} \frac{\partial a_j}{\partial w_{ji}}. \quad (5.50)$$

We now introduce a useful notation

$$\delta_j = \frac{\partial E_n}{\partial a_j} \quad (5.51)$$

where the δ 's are often referred to as *errors* for reasons we shall see shortly. Using (5.48), we can write

$$\frac{\partial a_j}{\partial w_{ji}} = z_i. \quad (5.52)$$

Substituting (5.51) and (5.52) into (5.50), we then obtain

$$\frac{\partial E_n}{\partial w_{ji}} = \delta_j z_i. \quad (5.53)$$

Equation (5.53) tells us that the required derivative is obtained simply by multiplying the value of δ for the unit at the output end of the weight by the value of z for the unit at the input end of the weight (where $z = 1$ in the case of a bias). Note that this takes the same form as for the simple linear model considered at the start of this section. Thus, in order to evaluate the derivatives, we need only to calculate the value of δ_j for each hidden and output unit in the network, and then apply (5.53).

As we have seen already, for the output units, we have

$$\delta_k = y_k - t_k \quad (5.54)$$

Figure 5.7 Illustration of the calculation of δ_j for hidden unit j by backpropagation of the δ 's from those units k to which unit j sends connections. The blue arrow denotes the direction of information flow during forward propagation, and the red arrows indicate the backward propagation of error information.



provided we are using the canonical link as the output-unit activation function. To evaluate the δ 's for hidden units, we again make use of the chain rule for partial derivatives,

$$\delta_j \equiv \frac{\partial E_n}{\partial a_j} = \sum_k \frac{\partial E_n}{\partial a_k} \frac{\partial a_k}{\partial a_j} \quad (5.55)$$

where the sum runs over all units k to which unit j sends connections. The arrangement of units and weights is illustrated in Figure 5.7. Note that the units labelled k could include other hidden units and/or output units. In writing down (5.55), we are making use of the fact that variations in a_j give rise to variations in the error function only through variations in the variables a_k . If we now substitute the definition of δ given by (5.51) into (5.55), and make use of (5.48) and (5.49), we obtain the following *backpropagation* formula

$$\delta_j = h'(a_j) \sum_k w_{kj} \delta_k \quad (5.56)$$

which tells us that the value of δ for a particular hidden unit can be obtained by propagating the δ 's backwards from units higher up in the network, as illustrated in Figure 5.7. Note that the summation in (5.56) is taken over the first index on w_{kj} (corresponding to backward propagation of information through the network), whereas in the forward propagation equation (5.10) it is taken over the second index. Because we already know the values of the δ 's for the output units, it follows that by recursively applying (5.56) we can evaluate the δ 's for all of the hidden units in a feed-forward network, regardless of its topology.

The backpropagation procedure can therefore be summarized as follows.

Error Backpropagation

1. Apply an input vector \mathbf{x}_n to the network and forward propagate through the network using (5.48) and (5.49) to find the activations of all the hidden and output units.
2. Evaluate the δ_k for all the output units using (5.54).
3. Backpropagate the δ 's using (5.56) to obtain δ_j for each hidden unit in the network.
4. Use (5.53) to evaluate the required derivatives.

For batch methods, the derivative of the total error E can then be obtained by repeating the above steps for each pattern in the training set and then summing over all patterns:

$$\frac{\partial E}{\partial w_{ji}} = \sum_n \frac{\partial E_n}{\partial w_{ji}}. \quad (5.57)$$

In the above derivation we have implicitly assumed that each hidden or output unit in the network has the same activation function $h(\cdot)$. The derivation is easily generalized, however, to allow different units to have individual activation functions, simply by keeping track of which form of $h(\cdot)$ goes with which unit.

5.3.2 A simple example

The above derivation of the backpropagation procedure allowed for general forms for the error function, the activation functions, and the network topology. In order to illustrate the application of this algorithm, we shall consider a particular example. This is chosen both for its simplicity and for its practical importance, because many applications of neural networks reported in the literature make use of this type of network. Specifically, we shall consider a two-layer network of the form illustrated in Figure 5.1, together with a sum-of-squares error, in which the output units have linear activation functions, so that $y_k = a_k$, while the hidden units have logistic sigmoid activation functions given by

$$h(a) \equiv \tanh(a) \quad (5.58)$$

where

$$\tanh(a) = \frac{e^a - e^{-a}}{e^a + e^{-a}}. \quad (5.59)$$

A useful feature of this function is that its derivative can be expressed in a particularly simple form:

$$h'(a) = 1 - h(a)^2. \quad (5.60)$$

We also consider a standard sum-of-squares error function, so that for pattern n the error is given by

$$E_n = \frac{1}{2} \sum_{k=1}^K (y_k - t_k)^2 \quad (5.61)$$

where y_k is the activation of output unit k , and t_k is the corresponding target, for a particular input pattern \mathbf{x}_n .

For each pattern in the training set in turn, we first perform a forward propagation using

$$a_j = \sum_{i=0}^D w_{ji}^{(1)} x_i \quad (5.62)$$

$$z_j = \tanh(a_j) \quad (5.63)$$

$$y_k = \sum_{j=0}^M w_{kj}^{(2)} z_j. \quad (5.64)$$

Next we compute the δ 's for each output unit using

$$\delta_k = y_k - t_k. \quad (5.65)$$

Then we backpropagate these to obtain δ s for the hidden units using

$$\delta_j = (1 - z_j^2) \sum_{k=1}^K w_{kj} \delta_k. \quad (5.66)$$

Finally, the derivatives with respect to the first-layer and second-layer weights are given by

$$\frac{\partial E_n}{\partial w_{ji}^{(1)}} = \delta_j x_i, \quad \frac{\partial E_n}{\partial w_{kj}^{(2)}} = \delta_k z_j. \quad (5.67)$$

5.3.3 Efficiency of backpropagation

One of the most important aspects of backpropagation is its computational efficiency. To understand this, let us examine how the number of computer operations required to evaluate the derivatives of the error function scales with the total number W of weights and biases in the network. A single evaluation of the error function (for a given input pattern) would require $O(W)$ operations, for sufficiently large W . This follows from the fact that, except for a network with very sparse connections, the number of weights is typically much greater than the number of units, and so the bulk of the computational effort in forward propagation is concerned with evaluating the sums in (5.48), with the evaluation of the activation functions representing a small overhead. Each term in the sum in (5.48) requires one multiplication and one addition, leading to an overall computational cost that is $O(W)$.

An alternative approach to backpropagation for computing the derivatives of the error function is to use finite differences. This can be done by perturbing each weight in turn, and approximating the derivatives by the expression

$$\frac{\partial E_n}{\partial w_{ji}} = \frac{E_n(w_{ji} + \epsilon) - E_n(w_{ji})}{\epsilon} + O(\epsilon) \quad (5.68)$$

where $\epsilon \ll 1$. In a software simulation, the accuracy of the approximation to the derivatives can be improved by making ϵ smaller, until numerical roundoff problems arise. The accuracy of the finite differences method can be improved significantly by using symmetrical *central differences* of the form

$$\frac{\partial E_n}{\partial w_{ji}} = \frac{E_n(w_{ji} + \epsilon) - E_n(w_{ji} - \epsilon)}{2\epsilon} + O(\epsilon^2). \quad (5.69)$$

Exercise 5.14

In this case, the $O(\epsilon)$ corrections cancel, as can be verified by Taylor expansion on the right-hand side of (5.69), and so the residual corrections are $O(\epsilon^2)$. The number of computational steps is, however, roughly doubled compared with (5.68).

The main problem with numerical differentiation is that the highly desirable $O(W)$ scaling has been lost. Each forward propagation requires $O(W)$ steps, and

Figure 5.8 Illustration of a modular pattern recognition system in which the Jacobian matrix can be used to backpropagate error signals from the outputs through to earlier modules in the system.



there are W weights in the network each of which must be perturbed individually, so that the overall scaling is $O(W^2)$.

However, numerical differentiation plays an important role in practice, because a comparison of the derivatives calculated by backpropagation with those obtained using central differences provides a powerful check on the correctness of any software implementation of the backpropagation algorithm. When training networks in practice, derivatives should be evaluated using backpropagation, because this gives the greatest accuracy and numerical efficiency. However, the results should be compared with numerical differentiation using (5.69) for some test cases in order to check the correctness of the implementation.

5.3.4 The Jacobian matrix

We have seen how the derivatives of an error function with respect to the weights can be obtained by the propagation of errors backwards through the network. The technique of backpropagation can also be applied to the calculation of other derivatives. Here we consider the evaluation of the *Jacobian* matrix, whose elements are given by the derivatives of the network outputs with respect to the inputs

$$J_{ki} \equiv \frac{\partial y_k}{\partial x_i} \quad (5.70)$$

where each such derivative is evaluated with all other inputs held fixed. Jacobian matrices play a useful role in systems built from a number of distinct modules, as illustrated in Figure 5.8. Each module can comprise a fixed or adaptive function, which can be linear or nonlinear, so long as it is differentiable. Suppose we wish to minimize an error function E with respect to the parameter w in Figure 5.8. The derivative of the error function is given by

$$\frac{\partial E}{\partial w} = \sum_{k,j} \frac{\partial E}{\partial y_k} \frac{\partial y_k}{\partial z_j} \frac{\partial z_j}{\partial w} \quad (5.71)$$

in which the Jacobian matrix for the red module in Figure 5.8 appears in the middle term.

Because the Jacobian matrix provides a measure of the local sensitivity of the outputs to changes in each of the input variables, it also allows any known errors Δx_i

associated with the inputs to be propagated through the trained network in order to estimate their contribution Δy_k to the errors at the outputs, through the relation

$$\Delta y_k \simeq \sum_i \frac{\partial y_k}{\partial x_i} \Delta x_i \quad (5.72)$$

which is valid provided the $|\Delta x_i|$ are small. In general, the network mapping represented by a trained neural network will be nonlinear, and so the elements of the Jacobian matrix will not be constants but will depend on the particular input vector used. Thus (5.72) is valid only for small perturbations of the inputs, and the Jacobian itself must be re-evaluated for each new input vector.

The Jacobian matrix can be evaluated using a backpropagation procedure that is similar to the one derived earlier for evaluating the derivatives of an error function with respect to the weights. We start by writing the element J_{ki} in the form

$$\begin{aligned} J_{ki} = \frac{\partial y_k}{\partial x_i} &= \sum_j \frac{\partial y_k}{\partial a_j} \frac{\partial a_j}{\partial x_i} \\ &= \sum_j w_{ji} \frac{\partial y_k}{\partial a_j} \end{aligned} \quad (5.73)$$

where we have made use of (5.48). The sum in (5.73) runs over all units j to which the input unit i sends connections (for example, over all units in the first hidden layer in the layered topology considered earlier). We now write down a recursive backpropagation formula to determine the derivatives $\partial y_k / \partial a_j$

$$\begin{aligned} \frac{\partial y_k}{\partial a_j} &= \sum_l \frac{\partial y_k}{\partial a_l} \frac{\partial a_l}{\partial a_j} \\ &= h'(a_j) \sum_l w_{lj} \frac{\partial y_k}{\partial a_l} \end{aligned} \quad (5.74)$$

where the sum runs over all units l to which unit j sends connections (corresponding to the first index of w_{lj}). Again, we have made use of (5.48) and (5.49). This backpropagation starts at the output units for which the required derivatives can be found directly from the functional form of the output-unit activation function. For instance, if we have individual sigmoidal activation functions at each output unit, then

$$\frac{\partial y_k}{\partial a_j} = \delta_{kj} \sigma'(a_j) \quad (5.75)$$

whereas for softmax outputs we have

$$\frac{\partial y_k}{\partial a_j} = \delta_{kj} y_k - y_k y_j. \quad (5.76)$$

We can summarize the procedure for evaluating the Jacobian matrix as follows. Apply the input vector corresponding to the point in input space at which the Jacobian matrix is to be found, and forward propagate in the usual way to obtain the

activations of all of the hidden and output units in the network. Next, for each row k of the Jacobian matrix, corresponding to the output unit k , backpropagate using the recursive relation (5.74), starting with (5.75) or (5.76), for all of the hidden units in the network. Finally, use (5.73) to do the backpropagation to the inputs. The Jacobian can also be evaluated using an alternative *forward* propagation formalism, which can be derived in an analogous way to the backpropagation approach given here.

Exercise 5.15

Again, the implementation of such algorithms can be checked by using numerical differentiation in the form

$$\frac{\partial y_k}{\partial x_i} = \frac{y_k(x_i + \epsilon) - y_k(x_i - \epsilon)}{2\epsilon} + O(\epsilon^2) \quad (5.77)$$

which involves $2D$ forward propagations for a network having D inputs.

5.4. The Hessian Matrix

We have shown how the technique of backpropagation can be used to obtain the first derivatives of an error function with respect to the weights in the network. Backpropagation can also be used to evaluate the second derivatives of the error, given by

$$\frac{\partial^2 E}{\partial w_{ji} \partial w_{lk}}. \quad (5.78)$$

Note that it is sometimes convenient to consider all of the weight and bias parameters as elements w_i of a single vector, denoted \mathbf{w} , in which case the second derivatives form the elements H_{ij} of the *Hessian* matrix \mathbf{H} , where $i, j \in \{1, \dots, W\}$ and W is the total number of weights and biases. The Hessian plays an important role in many aspects of neural computing, including the following:

1. Several nonlinear optimization algorithms used for training neural networks are based on considerations of the second-order properties of the error surface, which are controlled by the Hessian matrix (Bishop and Nabney, 2008).
2. The Hessian forms the basis of a fast procedure for re-training a feed-forward network following a small change in the training data (Bishop, 1991).
3. The inverse of the Hessian has been used to identify the least significant weights in a network as part of network ‘pruning’ algorithms (Le Cun *et al.*, 1990).
4. The Hessian plays a central role in the Laplace approximation for a Bayesian neural network (see Section 5.7). Its inverse is used to determine the predictive distribution for a trained network, its eigenvalues determine the values of hyperparameters, and its determinant is used to evaluate the model evidence.

Various approximation schemes have been used to evaluate the Hessian matrix for a neural network. However, the Hessian can also be calculated exactly using an extension of the backpropagation technique.

An important consideration for many applications of the Hessian is the efficiency with which it can be evaluated. If there are W parameters (weights and biases) in the network, then the Hessian matrix has dimensions $W \times W$ and so the computational effort needed to evaluate the Hessian will scale like $O(W^2)$ for each pattern in the data set. As we shall see, there are efficient methods for evaluating the Hessian whose scaling is indeed $O(W^2)$.

5.4.1 Diagonal approximation

Some of the applications for the Hessian matrix discussed above require the inverse of the Hessian, rather than the Hessian itself. For this reason, there has been some interest in using a diagonal approximation to the Hessian, in other words one that simply replaces the off-diagonal elements with zeros, because its inverse is trivial to evaluate. Again, we shall consider an error function that consists of a sum of terms, one for each pattern in the data set, so that $E = \sum_n E_n$. The Hessian can then be obtained by considering one pattern at a time, and then summing the results over all patterns. From (5.48), the diagonal elements of the Hessian, for pattern n , can be written

$$\frac{\partial^2 E_n}{\partial w_{ji}^2} = \frac{\partial^2 E_n}{\partial a_j^2} z_i^2. \quad (5.79)$$

Using (5.48) and (5.49), the second derivatives on the right-hand side of (5.79) can be found recursively using the chain rule of differential calculus to give a backpropagation equation of the form

$$\frac{\partial^2 E_n}{\partial a_j^2} = h'(a_j)^2 \sum_k \sum_{k'} w_{kj} w_{k'j} \frac{\partial^2 E_n}{\partial a_k \partial a_{k'}} + h''(a_j) \sum_k w_{kj} \frac{\partial E_n}{\partial a_k}. \quad (5.80)$$

If we now neglect off-diagonal elements in the second-derivative terms, we obtain (Becker and Le Cun, 1989; Le Cun *et al.*, 1990)

$$\frac{\partial^2 E_n}{\partial a_j^2} = h'(a_j)^2 \sum_k w_{kj}^2 \frac{\partial^2 E_n}{\partial a_k^2} + h''(a_j) \sum_k w_{kj} \frac{\partial E_n}{\partial a_k}. \quad (5.81)$$

Note that the number of computational steps required to evaluate this approximation is $O(W)$, where W is the total number of weight and bias parameters in the network, compared with $O(W^2)$ for the full Hessian.

Ricotti *et al.* (1988) also used the diagonal approximation to the Hessian, but they retained all terms in the evaluation of $\partial^2 E_n / \partial a_j^2$ and so obtained exact expressions for the diagonal terms. Note that this no longer has $O(W)$ scaling. The major problem with diagonal approximations, however, is that in practice the Hessian is typically found to be strongly nondiagonal, and so these approximations, which are driven mainly by computational convenience, must be treated with care.

5.4.2 Outer product approximation

When neural networks are applied to regression problems, it is common to use a sum-of-squares error function of the form

$$E = \frac{1}{2} \sum_{n=1}^N (y_n - t_n)^2 \quad (5.82)$$

where we have considered the case of a single output in order to keep the notation simple (the extension to several outputs is straightforward). We can then write the Hessian matrix in the form

$$\mathbf{H} = \nabla \nabla E = \sum_{n=1}^N \nabla y_n \nabla y_n + \sum_{n=1}^N (y_n - t_n) \nabla \nabla y_n. \quad (5.83)$$

If the network has been trained on the data set, and its outputs y_n happen to be very close to the target values t_n , then the second term in (5.83) will be small and can be neglected. More generally, however, it may be appropriate to neglect this term by the following argument. Recall from Section 1.5.5 that the optimal function that minimizes a sum-of-squares loss is the conditional average of the target data. The quantity $(y_n - t_n)$ is then a random variable with zero mean. If we assume that its value is uncorrelated with the value of the second derivative term on the right-hand side of (5.83), then the whole term will average to zero in the summation over n .

By neglecting the second term in (5.83), we arrive at the *Levenberg–Marquardt* approximation or *outer product* approximation (because the Hessian matrix is built up from a sum of outer products of vectors), given by

$$\mathbf{H} \simeq \sum_{n=1}^N \mathbf{b}_n \mathbf{b}_n^T \quad (5.84)$$

where $\mathbf{b}_n = \nabla y_n = \nabla a_n$ because the activation function for the output units is simply the identity. Evaluation of the outer product approximation for the Hessian is straightforward as it only involves first derivatives of the error function, which can be evaluated efficiently in $O(W)$ steps using standard backpropagation. The elements of the matrix can then be found in $O(W^2)$ steps by simple multiplication. It is important to emphasize that this approximation is only likely to be valid for a network that has been trained appropriately, and that for a general network mapping the second derivative terms on the right-hand side of (5.83) will typically not be negligible.

In the case of the cross-entropy error function for a network with logistic sigmoid output-unit activation functions, the corresponding approximation is given by

$$\mathbf{H} \simeq \sum_{n=1}^N y_n(1 - y_n) \mathbf{b}_n \mathbf{b}_n^T. \quad (5.85)$$

An analogous result can be obtained for multiclass networks having softmax output-unit activation functions.

Exercise 5.16

Exercise 5.17

Exercise 5.19

Exercise 5.20

5.4.3 Inverse Hessian

We can use the outer-product approximation to develop a computationally efficient procedure for approximating the inverse of the Hessian (Hassibi and Stork, 1993). First we write the outer-product approximation in matrix notation as

$$\mathbf{H}_N = \sum_{n=1}^N \mathbf{b}_n \mathbf{b}_n^T \quad (5.86)$$

where $\mathbf{b}_n \equiv \nabla_{\mathbf{w}} a_n$ is the contribution to the gradient of the output unit activation arising from data point n . We now derive a sequential procedure for building up the Hessian by including data points one at a time. Suppose we have already obtained the inverse Hessian using the first L data points. By separating off the contribution from data point $L + 1$, we obtain

$$\mathbf{H}_{L+1} = \mathbf{H}_L + \mathbf{b}_{L+1} \mathbf{b}_{L+1}^T. \quad (5.87)$$

In order to evaluate the inverse of the Hessian, we now consider the matrix identity

$$(\mathbf{M} + \mathbf{v}\mathbf{v}^T)^{-1} = \mathbf{M}^{-1} - \frac{(\mathbf{M}^{-1}\mathbf{v})(\mathbf{v}^T\mathbf{M}^{-1})}{1 + \mathbf{v}^T\mathbf{M}^{-1}\mathbf{v}} \quad (5.88)$$

where \mathbf{I} is the unit matrix, which is simply a special case of the Woodbury identity (C.7). If we now identify \mathbf{H}_L with \mathbf{M} and \mathbf{b}_{L+1} with \mathbf{v} , we obtain

$$\mathbf{H}_{L+1}^{-1} = \mathbf{H}_L^{-1} - \frac{\mathbf{H}_L^{-1}\mathbf{b}_{L+1}\mathbf{b}_{L+1}^T\mathbf{H}_L^{-1}}{1 + \mathbf{b}_{L+1}^T\mathbf{H}_L^{-1}\mathbf{b}_{L+1}}. \quad (5.89)$$

In this way, data points are sequentially absorbed until $L + 1 = N$ and the whole data set has been processed. This result therefore represents a procedure for evaluating the inverse of the Hessian using a single pass through the data set. The initial matrix \mathbf{H}_0 is chosen to be $\alpha\mathbf{I}$, where α is a small quantity, so that the algorithm actually finds the inverse of $\mathbf{H} + \alpha\mathbf{I}$. The results are not particularly sensitive to the precise value of α . Extension of this algorithm to networks having more than one output is straightforward.

Exercise 5.21

We note here that the Hessian matrix can sometimes be calculated indirectly as part of the network training algorithm. In particular, quasi-Newton nonlinear optimization algorithms gradually build up an approximation to the inverse of the Hessian during training. Such algorithms are discussed in detail in Bishop and Nabney (2008).

5.4.4 Finite differences

As in the case of the first derivatives of the error function, we can find the second derivatives by using finite differences, with accuracy limited by numerical precision. If we perturb each possible pair of weights in turn, we obtain

$$\begin{aligned} \frac{\partial^2 E}{\partial w_{ji} \partial w_{lk}} &= \frac{1}{4\epsilon^2} \{E(w_{ji} + \epsilon, w_{lk} + \epsilon) - E(w_{ji} + \epsilon, w_{lk} - \epsilon) \\ &\quad - E(w_{ji} - \epsilon, w_{lk} + \epsilon) + E(w_{ji} - \epsilon, w_{lk} - \epsilon)\} + O(\epsilon^2). \end{aligned} \quad (5.90)$$

Again, by using a symmetrical central differences formulation, we ensure that the residual errors are $O(\epsilon^2)$ rather than $O(\epsilon)$. Because there are W^2 elements in the Hessian matrix, and because the evaluation of each element requires four forward propagations each needing $O(W)$ operations (per pattern), we see that this approach will require $O(W^3)$ operations to evaluate the complete Hessian. It therefore has poor scaling properties, although in practice it is very useful as a check on the software implementation of backpropagation methods.

A more efficient version of numerical differentiation can be found by applying central differences to the first derivatives of the error function, which are themselves calculated using backpropagation. This gives

$$\frac{\partial^2 E}{\partial w_{ji} \partial w_{lk}} = \frac{1}{2\epsilon} \left\{ \frac{\partial E}{\partial w_{ji}}(w_{lk} + \epsilon) - \frac{\partial E}{\partial w_{ji}}(w_{lk} - \epsilon) \right\} + O(\epsilon^2). \quad (5.91)$$

Because there are now only W weights to be perturbed, and because the gradients can be evaluated in $O(W)$ steps, we see that this method gives the Hessian in $O(W^2)$ operations.

5.4.5 Exact evaluation of the Hessian

So far, we have considered various approximation schemes for evaluating the Hessian matrix or its inverse. The Hessian can also be evaluated exactly, for a network of arbitrary feed-forward topology, using extension of the technique of back-propagation used to evaluate first derivatives, which shares many of its desirable features including computational efficiency (Bishop, 1991; Bishop, 1992). It can be applied to any differentiable error function that can be expressed as a function of the network outputs and to networks having arbitrary differentiable activation functions. The number of computational steps needed to evaluate the Hessian scales like $O(W^2)$. Similar algorithms have also been considered by Buntine and Weigend (1993).

Here we consider the specific case of a network having two layers of weights, for which the required equations are easily derived. We shall use indices i and i' to denote inputs, indices j and j' to denote hidden units, and indices k and k' to denote outputs. We first define

$$\delta_k = \frac{\partial E_n}{\partial a_k}, \quad M_{kk'} \equiv \frac{\partial^2 E_n}{\partial a_k \partial a_{k'}} \quad (5.92)$$

where E_n is the contribution to the error from data point n . The Hessian matrix for this network can then be considered in three separate blocks as follows.

1. Both weights in the second layer:

$$\frac{\partial^2 E_n}{\partial w_{kj}^{(2)} \partial w_{k'j'}^{(2)}} = z_j z_{j'} M_{kk'}. \quad (5.93)$$

Exercise 5.22

2. Both weights in the first layer:

$$\begin{aligned} \frac{\partial^2 E_n}{\partial w_{ji}^{(1)} \partial w_{j'i'}^{(1)}} &= x_i x_{i'} h''(a_{j'}) I_{jj'} \sum_k w_{kj'}^{(2)} \delta_k \\ &+ x_i x_{i'} h'(a_{j'}) h'(a_j) \sum_k \sum_{k'} w_{k'j'}^{(2)} w_{kj}^{(2)} M_{kk'}. \end{aligned} \quad (5.94)$$

3. One weight in each layer:

$$\frac{\partial^2 E_n}{\partial w_{ji}^{(1)} \partial w_{kj'}^{(2)}} = x_i h'(a_{j'}) \left\{ \delta_k I_{jj'} + z_j \sum_{k'} w_{k'j'}^{(2)} H_{kk'} \right\}. \quad (5.95)$$

Here $I_{jj'}$ is the j, j' element of the identity matrix. If one or both of the weights is a bias term, then the corresponding expressions are obtained simply by setting the appropriate activation(s) to 1. Inclusion of skip-layer connections is straightforward.

Exercise 5.23

5.4.6 Fast multiplication by the Hessian

For many applications of the Hessian, the quantity of interest is not the Hessian matrix \mathbf{H} itself but the product of \mathbf{H} with some vector \mathbf{v} . We have seen that the evaluation of the Hessian takes $O(W^2)$ operations, and it also requires storage that is $O(W^2)$. The vector $\mathbf{v}^T \mathbf{H}$ that we wish to calculate, however, has only W elements, so instead of computing the Hessian as an intermediate step, we can instead try to find an efficient approach to evaluating $\mathbf{v}^T \mathbf{H}$ directly in a way that requires only $O(W)$ operations.

To do this, we first note that

$$\mathbf{v}^T \mathbf{H} = \mathbf{v}^T \nabla(\nabla E) \quad (5.96)$$

where ∇ denotes the gradient operator in weight space. We can then write down the standard forward-propagation and backpropagation equations for the evaluation of ∇E and apply (5.96) to these equations to give a set of forward-propagation and backpropagation equations for the evaluation of $\mathbf{v}^T \mathbf{H}$ (Møller, 1993; Pearlmutter, 1994). This corresponds to acting on the original forward-propagation and backpropagation equations with a differential operator $\mathbf{v}^T \nabla$. Pearlmutter (1994) used the notation $\mathcal{R}\{\cdot\}$ to denote the operator $\mathbf{v}^T \nabla$, and we shall follow this convention. The analysis is straightforward and makes use of the usual rules of differential calculus, together with the result

$$\mathcal{R}\{\mathbf{w}\} = \mathbf{v}. \quad (5.97)$$

The technique is best illustrated with a simple example, and again we choose a two-layer network of the form shown in Figure 5.1, with linear output units and a sum-of-squares error function. As before, we consider the contribution to the error function from one pattern in the data set. The required vector is then obtained as

usual by summing over the contributions from each of the patterns separately. For the two-layer network, the forward-propagation equations are given by

$$a_j = \sum_i w_{ji}x_i \quad (5.98)$$

$$z_j = h(a_j) \quad (5.99)$$

$$y_k = \sum_j w_{kj}z_j. \quad (5.100)$$

We now act on these equations using the $\mathcal{R}\{\cdot\}$ operator to obtain a set of forward propagation equations in the form

$$\mathcal{R}\{a_j\} = \sum_i v_{ji}x_i \quad (5.101)$$

$$\mathcal{R}\{z_j\} = h'(a_j)\mathcal{R}\{a_j\} \quad (5.102)$$

$$\mathcal{R}\{y_k\} = \sum_j w_{kj}\mathcal{R}\{z_j\} + \sum_j v_{kj}z_j \quad (5.103)$$

where v_{ji} is the element of the vector \mathbf{v} that corresponds to the weight w_{ji} . Quantities of the form $\mathcal{R}\{z_j\}$, $\mathcal{R}\{a_j\}$ and $\mathcal{R}\{y_k\}$ are to be regarded as new variables whose values are found using the above equations.

Because we are considering a sum-of-squares error function, we have the following standard backpropagation expressions:

$$\delta_k = y_k - t_k \quad (5.104)$$

$$\delta_j = h'(a_j) \sum_k w_{kj}\delta_k. \quad (5.105)$$

Again, we act on these equations with the $\mathcal{R}\{\cdot\}$ operator to obtain a set of backpropagation equations in the form

$$\mathcal{R}\{\delta_k\} = \mathcal{R}\{y_k\} \quad (5.106)$$

$$\begin{aligned} \mathcal{R}\{\delta_j\} &= h''(a_j)\mathcal{R}\{a_j\} \sum_k w_{kj}\delta_k \\ &\quad + h'(a_j) \sum_k v_{kj}\delta_k + h'(a_j) \sum_k w_{kj}\mathcal{R}\{\delta_k\}. \end{aligned} \quad (5.107)$$

Finally, we have the usual equations for the first derivatives of the error

$$\frac{\partial E}{\partial w_{kj}} = \delta_k z_j \quad (5.108)$$

$$\frac{\partial E}{\partial w_{ji}} = \delta_j x_i \quad (5.109)$$

and acting on these with the $\mathcal{R}\{\cdot\}$ operator, we obtain expressions for the elements of the vector $\mathbf{v}^T \mathbf{H}$

$$\mathcal{R}\left\{\frac{\partial E}{\partial w_{kj}}\right\} = \mathcal{R}\{\delta_k\}z_j + \delta_k \mathcal{R}\{z_j\} \quad (5.110)$$

$$\mathcal{R}\left\{\frac{\partial E}{\partial w_{ji}}\right\} = x_i \mathcal{R}\{\delta_j\}. \quad (5.111)$$

The implementation of this algorithm involves the introduction of additional variables $\mathcal{R}\{a_j\}$, $\mathcal{R}\{z_j\}$ and $\mathcal{R}\{\delta_j\}$ for the hidden units and $\mathcal{R}\{\delta_k\}$ and $\mathcal{R}\{y_k\}$ for the output units. For each input pattern, the values of these quantities can be found using the above results, and the elements of $\mathbf{v}^T \mathbf{H}$ are then given by (5.110) and (5.111). An elegant aspect of this technique is that the equations for evaluating $\mathbf{v}^T \mathbf{H}$ mirror closely those for standard forward and backward propagation, and so the extension of existing software to compute this product is typically straightforward.

If desired, the technique can be used to evaluate the full Hessian matrix by choosing the vector \mathbf{v} to be given successively by a series of unit vectors of the form $(0, 0, \dots, 1, \dots, 0)$ each of which picks out one column of the Hessian. This leads to a formalism that is analytically equivalent to the backpropagation procedure of Bishop (1992), as described in Section 5.4.5, though with some loss of efficiency due to redundant calculations.

5.5. Regularization in Neural Networks

The number of input and outputs units in a neural network is generally determined by the dimensionality of the data set, whereas the number M of hidden units is a free parameter that can be adjusted to give the best predictive performance. Note that M controls the number of parameters (weights and biases) in the network, and so we might expect that in a maximum likelihood setting there will be an optimum value of M that gives the best generalization performance, corresponding to the optimum balance between under-fitting and over-fitting. Figure 5.9 shows an example of the effect of different values of M for the sinusoidal regression problem.

The generalization error, however, is not a simple function of M due to the presence of local minima in the error function, as illustrated in Figure 5.10. Here we see the effect of choosing multiple random initializations for the weight vector for a range of values of M . The overall best validation set performance in this case occurred for a particular solution having $M = 8$. In practice, one approach to choosing M is in fact to plot a graph of the kind shown in Figure 5.10 and then to choose the specific solution having the smallest validation set error.

There are, however, other ways to control the complexity of a neural network model in order to avoid over-fitting. From our discussion of polynomial curve fitting in Chapter 1, we see that an alternative approach is to choose a relatively large value for M and then to control complexity by the addition of a regularization term to the error function. The simplest regularizer is the quadratic, giving a regularized error



Figure 5.9 Examples of two-layer networks trained on 10 data points drawn from the sinusoidal data set. The graphs show the result of fitting networks having $M = 1, 3$ and 10 hidden units, respectively, by minimizing a sum-of-squares error function using a scaled conjugate-gradient algorithm.

of the form

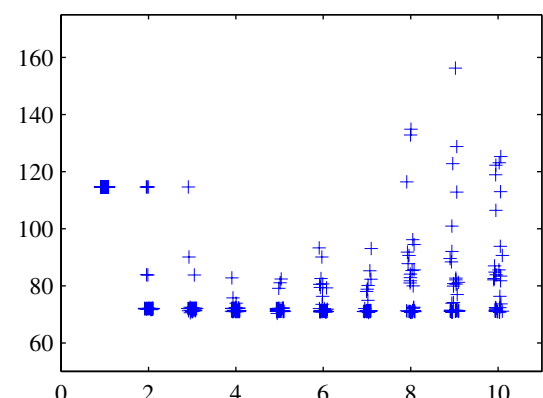
$$\tilde{E}(\mathbf{w}) = E(\mathbf{w}) + \frac{\lambda}{2} \mathbf{w}^T \mathbf{w}. \quad (5.112)$$

This regularizer is also known as *weight decay* and has been discussed at length in Chapter 3. The effective model complexity is then determined by the choice of the regularization coefficient λ . As we have seen previously, this regularizer can be interpreted as the negative logarithm of a zero-mean Gaussian prior distribution over the weight vector \mathbf{w} .

5.5.1 Consistent Gaussian priors

One of the limitations of simple weight decay in the form (5.112) is that is inconsistent with certain scaling properties of network mappings. To illustrate this, consider a multilayer perceptron network having two layers of weights and linear output units, which performs a mapping from a set of input variables $\{x_i\}$ to a set of output variables $\{y_k\}$. The activations of the hidden units in the first hidden layer

Figure 5.10 Plot of the sum-of-squares test-set error for the polynomial data set versus the number of hidden units in the network, with 30 random starts for each network size, showing the effect of local minima. For each new start, the weight vector was initialized by sampling from an isotropic Gaussian distribution having a mean of zero and a variance of 10.



take the form

$$z_j = h \left(\sum_i w_{ji} x_i + w_{j0} \right) \quad (5.113)$$

while the activations of the output units are given by

$$y_k = \sum_j w_{kj} z_j + w_{k0}. \quad (5.114)$$

Suppose we perform a linear transformation of the input data of the form

$$x_i \rightarrow \tilde{x}_i = ax_i + b. \quad (5.115)$$

Then we can arrange for the mapping performed by the network to be unchanged by making a corresponding linear transformation of the weights and biases from the inputs to the units in the hidden layer of the form

$$w_{ji} \rightarrow \tilde{w}_{ji} = \frac{1}{a} w_{ji} \quad (5.116)$$

$$w_{j0} \rightarrow \tilde{w}_{j0} = w_{j0} - \frac{b}{a} \sum_i w_{ji}. \quad (5.117)$$

Similarly, a linear transformation of the output variables of the network of the form

$$y_k \rightarrow \tilde{y}_k = cy_k + d \quad (5.118)$$

can be achieved by making a transformation of the second-layer weights and biases using

$$w_{kj} \rightarrow \tilde{w}_{kj} = cw_{kj} \quad (5.119)$$

$$w_{k0} \rightarrow \tilde{w}_{k0} = cw_{k0} + d. \quad (5.120)$$

If we train one network using the original data and one network using data for which the input and/or target variables are transformed by one of the above linear transformations, then consistency requires that we should obtain equivalent networks that differ only by the linear transformation of the weights as given. Any regularizer should be consistent with this property, otherwise it arbitrarily favours one solution over another, equivalent one. Clearly, simple weight decay (5.112), that treats all weights and biases on an equal footing, does not satisfy this property.

We therefore look for a regularizer which is invariant under the linear transformations (5.116), (5.117), (5.119) and (5.120). These require that the regularizer should be invariant to re-scaling of the weights and to shifts of the biases. Such a regularizer is given by

$$\frac{\lambda_1}{2} \sum_{w \in \mathcal{W}_1} w^2 + \frac{\lambda_2}{2} \sum_{w \in \mathcal{W}_2} w^2 \quad (5.121)$$

where \mathcal{W}_1 denotes the set of weights in the first layer, \mathcal{W}_2 denotes the set of weights in the second layer, and biases are excluded from the summations. This regularizer

Exercise 5.24

will remain unchanged under the weight transformations provided the regularization parameters are re-scaled using $\lambda_1 \rightarrow a^{1/2}\lambda_1$ and $\lambda_2 \rightarrow c^{-1/2}\lambda_2$.

The regularizer (5.121) corresponds to a prior of the form

$$p(\mathbf{w}|\alpha_1, \alpha_2) \propto \exp\left(-\frac{\alpha_1}{2} \sum_{w \in \mathcal{W}_1} w^2 - \frac{\alpha_2}{2} \sum_{w \in \mathcal{W}_2} w^2\right). \quad (5.122)$$

Note that priors of this form are *improper* (they cannot be normalized) because the bias parameters are unconstrained. The use of improper priors can lead to difficulties in selecting regularization coefficients and in model comparison within the Bayesian framework, because the corresponding evidence is zero. It is therefore common to include separate priors for the biases (which then break shift invariance) having their own hyperparameters. We can illustrate the effect of the resulting four hyperparameters by drawing samples from the prior and plotting the corresponding network functions, as shown in Figure 5.11.

More generally, we can consider priors in which the weights are divided into any number of groups \mathcal{W}_k so that

$$p(\mathbf{w}) \propto \exp\left(-\frac{1}{2} \sum_k \alpha_k \|\mathbf{w}\|_k^2\right) \quad (5.123)$$

where

$$\|\mathbf{w}\|_k^2 = \sum_{j \in \mathcal{W}_k} w_j^2. \quad (5.124)$$

As a special case of this prior, if we choose the groups to correspond to the sets of weights associated with each of the input units, and we optimize the marginal likelihood with respect to the corresponding parameters α_k , we obtain *automatic relevance determination* as discussed in Section 7.2.2.

5.5.2 Early stopping

An alternative to regularization as a way of controlling the effective complexity of a network is the procedure of *early stopping*. The training of nonlinear network models corresponds to an iterative reduction of the error function defined with respect to a set of training data. For many of the optimization algorithms used for network training, such as conjugate gradients, the error is a nonincreasing function of the iteration index. However, the error measured with respect to independent data, generally called a validation set, often shows a decrease at first, followed by an increase as the network starts to over-fit. Training can therefore be stopped at the point of smallest error with respect to the validation data set, as indicated in Figure 5.12, in order to obtain a network having good generalization performance.

The behaviour of the network in this case is sometimes explained qualitatively in terms of the effective number of degrees of freedom in the network, in which this number starts out small and then grows during the training process, corresponding to a steady increase in the effective complexity of the model. Halting training before



Figure 5.11 Illustration of the effect of the hyperparameters governing the prior distribution over weights and biases in a two-layer network having a single input, a single linear output, and 12 hidden units having ‘tanh’ activation functions. The priors are governed by four hyperparameters α_1^b , α_1^w , α_2^b , and α_2^w , which represent the precisions of the Gaussian distributions of the first-layer biases, first-layer weights, second-layer biases, and second-layer weights, respectively. We see that the parameter α_2^w governs the vertical scale of functions (note the different vertical axis ranges on the top two diagrams), α_1^w governs the horizontal scale of variations in the function values, and α_1^b governs the horizontal range over which variations occur. The parameter α_2^b , whose effect is not illustrated here, governs the range of vertical offsets of the functions.

a minimum of the training error has been reached then represents a way of limiting the effective network complexity.

In the case of a quadratic error function, we can verify this insight, and show that early stopping should exhibit similar behaviour to regularization using a simple weight-decay term. This can be understood from Figure 5.13, in which the axes in weight space have been rotated to be parallel to the eigenvectors of the Hessian matrix. If, in the absence of weight decay, the weight vector starts at the origin and proceeds during training along a path that follows the local negative gradient vector, then the weight vector will move initially parallel to the w_2 axis through a point corresponding roughly to \tilde{w} and then move towards the minimum of the error function w_{ML} . This follows from the shape of the error surface and the widely differing eigenvalues of the Hessian. Stopping at a point near \tilde{w} is therefore similar to weight decay. The relationship between early stopping and weight decay can be made quantitative, thereby showing that the quantity $\tau\eta$ (where τ is the iteration index, and η is the learning rate parameter) plays the role of the reciprocal of the regularization

Exercise 5.25



Figure 5.12 An illustration of the behaviour of training set error (left) and validation set error (right) during a typical training session, as a function of the iteration step, for the sinusoidal data set. The goal of achieving the best generalization performance suggests that training should be stopped at the point shown by the vertical dashed lines, corresponding to the minimum of the validation set error.

parameter λ . The effective number of parameters in the network therefore grows during the course of training.

5.5.3 Invariances

In many applications of pattern recognition, it is known that predictions should be unchanged, or *invariant*, under one or more transformations of the input variables. For example, in the classification of objects in two-dimensional images, such as handwritten digits, a particular object should be assigned the same classification irrespective of its position within the image (*translation invariance*) or of its size (*scale invariance*). Such transformations produce significant changes in the raw data, expressed in terms of the intensities at each of the pixels in the image, and yet should give rise to the same output from the classification system. Similarly in speech recognition, small levels of nonlinear warping along the time axis, which preserve temporal ordering, should not change the interpretation of the signal.

If sufficiently large numbers of training patterns are available, then an adaptive model such as a neural network can learn the invariance, at least approximately. This involves including within the training set a sufficiently large number of examples of the effects of the various transformations. Thus, for translation invariance in an image, the training set should include examples of objects at many different positions.

This approach may be impractical, however, if the number of training examples is limited, or if there are several invariants (because the number of combinations of transformations grows exponentially with the number of such transformations). We therefore seek alternative approaches for encouraging an adaptive model to exhibit the required invariances. These can broadly be divided into four categories:

1. The training set is augmented using replicas of the training patterns, transformed according to the desired invariances. For instance, in our digit recognition example, we could make multiple copies of each example in which the

Figure 5.13 A schematic illustration of why early stopping can give similar results to weight decay in the case of a quadratic error function. The ellipse shows a contour of constant error, and \mathbf{w}_{ML} denotes the minimum of the error function. If the weight vector starts at the origin and moves according to the local negative gradient direction, then it will follow the path shown by the curve. By stopping training early, a weight vector $\tilde{\mathbf{w}}$ is found that is qualitatively similar to that obtained with a simple weight-decay regularizer and training to the minimum of the regularized error, as can be seen by comparing with Figure 3.15.



digit is shifted to a different position in each image.

2. A regularization term is added to the error function that penalizes changes in the model output when the input is transformed. This leads to the technique of *tangent propagation*, discussed in Section 5.5.4.
3. Invariance is built into the pre-processing by extracting features that are invariant under the required transformations. Any subsequent regression or classification system that uses such features as inputs will necessarily also respect these invariances.
4. The final option is to build the invariance properties into the structure of a neural network (or into the definition of a kernel function in the case of techniques such as the relevance vector machine). One way to achieve this is through the use of local receptive fields and shared weights, as discussed in the context of convolutional neural networks in Section 5.5.6.

Approach 1 is often relatively easy to implement and can be used to encourage complex invariances such as those illustrated in Figure 5.14. For sequential training algorithms, this can be done by transforming each input pattern before it is presented to the model so that, if the patterns are being recycled, a different transformation (drawn from an appropriate distribution) is added each time. For batch methods, a similar effect can be achieved by replicating each data point a number of times and transforming each copy independently. The use of such augmented data can lead to significant improvements in generalization (Simard *et al.*, 2003), although it can also be computationally costly.

Approach 2 leaves the data set unchanged but modifies the error function through the addition of a regularizer. In Section 5.5.5, we shall show that this approach is closely related to approach 2.



Figure 5.14 Illustration of the synthetic warping of a handwritten digit. The original image is shown on the left. On the right, the top row shows three examples of warped digits, with the corresponding displacement fields shown on the bottom row. These displacement fields are generated by sampling random displacements $\Delta x, \Delta y \in (0, 1)$ at each pixel and then smoothing by convolution with Gaussians of width 0.01, 30 and 60 respectively.

One advantage of approach 3 is that it can correctly extrapolate well beyond the range of transformations included in the training set. However, it can be difficult to find hand-crafted features with the required invariances that do not also discard information that can be useful for discrimination.

5.5.4 Tangent propagation

We can use regularization to encourage models to be invariant to transformations of the input through the technique of *tangent propagation* (Simard *et al.*, 1992). Consider the effect of a transformation on a particular input vector x_n . Provided the transformation is continuous (such as translation or rotation, but not mirror reflection for instance), then the transformed pattern will sweep out a manifold \mathcal{M} within the D -dimensional input space. This is illustrated in Figure 5.15, for the case of $D = 2$ for simplicity. Suppose the transformation is governed by a single parameter ξ (which might be rotation angle for instance). Then the subspace \mathcal{M} swept out by x_n

Figure 5.15 Illustration of a two-dimensional input space showing the effect of a continuous transformation on a particular input vector x_n . A one-dimensional transformation, parameterized by the continuous variable ξ , applied to x_n causes it to sweep out a one-dimensional manifold \mathcal{M} . Locally, the effect of the transformation can be approximated by the tangent vector τ_n .



will be one-dimensional, and will be parameterized by ξ . Let the vector that results from acting on \mathbf{x}_n by this transformation be denoted by $\mathbf{s}(\mathbf{x}_n, \xi)$, which is defined so that $\mathbf{s}(\mathbf{x}, 0) = \mathbf{x}$. Then the tangent to the curve \mathcal{M} is given by the directional derivative $\boldsymbol{\tau} = \partial \mathbf{s} / \partial \xi$, and the tangent vector at the point \mathbf{x}_n is given by

$$\boldsymbol{\tau}_n = \left. \frac{\partial \mathbf{s}(\mathbf{x}_n, \xi)}{\partial \xi} \right|_{\xi=0}. \quad (5.125)$$

Under a transformation of the input vector, the network output vector will, in general, change. The derivative of output k with respect to ξ is given by

$$\left. \frac{\partial y_k}{\partial \xi} \right|_{\xi=0} = \sum_{i=1}^D \left. \frac{\partial y_k}{\partial x_i} \frac{\partial x_i}{\partial \xi} \right|_{\xi=0} = \sum_{i=1}^D J_{ki} \tau_i \quad (5.126)$$

where J_{ki} is the (k, i) element of the Jacobian matrix \mathbf{J} , as discussed in Section 5.3.4. The result (5.126) can be used to modify the standard error function, so as to encourage local invariance in the neighbourhood of the data points, by the addition to the original error function E of a regularization function Ω to give a total error function of the form

$$\tilde{E} = E + \lambda \Omega \quad (5.127)$$

where λ is a regularization coefficient and

$$\Omega = \frac{1}{2} \sum_n \sum_k \left(\left. \frac{\partial y_{nk}}{\partial \xi} \right|_{\xi=0} \right)^2 = \frac{1}{2} \sum_n \sum_k \left(\sum_{i=1}^D J_{nki} \tau_{ni} \right)^2. \quad (5.128)$$

The regularization function will be zero when the network mapping function is invariant under the transformation in the neighbourhood of each pattern vector, and the value of the parameter λ determines the balance between fitting the training data and learning the invariance property.

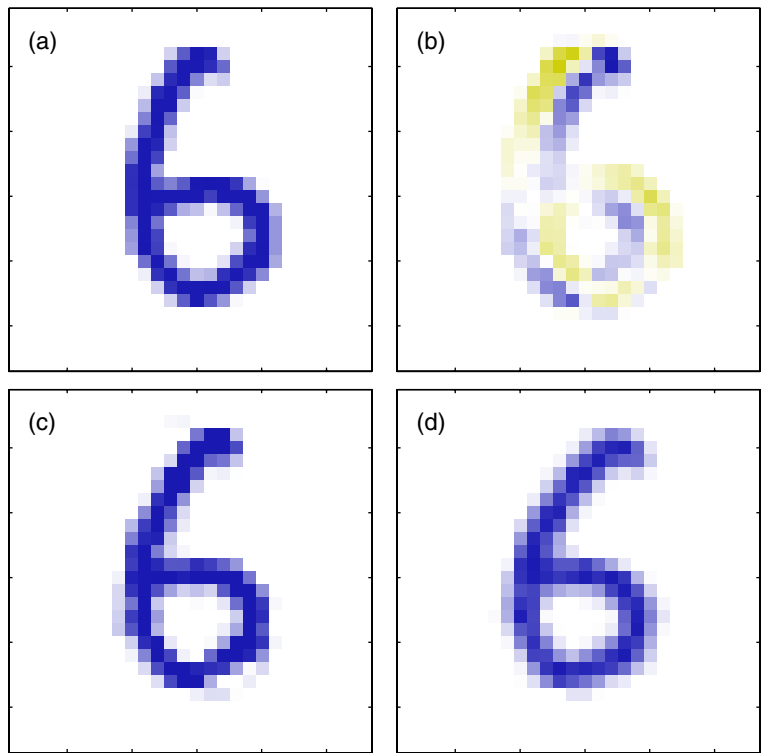
In a practical implementation, the tangent vector $\boldsymbol{\tau}_n$ can be approximated using finite differences, by subtracting the original vector \mathbf{x}_n from the corresponding vector after transformation using a small value of ξ , and then dividing by ξ . This is illustrated in Figure 5.16.

The regularization function depends on the network weights through the Jacobian \mathbf{J} . A backpropagation formalism for computing the derivatives of the regularizer with respect to the network weights is easily obtained by extension of the techniques introduced in Section 5.3.

If the transformation is governed by L parameters (e.g., $L = 3$ for the case of translations combined with in-plane rotations in a two-dimensional image), then the manifold \mathcal{M} will have dimensionality L , and the corresponding regularizer is given by the sum of terms of the form (5.128), one for each transformation. If several transformations are considered at the same time, and the network mapping is made invariant to each separately, then it will be (locally) invariant to combinations of the transformations (Simard *et al.*, 1992).

Exercise 5.26

Figure 5.16 Illustration showing (a) the original image \mathbf{x} of a handwritten digit, (b) the tangent vector τ corresponding to an infinitesimal clockwise rotation, (c) the result of adding a small contribution from the tangent vector to the original image giving $\mathbf{x} + \epsilon\tau$ with $\epsilon = 15$ degrees, and (d) the true image rotated for comparison.



A related technique, called *tangent distance*, can be used to build invariance properties into distance-based methods such as nearest-neighbour classifiers (Simard *et al.*, 1993).

5.5.5 Training with transformed data

We have seen that one way to encourage invariance of a model to a set of transformations is to expand the training set using transformed versions of the original input patterns. Here we show that this approach is closely related to the technique of tangent propagation (Bishop, 1995b; Leen, 1995).

As in Section 5.5.4, we shall consider a transformation governed by a single parameter ξ and described by the function $s(\mathbf{x}, \xi)$, with $s(\mathbf{x}, 0) = \mathbf{x}$. We shall also consider a sum-of-squares error function. The error function for untransformed inputs can be written (in the infinite data set limit) in the form

$$E = \frac{1}{2} \iint \{y(\mathbf{x}) - t\}^2 p(t|\mathbf{x}) p(\mathbf{x}) \, d\mathbf{x} \, dt \quad (5.129)$$

as discussed in Section 1.5.5. Here we have considered a network having a single output, in order to keep the notation uncluttered. If we now consider an infinite number of copies of each data point, each of which is perturbed by the transformation

in which the parameter ξ is drawn from a distribution $p(\xi)$, then the error function defined over this expanded data set can be written as

$$\tilde{E} = \frac{1}{2} \iint \{y(\mathbf{s}(\mathbf{x}, \xi)) - t\}^2 p(t|\mathbf{x}) p(\mathbf{x}) p(\xi) d\mathbf{x} dt d\xi. \quad (5.130)$$

We now assume that the distribution $p(\xi)$ has zero mean with small variance, so that we are only considering small transformations of the original input vectors. We can then expand the transformation function as a Taylor series in powers of ξ to give

$$\begin{aligned} \mathbf{s}(\mathbf{x}, \xi) &= \mathbf{s}(\mathbf{x}, 0) + \xi \frac{\partial}{\partial \xi} \mathbf{s}(\mathbf{x}, \xi) \Big|_{\xi=0} + \frac{\xi^2}{2} \frac{\partial^2}{\partial \xi^2} \mathbf{s}(\mathbf{x}, \xi) \Big|_{\xi=0} + O(\xi^3) \\ &= \mathbf{x} + \xi \boldsymbol{\tau} + \frac{1}{2} \xi^2 \boldsymbol{\tau}' + O(\xi^3) \end{aligned}$$

where $\boldsymbol{\tau}'$ denotes the second derivative of $\mathbf{s}(\mathbf{x}, \xi)$ with respect to ξ evaluated at $\xi = 0$. This allows us to expand the model function to give

$$y(\mathbf{s}(\mathbf{x}, \xi)) = y(\mathbf{x}) + \xi \boldsymbol{\tau}^T \nabla y(\mathbf{x}) + \frac{\xi^2}{2} \left[(\boldsymbol{\tau}')^T \nabla y(\mathbf{x}) + \boldsymbol{\tau}^T \nabla \nabla y(\mathbf{x}) \boldsymbol{\tau} \right] + O(\xi^3).$$

Substituting into the mean error function (5.130) and expanding, we then have

$$\begin{aligned} \tilde{E} &= \frac{1}{2} \iint \{y(\mathbf{x}) - t\}^2 p(t|\mathbf{x}) p(\mathbf{x}) d\mathbf{x} dt \\ &+ \mathbb{E}[\xi] \iint \{y(\mathbf{x}) - t\} \boldsymbol{\tau}^T \nabla y(\mathbf{x}) p(t|\mathbf{x}) p(\mathbf{x}) d\mathbf{x} dt \\ &+ \mathbb{E}[\xi^2] \iint \left[\{y(\mathbf{x}) - t\} \frac{1}{2} \left\{ (\boldsymbol{\tau}')^T \nabla y(\mathbf{x}) + \boldsymbol{\tau}^T \nabla \nabla y(\mathbf{x}) \boldsymbol{\tau} \right\} \right. \\ &\quad \left. + (\boldsymbol{\tau}^T \nabla y(\mathbf{x}))^2 \right] p(t|\mathbf{x}) p(\mathbf{x}) d\mathbf{x} dt + O(\xi^3). \end{aligned}$$

Because the distribution of transformations has zero mean we have $\mathbb{E}[\xi] = 0$. Also, we shall denote $\mathbb{E}[\xi^2]$ by λ . Omitting terms of $O(\xi^3)$, the average error function then becomes

$$\tilde{E} = E + \lambda \Omega \quad (5.131)$$

where E is the original sum-of-squares error, and the regularization term Ω takes the form

$$\begin{aligned} \Omega &= \int \left[\{y(\mathbf{x}) - \mathbb{E}[t|\mathbf{x}]\} \frac{1}{2} \left\{ (\boldsymbol{\tau}')^T \nabla y(\mathbf{x}) + \boldsymbol{\tau}^T \nabla \nabla y(\mathbf{x}) \boldsymbol{\tau} \right\} \right. \\ &\quad \left. + (\boldsymbol{\tau}^T \nabla y(\mathbf{x}))^2 \right] p(\mathbf{x}) d\mathbf{x} \end{aligned} \quad (5.132)$$

in which we have performed the integration over t .

We can further simplify this regularization term as follows. In Section 1.5.5 we saw that the function that minimizes the sum-of-squares error is given by the conditional average $\mathbb{E}[t|\mathbf{x}]$ of the target values t . From (5.131) we see that the regularized error will equal the unregularized sum-of-squares plus terms which are $O(\xi)$, and so the network function that minimizes the total error will have the form

$$y(\mathbf{x}) = \mathbb{E}[t|\mathbf{x}] + O(\xi). \quad (5.133)$$

Thus, to leading order in ξ , the first term in the regularizer vanishes and we are left with

$$\Omega = \frac{1}{2} \int (\boldsymbol{\tau}^T \nabla y(\mathbf{x}))^2 p(\mathbf{x}) d\mathbf{x} \quad (5.134)$$

which is equivalent to the tangent propagation regularizer (5.128).

If we consider the special case in which the transformation of the inputs simply consists of the addition of random noise, so that $\mathbf{x} \rightarrow \mathbf{x} + \boldsymbol{\xi}$, then the regularizer takes the form

$$\Omega = \frac{1}{2} \int \|\nabla y(\mathbf{x})\|^2 p(\mathbf{x}) d\mathbf{x} \quad (5.135)$$

which is known as *Tikhonov* regularization (Tikhonov and Arsenin, 1977; Bishop, 1995b). Derivatives of this regularizer with respect to the network weights can be found using an extended backpropagation algorithm (Bishop, 1993). We see that, for small noise amplitudes, Tikhonov regularization is related to the addition of random noise to the inputs, which has been shown to improve generalization in appropriate circumstances (Sietsma and Dow, 1991).

5.5.6 Convolutional networks

Another approach to creating models that are invariant to certain transformation of the inputs is to build the invariance properties into the structure of a neural network. This is the basis for the *convolutional neural network* (Le Cun *et al.*, 1989; LeCun *et al.*, 1998), which has been widely applied to image data.

Consider the specific task of recognizing handwritten digits. Each input image comprises a set of pixel intensity values, and the desired output is a posterior probability distribution over the ten digit classes. We know that the identity of the digit is invariant under translations and scaling as well as (small) rotations. Furthermore, the network must also exhibit invariance to more subtle transformations such as elastic deformations of the kind illustrated in Figure 5.14. One simple approach would be to treat the image as the input to a fully connected network, such as the kind shown in Figure 5.1. Given a sufficiently large training set, such a network could in principle yield a good solution to this problem and would learn the appropriate invariances by example.

However, this approach ignores a key property of images, which is that nearby pixels are more strongly correlated than more distant pixels. Many of the modern approaches to computer vision exploit this property by extracting *local* features that depend only on small subregions of the image. Information from such features can then be merged in later stages of processing in order to detect higher-order features

Exercise 5.27



Figure 5.17 Diagram illustrating part of a convolutional neural network, showing a layer of convolutional units followed by a layer of subsampling units. Several successive pairs of such layers may be used.

and ultimately to yield information about the image as whole. Also, local features that are useful in one region of the image are likely to be useful in other regions of the image, for instance if the object of interest is translated.

These notions are incorporated into convolutional neural networks through three mechanisms: (i) local receptive fields, (ii) weight sharing, and (iii) subsampling. The structure of a convolutional network is illustrated in Figure 5.17. In the convolutional layer the units are organized into planes, each of which is called a *feature map*. Units in a feature map each take inputs only from a small subregion of the image, and all of the units in a feature map are constrained to share the same weight values. For instance, a feature map might consist of 100 units arranged in a 10×10 grid, with each unit taking inputs from a 5×5 pixel patch of the image. The whole feature map therefore has 25 adjustable weight parameters plus one adjustable bias parameter. Input values from a patch are linearly combined using the weights and the bias, and the result transformed by a sigmoidal nonlinearity using (5.1). If we think of the units as feature detectors, then all of the units in a feature map detect the same pattern but at different locations in the input image. Due to the weight sharing, the evaluation of the activations of these units is equivalent to a convolution of the image pixel intensities with a ‘kernel’ comprising the weight parameters. If the input image is shifted, the activations of the feature map will be shifted by the same amount but will otherwise be unchanged. This provides the basis for the (approximate) invariance of

the network outputs to translations and distortions of the input image. Because we will typically need to detect multiple features in order to build an effective model, there will generally be multiple feature maps in the convolutional layer, each having its own set of weight and bias parameters.

The outputs of the convolutional units form the inputs to the subsampling layer of the network. For each feature map in the convolutional layer, there is a plane of units in the subsampling layer and each unit takes inputs from a small receptive field in the corresponding feature map of the convolutional layer. These units perform subsampling. For instance, each subsampling unit might take inputs from a 2×2 unit region in the corresponding feature map and would compute the average of those inputs, multiplied by an adaptive weight with the addition of an adaptive bias parameter, and then transformed using a sigmoidal nonlinear activation function. The receptive fields are chosen to be contiguous and nonoverlapping so that there are half the number of rows and columns in the subsampling layer compared with the convolutional layer. In this way, the response of a unit in the subsampling layer will be relatively insensitive to small shifts of the image in the corresponding regions of the input space.

In a practical architecture, there may be several pairs of convolutional and subsampling layers. At each stage there is a larger degree of invariance to input transformations compared to the previous layer. There may be several feature maps in a given convolutional layer for each plane of units in the previous subsampling layer, so that the gradual reduction in spatial resolution is then compensated by an increasing number of features. The final layer of the network would typically be a fully connected, fully adaptive layer, with a softmax output nonlinearity in the case of multiclass classification.

The whole network can be trained by error minimization using backpropagation to evaluate the gradient of the error function. This involves a slight modification of the usual backpropagation algorithm to ensure that the shared-weight constraints are satisfied. Due to the use of local receptive fields, the number of weights in the network is smaller than if the network were fully connected. Furthermore, the number of independent parameters to be learned from the data is much smaller still, due to the substantial numbers of constraints on the weights.

Exercise 5.28

5.5.7 Soft weight sharing

One way to reduce the effective complexity of a network with a large number of weights is to constrain weights within certain groups to be equal. This is the technique of weight sharing that was discussed in Section 5.5.6 as a way of building translation invariance into networks used for image interpretation. It is only applicable, however, to particular problems in which the form of the constraints can be specified in advance. Here we consider a form of *soft weight sharing* (Nowlan and Hinton, 1992) in which the hard constraint of equal weights is replaced by a form of regularization in which groups of weights are encouraged to have similar values. Furthermore, the division of weights into groups, the mean weight value for each group, and the spread of values within the groups are all determined as part of the learning process.

Section 2.3.9

Recall that the simple weight decay regularizer, given in (5.112), can be viewed as the negative log of a Gaussian prior distribution over the weights. We can encourage the weight values to form several groups, rather than just one group, by considering instead a probability distribution that is a *mixture* of Gaussians. The centres and variances of the Gaussian components, as well as the mixing coefficients, will be considered as adjustable parameters to be determined as part of the learning process. Thus, we have a probability density of the form

$$p(\mathbf{w}) = \prod_i p(w_i) \quad (5.136)$$

where

$$p(w_i) = \sum_{j=1}^M \pi_j \mathcal{N}(w_i | \mu_j, \sigma_j^2) \quad (5.137)$$

and π_j are the mixing coefficients. Taking the negative logarithm then leads to a regularization function of the form

$$\Omega(\mathbf{w}) = - \sum_i \ln \left(\sum_{j=1}^M \pi_j \mathcal{N}(w_i | \mu_j, \sigma_j^2) \right). \quad (5.138)$$

The total error function is then given by

$$\tilde{E}(\mathbf{w}) = E(\mathbf{w}) + \lambda \Omega(\mathbf{w}) \quad (5.139)$$

where λ is the regularization coefficient. This error is minimized both with respect to the weights w_i and with respect to the parameters $\{\pi_j, \mu_j, \sigma_j\}$ of the mixture model. If the weights were constant, then the parameters of the mixture model could be determined by using the EM algorithm discussed in Chapter 9. However, the distribution of weights is itself evolving during the learning process, and so to avoid numerical instability, a joint optimization is performed simultaneously over the weights and the mixture-model parameters. This can be done using a standard optimization algorithm such as conjugate gradients or quasi-Newton methods.

In order to minimize the total error function, it is necessary to be able to evaluate its derivatives with respect to the various adjustable parameters. To do this it is convenient to regard the $\{\pi_j\}$ as *prior* probabilities and to introduce the corresponding posterior probabilities which, following (2.192), are given by Bayes' theorem in the form

$$\gamma_j(w) = \frac{\pi_j \mathcal{N}(w | \mu_j, \sigma_j^2)}{\sum_k \pi_k \mathcal{N}(w | \mu_k, \sigma_k^2)}. \quad (5.140)$$

Exercise 5.29

The derivatives of the total error function with respect to the weights are then given by

$$\frac{\partial \tilde{E}}{\partial w_i} = \frac{\partial E}{\partial w_i} + \lambda \sum_j \gamma_j(w_i) \frac{(w_i - \mu_j)}{\sigma_j^2}. \quad (5.141)$$

The effect of the regularization term is therefore to pull each weight towards the centre of the j^{th} Gaussian, with a force proportional to the posterior probability of that Gaussian for the given weight. This is precisely the kind of effect that we are seeking.

Derivatives of the error with respect to the centres of the Gaussians are also easily computed to give

$$\frac{\partial \tilde{E}}{\partial \mu_j} = \lambda \sum_i \gamma_j(w_i) \frac{(\mu_i - w_j)}{\sigma_j^2} \quad (5.142)$$

which has a simple intuitive interpretation, because it pushes μ_j towards an average of the weight values, weighted by the posterior probabilities that the respective weight parameters were generated by component j . Similarly, the derivatives with respect to the variances are given by

$$\frac{\partial \tilde{E}}{\partial \sigma_j} = \lambda \sum_i \gamma_j(w_i) \left(\frac{1}{\sigma_j} - \frac{(w_i - \mu_j)^2}{\sigma_j^3} \right) \quad (5.143)$$

which drives σ_j towards the weighted average of the squared deviations of the weights around the corresponding centre μ_j , where the weighting coefficients are again given by the posterior probability that each weight is generated by component j . Note that in a practical implementation, new variables η_j defined by

$$\sigma_j^2 = \exp(\eta_j) \quad (5.144)$$

are introduced, and the minimization is performed with respect to the η_j . This ensures that the parameters σ_j remain positive. It also has the effect of discouraging pathological solutions in which one or more of the σ_j goes to zero, corresponding to a Gaussian component collapsing onto one of the weight parameter values. Such solutions are discussed in more detail in the context of Gaussian mixture models in Section 9.2.1.

For the derivatives with respect to the mixing coefficients π_j , we need to take account of the constraints

$$\sum_j \pi_j = 1, \quad 0 \leq \pi_i \leq 1 \quad (5.145)$$

which follow from the interpretation of the π_j as prior probabilities. This can be done by expressing the mixing coefficients in terms of a set of auxiliary variables $\{\eta_j\}$ using the *softmax* function given by

$$\pi_j = \frac{\exp(\eta_j)}{\sum_{k=1}^M \exp(\eta_k)}. \quad (5.146)$$

The derivatives of the regularized error function with respect to the $\{\eta_j\}$ then take the form

Exercise 5.30

Exercise 5.31

Exercise 5.32

Figure 5.18 The left figure shows a two-link robot arm, in which the Cartesian coordinates (x_1, x_2) of the end effector are determined uniquely by the two joint angles θ_1 and θ_2 and the (fixed) lengths L_1 and L_2 of the arms. This is known as the *forward kinematics* of the arm. In practice, we have to find the joint angles that will give rise to a desired end effector position and, as shown in the right figure, this *inverse kinematics* has two solutions corresponding to ‘elbow up’ and ‘elbow down’.



$$\frac{\partial \tilde{E}}{\partial \eta_j} = \sum_i \{\pi_j - \gamma_j(w_i)\}. \quad (5.147)$$

We see that π_j is therefore driven towards the average posterior probability for component j .

5.6. Mixture Density Networks

The goal of supervised learning is to model a conditional distribution $p(\mathbf{t}|\mathbf{x})$, which for many simple regression problems is chosen to be Gaussian. However, practical machine learning problems can often have significantly non-Gaussian distributions. These can arise, for example, with *inverse problems* in which the distribution can be multimodal, in which case the Gaussian assumption can lead to very poor predictions.

Exercise 5.33

As a simple example of an inverse problem, consider the kinematics of a robot arm, as illustrated in Figure 5.18. The *forward problem* involves finding the end effector position given the joint angles and has a unique solution. However, in practice we wish to move the end effector of the robot to a specific position, and to do this we must set appropriate joint angles. We therefore need to solve the inverse problem, which has two solutions as seen in Figure 5.18.

Forward problems often correspond to causality in a physical system and generally have a unique solution. For instance, a specific pattern of symptoms in the human body may be caused by the presence of a particular disease. In pattern recognition, however, we typically have to solve an inverse problem, such as trying to predict the presence of a disease given a set of symptoms. If the forward problem involves a many-to-one mapping, then the inverse problem will have multiple solutions. For instance, several different diseases may result in the same symptoms.

In the robotics example, the kinematics is defined by geometrical equations, and the multimodality is readily apparent. However, in many machine learning problems the presence of multimodality, particularly in problems involving spaces of high dimensionality, can be less obvious. For tutorial purposes, however, we shall consider a simple toy problem for which we can easily visualize the multimodality. Data for this problem is generated by sampling a variable x uniformly over the interval $(0, 1)$, to give a set of values $\{x_n\}$, and the corresponding target values t_n are obtained

Figure 5.19 On the left is the data set for a simple ‘forward problem’ in which the red curve shows the result of fitting a two-layer neural network by minimizing the sum-of-squares error function. The corresponding inverse problem, shown on the right, is obtained by exchanging the roles of x and t . Here the same network trained again by minimizing the sum-of-squares error function gives a very poor fit to the data due to the multimodality of the data set.



by computing the function $x_n + 0.3 \sin(2\pi x_n)$ and then adding uniform noise over the interval $(-0.1, 0.1)$. The inverse problem is then obtained by keeping the same data points but exchanging the roles of x and t . Figure 5.19 shows the data sets for the forward and inverse problems, along with the results of fitting two-layer neural networks having 6 hidden units and a single linear output unit by minimizing a sum-of-squares error function. Least squares corresponds to maximum likelihood under a Gaussian assumption. We see that this leads to a very poor model for the highly non-Gaussian inverse problem.

We therefore seek a general framework for modelling conditional probability distributions. This can be achieved by using a mixture model for $p(t|x)$ in which both the mixing coefficients as well as the component densities are flexible functions of the input vector x , giving rise to the *mixture density network*. For any given value of x , the mixture model provides a general formalism for modelling an arbitrary conditional density function $p(t|x)$. Provided we consider a sufficiently flexible network, we then have a framework for approximating arbitrary conditional distributions.

Here we shall develop the model explicitly for Gaussian components, so that

$$p(t|x) = \sum_{k=1}^K \pi_k(x) \mathcal{N}(t|\mu_k(x), \sigma_k^2(x)). \quad (5.148)$$

This is an example of a *heteroscedastic* model since the noise variance on the data is a function of the input vector x . Instead of Gaussians, we can use other distributions for the components, such as Bernoulli distributions if the target variables are binary rather than continuous. We have also specialized to the case of isotropic covariances for the components, although the mixture density network can readily be extended to allow for general covariance matrices by representing the covariances using a Cholesky factorization (Williams, 1996). Even with isotropic components, the conditional distribution $p(t|x)$ does not assume factorization with respect to the components of t (in contrast to the standard sum-of-squares regression model) as a consequence of the mixture distribution.

We now take the various parameters of the mixture model, namely the mixing coefficients $\pi_k(x)$, the means $\mu_k(x)$, and the variances $\sigma_k^2(x)$, to be governed by

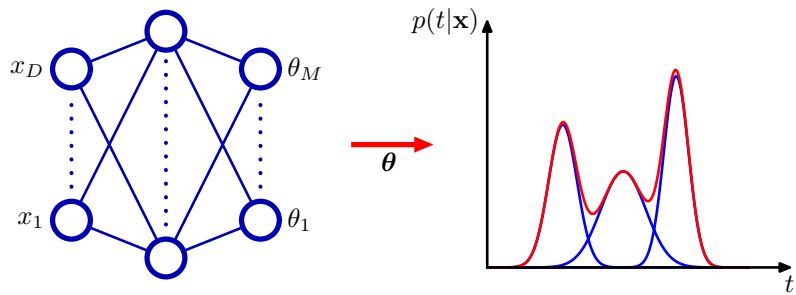


Figure 5.20 The *mixture density network* can represent general conditional probability densities $p(t|x)$ by considering a parametric mixture model for the distribution of t whose parameters are determined by the outputs of a neural network that takes x as its input vector.

the outputs of a conventional neural network that takes x as its input. The structure of this mixture density network is illustrated in Figure 5.20. The mixture density network is closely related to the mixture of experts discussed in Section 14.5.3. The principle difference is that in the mixture density network the same function is used to predict the parameters of all of the component densities as well as the mixing coefficients, and so the nonlinear hidden units are shared amongst the input-dependent functions.

The neural network in Figure 5.20 can, for example, be a two-layer network having sigmoidal ('tanh') hidden units. If there are L components in the mixture model (5.148), and if \mathbf{t} has K components, then the network will have L output unit activations denoted by a_k^π that determine the mixing coefficients $\pi_k(\mathbf{x})$, K outputs denoted by a_k^σ that determine the kernel widths $\sigma_k(\mathbf{x})$, and $L \times K$ outputs denoted by a_{kj}^μ that determine the components $\mu_{kj}(\mathbf{x})$ of the kernel centres $\mu_k(\mathbf{x})$. The total number of network outputs is given by $(K + 2)L$, as compared with the usual K outputs for a network, which simply predicts the conditional means of the target variables.

The mixing coefficients must satisfy the constraints

$$\sum_{k=1}^K \pi_k(\mathbf{x}) = 1, \quad 0 \leq \pi_k(\mathbf{x}) \leq 1 \quad (5.149)$$

which can be achieved using a set of softmax outputs

$$\pi_k(\mathbf{x}) = \frac{\exp(a_k^\pi)}{\sum_{l=1}^K \exp(a_l^\pi)}. \quad (5.150)$$

Similarly, the variances must satisfy $\sigma_k^2(\mathbf{x}) \geq 0$ and so can be represented in terms of the exponentials of the corresponding network activations using

$$\sigma_k(\mathbf{x}) = \exp(a_k^\sigma). \quad (5.151)$$

Finally, because the means $\mu_k(\mathbf{x})$ have real components, they can be represented

directly by the network output activations

$$\mu_{kj}(\mathbf{x}) = a_{kj}^\mu. \quad (5.152)$$

The adaptive parameters of the mixture density network comprise the vector \mathbf{w} of weights and biases in the neural network, that can be set by maximum likelihood, or equivalently by minimizing an error function defined to be the negative logarithm of the likelihood. For independent data, this error function takes the form

$$E(\mathbf{w}) = - \sum_{n=1}^N \ln \left\{ \sum_{k=1}^K \pi_k(\mathbf{x}_n, \mathbf{w}) \mathcal{N}(\mathbf{t}_n | \boldsymbol{\mu}_k(\mathbf{x}_n, \mathbf{w}), \sigma_k^2(\mathbf{x}_n, \mathbf{w})) \right\} \quad (5.153)$$

where we have made the dependencies on \mathbf{w} explicit.

In order to minimize the error function, we need to calculate the derivatives of the error $E(\mathbf{w})$ with respect to the components of \mathbf{w} . These can be evaluated by using the standard backpropagation procedure, provided we obtain suitable expressions for the derivatives of the error with respect to the output-unit activations. These represent error signals δ for each pattern and for each output unit, and can be back-propagated to the hidden units and the error function derivatives evaluated in the usual way. Because the error function (5.153) is composed of a sum of terms, one for each training data point, we can consider the derivatives for a particular pattern n and then find the derivatives of E by summing over all patterns.

Because we are dealing with mixture distributions, it is convenient to view the mixing coefficients $\pi_k(\mathbf{x})$ as \mathbf{x} -dependent prior probabilities and to introduce the corresponding posterior probabilities given by

$$\gamma_k(\mathbf{t}|\mathbf{x}) = \frac{\pi_k \mathcal{N}_{nk}}{\sum_{l=1}^K \pi_l \mathcal{N}_{nl}} \quad (5.154)$$

where \mathcal{N}_{nk} denotes $\mathcal{N}(\mathbf{t}_n | \boldsymbol{\mu}_k(\mathbf{x}_n), \sigma_k^2(\mathbf{x}_n))$.

Exercise 5.34

The derivatives with respect to the network output activations governing the mixing coefficients are given by

$$\frac{\partial E_n}{\partial a_k^\pi} = \pi_k - \gamma_k. \quad (5.155)$$

Exercise 5.35

Similarly, the derivatives with respect to the output activations controlling the component means are given by

$$\frac{\partial E_n}{\partial a_{kl}^\mu} = \gamma_k \left\{ \frac{\mu_{kl} - t_l}{\sigma_k^2} \right\}. \quad (5.156)$$

Exercise 5.36

Finally, the derivatives with respect to the output activations controlling the component variances are given by

$$\frac{\partial E_n}{\partial a_k^\sigma} = -\gamma_k \left\{ \frac{\|\mathbf{t} - \boldsymbol{\mu}_k\|^2}{\sigma_k^3} - \frac{1}{\sigma_k} \right\}. \quad (5.157)$$

Figure 5.21 (a) Plot of the mixing coefficients $\pi_k(x)$ as a function of x for the three kernel functions in a mixture density network trained on the data shown in Figure 5.19. The model has three Gaussian components, and uses a two-layer multi-layer perceptron with five ‘tanh’ sigmoidal units in the hidden layer, and nine outputs (corresponding to the 3 means and 3 variances of the Gaussian components and the 3 mixing coefficients). At both small and large values of x , where the conditional probability density of the target data is unimodal, only one of the kernels has a high value for its prior probability, while at intermediate values of x , where the conditional density is trimodal, the three mixing coefficients have comparable values. (b) Plots of the means $\mu_k(x)$ using the same colour coding as for the mixing coefficients. (c) Plot of the contours of the corresponding conditional probability density of the target data for the same mixture density network. (d) Plot of the approximate conditional mode, shown by the red points, of the conditional density.



We illustrate the use of a mixture density network by returning to the toy example of an inverse problem shown in Figure 5.19. Plots of the mixing coefficients $\pi_k(x)$, the means $\mu_k(x)$, and the conditional density contours corresponding to $p(t|x)$, are shown in Figure 5.21. The outputs of the neural network, and hence the parameters in the mixture model, are necessarily continuous single-valued functions of the input variables. However, we see from Figure 5.21(c) that the model is able to produce a conditional density that is unimodal for some values of x and trimodal for other values by modulating the amplitudes of the mixing components $\pi_k(x)$.

Once a mixture density network has been trained, it can predict the conditional density function of the target data for any given value of the input vector. This conditional density represents a complete description of the generator of the data, so far as the problem of predicting the value of the output vector is concerned. From this density function we can calculate more specific quantities that may be of interest in different applications. One of the simplest of these is the mean, corresponding to the conditional average of the target data, and is given by

$$\mathbb{E}[\mathbf{t}|\mathbf{x}] = \int \mathbf{t} p(\mathbf{t}|\mathbf{x}) d\mathbf{t} = \sum_{k=1}^K \pi_k(\mathbf{x}) \boldsymbol{\mu}_k(\mathbf{x}) \quad (5.158)$$

where we have used (5.148). Because a standard network trained by least squares is approximating the conditional mean, we see that a mixture density network can reproduce the conventional least-squares result as a special case. Of course, as we have already noted, for a multimodal distribution the conditional mean is of limited value.

We can similarly evaluate the variance of the density function about the conditional average, to give

$$s^2(\mathbf{x}) = \mathbb{E} [\|\mathbf{t} - \mathbb{E}[\mathbf{t}|\mathbf{x}]\|^2 | \mathbf{x}] \quad (5.159)$$

$$= \sum_{k=1}^K \pi_k(\mathbf{x}) \left\{ \sigma_k^2(\mathbf{x}) + \left\| \boldsymbol{\mu}_k(\mathbf{x}) - \sum_{l=1}^K \pi_l(\mathbf{x}) \boldsymbol{\mu}_l(\mathbf{x}) \right\|^2 \right\} \quad (5.160)$$

where we have used (5.148) and (5.158). This is more general than the corresponding least-squares result because the variance is a function of \mathbf{x} .

We have seen that for multimodal distributions, the conditional mean can give a poor representation of the data. For instance, in controlling the simple robot arm shown in Figure 5.18, we need to pick one of the two possible joint angle settings in order to achieve the desired end-effector location, whereas the average of the two solutions is not itself a solution. In such cases, the conditional mode may be of more value. Because the conditional mode for the mixture density network does not have a simple analytical solution, this would require numerical iteration. A simple alternative is to take the mean of the most probable component (i.e., the one with the largest mixing coefficient) at each value of \mathbf{x} . This is shown for the toy data set in Figure 5.21(d).

5.7. Bayesian Neural Networks

So far, our discussion of neural networks has focussed on the use of maximum likelihood to determine the network parameters (weights and biases). Regularized maximum likelihood can be interpreted as a MAP (maximum posterior) approach in which the regularizer can be viewed as the logarithm of a prior parameter distribution. However, in a Bayesian treatment we need to marginalize over the distribution of parameters in order to make predictions.

In Section 3.3, we developed a Bayesian solution for a simple linear regression model under the assumption of Gaussian noise. We saw that the posterior distribution, which is Gaussian, could be evaluated exactly and that the predictive distribution could also be found in closed form. In the case of a multilayered network, the highly nonlinear dependence of the network function on the parameter values means that an exact Bayesian treatment can no longer be found. In fact, the log of the posterior distribution will be nonconvex, corresponding to the multiple local minima in the error function.

The technique of variational inference, to be discussed in Chapter 10, has been applied to Bayesian neural networks using a factorized Gaussian approximation

Exercise 5.37

to the posterior distribution (Hinton and van Camp, 1993) and also using a full-covariance Gaussian (Barber and Bishop, 1998a; Barber and Bishop, 1998b). The most complete treatment, however, has been based on the Laplace approximation (MacKay, 1992c; MacKay, 1992b) and forms the basis for the discussion given here. We will approximate the posterior distribution by a Gaussian, centred at a mode of the true posterior. Furthermore, we shall assume that the covariance of this Gaussian is small so that the network function is approximately linear with respect to the parameters over the region of parameter space for which the posterior probability is significantly nonzero. With these two approximations, we will obtain models that are analogous to the linear regression and classification models discussed in earlier chapters and so we can exploit the results obtained there. We can then make use of the evidence framework to provide point estimates for the hyperparameters and to compare alternative models (for example, networks having different numbers of hidden units). To start with, we shall discuss the regression case and then later consider the modifications needed for solving classification tasks.

5.7.1 Posterior parameter distribution

Consider the problem of predicting a single continuous target variable t from a vector \mathbf{x} of inputs (the extension to multiple targets is straightforward). We shall suppose that the conditional distribution $p(t|\mathbf{x})$ is Gaussian, with an \mathbf{x} -dependent mean given by the output of a neural network model $y(\mathbf{x}, \mathbf{w})$, and with precision (inverse variance) β

$$p(t|\mathbf{x}, \mathbf{w}, \beta) = \mathcal{N}(t|y(\mathbf{x}, \mathbf{w}), \beta^{-1}). \quad (5.161)$$

Similarly, we shall choose a prior distribution over the weights \mathbf{w} that is Gaussian of the form

$$p(\mathbf{w}|\alpha) = \mathcal{N}(\mathbf{w}|\mathbf{0}, \alpha^{-1}\mathbf{I}). \quad (5.162)$$

For an i.i.d. data set of N observations $\mathbf{x}_1, \dots, \mathbf{x}_N$, with a corresponding set of target values $\mathcal{D} = \{t_1, \dots, t_N\}$, the likelihood function is given by

$$p(\mathcal{D}|\mathbf{w}, \beta) = \prod_{n=1}^N \mathcal{N}(t_n|y(\mathbf{x}_n, \mathbf{w}), \beta^{-1}) \quad (5.163)$$

and so the resulting posterior distribution is then

$$p(\mathbf{w}|\mathcal{D}, \alpha, \beta) \propto p(\mathbf{w}|\alpha)p(\mathcal{D}|\mathbf{w}, \beta). \quad (5.164)$$

which, as a consequence of the nonlinear dependence of $y(\mathbf{x}, \mathbf{w})$ on \mathbf{w} , will be non-Gaussian.

We can find a Gaussian approximation to the posterior distribution by using the Laplace approximation. To do this, we must first find a (local) maximum of the posterior, and this must be done using iterative numerical optimization. As usual, it is convenient to maximize the logarithm of the posterior, which can be written in the

form

$$\ln p(\mathbf{w}|\mathcal{D}) = -\frac{\alpha}{2}\mathbf{w}^T\mathbf{w} - \frac{\beta}{2} \sum_{n=1}^N \{y(\mathbf{x}_n, \mathbf{w}) - t_n\}^2 + \text{const} \quad (5.165)$$

which corresponds to a regularized sum-of-squares error function. Assuming for the moment that α and β are fixed, we can find a maximum of the posterior, which we denote \mathbf{w}_{MAP} , by standard nonlinear optimization algorithms such as conjugate gradients, using error backpropagation to evaluate the required derivatives.

Having found a mode \mathbf{w}_{MAP} , we can then build a local Gaussian approximation by evaluating the matrix of second derivatives of the negative log posterior distribution. From (5.165), this is given by

$$\mathbf{A} = -\nabla\nabla \ln p(\mathbf{w}|\mathcal{D}, \alpha, \beta) = \alpha\mathbf{I} + \beta\mathbf{H} \quad (5.166)$$

where \mathbf{H} is the Hessian matrix comprising the second derivatives of the sum-of-squares error function with respect to the components of \mathbf{w} . Algorithms for computing and approximating the Hessian were discussed in Section 5.4. The corresponding Gaussian approximation to the posterior is then given from (4.134) by

$$q(\mathbf{w}|\mathcal{D}) = \mathcal{N}(\mathbf{w}|\mathbf{w}_{\text{MAP}}, \mathbf{A}^{-1}). \quad (5.167)$$

Similarly, the predictive distribution is obtained by marginalizing with respect to this posterior distribution

$$p(t|\mathbf{x}, \mathcal{D}) = \int p(t|\mathbf{x}, \mathbf{w})q(\mathbf{w}|\mathcal{D}) d\mathbf{w}. \quad (5.168)$$

However, even with the Gaussian approximation to the posterior, this integration is still analytically intractable due to the nonlinearity of the network function $y(\mathbf{x}, \mathbf{w})$ as a function of \mathbf{w} . To make progress, we now assume that the posterior distribution has small variance compared with the characteristic scales of \mathbf{w} over which $y(\mathbf{x}, \mathbf{w})$ is varying. This allows us to make a Taylor series expansion of the network function around \mathbf{w}_{MAP} and retain only the linear terms

$$y(\mathbf{x}, \mathbf{w}) \simeq y(\mathbf{x}, \mathbf{w}_{\text{MAP}}) + \mathbf{g}^T(\mathbf{w} - \mathbf{w}_{\text{MAP}}) \quad (5.169)$$

where we have defined

$$\mathbf{g} = \nabla_{\mathbf{w}} y(\mathbf{x}, \mathbf{w})|_{\mathbf{w}=\mathbf{w}_{\text{MAP}}}. \quad (5.170)$$

With this approximation, we now have a linear-Gaussian model with a Gaussian distribution for $p(\mathbf{w})$ and a Gaussian for $p(t|\mathbf{w})$ whose mean is a linear function of \mathbf{w} of the form

$$p(t|\mathbf{x}, \mathbf{w}, \beta) \simeq \mathcal{N}(t|y(\mathbf{x}, \mathbf{w}_{\text{MAP}}) + \mathbf{g}^T(\mathbf{w} - \mathbf{w}_{\text{MAP}}), \beta^{-1}). \quad (5.171)$$

Exercise 5.38

We can therefore make use of the general result (2.115) for the marginal $p(t)$ to give

$$p(t|\mathbf{x}, \mathcal{D}, \alpha, \beta) = \mathcal{N}(t|y(\mathbf{x}, \mathbf{w}_{\text{MAP}}), \sigma^2(\mathbf{x})) \quad (5.172)$$

where the input-dependent variance is given by

$$\sigma^2(\mathbf{x}) = \beta^{-1} + \mathbf{g}^T \mathbf{A}^{-1} \mathbf{g}. \quad (5.173)$$

We see that the predictive distribution $p(t|\mathbf{x}, \mathcal{D})$ is a Gaussian whose mean is given by the network function $y(\mathbf{x}, \mathbf{w}_{\text{MAP}})$ with the parameter set to their MAP value. The variance has two terms, the first of which arises from the intrinsic noise on the target variable, whereas the second is an \mathbf{x} -dependent term that expresses the uncertainty in the interpolant due to the uncertainty in the model parameters \mathbf{w} . This should be compared with the corresponding predictive distribution for the linear regression model, given by (3.58) and (3.59).

5.7.2 Hyperparameter optimization

So far, we have assumed that the hyperparameters α and β are fixed and known. We can make use of the evidence framework, discussed in Section 3.5, together with the Gaussian approximation to the posterior obtained using the Laplace approximation, to obtain a practical procedure for choosing the values of such hyperparameters.

The marginal likelihood, or evidence, for the hyperparameters is obtained by integrating over the network weights

$$p(\mathcal{D}|\alpha, \beta) = \int p(\mathcal{D}|\mathbf{w}, \beta) p(\mathbf{w}|\alpha) d\mathbf{w}. \quad (5.174)$$

Exercise 5.39

This is easily evaluated by making use of the Laplace approximation result (4.135). Taking logarithms then gives

$$\ln p(\mathcal{D}|\alpha, \beta) \simeq -E(\mathbf{w}_{\text{MAP}}) - \frac{1}{2} \ln |\mathbf{A}| + \frac{W}{2} \ln \alpha + \frac{N}{2} \ln \beta - \frac{N}{2} \ln(2\pi) \quad (5.175)$$

where W is the total number of parameters in \mathbf{w} , and the regularized error function is defined by

$$E(\mathbf{w}_{\text{MAP}}) = \frac{\beta}{2} \sum_{n=1}^N \{y(\mathbf{x}_n, \mathbf{w}_{\text{MAP}}) - t_n\}^2 + \frac{\alpha}{2} \mathbf{w}_{\text{MAP}}^T \mathbf{w}_{\text{MAP}}. \quad (5.176)$$

We see that this takes the same form as the corresponding result (3.86) for the linear regression model.

In the evidence framework, we make point estimates for α and β by maximizing $\ln p(\mathcal{D}|\alpha, \beta)$. Consider first the maximization with respect to α , which can be done by analogy with the linear regression case discussed in Section 3.5.2. We first define the eigenvalue equation

$$\beta \mathbf{H} \mathbf{u}_i = \lambda_i \mathbf{u}_i \quad (5.177)$$

where \mathbf{H} is the Hessian matrix comprising the second derivatives of the sum-of-squares error function, evaluated at $\mathbf{w} = \mathbf{w}_{\text{MAP}}$. By analogy with (3.92), we obtain

$$\alpha = \frac{\gamma}{\mathbf{w}_{\text{MAP}}^T \mathbf{w}_{\text{MAP}}} \quad (5.178)$$

Section 3.5.3

where γ represents the effective number of parameters and is defined by

$$\gamma = \sum_{i=1}^W \frac{\lambda_i}{\alpha + \lambda_i}. \quad (5.179)$$

Note that this result was exact for the linear regression case. For the nonlinear neural network, however, it ignores the fact that changes in α will cause changes in the Hessian \mathbf{H} , which in turn will change the eigenvalues. We have therefore implicitly ignored terms involving the derivatives of λ_i with respect to α .

Similarly, from (3.95) we see that maximizing the evidence with respect to β gives the re-estimation formula

$$\frac{1}{\beta} = \frac{1}{N - \gamma} \sum_{n=1}^N \{y(\mathbf{x}_n, \mathbf{w}_{\text{MAP}}) - t_n\}^2. \quad (5.180)$$

Section 5.1.1

As with the linear model, we need to alternate between re-estimation of the hyperparameters α and β and updating of the posterior distribution. The situation with a neural network model is more complex, however, due to the multimodality of the posterior distribution. As a consequence, the solution for \mathbf{w}_{MAP} found by maximizing the log posterior will depend on the initialization of \mathbf{w} . Solutions that differ only as a consequence of the interchange and sign reversal symmetries in the hidden units are identical so far as predictions are concerned, and it is irrelevant which of the equivalent solutions is found. However, there may be inequivalent solutions as well, and these will generally yield different values for the optimized hyperparameters.

In order to compare different models, for example neural networks having different numbers of hidden units, we need to evaluate the model evidence $p(\mathcal{D})$. This can be approximated by taking (5.175) and substituting the values of α and β obtained from the iterative optimization of these hyperparameters. A more careful evaluation is obtained by marginalizing over α and β , again by making a Gaussian approximation (MacKay, 1992c; Bishop, 1995a). In either case, it is necessary to evaluate the determinant $|\mathbf{A}|$ of the Hessian matrix. This can be problematic in practice because the determinant, unlike the trace, is sensitive to the small eigenvalues that are often difficult to determine accurately.

The Laplace approximation is based on a local quadratic expansion around a mode of the posterior distribution over weights. We have seen in Section 5.1.1 that any given mode in a two-layer network is a member of a set of $M!2^M$ equivalent modes that differ by interchange and sign-change symmetries, where M is the number of hidden units. When comparing networks having different numbers of hidden units, this can be taken into account by multiplying the evidence by a factor of $M!2^M$.

5.7.3 Bayesian neural networks for classification

So far, we have used the Laplace approximation to develop a Bayesian treatment of neural network regression models. We now discuss the modifications to

this framework that arise when it is applied to classification. Here we shall consider a network having a single logistic sigmoid output corresponding to a two-class classification problem. The extension to networks with multiclass softmax outputs is straightforward. We shall build extensively on the analogous results for linear classification models discussed in Section 4.5, and so we encourage the reader to familiarize themselves with that material before studying this section.

Exercise 5.40

The log likelihood function for this model is given by

$$\ln p(\mathcal{D}|\mathbf{w}) = \sum_n = 1^N \{t_n \ln y_n + (1 - t_n) \ln(1 - y_n)\} \quad (5.181)$$

where $t_n \in \{0, 1\}$ are the target values, and $y_n \equiv y(\mathbf{x}_n, \mathbf{w})$. Note that there is no hyperparameter β , because the data points are assumed to be correctly labelled. As before, the prior is taken to be an isotropic Gaussian of the form (5.162).

The first stage in applying the Laplace framework to this model is to initialize the hyperparameter α , and then to determine the parameter vector \mathbf{w} by maximizing the log posterior distribution. This is equivalent to minimizing the regularized error function

$$E(\mathbf{w}) = -\ln p(\mathcal{D}|\mathbf{w}) + \frac{\alpha}{2} \mathbf{w}^T \mathbf{w} \quad (5.182)$$

and can be achieved using error backpropagation combined with standard optimization algorithms, as discussed in Section 5.3.

Having found a solution \mathbf{w}_{MAP} for the weight vector, the next step is to evaluate the Hessian matrix \mathbf{H} comprising the second derivatives of the negative log likelihood function. This can be done, for instance, using the exact method of Section 5.4.5, or using the outer product approximation given by (5.85). The second derivatives of the negative log posterior can again be written in the form (5.166), and the Gaussian approximation to the posterior is then given by (5.167).

Exercise 5.41

To optimize the hyperparameter α , we again maximize the marginal likelihood, which is easily shown to take the form

$$\ln p(\mathcal{D}|\alpha) \simeq -E(\mathbf{w}_{MAP}) - \frac{1}{2} \ln |\mathbf{A}| + \frac{W}{2} \ln \alpha + \text{const} \quad (5.183)$$

where the regularized error function is defined by

$$E(\mathbf{w}_{MAP}) = -\sum_{n=1}^N \{t_n \ln y_n + (1 - t_n) \ln(1 - y_n)\} + \frac{\alpha}{2} \mathbf{w}_{MAP}^T \mathbf{w}_{MAP} \quad (5.184)$$

in which $y_n \equiv y(\mathbf{x}_n, \mathbf{w}_{MAP})$. Maximizing this evidence function with respect to α again leads to the re-estimation equation given by (5.178).

The use of the evidence procedure to determine α is illustrated in Figure 5.22 for the synthetic two-dimensional data discussed in Appendix A.

Finally, we need the predictive distribution, which is defined by (5.168). Again, this integration is intractable due to the nonlinearity of the network function. The

Figure 5.22 Illustration of the evidence framework applied to a synthetic two-class data set. The green curve shows the optimal decision boundary, the black curve shows the result of fitting a two-layer network with 8 hidden units by maximum likelihood, and the red curve shows the result of including a regularizer in which α is optimized using the evidence procedure, starting from the initial value $\alpha = 0$. Note that the evidence procedure greatly reduces the over-fitting of the network.



simplest approximation is to assume that the posterior distribution is very narrow and hence make the approximation

$$p(t|\mathbf{x}, \mathcal{D}) \simeq p(t|\mathbf{x}, \mathbf{w}_{\text{MAP}}). \quad (5.185)$$

We can improve on this, however, by taking account of the variance of the posterior distribution. In this case, a linear approximation for the network outputs, as was used in the case of regression, would be inappropriate due to the logistic sigmoid output-unit activation function that constrains the output to lie in the range $(0, 1)$. Instead, we make a linear approximation for the output unit activation in the form

$$a(\mathbf{x}, \mathbf{w}) \simeq a_{\text{MAP}}(\mathbf{x}) + \mathbf{b}^T(\mathbf{w} - \mathbf{w}_{\text{MAP}}) \quad (5.186)$$

where $a_{\text{MAP}}(\mathbf{x}) = a(\mathbf{x}, \mathbf{w}_{\text{MAP}})$, and the vector $\mathbf{b} \equiv \nabla a(\mathbf{x}, \mathbf{w}_{\text{MAP}})$ can be found by backpropagation.

Because we now have a Gaussian approximation for the posterior distribution over \mathbf{w} , and a model for a that is a linear function of \mathbf{w} , we can now appeal to the results of Section 4.5.2. The distribution of output unit activation values, induced by the distribution over network weights, is given by

$$p(a|\mathbf{x}, \mathcal{D}) = \int \delta(a - a_{\text{MAP}}(\mathbf{x}) - \mathbf{b}^T(\mathbf{x})(\mathbf{w} - \mathbf{w}_{\text{MAP}})) q(\mathbf{w}|\mathcal{D}) d\mathbf{w} \quad (5.187)$$

where $q(\mathbf{w}|\mathcal{D})$ is the Gaussian approximation to the posterior distribution given by (5.167). From Section 4.5.2, we see that this distribution is Gaussian with mean $a_{\text{MAP}} \equiv a(\mathbf{x}, \mathbf{w}_{\text{MAP}})$, and variance

$$\sigma_a^2(\mathbf{x}) = \mathbf{b}^T(\mathbf{x}) \mathbf{A}^{-1} \mathbf{b}(\mathbf{x}). \quad (5.188)$$

Finally, to obtain the predictive distribution, we must marginalize over a using

$$p(t = 1|\mathbf{x}, \mathcal{D}) = \int \sigma(a)p(a|\mathbf{x}, \mathcal{D}) da. \quad (5.189)$$



Figure 5.23 An illustration of the Laplace approximation for a Bayesian neural network having 8 hidden units with ‘tanh’ activation functions and a single logistic-sigmoid output unit. The weight parameters were found using scaled conjugate gradients, and the hyperparameter α was optimized using the evidence framework. On the left is the result of using the simple approximation (5.185) based on a point estimate \mathbf{w}_{MAP} of the parameters, in which the green curve shows the $y = 0.5$ decision boundary, and the other contours correspond to output probabilities of $y = 0.1, 0.3, 0.7, \text{ and } 0.9$. On the right is the corresponding result obtained using (5.190). Note that the effect of marginalization is to spread out the contours and to make the predictions less confident, so that at each input point \mathbf{x} , the posterior probabilities are shifted towards 0.5, while the $y = 0.5$ contour itself is unaffected.

The convolution of a Gaussian with a logistic sigmoid is intractable. We therefore apply the approximation (4.153) to (5.189) giving

$$p(t=1|\mathbf{x}, \mathcal{D}) = \sigma(\kappa(\sigma_a^2) \mathbf{b}^T \mathbf{w}_{\text{MAP}}) \quad (5.190)$$

where $\kappa(\cdot)$ is defined by (4.154). Recall that both σ_a^2 and \mathbf{b} are functions of \mathbf{x} .

Figure 5.23 shows an example of this framework applied to the synthetic classification data set described in Appendix A.

Exercises

- 5.1** (**) Consider a two-layer network function of the form (5.7) in which the hidden-unit nonlinear activation functions $g(\cdot)$ are given by logistic sigmoid functions of the form

$$\sigma(a) = \{1 + \exp(-a)\}^{-1}. \quad (5.191)$$

Show that there exists an equivalent network, which computes exactly the same function, but with hidden unit activation functions given by $\tanh(a)$ where the \tanh function is defined by (5.59). Hint: first find the relation between $\sigma(a)$ and $\tanh(a)$, and then show that the parameters of the two networks differ by linear transformations.

- 5.2** (*) [www](#) Show that maximizing the likelihood function under the conditional distribution (5.16) for a multioutput neural network is equivalent to minimizing the sum-of-squares error function (5.11).

- 5.3** (**) Consider a regression problem involving multiple target variables in which it is assumed that the distribution of the targets, conditioned on the input vector \mathbf{x} , is a Gaussian of the form

$$p(\mathbf{t}|\mathbf{x}, \mathbf{w}) = \mathcal{N}(\mathbf{t}|\mathbf{y}(\mathbf{x}, \mathbf{w}), \Sigma) \quad (5.192)$$

where $\mathbf{y}(\mathbf{x}, \mathbf{w})$ is the output of a neural network with input vector \mathbf{x} and weight vector \mathbf{w} , and Σ is the covariance of the assumed Gaussian noise on the targets. Given a set of independent observations of \mathbf{x} and \mathbf{t} , write down the error function that must be minimized in order to find the maximum likelihood solution for \mathbf{w} , if we assume that Σ is fixed and known. Now assume that Σ is also to be determined from the data, and write down an expression for the maximum likelihood solution for Σ . Note that the optimizations of \mathbf{w} and Σ are now coupled, in contrast to the case of independent target variables discussed in Section 5.2.

- 5.4** (**) Consider a binary classification problem in which the target values are $t \in \{0, 1\}$, with a network output $y(\mathbf{x}, \mathbf{w})$ that represents $p(t = 1|\mathbf{x})$, and suppose that there is a probability ϵ that the class label on a training data point has been incorrectly set. Assuming independent and identically distributed data, write down the error function corresponding to the negative log likelihood. Verify that the error function (5.21) is obtained when $\epsilon = 0$. Note that this error function makes the model robust to incorrectly labelled data, in contrast to the usual error function.
- 5.5** (*) **www** Show that maximizing likelihood for a multiclass neural network model in which the network outputs have the interpretation $y_k(\mathbf{x}, \mathbf{w}) = p(t_k = 1|\mathbf{x})$ is equivalent to the minimization of the cross-entropy error function (5.24).
- 5.6** (*) **www** Show the derivative of the error function (5.21) with respect to the activation a_k for an output unit having a logistic sigmoid activation function satisfies (5.18).
- 5.7** (*) Show the derivative of the error function (5.24) with respect to the activation a_k for output units having a softmax activation function satisfies (5.18).
- 5.8** (*) We saw in (4.88) that the derivative of the logistic sigmoid activation function can be expressed in terms of the function value itself. Derive the corresponding result for the ‘tanh’ activation function defined by (5.59).
- 5.9** (*) **www** The error function (5.21) for binary classification problems was derived for a network having a logistic-sigmoid output activation function, so that $0 \leq y(\mathbf{x}, \mathbf{w}) \leq 1$, and data having target values $t \in \{0, 1\}$. Derive the corresponding error function if we consider a network having an output $-1 \leq y(\mathbf{x}, \mathbf{w}) \leq 1$ and target values $t = 1$ for class C_1 and $t = -1$ for class C_2 . What would be the appropriate choice of output unit activation function?
- 5.10** (*) **www** Consider a Hessian matrix \mathbf{H} with eigenvector equation (5.33). By setting the vector \mathbf{v} in (5.39) equal to each of the eigenvectors \mathbf{u}_i in turn, show that \mathbf{H} is positive definite if, and only if, all of its eigenvalues are positive.

- 5.11** (**) **www** Consider a quadratic error function defined by (5.32), in which the Hessian matrix \mathbf{H} has an eigenvalue equation given by (5.33). Show that the contours of constant error are ellipses whose axes are aligned with the eigenvectors \mathbf{u}_i , with lengths that are inversely proportional to the square root of the corresponding eigenvalues λ_i .
- 5.12** (**) **www** By considering the local Taylor expansion (5.32) of an error function about a stationary point \mathbf{w}^* , show that the necessary and sufficient condition for the stationary point to be a local minimum of the error function is that the Hessian matrix \mathbf{H} , defined by (5.30) with $\widehat{\mathbf{w}} = \mathbf{w}^*$, be positive definite.
- 5.13** (*) Show that as a consequence of the symmetry of the Hessian matrix \mathbf{H} , the number of independent elements in the quadratic error function (5.28) is given by $W(W + 3)/2$.
- 5.14** (*) By making a Taylor expansion, verify that the terms that are $O(\epsilon)$ cancel on the right-hand side of (5.69).
- 5.15** (**) In Section 5.3.4, we derived a procedure for evaluating the Jacobian matrix of a neural network using a backpropagation procedure. Derive an alternative formalism for finding the Jacobian based on *forward propagation* equations.
- 5.16** (*) The outer product approximation to the Hessian matrix for a neural network using a sum-of-squares error function is given by (5.84). Extend this result to the case of multiple outputs.
- 5.17** (*) Consider a squared loss function of the form

$$E = \frac{1}{2} \iint \{y(\mathbf{x}, \mathbf{w}) - t\}^2 p(\mathbf{x}, t) \, d\mathbf{x} \, dt \quad (5.193)$$

where $y(\mathbf{x}, \mathbf{w})$ is a parametric function such as a neural network. The result (1.89) shows that the function $y(\mathbf{x}, \mathbf{w})$ that minimizes this error is given by the conditional expectation of t given \mathbf{x} . Use this result to show that the second derivative of E with respect to two elements w_r and w_s of the vector \mathbf{w} , is given by

$$\frac{\partial^2 E}{\partial w_r \partial w_s} = \int \frac{\partial y}{\partial w_r} \frac{\partial y}{\partial w_s} p(\mathbf{x}) \, d\mathbf{x}. \quad (5.194)$$

Note that, for a finite sample from $p(\mathbf{x})$, we obtain (5.84).

- 5.18** (*) Consider a two-layer network of the form shown in Figure 5.1 with the addition of extra parameters corresponding to skip-layer connections that go directly from the inputs to the outputs. By extending the discussion of Section 5.3.2, write down the equations for the derivatives of the error function with respect to these additional parameters.
- 5.19** (*) **www** Derive the expression (5.85) for the outer product approximation to the Hessian matrix for a network having a single output with a logistic sigmoid output-unit activation function and a cross-entropy error function, corresponding to the result (5.84) for the sum-of-squares error function.

- 5.20** (★) Derive an expression for the outer product approximation to the Hessian matrix for a network having K outputs with a softmax output-unit activation function and a cross-entropy error function, corresponding to the result (5.84) for the sum-of-squares error function.
- 5.21** (★★★) Extend the expression (5.86) for the outer product approximation of the Hessian matrix to the case of $K > 1$ output units. Hence, derive a recursive expression analogous to (5.87) for incrementing the number N of patterns and a similar expression for incrementing the number K of outputs. Use these results, together with the identity (5.88), to find sequential update expressions analogous to (5.89) for finding the inverse of the Hessian by incrementally including both extra patterns and extra outputs.
- 5.22** (★★) Derive the results (5.93), (5.94), and (5.95) for the elements of the Hessian matrix of a two-layer feed-forward network by application of the chain rule of calculus.
- 5.23** (★★) Extend the results of Section 5.4.5 for the exact Hessian of a two-layer network to include skip-layer connections that go directly from inputs to outputs.
- 5.24** (★) Verify that the network function defined by (5.113) and (5.114) is invariant under the transformation (5.115) applied to the inputs, provided the weights and biases are simultaneously transformed using (5.116) and (5.117). Similarly, show that the network outputs can be transformed according (5.118) by applying the transformation (5.119) and (5.120) to the second-layer weights and biases.
- 5.25** (★★★) **www** Consider a quadratic error function of the form

$$E = E_0 + \frac{1}{2}(\mathbf{w} - \mathbf{w}^*)^T \mathbf{H} (\mathbf{w} - \mathbf{w}^*) \quad (5.195)$$

where \mathbf{w}^* represents the minimum, and the Hessian matrix \mathbf{H} is positive definite and constant. Suppose the initial weight vector $\mathbf{w}^{(0)}$ is chosen to be at the origin and is updated using simple gradient descent

$$\mathbf{w}^{(\tau)} = \mathbf{w}^{(\tau-1)} - \rho \nabla E \quad (5.196)$$

where τ denotes the step number, and ρ is the learning rate (which is assumed to be small). Show that, after τ steps, the components of the weight vector parallel to the eigenvectors of \mathbf{H} can be written

$$w_j^{(\tau)} = \{1 - (1 - \rho \eta_j)^\tau\} w_j^* \quad (5.197)$$

where $w_j = \mathbf{w}^T \mathbf{u}_j$, and \mathbf{u}_j and η_j are the eigenvectors and eigenvalues, respectively, of \mathbf{H} so that

$$\mathbf{H} \mathbf{u}_j = \eta_j \mathbf{u}_j. \quad (5.198)$$

Show that as $\tau \rightarrow \infty$, this gives $\mathbf{w}^{(\tau)} \rightarrow \mathbf{w}^*$ as expected, provided $|1 - \rho \eta_j| < 1$. Now suppose that training is halted after a finite number τ of steps. Show that the

components of the weight vector parallel to the eigenvectors of the Hessian satisfy

$$w_j^{(\tau)} \simeq w_j^* \quad \text{when} \quad \eta_j \gg (\rho\tau)^{-1} \quad (5.199)$$

$$|w_j^{(\tau)}| \ll |w_j^*| \quad \text{when} \quad \eta_j \ll (\rho\tau)^{-1}. \quad (5.200)$$

Compare this result with the discussion in Section 3.5.3 of regularization with simple weight decay, and hence show that $(\rho\tau)^{-1}$ is analogous to the regularization parameter λ . The above results also show that the effective number of parameters in the network, as defined by (3.91), grows as the training progresses.

- 5.26** (**) Consider a multilayer perceptron with arbitrary feed-forward topology, which is to be trained by minimizing the *tangent propagation* error function (5.127) in which the regularizing function is given by (5.128). Show that the regularization term Ω can be written as a sum over patterns of terms of the form

$$\Omega_n = \frac{1}{2} \sum_k (\mathcal{G}y_k)^2 \quad (5.201)$$

where \mathcal{G} is a differential operator defined by

$$\mathcal{G} \equiv \sum_i \tau_i \frac{\partial}{\partial x_i}. \quad (5.202)$$

By acting on the forward propagation equations

$$z_j = h(a_j), \quad a_j = \sum_i w_{ji} z_i \quad (5.203)$$

with the operator \mathcal{G} , show that Ω_n can be evaluated by forward propagation using the following equations:

$$\alpha_j = h'(a_j)\beta_j, \quad \beta_j = \sum_i w_{ji}\alpha_i. \quad (5.204)$$

where we have defined the new variables

$$\alpha_j \equiv \mathcal{G}z_j, \quad \beta_j \equiv \mathcal{G}a_j. \quad (5.205)$$

Now show that the derivatives of Ω_n with respect to a weight w_{rs} in the network can be written in the form

$$\frac{\partial \Omega_n}{\partial w_{rs}} = \sum_k \alpha_k \{ \phi_{kr} z_s + \delta_{kr} \alpha_s \} \quad (5.206)$$

where we have defined

$$\delta_{kr} \equiv \frac{\partial y_k}{\partial a_r}, \quad \phi_{kr} \equiv \mathcal{G}\delta_{kr}. \quad (5.207)$$

Write down the backpropagation equations for δ_{kr} , and hence derive a set of back-propagation equations for the evaluation of the ϕ_{kr} .

- 5.27** (**) **www** Consider the framework for training with transformed data in the special case in which the transformation consists simply of the addition of random noise $\mathbf{x} \rightarrow \mathbf{x} + \boldsymbol{\xi}$ where $\boldsymbol{\xi}$ has a Gaussian distribution with zero mean and unit covariance. By following an argument analogous to that of Section 5.5.5, show that the resulting regularizer reduces to the Tikhonov form (5.135).
- 5.28** (*) **www** Consider a neural network, such as the convolutional network discussed in Section 5.5.6, in which multiple weights are constrained to have the same value. Discuss how the standard backpropagation algorithm must be modified in order to ensure that such constraints are satisfied when evaluating the derivatives of an error function with respect to the adjustable parameters in the network.
- 5.29** (*) **www** Verify the result (5.141).
- 5.30** (*) Verify the result (5.142).
- 5.31** (*) Verify the result (5.143).
- 5.32** (**) Show that the derivatives of the mixing coefficients $\{\pi_k\}$, defined by (5.146), with respect to the auxiliary parameters $\{\eta_j\}$ are given by

$$\frac{\partial \pi_k}{\partial \eta_j} = \delta_{jk} \pi_j - \pi_j \pi_k. \quad (5.208)$$

Hence, by making use of the constraint $\sum_k \pi_k = 1$, derive the result (5.147).

- 5.33** (*) Write down a pair of equations that express the Cartesian coordinates (x_1, x_2) for the robot arm shown in Figure 5.18 in terms of the joint angles θ_1 and θ_2 and the lengths L_1 and L_2 of the links. Assume the origin of the coordinate system is given by the attachment point of the lower arm. These equations define the ‘forward kinematics’ of the robot arm.
- 5.34** (*) **www** Derive the result (5.155) for the derivative of the error function with respect to the network output activations controlling the mixing coefficients in the mixture density network.
- 5.35** (*) Derive the result (5.156) for the derivative of the error function with respect to the network output activations controlling the component means in the mixture density network.
- 5.36** (*) Derive the result (5.157) for the derivative of the error function with respect to the network output activations controlling the component variances in the mixture density network.
- 5.37** (*) Verify the results (5.158) and (5.160) for the conditional mean and variance of the mixture density network model.
- 5.38** (*) Using the general result (2.115), derive the predictive distribution (5.172) for the Laplace approximation to the Bayesian neural network model.

- 5.39** (*) **www** Make use of the Laplace approximation result (4.135) to show that the evidence function for the hyperparameters α and β in the Bayesian neural network model can be approximated by (5.175).
- 5.40** (*) **www** Outline the modifications needed to the framework for Bayesian neural networks, discussed in Section 5.7.3, to handle multiclass problems using networks having softmax output-unit activation functions.
- 5.41** (**) By following analogous steps to those given in Section 5.7.1 for regression networks, derive the result (5.183) for the marginal likelihood in the case of a network having a cross-entropy error function and logistic-sigmoid output-unit activation function.

6

Kernel Methods

In Chapters 3 and 4, we considered linear parametric models for regression and classification in which the form of the mapping $y(\mathbf{x}, \mathbf{w})$ from input \mathbf{x} to output y is governed by a vector \mathbf{w} of adaptive parameters. During the learning phase, a set of training data is used either to obtain a point estimate of the parameter vector or to determine a posterior distribution over this vector. The training data is then discarded, and predictions for new inputs are based purely on the learned parameter vector \mathbf{w} . This approach is also used in nonlinear parametric models such as neural networks.

Chapter 5

Section 2.5.1

However, there is a class of pattern recognition techniques, in which the training data points, or a subset of them, are kept and used also during the prediction phase. For instance, the Parzen probability density model comprised a linear combination of ‘kernel’ functions each one centred on one of the training data points. Similarly, in Section 2.5.2 we introduced a simple technique for classification called nearest neighbours, which involved assigning to each new test vector the same label as the

closest example from the training set. These are examples of *memory-based* methods that involve storing the entire training set in order to make predictions for future data points. They typically require a metric to be defined that measures the similarity of any two vectors in input space, and are generally fast to ‘train’ but slow at making predictions for test data points.

Many linear parametric models can be re-cast into an equivalent ‘dual representation’ in which the predictions are also based on linear combinations of a *kernel function* evaluated at the training data points. As we shall see, for models which are based on a fixed nonlinear *feature space* mapping $\phi(\mathbf{x})$, the kernel function is given by the relation

$$k(\mathbf{x}, \mathbf{x}') = \phi(\mathbf{x})^T \phi(\mathbf{x}'). \quad (6.1)$$

From this definition, we see that the kernel is a symmetric function of its arguments so that $k(\mathbf{x}, \mathbf{x}') = k(\mathbf{x}', \mathbf{x})$. The kernel concept was introduced into the field of pattern recognition by Aizerman *et al.* (1964) in the context of the method of potential functions, so-called because of an analogy with electrostatics. Although neglected for many years, it was re-introduced into machine learning in the context of large-margin classifiers by Boser *et al.* (1992) giving rise to the technique of *support vector machines*. Since then, there has been considerable interest in this topic, both in terms of theory and applications. One of the most significant developments has been the extension of kernels to handle symbolic objects, thereby greatly expanding the range of problems that can be addressed.

The simplest example of a kernel function is obtained by considering the identity mapping for the feature space in (6.1) so that $\phi(\mathbf{x}) = \mathbf{x}$, in which case $k(\mathbf{x}, \mathbf{x}') = \mathbf{x}^T \mathbf{x}'$. We shall refer to this as the linear kernel.

The concept of a kernel formulated as an inner product in a feature space allows us to build interesting extensions of many well-known algorithms by making use of the *kernel trick*, also known as *kernel substitution*. The general idea is that, if we have an algorithm formulated in such a way that the input vector \mathbf{x} enters only in the form of scalar products, then we can replace that scalar product with some other choice of kernel. For instance, the technique of kernel substitution can be applied to principal component analysis in order to develop a nonlinear variant of PCA (Schölkopf *et al.*, 1998). Other examples of kernel substitution include nearest-neighbour classifiers and the kernel Fisher discriminant (Mika *et al.*, 1999; Roth and Steinhage, 2000; Baudat and Anouar, 2000).

There are numerous forms of kernel functions in common use, and we shall encounter several examples in this chapter. Many have the property of being a function only of the difference between the arguments, so that $k(\mathbf{x}, \mathbf{x}') = k(\mathbf{x} - \mathbf{x}')$, which are known as *stationary* kernels because they are invariant to translations in input space. A further specialization involves *homogeneous* kernels, also known as *radial basis functions*, which depend only on the magnitude of the distance (typically Euclidean) between the arguments so that $k(\mathbf{x}, \mathbf{x}') = k(\|\mathbf{x} - \mathbf{x}'\|)$.

For recent textbooks on kernel methods, see Schölkopf and Smola (2002), Herbrich (2002), and Shawe-Taylor and Cristianini (2004).

Chapter 7

Section 12.3

Section 6.3

6.1. Dual Representations

Many linear models for regression and classification can be reformulated in terms of a dual representation in which the kernel function arises naturally. This concept will play an important role when we consider support vector machines in the next chapter. Here we consider a linear regression model whose parameters are determined by minimizing a regularized sum-of-squares error function given by

$$J(\mathbf{w}) = \frac{1}{2} \sum_{n=1}^N \{\mathbf{w}^T \phi(\mathbf{x}_n) - t_n\}^2 + \frac{\lambda}{2} \mathbf{w}^T \mathbf{w} \quad (6.2)$$

where $\lambda \geq 0$. If we set the gradient of $J(\mathbf{w})$ with respect to \mathbf{w} equal to zero, we see that the solution for \mathbf{w} takes the form of a linear combination of the vectors $\phi(\mathbf{x}_n)$, with coefficients that are functions of \mathbf{w} , of the form

$$\mathbf{w} = -\frac{1}{\lambda} \sum_{n=1}^N \{\mathbf{w}^T \phi(\mathbf{x}_n) - t_n\} \phi(\mathbf{x}_n) = \sum_{n=1}^N a_n \phi(\mathbf{x}_n) = \Phi^T \mathbf{a} \quad (6.3)$$

where Φ is the design matrix, whose n^{th} row is given by $\phi(\mathbf{x}_n)^T$. Here the vector $\mathbf{a} = (a_1, \dots, a_N)^T$, and we have defined

$$a_n = -\frac{1}{\lambda} \{\mathbf{w}^T \phi(\mathbf{x}_n) - t_n\}. \quad (6.4)$$

Instead of working with the parameter vector \mathbf{w} , we can now reformulate the least-squares algorithm in terms of the parameter vector \mathbf{a} , giving rise to a *dual representation*. If we substitute $\mathbf{w} = \Phi^T \mathbf{a}$ into $J(\mathbf{w})$, we obtain

$$J(\mathbf{a}) = \frac{1}{2} \mathbf{a}^T \Phi \Phi^T \Phi \Phi^T \mathbf{a} - \mathbf{a}^T \Phi \Phi^T \mathbf{t} + \frac{1}{2} \mathbf{t}^T \mathbf{t} + \frac{\lambda}{2} \mathbf{a}^T \Phi \Phi^T \mathbf{a} \quad (6.5)$$

where $\mathbf{t} = (t_1, \dots, t_N)^T$. We now define the *Gram matrix* $\mathbf{K} = \Phi \Phi^T$, which is an $N \times N$ symmetric matrix with elements

$$K_{nm} = \phi(\mathbf{x}_n)^T \phi(\mathbf{x}_m) = k(\mathbf{x}_n, \mathbf{x}_m) \quad (6.6)$$

where we have introduced the *kernel function* $k(\mathbf{x}, \mathbf{x}')$ defined by (6.1). In terms of the Gram matrix, the sum-of-squares error function can be written as

$$J(\mathbf{a}) = \frac{1}{2} \mathbf{a}^T \mathbf{K} \mathbf{K} \mathbf{a} - \mathbf{a}^T \mathbf{K} \mathbf{t} + \frac{1}{2} \mathbf{t}^T \mathbf{t} + \frac{\lambda}{2} \mathbf{a}^T \mathbf{K} \mathbf{a}. \quad (6.7)$$

Setting the gradient of $J(\mathbf{a})$ with respect to \mathbf{a} to zero, we obtain the following solution

$$\mathbf{a} = (\mathbf{K} + \lambda \mathbf{I}_N)^{-1} \mathbf{t}. \quad (6.8)$$

If we substitute this back into the linear regression model, we obtain the following prediction for a new input \mathbf{x}

$$y(\mathbf{x}) = \mathbf{w}^T \phi(\mathbf{x}) = \mathbf{a}^T \Phi \phi(\mathbf{x}) = \mathbf{k}(\mathbf{x})^T (\mathbf{K} + \lambda \mathbf{I}_N)^{-1} \mathbf{t} \quad (6.9)$$

where we have defined the vector $\mathbf{k}(\mathbf{x})$ with elements $k_n(\mathbf{x}) = k(\mathbf{x}_n, \mathbf{x})$. Thus we see that the dual formulation allows the solution to the least-squares problem to be expressed entirely in terms of the kernel function $k(\mathbf{x}, \mathbf{x}')$. This is known as a dual formulation because, by noting that the solution for \mathbf{a} can be expressed as a linear combination of the elements of $\phi(\mathbf{x})$, we recover the original formulation in terms of the parameter vector \mathbf{w} . Note that the prediction at \mathbf{x} is given by a linear combination of the target values from the training set. In fact, we have already obtained this result, using a slightly different notation, in Section 3.3.3.

Exercise 6.1

In the dual formulation, we determine the parameter vector \mathbf{a} by inverting an $N \times N$ matrix, whereas in the original parameter space formulation we had to invert an $M \times M$ matrix in order to determine \mathbf{w} . Because N is typically much larger than M , the dual formulation does not seem to be particularly useful. However, the advantage of the dual formulation, as we shall see, is that it is expressed entirely in terms of the kernel function $k(\mathbf{x}, \mathbf{x}')$. We can therefore work directly in terms of kernels and avoid the explicit introduction of the feature vector $\phi(\mathbf{x})$, which allows us implicitly to use feature spaces of high, even infinite, dimensionality.

Exercise 6.2

The existence of a dual representation based on the Gram matrix is a property of many linear models, including the perceptron. In Section 6.4, we will develop a duality between probabilistic linear models for regression and the technique of Gaussian processes. Duality will also play an important role when we discuss support vector machines in Chapter 7.

6.2. Constructing Kernels

In order to exploit kernel substitution, we need to be able to construct valid kernel functions. One approach is to choose a feature space mapping $\phi(\mathbf{x})$ and then use this to find the corresponding kernel, as is illustrated in Figure 6.1. Here the kernel function is defined for a one-dimensional input space by

$$k(x, x') = \phi(x)^T \phi(x') = \sum_{i=1}^M \phi_i(x) \phi_i(x') \quad (6.10)$$

where $\phi_i(x)$ are the basis functions.

An alternative approach is to construct kernel functions directly. In this case, we must ensure that the function we choose is a valid kernel, in other words that it corresponds to a scalar product in some (perhaps infinite dimensional) feature space. As a simple example, consider a kernel function given by

$$k(\mathbf{x}, \mathbf{z}) = (\mathbf{x}^T \mathbf{z})^2. \quad (6.11)$$



Figure 6.1 Illustration of the construction of kernel functions starting from a corresponding set of basis functions. In each column the lower plot shows the kernel function $k(x, x')$ defined by (6.10) plotted as a function of x for $x' = 0$, while the upper plot shows the corresponding basis functions given by polynomials (left column), ‘Gaussians’ (centre column), and logistic sigmoids (right column).

If we take the particular case of a two-dimensional input space $\mathbf{x} = (x_1, x_2)$ we can expand out the terms and thereby identify the corresponding nonlinear feature mapping

$$\begin{aligned}
 k(\mathbf{x}, \mathbf{z}) &= (\mathbf{x}^T \mathbf{z})^2 = (x_1 z_1 + x_2 z_2)^2 \\
 &= x_1^2 z_1^2 + 2x_1 z_1 x_2 z_2 + x_2^2 z_2^2 \\
 &= (x_1^2, \sqrt{2}x_1 x_2, x_2^2)(z_1^2, \sqrt{2}z_1 z_2, z_2^2)^T \\
 &= \phi(\mathbf{x})^T \phi(\mathbf{z}).
 \end{aligned} \tag{6.12}$$

We see that the feature mapping takes the form $\phi(\mathbf{x}) = (x_1^2, \sqrt{2}x_1 x_2, x_2^2)^T$ and therefore comprises all possible second order terms, with a specific weighting between them.

More generally, however, we need a simple way to test whether a function constitutes a valid kernel without having to construct the function $\phi(\mathbf{x})$ explicitly. A necessary and sufficient condition for a function $k(\mathbf{x}, \mathbf{x}')$ to be a valid kernel (Shawe-Taylor and Cristianini, 2004) is that the Gram matrix \mathbf{K} , whose elements are given by $k(\mathbf{x}_n, \mathbf{x}_m)$, should be positive semidefinite for all possible choices of the set $\{\mathbf{x}_n\}$. Note that a positive semidefinite matrix is not the same thing as a matrix whose elements are nonnegative.

Appendix C

One powerful technique for constructing new kernels is to build them out of simpler kernels as building blocks. This can be done using the following properties:

Techniques for Constructing New Kernels.

Given valid kernels $k_1(\mathbf{x}, \mathbf{x}')$ and $k_2(\mathbf{x}, \mathbf{x}')$, the following new kernels will also be valid:

$$k(\mathbf{x}, \mathbf{x}') = ck_1(\mathbf{x}, \mathbf{x}') \quad (6.13)$$

$$k(\mathbf{x}, \mathbf{x}') = f(\mathbf{x})k_1(\mathbf{x}, \mathbf{x}')f(\mathbf{x}') \quad (6.14)$$

$$k(\mathbf{x}, \mathbf{x}') = q(k_1(\mathbf{x}, \mathbf{x}')) \quad (6.15)$$

$$k(\mathbf{x}, \mathbf{x}') = \exp(k_1(\mathbf{x}, \mathbf{x}')) \quad (6.16)$$

$$k(\mathbf{x}, \mathbf{x}') = k_1(\mathbf{x}, \mathbf{x}') + k_2(\mathbf{x}, \mathbf{x}') \quad (6.17)$$

$$k(\mathbf{x}, \mathbf{x}') = k_1(\mathbf{x}, \mathbf{x}')k_2(\mathbf{x}, \mathbf{x}') \quad (6.18)$$

$$k(\mathbf{x}, \mathbf{x}') = k_3(\phi(\mathbf{x}), \phi(\mathbf{x}')) \quad (6.19)$$

$$k(\mathbf{x}, \mathbf{x}') = \mathbf{x}^T \mathbf{A} \mathbf{x}' \quad (6.20)$$

$$k(\mathbf{x}, \mathbf{x}') = k_a(\mathbf{x}_a, \mathbf{x}'_a) + k_b(\mathbf{x}_b, \mathbf{x}'_b) \quad (6.21)$$

$$k(\mathbf{x}, \mathbf{x}') = k_a(\mathbf{x}_a, \mathbf{x}'_a)k_b(\mathbf{x}_b, \mathbf{x}'_b) \quad (6.22)$$

where $c > 0$ is a constant, $f(\cdot)$ is any function, $q(\cdot)$ is a polynomial with nonnegative coefficients, $\phi(\mathbf{x})$ is a function from \mathbf{x} to \mathbb{R}^M , $k_3(\cdot, \cdot)$ is a valid kernel in \mathbb{R}^M , \mathbf{A} is a symmetric positive semidefinite matrix, \mathbf{x}_a and \mathbf{x}_b are variables (not necessarily disjoint) with $\mathbf{x} = (\mathbf{x}_a, \mathbf{x}_b)$, and k_a and k_b are valid kernel functions over their respective spaces.

Equipped with these properties, we can now embark on the construction of more complex kernels appropriate to specific applications. We require that the kernel $k(\mathbf{x}, \mathbf{x}')$ be symmetric and positive semidefinite and that it expresses the appropriate form of similarity between \mathbf{x} and \mathbf{x}' according to the intended application. Here we consider a few common examples of kernel functions. For a more extensive discussion of ‘kernel engineering’, see Shawe-Taylor and Cristianini (2004).

We saw that the simple polynomial kernel $k(\mathbf{x}, \mathbf{x}') = (\mathbf{x}^T \mathbf{x}')^2$ contains only terms of degree two. If we consider the slightly generalized kernel $k(\mathbf{x}, \mathbf{x}') = (\mathbf{x}^T \mathbf{x}' + c)^2$ with $c > 0$, then the corresponding feature mapping $\phi(\mathbf{x})$ contains constant and linear terms as well as terms of order two. Similarly, $k(\mathbf{x}, \mathbf{x}') = (\mathbf{x}^T \mathbf{x}')^M$ contains all monomials of order M . For instance, if \mathbf{x} and \mathbf{x}' are two images, then the kernel represents a particular weighted sum of all possible products of M pixels in the first image with M pixels in the second image. This can similarly be generalized to include all terms up to degree M by considering $k(\mathbf{x}, \mathbf{x}') = (\mathbf{x}^T \mathbf{x}' + c)^M$ with $c > 0$. Using the results (6.17) and (6.18) for combining kernels we see that these will all be valid kernel functions.

Another commonly used kernel takes the form

$$k(\mathbf{x}, \mathbf{x}') = \exp(-\|\mathbf{x} - \mathbf{x}'\|^2 / 2\sigma^2) \quad (6.23)$$

and is often called a ‘Gaussian’ kernel. Note, however, that in this context it is not interpreted as a probability density, and hence the normalization coefficient is

omitted. We can see that this is a valid kernel by expanding the square

$$\|\mathbf{x} - \mathbf{x}'\|^2 = \mathbf{x}^T \mathbf{x} + (\mathbf{x}')^T \mathbf{x}' - 2\mathbf{x}^T \mathbf{x}' \quad (6.24)$$

to give

$$k(\mathbf{x}, \mathbf{x}') = \exp(-\mathbf{x}^T \mathbf{x}/2\sigma^2) \exp(\mathbf{x}^T \mathbf{x}'/\sigma^2) \exp(-(\mathbf{x}')^T \mathbf{x}'/2\sigma^2) \quad (6.25)$$

and then making use of (6.14) and (6.16), together with the validity of the linear kernel $k(\mathbf{x}, \mathbf{x}') = \mathbf{x}^T \mathbf{x}'$. Note that the feature vector that corresponds to the Gaussian kernel has infinite dimensionality.

Exercise 6.11

The Gaussian kernel is not restricted to the use of Euclidean distance. If we use kernel substitution in (6.24) to replace $\mathbf{x}^T \mathbf{x}'$ with a nonlinear kernel $\kappa(\mathbf{x}, \mathbf{x}')$, we obtain

$$k(\mathbf{x}, \mathbf{x}') = \exp\left\{-\frac{1}{2\sigma^2} (\kappa(\mathbf{x}, \mathbf{x}) + \kappa(\mathbf{x}', \mathbf{x}') - 2\kappa(\mathbf{x}, \mathbf{x}'))\right\}. \quad (6.26)$$

An important contribution to arise from the kernel viewpoint has been the extension to inputs that are symbolic, rather than simply vectors of real numbers. Kernel functions can be defined over objects as diverse as graphs, sets, strings, and text documents. Consider, for instance, a fixed set and define a nonvectorial space consisting of all possible subsets of this set. If A_1 and A_2 are two such subsets then one simple choice of kernel would be

$$k(A_1, A_2) = 2^{|A_1 \cap A_2|} \quad (6.27)$$

where $A_1 \cap A_2$ denotes the intersection of sets A_1 and A_2 , and $|A|$ denotes the number of subsets in A . This is a valid kernel function because it can be shown to correspond to an inner product in a feature space.

Exercise 6.12

One powerful approach to the construction of kernels starts from a probabilistic generative model (Haussler, 1999), which allows us to apply generative models in a discriminative setting. Generative models can deal naturally with missing data and in the case of hidden Markov models can handle sequences of varying length. By contrast, discriminative models generally give better performance on discriminative tasks than generative models. It is therefore of some interest to combine these two approaches (Lasserre *et al.*, 2006). One way to combine them is to use a generative model to define a kernel, and then use this kernel in a discriminative approach.

Given a generative model $p(\mathbf{x})$ we can define a kernel by

$$k(\mathbf{x}, \mathbf{x}') = p(\mathbf{x})p(\mathbf{x}'). \quad (6.28)$$

This is clearly a valid kernel function because we can interpret it as an inner product in the one-dimensional feature space defined by the mapping $p(\mathbf{x})$. It says that two inputs \mathbf{x} and \mathbf{x}' are similar if they both have high probabilities. We can use (6.13) and (6.17) to extend this class of kernels by considering sums over products of different probability distributions, with positive weighting coefficients $p(i)$, of the form

$$k(\mathbf{x}, \mathbf{x}') = \sum_i p(\mathbf{x}|i)p(\mathbf{x}'|i)p(i). \quad (6.29)$$

Section 9.2

This is equivalent, up to an overall multiplicative constant, to a mixture distribution in which the components factorize, with the index i playing the role of a ‘latent’ variable. Two inputs \mathbf{x} and \mathbf{x}' will give a large value for the kernel function, and hence appear similar, if they have significant probability under a range of different components. Taking the limit of an infinite sum, we can also consider kernels of the form

$$k(\mathbf{x}, \mathbf{x}') = \int p(\mathbf{x}|\mathbf{z})p(\mathbf{x}'|\mathbf{z})p(\mathbf{z}) d\mathbf{z} \quad (6.30)$$

where \mathbf{z} is a continuous latent variable.

Section 13.2

Now suppose that our data consists of ordered sequences of length L so that an observation is given by $\mathbf{X} = \{\mathbf{x}_1, \dots, \mathbf{x}_L\}$. A popular generative model for sequences is the hidden Markov model, which expresses the distribution $p(\mathbf{X})$ as a marginalization over a corresponding sequence of hidden states $\mathbf{Z} = \{\mathbf{z}_1, \dots, \mathbf{z}_L\}$. We can use this approach to define a kernel function measuring the similarity of two sequences \mathbf{X} and \mathbf{X}' by extending the mixture representation (6.29) to give

$$k(\mathbf{X}, \mathbf{X}') = \sum_{\mathbf{Z}} p(\mathbf{X}|\mathbf{Z})p(\mathbf{X}'|\mathbf{Z})p(\mathbf{Z}) \quad (6.31)$$

so that both observed sequences are generated by the same hidden sequence \mathbf{Z} . This model can easily be extended to allow sequences of differing length to be compared.

An alternative technique for using generative models to define kernel functions is known as the *Fisher kernel* (Jaakkola and Haussler, 1999). Consider a parametric generative model $p(\mathbf{x}|\boldsymbol{\theta})$ where $\boldsymbol{\theta}$ denotes the vector of parameters. The goal is to find a kernel that measures the similarity of two input vectors \mathbf{x} and \mathbf{x}' induced by the generative model. Jaakkola and Haussler (1999) consider the gradient with respect to $\boldsymbol{\theta}$, which defines a vector in a ‘feature’ space having the same dimensionality as $\boldsymbol{\theta}$. In particular, they consider the *Fisher score*

$$\mathbf{g}(\boldsymbol{\theta}, \mathbf{x}) = \nabla_{\boldsymbol{\theta}} \ln p(\mathbf{x}|\boldsymbol{\theta}) \quad (6.32)$$

from which the Fisher kernel is defined by

$$k(\mathbf{x}, \mathbf{x}') = \mathbf{g}(\boldsymbol{\theta}, \mathbf{x})^T \mathbf{F}^{-1} \mathbf{g}(\boldsymbol{\theta}, \mathbf{x}'). \quad (6.33)$$

Here \mathbf{F} is the *Fisher information matrix*, given by

$$\mathbf{F} = \mathbb{E}_{\mathbf{x}} [\mathbf{g}(\boldsymbol{\theta}, \mathbf{x}) \mathbf{g}(\boldsymbol{\theta}, \mathbf{x})^T] \quad (6.34)$$

Exercise 6.13

where the expectation is with respect to \mathbf{x} under the distribution $p(\mathbf{x}|\boldsymbol{\theta})$. This can be motivated from the perspective of *information geometry* (Amari, 1998), which considers the differential geometry of the space of model parameters. Here we simply note that the presence of the Fisher information matrix causes this kernel to be invariant under a nonlinear re-parameterization of the density model $\boldsymbol{\theta} \rightarrow \psi(\boldsymbol{\theta})$.

In practice, it is often infeasible to evaluate the Fisher information matrix. One approach is simply to replace the expectation in the definition of the Fisher information with the sample average, giving

$$\mathbf{F} \simeq \frac{1}{N} \sum_{n=1}^N \mathbf{g}(\boldsymbol{\theta}, \mathbf{x}_n) \mathbf{g}(\boldsymbol{\theta}, \mathbf{x}_n)^T. \quad (6.35)$$

Section 12.1.3

This is the covariance matrix of the Fisher scores, and so the Fisher kernel corresponds to a whitening of these scores. More simply, we can just omit the Fisher information matrix altogether and use the noninvariant kernel

$$k(\mathbf{x}, \mathbf{x}') = \mathbf{g}(\boldsymbol{\theta}, \mathbf{x})^T \mathbf{g}(\boldsymbol{\theta}, \mathbf{x}'). \quad (6.36)$$

An application of Fisher kernels to document retrieval is given by Hofmann (2000).

A final example of a kernel function is the sigmoidal kernel given by

$$k(\mathbf{x}, \mathbf{x}') = \tanh(a \mathbf{x}^T \mathbf{x}' + b) \quad (6.37)$$

Section 6.4.7

whose Gram matrix in general is not positive semidefinite. This form of kernel has, however, been used in practice (Vapnik, 1995), possibly because it gives kernel expansions such as the support vector machine a superficial resemblance to neural network models. As we shall see, in the limit of an infinite number of basis functions, a Bayesian neural network with an appropriate prior reduces to a Gaussian process, thereby providing a deeper link between neural networks and kernel methods.

6.3. Radial Basis Function Networks

In Chapter 3, we discussed regression models based on linear combinations of fixed basis functions, although we did not discuss in detail what form those basis functions might take. One choice that has been widely used is that of *radial basis functions*, which have the property that each basis function depends only on the radial distance (typically Euclidean) from a centre $\boldsymbol{\mu}_j$, so that $\phi_j(\mathbf{x}) = h(\|\mathbf{x} - \boldsymbol{\mu}_j\|)$.

Historically, radial basis functions were introduced for the purpose of exact function interpolation (Powell, 1987). Given a set of input vectors $\{\mathbf{x}_1, \dots, \mathbf{x}_N\}$ along with corresponding target values $\{t_1, \dots, t_N\}$, the goal is to find a smooth function $f(\mathbf{x})$ that fits every target value exactly, so that $f(\mathbf{x}_n) = t_n$ for $n = 1, \dots, N$. This is achieved by expressing $f(\mathbf{x})$ as a linear combination of radial basis functions, one centred on every data point

$$f(\mathbf{x}) = \sum_{n=1}^N w_n h(\|\mathbf{x} - \mathbf{x}_n\|). \quad (6.38)$$

The values of the coefficients $\{w_n\}$ are found by least squares, and because there are the same number of coefficients as there are constraints, the result is a function that fits every target value exactly. In pattern recognition applications, however, the target values are generally noisy, and exact interpolation is undesirable because this corresponds to an over-fitted solution.

Expansions in radial basis functions also arise from regularization theory (Poggio and Girosi, 1990; Bishop, 1995a). For a sum-of-squares error function with a regularizer defined in terms of a differential operator, the optimal solution is given by an expansion in the *Green's functions* of the operator (which are analogous to the eigenvectors of a discrete matrix), again with one basis function centred on each data

point. If the differential operator is isotropic then the Green's functions depend only on the radial distance from the corresponding data point. Due to the presence of the regularizer, the solution no longer interpolates the training data exactly.

Another motivation for radial basis functions comes from a consideration of the interpolation problem when the input (rather than the target) variables are noisy (Webb, 1994; Bishop, 1995a). If the noise on the input variable \mathbf{x} is described by a variable ξ having a distribution $\nu(\xi)$, then the sum-of-squares error function becomes

$$E = \frac{1}{2} \sum_{n=1}^N \int \{y(\mathbf{x}_n + \xi) - t_n\}^2 \nu(\xi) d\xi. \quad (6.39)$$

Appendix D

Exercise 6.17

Using the calculus of variations, we can optimize with respect to the function $f(\mathbf{x})$ to give

$$y(\mathbf{x}_n) = \sum_{n=1}^N t_n h(\mathbf{x} - \mathbf{x}_n) \quad (6.40)$$

where the basis functions are given by

$$h(\mathbf{x} - \mathbf{x}_n) = \frac{\nu(\mathbf{x} - \mathbf{x}_n)}{\sum_{n=1}^N \nu(\mathbf{x} - \mathbf{x}_n)}. \quad (6.41)$$

We see that there is one basis function centred on every data point. This is known as the *Nadaraya-Watson* model and will be derived again from a different perspective in Section 6.3.1. If the noise distribution $\nu(\xi)$ is isotropic, so that it is a function only of $\|\xi\|$, then the basis functions will be radial.

Note that the basis functions (6.41) are normalized, so that $\sum_n h(\mathbf{x} - \mathbf{x}_n) = 1$ for any value of \mathbf{x} . The effect of such normalization is shown in Figure 6.2. Normalization is sometimes used in practice as it avoids having regions of input space where all of the basis functions take small values, which would necessarily lead to predictions in such regions that are either small or controlled purely by the bias parameter.

Another situation in which expansions in normalized radial basis functions arise is in the application of kernel density estimation to the problem of regression, as we shall discuss in Section 6.3.1.

Because there is one basis function associated with every data point, the corresponding model can be computationally costly to evaluate when making predictions for new data points. Models have therefore been proposed (Broomhead and Lowe, 1988; Moody and Darken, 1989; Poggio and Girosi, 1990), which retain the expansion in radial basis functions but where the number M of basis functions is smaller than the number N of data points. Typically, the number of basis functions, and the locations μ_i of their centres, are determined based on the input data $\{\mathbf{x}_n\}$ alone. The basis functions are then kept fixed and the coefficients $\{w_i\}$ are determined by least squares by solving the usual set of linear equations, as discussed in Section 3.1.1.



Figure 6.2 Plot of a set of Gaussian basis functions on the left, together with the corresponding normalized basis functions on the right.

One of the simplest ways of choosing basis function centres is to use a randomly chosen subset of the data points. A more systematic approach is called *orthogonal least squares* (Chen *et al.*, 1991). This is a sequential selection process in which at each step the next data point to be chosen as a basis function centre corresponds to the one that gives the greatest reduction in the sum-of-squares error. Values for the expansion coefficients are determined as part of the algorithm. Clustering algorithms such as K -means have also been used, which give a set of basis function centres that no longer coincide with training data points.

Section 9.1

6.3.1 Nadaraya-Watson model

In Section 3.3.3, we saw that the prediction of a linear regression model for a new input \mathbf{x} takes the form of a linear combination of the training set target values with coefficients given by the ‘equivalent kernel’ (3.62) where the equivalent kernel satisfies the summation constraint (3.64).

Section 2.5.1

We can motivate the kernel regression model (3.61) from a different perspective, starting with kernel density estimation. Suppose we have a training set $\{\mathbf{x}_n, t_n\}$ and we use a Parzen density estimator to model the joint distribution $p(\mathbf{x}, t)$, so that

$$p(\mathbf{x}, t) = \frac{1}{N} \sum_{n=1}^N f(\mathbf{x} - \mathbf{x}_n, t - t_n) \quad (6.42)$$

where $f(\mathbf{x}, t)$ is the component density function, and there is one such component centred on each data point. We now find an expression for the regression function $y(\mathbf{x})$, corresponding to the conditional average of the target variable conditioned on

the input variable, which is given by

$$\begin{aligned}
 y(\mathbf{x}) &= \mathbb{E}[t|\mathbf{x}] = \int_{-\infty}^{\infty} tp(t|\mathbf{x}) dt \\
 &= \frac{\int tp(\mathbf{x}, t) dt}{\int p(\mathbf{x}, t) dt} \\
 &= \frac{\sum_n \int tf(\mathbf{x} - \mathbf{x}_n, t - t_n) dt}{\sum_m \int f(\mathbf{x} - \mathbf{x}_m, t - t_m) dt}. \tag{6.43}
 \end{aligned}$$

We now assume for simplicity that the component density functions have zero mean so that

$$\int_{-\infty}^{\infty} f(\mathbf{x}, t)t dt = 0 \tag{6.44}$$

for all values of \mathbf{x} . Using a simple change of variable, we then obtain

$$\begin{aligned}
 y(\mathbf{x}) &= \frac{\sum_n g(\mathbf{x} - \mathbf{x}_n) t_n}{\sum_m g(\mathbf{x} - \mathbf{x}_m)} \\
 &= \sum_n k(\mathbf{x}, \mathbf{x}_n) t_n \tag{6.45}
 \end{aligned}$$

where $n, m = 1, \dots, N$ and the kernel function $k(\mathbf{x}, \mathbf{x}_n)$ is given by

$$k(\mathbf{x}, \mathbf{x}_n) = \frac{g(\mathbf{x} - \mathbf{x}_n)}{\sum_m g(\mathbf{x} - \mathbf{x}_m)} \tag{6.46}$$

and we have defined

$$g(\mathbf{x}) = \int_{-\infty}^{\infty} f(\mathbf{x}, t) dt. \tag{6.47}$$

The result (6.45) is known as the *Nadaraya-Watson* model, or *kernel regression* (Nadaraya, 1964; Watson, 1964). For a localized kernel function, it has the property of giving more weight to the data points \mathbf{x}_n that are close to \mathbf{x} . Note that the kernel (6.46) satisfies the summation constraint

$$\sum_{n=1}^N k(\mathbf{x}, \mathbf{x}_n) = 1.$$

Figure 6.3 Illustration of the Nadaraya-Watson kernel regression model using isotropic Gaussian kernels, for the sinusoidal data set. The original sine function is shown by the green curve, the data points are shown in blue, and each is the centre of an isotropic Gaussian kernel. The resulting regression function, given by the conditional mean, is shown by the red line, along with the two-standard-deviation region for the conditional distribution $p(t|x)$ shown by the red shading. The blue ellipse around each data point shows one standard deviation contour for the corresponding kernel. These appear noncircular due to the different scales on the horizontal and vertical axes.



In fact, this model defines not only a conditional expectation but also a full conditional distribution given by

$$p(t|\mathbf{x}) = \frac{p(t, \mathbf{x})}{\int p(t, \mathbf{x}) dt} = \frac{\sum_n f(\mathbf{x} - \mathbf{x}_n, t - t_n)}{\sum_m \int f(\mathbf{x} - \mathbf{x}_m, t - t_m) dt} \quad (6.48)$$

from which other expectations can be evaluated.

As an illustration we consider the case of a single input variable x in which $f(x, t)$ is given by a zero-mean isotropic Gaussian over the variable $\mathbf{z} = (x, t)$ with variance σ^2 . The corresponding conditional distribution (6.48) is given by a Gaussian mixture, and is shown, together with the conditional mean, for the sinusoidal synthetic data set in Figure 6.3.

Exercise 6.18

An obvious extension of this model is to allow for more flexible forms of Gaussian components, for instance having different variance parameters for the input and target variables. More generally, we could model the joint distribution $p(t, \mathbf{x})$ using a Gaussian mixture model, trained using techniques discussed in Chapter 9 (Ghahramani and Jordan, 1994), and then find the corresponding conditional distribution $p(t|\mathbf{x})$. In this latter case we no longer have a representation in terms of kernel functions evaluated at the training set data points. However, the number of components in the mixture model can be smaller than the number of training set points, resulting in a model that is faster to evaluate for test data points. We have thereby accepted an increased computational cost during the training phase in order to have a model that is faster at making predictions.

6.4. Gaussian Processes

In Section 6.1, we introduced kernels by applying the concept of duality to a non-probabilistic model for regression. Here we extend the role of kernels to probabilis-

tic discriminative models, leading to the framework of Gaussian processes. We shall thereby see how kernels arise naturally in a Bayesian setting.

In Chapter 3, we considered linear regression models of the form $y(\mathbf{x}, \mathbf{w}) = \mathbf{w}^T \phi(\mathbf{x})$ in which \mathbf{w} is a vector of parameters and $\phi(\mathbf{x})$ is a vector of fixed nonlinear basis functions that depend on the input vector \mathbf{x} . We showed that a prior distribution over \mathbf{w} induced a corresponding prior distribution over functions $y(\mathbf{x}, \mathbf{w})$. Given a training data set, we then evaluated the posterior distribution over \mathbf{w} and thereby obtained the corresponding posterior distribution over regression functions, which in turn (with the addition of noise) implies a predictive distribution $p(t|\mathbf{x})$ for new input vectors \mathbf{x} .

In the Gaussian process viewpoint, we dispense with the parametric model and instead define a prior probability distribution over functions directly. At first sight, it might seem difficult to work with a distribution over the uncountably infinite space of functions. However, as we shall see, for a finite training set we only need to consider the values of the function at the discrete set of input values \mathbf{x}_n corresponding to the training set and test set data points, and so in practice we can work in a finite space.

Models equivalent to Gaussian processes have been widely studied in many different fields. For instance, in the geostatistics literature Gaussian process regression is known as *kriging* (Cressie, 1993). Similarly, ARMA (autoregressive moving average) models, Kalman filters, and radial basis function networks can all be viewed as forms of Gaussian process models. Reviews of Gaussian processes from a machine learning perspective can be found in MacKay (1998), Williams (1999), and MacKay (2003), and a comparison of Gaussian process models with alternative approaches is given in Rasmussen (1996). See also Rasmussen and Williams (2006) for a recent textbook on Gaussian processes.

6.4.1 Linear regression revisited

In order to motivate the Gaussian process viewpoint, let us return to the linear regression example and re-derive the predictive distribution by working in terms of distributions over functions $y(\mathbf{x}, \mathbf{w})$. This will provide a specific example of a Gaussian process.

Consider a model defined in terms of a linear combination of M fixed basis functions given by the elements of the vector $\phi(\mathbf{x})$ so that

$$y(\mathbf{x}) = \mathbf{w}^T \phi(\mathbf{x}) \quad (6.49)$$

where \mathbf{x} is the input vector and \mathbf{w} is the M -dimensional weight vector. Now consider a prior distribution over \mathbf{w} given by an isotropic Gaussian of the form

$$p(\mathbf{w}) = \mathcal{N}(\mathbf{w} | \mathbf{0}, \alpha^{-1} \mathbf{I}) \quad (6.50)$$

governed by the hyperparameter α , which represents the precision (inverse variance) of the distribution. For any given value of \mathbf{w} , the definition (6.49) defines a particular function of \mathbf{x} . The probability distribution over \mathbf{w} defined by (6.50) therefore induces a probability distribution over functions $y(\mathbf{x})$. In practice, we wish to evaluate this function at specific values of \mathbf{x} , for example at the training data points

$\mathbf{x}_1, \dots, \mathbf{x}_N$. We are therefore interested in the joint distribution of the function values $y(\mathbf{x}_1), \dots, y(\mathbf{x}_N)$, which we denote by the vector \mathbf{y} with elements $y_n = y(\mathbf{x}_n)$ for $n = 1, \dots, N$. From (6.49), this vector is given by

$$\mathbf{y} = \Phi \mathbf{w} \quad (6.51)$$

where Φ is the design matrix with elements $\Phi_{nk} = \phi_k(\mathbf{x}_n)$. We can find the probability distribution of \mathbf{y} as follows. First of all we note that \mathbf{y} is a linear combination of Gaussian distributed variables given by the elements of \mathbf{w} and hence is itself Gaussian. We therefore need only to find its mean and covariance, which are given from (6.50) by

$$\mathbb{E}[\mathbf{y}] = \Phi \mathbb{E}[\mathbf{w}] = \mathbf{0} \quad (6.52)$$

$$\text{cov}[\mathbf{y}] = \mathbb{E}[\mathbf{y}\mathbf{y}^T] = \Phi \mathbb{E}[\mathbf{w}\mathbf{w}^T] \Phi^T = \frac{1}{\alpha} \Phi \Phi^T = \mathbf{K} \quad (6.53)$$

where \mathbf{K} is the Gram matrix with elements

$$K_{nm} = k(\mathbf{x}_n, \mathbf{x}_m) = \frac{1}{\alpha} \phi(\mathbf{x}_n)^T \phi(\mathbf{x}_m) \quad (6.54)$$

and $k(\mathbf{x}, \mathbf{x}')$ is the kernel function.

This model provides us with a particular example of a Gaussian process. In general, a Gaussian process is defined as a probability distribution over functions $y(\mathbf{x})$ such that the set of values of $y(\mathbf{x})$ evaluated at an arbitrary set of points $\mathbf{x}_1, \dots, \mathbf{x}_N$ jointly have a Gaussian distribution. In cases where the input vector \mathbf{x} is two dimensional, this may also be known as a *Gaussian random field*. More generally, a *stochastic process* $y(\mathbf{x})$ is specified by giving the joint probability distribution for any finite set of values $y(\mathbf{x}_1), \dots, y(\mathbf{x}_N)$ in a consistent manner.

A key point about Gaussian stochastic processes is that the joint distribution over N variables y_1, \dots, y_N is specified completely by the second-order statistics, namely the mean and the covariance. In most applications, we will not have any prior knowledge about the mean of $y(\mathbf{x})$ and so by symmetry we take it to be zero. This is equivalent to choosing the mean of the prior over weight values $p(\mathbf{w}|\alpha)$ to be zero in the basis function viewpoint. The specification of the Gaussian process is then completed by giving the covariance of $y(\mathbf{x})$ evaluated at any two values of \mathbf{x} , which is given by the kernel function

$$\mathbb{E}[y(\mathbf{x}_n)y(\mathbf{x}_m)] = k(\mathbf{x}_n, \mathbf{x}_m). \quad (6.55)$$

For the specific case of a Gaussian process defined by the linear regression model (6.49) with a weight prior (6.50), the kernel function is given by (6.54).

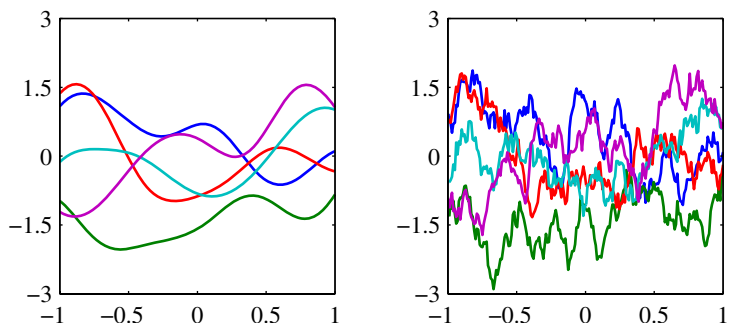
We can also define the kernel function directly, rather than indirectly through a choice of basis function. Figure 6.4 shows samples of functions drawn from Gaussian processes for two different choices of kernel function. The first of these is a ‘Gaussian’ kernel of the form (6.23), and the second is the exponential kernel given by

$$k(x, x') = \exp(-\theta |x - x'|) \quad (6.56)$$

which corresponds to the *Ornstein-Uhlenbeck process* originally introduced by Uhlenbeck and Ornstein (1930) to describe Brownian motion.

Exercise 2.31

Figure 6.4 Samples from Gaussian processes for a ‘Gaussian’ kernel (left) and an exponential kernel (right).



6.4.2 Gaussian processes for regression

In order to apply Gaussian process models to the problem of regression, we need to take account of the noise on the observed target values, which are given by

$$t_n = y_n + \epsilon_n \quad (6.57)$$

where $y_n = y(\mathbf{x}_n)$, and ϵ_n is a random noise variable whose value is chosen independently for each observation n . Here we shall consider noise processes that have a Gaussian distribution, so that

$$p(t_n|y_n) = \mathcal{N}(t_n|y_n, \beta^{-1}) \quad (6.58)$$

where β is a hyperparameter representing the precision of the noise. Because the noise is independent for each data point, the joint distribution of the target values $\mathbf{t} = (t_1, \dots, t_N)^T$ conditioned on the values of $\mathbf{y} = (y_1, \dots, y_N)^T$ is given by an isotropic Gaussian of the form

$$p(\mathbf{t}|\mathbf{y}) = \mathcal{N}(\mathbf{t}|\mathbf{y}, \beta^{-1} \mathbf{I}_N) \quad (6.59)$$

where \mathbf{I}_N denotes the $N \times N$ unit matrix. From the definition of a Gaussian process, the marginal distribution $p(\mathbf{y})$ is given by a Gaussian whose mean is zero and whose covariance is defined by a Gram matrix \mathbf{K} so that

$$p(\mathbf{y}) = \mathcal{N}(\mathbf{y}|\mathbf{0}, \mathbf{K}). \quad (6.60)$$

The kernel function that determines \mathbf{K} is typically chosen to express the property that, for points \mathbf{x}_n and \mathbf{x}_m that are similar, the corresponding values $y(\mathbf{x}_n)$ and $y(\mathbf{x}_m)$ will be more strongly correlated than for dissimilar points. Here the notion of similarity will depend on the application.

In order to find the marginal distribution $p(\mathbf{t})$, conditioned on the input values $\mathbf{x}_1, \dots, \mathbf{x}_N$, we need to integrate over \mathbf{y} . This can be done by making use of the results from Section 2.3.3 for the linear-Gaussian model. Using (2.115), we see that the marginal distribution of \mathbf{t} is given by

$$p(\mathbf{t}) = \int p(\mathbf{t}|\mathbf{y})p(\mathbf{y}) d\mathbf{y} = \mathcal{N}(\mathbf{t}|\mathbf{0}, \mathbf{C}) \quad (6.61)$$

where the covariance matrix \mathbf{C} has elements

$$C(\mathbf{x}_n, \mathbf{x}_m) = k(\mathbf{x}_n, \mathbf{x}_m) + \beta^{-1} \delta_{nm}. \quad (6.62)$$

This result reflects the fact that the two Gaussian sources of randomness, namely that associated with $y(\mathbf{x})$ and that associated with ϵ , are independent and so their covariances simply add.

One widely used kernel function for Gaussian process regression is given by the exponential of a quadratic form, with the addition of constant and linear terms to give

$$k(\mathbf{x}_n, \mathbf{x}_m) = \theta_0 \exp \left\{ -\frac{\theta_1}{2} \|\mathbf{x}_n - \mathbf{x}_m\|^2 \right\} + \theta_2 + \theta_3 \mathbf{x}_n^T \mathbf{x}_m. \quad (6.63)$$

Note that the term involving θ_3 corresponds to a parametric model that is a linear function of the input variables. Samples from this prior are plotted for various values of the parameters $\theta_0, \dots, \theta_3$ in Figure 6.5, and Figure 6.6 shows a set of points sampled from the joint distribution (6.60) along with the corresponding values defined by (6.61).

So far, we have used the Gaussian process viewpoint to build a model of the joint distribution over sets of data points. Our goal in regression, however, is to make predictions of the target variables for new inputs, given a set of training data. Let us suppose that $\mathbf{t}_N = (t_1, \dots, t_N)^T$, corresponding to input values $\mathbf{x}_1, \dots, \mathbf{x}_N$, comprise the observed training set, and our goal is to predict the target variable t_{N+1} for a new input vector \mathbf{x}_{N+1} . This requires that we evaluate the predictive distribution $p(t_{N+1} | \mathbf{t}_N)$. Note that this distribution is conditioned also on the variables $\mathbf{x}_1, \dots, \mathbf{x}_N$ and \mathbf{x}_{N+1} . However, to keep the notation simple we will not show these conditioning variables explicitly.

To find the conditional distribution $p(t_{N+1} | \mathbf{t})$, we begin by writing down the joint distribution $p(\mathbf{t}_{N+1})$, where \mathbf{t}_{N+1} denotes the vector $(t_1, \dots, t_N, t_{N+1})^T$. We then apply the results from Section 2.3.1 to obtain the required conditional distribution, as illustrated in Figure 6.7.

From (6.61), the joint distribution over t_1, \dots, t_{N+1} will be given by

$$p(\mathbf{t}_{N+1}) = \mathcal{N}(\mathbf{t}_{N+1} | \mathbf{0}, \mathbf{C}_{N+1}) \quad (6.64)$$

where \mathbf{C}_{N+1} is an $(N + 1) \times (N + 1)$ covariance matrix with elements given by (6.62). Because this joint distribution is Gaussian, we can apply the results from Section 2.3.1 to find the conditional Gaussian distribution. To do this, we partition the covariance matrix as follows

$$\mathbf{C}_{N+1} = \begin{pmatrix} \mathbf{C}_N & \mathbf{k} \\ \mathbf{k}^T & c \end{pmatrix} \quad (6.65)$$

where \mathbf{C}_N is the $N \times N$ covariance matrix with elements given by (6.62) for $n, m = 1, \dots, N$, the vector \mathbf{k} has elements $k(\mathbf{x}_n, \mathbf{x}_{N+1})$ for $n = 1, \dots, N$, and the scalar



Figure 6.5 Samples from a Gaussian process prior defined by the covariance function (6.63). The title above each plot denotes $(\theta_0, \theta_1, \theta_2, \theta_3)$.

$c = k(\mathbf{x}_{N+1}, \mathbf{x}_{N+1}) + \beta^{-1}$. Using the results (2.81) and (2.82), we see that the conditional distribution $p(t_{N+1} | \mathbf{t})$ is a Gaussian distribution with mean and covariance given by

$$m(\mathbf{x}_{N+1}) = \mathbf{k}^T \mathbf{C}_N^{-1} \mathbf{t} \quad (6.66)$$

$$\sigma^2(\mathbf{x}_{N+1}) = c - \mathbf{k}^T \mathbf{C}_N^{-1} \mathbf{k}. \quad (6.67)$$

These are the key results that define Gaussian process regression. Because the vector \mathbf{k} is a function of the test point input value \mathbf{x}_{N+1} , we see that the predictive distribution is a Gaussian whose mean and variance both depend on \mathbf{x}_{N+1} . An example of Gaussian process regression is shown in Figure 6.8.

The only restriction on the kernel function is that the covariance matrix given by (6.62) must be positive definite. If λ_i is an eigenvalue of \mathbf{K} , then the corresponding eigenvalue of \mathbf{C} will be $\lambda_i + \beta^{-1}$. It is therefore sufficient that the kernel matrix $k(\mathbf{x}_n, \mathbf{x}_m)$ be positive semidefinite for any pair of points \mathbf{x}_n and \mathbf{x}_m , so that $\lambda_i \geq 0$, because any eigenvalue λ_i that is zero will still give rise to a positive eigenvalue for \mathbf{C} because $\beta > 0$. This is the same restriction on the kernel function discussed earlier, and so we can again exploit all of the techniques in Section 6.2 to construct

Figure 6.6 Illustration of the sampling of data points $\{t_n\}$ from a Gaussian process. The blue curve shows a sample function from the Gaussian process prior over functions, and the red points show the values of y_n obtained by evaluating the function at a set of input values $\{x_n\}$. The corresponding values of $\{t_n\}$, shown in green, are obtained by adding independent Gaussian noise to each of the $\{y_n\}$.



suitable kernels.

Note that the mean (6.66) of the predictive distribution can be written, as a function of \mathbf{x}_{N+1} , in the form

$$m(\mathbf{x}_{N+1}) = \sum_{n=1}^N a_n k(\mathbf{x}_n, \mathbf{x}_{N+1}) \quad (6.68)$$

where a_n is the n^{th} component of $\mathbf{C}_N^{-1}\mathbf{t}$. Thus, if the kernel function $k(\mathbf{x}_n, \mathbf{x}_m)$ depends only on the distance $\|\mathbf{x}_n - \mathbf{x}_m\|$, then we obtain an expansion in radial basis functions.

The results (6.66) and (6.67) define the predictive distribution for Gaussian process regression with an arbitrary kernel function $k(\mathbf{x}_n, \mathbf{x}_m)$. In the particular case in which the kernel function $k(\mathbf{x}, \mathbf{x}')$ is defined in terms of a finite set of basis functions, we can derive the results obtained previously in Section 3.3.2 for linear regression starting from the Gaussian process viewpoint.

For such models, we can therefore obtain the predictive distribution either by taking a parameter space viewpoint and using the linear regression result or by taking a function space viewpoint and using the Gaussian process result.

The central computational operation in using Gaussian processes will involve the inversion of a matrix of size $N \times N$, for which standard methods require $O(N^3)$ computations. By contrast, in the basis function model we have to invert a matrix \mathbf{S}_N of size $M \times M$, which has $O(M^3)$ computational complexity. Note that for both viewpoints, the matrix inversion must be performed once for the given training set. For each new test point, both methods require a vector-matrix multiply, which has cost $O(N^2)$ in the Gaussian process case and $O(M^2)$ for the linear basis function model. If the number M of basis functions is smaller than the number N of data points, it will be computationally more efficient to work in the basis function

Exercise 6.21

Figure 6.7 Illustration of the mechanism of Gaussian process regression for the case of one training point and one test point, in which the red ellipses show contours of the joint distribution $p(t_1, t_2)$. Here t_1 is the training data point, and conditioning on the value of t_1 , corresponding to the vertical blue line, we obtain $p(t_2|t_1)$ shown as a function of t_2 by the green curve.



framework. However, an advantage of a Gaussian processes viewpoint is that we can consider covariance functions that can only be expressed in terms of an infinite number of basis functions.

For large training data sets, however, the direct application of Gaussian process methods can become infeasible, and so a range of approximation schemes have been developed that have better scaling with training set size than the exact approach (Gibbs, 1997; Tresp, 2001; Smola and Bartlett, 2001; Williams and Seeger, 2001; Csató and Opper, 2002; Seeger *et al.*, 2003). Practical issues in the application of Gaussian processes are discussed in Bishop and Nabney (2008).

We have introduced Gaussian process regression for the case of a single target variable. The extension of this formalism to multiple target variables, known as co-kriging (Cressie, 1993), is straightforward. Various other extensions of Gaus-

Exercise 6.23

Figure 6.8 Illustration of Gaussian process regression applied to the sinusoidal data set in Figure A.6 in which the three right-most data points have been omitted. The green curve shows the sinusoidal function from which the data points, shown in blue, are obtained by sampling and addition of Gaussian noise. The red line shows the mean of the Gaussian process predictive distribution, and the shaded region corresponds to plus and minus two standard deviations. Notice how the uncertainty increases in the region to the right of the data points.



sian process regression have also been considered, for purposes such as modelling the distribution over low-dimensional manifolds for unsupervised learning (Bishop *et al.*, 1998a) and the solution of stochastic differential equations (Graepel, 2003).

6.4.3 Learning the hyperparameters

The predictions of a Gaussian process model will depend, in part, on the choice of covariance function. In practice, rather than fixing the covariance function, we may prefer to use a parametric family of functions and then infer the parameter values from the data. These parameters govern such things as the length scale of the correlations and the precision of the noise and correspond to the hyperparameters in a standard parametric model.

Techniques for learning the hyperparameters are based on the evaluation of the likelihood function $p(\mathbf{t}|\boldsymbol{\theta})$ where $\boldsymbol{\theta}$ denotes the hyperparameters of the Gaussian process model. The simplest approach is to make a point estimate of $\boldsymbol{\theta}$ by maximizing the log likelihood function. Because $\boldsymbol{\theta}$ represents a set of hyperparameters for the regression problem, this can be viewed as analogous to the type 2 maximum likelihood procedure for linear regression models. Maximization of the log likelihood can be done using efficient gradient-based optimization algorithms such as conjugate gradients (Fletcher, 1987; Nocedal and Wright, 1999; Bishop and Nabney, 2008).

Section 3.5

The log likelihood function for a Gaussian process regression model is easily evaluated using the standard form for a multivariate Gaussian distribution, giving

$$\ln p(\mathbf{t}|\boldsymbol{\theta}) = -\frac{1}{2} \ln |\mathbf{C}_N| - \frac{1}{2} \mathbf{t}^T \mathbf{C}_N^{-1} \mathbf{t} - \frac{N}{2} \ln(2\pi). \quad (6.69)$$

For nonlinear optimization, we also need the gradient of the log likelihood function with respect to the parameter vector $\boldsymbol{\theta}$. We shall assume that evaluation of the derivatives of \mathbf{C}_N is straightforward, as would be the case for the covariance functions considered in this chapter. Making use of the result (C.21) for the derivative of \mathbf{C}_N^{-1} , together with the result (C.22) for the derivative of $\ln |\mathbf{C}_N|$, we obtain

$$\frac{\partial}{\partial \theta_i} \ln p(\mathbf{t}|\boldsymbol{\theta}) = -\frac{1}{2} \text{Tr} \left(\mathbf{C}_N^{-1} \frac{\partial \mathbf{C}_N}{\partial \theta_i} \right) + \frac{1}{2} \mathbf{t}^T \mathbf{C}_N^{-1} \frac{\partial \mathbf{C}_N}{\partial \theta_i} \mathbf{C}_N^{-1} \mathbf{t}. \quad (6.70)$$

Because $\ln p(\mathbf{t}|\boldsymbol{\theta})$ will in general be a nonconvex function, it can have multiple maxima.

It is straightforward to introduce a prior over $\boldsymbol{\theta}$ and to maximize the log posterior using gradient-based methods. In a fully Bayesian treatment, we need to evaluate marginals over $\boldsymbol{\theta}$ weighted by the product of the prior $p(\boldsymbol{\theta})$ and the likelihood function $p(\mathbf{t}|\boldsymbol{\theta})$. In general, however, exact marginalization will be intractable, and we must resort to approximations.

The Gaussian process regression model gives a predictive distribution whose mean and variance are functions of the input vector \mathbf{x} . However, we have assumed that the contribution to the predictive variance arising from the additive noise, governed by the parameter β , is a constant. For some problems, known as *heteroscedastic*, the noise variance itself will also depend on \mathbf{x} . To model this, we can extend the

Figure 6.9 Samples from the ARD prior for Gaussian processes, in which the kernel function is given by (6.71). The left plot corresponds to $\eta_1 = \eta_2 = 1$, and the right plot corresponds to $\eta_1 = 1, \eta_2 = 0.01$.



Gaussian process framework by introducing a second Gaussian process to represent the dependence of β on the input \mathbf{x} (Goldberg *et al.*, 1998). Because β is a variance, and hence nonnegative, we use the Gaussian process to model $\ln \beta(\mathbf{x})$.

6.4.4 Automatic relevance determination

In the previous section, we saw how maximum likelihood could be used to determine a value for the correlation length-scale parameter in a Gaussian process. This technique can usefully be extended by incorporating a separate parameter for each input variable (Rasmussen and Williams, 2006). The result, as we shall see, is that the optimization of these parameters by maximum likelihood allows the relative importance of different inputs to be inferred from the data. This represents an example in the Gaussian process context of *automatic relevance determination*, or *ARD*, which was originally formulated in the framework of neural networks (MacKay, 1994; Neal, 1996). The mechanism by which appropriate inputs are preferred is discussed in Section 7.2.2.

Consider a Gaussian process with a two-dimensional input space $\mathbf{x} = (x_1, x_2)$, having a kernel function of the form

$$k(\mathbf{x}, \mathbf{x}') = \theta_0 \exp \left\{ -\frac{1}{2} \sum_{i=1}^2 \eta_i (x_i - x'_i)^2 \right\}. \quad (6.71)$$

Samples from the resulting prior over functions $y(\mathbf{x})$ are shown for two different settings of the precision parameters η_i in Figure 6.9. We see that, as a particular parameter η_i becomes small, the function becomes relatively insensitive to the corresponding input variable x_i . By adapting these parameters to a data set using maximum likelihood, it becomes possible to detect input variables that have little effect on the predictive distribution, because the corresponding values of η_i will be small. This can be useful in practice because it allows such inputs to be discarded. ARD is illustrated using a simple synthetic data set having three inputs x_1, x_2 and x_3 (Nabney, 2002) in Figure 6.10. The target variable t , is generated by sampling 100 values of x_1 from a Gaussian, evaluating the function $\sin(2\pi x_1)$, and then adding

Figure 6.10 Illustration of automatic relevance determination in a Gaussian process for a synthetic problem having three inputs x_1 , x_2 , and x_3 , for which the curves show the corresponding values of the hyperparameters η_1 (red), η_2 (green), and η_3 (blue) as a function of the number of iterations when optimizing the marginal likelihood. Details are given in the text. Note the logarithmic scale on the vertical axis.



Gaussian noise. Values of x_2 are given by copying the corresponding values of x_1 and adding noise, and values of x_3 are sampled from an independent Gaussian distribution. Thus x_1 is a good predictor of t , x_2 is a more noisy predictor of t , and x_3 has only chance correlations with t . The marginal likelihood for a Gaussian process with ARD parameters η_1, η_2, η_3 is optimized using the scaled conjugate gradients algorithm. We see from Figure 6.10 that η_1 converges to a relatively large value, η_2 converges to a much smaller value, and η_3 becomes very small indicating that x_3 is irrelevant for predicting t .

The ARD framework is easily incorporated into the exponential-quadratic kernel (6.63) to give the following form of kernel function, which has been found useful for applications of Gaussian processes to a range of regression problems

$$k(\mathbf{x}_n, \mathbf{x}_m) = \theta_0 \exp \left\{ -\frac{1}{2} \sum_{i=1}^D \eta_i (x_{ni} - x_{mi})^2 \right\} + \theta_2 + \theta_3 \sum_{i=1}^D x_{ni} x_{mi} \quad (6.72)$$

where D is the dimensionality of the input space.

6.4.5 Gaussian processes for classification

In a probabilistic approach to classification, our goal is to model the posterior probabilities of the target variable for a new input vector, given a set of training data. These probabilities must lie in the interval $(0, 1)$, whereas a Gaussian process model makes predictions that lie on the entire real axis. However, we can easily adapt Gaussian processes to classification problems by transforming the output of the Gaussian process using an appropriate nonlinear activation function.

Consider first the two-class problem with a target variable $t \in \{0, 1\}$. If we define a Gaussian process over a function $a(\mathbf{x})$ and then transform the function using a logistic sigmoid $y = \sigma(a)$, given by (4.59), then we will obtain a non-Gaussian stochastic process over functions $y(\mathbf{x})$ where $y \in (0, 1)$. This is illustrated for the case of a one-dimensional input space in Figure 6.11 in which the probability distri-

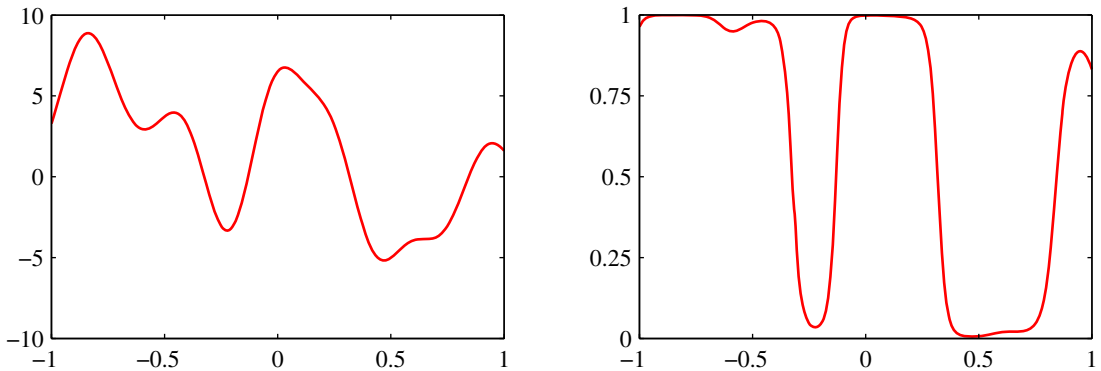


Figure 6.11 The left plot shows a sample from a Gaussian process prior over functions $a(\mathbf{x})$, and the right plot shows the result of transforming this sample using a logistic sigmoid function.

bution over the target variable t is then given by the Bernoulli distribution

$$p(t|a) = \sigma(a)^t(1 - \sigma(a))^{1-t}. \quad (6.73)$$

As usual, we denote the training set inputs by $\mathbf{x}_1, \dots, \mathbf{x}_N$ with corresponding observed target variables $\mathbf{t} = (t_1, \dots, t_N)^\top$. We also consider a single test point \mathbf{x}_{N+1} with target value t_{N+1} . Our goal is to determine the predictive distribution $p(t_{N+1}|\mathbf{t})$, where we have left the conditioning on the input variables implicit. To do this we introduce a Gaussian process prior over the vector \mathbf{a}_{N+1} , which has components $a(\mathbf{x}_1), \dots, a(\mathbf{x}_{N+1})$. This in turn defines a non-Gaussian process over \mathbf{t}_{N+1} , and by conditioning on the training data \mathbf{t}_N we obtain the required predictive distribution. The Gaussian process prior for \mathbf{a}_{N+1} takes the form

$$p(\mathbf{a}_{N+1}) = \mathcal{N}(\mathbf{a}_{N+1} | \mathbf{0}, \mathbf{C}_{N+1}). \quad (6.74)$$

Unlike the regression case, the covariance matrix no longer includes a noise term because we assume that all of the training data points are correctly labelled. However, for numerical reasons it is convenient to introduce a noise-like term governed by a parameter ν that ensures that the covariance matrix is positive definite. Thus the covariance matrix \mathbf{C}_{N+1} has elements given by

$$C(\mathbf{x}_n, \mathbf{x}_m) = k(\mathbf{x}_n, \mathbf{x}_m) + \nu \delta_{nm} \quad (6.75)$$

where $k(\mathbf{x}_n, \mathbf{x}_m)$ is any positive semidefinite kernel function of the kind considered in Section 6.2, and the value of ν is typically fixed in advance. We shall assume that the kernel function $k(\mathbf{x}, \mathbf{x}')$ is governed by a vector $\boldsymbol{\theta}$ of parameters, and we shall later discuss how $\boldsymbol{\theta}$ may be learned from the training data.

For two-class problems, it is sufficient to predict $p(t_{N+1} = 1|\mathbf{t}_N)$ because the value of $p(t_{N+1} = 0|\mathbf{t}_N)$ is then given by $1 - p(t_{N+1} = 1|\mathbf{t}_N)$. The required

predictive distribution is given by

$$p(t_{N+1} = 1 | \mathbf{t}_N) = \int p(t_{N+1} = 1 | a_{N+1}) p(a_{N+1} | \mathbf{t}_N) da_{N+1} \quad (6.76)$$

where $p(t_{N+1} = 1 | a_{N+1}) = \sigma(a_{N+1})$.

This integral is analytically intractable, and so may be approximated using sampling methods (Neal, 1997). Alternatively, we can consider techniques based on an analytical approximation. In Section 4.5.2, we derived the approximate formula (4.153) for the convolution of a logistic sigmoid with a Gaussian distribution. We can use this result to evaluate the integral in (6.76) provided we have a Gaussian approximation to the posterior distribution $p(a_{N+1} | \mathbf{t}_N)$. The usual justification for a Gaussian approximation to a posterior distribution is that the true posterior will tend to a Gaussian as the number of data points increases as a consequence of the central limit theorem. In the case of Gaussian processes, the number of variables grows with the number of data points, and so this argument does not apply directly. However, if we consider increasing the number of data points falling in a fixed region of \mathbf{x} space, then the corresponding uncertainty in the function $a(\mathbf{x})$ will decrease, again leading asymptotically to a Gaussian (Williams and Barber, 1998).

Section 2.3

Section 10.1

Section 10.7

Section 4.4

Three different approaches to obtaining a Gaussian approximation have been considered. One technique is based on *variational inference* (Gibbs and MacKay, 2000) and makes use of the local variational bound (10.144) on the logistic sigmoid. This allows the product of sigmoid functions to be approximated by a product of Gaussians thereby allowing the marginalization over \mathbf{a}_N to be performed analytically. The approach also yields a lower bound on the likelihood function $p(\mathbf{t}_N | \theta)$. The variational framework for Gaussian process classification can also be extended to multiclass ($K > 2$) problems by using a Gaussian approximation to the softmax function (Gibbs, 1997).

A second approach uses *expectation propagation* (Opper and Winther, 2000b; Minka, 2001b; Seeger, 2003). Because the true posterior distribution is unimodal, as we shall see shortly, the expectation propagation approach can give good results.

6.4.6 Laplace approximation

The third approach to Gaussian process classification is based on the Laplace approximation, which we now consider in detail. In order to evaluate the predictive distribution (6.76), we seek a Gaussian approximation to the posterior distribution over a_{N+1} , which, using Bayes' theorem, is given by

$$\begin{aligned} p(a_{N+1} | \mathbf{t}_N) &= \int p(a_{N+1}, \mathbf{a}_N | \mathbf{t}_N) d\mathbf{a}_N \\ &= \frac{1}{p(\mathbf{t}_N)} \int p(a_{N+1}, \mathbf{a}_N) p(\mathbf{t}_N | a_{N+1}, \mathbf{a}_N) d\mathbf{a}_N \\ &= \frac{1}{p(\mathbf{t}_N)} \int p(a_{N+1} | \mathbf{a}_N) p(\mathbf{a}_N) p(\mathbf{t}_N | \mathbf{a}_N) d\mathbf{a}_N \\ &= \int p(a_{N+1} | \mathbf{a}_N) p(\mathbf{a}_N | \mathbf{t}_N) d\mathbf{a}_N \end{aligned} \quad (6.77)$$

where we have used $p(\mathbf{t}_N | a_{N+1}, \mathbf{a}_N) = p(\mathbf{t}_N | \mathbf{a}_N)$. The conditional distribution $p(a_{N+1} | \mathbf{a}_N)$ is obtained by invoking the results (6.66) and (6.67) for Gaussian process regression, to give

$$p(a_{N+1} | \mathbf{a}_N) = \mathcal{N}(a_{N+1} | \mathbf{k}^T \mathbf{C}_N^{-1} \mathbf{a}_N, c - \mathbf{k}^T \mathbf{C}_N^{-1} \mathbf{k}). \quad (6.78)$$

We can therefore evaluate the integral in (6.77) by finding a Laplace approximation for the posterior distribution $p(\mathbf{a}_N | \mathbf{t}_N)$, and then using the standard result for the convolution of two Gaussian distributions.

The prior $p(\mathbf{a}_N)$ is given by a zero-mean Gaussian process with covariance matrix \mathbf{C}_N , and the data term (assuming independence of the data points) is given by

$$p(\mathbf{t}_N | \mathbf{a}_N) = \prod_{n=1}^N \sigma(a_n)^{t_n} (1 - \sigma(a_n))^{1-t_n} = \prod_{n=1}^N e^{a_n t_n} \sigma(-a_n). \quad (6.79)$$

We then obtain the Laplace approximation by Taylor expanding the logarithm of $p(\mathbf{a}_N | \mathbf{t}_N)$, which up to an additive normalization constant is given by the quantity

$$\begin{aligned} \Psi(\mathbf{a}_N) &= \ln p(\mathbf{a}_N) + \ln p(\mathbf{t}_N | \mathbf{a}_N) \\ &= -\frac{1}{2} \mathbf{a}_N^T \mathbf{C}_N^{-1} \mathbf{a}_N - \frac{N}{2} \ln(2\pi) - \frac{1}{2} \ln |\mathbf{C}_N| + \mathbf{t}_N^T \mathbf{a}_N \\ &\quad - \sum_{n=1}^N \ln(1 + e^{a_n}) + \text{const.} \end{aligned} \quad (6.80)$$

First we need to find the mode of the posterior distribution, and this requires that we evaluate the gradient of $\Psi(\mathbf{a}_N)$, which is given by

$$\nabla \Psi(\mathbf{a}_N) = \mathbf{t}_N - \boldsymbol{\sigma}_N - \mathbf{C}_N^{-1} \mathbf{a}_N \quad (6.81)$$

where $\boldsymbol{\sigma}_N$ is a vector with elements $\sigma(a_n)$. We cannot simply find the mode by setting this gradient to zero, because $\boldsymbol{\sigma}_N$ depends nonlinearly on \mathbf{a}_N , and so we resort to an iterative scheme based on the Newton-Raphson method, which gives rise to an iterative reweighted least squares (IRLS) algorithm. This requires the second derivatives of $\Psi(\mathbf{a}_N)$, which we also require for the Laplace approximation anyway, and which are given by

$$\nabla \nabla \Psi(\mathbf{a}_N) = -\mathbf{W}_N - \mathbf{C}_N^{-1} \quad (6.82)$$

where \mathbf{W}_N is a diagonal matrix with elements $\sigma(a_n)(1 - \sigma(a_n))$, and we have used the result (4.88) for the derivative of the logistic sigmoid function. Note that these diagonal elements lie in the range $(0, 1/4)$, and hence \mathbf{W}_N is a positive definite matrix. Because \mathbf{C}_N (and hence its inverse) is positive definite by construction, and because the sum of two positive definite matrices is also positive definite, we see that the Hessian matrix $\mathbf{A} = -\nabla \nabla \Psi(\mathbf{a}_N)$ is positive definite and so the posterior distribution $p(\mathbf{a}_N | \mathbf{t}_N)$ is log convex and therefore has a single mode that is the global

Section 4.3.3

Exercise 6.24

maximum. The posterior distribution is not Gaussian, however, because the Hessian is a function of \mathbf{a}_N .

Exercise 6.25

Using the Newton-Raphson formula (4.92), the iterative update equation for \mathbf{a}_N is given by

$$\mathbf{a}_N^{\text{new}} = \mathbf{C}_N(\mathbf{I} + \mathbf{W}_N \mathbf{C}_N)^{-1} \{ \mathbf{t}_N - \boldsymbol{\sigma}_N + \mathbf{W}_N \mathbf{a}_N \}. \quad (6.83)$$

These equations are iterated until they converge to the mode which we denote by \mathbf{a}_N^* . At the mode, the gradient $\nabla\Psi(\mathbf{a}_N)$ will vanish, and hence \mathbf{a}_N^* will satisfy

$$\mathbf{a}_N^* = \mathbf{C}_N(\mathbf{t}_N - \boldsymbol{\sigma}_N). \quad (6.84)$$

Once we have found the mode \mathbf{a}_N^* of the posterior, we can evaluate the Hessian matrix given by

$$\mathbf{H} = -\nabla\nabla\Psi(\mathbf{a}_N) = \mathbf{W}_N + \mathbf{C}_N^{-1} \quad (6.85)$$

where the elements of \mathbf{W}_N are evaluated using \mathbf{a}_N^* . This defines our Gaussian approximation to the posterior distribution $p(\mathbf{a}_N|\mathbf{t}_N)$ given by

$$q(\mathbf{a}_N) = \mathcal{N}(\mathbf{a}_N|\mathbf{a}_N^*, \mathbf{H}^{-1}). \quad (6.86)$$

We can now combine this with (6.78) and hence evaluate the integral (6.77). Because this corresponds to a linear-Gaussian model, we can use the general result (2.115) to give

$$\mathbb{E}[a_{N+1}|\mathbf{t}_N] = \mathbf{k}^T(\mathbf{t}_N - \boldsymbol{\sigma}_N) \quad (6.87)$$

$$\text{var}[a_{N+1}|\mathbf{t}_N] = c - \mathbf{k}^T(\mathbf{W}_N^{-1} + \mathbf{C}_N)^{-1}\mathbf{k}. \quad (6.88)$$

Now that we have a Gaussian distribution for $p(a_{N+1}|\mathbf{t}_N)$, we can approximate the integral (6.76) using the result (4.153). As with the Bayesian logistic regression model of Section 4.5, if we are only interested in the decision boundary corresponding to $p(t_{N+1}|\mathbf{t}_N) = 0.5$, then we need only consider the mean and we can ignore the effect of the variance.

We also need to determine the parameters $\boldsymbol{\theta}$ of the covariance function. One approach is to maximize the likelihood function given by $p(\mathbf{t}_N|\boldsymbol{\theta})$ for which we need expressions for the log likelihood and its gradient. If desired, suitable regularization terms can also be added, leading to a penalized maximum likelihood solution. The likelihood function is defined by

$$p(\mathbf{t}_N|\boldsymbol{\theta}) = \int p(\mathbf{t}_N|\mathbf{a}_N)p(\mathbf{a}_N|\boldsymbol{\theta}) d\mathbf{a}_N. \quad (6.89)$$

This integral is analytically intractable, so again we make use of the Laplace approximation. Using the result (4.135), we obtain the following approximation for the log of the likelihood function

$$\ln p(\mathbf{t}_N|\boldsymbol{\theta}) = \Psi(\mathbf{a}_N^*) - \frac{1}{2} \ln |\mathbf{W}_N + \mathbf{C}_N^{-1}| + \frac{N}{2} \ln(2\pi) \quad (6.90)$$

where $\Psi(\mathbf{a}_N^*) = \ln p(\mathbf{a}_N^* | \boldsymbol{\theta}) + \ln p(\mathbf{t}_N | \mathbf{a}_N^*)$. We also need to evaluate the gradient of $\ln p(\mathbf{t}_N | \boldsymbol{\theta})$ with respect to the parameter vector $\boldsymbol{\theta}$. Note that changes in $\boldsymbol{\theta}$ will cause changes in \mathbf{a}_N^* , leading to additional terms in the gradient. Thus, when we differentiate (6.90) with respect to $\boldsymbol{\theta}$, we obtain two sets of terms, the first arising from the dependence of the covariance matrix \mathbf{C}_N on $\boldsymbol{\theta}$, and the rest arising from dependence of \mathbf{a}_N^* on $\boldsymbol{\theta}$.

The terms arising from the explicit dependence on $\boldsymbol{\theta}$ can be found by using (6.80) together with the results (C.21) and (C.22), and are given by

$$\begin{aligned} \frac{\partial \ln p(\mathbf{t}_N | \boldsymbol{\theta})}{\partial \theta_j} &= \frac{1}{2} \mathbf{a}_N^{*\top} \mathbf{C}_N^{-1} \frac{\partial \mathbf{C}_N}{\partial \theta_j} \mathbf{C}_N^{-1} \mathbf{a}_N^* \\ &\quad - \frac{1}{2} \text{Tr} \left[(\mathbf{I} + \mathbf{C}_N \mathbf{W}_N)^{-1} \mathbf{W}_N \frac{\partial \mathbf{C}_N}{\partial \theta_j} \right]. \end{aligned} \quad (6.91)$$

To compute the terms arising from the dependence of \mathbf{a}_N^* on $\boldsymbol{\theta}$, we note that the Laplace approximation has been constructed such that $\Psi(\mathbf{a}_N)$ has zero gradient at $\mathbf{a}_N = \mathbf{a}_N^*$, and so $\Psi(\mathbf{a}_N^*)$ gives no contribution to the gradient as a result of its dependence on \mathbf{a}_N^* . This leaves the following contribution to the derivative with respect to a component θ_j of $\boldsymbol{\theta}$

$$\begin{aligned} &- \frac{1}{2} \sum_{n=1}^N \frac{\partial \ln |\mathbf{W}_N + \mathbf{C}_N^{-1}|}{\partial a_n^*} \frac{\partial a_n^*}{\partial \theta_j} \\ &= - \frac{1}{2} \sum_{n=1}^N [(\mathbf{I} + \mathbf{C}_N \mathbf{W}_N)^{-1} \mathbf{C}_N]_{nn} \sigma_n^* (1 - \sigma_n^*) (1 - 2\sigma_n^*) \frac{\partial a_n^*}{\partial \theta_j} \end{aligned} \quad (6.92)$$

where $\sigma_n^* = \sigma(a_n^*)$, and again we have used the result (C.22) together with the definition of \mathbf{W}_N . We can evaluate the derivative of a_N^* with respect to θ_j by differentiating the relation (6.84) with respect to θ_j to give

$$\frac{\partial a_n^*}{\partial \theta_j} = \frac{\partial \mathbf{C}_N}{\partial \theta_j} (\mathbf{t}_N - \boldsymbol{\sigma}_N) - \mathbf{C}_N \mathbf{W}_N \frac{\partial a_n^*}{\partial \theta_j}. \quad (6.93)$$

Rearranging then gives

$$\frac{\partial a_n^*}{\partial \theta_j} = (\mathbf{I} + \mathbf{W}_N \mathbf{C}_N)^{-1} \frac{\partial \mathbf{C}_N}{\partial \theta_j} (\mathbf{t}_N - \boldsymbol{\sigma}_N). \quad (6.94)$$

Combining (6.91), (6.92), and (6.94), we can evaluate the gradient of the log likelihood function, which can be used with standard nonlinear optimization algorithms in order to determine a value for $\boldsymbol{\theta}$.

We can illustrate the application of the Laplace approximation for Gaussian processes using the synthetic two-class data set shown in Figure 6.12. Extension of the Laplace approximation to Gaussian processes involving $K > 2$ classes, using the softmax activation function, is straightforward (Williams and Barber, 1998).



Figure 6.12 Illustration of the use of a Gaussian process for classification, showing the data on the left together with the optimal decision boundary from the true distribution in green, and the decision boundary from the Gaussian process classifier in black. On the right is the predicted posterior probability for the blue and red classes together with the Gaussian process decision boundary.

6.4.7 Connection to neural networks

We have seen that the range of functions which can be represented by a neural network is governed by the number M of hidden units, and that, for sufficiently large M , a two-layer network can approximate any given function with arbitrary accuracy. In the framework of maximum likelihood, the number of hidden units needs to be limited (to a level dependent on the size of the training set) in order to avoid over-fitting. However, from a Bayesian perspective it makes little sense to limit the number of parameters in the network according to the size of the training set.

In a Bayesian neural network, the prior distribution over the parameter vector \mathbf{w} , in conjunction with the network function $f(\mathbf{x}, \mathbf{w})$, produces a prior distribution over functions from $y(\mathbf{x})$ where y is the vector of network outputs. Neal (1996) has shown that, for a broad class of prior distributions over \mathbf{w} , the distribution of functions generated by a neural network will tend to a Gaussian process in the limit $M \rightarrow \infty$. It should be noted, however, that in this limit the output variables of the neural network become independent. One of the great merits of neural networks is that the outputs share the hidden units and so they can ‘borrow statistical strength’ from each other, that is, the weights associated with each hidden unit are influenced by all of the output variables not just by one of them. This property is therefore lost in the Gaussian process limit.

We have seen that a Gaussian process is determined by its covariance (kernel) function. Williams (1998) has given explicit forms for the covariance in the case of two specific choices for the hidden unit activation function (probit and Gaussian). These kernel functions $k(\mathbf{x}, \mathbf{x}')$ are nonstationary, i.e. they cannot be expressed as a function of the difference $\mathbf{x} - \mathbf{x}'$, as a consequence of the Gaussian weight prior being centred on zero which breaks translation invariance in weight space.

By working directly with the covariance function we have implicitly marginalized over the distribution of weights. If the weight prior is governed by hyperparameters, then their values will determine the length scales of the distribution over functions, as can be understood by studying the examples in Figure 5.11 for the case of a finite number of hidden units. Note that we cannot marginalize out the hyperparameters analytically, and must instead resort to techniques of the kind discussed in Section 6.4.

Exercises

- 6.1** (**) **www** Consider the dual formulation of the least squares linear regression problem given in Section 6.1. Show that the solution for the components a_n of the vector \mathbf{a} can be expressed as a linear combination of the elements of the vector $\phi(\mathbf{x}_n)$. Denoting these coefficients by the vector \mathbf{w} , show that the dual of the dual formulation is given by the original representation in terms of the parameter vector \mathbf{w} .
- 6.2** (**) In this exercise, we develop a dual formulation of the perceptron learning algorithm. Using the perceptron learning rule (4.55), show that the learned weight vector \mathbf{w} can be written as a linear combination of the vectors $t_n \phi(\mathbf{x}_n)$ where $t_n \in \{-1, +1\}$. Denote the coefficients of this linear combination by α_n and derive a formulation of the perceptron learning algorithm, and the predictive function for the perceptron, in terms of the α_n . Show that the feature vector $\phi(\mathbf{x})$ enters only in the form of the kernel function $k(\mathbf{x}, \mathbf{x}') = \phi(\mathbf{x})^\top \phi(\mathbf{x}')$.
- 6.3** (*) The nearest-neighbour classifier (Section 2.5.2) assigns a new input vector \mathbf{x} to the same class as that of the nearest input vector \mathbf{x}_n from the training set, where in the simplest case, the distance is defined by the Euclidean metric $\|\mathbf{x} - \mathbf{x}_n\|^2$. By expressing this rule in terms of scalar products and then making use of kernel substitution, formulate the nearest-neighbour classifier for a general nonlinear kernel.
- 6.4** (*) In Appendix C, we give an example of a matrix that has positive elements but that has a negative eigenvalue and hence that is not positive definite. Find an example of the converse property, namely a 2×2 matrix with positive eigenvalues yet that has at least one negative element.
- 6.5** (*) **www** Verify the results (6.13) and (6.14) for constructing valid kernels.
- 6.6** (*) Verify the results (6.15) and (6.16) for constructing valid kernels.
- 6.7** (*) **www** Verify the results (6.17) and (6.18) for constructing valid kernels.
- 6.8** (*) Verify the results (6.19) and (6.20) for constructing valid kernels.
- 6.9** (*) Verify the results (6.21) and (6.22) for constructing valid kernels.
- 6.10** (*) Show that an excellent choice of kernel for learning a function $f(\mathbf{x})$ is given by $k(\mathbf{x}, \mathbf{x}') = f(\mathbf{x})f(\mathbf{x}')$ by showing that a linear learning machine based on this kernel will always find a solution proportional to $f(\mathbf{x})$.

6.11 (★) By making use of the expansion (6.25), and then expanding the middle factor as a power series, show that the Gaussian kernel (6.23) can be expressed as the inner product of an infinite-dimensional feature vector.

6.12 (★★) **www** Consider the space of all possible subsets A of a given fixed set D . Show that the kernel function (6.27) corresponds to an inner product in a feature space of dimensionality $2^{|D|}$ defined by the mapping $\phi(A)$ where A is a subset of D and the element $\phi_U(A)$, indexed by the subset U , is given by

$$\phi_U(A) = \begin{cases} 1, & \text{if } U \subseteq A; \\ 0, & \text{otherwise.} \end{cases} \quad (6.95)$$

Here $U \subseteq A$ denotes that U is either a subset of A or is equal to A .

6.13 (★) Show that the Fisher kernel, defined by (6.33), remains invariant if we make a nonlinear transformation of the parameter vector $\theta \rightarrow \psi(\theta)$, where the function $\psi(\cdot)$ is invertible and differentiable.

6.14 (★) **www** Write down the form of the Fisher kernel, defined by (6.33), for the case of a distribution $p(\mathbf{x}|\boldsymbol{\mu}) = \mathcal{N}(\mathbf{x}|\boldsymbol{\mu}, \mathbf{S})$ that is Gaussian with mean $\boldsymbol{\mu}$ and fixed covariance \mathbf{S} .

6.15 (★) By considering the determinant of a 2×2 Gram matrix, show that a positive-definite kernel function $k(x, x')$ satisfies the Cauchy-Schwartz inequality

$$k(x_1, x_2)^2 \leq k(x_1, x_1)k(x_2, x_2). \quad (6.96)$$

6.16 (★★) Consider a parametric model governed by the parameter vector \mathbf{w} together with a data set of input values $\mathbf{x}_1, \dots, \mathbf{x}_N$ and a nonlinear feature mapping $\phi(\mathbf{x})$. Suppose that the dependence of the error function on \mathbf{w} takes the form

$$J(\mathbf{w}) = f(\mathbf{w}^T \phi(\mathbf{x}_1), \dots, \mathbf{w}^T \phi(\mathbf{x}_N)) + g(\mathbf{w}^T \mathbf{w}) \quad (6.97)$$

where $g(\cdot)$ is a monotonically increasing function. By writing \mathbf{w} in the form

$$\mathbf{w} = \sum_{n=1}^N \alpha_n \phi(\mathbf{x}_n) + \mathbf{w}_\perp \quad (6.98)$$

show that the value of \mathbf{w} that minimizes $J(\mathbf{w})$ takes the form of a linear combination of the basis functions $\phi(\mathbf{x}_n)$ for $n = 1, \dots, N$.

6.17 (★★) **www** Consider the sum-of-squares error function (6.39) for data having noisy inputs, where $\nu(\xi)$ is the distribution of the noise. Use the calculus of variations to minimize this error function with respect to the function $y(\mathbf{x})$, and hence show that the optimal solution is given by an expansion of the form (6.40) in which the basis functions are given by (6.41).

- 6.18** (*) Consider a Nadaraya-Watson model with one input variable x and one target variable t having Gaussian components with isotropic covariances, so that the covariance matrix is given by $\sigma^2 \mathbf{I}$ where \mathbf{I} is the unit matrix. Write down expressions for the conditional density $p(t|x)$ and for the conditional mean $\mathbb{E}[t|x]$ and variance $\text{var}[t|x]$, in terms of the kernel function $k(x, x_n)$.
- 6.19** (**) Another viewpoint on kernel regression comes from a consideration of regression problems in which the input variables as well as the target variables are corrupted with additive noise. Suppose each target value t_n is generated as usual by taking a function $y(\mathbf{z}_n)$ evaluated at a point \mathbf{z}_n , and adding Gaussian noise. The value of \mathbf{z}_n is not directly observed, however, but only a noise corrupted version $\mathbf{x}_n = \mathbf{z}_n + \boldsymbol{\xi}_n$ where the random variable $\boldsymbol{\xi}$ is governed by some distribution $g(\boldsymbol{\xi})$. Consider a set of observations $\{\mathbf{x}_n, t_n\}$, where $n = 1, \dots, N$, together with a corresponding sum-of-squares error function defined by averaging over the distribution of input noise to give
- $$E = \frac{1}{2} \sum_{n=1}^N \int \{y(\mathbf{x}_n - \boldsymbol{\xi}_n) - t_n\}^2 g(\boldsymbol{\xi}_n) d\boldsymbol{\xi}_n. \quad (6.99)$$
- By minimizing E with respect to the function $y(\mathbf{z})$ using the calculus of variations (Appendix D), show that optimal solution for $y(\mathbf{x})$ is given by a Nadaraya-Watson kernel regression solution of the form (6.45) with a kernel of the form (6.46).
- 6.20** (**) **www** Verify the results (6.66) and (6.67).
- 6.21** (**) **www** Consider a Gaussian process regression model in which the kernel function is defined in terms of a fixed set of nonlinear basis functions. Show that the predictive distribution is identical to the result (3.58) obtained in Section 3.3.2 for the Bayesian linear regression model. To do this, note that both models have Gaussian predictive distributions, and so it is only necessary to show that the conditional mean and variance are the same. For the mean, make use of the matrix identity (C.6), and for the variance, make use of the matrix identity (C.7).
- 6.22** (**) Consider a regression problem with N training set input vectors $\mathbf{x}_1, \dots, \mathbf{x}_N$ and L test set input vectors $\mathbf{x}_{N+1}, \dots, \mathbf{x}_{N+L}$, and suppose we define a Gaussian process prior over functions $t(\mathbf{x})$. Derive an expression for the joint predictive distribution for $t(\mathbf{x}_{N+1}), \dots, t(\mathbf{x}_{N+L})$, given the values of $t(\mathbf{x}_1), \dots, t(\mathbf{x}_N)$. Show the marginal of this distribution for one of the test observations t_j where $N+1 \leq j \leq N+L$ is given by the usual Gaussian process regression result (6.66) and (6.67).
- 6.23** (**) **www** Consider a Gaussian process regression model in which the target variable \mathbf{t} has dimensionality D . Write down the conditional distribution of \mathbf{t}_{N+1} for a test input vector \mathbf{x}_{N+1} , given a training set of input vectors $\mathbf{x}_1, \dots, \mathbf{x}_{N+1}$ and corresponding target observations $\mathbf{t}_1, \dots, \mathbf{t}_N$.
- 6.24** (*) Show that a diagonal matrix \mathbf{W} whose elements satisfy $0 < W_{ii} < 1$ is positive definite. Show that the sum of two positive definite matrices is itself positive definite.

- 6.25** (★) **www** Using the Newton-Raphson formula (4.92), derive the iterative update formula (6.83) for finding the mode \mathbf{a}_N^* of the posterior distribution in the Gaussian process classification model.
- 6.26** (★) Using the result (2.115), derive the expressions (6.87) and (6.88) for the mean and variance of the posterior distribution $p(a_{N+1}|\mathbf{t}_N)$ in the Gaussian process classification model.
- 6.27** (★★★) Derive the result (6.90) for the log likelihood function in the Laplace approximation framework for Gaussian process classification. Similarly, derive the results (6.91), (6.92), and (6.94) for the terms in the gradient of the log likelihood.

7

Sparse Kernel Machines

In the previous chapter, we explored a variety of learning algorithms based on non-linear kernels. One of the significant limitations of many such algorithms is that the kernel function $k(\mathbf{x}_n, \mathbf{x}_m)$ must be evaluated for all possible pairs \mathbf{x}_n and \mathbf{x}_m of training points, which can be computationally infeasible during training and can lead to excessive computation times when making predictions for new data points. In this chapter we shall look at kernel-based algorithms that have *sparse* solutions, so that predictions for new inputs depend only on the kernel function evaluated at a subset of the training data points.

We begin by looking in some detail at the *support vector machine* (SVM), which became popular in some years ago for solving problems in classification, regression, and novelty detection. An important property of support vector machines is that the determination of the model parameters corresponds to a convex optimization problem, and so any local solution is also a global optimum. Because the discussion of support vector machines makes extensive use of Lagrange multipliers, the reader is

encouraged to review the key concepts covered in Appendix E. Additional information on support vector machines can be found in Vapnik (1995), Burges (1998), Cristianini and Shawe-Taylor (2000), Müller *et al.* (2001), Schölkopf and Smola (2002), and Herbrich (2002).

The SVM is a decision machine and so does not provide posterior probabilities. We have already discussed some of the benefits of determining probabilities in Section 1.5.4. An alternative sparse kernel technique, known as the *relevance vector machine* (RVM), is based on a Bayesian formulation and provides posterior probabilistic outputs, as well as having typically much sparser solutions than the SVM.

Section 7.2

7.1. Maximum Margin Classifiers

We begin our discussion of support vector machines by returning to the two-class classification problem using linear models of the form

$$y(\mathbf{x}) = \mathbf{w}^T \phi(\mathbf{x}) + b \quad (7.1)$$

where $\phi(\mathbf{x})$ denotes a fixed feature-space transformation, and we have made the bias parameter b explicit. Note that we shall shortly introduce a dual representation expressed in terms of kernel functions, which avoids having to work explicitly in feature space. The training data set comprises N input vectors $\mathbf{x}_1, \dots, \mathbf{x}_N$, with corresponding target values t_1, \dots, t_N where $t_n \in \{-1, 1\}$, and new data points \mathbf{x} are classified according to the sign of $y(\mathbf{x})$.

We shall assume for the moment that the training data set is linearly separable in feature space, so that by definition there exists at least one choice of the parameters \mathbf{w} and b such that a function of the form (7.1) satisfies $y(\mathbf{x}_n) > 0$ for points having $t_n = +1$ and $y(\mathbf{x}_n) < 0$ for points having $t_n = -1$, so that $t_n y(\mathbf{x}_n) > 0$ for all training data points.

There may of course exist many such solutions that separate the classes exactly. In Section 4.1.7, we described the perceptron algorithm that is guaranteed to find a solution in a finite number of steps. The solution that it finds, however, will be dependent on the (arbitrary) initial values chosen for \mathbf{w} and b as well as on the order in which the data points are presented. If there are multiple solutions all of which classify the training data set exactly, then we should try to find the one that will give the smallest generalization error. The support vector machine approaches this problem through the concept of the *margin*, which is defined to be the smallest distance between the decision boundary and any of the samples, as illustrated in Figure 7.1.

In support vector machines the decision boundary is chosen to be the one for which the margin is maximized. The maximum margin solution can be motivated using *computational learning theory*, also known as *statistical learning theory*. However, a simple insight into the origins of maximum margin has been given by Tong and Koller (2000) who consider a framework for classification based on a hybrid of generative and discriminative approaches. They first model the distribution over input vectors \mathbf{x} for each class using a Parzen density estimator with Gaussian kernels

Section 7.1.5



Figure 7.1 The margin is defined as the perpendicular distance between the decision boundary and the closest of the data points, as shown on the left figure. Maximizing the margin leads to a particular choice of decision boundary, as shown on the right. The location of this boundary is determined by a subset of the data points, known as support vectors, which are indicated by the circles.

having a common parameter σ^2 . Together with the class priors, this defines an optimal misclassification-rate decision boundary. However, instead of using this optimal boundary, they determine the best hyperplane by minimizing the probability of error relative to the learned density model. In the limit $\sigma^2 \rightarrow 0$, the optimal hyperplane is shown to be the one having maximum margin. The intuition behind this result is that as σ^2 is reduced, the hyperplane is increasingly dominated by nearby data points relative to more distant ones. In the limit, the hyperplane becomes independent of data points that are not support vectors.

We shall see in Figure 10.13 that marginalization with respect to the prior distribution of the parameters in a Bayesian approach for a simple linearly separable data set leads to a decision boundary that lies in the middle of the region separating the data points. The large margin solution has similar behaviour.

Recall from Figure 4.1 that the perpendicular distance of a point \mathbf{x} from a hyperplane defined by $y(\mathbf{x}) = 0$ where $y(\mathbf{x})$ takes the form (7.1) is given by $|y(\mathbf{x})|/\|\mathbf{w}\|$. Furthermore, we are only interested in solutions for which all data points are correctly classified, so that $t_n y(\mathbf{x}_n) > 0$ for all n . Thus the distance of a point \mathbf{x}_n to the decision surface is given by

$$\frac{t_n y(\mathbf{x}_n)}{\|\mathbf{w}\|} = \frac{t_n (\mathbf{w}^T \phi(\mathbf{x}_n) + b)}{\|\mathbf{w}\|}. \quad (7.2)$$

The margin is given by the perpendicular distance to the closest point \mathbf{x}_n from the data set, and we wish to optimize the parameters \mathbf{w} and b in order to maximize this distance. Thus the maximum margin solution is found by solving

$$\arg \max_{\mathbf{w}, b} \left\{ \frac{1}{\|\mathbf{w}\|} \min_n [t_n (\mathbf{w}^T \phi(\mathbf{x}_n) + b)] \right\} \quad (7.3)$$

where we have taken the factor $1/\|\mathbf{w}\|$ outside the optimization over n because \mathbf{w}

does not depend on n . Direct solution of this optimization problem would be very complex, and so we shall convert it into an equivalent problem that is much easier to solve. To do this we note that if we make the rescaling $\mathbf{w} \rightarrow \kappa\mathbf{w}$ and $b \rightarrow \kappa b$, then the distance from any point \mathbf{x}_n to the decision surface, given by $t_n y(\mathbf{x}_n)/\|\mathbf{w}\|$, is unchanged. We can use this freedom to set

$$t_n (\mathbf{w}^T \phi(\mathbf{x}_n) + b) = 1 \quad (7.4)$$

for the point that is closest to the surface. In this case, all data points will satisfy the constraints

$$t_n (\mathbf{w}^T \phi(\mathbf{x}_n) + b) \geq 1, \quad n = 1, \dots, N. \quad (7.5)$$

This is known as the canonical representation of the decision hyperplane. In the case of data points for which the equality holds, the constraints are said to be *active*, whereas for the remainder they are said to be *inactive*. By definition, there will always be at least one active constraint, because there will always be a closest point, and once the margin has been maximized there will be at least two active constraints. The optimization problem then simply requires that we maximize $\|\mathbf{w}\|^{-1}$, which is equivalent to minimizing $\|\mathbf{w}\|^2$, and so we have to solve the optimization problem

$$\arg \min_{\mathbf{w}, b} \frac{1}{2} \|\mathbf{w}\|^2 \quad (7.6)$$

subject to the constraints given by (7.5). The factor of $1/2$ in (7.6) is included for later convenience. This is an example of a *quadratic programming* problem in which we are trying to minimize a quadratic function subject to a set of linear inequality constraints. It appears that the bias parameter b has disappeared from the optimization. However, it is determined implicitly via the constraints, because these require that changes to $\|\mathbf{w}\|$ be compensated by changes to b . We shall see how this works shortly.

Appendix E In order to solve this constrained optimization problem, we introduce Lagrange multipliers $a_n \geq 0$, with one multiplier a_n for each of the constraints in (7.5), giving the Lagrangian function

$$L(\mathbf{w}, b, \mathbf{a}) = \frac{1}{2} \|\mathbf{w}\|^2 - \sum_{n=1}^N a_n \{ t_n (\mathbf{w}^T \phi(\mathbf{x}_n) + b) - 1 \} \quad (7.7)$$

where $\mathbf{a} = (a_1, \dots, a_N)^T$. Note the minus sign in front of the Lagrange multiplier term, because we are minimizing with respect to \mathbf{w} and b , and maximizing with respect to \mathbf{a} . Setting the derivatives of $L(\mathbf{w}, b, \mathbf{a})$ with respect to \mathbf{w} and b equal to zero, we obtain the following two conditions

$$\mathbf{w} = \sum_{n=1}^N a_n t_n \phi(\mathbf{x}_n) \quad (7.8)$$

$$0 = \sum_{n=1}^N a_n t_n. \quad (7.9)$$

Eliminating \mathbf{w} and b from $L(\mathbf{w}, b, \mathbf{a})$ using these conditions then gives the *dual representation* of the maximum margin problem in which we maximize

$$\tilde{L}(\mathbf{a}) = \sum_{n=1}^N a_n - \frac{1}{2} \sum_{n=1}^N \sum_{m=1}^N a_n a_m t_n t_m k(\mathbf{x}_n, \mathbf{x}_m) \quad (7.10)$$

with respect to \mathbf{a} subject to the constraints

$$a_n \geq 0, \quad n = 1, \dots, N, \quad (7.11)$$

$$\sum_{n=1}^N a_n t_n = 0. \quad (7.12)$$

Here the kernel function is defined by $k(\mathbf{x}, \mathbf{x}') = \phi(\mathbf{x})^T \phi(\mathbf{x}')$. Again, this takes the form of a quadratic programming problem in which we optimize a quadratic function of \mathbf{a} subject to a set of inequality constraints. We shall discuss techniques for solving such quadratic programming problems in Section 7.1.1.

The solution to a quadratic programming problem in M variables in general has computational complexity that is $O(M^3)$. In going to the dual formulation we have turned the original optimization problem, which involved minimizing (7.6) over M variables, into the dual problem (7.10), which has N variables. For a fixed set of basis functions whose number M is smaller than the number N of data points, the move to the dual problem appears disadvantageous. However, it allows the model to be reformulated using kernels, and so the maximum margin classifier can be applied efficiently to feature spaces whose dimensionality exceeds the number of data points, including infinite feature spaces. The kernel formulation also makes clear the role of the constraint that the kernel function $k(\mathbf{x}, \mathbf{x}')$ be positive definite, because this ensures that the Lagrangian function $\tilde{L}(\mathbf{a})$ is bounded below, giving rise to a well-defined optimization problem.

In order to classify new data points using the trained model, we evaluate the sign of $y(\mathbf{x})$ defined by (7.1). This can be expressed in terms of the parameters $\{a_n\}$ and the kernel function by substituting for \mathbf{w} using (7.8) to give

$$y(\mathbf{x}) = \sum_{n=1}^N a_n t_n k(\mathbf{x}, \mathbf{x}_n) + b. \quad (7.13)$$



Joseph-Louis Lagrange
1736–1813

Although widely considered to be a French mathematician, Lagrange was born in Turin in Italy. By the age of nineteen, he had already made important contributions mathematics and had been appointed as Professor at the Royal Artillery School in Turin. For many

years, Euler worked hard to persuade Lagrange to move to Berlin, which he eventually did in 1766 where he succeeded Euler as Director of Mathematics at the Berlin Academy. Later he moved to Paris, narrowly escaping with his life during the French revolution thanks to the personal intervention of Lavoisier (the French chemist who discovered oxygen) who himself was later executed at the guillotine. Lagrange made key contributions to the calculus of variations and the foundations of dynamics.

In Appendix E, we show that a constrained optimization of this form satisfies the *Karush-Kuhn-Tucker* (KKT) conditions, which in this case require that the following three properties hold

$$a_n \geq 0 \quad (7.14)$$

$$t_n y(\mathbf{x}_n) - 1 \geq 0 \quad (7.15)$$

$$a_n \{t_n y(\mathbf{x}_n) - 1\} = 0. \quad (7.16)$$

Thus for every data point, either $a_n = 0$ or $t_n y(\mathbf{x}_n) = 1$. Any data point for which $a_n = 0$ will not appear in the sum in (7.13) and hence plays no role in making predictions for new data points. The remaining data points are called *support vectors*, and because they satisfy $t_n y(\mathbf{x}_n) = 1$, they correspond to points that lie on the maximum margin hyperplanes in feature space, as illustrated in Figure 7.1. This property is central to the practical applicability of support vector machines. Once the model is trained, a significant proportion of the data points can be discarded and only the support vectors retained.

Having solved the quadratic programming problem and found a value for \mathbf{a} , we can then determine the value of the threshold parameter b by noting that any support vector \mathbf{x}_n satisfies $t_n y(\mathbf{x}_n) = 1$. Using (7.13) this gives

$$t_n \left(\sum_{m \in \mathcal{S}} a_m t_m k(\mathbf{x}_n, \mathbf{x}_m) + b \right) = 1 \quad (7.17)$$

where \mathcal{S} denotes the set of indices of the support vectors. Although we can solve this equation for b using an arbitrarily chosen support vector \mathbf{x}_n , a numerically more stable solution is obtained by first multiplying through by t_n , making use of $t_n^2 = 1$, and then averaging these equations over all support vectors and solving for b to give

$$b = \frac{1}{N_{\mathcal{S}}} \sum_{n \in \mathcal{S}} \left(t_n - \sum_{m \in \mathcal{S}} a_m t_m k(\mathbf{x}_n, \mathbf{x}_m) \right) \quad (7.18)$$

where $N_{\mathcal{S}}$ is the total number of support vectors.

For later comparison with alternative models, we can express the maximum-margin classifier in terms of the minimization of an error function, with a simple quadratic regularizer, in the form

$$\sum_{n=1}^N E_\infty(y(\mathbf{x}_n)t_n - 1) + \lambda \|\mathbf{w}\|^2 \quad (7.19)$$

where $E_\infty(z)$ is a function that is zero if $z \geq 0$ and ∞ otherwise and ensures that the constraints (7.5) are satisfied. Note that as long as the regularization parameter satisfies $\lambda > 0$, its precise value plays no role.

Figure 7.2 shows an example of the classification resulting from training a support vector machine on a simple synthetic data set using a Gaussian kernel of the

Figure 7.2 Example of synthetic data from two classes in two dimensions showing contours of constant $y(\mathbf{x})$ obtained from a support vector machine having a Gaussian kernel function. Also shown are the decision boundary, the margin boundaries, and the support vectors.



form (6.23). Although the data set is not linearly separable in the two-dimensional data space \mathbf{x} , it is linearly separable in the nonlinear feature space defined implicitly by the nonlinear kernel function. Thus the training data points are perfectly separated in the original data space.

This example also provides a geometrical insight into the origin of sparsity in the SVM. The maximum margin hyperplane is defined by the location of the support vectors. Other data points can be moved around freely (so long as they remain outside the margin region) without changing the decision boundary, and so the solution will be independent of such data points.

7.1.1 Overlapping class distributions

So far, we have assumed that the training data points are linearly separable in the feature space $\phi(\mathbf{x})$. The resulting support vector machine will give exact separation of the training data in the original input space \mathbf{x} , although the corresponding decision boundary will be nonlinear. In practice, however, the class-conditional distributions may overlap, in which case exact separation of the training data can lead to poor generalization.

We therefore need a way to modify the support vector machine so as to allow some of the training points to be misclassified. From (7.19) we see that in the case of separable classes, we implicitly used an error function that gave infinite error if a data point was misclassified and zero error if it was classified correctly, and then optimized the model parameters to maximize the margin. We now modify this approach so that data points are allowed to be on the ‘wrong side’ of the margin boundary, but with a penalty that increases with the distance from that boundary. For the subsequent optimization problem, it is convenient to make this penalty a linear function of this distance. To do this, we introduce *slack variables*, $\xi_n \geq 0$ where $n = 1, \dots, N$, with one slack variable for each training data point (Bennett, 1992; Cortes and Vapnik, 1995). These are defined by $\xi_n = 0$ for data points that are on or inside the correct margin boundary and $\xi_n = |t_n - y(\mathbf{x}_n)|$ for other points. Thus a data point that is on the decision boundary $y(\mathbf{x}_n) = 0$ will have $\xi_n = 1$, and points

Figure 7.3 Illustration of the slack variables $\xi_n \geq 0$. Data points with circles around them are support vectors.



with $\xi_n > 1$ will be misclassified. The exact classification constraints (7.5) are then replaced with

$$t_n y(\mathbf{x}_n) \geq 1 - \xi_n, \quad n = 1, \dots, N \quad (7.20)$$

in which the slack variables are constrained to satisfy $\xi_n \geq 0$. Data points for which $\xi_n = 0$ are correctly classified and are either on the margin or on the correct side of the margin. Points for which $0 < \xi_n \leq 1$ lie inside the margin, but on the correct side of the decision boundary, and those data points for which $\xi_n > 1$ lie on the wrong side of the decision boundary and are misclassified, as illustrated in Figure 7.3. This is sometimes described as relaxing the hard margin constraint to give a *soft margin* and allows some of the training set data points to be misclassified. Note that while slack variables allow for overlapping class distributions, this framework is still sensitive to outliers because the penalty for misclassification increases linearly with ξ .

Our goal is now to maximize the margin while softly penalizing points that lie on the wrong side of the margin boundary. We therefore minimize

$$C \sum_{n=1}^N \xi_n + \frac{1}{2} \|\mathbf{w}\|^2 \quad (7.21)$$

where the parameter $C > 0$ controls the trade-off between the slack variable penalty and the margin. Because any point that is misclassified has $\xi_n > 1$, it follows that $\sum_n \xi_n$ is an upper bound on the number of misclassified points. The parameter C is therefore analogous to (the inverse of) a regularization coefficient because it controls the trade-off between minimizing training errors and controlling model complexity. In the limit $C \rightarrow \infty$, we will recover the earlier support vector machine for separable data.

We now wish to minimize (7.21) subject to the constraints (7.20) together with $\xi_n \geq 0$. The corresponding Lagrangian is given by

$$L(\mathbf{w}, b, \mathbf{a}) = \frac{1}{2} \|\mathbf{w}\|^2 + C \sum_{n=1}^N \xi_n - \sum_{n=1}^N a_n \{t_n y(\mathbf{x}_n) - 1 + \xi_n\} - \sum_{n=1}^N \mu_n \xi_n \quad (7.22)$$

Appendix E

where $\{a_n \geq 0\}$ and $\{\mu_n \geq 0\}$ are Lagrange multipliers. The corresponding set of KKT conditions are given by

$$a_n \geq 0 \quad (7.23)$$

$$t_n y(\mathbf{x}_n) - 1 + \xi_n \geq 0 \quad (7.24)$$

$$a_n (t_n y(\mathbf{x}_n) - 1 + \xi_n) = 0 \quad (7.25)$$

$$\mu_n \geq 0 \quad (7.26)$$

$$\xi_n \geq 0 \quad (7.27)$$

$$\mu_n \xi_n = 0 \quad (7.28)$$

where $n = 1, \dots, N$.

We now optimize out \mathbf{w} , b , and $\{\xi_n\}$ making use of the definition (7.1) of $y(\mathbf{x})$ to give

$$\frac{\partial L}{\partial \mathbf{w}} = 0 \Rightarrow \mathbf{w} = \sum_{n=1}^N a_n t_n \phi(\mathbf{x}_n) \quad (7.29)$$

$$\frac{\partial L}{\partial b} = 0 \Rightarrow \sum_{n=1}^N a_n t_n = 0 \quad (7.30)$$

$$\frac{\partial L}{\partial \xi_n} = 0 \Rightarrow a_n = C - \mu_n. \quad (7.31)$$

Using these results to eliminate \mathbf{w} , b , and $\{\xi_n\}$ from the Lagrangian, we obtain the dual Lagrangian in the form

$$\tilde{L}(\mathbf{a}) = \sum_{n=1}^N a_n - \frac{1}{2} \sum_{n=1}^N \sum_{m=1}^N a_n a_m t_n t_m k(\mathbf{x}_n, \mathbf{x}_m) \quad (7.32)$$

which is identical to the separable case, except that the constraints are somewhat different. To see what these constraints are, we note that $a_n \geq 0$ is required because these are Lagrange multipliers. Furthermore, (7.31) together with $\mu_n \geq 0$ implies $a_n \leq C$. We therefore have to minimize (7.32) with respect to the dual variables $\{a_n\}$ subject to

$$0 \leq a_n \leq C \quad (7.33)$$

$$\sum_{n=1}^N a_n t_n = 0 \quad (7.34)$$

for $n = 1, \dots, N$, where (7.33) are known as *box constraints*. This again represents a quadratic programming problem. If we substitute (7.29) into (7.1), we see that predictions for new data points are again made by using (7.13).

We can now interpret the resulting solution. As before, a subset of the data points may have $a_n = 0$, in which case they do not contribute to the predictive

model (7.13). The remaining data points constitute the support vectors. These have $a_n > 0$ and hence from (7.25) must satisfy

$$t_n y(\mathbf{x}_n) = 1 - \xi_n. \quad (7.35)$$

If $a_n < C$, then (7.31) implies that $\mu_n > 0$, which from (7.28) requires $\xi_n = 0$ and hence such points lie on the margin. Points with $a_n = C$ can lie inside the margin and can either be correctly classified if $\xi_n \leq 1$ or misclassified if $\xi_n > 1$.

To determine the parameter b in (7.1), we note that those support vectors for which $0 < a_n < C$ have $\xi_n = 0$ so that $t_n y(\mathbf{x}_n) = 1$ and hence will satisfy

$$t_n \left(\sum_{m \in \mathcal{S}} a_m t_m k(\mathbf{x}_n, \mathbf{x}_m) + b \right) = 1. \quad (7.36)$$

Again, a numerically stable solution is obtained by averaging to give

$$b = \frac{1}{N_{\mathcal{M}}} \sum_{n \in \mathcal{M}} \left(t_n - \sum_{m \in \mathcal{S}} a_m t_m k(\mathbf{x}_n, \mathbf{x}_m) \right) \quad (7.37)$$

where \mathcal{M} denotes the set of indices of data points having $0 < a_n < C$.

An alternative, equivalent formulation of the support vector machine, known as the ν -SVM, has been proposed by Schölkopf *et al.* (2000). This involves maximizing

$$\tilde{L}(\mathbf{a}) = -\frac{1}{2} \sum_{n=1}^N \sum_{m=1}^N a_n a_m t_n t_m k(\mathbf{x}_n, \mathbf{x}_m) \quad (7.38)$$

subject to the constraints

$$0 \leq a_n \leq 1/N \quad (7.39)$$

$$\sum_{n=1}^N a_n t_n = 0 \quad (7.40)$$

$$\sum_{n=1}^N a_n \geq \nu. \quad (7.41)$$

This approach has the advantage that the parameter ν , which replaces C , can be interpreted as both an upper bound on the fraction of *margin errors* (points for which $\xi_n > 0$ and hence which lie on the wrong side of the margin boundary and which may or may not be misclassified) and a lower bound on the fraction of support vectors. An example of the ν -SVM applied to a synthetic data set is shown in Figure 7.4. Here Gaussian kernels of the form $\exp(-\gamma \|\mathbf{x} - \mathbf{x}'\|^2)$ have been used, with $\gamma = 0.45$.

Although predictions for new inputs are made using only the support vectors, the training phase (i.e., the determination of the parameters \mathbf{a} and b) makes use of the whole data set, and so it is important to have efficient algorithms for solving

Figure 7.4 Illustration of the ν -SVM applied to a nonseparable data set in two dimensions. The support vectors are indicated by circles.



the quadratic programming problem. We first note that the objective function $\tilde{L}(\mathbf{a})$ given by (7.10) or (7.32) is quadratic and so any local optimum will also be a global optimum provided the constraints define a convex region (which they do as a consequence of being linear). Direct solution of the quadratic programming problem using traditional techniques is often infeasible due to the demanding computation and memory requirements, and so more practical approaches need to be found. The technique of *chunking* (Vapnik, 1982) exploits the fact that the value of the Lagrangian is unchanged if we remove the rows and columns of the kernel matrix corresponding to Lagrange multipliers that have value zero. This allows the full quadratic programming problem to be broken down into a series of smaller ones, whose goal is eventually to identify all of the nonzero Lagrange multipliers and discard the others. Chunking can be implemented using *protected conjugate gradients* (Burges, 1998). Although chunking reduces the size of the matrix in the quadratic function from the number of data points squared to approximately the number of nonzero Lagrange multipliers squared, even this may be too big to fit in memory for large-scale applications. *Decomposition methods* (Osuna *et al.*, 1996) also solve a series of smaller quadratic programming problems but are designed so that each of these is of a fixed size, and so the technique can be applied to arbitrarily large data sets. However, it still involves numerical solution of quadratic programming subproblems and these can be problematic and expensive. One of the most popular approaches to training support vector machines is called *sequential minimal optimization*, or *SMO* (Platt, 1999). It takes the concept of chunking to the extreme limit and considers just two Lagrange multipliers at a time. In this case, the subproblem can be solved analytically, thereby avoiding numerical quadratic programming altogether. Heuristics are given for choosing the pair of Lagrange multipliers to be considered at each step. In practice, SMO is found to have a scaling with the number of data points that is somewhere between linear and quadratic depending on the particular application.

We have seen that kernel functions correspond to inner products in feature spaces that can have high, or even infinite, dimensionality. By working directly in terms of the kernel function, without introducing the feature space explicitly, it might therefore seem that support vector machines somehow manage to avoid the curse of di-

Section 1.4

mensionality. This is not the case, however, because there are constraints amongst the feature values that restrict the effective dimensionality of feature space. To see this consider a simple second-order polynomial kernel that we can expand in terms of its components

$$\begin{aligned}
 k(\mathbf{x}, \mathbf{z}) &= (1 + \mathbf{x}^T \mathbf{z})^2 = (1 + x_1 z_1 + x_2 z_2)^2 \\
 &= 1 + 2x_1 z_1 + 2x_2 z_2 + x_1^2 z_1^2 + 2x_1 x_2 z_2 + x_2^2 z_2^2 \\
 &= (1, \sqrt{2}x_1, \sqrt{2}x_2, x_1^2, \sqrt{2}x_1 x_2, x_2^2)(1, \sqrt{2}z_1, \sqrt{2}z_2, z_1^2, \sqrt{2}z_1 z_2, z_2^2)^T \\
 &= \phi(\mathbf{x})^T \phi(\mathbf{z}).
 \end{aligned} \tag{7.42}$$

This kernel function therefore represents an inner product in a feature space having six dimensions, in which the mapping from input space to feature space is described by the vector function $\phi(\mathbf{x})$. However, the coefficients weighting these different features are constrained to have specific forms. Thus any set of points in the original two-dimensional space \mathbf{x} would be constrained to lie exactly on a two-dimensional nonlinear manifold embedded in the six-dimensional feature space.

We have already highlighted the fact that the support vector machine does not provide probabilistic outputs but instead makes classification decisions for new input vectors. Veropoulos *et al.* (1999) discuss modifications to the SVM to allow the trade-off between false positive and false negative errors to be controlled. However, if we wish to use the SVM as a module in a larger probabilistic system, then probabilistic predictions of the class label t for new inputs \mathbf{x} are required.

To address this issue, Platt (2000) has proposed fitting a logistic sigmoid to the outputs of a previously trained support vector machine. Specifically, the required conditional probability is assumed to be of the form

$$p(t = 1 | \mathbf{x}) = \sigma(Ay(\mathbf{x}) + B) \tag{7.43}$$

where $y(\mathbf{x})$ is defined by (7.1). Values for the parameters A and B are found by minimizing the cross-entropy error function defined by a training set consisting of pairs of values $y(\mathbf{x}_n)$ and t_n . The data used to fit the sigmoid needs to be independent of that used to train the original SVM in order to avoid severe over-fitting. This two-stage approach is equivalent to assuming that the output $y(\mathbf{x})$ of the support vector machine represents the log-odds of \mathbf{x} belonging to class $t = 1$. Because the SVM training procedure is not specifically intended to encourage this, the SVM can give a poor approximation to the posterior probabilities (Tipping, 2001).

7.1.2 Relation to logistic regression

As with the separable case, we can re-cast the SVM for nonseparable distributions in terms of the minimization of a regularized error function. This will also allow us to highlight similarities, and differences, compared to the logistic regression model.

We have seen that for data points that are on the correct side of the margin boundary, and which therefore satisfy $y_n t_n \geq 1$, we have $\xi_n = 0$, and for the

Section 4.3.2

Figure 7.5 Plot of the ‘hinge’ error function used in support vector machines, shown in blue, along with the error function for logistic regression, rescaled by a factor of $1/\ln(2)$ so that it passes through the point $(0, 1)$, shown in red. Also shown are the misclassification error in black and the squared error in green.



remaining points we have $\xi_n = 1 - y_n t_n$. Thus the objective function (7.21) can be written (up to an overall multiplicative constant) in the form

$$\sum_{n=1}^N E_{\text{SV}}(y_n t_n) + \lambda \|\mathbf{w}\|^2 \quad (7.44)$$

where $\lambda = (2C)^{-1}$, and $E_{\text{SV}}(\cdot)$ is the *hinge* error function defined by

$$E_{\text{SV}}(y_n t_n) = [1 - y_n t_n]_+ \quad (7.45)$$

where $[\cdot]_+$ denotes the positive part. The hinge error function, so-called because of its shape, is plotted in Figure 7.5. It can be viewed as an approximation to the misclassification error, i.e., the error function that ideally we would like to minimize, which is also shown in Figure 7.5.

When we considered the logistic regression model in Section 4.3.2, we found it convenient to work with target variable $t \in \{0, 1\}$. For comparison with the support vector machine, we first reformulate maximum likelihood logistic regression using the target variable $t \in \{-1, 1\}$. To do this, we note that $p(t = 1|y) = \sigma(y)$ where $y(\mathbf{x})$ is given by (7.1), and $\sigma(y)$ is the logistic sigmoid function defined by (4.59). It follows that $p(t = -1|y) = 1 - \sigma(y) = \sigma(-y)$, where we have used the properties of the logistic sigmoid function, and so we can write

$$p(t|y) = \sigma(yt). \quad (7.46)$$

From this we can construct an error function by taking the negative logarithm of the likelihood function that, with a quadratic regularizer, takes the form

$$\sum_{n=1}^N E_{\text{LR}}(y_n t_n) + \lambda \|\mathbf{w}\|^2. \quad (7.47)$$

where

$$E_{\text{LR}}(yt) = \ln(1 + \exp(-yt)). \quad (7.48)$$

For comparison with other error functions, we can divide by $\ln(2)$ so that the error function passes through the point $(0, 1)$. This rescaled error function is also plotted in Figure 7.5 and we see that it has a similar form to the support vector error function. The key difference is that the flat region in $E_{SV}(yt)$ leads to sparse solutions.

Both the logistic error and the hinge loss can be viewed as continuous approximations to the misclassification error. Another continuous error function that has sometimes been used to solve classification problems is the squared error, which is again plotted in Figure 7.5. It has the property, however, of placing increasing emphasis on data points that are correctly classified but that are a long way from the decision boundary on the correct side. Such points will be strongly weighted at the expense of misclassified points, and so if the objective is to minimize the misclassification rate, then a monotonically decreasing error function would be a better choice.

7.1.3 Multiclass SVMs

The support vector machine is fundamentally a two-class classifier. In practice, however, we often have to tackle problems involving $K > 2$ classes. Various methods have therefore been proposed for combining multiple two-class SVMs in order to build a multiclass classifier.

One commonly used approach (Vapnik, 1998) is to construct K separate SVMs, in which the k^{th} model $y_k(\mathbf{x})$ is trained using the data from class C_k as the positive examples and the data from the remaining $K - 1$ classes as the negative examples. This is known as the *one-versus-the-rest* approach. However, in Figure 4.2 we saw that using the decisions of the individual classifiers can lead to inconsistent results in which an input is assigned to multiple classes simultaneously. This problem is sometimes addressed by making predictions for new inputs \mathbf{x} using

$$y(\mathbf{x}) = \max_k y_k(\mathbf{x}). \quad (7.49)$$

Unfortunately, this heuristic approach suffers from the problem that the different classifiers were trained on different tasks, and there is no guarantee that the real-valued quantities $y_k(\mathbf{x})$ for different classifiers will have appropriate scales.

Another problem with the one-versus-the-rest approach is that the training sets are imbalanced. For instance, if we have ten classes each with equal numbers of training data points, then the individual classifiers are trained on data sets comprising 90% negative examples and only 10% positive examples, and the symmetry of the original problem is lost. A variant of the one-versus-the-rest scheme was proposed by Lee *et al.* (2001) who modify the target values so that the positive class has target $+1$ and the negative class has target $-1/(K - 1)$.

Weston and Watkins (1999) define a single objective function for training all K SVMs simultaneously, based on maximizing the margin from each to remaining classes. However, this can result in much slower training because, instead of solving K separate optimization problems each over N data points with an overall cost of $O(KN^2)$, a single optimization problem of size $(K - 1)N$ must be solved giving an overall cost of $O(K^2N^2)$.

Another approach is to train $K(K - 1)/2$ different 2-class SVMs on all possible pairs of classes, and then to classify test points according to which class has the highest number of ‘votes’, an approach that is sometimes called *one-versus-one*. Again, we saw in Figure 4.2 that this can lead to ambiguities in the resulting classification. Also, for large K this approach requires significantly more training time than the one-versus-the-rest approach. Similarly, to evaluate test points, significantly more computation is required.

The latter problem can be alleviated by organizing the pairwise classifiers into a directed acyclic graph (not to be confused with a probabilistic graphical model) leading to the *DAGSVM* (Platt *et al.*, 2000). For K classes, the DAGSVM has a total of $K(K - 1)/2$ classifiers, and to classify a new test point only $K - 1$ pairwise classifiers need to be evaluated, with the particular classifiers used depending on which path through the graph is traversed.

A different approach to multiclass classification, based on error-correcting output codes, was developed by Dietterich and Bakiri (1995) and applied to support vector machines by Allwein *et al.* (2000). This can be viewed as a generalization of the voting scheme of the one-versus-one approach in which more general partitions of the classes are used to train the individual classifiers. The K classes themselves are represented as particular sets of responses from the two-class classifiers chosen, and together with a suitable decoding scheme, this gives robustness to errors and to ambiguity in the outputs of the individual classifiers. Although the application of SVMs to multiclass classification problems remains an open issue, in practice the one-versus-the-rest approach is the most widely used in spite of its ad-hoc formulation and its practical limitations.

There are also *single-class* support vector machines, which solve an unsupervised learning problem related to probability density estimation. Instead of modelling the density of data, however, these methods aim to find a smooth boundary enclosing a region of high density. The boundary is chosen to represent a quantile of the density, that is, the probability that a data point drawn from the distribution will land inside that region is given by a fixed number between 0 and 1 that is specified in advance. This is a more restricted problem than estimating the full density but may be sufficient in specific applications. Two approaches to this problem using support vector machines have been proposed. The algorithm of Schölkopf *et al.* (2001) tries to find a hyperplane that separates all but a fixed fraction ν of the training data from the origin while at the same time maximizing the distance (margin) of the hyperplane from the origin, while Tax and Duin (1999) look for the smallest sphere in feature space that contains all but a fraction ν of the data points. For kernels $k(\mathbf{x}, \mathbf{x}')$ that are functions only of $\mathbf{x} - \mathbf{x}'$, the two algorithms are equivalent.

7.1.4 SVMs for regression

Section 3.1.4

We now extend support vector machines to regression problems while at the same time preserving the property of sparseness. In simple linear regression, we

Figure 7.6 Plot of an ϵ -insensitive error function (in red) in which the error increases linearly with distance beyond the insensitive region. Also shown for comparison is the quadratic error function (in green).



minimize a regularized error function given by

$$\frac{1}{2} \sum_{n=1}^N \{y_n - t_n\}^2 + \frac{\lambda}{2} \|\mathbf{w}\|^2. \quad (7.50)$$

To obtain sparse solutions, the quadratic error function is replaced by an ϵ -insensitive error function (Vapnik, 1995), which gives zero error if the absolute difference between the prediction $y(\mathbf{x})$ and the target t is less than ϵ where $\epsilon > 0$. A simple example of an ϵ -insensitive error function, having a linear cost associated with errors outside the insensitive region, is given by

$$E_\epsilon(y(\mathbf{x}) - t) = \begin{cases} 0, & \text{if } |y(\mathbf{x}) - t| < \epsilon; \\ |y(\mathbf{x}) - t| - \epsilon, & \text{otherwise} \end{cases} \quad (7.51)$$

and is illustrated in Figure 7.6.

We therefore minimize a regularized error function given by

$$C \sum_{n=1}^N E_\epsilon(y(\mathbf{x}_n) - t_n) + \frac{1}{2} \|\mathbf{w}\|^2 \quad (7.52)$$

where $y(\mathbf{x})$ is given by (7.1). By convention the (inverse) regularization parameter, denoted C , appears in front of the error term.

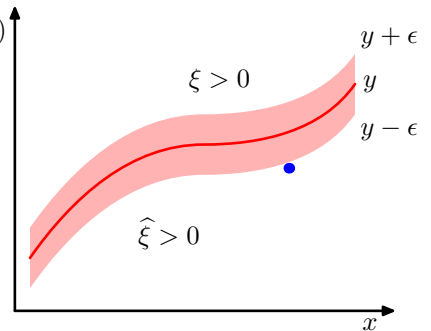
As before, we can re-express the optimization problem by introducing slack variables. For each data point \mathbf{x}_n , we now need two slack variables $\xi_n \geq 0$ and $\hat{\xi}_n \geq 0$, where $\xi_n > 0$ corresponds to a point for which $t_n > y(\mathbf{x}_n) + \epsilon$, and $\hat{\xi}_n > 0$ corresponds to a point for which $t_n < y(\mathbf{x}_n) - \epsilon$, as illustrated in Figure 7.7.

The condition for a target point to lie inside the ϵ -tube is that $y_n - \epsilon \leq t_n \leq y_n + \epsilon$, where $y_n = y(\mathbf{x}_n)$. Introducing the slack variables allows points to lie outside the tube provided the slack variables are nonzero, and the corresponding conditions are

$$t_n \leq y(\mathbf{x}_n) + \epsilon + \xi_n \quad (7.53)$$

$$t_n \geq y(\mathbf{x}_n) - \epsilon - \hat{\xi}_n. \quad (7.54)$$

Figure 7.7 Illustration of SVM regression, showing the regression curve together with the ϵ -insensitive ‘tube’. Also shown are examples of the slack variables ξ and $\hat{\xi}$. Points above the ϵ -tube have $\xi > 0$ and $\hat{\xi} = 0$, points below the ϵ -tube have $\xi = 0$ and $\hat{\xi} > 0$, and points inside the ϵ -tube have $\xi = \hat{\xi} = 0$.



The error function for support vector regression can then be written as

$$C \sum_{n=1}^N (\xi_n + \hat{\xi}_n) + \frac{1}{2} \|\mathbf{w}\|^2 \quad (7.55)$$

which must be minimized subject to the constraints $\xi_n \geq 0$ and $\hat{\xi}_n \geq 0$ as well as (7.53) and (7.54). This can be achieved by introducing Lagrange multipliers $a_n \geq 0$, $\hat{a}_n \geq 0$, $\mu_n \geq 0$, and $\hat{\mu}_n \geq 0$ and optimizing the Lagrangian

$$\begin{aligned} L = & C \sum_{n=1}^N (\xi_n + \hat{\xi}_n) + \frac{1}{2} \|\mathbf{w}\|^2 - \sum_{n=1}^N (\mu_n \xi_n + \hat{\mu}_n \hat{\xi}_n) \\ & - \sum_{n=1}^N a_n (\epsilon + \xi_n + y_n - t_n) - \sum_{n=1}^N \hat{a}_n (\epsilon + \hat{\xi}_n - y_n + t_n). \end{aligned} \quad (7.56)$$

We now substitute for $y(\mathbf{x})$ using (7.1) and then set the derivatives of the Lagrangian with respect to \mathbf{w} , b , ξ_n , and $\hat{\xi}_n$ to zero, giving

$$\frac{\partial L}{\partial \mathbf{w}} = 0 \Rightarrow \mathbf{w} = \sum_{n=1}^N (a_n - \hat{a}_n) \phi(\mathbf{x}_n) \quad (7.57)$$

$$\frac{\partial L}{\partial b} = 0 \Rightarrow \sum_{n=1}^N (a_n - \hat{a}_n) = 0 \quad (7.58)$$

$$\frac{\partial L}{\partial \xi_n} = 0 \Rightarrow a_n + \mu_n = C \quad (7.59)$$

$$\frac{\partial L}{\partial \hat{\xi}_n} = 0 \Rightarrow \hat{a}_n + \hat{\mu}_n = C. \quad (7.60)$$

Using these results to eliminate the corresponding variables from the Lagrangian, we see that the dual problem involves maximizing

$$\begin{aligned}\tilde{L}(\mathbf{a}, \hat{\mathbf{a}}) &= -\frac{1}{2} \sum_{n=1}^N \sum_{m=1}^N (a_n - \hat{a}_n)(a_m - \hat{a}_m) k(\mathbf{x}_n, \mathbf{x}_m) \\ &\quad - \epsilon \sum_{n=1}^N (a_n + \hat{a}_n) + \sum_{n=1}^N (a_n - \hat{a}_n)t_n\end{aligned}\quad (7.61)$$

with respect to $\{a_n\}$ and $\{\hat{a}_n\}$, where we have introduced the kernel $k(\mathbf{x}, \mathbf{x}') = \phi(\mathbf{x})^T \phi(\mathbf{x}')$. Again, this is a constrained maximization, and to find the constraints we note that $a_n \geq 0$ and $\hat{a}_n \geq 0$ are both required because these are Lagrange multipliers. Also $\mu_n \geq 0$ and $\hat{\mu}_n \geq 0$ together with (7.59) and (7.60), require $a_n \leq C$ and $\hat{a}_n \leq C$, and so again we have the box constraints

$$0 \leq a_n \leq C \quad (7.62)$$

$$0 \leq \hat{a}_n \leq C \quad (7.63)$$

together with the condition (7.58).

Substituting (7.57) into (7.1), we see that predictions for new inputs can be made using

$$y(\mathbf{x}) = \sum_{n=1}^N (a_n - \hat{a}_n) k(\mathbf{x}, \mathbf{x}_n) + b \quad (7.64)$$

which is again expressed in terms of the kernel function.

The corresponding Karush-Kuhn-Tucker (KKT) conditions, which state that at the solution the product of the dual variables and the constraints must vanish, are given by

$$a_n(\epsilon + \xi_n + y_n - t_n) = 0 \quad (7.65)$$

$$\hat{a}_n(\epsilon + \hat{\xi}_n - y_n + t_n) = 0 \quad (7.66)$$

$$(C - a_n)\xi_n = 0 \quad (7.67)$$

$$(C - \hat{a}_n)\hat{\xi}_n = 0. \quad (7.68)$$

From these we can obtain several useful results. First of all, we note that a coefficient a_n can only be nonzero if $\epsilon + \xi_n + y_n - t_n = 0$, which implies that the data point either lies on the upper boundary of the ϵ -tube ($\xi_n = 0$) or lies above the upper boundary ($\xi_n > 0$). Similarly, a nonzero value for \hat{a}_n implies $\epsilon + \hat{\xi}_n - y_n + t_n = 0$, and such points must lie either on or below the lower boundary of the ϵ -tube.

Furthermore, the two constraints $\epsilon + \xi_n + y_n - t_n = 0$ and $\epsilon + \hat{\xi}_n - y_n + t_n = 0$ are incompatible, as is easily seen by adding them together and noting that ξ_n and $\hat{\xi}_n$ are nonnegative while ϵ is strictly positive, and so for every data point \mathbf{x}_n , either a_n or \hat{a}_n (or both) must be zero.

The support vectors are those data points that contribute to predictions given by (7.64), in other words those for which either $a_n \neq 0$ or $\hat{a}_n \neq 0$. These are points that lie on the boundary of the ϵ -tube or outside the tube. All points within the tube have

$a_n = \hat{a}_n = 0$. We again have a sparse solution, and the only terms that have to be evaluated in the predictive model (7.64) are those that involve the support vectors.

The parameter b can be found by considering a data point for which $0 < a_n < C$, which from (7.67) must have $\xi_n = 0$, and from (7.65) must therefore satisfy $\epsilon + y_n - t_n = 0$. Using (7.1) and solving for b , we obtain

$$\begin{aligned} b &= t_n - \epsilon - \mathbf{w}^T \phi(\mathbf{x}_n) \\ &= t_n - \epsilon - \sum_{m=1}^N (a_m - \hat{a}_m) k(\mathbf{x}_n, \mathbf{x}_m) \end{aligned} \quad (7.69)$$

where we have used (7.57). We can obtain an analogous result by considering a point for which $0 < \hat{a}_n < C$. In practice, it is better to average over all such estimates of b .

As with the classification case, there is an alternative formulation of the SVM for regression in which the parameter governing complexity has a more intuitive interpretation (Schölkopf *et al.*, 2000). In particular, instead of fixing the width ϵ of the insensitive region, we fix instead a parameter ν that bounds the fraction of points lying outside the tube. This involves maximizing

$$\begin{aligned} \tilde{L}(\mathbf{a}, \hat{\mathbf{a}}) &= -\frac{1}{2} \sum_{n=1}^N \sum_{m=1}^N (a_n - \hat{a}_n)(a_m - \hat{a}_m) k(\mathbf{x}_n, \mathbf{x}_m) \\ &\quad + \sum_{n=1}^N (a_n - \hat{a}_n)t_n \end{aligned} \quad (7.70)$$

subject to the constraints

$$0 \leq a_n \leq C/N \quad (7.71)$$

$$0 \leq \hat{a}_n \leq C/N \quad (7.72)$$

$$\sum_{n=1}^N (a_n - \hat{a}_n) = 0 \quad (7.73)$$

$$\sum_{n=1}^N (a_n + \hat{a}_n) \leq \nu C. \quad (7.74)$$

It can be shown that there are at most νN data points falling outside the insensitive tube, while at least νN data points are support vectors and so lie either on the tube or outside it.

The use of a support vector machine to solve a regression problem is illustrated using the sinusoidal data set in Figure 7.8. Here the parameters ν and C have been chosen by hand. In practice, their values would typically be determined by cross-validation.

Figure 7.8 Illustration of the ν -SVM for regression applied to the sinusoidal synthetic data set using Gaussian kernels. The predicted regression curve is shown by the red line, and the ϵ -insensitive tube corresponds to the shaded region. Also, the data points are shown in green, and those with support vectors are indicated by blue circles.



7.1.5 Computational learning theory

Historically, support vector machines have largely been motivated and analysed using a theoretical framework known as *computational learning theory*, also sometimes called *statistical learning theory* (Anthony and Biggs, 1992; Kearns and Vazirani, 1994; Vapnik, 1995; Vapnik, 1998). This has its origins with Valiant (1984) who formulated the *probably approximately correct*, or PAC, learning framework. The goal of the PAC framework is to understand how large a data set needs to be in order to give good generalization. It also gives bounds for the computational cost of learning, although we do not consider these here.

Suppose that a data set \mathcal{D} of size N is drawn from some joint distribution $p(\mathbf{x}, \mathbf{t})$ where \mathbf{x} is the input variable and \mathbf{t} represents the class label, and that we restrict attention to ‘noise free’ situations in which the class labels are determined by some (unknown) deterministic function $\mathbf{t} = \mathbf{g}(\mathbf{x})$. In PAC learning we say that a function $\mathbf{f}(\mathbf{x}; \mathcal{D})$, drawn from a space \mathcal{F} of such functions on the basis of the training set \mathcal{D} , has good generalization if its expected error rate is below some pre-specified threshold ϵ , so that

$$\mathbb{E}_{\mathbf{x}, \mathbf{t}} [I(\mathbf{f}(\mathbf{x}; \mathcal{D}) \neq \mathbf{t})] < \epsilon \quad (7.75)$$

where $I(\cdot)$ is the indicator function, and the expectation is with respect to the distribution $p(\mathbf{x}, \mathbf{t})$. The quantity on the left-hand side is a random variable, because it depends on the training set \mathcal{D} , and the PAC framework requires that (7.75) holds, with probability greater than $1 - \delta$, for a data set \mathcal{D} drawn randomly from $p(\mathbf{x}, \mathbf{t})$. Here δ is another pre-specified parameter, and the terminology ‘probably approximately correct’ comes from the requirement that with high probability (greater than $1 - \delta$), the error rate be small (less than ϵ). For a given choice of model space \mathcal{F} , and for given parameters ϵ and δ , PAC learning aims to provide bounds on the minimum size N of data set needed to meet this criterion. A key quantity in PAC learning is the *Vapnik-Chervonenkis dimension*, or VC dimension, which provides a measure of the complexity of a space of functions, and which allows the PAC framework to be extended to spaces containing an infinite number of functions.

The bounds derived within the PAC framework are often described as worst-

case, because they apply to *any* choice for the distribution $p(\mathbf{x}, \mathbf{t})$, so long as both the training and the test examples are drawn (independently) from the same distribution, and for *any* choice for the function $\mathbf{f}(\mathbf{x})$ so long as it belongs to \mathcal{F} . In real-world applications of machine learning, we deal with distributions that have significant regularity, for example in which large regions of input space carry the same class label. As a consequence of the lack of any assumptions about the form of the distribution, the PAC bounds are very conservative, in other words they strongly over-estimate the size of data sets required to achieve a given generalization performance. For this reason, PAC bounds have found few, if any, practical applications.

One attempt to improve the tightness of the PAC bounds is the *PAC-Bayesian* framework (McAllester, 2003), which considers a distribution over the space \mathcal{F} of functions, somewhat analogous to the prior in a Bayesian treatment. This still considers any possible choice for $p(\mathbf{x}, \mathbf{t})$, and so although the bounds are tighter, they are still very conservative.

7.2. Relevance Vector Machines

Support vector machines have been used in a variety of classification and regression applications. Nevertheless, they suffer from a number of limitations, several of which have been highlighted already in this chapter. In particular, the outputs of an SVM represent decisions rather than posterior probabilities. Also, the SVM was originally formulated for two classes, and the extension to $K > 2$ classes is problematic. There is a complexity parameter C , or ν (as well as a parameter ϵ in the case of regression), that must be found using a hold-out method such as cross-validation. Finally, predictions are expressed as linear combinations of kernel functions that are centred on training data points and that are required to be positive definite.

The *relevance vector machine* or RVM (Tipping, 2001) is a Bayesian sparse kernel technique for regression and classification that shares many of the characteristics of the SVM whilst avoiding its principal limitations. Additionally, it typically leads to much sparser models resulting in correspondingly faster performance on test data whilst maintaining comparable generalization error.

In contrast to the SVM we shall find it more convenient to introduce the regression form of the RVM first and then consider the extension to classification tasks.

7.2.1 RVM for regression

The relevance vector machine for regression is a linear model of the form studied in Chapter 3 but with a modified prior that results in sparse solutions. The model defines a conditional distribution for a real-valued target variable t , given an input vector \mathbf{x} , which takes the form

$$p(t|\mathbf{x}, \mathbf{w}, \beta) = \mathcal{N}(t|y(\mathbf{x}), \beta^{-1}) \quad (7.76)$$

where $\beta = \sigma^{-2}$ is the noise precision (inverse noise variance), and the mean is given by a linear model of the form

$$y(\mathbf{x}) = \sum_{i=1}^M w_i \phi_i(\mathbf{x}) = \mathbf{w}^T \boldsymbol{\phi}(\mathbf{x}) \quad (7.77)$$

with fixed nonlinear basis functions $\phi_i(\mathbf{x})$, which will typically include a constant term so that the corresponding weight parameter represents a ‘bias’.

The relevance vector machine is a specific instance of this model, which is intended to mirror the structure of the support vector machine. In particular, the basis functions are given by kernels, with one kernel associated with each of the data points from the training set. The general expression (7.77) then takes the SVM-like form

$$y(\mathbf{x}) = \sum_{n=1}^N w_n k(\mathbf{x}, \mathbf{x}_n) + b \quad (7.78)$$

where b is a bias parameter. The number of parameters in this case is $M = N + 1$, and $y(\mathbf{x})$ has the same form as the predictive model (7.64) for the SVM, except that the coefficients a_n are here denoted w_n . It should be emphasized that the subsequent analysis is valid for arbitrary choices of basis function, and for generality we shall work with the form (7.77). In contrast to the SVM, there is no restriction to positive-definite kernels, nor are the basis functions tied in either number or location to the training data points.

Suppose we are given a set of N observations of the input vector \mathbf{x} , which we denote collectively by a data matrix \mathbf{X} whose n^{th} row is \mathbf{x}_n^T with $n = 1, \dots, N$. The corresponding target values are given by $\mathbf{t} = (t_1, \dots, t_N)^T$. Thus, the likelihood function is given by

$$p(\mathbf{t}|\mathbf{X}, \mathbf{w}, \beta) = \prod_{n=1}^N p(t_n | \mathbf{x}_n, \mathbf{w}, \beta^{-1}). \quad (7.79)$$

Next we introduce a prior distribution over the parameter vector \mathbf{w} and as in Chapter 3, we shall consider a zero-mean Gaussian prior. However, the key difference in the RVM is that we introduce a separate hyperparameter α_i for each of the weight parameters w_i instead of a single shared hyperparameter. Thus the weight prior takes the form

$$p(\mathbf{w}|\boldsymbol{\alpha}) = \prod_{i=1}^M \mathcal{N}(w_i | 0, \alpha_i^{-1}) \quad (7.80)$$

where α_i represents the precision of the corresponding parameter w_i , and $\boldsymbol{\alpha}$ denotes $(\alpha_1, \dots, \alpha_M)^T$. We shall see that, when we maximize the evidence with respect to these hyperparameters, a significant proportion of them go to infinity, and the corresponding weight parameters have posterior distributions that are concentrated at zero. The basis functions associated with these parameters therefore play no role

in the predictions made by the model and so are effectively pruned out, resulting in a sparse model.

Using the result (3.49) for linear regression models, we see that the posterior distribution for the weights is again Gaussian and takes the form

$$p(\mathbf{w}|\mathbf{t}, \mathbf{X}, \boldsymbol{\alpha}, \beta) = \mathcal{N}(\mathbf{w}|\mathbf{m}, \boldsymbol{\Sigma}) \quad (7.81)$$

where the mean and covariance are given by

$$\mathbf{m} = \beta \boldsymbol{\Phi}^T \mathbf{t} \quad (7.82)$$

$$\boldsymbol{\Sigma} = (\mathbf{A} + \beta \boldsymbol{\Phi}^T \boldsymbol{\Phi})^{-1} \quad (7.83)$$

where $\boldsymbol{\Phi}$ is the $N \times M$ design matrix with elements $\Phi_{ni} = \phi_i(\mathbf{x}_n)$, and $\mathbf{A} = \text{diag}(\alpha_i)$. Note that in the specific case of the model (7.78), we have $\boldsymbol{\Phi} = \mathbf{K}$, where \mathbf{K} is the symmetric $(N+1) \times (N+1)$ kernel matrix with elements $k(\mathbf{x}_n, \mathbf{x}_m)$.

The values of $\boldsymbol{\alpha}$ and β are determined using type-2 maximum likelihood, also known as the *evidence approximation*, in which we maximize the marginal likelihood function obtained by integrating out the weight parameters

$$p(\mathbf{t}|\mathbf{X}, \boldsymbol{\alpha}, \beta) = \int p(\mathbf{t}|\mathbf{X}, \mathbf{w}, \beta) p(\mathbf{w}|\boldsymbol{\alpha}) d\mathbf{w}. \quad (7.84)$$

Section 3.5

Exercise 7.10

Because this represents the convolution of two Gaussians, it is readily evaluated to give the log marginal likelihood in the form

$$\begin{aligned} \ln p(\mathbf{t}|\mathbf{X}, \boldsymbol{\alpha}, \beta) &= \ln \mathcal{N}(\mathbf{t}|\mathbf{0}, \mathbf{C}) \\ &= -\frac{1}{2} \{ N \ln(2\pi) + \ln |\mathbf{C}| + \mathbf{t}^T \mathbf{C}^{-1} \mathbf{t} \} \end{aligned} \quad (7.85)$$

where $\mathbf{t} = (t_1, \dots, t_N)^T$, and we have defined the $N \times N$ matrix \mathbf{C} given by

$$\mathbf{C} = \beta^{-1} \mathbf{I} + \boldsymbol{\Phi} \mathbf{A}^{-1} \boldsymbol{\Phi}^T. \quad (7.86)$$

Our goal is now to maximize (7.85) with respect to the hyperparameters $\boldsymbol{\alpha}$ and β . This requires only a small modification to the results obtained in Section 3.5 for the evidence approximation in the linear regression model. Again, we can identify two approaches. In the first, we simply set the required derivatives of the marginal likelihood to zero and obtain the following re-estimation equations

$$\alpha_i^{\text{new}} = \frac{\gamma_i}{m_i^2} \quad (7.87)$$

$$(\beta^{\text{new}})^{-1} = \frac{\|\mathbf{t} - \boldsymbol{\Phi} \mathbf{m}\|^2}{N - \sum_i \gamma_i} \quad (7.88)$$

where m_i is the i^{th} component of the posterior mean \mathbf{m} defined by (7.82). The quantity γ_i measures how well the corresponding parameter w_i is determined by the data and is defined by

Section 3.5.3

$$\gamma_i = 1 - \alpha_i \Sigma_{ii} \quad (7.89)$$

in which Σ_{ii} is the i^{th} diagonal component of the posterior covariance Σ given by (7.83). Learning therefore proceeds by choosing initial values for α and β , evaluating the mean and covariance of the posterior using (7.82) and (7.83), respectively, and then alternately re-estimating the hyperparameters, using (7.87) and (7.88), and re-estimating the posterior mean and covariance, using (7.82) and (7.83), until a suitable convergence criterion is satisfied.

The second approach is to use the EM algorithm, and is discussed in Section 9.3.4. These two approaches to finding the values of the hyperparameters that maximize the evidence are formally equivalent. Numerically, however, it is found that the direct optimization approach corresponding to (7.87) and (7.88) gives somewhat faster convergence (Tipping, 2001).

Exercise 9.23

Section 7.2.2

As a result of the optimization, we find that a proportion of the hyperparameters $\{\alpha_i\}$ are driven to large (in principle infinite) values, and so the weight parameters w_i corresponding to these hyperparameters have posterior distributions with mean and variance both zero. Thus those parameters, and the corresponding basis functions $\phi_i(\mathbf{x})$, are removed from the model and play no role in making predictions for new inputs. In the case of models of the form (7.78), the inputs \mathbf{x}_n corresponding to the remaining nonzero weights are called *relevance vectors*, because they are identified through the mechanism of automatic relevance determination, and are analogous to the support vectors of an SVM. It is worth emphasizing, however, that this mechanism for achieving sparsity in probabilistic models through automatic relevance determination is quite general and can be applied to any model expressed as an adaptive linear combination of basis functions.

Having found values α^* and β^* for the hyperparameters that maximize the marginal likelihood, we can evaluate the predictive distribution over t for a new input \mathbf{x} . Using (7.76) and (7.81), this is given by

$$\begin{aligned} p(t|\mathbf{x}, \mathbf{X}, \mathbf{t}, \alpha^*, \beta^*) &= \int p(t|\mathbf{w}, \beta^*) p(\mathbf{w}|\mathbf{X}, \mathbf{t}, \alpha^*, \beta^*) d\mathbf{w} \\ &= \mathcal{N}(t|\mathbf{m}^T \phi(\mathbf{x}), \sigma^2(\mathbf{x})). \end{aligned} \quad (7.90)$$

Exercise 7.14

Thus the predictive mean is given by (7.76) with \mathbf{w} set equal to the posterior mean \mathbf{m} , and the variance of the predictive distribution is given by

$$\sigma^2(\mathbf{x}) = (\beta^*)^{-1} + \phi(\mathbf{x})^T \Sigma \phi(\mathbf{x}) \quad (7.91)$$

Section 6.4.2

where Σ is given by (7.83) in which α and β are set to their optimized values α^* and β^* . This is just the familiar result (3.59) obtained in the context of linear regression. Recall that for localized basis functions, the predictive variance for linear regression models becomes small in regions of input space where there are no basis functions. In the case of an RVM with the basis functions centred on data points, the model will therefore become increasingly certain of its predictions when extrapolating outside the domain of the data (Rasmussen and Quiñonero-Candela, 2005), which of course is undesirable. The predictive distribution in Gaussian process regression does not

Figure 7.9 Illustration of RVM regression using the same data set, and the same Gaussian kernel functions, as used in Figure 7.8 for the ν -SVM regression model. The mean of the predictive distribution for the RVM is shown by the red line, and the one standard-deviation predictive distribution is shown by the shaded region. Also, the data points are shown in green, and the relevance vectors are indicated by blue circles. Note that there are only 3 relevance vectors compared to 7 support vectors for the ν -SVM in Figure 7.8.



suffer from this problem. However, the computational cost of making predictions with a Gaussian processes is typically much higher than with an RVM.

Figure 7.9 shows an example of the RVM applied to the sinusoidal regression data set. Here the noise precision parameter β is also determined through evidence maximization. We see that the number of relevance vectors in the RVM is significantly smaller than the number of support vectors used by the SVM. For a wide range of regression and classification tasks, the RVM is found to give models that are typically an order of magnitude more compact than the corresponding support vector machine, resulting in a significant improvement in the speed of processing on test data. Remarkably, this greater sparsity is achieved with little or no reduction in generalization error compared with the corresponding SVM.

The principal disadvantage of the RVM compared to the SVM is that training involves optimizing a nonconvex function, and training times can be longer than for a comparable SVM. For a model with M basis functions, the RVM requires inversion of a matrix of size $M \times M$, which in general requires $O(M^3)$ computation. In the specific case of the SVM-like model (7.78), we have $M = N + 1$. As we have noted, there are techniques for training SVMs whose cost is roughly quadratic in N . Of course, in the case of the RVM we always have the option of starting with a smaller number of basis functions than $N + 1$. More significantly, in the relevance vector machine the parameters governing complexity and noise variance are determined automatically from a single training run, whereas in the support vector machine the parameters C and ϵ (or ν) are generally found using cross-validation, which involves multiple training runs. Furthermore, in the next section we shall derive an alternative procedure for training the relevance vector machine that improves training speed significantly.

7.2.2 Analysis of sparsity

We have noted earlier that the mechanism of *automatic relevance determination* causes a subset of parameters to be driven to zero. We now examine in more detail



Figure 7.10 Illustration of the mechanism for sparsity in a Bayesian linear regression model, showing a training set vector of target values given by $\mathbf{t} = (t_1, t_2)^T$, indicated by the cross, for a model with one basis vector $\varphi = (\phi(\mathbf{x}_1), \phi(\mathbf{x}_2))^T$, which is poorly aligned with the target data vector \mathbf{t} . On the left we see a model having only isotropic noise, so that $\mathbf{C} = \beta^{-1}\mathbf{I}$, corresponding to $\alpha = \infty$, with β set to its most probable value. On the right we see the same model but with a finite value of α . In each case the red ellipse corresponds to unit Mahalanobis distance, with $|\mathbf{C}|$ taking the same value for both plots, while the dashed green circle shows the contrition arising from the noise term β^{-1} . We see that any finite value of α reduces the probability of the observed data, and so for the most probable solution the basis vector is removed.

the mechanism of sparsity in the context of the relevance vector machine. In the process, we will arrive at a significantly faster procedure for optimizing the hyperparameters compared to the direct techniques given above.

Before proceeding with a mathematical analysis, we first give some informal insight into the origin of sparsity in Bayesian linear models. Consider a data set comprising $N = 2$ observations t_1 and t_2 , together with a model having a single basis function $\phi(\mathbf{x})$, with hyperparameter α , along with isotropic noise having precision β . From (7.85), the marginal likelihood is given by $p(\mathbf{t}|\alpha, \beta) = \mathcal{N}(\mathbf{t}|\mathbf{0}, \mathbf{C})$ in which the covariance matrix takes the form

$$\mathbf{C} = \frac{1}{\beta}\mathbf{I} + \frac{1}{\alpha}\varphi\varphi^T \quad (7.92)$$

where φ denotes the N -dimensional vector $(\phi(\mathbf{x}_1), \phi(\mathbf{x}_2))^T$, and similarly $\mathbf{t} = (t_1, t_2)^T$. Notice that this is just a zero-mean Gaussian process model over \mathbf{t} with covariance \mathbf{C} . Given a particular observation for \mathbf{t} , our goal is to find α^* and β^* by maximizing the marginal likelihood. We see from Figure 7.10 that, if there is a poor alignment between the direction of φ and that of the training data vector \mathbf{t} , then the corresponding hyperparameter α will be driven to ∞ , and the basis vector will be pruned from the model. This arises because any finite value for α will always assign a lower probability to the data, thereby decreasing the value of the density at \mathbf{t} , provided that β is set to its optimal value. We see that any finite value for α would cause the distribution to be elongated in a direction away from the data, thereby increasing the probability mass in regions away from the observed data and hence reducing the value of the density at the target data vector itself. For the more general case of M

basis vectors $\varphi_1, \dots, \varphi_M$ a similar intuition holds, namely that if a particular basis vector is poorly aligned with the data vector t , then it is likely to be pruned from the model.

We now investigate the mechanism for sparsity from a more mathematical perspective, for a general case involving M basis functions. To motivate this analysis we first note that, in the result (7.87) for re-estimating the parameter α_i , the terms on the right-hand side are themselves also functions of α_i . These results therefore represent implicit solutions, and iteration would be required even to determine a single α_i with all other α_j for $j \neq i$ fixed.

This suggests a different approach to solving the optimization problem for the RVM, in which we make explicit all of the dependence of the marginal likelihood (7.85) on a particular α_i and then determine its stationary points explicitly (Faul and Tipping, 2002; Tipping and Faul, 2003). To do this, we first pull out the contribution from α_i in the matrix C defined by (7.86) to give

$$\begin{aligned} C &= \beta^{-1}I + \sum_{j \neq i} \alpha_j^{-1} \varphi_j \varphi_j^T + \alpha_i^{-1} \varphi_i \varphi_i^T \\ &= C_{-i} + \alpha_i^{-1} \varphi_i \varphi_i^T \end{aligned} \quad (7.93)$$

where φ_i denotes the i^{th} column of Φ , in other words the N -dimensional vector with elements $(\phi_i(x_1), \dots, \phi_i(x_N))$, in contrast to ϕ_n , which denotes the n^{th} row of Φ . The matrix C_{-i} represents the matrix C with the contribution from basis function i removed. Using the matrix identities (C.7) and (C.15), the determinant and inverse of C can then be written

$$|C| = |C_{-i}| |1 + \alpha_i^{-1} \varphi_i^T C_{-i}^{-1} \varphi_i| \quad (7.94)$$

$$C^{-1} = C_{-i}^{-1} - \frac{C_{-i}^{-1} \varphi_i \varphi_i^T C_{-i}^{-1}}{\alpha_i + \varphi_i^T C_{-i}^{-1} \varphi_i}. \quad (7.95)$$

Using these results, we can then write the log marginal likelihood function (7.85) in the form

$$L(\alpha) = L(\alpha_{-i}) + \lambda(\alpha_i) \quad (7.96)$$

where $L(\alpha_{-i})$ is simply the log marginal likelihood with basis function φ_i omitted, and the quantity $\lambda(\alpha_i)$ is defined by

$$\lambda(\alpha_i) = \frac{1}{2} \left[\ln \alpha_i - \ln (\alpha_i + s_i) + \frac{q_i^2}{\alpha_i + s_i} \right] \quad (7.97)$$

and contains all of the dependence on α_i . Here we have introduced the two quantities

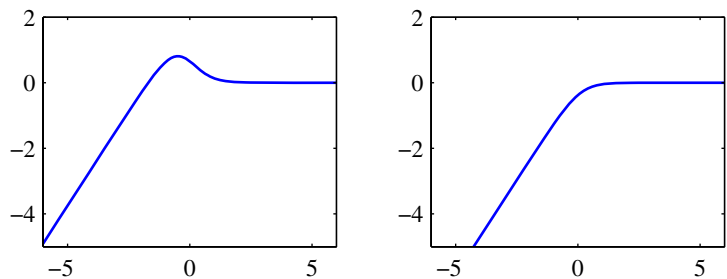
$$s_i = \varphi_i^T C_{-i}^{-1} \varphi_i \quad (7.98)$$

$$q_i = \varphi_i^T C_{-i}^{-1} t. \quad (7.99)$$

Here s_i is called the *sparsity* and q_i is known as the *quality* of φ_i , and as we shall see, a large value of s_i relative to the value of q_i means that the basis function φ_i

Exercise 7.15

Figure 7.11 Plots of the log marginal likelihood $\lambda(\alpha_i)$ versus $\ln \alpha_i$ showing on the left, the single maximum at a finite α_i for $q_i^2 = 4$ and $s_i = 1$ (so that $q_i^2 > s_i$) and on the right, the maximum at $\alpha_i = \infty$ for $q_i^2 = 1$ and $s_i = 2$ (so that $q_i^2 < s_i$).



is more likely to be pruned from the model. The ‘sparsity’ measures the extent to which basis function φ_i overlaps with the other basis vectors in the model, and the ‘quality’ represents a measure of the alignment of the basis vector φ_n with the error between the training set values $\mathbf{t} = (t_1, \dots, t_N)^T$ and the vector \mathbf{y}_{-i} of predictions that would result from the model with the vector φ_i excluded (Tipping and Faul, 2003).

The stationary points of the marginal likelihood with respect to α_i occur when the derivative

$$\frac{d\lambda(\alpha_i)}{d\alpha_i} = \frac{\alpha_i^{-1}s_i^2 - (q_i^2 - s_i)}{2(\alpha_i + s_i)^2} \quad (7.100)$$

is equal to zero. There are two possible forms for the solution. Recalling that $\alpha_i \geq 0$, we see that if $q_i^2 < s_i$, then $\alpha_i \rightarrow \infty$ provides a solution. Conversely, if $q_i^2 > s_i$, we can solve for α_i to obtain

$$\alpha_i = \frac{s_i^2}{q_i^2 - s_i}. \quad (7.101)$$

These two solutions are illustrated in Figure 7.11. We see that the relative size of the quality and sparsity terms determines whether a particular basis vector will be pruned from the model or not. A more complete analysis (Faul and Tipping, 2002), based on the second derivatives of the marginal likelihood, confirms these solutions are indeed the unique maxima of $\lambda(\alpha_i)$.

Exercise 7.16

Note that this approach has yielded a closed-form solution for α_i , for given values of the other hyperparameters. As well as providing insight into the origin of sparsity in the RVM, this analysis also leads to a practical algorithm for optimizing the hyperparameters that has significant speed advantages. This uses a fixed set of candidate basis vectors, and then cycles through them in turn to decide whether each vector should be included in the model or not. The resulting sequential sparse Bayesian learning algorithm is described below.

Sequential Sparse Bayesian Learning Algorithm

1. If solving a regression problem, initialize β .
2. Initialize using one basis function φ_1 , with hyperparameter α_1 set using (7.101), with the remaining hyperparameters α_j for $j \neq i$ initialized to infinity, so that only φ_1 is included in the model.

3. Evaluate Σ and \mathbf{m} , along with q_i and s_i for all basis functions.
4. Select a candidate basis function φ_i .
5. If $q_i^2 > s_i$, and $\alpha_i < \infty$, so that the basis vector φ_i is already included in the model, then update α_i using (7.101).
6. If $q_i^2 > s_i$, and $\alpha_i = \infty$, then add φ_i to the model, and evaluate hyperparameter α_i using (7.101).
7. If $q_i^2 \leq s_i$, and $\alpha_i < \infty$ then remove basis function φ_i from the model, and set $\alpha_i = \infty$.
8. If solving a regression problem, update β .
9. If converged terminate, otherwise go to 3.

Note that if $q_i^2 \leq s_i$ and $\alpha_i = \infty$, then the basis function φ_i is already excluded from the model and no action is required.

In practice, it is convenient to evaluate the quantities

$$Q_i = \varphi_i^T \mathbf{C}^{-1} \mathbf{t} \quad (7.102)$$

$$S_i = \varphi_i^T \mathbf{C}^{-1} \varphi_i. \quad (7.103)$$

The quality and sparseness variables can then be expressed in the form

$$q_i = \frac{\alpha_i Q_i}{\alpha_i - S_i} \quad (7.104)$$

$$s_i = \frac{\alpha_i S_i}{\alpha_i - S_i}. \quad (7.105)$$

Exercise 7.17

Note that when $\alpha_i = \infty$, we have $q_i = Q_i$ and $s_i = S_i$. Using (C.7), we can write

$$Q_i = \beta \varphi_i^T \mathbf{t} - \beta^2 \varphi_i^T \Phi \Sigma \Phi^T \mathbf{t} \quad (7.106)$$

$$S_i = \beta \varphi_i^T \varphi_i - \beta^2 \varphi_i^T \Phi \Sigma \Phi^T \varphi_i \quad (7.107)$$

where Φ and Σ involve only those basis vectors that correspond to finite hyperparameters α_i . At each stage the required computations therefore scale like $O(M^3)$, where M is the number of active basis vectors in the model and is typically much smaller than the number N of training patterns.

7.2.3 RVM for classification

We can extend the relevance vector machine framework to classification problems by applying the ARD prior over weights to a probabilistic linear classification model of the kind studied in Chapter 4. To start with, we consider two-class problems with a binary target variable $t \in \{0, 1\}$. The model now takes the form of a linear combination of basis functions transformed by a logistic sigmoid function

$$y(\mathbf{x}, \mathbf{w}) = \sigma(\mathbf{w}^T \phi(\mathbf{x})) \quad (7.108)$$

where $\sigma(\cdot)$ is the logistic sigmoid function defined by (4.59). If we introduce a Gaussian prior over the weight vector \mathbf{w} , then we obtain the model that has been considered already in Chapter 4. The difference here is that in the RVM, this model uses the ARD prior (7.80) in which there is a separate precision hyperparameter associated with each weight parameter.

Section 4.4

In contrast to the regression model, we can no longer integrate analytically over the parameter vector \mathbf{w} . Here we follow Tipping (2001) and use the Laplace approximation, which was applied to the closely related problem of Bayesian logistic regression in Section 4.5.1.

We begin by initializing the hyperparameter vector α . For this given value of α , we then build a Gaussian approximation to the posterior distribution and thereby obtain an approximation to the marginal likelihood. Maximization of this approximate marginal likelihood then leads to a re-estimated value for α , and the process is repeated until convergence.

Let us consider the Laplace approximation for this model in more detail. For a fixed value of α , the mode of the posterior distribution over \mathbf{w} is obtained by maximizing

$$\begin{aligned} \ln p(\mathbf{w}|\mathbf{t}, \alpha) &= \ln \{p(\mathbf{t}|\mathbf{w})p(\mathbf{w}|\alpha)\} - \ln p(\mathbf{t}|\alpha) \\ &= \sum_{n=1}^N \{t_n \ln y_n + (1-t_n) \ln(1-y_n)\} - \frac{1}{2} \mathbf{w}^T \mathbf{A} \mathbf{w} + \text{const} \end{aligned} \quad (7.109)$$

Exercise 7.18

where $\mathbf{A} = \text{diag}(\alpha_i)$. This can be done using iterative reweighted least squares (IRLS) as discussed in Section 4.3.3. For this, we need the gradient vector and Hessian matrix of the log posterior distribution, which from (7.109) are given by

$$\nabla \ln p(\mathbf{w}|\mathbf{t}, \alpha) = \Phi^T(\mathbf{t} - \mathbf{y}) - \mathbf{A} \mathbf{w} \quad (7.110)$$

$$\nabla \nabla \ln p(\mathbf{w}|\mathbf{t}, \alpha) = -(\Phi^T \mathbf{B} \Phi + \mathbf{A}) \quad (7.111)$$

where \mathbf{B} is an $N \times N$ diagonal matrix with elements $b_n = y_n(1-y_n)$, the vector $\mathbf{y} = (y_1, \dots, y_N)^T$, and Φ is the design matrix with elements $\Phi_{ni} = \phi_i(\mathbf{x}_n)$. Here we have used the property (4.88) for the derivative of the logistic sigmoid function. At convergence of the IRLS algorithm, the negative Hessian represents the inverse covariance matrix for the Gaussian approximation to the posterior distribution.

The mode of the resulting approximation to the posterior distribution, corresponding to the mean of the Gaussian approximation, is obtained setting (7.110) to zero, giving the mean and covariance of the Laplace approximation in the form

$$\mathbf{w}^* = \mathbf{A}^{-1} \Phi^T (\mathbf{t} - \mathbf{y}) \quad (7.112)$$

$$\Sigma = (\Phi^T \mathbf{B} \Phi + \mathbf{A})^{-1}. \quad (7.113)$$

We can now use this Laplace approximation to evaluate the marginal likelihood. Using the general result (4.135) for an integral evaluated using the Laplace approxi-

mation, we have

$$\begin{aligned} p(\mathbf{t}|\boldsymbol{\alpha}) &= \int p(\mathbf{t}|\mathbf{w})p(\mathbf{w}|\boldsymbol{\alpha}) d\mathbf{w} \\ &\simeq p(\mathbf{t}|\mathbf{w}^*)p(\mathbf{w}^*|\boldsymbol{\alpha})(2\pi)^{M/2}|\boldsymbol{\Sigma}|^{1/2}. \end{aligned} \quad (7.114)$$

If we substitute for $p(\mathbf{t}|\mathbf{w}^*)$ and $p(\mathbf{w}^*|\boldsymbol{\alpha})$ and then set the derivative of the marginal likelihood with respect to α_i equal to zero, we obtain

$$-\frac{1}{2}(w_i^*)^2 + \frac{1}{2\alpha_i} - \frac{1}{2}\Sigma_{ii} = 0. \quad (7.115)$$

Defining $\gamma_i = 1 - \alpha_i\Sigma_{ii}$ and rearranging then gives

$$\alpha_i^{\text{new}} = \frac{\gamma_i}{(w_i^*)^2} \quad (7.116)$$

which is identical to the re-estimation formula (7.87) obtained for the regression RVM.

If we define

$$\hat{\mathbf{t}} = \Phi\mathbf{w}^* + \mathbf{B}^{-1}(\mathbf{t} - \mathbf{y}) \quad (7.117)$$

we can write the approximate log marginal likelihood in the form

$$\ln p(\mathbf{t}|\boldsymbol{\alpha}, \beta) = -\frac{1}{2} \left\{ N \ln(2\pi) + \ln |\mathbf{C}| + (\hat{\mathbf{t}})^T \mathbf{C}^{-1} \hat{\mathbf{t}} \right\} \quad (7.118)$$

where

$$\mathbf{C} = \mathbf{B} + \Phi\mathbf{A}\Phi^T. \quad (7.119)$$

This takes the same form as (7.85) in the regression case, and so we can apply the same analysis of sparsity and obtain the same fast learning algorithm in which we fully optimize a single hyperparameter α_i at each step.

Appendix A

Figure 7.12 shows the relevance vector machine applied to a synthetic classification data set. We see that the relevance vectors tend not to lie in the region of the decision boundary, in contrast to the support vector machine. This is consistent with our earlier discussion of sparsity in the RVM, because a basis function $\phi_i(\mathbf{x})$ centred on a data point near the boundary will have a vector φ_i that is poorly aligned with the training data vector \mathbf{t} .

Section 13.3

One of the potential advantages of the relevance vector machine compared with the SVM is that it makes probabilistic predictions. For example, this allows the RVM to be used to help construct an emission density in a nonlinear extension of the linear dynamical system for tracking faces in video sequences (Williams *et al.*, 2005).

So far, we have considered the RVM for binary classification problems. For $K > 2$ classes, we again make use of the probabilistic approach in Section 4.3.4 in which there are K linear models of the form

$$a_k = \mathbf{w}_k^T \mathbf{x} \quad (7.120)$$



Figure 7.12 Example of the relevance vector machine applied to a synthetic data set, in which the left-hand plot shows the decision boundary and the data points, with the relevance vectors indicated by circles. Comparison with the results shown in Figure 7.4 for the corresponding support vector machine shows that the RVM gives a much sparser model. The right-hand plot shows the posterior probability given by the RVM output in which the proportion of red (blue) ink indicates the probability of that point belonging to the red (blue) class.

which are combined using a softmax function to give outputs

$$y_k(\mathbf{x}) = \frac{\exp(a_k)}{\sum_j \exp(a_j)}. \quad (7.121)$$

The log likelihood function is then given by

$$\ln p(\mathbf{T}|\mathbf{w}_1, \dots, \mathbf{w}_K) = \prod_{n=1}^N \prod_{k=1}^K y_{nk}^{t_{nk}} \quad (7.122)$$

where the target values t_{nk} have a 1-of- K coding for each data point n , and \mathbf{T} is a matrix with elements t_{nk} . Again, the Laplace approximation can be used to optimize the hyperparameters (Tipping, 2001), in which the model and its Hessian are found using IRLS. This gives a more principled approach to multiclass classification than the pairwise method used in the support vector machine and also provides probabilistic predictions for new data points. The principal disadvantage is that the Hessian matrix has size $MK \times MK$, where M is the number of active basis functions, which gives an additional factor of K^3 in the computational cost of training compared with the two-class RVM.

The principal disadvantage of the relevance vector machine is the relatively long training times compared with the SVM. This is offset, however, by the avoidance of cross-validation runs to set the model complexity parameters. Furthermore, because it yields sparser models, the computation time on test points, which is usually the more important consideration in practice, is typically much less.

Exercises

- 7.1** (**) **www** Suppose we have a data set of input vectors $\{\mathbf{x}_n\}$ with corresponding target values $t_n \in \{-1, 1\}$, and suppose that we model the density of input vectors within each class separately using a Parzen kernel density estimator (see Section 2.5.1) with a kernel $k(\mathbf{x}, \mathbf{x}')$. Write down the minimum misclassification-rate decision rule assuming the two classes have equal prior probability. Show also that, if the kernel is chosen to be $k(\mathbf{x}, \mathbf{x}') = \mathbf{x}^T \mathbf{x}'$, then the classification rule reduces to simply assigning a new input vector to the class having the closest mean. Finally, show that, if the kernel takes the form $k(\mathbf{x}, \mathbf{x}') = \phi(\mathbf{x})^T \phi(\mathbf{x}')$, that the classification is based on the closest mean in the feature space $\phi(\mathbf{x})$.
- 7.2** (*) Show that, if the 1 on the right-hand side of the constraint (7.5) is replaced by some arbitrary constant $\gamma > 0$, the solution for the maximum margin hyperplane is unchanged.
- 7.3** (**) Show that, irrespective of the dimensionality of the data space, a data set consisting of just two data points, one from each class, is sufficient to determine the location of the maximum-margin hyperplane.
- 7.4** (**) **www** Show that the value ρ of the margin for the maximum-margin hyperplane is given by

$$\frac{1}{\rho^2} = \sum_{n=1}^N a_n \quad (7.123)$$

where $\{a_n\}$ are given by maximizing (7.10) subject to the constraints (7.11) and (7.12).

- 7.5** (**) Show that the values of ρ and $\{a_n\}$ in the previous exercise also satisfy

$$\frac{1}{\rho^2} = 2\tilde{L}(\mathbf{a}) \quad (7.124)$$

where $\tilde{L}(\mathbf{a})$ is defined by (7.10). Similarly, show that

$$\frac{1}{\rho^2} = \|\mathbf{w}\|^2. \quad (7.125)$$

- 7.6** (*) Consider the logistic regression model with a target variable $t \in \{-1, 1\}$. If we define $p(t = 1|y) = \sigma(y)$ where $y(\mathbf{x})$ is given by (7.1), show that the negative log likelihood, with the addition of a quadratic regularization term, takes the form (7.47).
- 7.7** (*) Consider the Lagrangian (7.56) for the regression support vector machine. By setting the derivatives of the Lagrangian with respect to \mathbf{w} , b , ξ_n , and $\hat{\xi}_n$ to zero and then back substituting to eliminate the corresponding variables, show that the dual Lagrangian is given by (7.61).

- 7.8** (★) **www** For the regression support vector machine considered in Section 7.1.4, show that all training data points for which $\xi_n > 0$ will have $a_n = C$, and similarly all points for which $\hat{\xi}_n > 0$ will have $\hat{a}_n = C$.
- 7.9** (★) Verify the results (7.82) and (7.83) for the mean and covariance of the posterior distribution over weights in the regression RVM.
- 7.10** (★★) **www** Derive the result (7.85) for the marginal likelihood function in the regression RVM, by performing the Gaussian integral over \mathbf{w} in (7.84) using the technique of completing the square in the exponential.
- 7.11** (★★) Repeat the above exercise, but this time make use of the general result (2.115).
- 7.12** (★★) **www** Show that direct maximization of the log marginal likelihood (7.85) for the regression relevance vector machine leads to the re-estimation equations (7.87) and (7.88) where γ_i is defined by (7.89).
- 7.13** (★★) In the evidence framework for RVM regression, we obtained the re-estimation formulae (7.87) and (7.88) by maximizing the marginal likelihood given by (7.85). Extend this approach by inclusion of hyperpriors given by gamma distributions of the form (B.26) and obtain the corresponding re-estimation formulae for α and β by maximizing the corresponding posterior probability $p(\mathbf{t}, \alpha, \beta | \mathbf{X})$ with respect to α and β .
- 7.14** (★★) Derive the result (7.90) for the predictive distribution in the relevance vector machine for regression. Show that the predictive variance is given by (7.91).
- 7.15** (★★) **www** Using the results (7.94) and (7.95), show that the marginal likelihood (7.85) can be written in the form (7.96), where $\lambda(\alpha_n)$ is defined by (7.97) and the sparsity and quality factors are defined by (7.98) and (7.99), respectively.
- 7.16** (★) By taking the second derivative of the log marginal likelihood (7.97) for the regression RVM with respect to the hyperparameter α_i , show that the stationary point given by (7.101) is a maximum of the marginal likelihood.
- 7.17** (★★) Using (7.83) and (7.86), together with the matrix identity (C.7), show that the quantities S_n and Q_n defined by (7.102) and (7.103) can be written in the form (7.106) and (7.107).
- 7.18** (★) **www** Show that the gradient vector and Hessian matrix of the log posterior distribution (7.109) for the classification relevance vector machine are given by (7.110) and (7.111).
- 7.19** (★★) Verify that maximization of the approximate log marginal likelihood function (7.114) for the classification relevance vector machine leads to the result (7.116) for re-estimation of the hyperparameters.